NASA/CP—1999–209144

The 1998 NASA Aerospace Battery Workshop

Compiled by
J.C. Brewer
Marshall Space Flight Center, Marshall Space Flight Center, Alabama

Proceedings of a conference sponsored by the
NASA Aerospace Flight Battery Systems Program
and held in Huntsville, Alabama, October 27–29, 1998

February 1999

The NASA STI Program Office...in Profile

Since its founding, NASA has been dedicated to the advancement of aeronautics and space science. The NASA Scientific and Technical Information (STI) Program Office plays a key part in helping NASA maintain this important role.

The NASA STI Program Office is operated by Langley Research Center, the lead center for NASA's scientific and technical information. The NASA STI Program Office provides access to the NASA STI Database, the largest collection of aeronautical and space science STI in the world. The Program Office is also NASA's institutional mechanism for disseminating the results of its research and development activities. These results are published by NASA in the NASA STI Report Series, which includes the following report types:

- TECHNICAL PUBLICATION. Reports of completed research or a major significant phase of research that present the results of NASA programs and include extensive data or theoretical analysis. Includes compilations of significant scientific and technical data and information deemed to be of continuing reference value. NASA's counterpart of peer-reviewed formal professional papers but has less stringent limitations on manuscript length and extent of graphic presentations.

- TECHNICAL MEMORANDUM. Scientific and technical findings that are preliminary or of specialized interest, e.g., quick release reports, working papers, and bibliographies that contain minimal annotation. Does not contain extensive analysis.

- CONTRACTOR REPORT. Scientific and technical findings by NASA-sponsored contractors and grantees.

- CONFERENCE PUBLICATION. Collected papers from scientific and technical conferences, symposia, seminars, or other meetings sponsored or cosponsored by NASA.

- SPECIAL PUBLICATION. Scientific, technical, or historical information from NASA programs, projects, and mission, often concerned with subjects having substantial public interest.

- TECHNICAL TRANSLATION. English-language translations of foreign scientific and technical material pertinent to NASA's mission.

Specialized services that complement the STI Program Office's diverse offerings include creating custom thesauri, building customized databases, organizing and publishing research results...even providing videos.

For more information about the NASA STI Program Office, see the following:

- Access the NASA STI Program Home Page at ***http://www.sti.nasa.gov***

- E-mail your question via the Internet to help@sti.nasa.gov

- Fax your question to the NASA Access Help Desk at (301) 621–0134

- Telephone the NASA Access Help Desk at (301) 621–0390

- Write to:
  NASA Access Help Desk
  NASA Center for AeroSpace Information
  800 Elkridge Landing Road
  Linthicum Heights, MD 21090–2934

NASA/CP—1999–209144

The 1998 NASA Aerospace Battery Workshop

Compiled by
J.C. Brewer
Marshall Space Flight Center, Marshall Space Flight Center, Alabama

Proceedings of a conference sponsored by the
NASA Aerospace Flight Battery Systems Program
and held in Huntsville, Alabama, October 27–29, 1998

National Aeronautics and
Space Administration

Marshall Space Flight Center • MSFC, Alabama 35812

February 1999

Available from:

NASA Center for AeroSpace Information
800 Elkridge Landing Road
Linthicum Heights, MD 21090–2934
(301) 621–0390

National Technical Information Service
5285 Port Royal Road
Springfield, VA 22161
(703) 487–4650

Preface

This document contains the proceedings of the 31st annual NASA Aerospace Battery Workshop, hosted by the Marshall Space Flight Center on October 27-29, 1998. The workshop was attended by scientists and engineers from various agencies of the U.S. Government, aerospace contractors, and battery manufacturers, as well as international participation in like kind from a number of countries around the world.

The subjects covered included nickel-hydrogen, silver-hydrogen, nickel-metal hydride, and lithium-based technologies, as well as results from destructive physical analyses on various cell chemistries.

Introduction

The NASA Aerospace Battery Workshop is an annual event hosted by the Marshall Space Flight Center. The workshop is sponsored by the NASA Aerospace Flight Battery Systems Program which is managed out of NASA Lewis Research Center and receives support in the form of overall objectives, guidelines, and funding from Code S, NASA Headquarters.

The 1998 Workshop was held on three consecutive days and was divided into five sessions. The first day consisted of a General Session and a Lithium-Ion / Nickel-Metal Hydride Session. The second day consisted of a Destructive Physical Analysis (DPA) Findings Focused Session and a Nickel-Hydrogen Session. The third and final day was devoted to an Advanced Nickel-Hydrogen / Silver-Hydrogen Session.

On a personal note, I would like to take this opportunity to thank all of the many people that contributed to the organization and production of this workshop:

The NASA Aerospace Flight Battery Systems Program, for their financial support as well as their input during the initial planning stages of the workshop;

Lawrence H. Thaller and **Albert H. Zimmerman**, The Aerospace Corporation, for serving as Focused Session Organizers, which involved soliciting presentations, organizing the session agenda, and orchestrating the session during the workshop;

Huntsville Hilton, for doing an outstanding job in providing an ideal setting for this workshop and for the hospitality that was shown to all who attended;

Marshall Space Flight Center employees, for their help in mailing the various correspondence, registering attendees, handling the audience microphones, and flipping transparencies during the workshop.

Finally, I want to thank all of you that attended and/or prepared and delivered presentations for this workshop. You were the key to the success of this workshop.

Jeff Brewer
NASA Marshall Space Flight Center

Table of Contents

Preface iii

Introduction v

General Session 1

Design Automation Associates, Inc. Rule Based Development Partner
John C. Lambert, Design Automation Associates, Inc. 3

Thermal Control Using Electrochromism
Hari Vaidyanathan, COMSAT Laboratories; and Gopalakrishna Rao, NASA Goddard Space Flight Center 39

Battery / Ultracapacitor Evaluation for X-38 Crew Return Vehicle (CRV)
Eric C. Darcy, NASA Johnson Space Center; and Bradley Strangways, Symmetry Resources, Inc. 61

DS-2 Mars Microprobe Battery
H. Frank, A. Kindler, F. Deligiannis, E. Davies, J. Blankevoort, B.V. Ratnakumar, and S. Surampudi, Jet Propulsion Laboratory 91

Design and Flight Performance of NOAA-K Spacecraft Batteries
Gopalakrishna M. Rao and Tom Spitzer, NASA Goddard Space Flight Center; P.R.K. Chetty, Kris Engineering, Inc.; and P. Chilelli, LMMS 113

Lithium-Ion / Nickel-Metal Hydride Session 139

Lithium-Ion Batteries for Aerospace Applications
S. Surampudi and G. Halpert, Jet Propulsion Laboratory; R.A. Marsh and R. James, U.S. Air Force Research Laboratory 141

The Applicability of Lithium-Ion Secondary Battery Cells to Space Programs
Yoshitsugu Sone, Hiroaki Kusawake, Koichi Kanno, and Saburo Kuwajima, NASDA 161

Testing of the Eagle-Picher Lithium-Ion System
Chad Kelly and Shellie Wilson, Eagle-Picher Technologies, LLC 193

Evaluation of Safety and Performance of Sony Lithium-Ion Cells
Judith A. Jeevarajan and Bobby J. Bragg, NASA Johnson Space Center 203

Bipolar Nickel-Metal Hydride Battery Development Project
John Cole, Electro Energy, Inc. 223

Battery Study for the Shuttle Orbiter EAPU Upgrade
B. Otzinger, S. Hwangbo, T. Farkas, G. Schwartz, M. Gajewski, S. Verzwyvelt, T. Barrera, B. Barrera, and C. Johnson, Boeing Defense and Space Group; and B. Irlbeck, NASA Johnson Space Center 265

DPA Findings Focused Session 295

Expert System for Nickel-Hydrogen Battery Cell Diagnostics
A. Zimmerman and L. Thaller, The Aerospace Corporation 297

Nickel Electrode Failure by Chemical De-activation of Active Material
A. Zimmerman, M. Quinzio, G. To, P. Adams, and L. Thaller, The Aerospace Corporation . . 317

Studies of Component Degradation and Silver Migration in Experimental Silver-Zinc Cells
Harlan L. Lewis, Naval Surface Warfare Center, Crane Division 329

Studies of Component Degradation During Testing of Nickel-Hydrogen Cells
Steve Wharton and Harry Brown, Naval Surface Warfare Center, Crane Division 349

Destructive Physical Analysis of Flight- and Ground-Tested Sodium-Sulfur Cells
Margot L. Wasz and Boyd J. Carter, The Aerospace Corporation; Lt. Charles M. Donet, Air Force Research Laboratory; and Richard S. Baldwin, NASA Lewis Research Center 377

Using DPA Results from Boiler Plate NiH_2 Cells to Help Understand Design Limitations and Validate New Cell Components
Thierry Jamin, French Space Agency CNES Toulouse 399

Destructive Physical Analysis of Lithium-Ion Cells
Nathan "Ned" Isaacs, John Baker, Joseph Bytella, Ken Richardson, and Brian Stein, Mine Safety Appliances Company 441

Nickel-Hydrogen Session 481

Proposed Convention for Assigning NiH_2 Cell Capacity
James R. Wheeler, Eagle-Picher Technologies, LLC 483

NiH_2 Reliability Update
Douglas P. Hafen, Lockheed Martin Missiles & Space 503

High DOD LEO Life Cycle Testing
Jeff Dermott, Eagle-Picher Technologies, LLC 521

Ni-H_2 Batteries Performance on Communication and Broadcasting Engineering Test Satellite
H. Kusawake, Y. Sone, T. Nakamura, and S. Kuwajima, National Space Development Agency of Japan 535

Reversal as a Tool for Assessing Precharge of Nickel-Hydrogen Cells
Jack N. Brill and Ron Smith, Eagle-Picher Technologies, LLC 559

Advanced Nickel-Hydrogen / Silver-Hydrogen Session 579

MGS 2-Cell CPV NiH_2 Batteries
Sal Di Stefano, Jet Propulsion Laboratory 581

CPV Flight Experience
William Cook and Jack Brill, Eagle-Picher Industries, LLC 605

Status of SPV/CPV Testing
Harry Brown & Steve Hall, Naval Surface Warfare Center, Crane Division 621

Nickel-Hydrogen Single Pressure Vessel (SPV) Battery Test Results
Steve Sterz, Beth Parmley, and Dwight Caldwell, Eagle-Picher Industries, LLC 647

Lightweight Silver-Hydrogen Cell Design
D.K. Coates, S.C. Cooper, and D.P. Bemis, Eagle-Picher Industries, LLC 669

ERRATA to 1997 NASA Aerospace Battery Workshop Proceedings
(NASA/CP-1998-208536, pages 83-112) 703

1998 NASA Aerospace Battery Workshop Attendance List 707

General Session

Design Automation Associates, Inc

Rule Based **d e v e l o p m e n t**

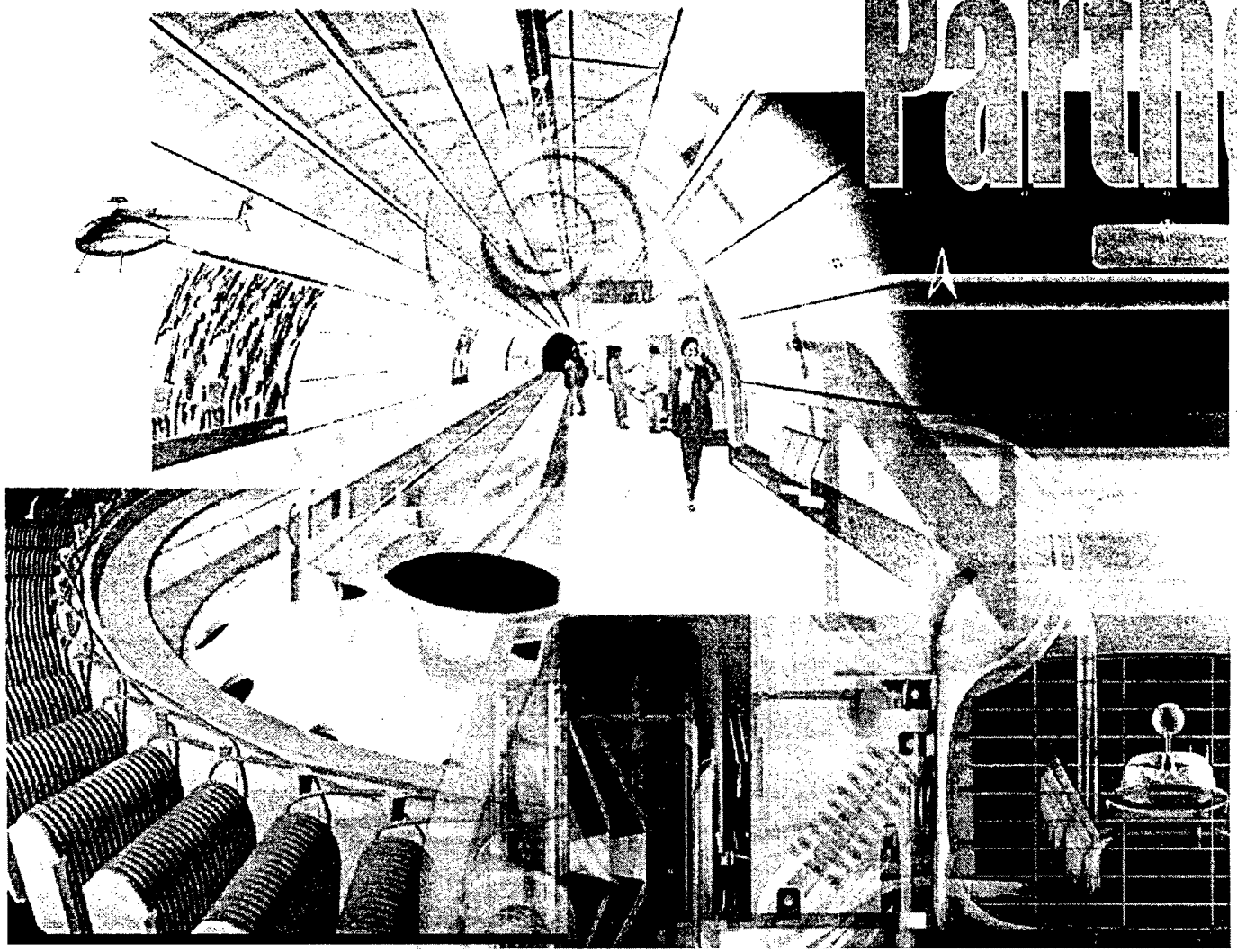

Your Presenter

Design Automation Associates, Inc.

- John C. Lambert
  - President & Co-Founder
  -

new ways to new solutions

Design By Intent!

1998 NASA Aerospace Workshop

Design Automation Associates, Inc.

Providers of:

- Engineering Automation
- Engineering Solutions
- Manufacturing Automation
- Sales Engineering Automation

new ways to new solutions

DESIGN BY INTENT!

Why are we here today?

- Brief overview of DAA
- Bi-Polar NiMH Battery Design System (LeRC)
- Ni-H_2 Battery Evaluation System (Goddard)
- Future Directions
- Classical Problems with Automation
- How RBT Fits into Automation
- Wrap Up

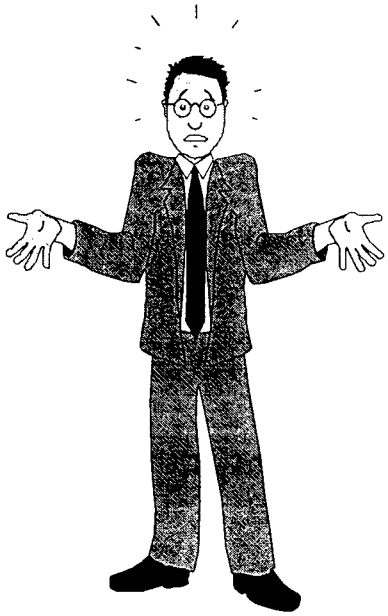

new ways to new solutions

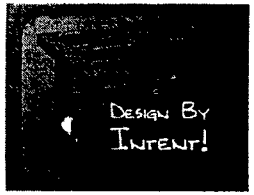

DAA Overview

- Engineering/Software Solution Provider
  - Environments: Intent!, ICAD, VB, LISP, FORTRAN, C, C++, CAD, MS Office, etc...
- Staff of Degreed Engineers
- DAA Engineers understand <u>your</u> mentality and can provide solutions that meet the real life application challenges.
- Completing or 5th year of Business.
- Major National Accounts, Numerous hardened, successful applications in production.
- <u>Commitment to following through</u> until success is achieved.
- **new ways to new solutions**

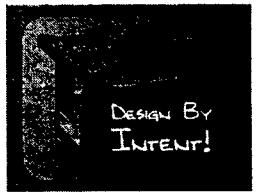

DAA's Core Competencies

- **Engineering Automation**
  - Optimization, Database and Logic Intensive Applications
  - Drawings, 2D & 3D, Wireframe, Solid Modeling
  - Custom Report Generation, Schematics and Diagrams
  - Finite Element Analysis Automation (Thermal/Structural)
  - Integration with in-house or Commercial off the Shelf Programs
  - Custom Assemblies & Designs
- **Manufacturing Automation**
  - Assembly & Machining Fixtures
  - Routings/Work Cell Selection/OP Sheets/Material Selection
  - Inspection Documents/Scheduling/ MRP Integration
  - Machine, Tool & Fixture Design
  -

new ways to new solutions

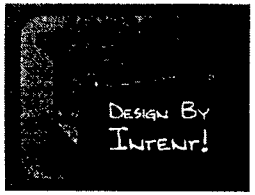

DAA's Core Competencies, (cont.

- **Special Services**
  - Hot-line Support
  - Intent! developer training
  - Documentation
  - Structural & Thermal FEA automation
  - Visual Basic, AutoLISP, C, FORTRAN, Basic
  - Project Management
  - DAA Intent!™ Extension
  - ***WEB Based support, Design and Configurations***
  - —

new ways **to new** solutions

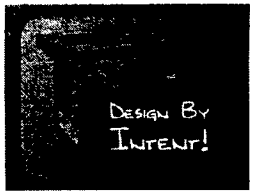

NiMH (Bi-Polar) Battery Design System

- Benefits
  - Allows Designers to Conduct Comprehensive Battery and Cell Trade Studies *rapidly*
  - Designers can conduct complex structural and thermal analysis without in depth knowledge of these specialized disciplines
  - Standardization
  - Error elimination
  - System Flexibility, Modularity and Long Term Longevity
  - Software Systems Integration
  - Expandable to other chemistries

new ways to new solutions

NiMH (Bi-Polar) Battery Design System

- Inputs
  - –
    - Graphical "MS Office" like User Interface
    - Performance Requirements or Envelope
    - Cell and Hardware Information
    - Cost information
    - Sensitivity Studies
    - Iteration based on cell orientations
    - Fully Automated Structural and Thermal Analysis (Finite Element)
  - –
  - –

new ways to new solutions

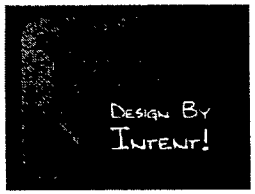

NiMH (Bi-Polar) Battery Design System

- System Highlights
  -
    - Prismatic or Cylindrical Designs
    - Hogged Out or Honeycomb end plates
    - Rapid Fatigue Analysis (LCF and HCF)
    - Rapid Thermal Analysis
    - Multiple battery designs can be considered simultaneously
      - Cell orientations
      - Sensitivity Studies
    - System is **extremely** flexible and expandable

new ways to new solutions

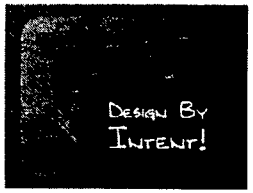

NiMH (Bi-Polar) Battery Design System

- Outputs
  - Battery Summary and 3D Model
  - Extensive Inputs Report
  - Weight summaries and breakdowns (Battery, Cell and Hardware)
  - Costed BOMS (Recurring and Non-Recurring)
  - Produciblity Report and Maintenance Guidelines
  - 2D Detailed drawings and details
  - Sensitivity Study Plots
  - Fatigue Life Summary

new ways to new solutions

Design By Intent!

NiMH (Bi-Polar) Battery Design System

- Demonstration
-

Ni-H_2 Battery Concept Design System

- Benefits
  - Allows Non-Expert Designers to Conduct Comprehensive Battery and Cell Trade Studies *rapidly*
  - Knowledge Capture, Retention and Control
  - Standardization
  - Error elimination
  - System Flexibility, Modularity and Long Term Longevity
  - Software Systems Integration
  - EXPANDABLE to other chemistries!
  - Expandable to include comprehensive database of all commercially available batteries and cells

new ways to new solutions

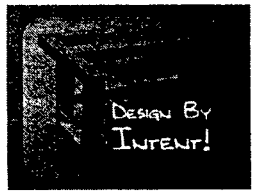

Ni-H_2 Battery Concept Design System

- Inputs
  -
  - High Level Mission requirements
  - Cell Configuration (IPC, CPV, etc…)
  - Ability to iterate and sort many cells by weight, footprint, height, cost, etc..
  -
  -
  -
-
-

new ways to new solutions

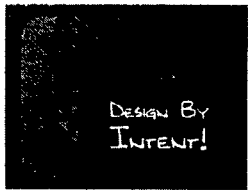

Ni-H_2 Battery Concept Design System

- System Highlights
  - Advanced User interface (UI)
  - Cell Evaluation and Battery Configuration System as opposed to a detailed design system.
  - Intensive iteration and trade study capability (up to 128 battery designs sorted by output driver)
  - Optimized cell arrangement
  - Accurate Depth of Discharge Calculation
  - Automated Thermal Analysis (Automated Finite Difference Model generation, execution and post processing)

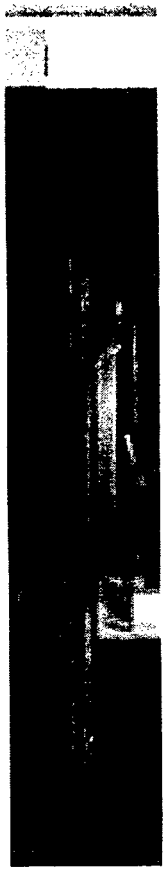

new ways to new solutions

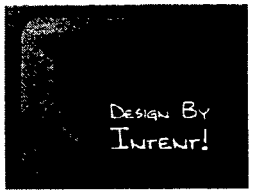

Ni-H_2 Battery Concept Design System

- System Highlights
  - Cells designs based on, and constrained by "Industry Standards".
  - Weights, Actual Geometry for Electrode Leads determined, etc…
  - Provides solid starting point to approach Ni-H_2 vendor
  -
  -
  -
  -

new ways to new solutions

Design By Intent!

Ni-H_2 Battery Concept Design System

- Outputs
  -
    - Viable Options Report.
    - Key Parameter Report.
    - Input Report.
    - Cell Cross Section.
    - Parts List.
    - Cell Arrangement in 3D Solids
    - Thermal Results (Finite Difference Model and Results)
    -

new ways to new solutions

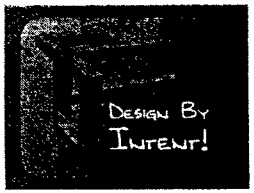

Ni-H_2 Battery Concept Design System

- Demonstration
-

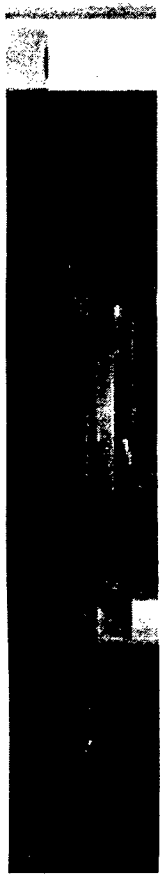

new ways **to new** solutions

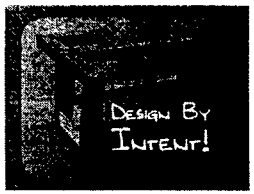

Future Direction

- Create an integrated Battery Evaluation System for Multiple Chemistries.
  - Expand current functionality for:
    - Ni-H_2
  - Includes new functionality to Include:
    - NiCd, Li-Ion
  - May also include new/expanded functionality for
    - NiMH (Traditional and Bi-Polar)

new ways to new solutions

Future Direction

- Create an integrated Battery Evaluation System.
  - Includes
    - Electro-Chemical Performance characteristics
    - Industry standard rules of battery configuration and/or design
    - Comprehensive industry standards database
    - Functionality as specified by Industry Battery Users
    - Targeted for Aerospace community initially(Battery manufacturers and battery users)
    - Expanded to commercial products (laptops, cell phones, camcorders, etc… 500M/year market)

new ways to new solutions

Future Direction

- Create an integrated Battery Evaluation System.
  - Customization Module that allows easy addition of organization specific design requirements and rules
  - Couple the system into Power System Design?
    - Solar Arrays, etc...

new ways to new solutions

Classical Problems with Automation

- Complete "visionary" picture required up-front
- Conflict between size and flexibility - application "dead ending"
- Continuum of changing requirements.
- Multiple "domains" involved in the Automation Effort
- Gaps in domain experts expectations vs. the programmer's.
- High Costs and/or "heavy" systems
-
-

new ways to new solutions

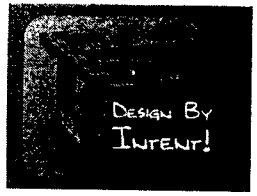

Classical Problems with Automation

- In Summary
  - Too Much Complexity
  - Not Enough Flexibility
  - Gaps in Expectations
  - Cost are too High
-
-

new ways to new solutions

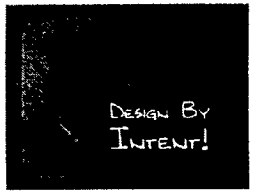

Complexity is Driven by Each Individual's Proces

Many Different Data Sources and Sub Processes Managed by the Engineer

Personal Knowledge

External Data

- Parts Libraries
- Catalogs/Tables
- Books/Manuals
- Standards/Codes

Specifications

- Customer Requirements
- Functional Requirements
- Constraints
- Specs

Other Experts

- Design
- Manufacturing
- Analysis
- Drafting
- Consultants

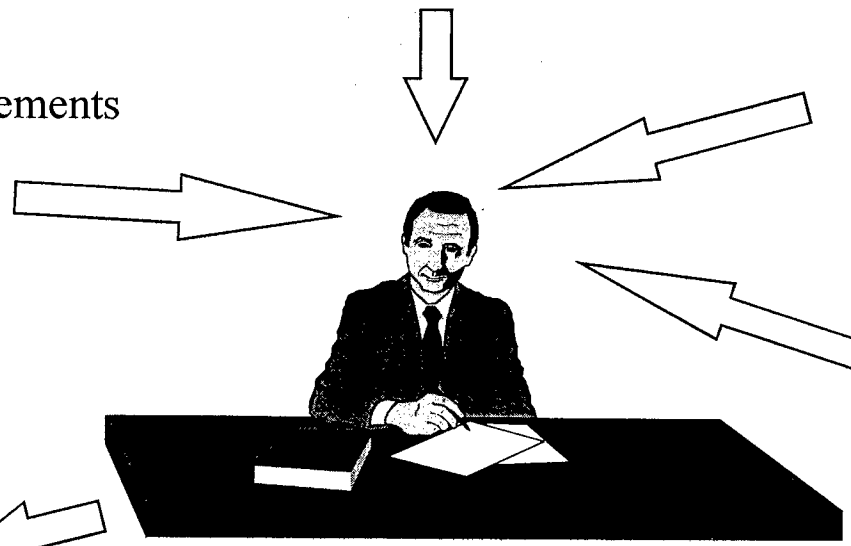

Engineer/Analyst

Outputs

- Analysis Results
- Data
- Reports/Documents
- Drawings, Schematics
- CAD Models

Computer Program

- COPs
- Legacy Programs

new ways to new solutions

Design By Intent!

RBT Can Simplify the Complexity

The *Only* Automation Environment that Encompasse all functional domains

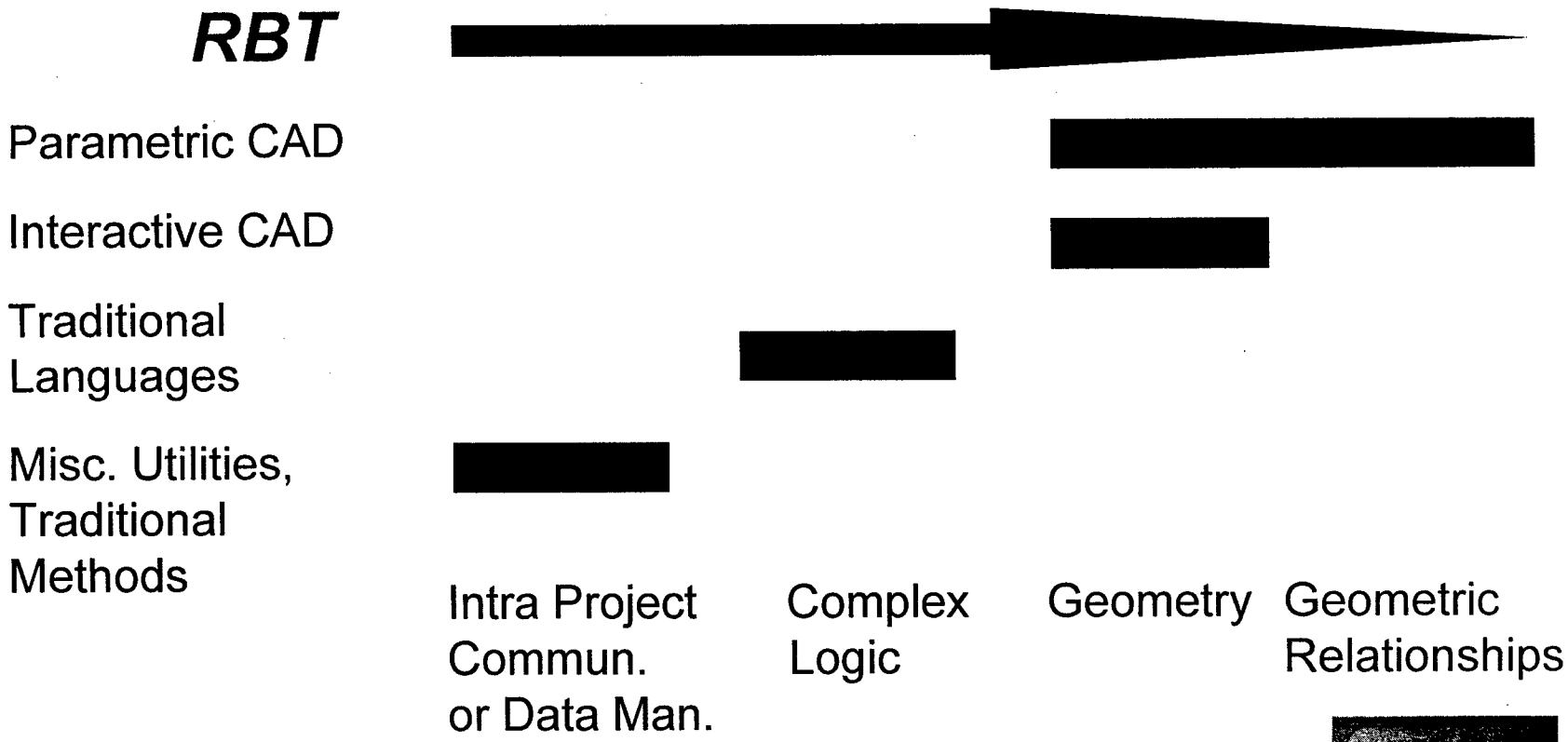

new ways to new solutions

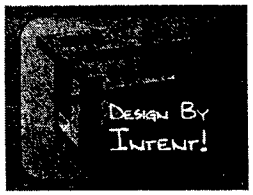

RBT Can Simplify the Complexity

- Seamless Functionality across all Domains
  - Optimization & *Rapid* Trade Studies (Geometric/Non Geometric)
  - Data base integration, Data Manipulation
  - Thermal and Structural Analysis
  - Geometry, Assemblies, Models, Drawings, S... ...s...
  - System Integration
  - Communication Automation
  - Knowledge Retention
  -

new ways to new solutions

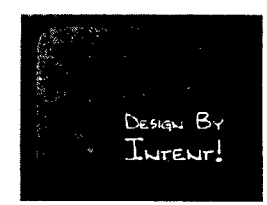

26

RBT adds Flexibility

- Programming Flexibility
  - Non-Procedural, Declarative Programming Style; No required order for rules!
  - Extremely Flexible Architecture (flexibility not a function of size)
  - Demand Driven Program Execution
  - Object Orientated

new ways to new solutions

Design By Intent!

RBT adds Flexibility

- Ease of Application Creation
  - Simple Language Syntax; Easy to learn
  - Visual Development Environment with Code Generation
  - Automated Memory Management
- Open Architecture
  - ODBC, C/C++, Active-X on its way
- Robust, Comprehensive Language
-
-
- **new ways to new solutions**

Design By Intent!

RBT adds Flexibility

Flexible Application Development

- Rule Based Applications can be as interactive or programmatic as necessary. (Often times engineers change the rules or don't even know what they want!)

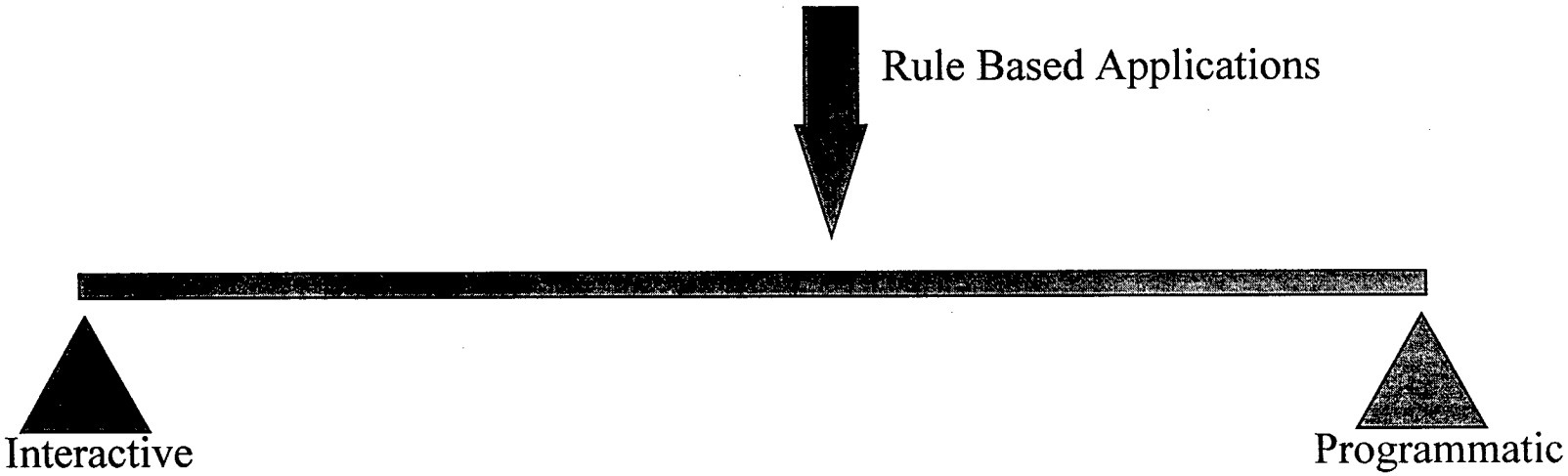

new ways to new solutions

Design By Intent!

RBT adds Flexibility

- Bottom Line:
  - Flexibility and Long Term Application Longevity

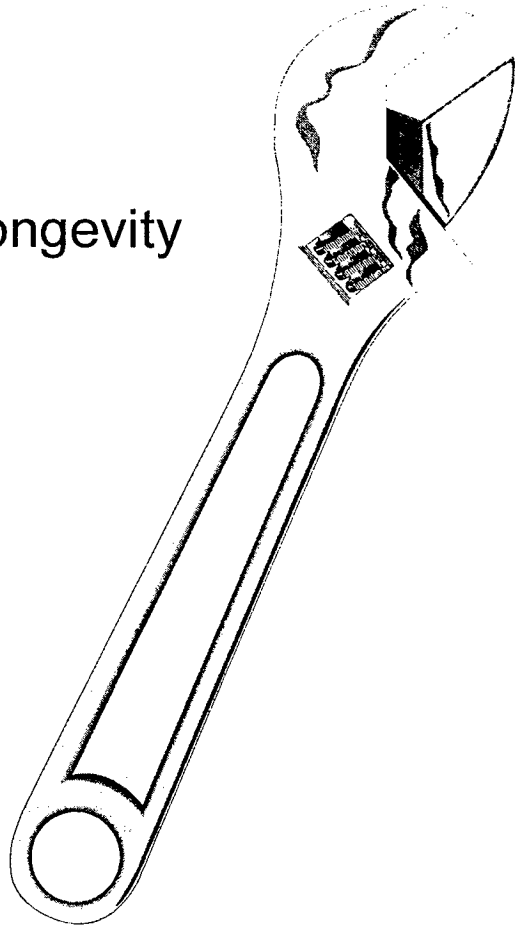

new ways to new solutions

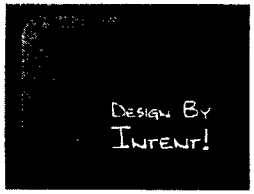

RBT Helps to Close Expectation Gaps

- DAA uses engineers as primary application developers
- RBT enables the domain expert and the developer to be one in the same.
- Communication between DAA engineers and the customer usually flows very smoothly.
-

new ways to new solutions

Design By Intent!

RBT is Cost Effective

- Lower Cost of Ownership than legacy RBT
  - Purchase Price
  - Maintenance
  - Platform (PC Based)
- Deployment costs have come down
- Runtime speeds of RBT languages have increased dramatically
- Application "dead ending" eliminated

new ways to new solutions

Design By Intent!

Wrap Up

- RBT and DAA Add Up To:
  - Less Complexity
  - Much Greater Flexibility and Long Term Longevity
  - Fewer Gaps in Customer/Developer Expectations
  - Automation made more Cost Effective
  - Deviation from the traditional programming model.
  - Guaranteed Success provided by DAA as your Integration Partner
  -
- **new ways to new solutions**

Design By Intent!

Acknowledgements

- NASA
  - LeRC - Michelle Manzo & Tom Miller
  - GSFC - Thomas Yi
- Electro Energy Inc
  - Martin Klein & John Cole
- DAA
  - Sean Sullivan & William Johnson

new ways to new solutions

Design By Intent!

End of Presentation

new ways to new solutions

DESIGN BY INTENT!

THERMAL CONTROL USING ELECTROCHROMISM

Hari Vaidyanathan
COMSAT Laboratories
Clarksburg, MD
And
Gopalakrishna Rao
NASA Goddard Space Flight Center
Greenbelt, MD

ABSTRACT

The applicability of a charge balanced electrochromic device to modulate the frequencies in the thermal infra red region is examined in this study. The device consisted of a transparent conductor, WO_3 anode, PMMA/$LiClO_4$ electrolyte,V_2O_5 cathode and transparent conductor. The supporting structure in the device is SnO_2 coated glass and the edges are sealed with epoxy to reduce moisture absorption. The performance evaluation comprised of cyclic voltammetric measurements and determination of transmittance at various wavelengths. The device was subjected to anodic and cathodic polarization by sweeping the potential at a rate of 10 mV/sec from –0.8V to 1.8V. The current versus voltage profile indicated no reaction between -0.5 and +0.5 V. The device is colored green at 1.8 V with a transmittance of 5% at a wavelength, λ =900 nm and colorless at -0.8 V with a transmittance of 74% at λ=500 nm. The optical modulation is limited to 400-1500 nm and there is no activity in the thermal infrared. The switching time is a function of temperature and time for coloring reaction was slower than the bleaching reaction. The device yielded reproducible values for transmittance when cycled between colored and bleached states by application of 1.8V and –0.8V, respectively.

INTRODUCTION

Electrochromism has been the subject of intense study in the past decade. The automatic dimming of rear view mirrors for motor vehicles is the first commercial product based on electrochromism. The electrochromic devices exhibit high optical contrast with continuous variation of transmittance, UV stability, optical memory and a wide temperature range of operation. An electrochromic device is a thin film rechargeable battery in which an electrochromic electrode is separated by a solid electrolyte from a counter electrode. The rechargeable battery uses the 'rocking chair concept' in which the lithium ions rock between cathode and anode. Charging and discharging of the device changes the spectral response. The performance of the device is based on the insertion of lithium ions into the lattice of the electrochromic electrode. The device can be constructed with electrochromic material on either the anode or cathode or in both.

The purpose of this study is to examine the applicability of the thin film electrochromic devices for thermal control in satellites. This device is a lightweight alternative for the heaters, louvers and heat pipes that regulate the satellite temperature. The experimental results obtained using a device supplied by NREL are reported in this study.

DESCRIPTION

The device consists of a solid-state battery composed of thin layers of anode, cathode, and electrolyte assembled in a glass case. The electrochromic layer consisted of WO_3 and it functions as a cathode. The active material in the anode was V_2O_5 and it functions as an ion storage layer. The stiffness to the structure is provided by indium tin oxide (ITO) that also functions as a transparent conductor. The solid electrolyte consists of polymethylmethacrylate mixed with $LiClO_4$ and propylene carbonate. The dimensions of the device are 5 cm X 6 cm X 0.5 cm. Figure 1 shows the schematic structure of the device.

The tests consisted of determining the voltage profile using cyclic voltammetry and measuring the optical spectrum using a spectrophotometer.

VOLTAGE PROFILE

The device was polarized anodically by sweeping the potential from –0.8 V to 1.8 V at a rate of 10 mV/sec and then, polarized back to – 0.8 V at the same rate in one cycle to obtain the current-voltage profile. The current was negligibly small from –0.5 to 0.5 V and then increased in an exponential manner until 1.8 V. The device turned green at 1.8 V and colorless at – 0.8 V. The coloring and bleaching of the device occurred when the potential sweeps were repeated. Figure 2 shows the potential-current curves for two consecutive cycles. There is hysterisis in the current-voltage profile and the coloring reaction has a higher current density than the bleaching reaction.

SPECTRAL RESPONSE

The device was mounted in the spectrophotometer and electrical connections were made to perform potentiostatic experiments. The transmittance of the device at an applied voltage of 1.7 V was measured as a function of wavelength. Then, the applied voltage was decreased to 0 V and the transmittance was again measured. The spectral data indicated that there is optical modulation between wavelength $\lambda = 450$ nm and 1100 nm. The transmittance of the device was

74% at $\lambda = 500$ nm (colorless state-bleached) and 5% at $\lambda = 900$ nm (green). The device switches from a transmittance of 71% to 10% at a wavelength of 680 nm as a result of the applied voltage. Figure 3 illustrates the activity of the device in the spectral region from 400 to 1400 nm.

SWITCHING TIME

The time taken by the device, to turn to the bleached state from a colored state at 45 °C, was determined by measuring the transmittance at $\lambda = 700$ nm as a function of time, after application of –0.8 V. Figure 4 shows the spectral transient. The transmittance increases to 60% in 240 seconds and to 72% in 900 seconds. The switching time for the reverse process, i.e. coloring was determined by applying 1.8 V and measuring the transmittance at 700 nm as a function of time. A switching time of 75 seconds was measured for the transmittance to decrease to 50%. A further 10% decrease in transmittance to 40%, occurred in 23 minutes.

The colored-to-bleached switching time was determined at 30°C and 0°C and the transients are shown in Figures 5 and 6 respectively. There is a marked increase in the switching observed at 0°C.

TEMPERATURE EFFECT

The optical spectrum was determined in the bleached state at 23°C, 30°C, 45°C and 0°C and the results are shown in Figure 7 through 10 respectively.. The percent transmittance is higher in the colored state at 30°C compared to 0°C, whereas in the bleached state the transmittance is lower at 30°C compared to 0°C. The variation of percent transmittance at $\lambda = 610$ nm as a function of temperature is plotted in Figure 11. The results indicated marginal increase in the transmittance when the temperature is increased from 23°C to 45°C. At 10°C the percent transmittance decreased by 6% compared to that measured at 23°C. The temperature dependency is attributed to the conductivity of the solid electrolyte which increases with increase in temperature. .

REPETITIVE CYCLING

The device was cycled between –0.8 V and 1.8 V a number of times and the transmittance at $\lambda = 700$ nm was measured at 23°C. Figure 12 shows the transients which were reproducible with cycling. The curves indicate a transmittance of 5.9% in the colored state and 69.5% in the bleached state.

THERMAL MODULATION

The spectrographic data indicates activity in the wavelength region 400- 1500 nm. The bleaching and coloring in the visible region demonstrates the ability to modulate energy in the visible region. There is no spectral response in the wavelength region 6-10 micron that corresponds to the infra red region.

CONCLUSIONS

The results of the evaluation point to the following conclusions:

1. The electrochemical current-voltage curves indicate that the device is colored at 1.8 V and bleached at - 0.8 V. There is no electrochemical reaction from –0.5 to 0.5 V and the coloring reaction has a higher current.
2. In the colored state the minimum transmittance observed is 5.9 % at a wavelength of 700 nm. In the bleached state the transmittance was 74 % at a wavelength of 500 nm.
3. The switching time for the coloring process from a bleached state was higher than that of the bleaching reaction in the reverse direction .
4. The data suggests modulation of energy in the visible region. There is no spectral activity from 6 – 10 microns that corresponds to the infrared region.
5. The device is capable repeated cycling

THERMAL CONTROL USING ELECTROCHROMISM

PURPOSE

TO DEVELOP FILM STRUCTURES BASED ON ELECTROCHROMISM FOR THERMAL CONTROL OF SATELLITE SUBSYSTEMS

COMSAT LABORATORIES

ADVANTAGES

- ELECTROCHROMIC DEVICE IS LIGHT WEIGHT, IT HAS OPTICAL MEMORY, ELECTRICALLY TUNABLE, SPECTRAL SELECTIVITY AND WIDE RANGE OF OPERATING TEMPERATURE.
- POTENTIAL REPLACEMENT FOR HEATERS, LOUVERS AND HEAT PIPES

COMSAT LABORATORIES

DESCRIPTION

- AN ELECTROCHROMIC DIVICE IS A THIN FILM BATTERY CONTAINING ELECTROCHROMIC ELECTRODES SEPARATED BY A SOLID ELECTROLYTE.
- CHARGING AND DISCHARGING CHANGE THE SPECTRAL RESPONSE
- LITHIUM INSERTION INDUCES SPECTRAL RESPONSE.

COMSAT LABORATORIES

FIGURE 1

SCHEMATIC OF THE ELECTROCHROMIC DEVICE

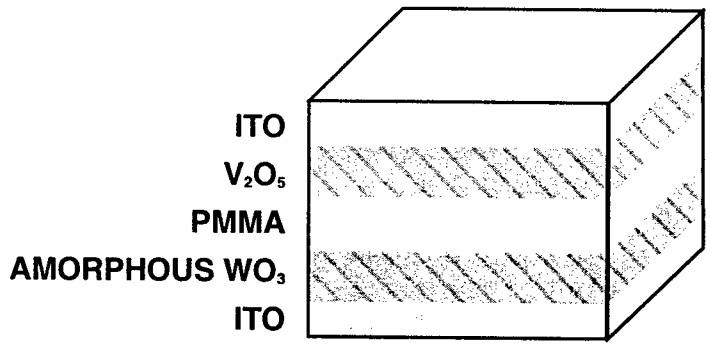

$$Li_xWO_3 + V_2O_5 \leftrightarrow WO_3 + Li_yV_2O_5$$

(COLORED) (BLEACHED)

COMSAT LABORATORIES

EVALUATION OF THE PROTOTYPE

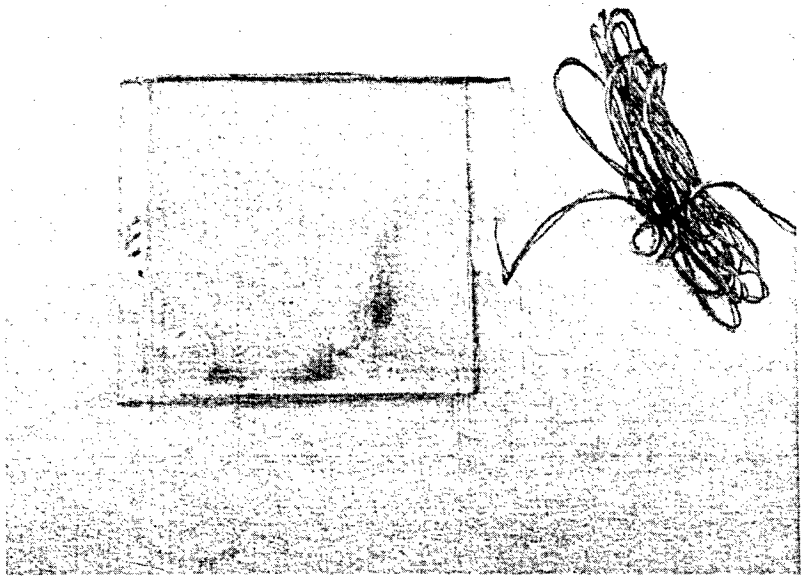

- DEVICE ASSEMBLED BY NREL
- USES WO_3 AND V_2O_5
- PARAMETERS: SPECTRAL RANGE, MODULATION, TEMP.,VOLTAGE PROFILE, AND CYCLE LIFE

COMSAT LABORATORIES

FIGURE 2

VOLTAMMOGRAMS OF THE ELECTROCHROMIC DEVICE AT 22°C AT A SWEEP RATE OF 10 mV/s

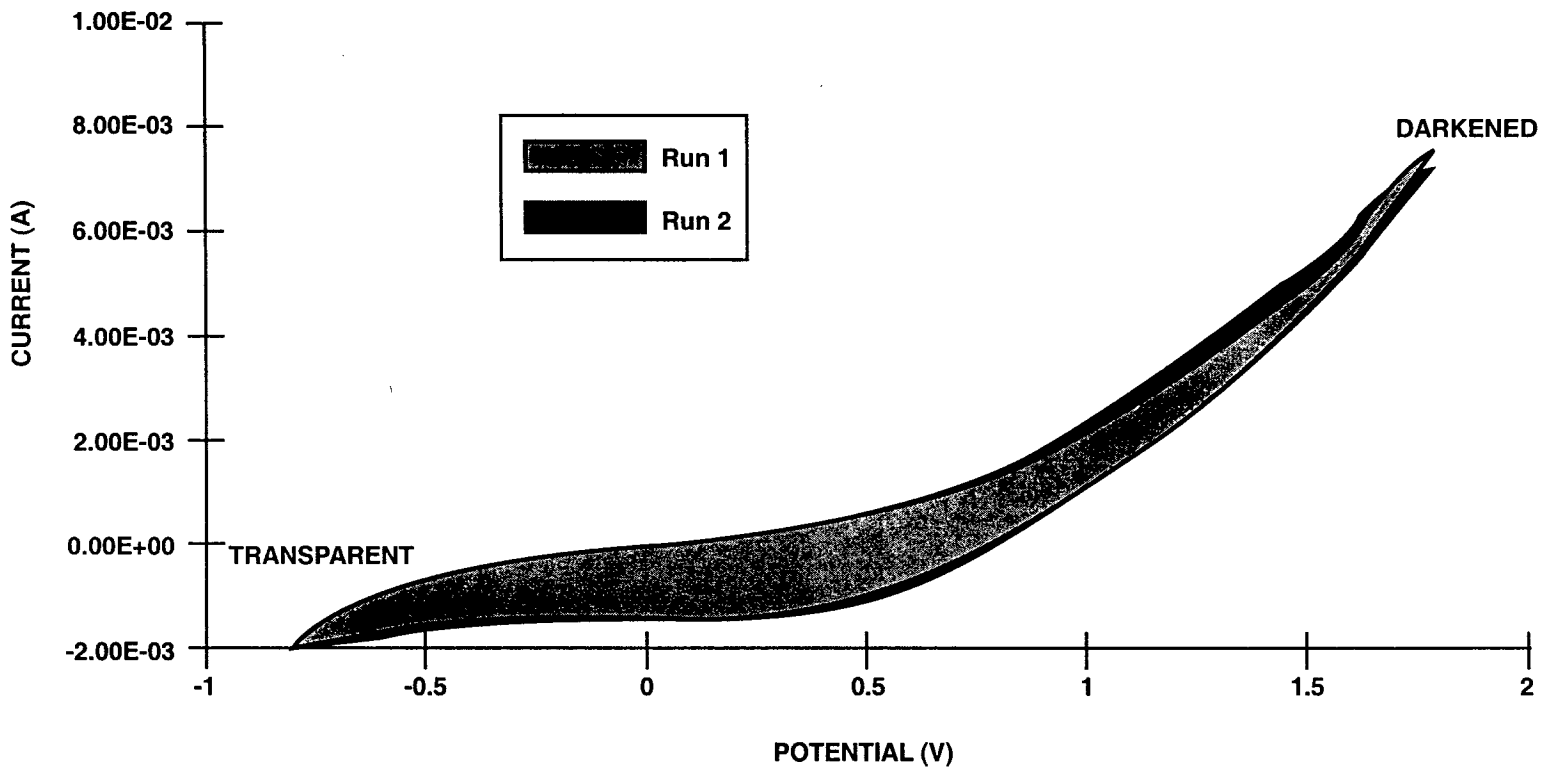

COMSAT LABORATORIES

FIGURE 3

TRANSMITTANCE AS A FUNCTION OF WAVELENGTH FOR THE ELECTROCHROMIC DEVICE

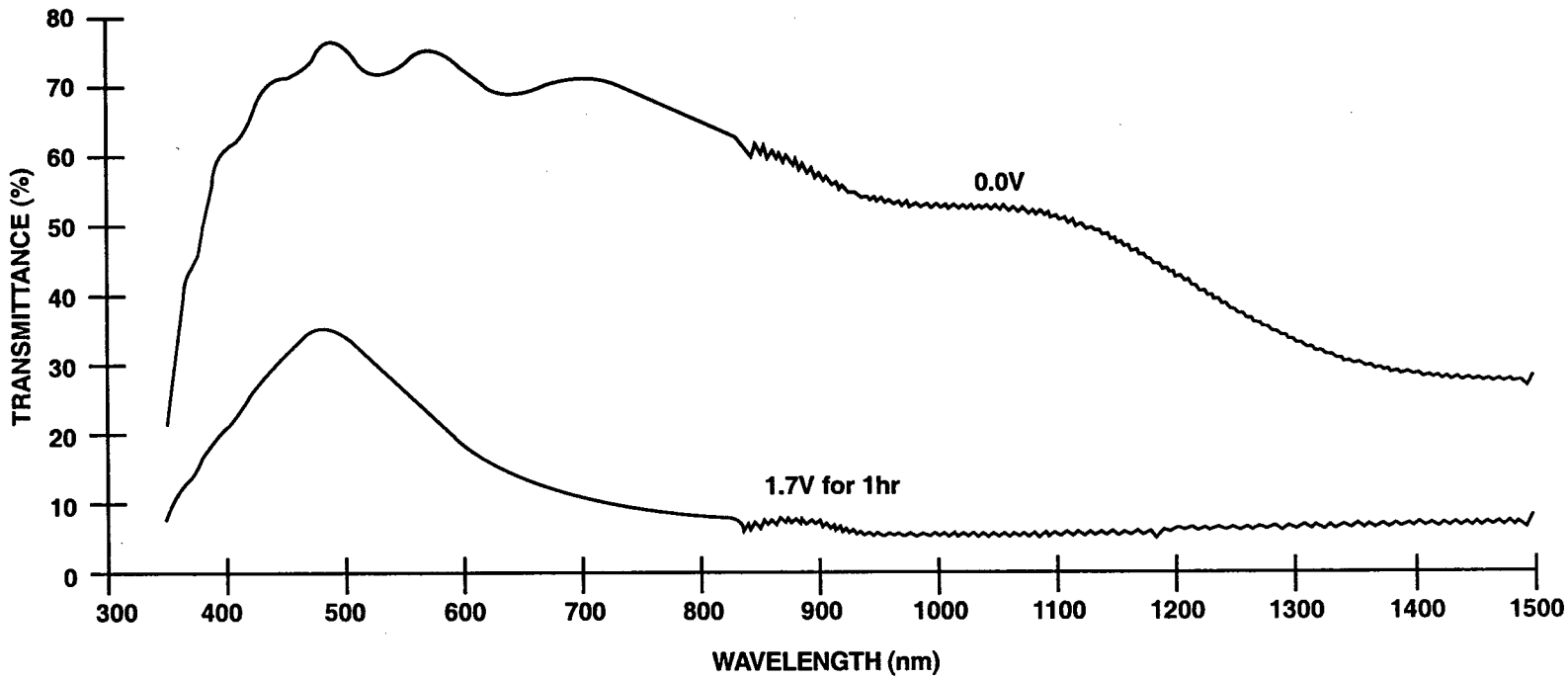

COMSAT LABORATORIES

FIGURE 4

COLORING/BLEACHING SWITCHING TRANSIENTS AT 45°C

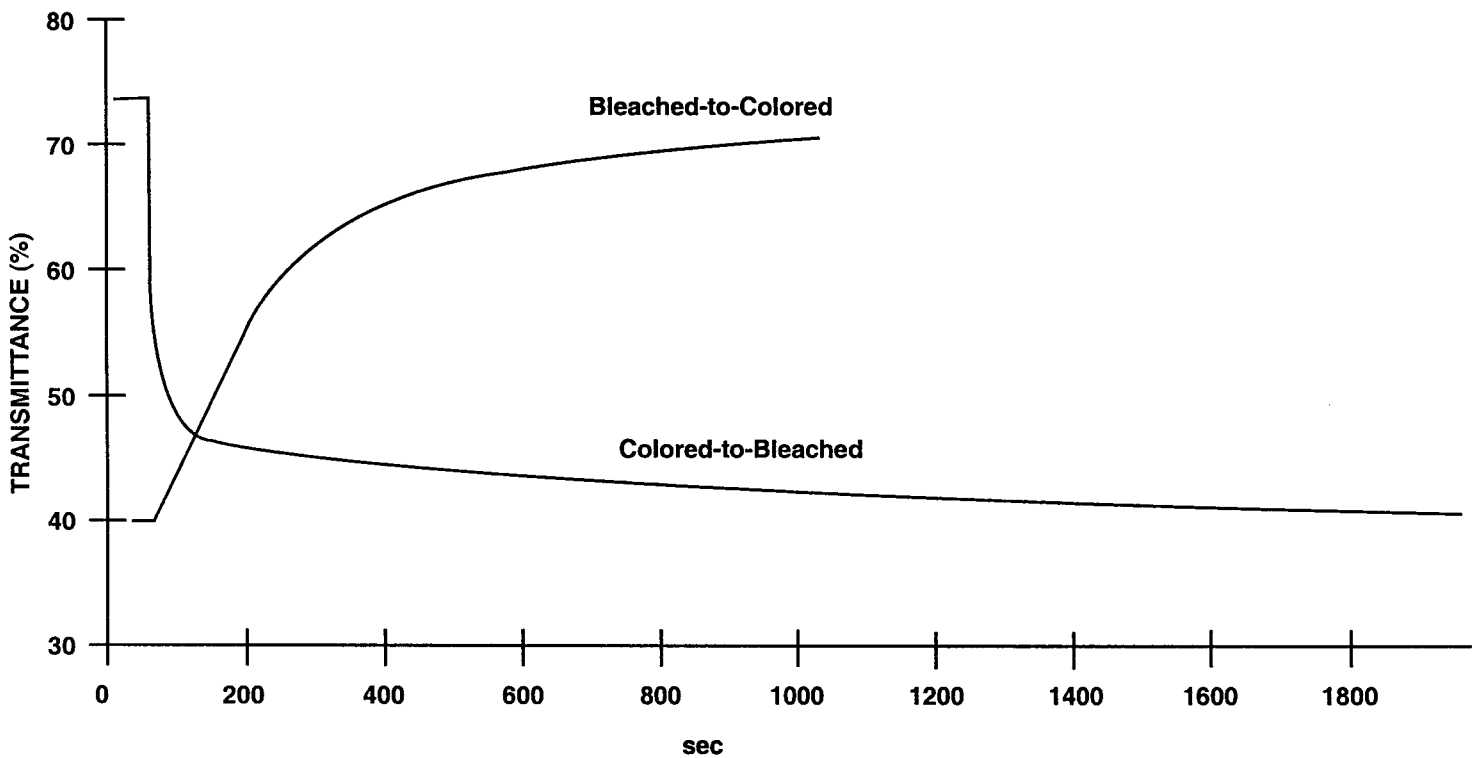

COMSAT LABORATORIES

FIGURE 5

COLORED-TO-BLEACHED SWITCHING TRANSIENT AT 30°C

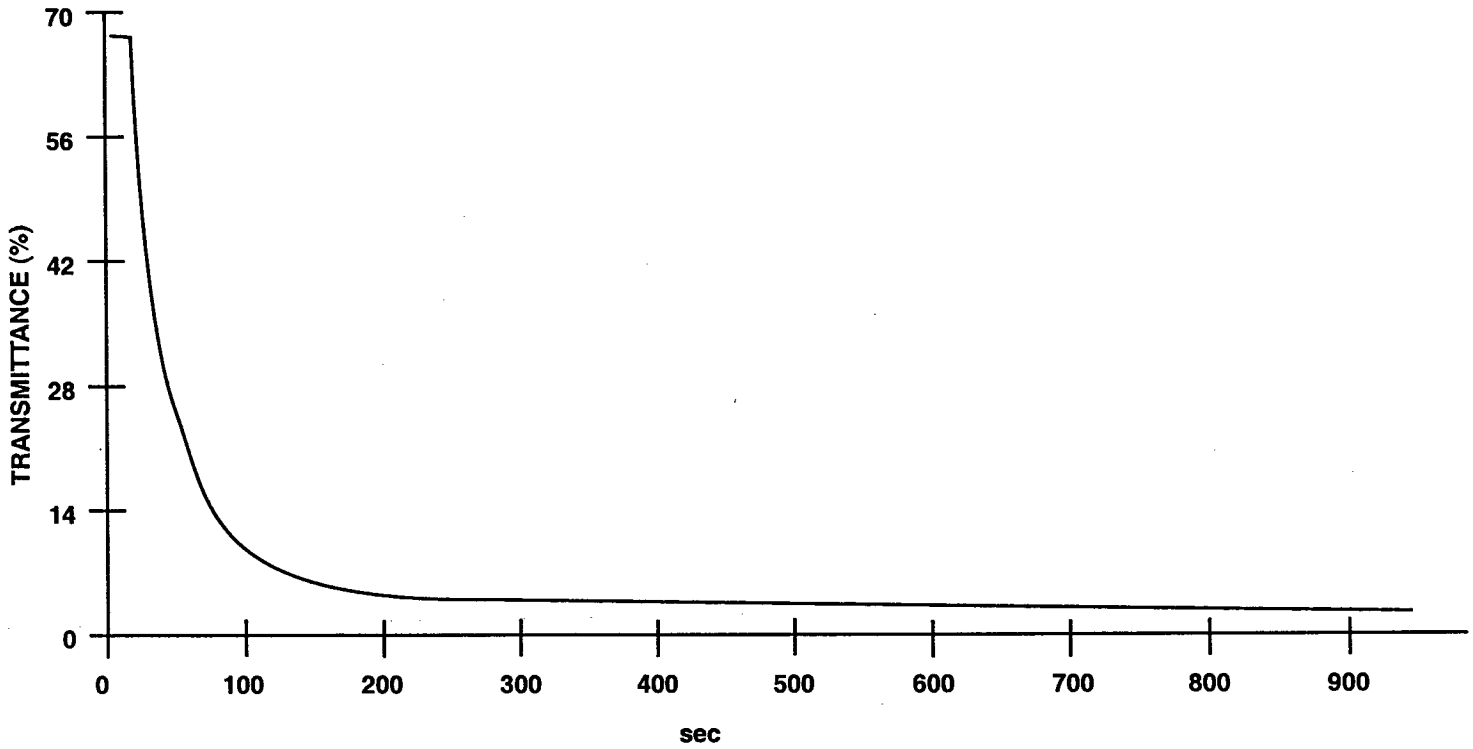

COMSAT LABORATORIES

FIGURE 6

COLORED-TO-BLEACHED SWITCHING TIME AT 0°C

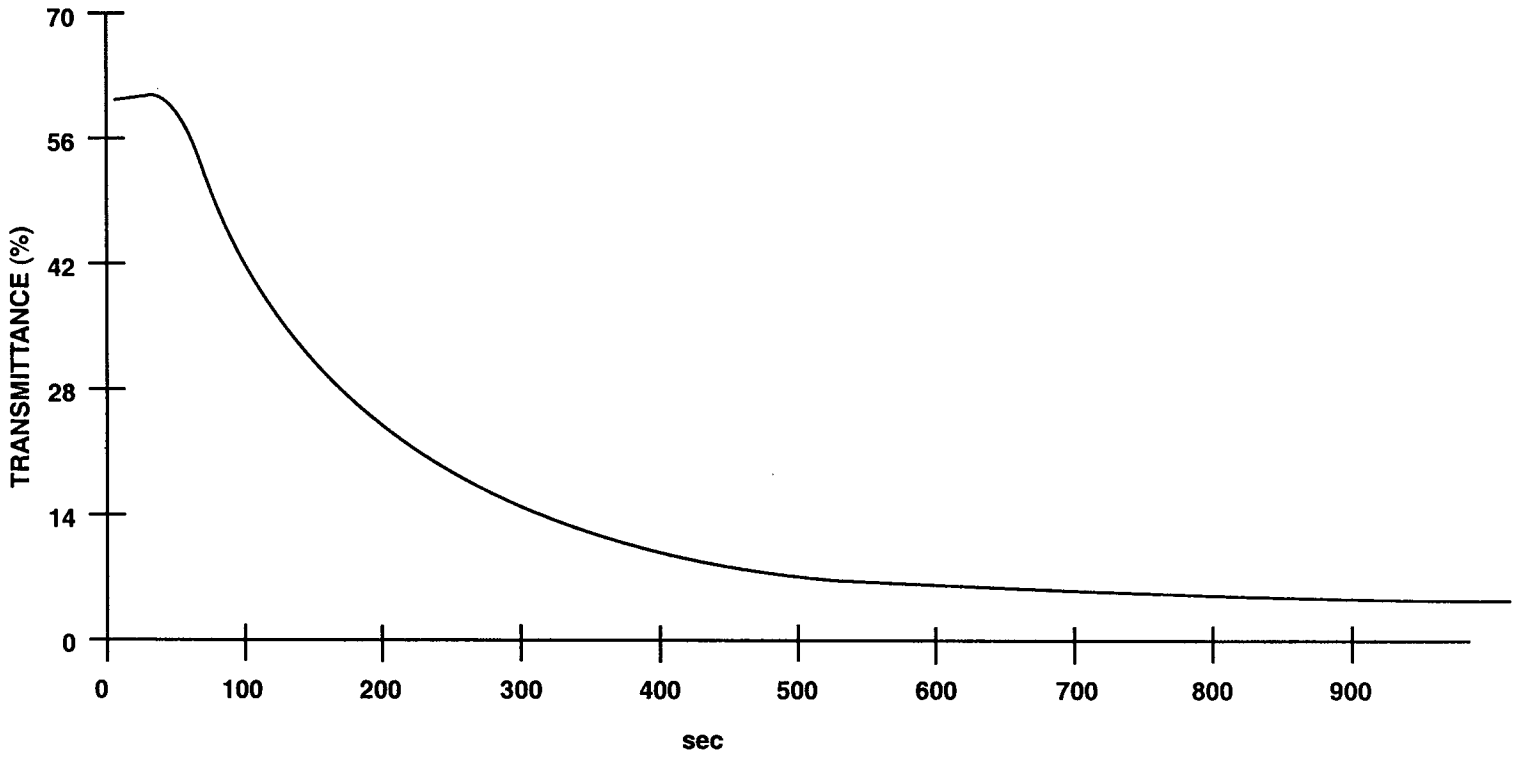

COMSAT LABORATORIES

FIGURE 7

SPECTRAL RESPONSE AT 23°C IN THE COLORED STATE

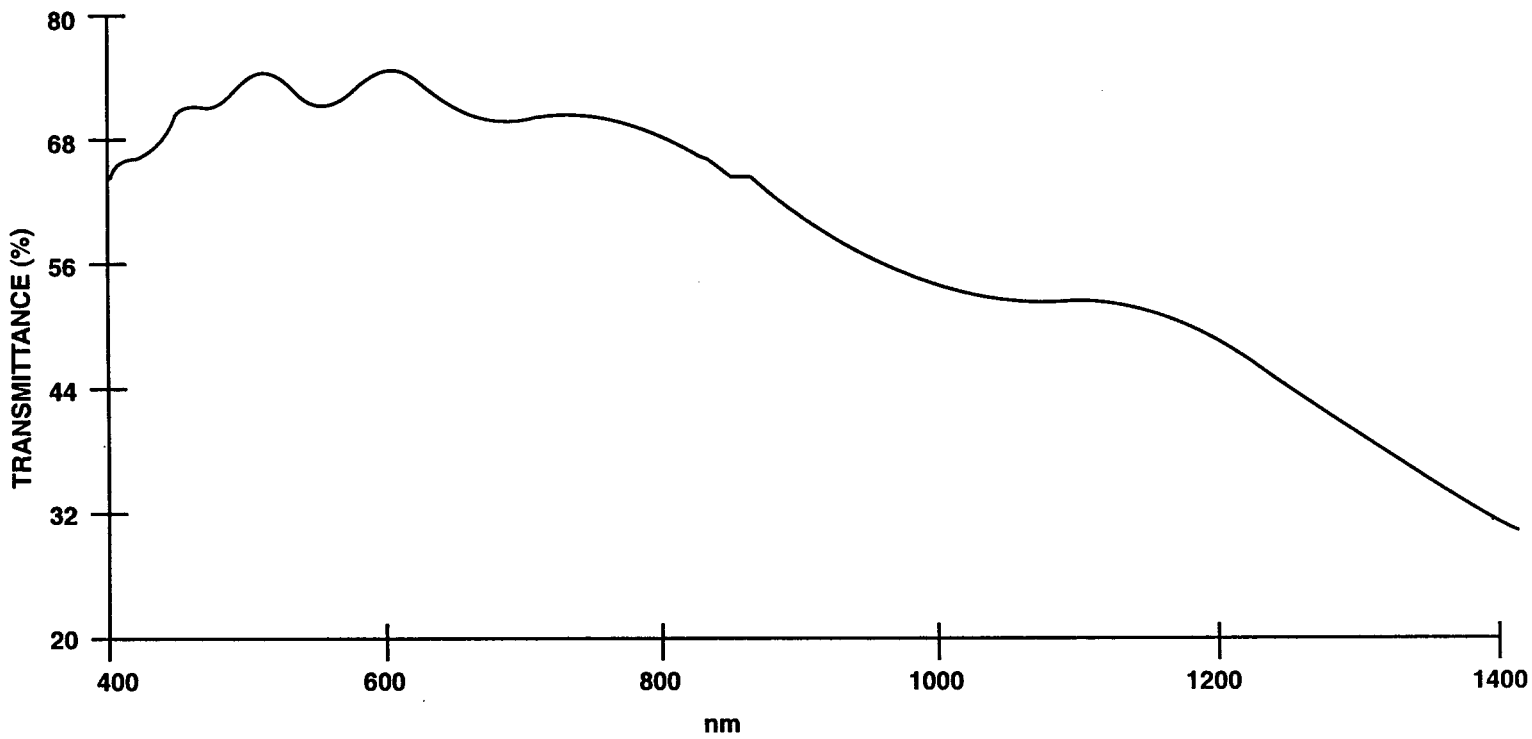

COMSAT LABORATORIES

FIGURE 8

SPECTRAL RESPONSE AT 30°C IN THE COLORED STATE

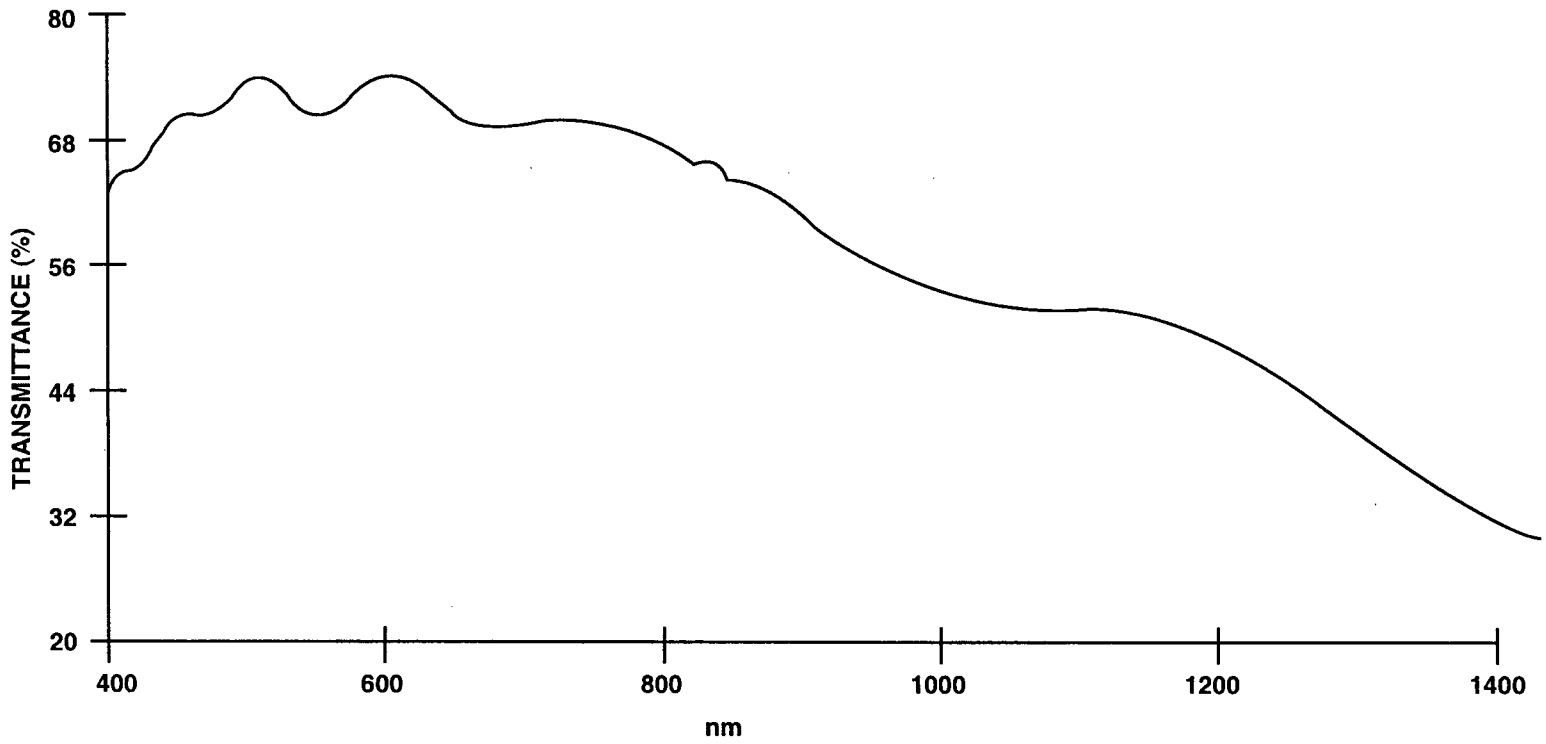

COMSAT LABORATORIES

FIGURE 9

SPECTRAL RESPONSE AT 45°C IN THE COLORED STATE

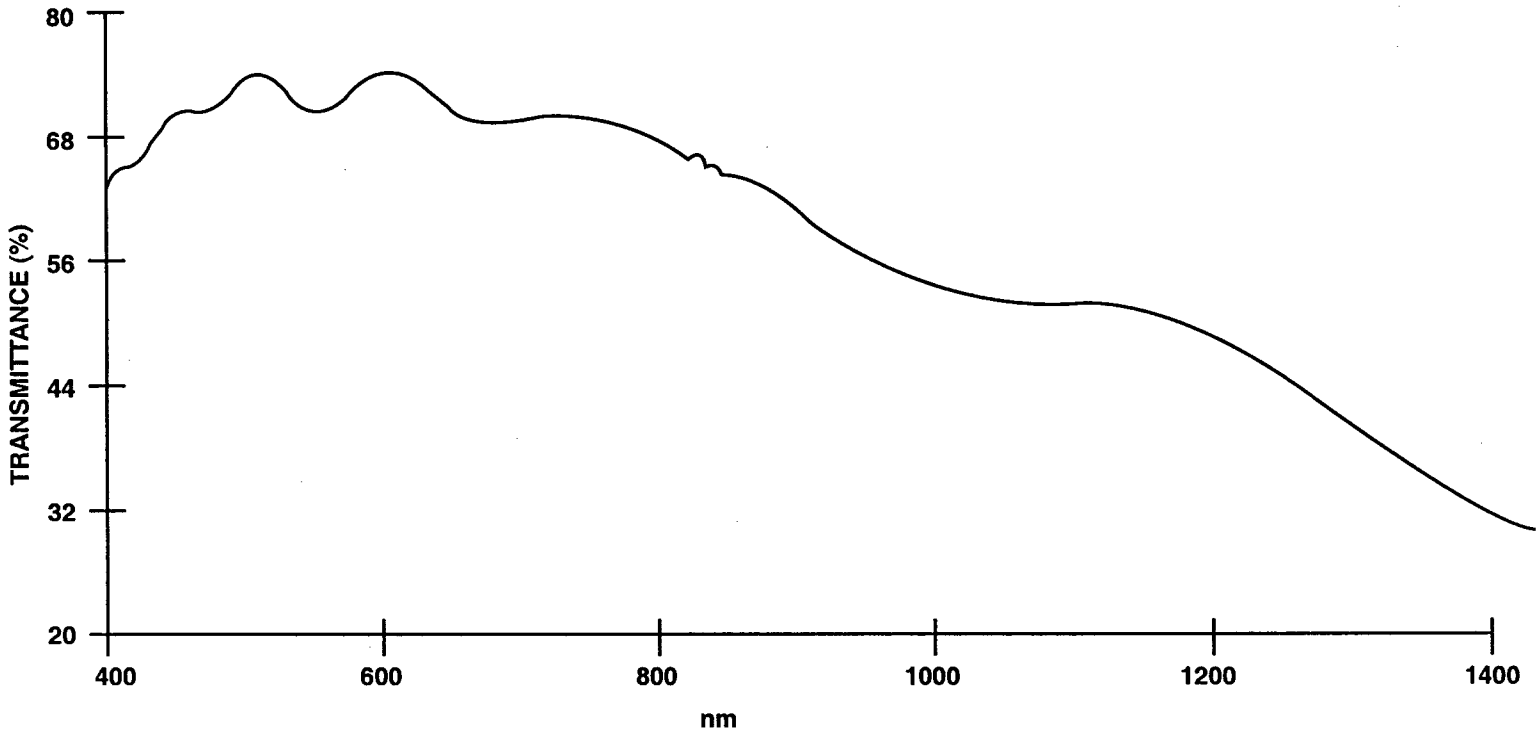

COMSAT LABORATORIES

FIGURE 10

SPECTRAL RESPONSE AT 0°C IN THE COLORED STATE

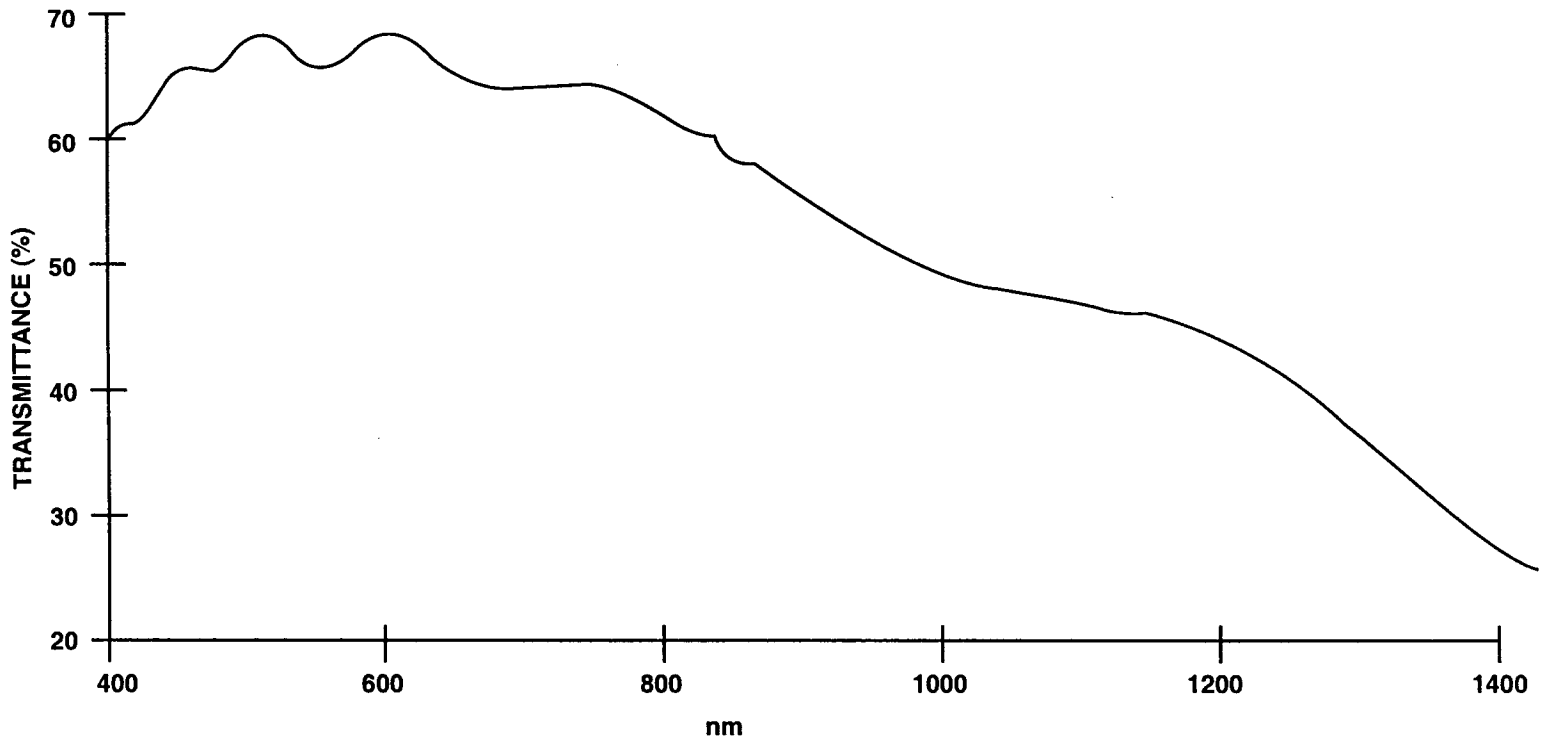

COMSAT LABORATORIES

FIGURE 11

VARIATION OF TRANSMITTANCE AT A WAVELENGTH OF 610 nm

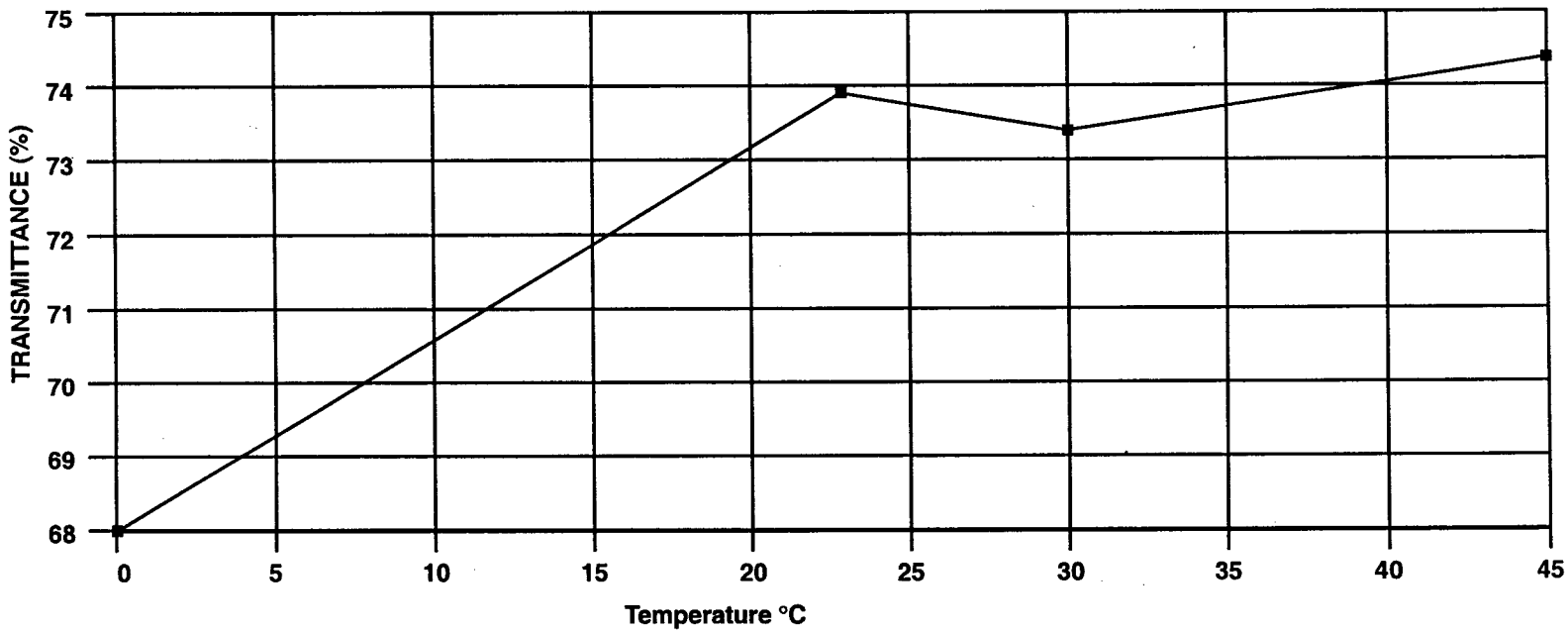

COMSAT LABORATORIES

FIGURE 12

TRANSMITTANCE AT λ = 700 nm DURING REPETITIVE CYCLING AT 30°C

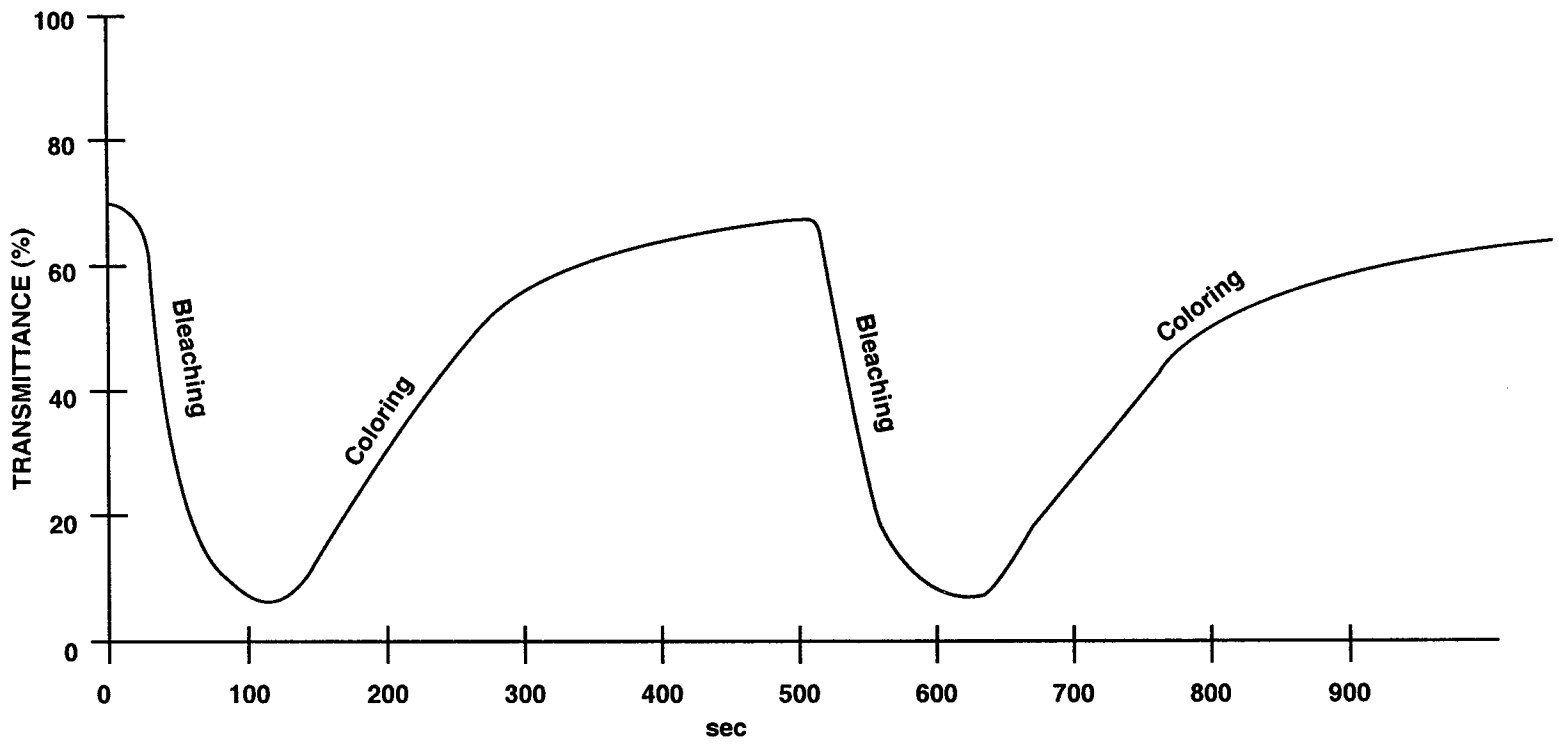

COMSAT LABORATORIES

CONCLUSIONS

- SPECTRAL REGULATION IN THE VISIBLE REGION
- THE TRANSMITTANCE IN THE COLORED STATE IS 5.9% AND THAT IN THE BLEACHED STATE IS 74%
- SWITCHING TIME FOR THE COLORING PROCESS IS HIGHER THAN THAT OF THE BLEACHING PROCESS
- CAPABLE OF REPEATED CYCLING

COMSAT LABORATORIES

Battery/Ultracapacitor Evaluation

for

X-38 Crew Return Vehicle (CRV)

by
Eric Darcy
NASA-Johnson Space Center
and
Bradley Strangways
Symmetry Resources, Inc.

1998 NASA Aerospace Battery Workshop

This Page Left Blank Intentionally

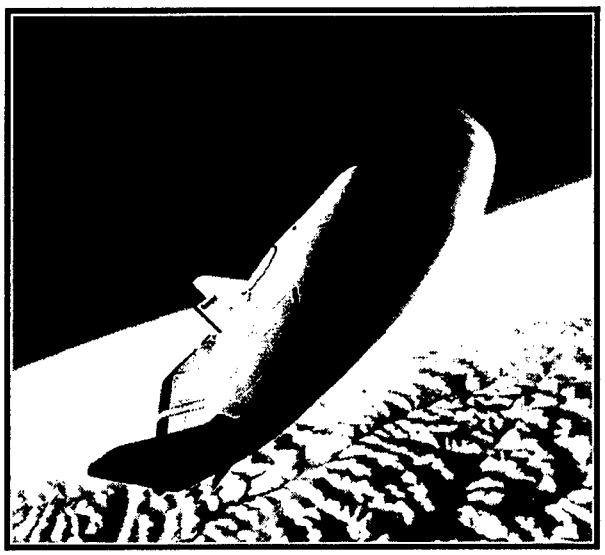

•Top Level CRV Requirements

•Provide for the safe return of ISS crew of zero to 7 in case

–emergency return of ill or injured crew person

–ISS can not maintain critical systems, pressure, attitude, or is contaminated

–Shuttle is not available to return crew

•Crew return without pressure suits

•On-orbit lifetime of 3 years

•700 nautical miles of cross range

•Land lander

•Separation time from ISS < 3 minutes

•Planned return mission time is 3 hours maximum

•Contigency return mission time is 9 hour maximum

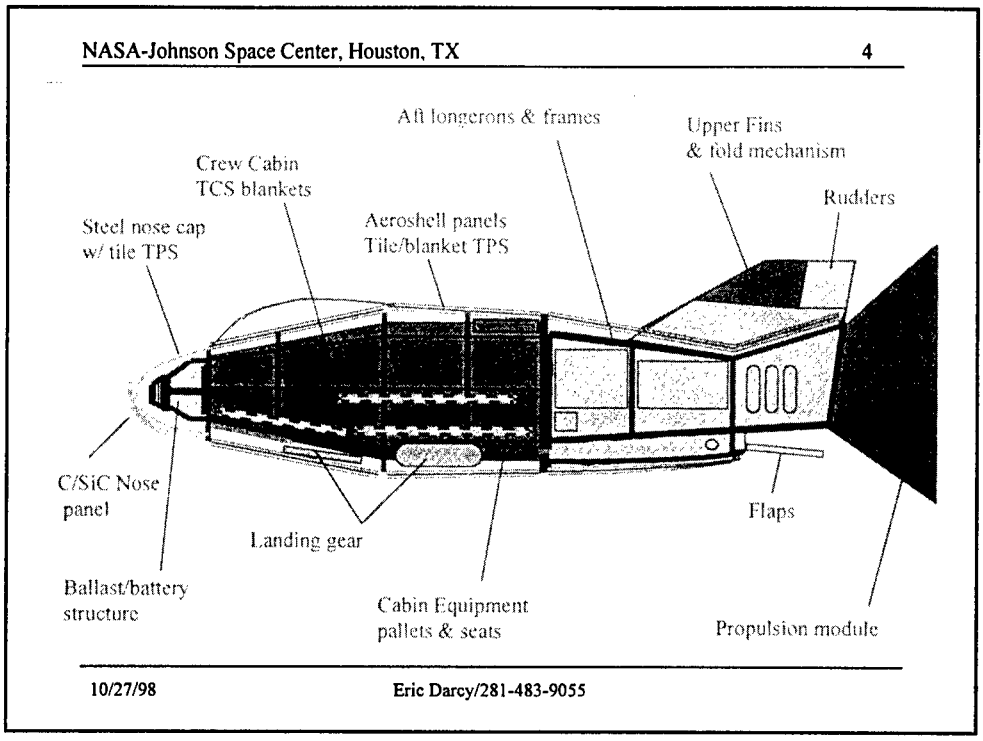

•Mission design

–V-201 mission objectives

- •Demonstrate launch on STS
- •Demonstrate on-orbit activation and checkout
- •Demonstrate RMS deployment
- •Access on-orbit handling qualities
- •Assess system performance
- •Demonstrate de-orbit burn
- •Demonstrate de-orbit module separation and entry attitude maneuvers
- •Assess entry and hypersonic flight performance
- •Assess atmospheric flight performance
- •Demonstrate parachute operations
- •Assess landing accuracy
- •Demonstrate landing performance
- •Demonstrate system shutdown

NASA-Johnson Space Center, Houston, TX 5

CRV 270V Battery Requirements

- Performance
  - 270 +60/-20Vduring discharge, 367V max during charge
  - Divide into eight batteries modules each capable of 2.09 Ah (1.70 Ah for EMAs)
    - 57A (or 27C), 80 ms peaks every 2 seconds for 15 minutes
    - 4.7A (or 2.3C) average current baseline during the 15 minutes on EMAs
    - 2.1A (or C-rate) average current baseline during the 10 minutes on chutes
    - 29A (or 14C), 5 second peak at the end of the 10 minutes for the flare
  - 36 five minute discharge cycles once a month
  - Outside cabin, vacuum exposed for 3 years (14 days for V201)
- Preliminary Oblique Trapezoid Volume in Nose of Vehicle
  - 38" tall flush with forward bulkhead
  - 17" tall forward face
  - 28" forward length (x-axis)
  - 19.6" wide (y-axis)
  - 247 L max

10/27/98 Eric Darcy/281-483-9055

•Unique Program Approach for X-38

•Design, Build, and Test in small increments for rapid feedback

–Pallet Drops (parachute weight tests)

–Dog House Drop (parachute drop test with a vehicle-like shape)

–V-131 (X-24 aero shape with fixed surfaces dropped from a B52)

–V-132 (same shape with EMA controlled surfaces)

–V-133 (20% bigger, again B52 dropped)

–V-201 (Shuttle launched, 5/00, unmanned return test)

–V-202 (Ariane launched, 3/02, unmanned return test)

•No prime contractor (except for Deorbit Propulsion Stage) thru V-202

•Later, a prime contractor will build operational CRVs for ISS

Battery Envelope (preliminary)

X-38 Vehicle 201
Crew Cabin Assy

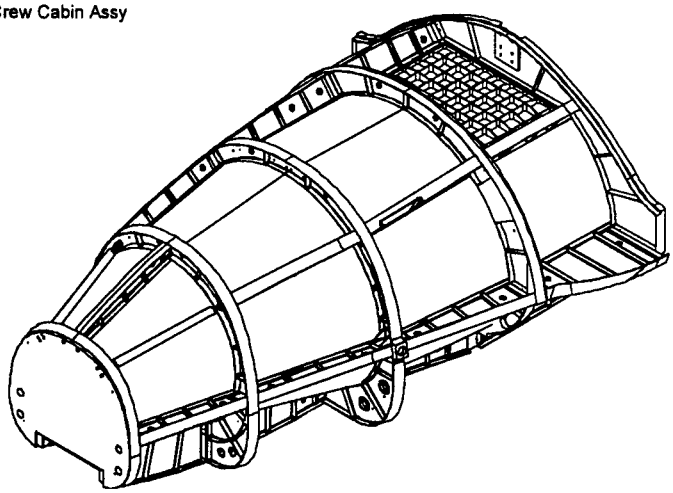

Early Battery Point Design and Test Results

- All testing performed by Symmetry Resources, Inc., in Arab, AL
- In early 1997, first pursued Hawker Cyclon Tall D-cell as baseline cell
- Resulting Point Design with Hawker Tall D-cell
  - 1P - 160S battery module
  - 67.5 kg/module
  - 540 kg/total battery
  - 340mm x 760mm x 112mm, (28.94 L/module)
  - 231.5 L/total battery
- Observations
  - Cell internal resistance = 7.9 mohms
  - Need lower impedance cell design and higher power density

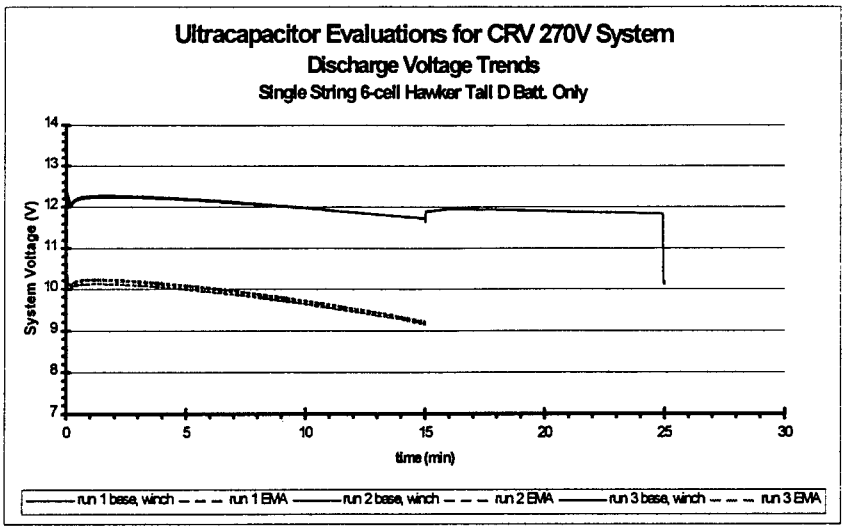

Test Conditions and Results

- Discharge at 25 deg C
- Minimum EMA voltage = 9.2V/6 cells (= 246V for 160S)
- Mininum Winch voltage = 10.2V/6 cells (= 272V for 160S)
- Maximum voltage sag = 2.4V/6 cells (= 64V for 160S) during last EMA pulse

Ultracapacitor Bank

- Capacitor bank of 7 capacitor in series
- Capacitor bank rated at 142 Farads using unit cell rated at
  - 1000 Farad, 2645 J
  - 390 g → 1.88 Wh/kg
  - 160mm x 75mm x 24mm → 2.55 Wh/L
  - ESR = 1.85 mohm
  - above values based on 2.3V float voltage
  - specific power = 4210 W/kg, power density = 5701 W/L
  - above values based on surge voltage = 2.7V
- Bank and cell are commercially available from Maxwell Technology
  - bank P/N PCM14014X
  - capacitor P/N PC2623

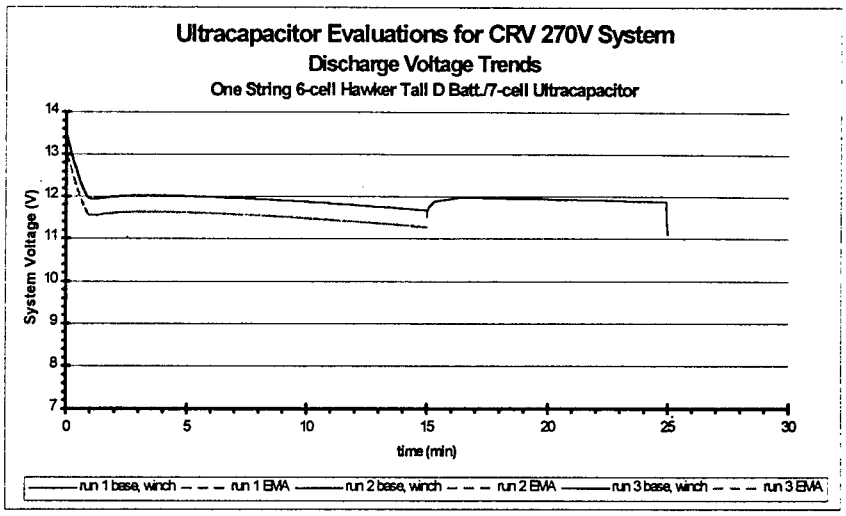

Test Method

- 1 Battery string and 1 capacitor bank were charged independently
- Hawker battery string was charged to 14.7 with a 6 amp limit for 16 hours
- Capacitor bank charged to a voltage = OCV of battery string (13.02V)
- Cells in capacitor bank were monitored and equalized for proper balancing
- Immediately after, battery and cap bank were paralleled and discharge began
- Original power profile was run (57A peak)
- Battery and total currents were measured throughout run

Results

- Minimum EMA voltage = 11.3V (1.88 V/LA cell)
- Minimum Winch voltage = 11.1V (1.85 V/LA cell)

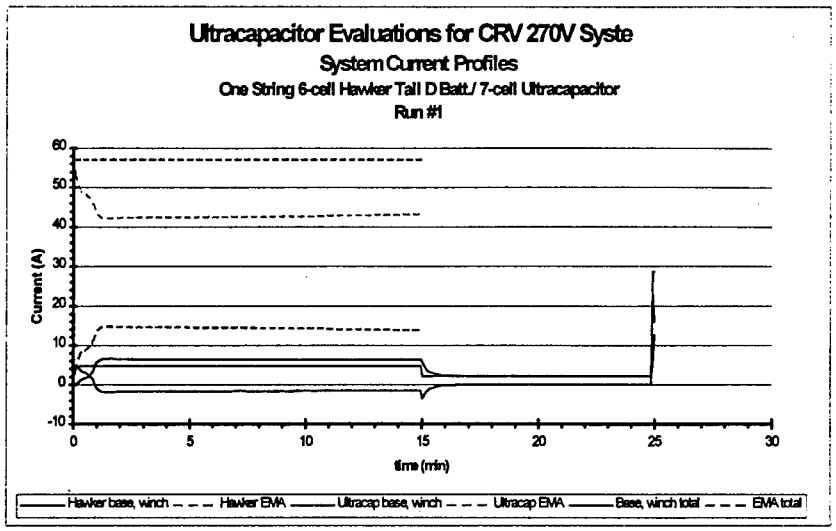

Results

- Capacitor current is 95% (54A) of total at first
- Capacitor current levels to 75% (43A) after 1 minute
- Battery is charging capacitor at 2A during EMA off peaks
- Capacitor bank absorbs most of Winch pulse at first
- Capacitor bank current fades about 10A at end of 5s Winch pulse

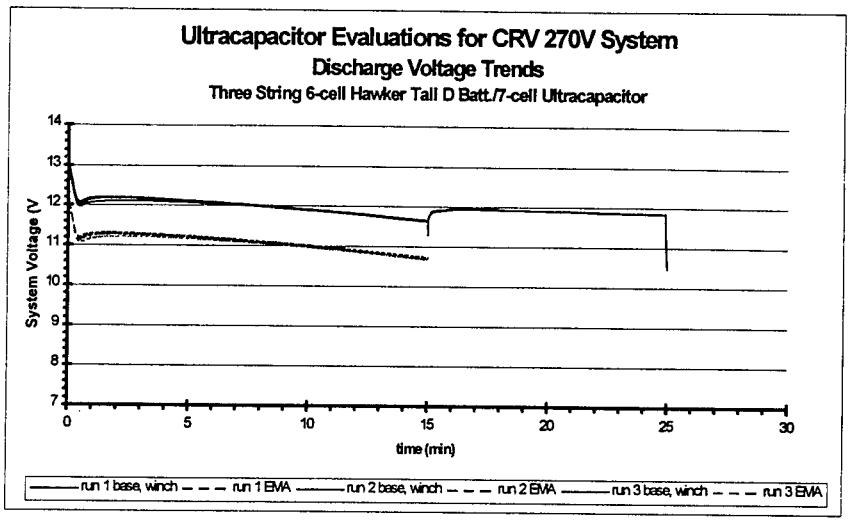

Test Method

- 3 Battery strings and 1 capacitor bank were charged independently
- Hawker battery strings were charged to 14.7 with a 6 amp limit for 16 hours
- Capacitor bank charged to a voltage = OCV of battery string (13.02V)
- Cells in capacitor bank were monitored and equalized for proper balancing
- Immediately after, batteries and cap bank were paralleled and discharge began
- 3X original power profile was run (171A peak)
- Total battery and total hybrid currents were measured throughout run

Results

- Minimum EMA voltage = 10.7V (1.78 V/LA cell)
- Minimum Winch voltage = 10.5V (1.75 V/LA cell)

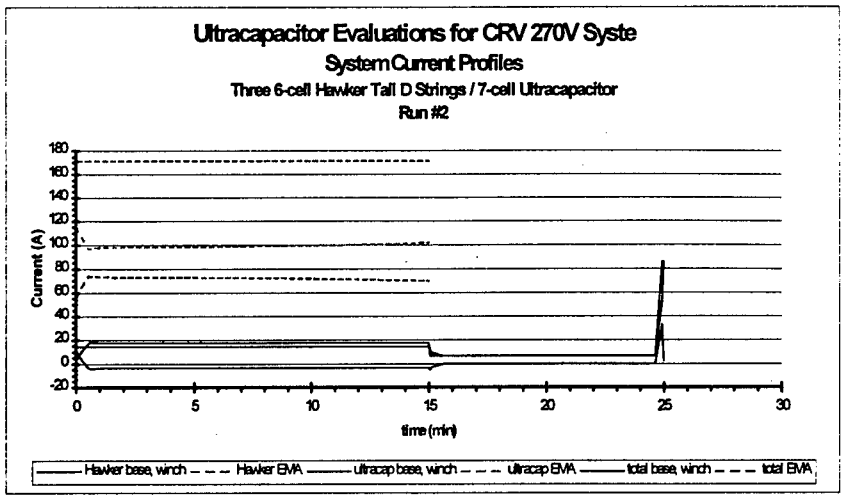

Results

- Capacitor current is 70% (120A) of total at first
- Capacitor current levels to 58% (100A) after 1 minute
- Battery is charging capacitor at 5A during EMA off peaks
- Capacitor bank absorbs only 40% (35A) of Winch pulse at first
- Capacitor bank current fades about 2A at end of 5s Winch pulse

Summary

- Results indicate
  - Battery/capacitor hybrid does load share as expected
  - At triple currents, one bank of capacitors in parallel with three batt strings
    - increases load voltage by 16% during last EMA pulse
    - increases load voltage by only 3% during 5 second winch pulse
  - 4x currents would result in capacitor bank sharing < 50% of peaks
  - 7 cap in parallel with 6 batteries results in caps charged to 1.91V/cap
  - Need better voltage matching to more fully charge caps
- Hybrid Point Design
  - starting at 2.7V/cap, 330V bank consists of 122 in series
  - 122S bank weighs 47.9 kg and consumes 35.2 L
  - 22% more volume than 1P-160S battery of Hawker Tall D-cells

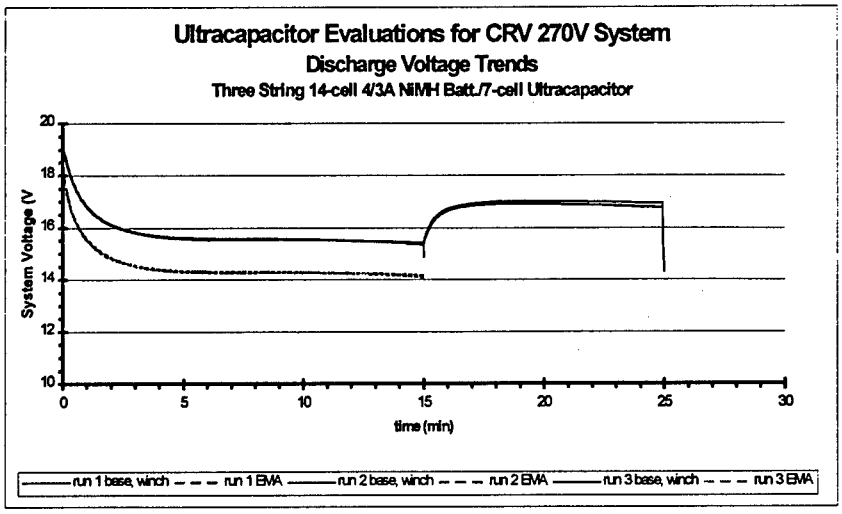

Test Method

- 3 Battery strings and 1 capacitor bank were charged independently
- 14S strings of Sanyo 4/3A NiMH cells charged to 0.35A for 16 hours
- Capacitor bank charged to a voltage = OCV of battery strings (19.2V)
- Cells in capacitor bank were monitored and equalized for proper balancing
- Immediately after, batteries and cap bank were paralleled and discharge began
- 3X original power profile was run (171A peak)
- Total battery and total hybrid currents were measured throughout run

Results

- Minimum EMA voltage = 14.1V (1.01 V/NiMH cell)
- Minimum Winch voltage = 14.4V (1.03 V/NiMH cell)

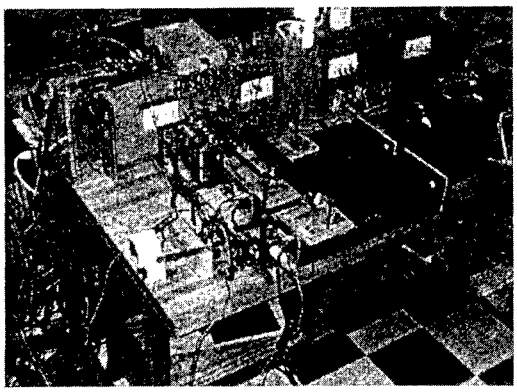

Test set-up at Symmetry Resources, Inc., in Arab, AL

Test set-up at Symmetry Resources, Inc., in Arab, AL

- Ultracapacitor bank is in background
- NiMH battery is in foreground

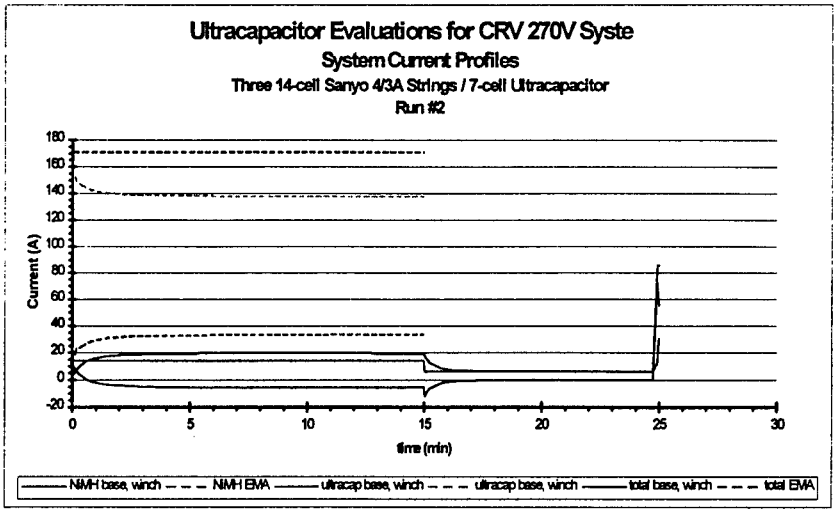

Results

- Capacitor current is 90% (154A) of total at first
- Capacitor current levels to 81% (138A) after 3 minutes
- Battery is charging capacitor at ~6.7A during EMA off peaks
- Capacitor bank absorbs only 84% (73A) of Winch pulse at first
- Capacitor bank current fades about 18A at end of 5s Winch pulse

Summary of NiMH/Capacitor Hybrid

- Test results indicate
  - Capacitors charged to 2.75V/ea when paralleled with 14-cell NiMH
  - Load voltage during EMA pulses barely > 1V/MH cell
  - Majority (> 80%) of pulse current absorbed by capacitor bank
  - non-peak EMA current provide entirely by MH cell
  - Better load voltage balance between EMA and Winch pulses
  - non-peak current reaches is ~7A/cell, which is too high for this cell
- Conclusions
  - Ultracapacitors can be paired with batteries with complimentary results
  - Impedance balance between battery & capacitor bank is crucial to results
  - Power density (W/L) of present ultracapacitor technology is not high enough for CRV in a straight parallel w/ batteries hybrid configuration

Modified CRV 270V Battery Requirements

- Performance
  - 270 +30/-65Vduring discharge, 345Vmax during charge
  - Divide into eight batteries modules each capable of 2.65 Ah (2.06 Ah for EMAs)
    - 81A (or 31C), 60 ms peaks every 2 seconds for 15 minutes
    - 6A (or 2.3C) average current baseline during the 15 minutes on EMAs
    - 3A (1.1C) average current baseline during the 10 minutes on chutes
    - 33A (or 12C), 10 second peak at the end of the 10 minutes for the flare
  - 36 five minute discharge cycles once a month
  - **Bus voltage < 300V during 40 kW regenerative charging (40.5A for 60 ms)**
  - Outside cabin, vacuum exposed for 3 years (14 days for V201)
  - 247 liters available in nose in an oblique trapezoid shape

High Power Cell Design Trades

Cell Design	Cell Size	Cell 1C Cap. (Ah)	Batt Module configuration	Max OCV (V)	Final EMA Volt (V)	Final Winch Volt (V)	Estimated Battery Module Mass (kg)	Estimated Battery Module Volume (L)
Hawker lead acid	D	1.90	2P-125S	274	211	229	62.30	31.46
Bolder lead acid	9/5C	1.00	3P-115S	252	215	204	43.47	19.92
Energizer Ni-MH	subC	2.00	3P-210S	286	213	241	46.75	20.52
Sanyo NiCd	D	4.00	1P-218S	301	209	243	45.78	23.75
Energizer NiCd	subC	1.70	3P-200S	274	220	235	45.38	19.44

Assumptions used
- Effective internal resistance (Re) of cells based on delta V:delta I performance under test
- Re was measured at 10% increments during 1C discharges with 10C, 80 ms pulses
- Cell interconnect resistance of 0.5 mohms used for each cell
- Total cell mass (volume) x 1.5 (x2.0) = estimated battery module mass (volume)

Conclusions
- NiCd Cs cell yields module with lowest volume, Bolder lead acid close second.
- 8 Hawker lead acid D-cell battery modules exceeds available volume (247L)

10/27/98 Eric Darcy/281-483-9055

Test Method
- Cells were charged per the manufacturer's recommendation
- Allowed to rest at OCV for > 1.5 hours
- Discharged at C-rate with 10C, 80 ms pulses every 5.987 minutes at 25 degC
- Data allows Re to be calculated at 10% SOC increments from 90 to 10%
- Re = deltaV/delta I

Bolder Technology Lead Acid Cell

- Thin metal film cell contruction yields very high power
  - 9/5C sized cell delivering 1.0 Ah
  - cell is 90g, 22.9 mm diameter x 70.1 mm tall
  - cell impedance < 2 mohm, similar to 1000F capacitor

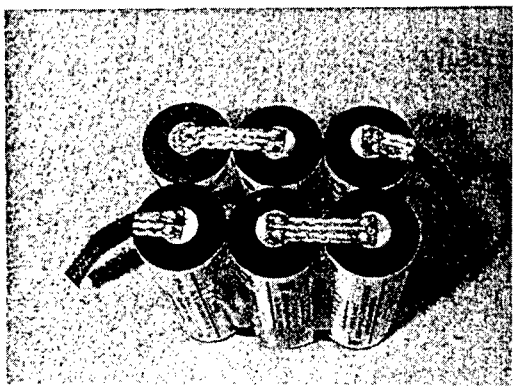

Impedances are very similar

- Bolder 9/5C LA cell (1F)
- Maxwell capacitor (1000F)

NASA-Johnson Space Center, Houston, TX 22

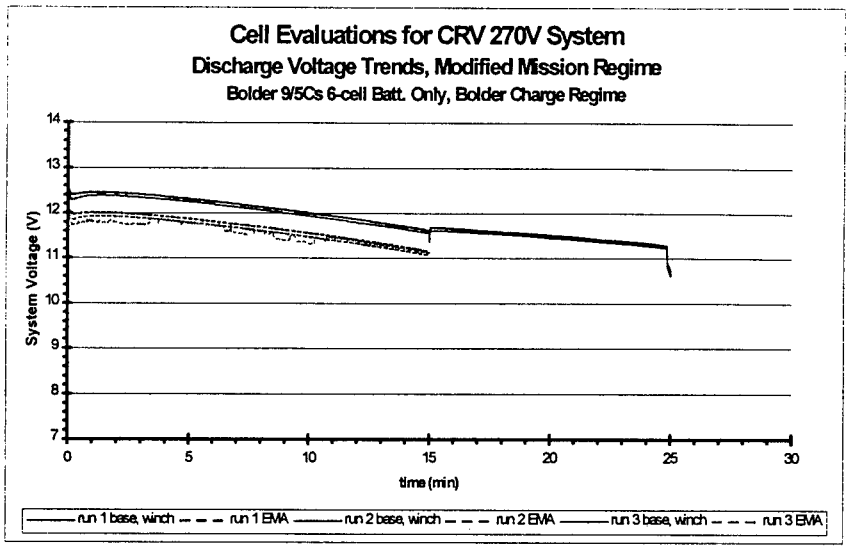

10/27/98 Eric Darcy/281-483-9055

Test Conditions and Results

- Charging followed Bolder's recommended "Current Regulated Taper Charge"
- Discharge at 25 deg C at 1/3 current levels of the new profile (27A peak)
- Minimum EMA voltage = 11.1V/6 cells (= 212V for 115S)
- Mininum Winch voltage = 10.7V/6 cells (= 204V for 115S)
- Maximum voltage sag = 0.9V/6 cells (= 17V for 115S) during winch pulse

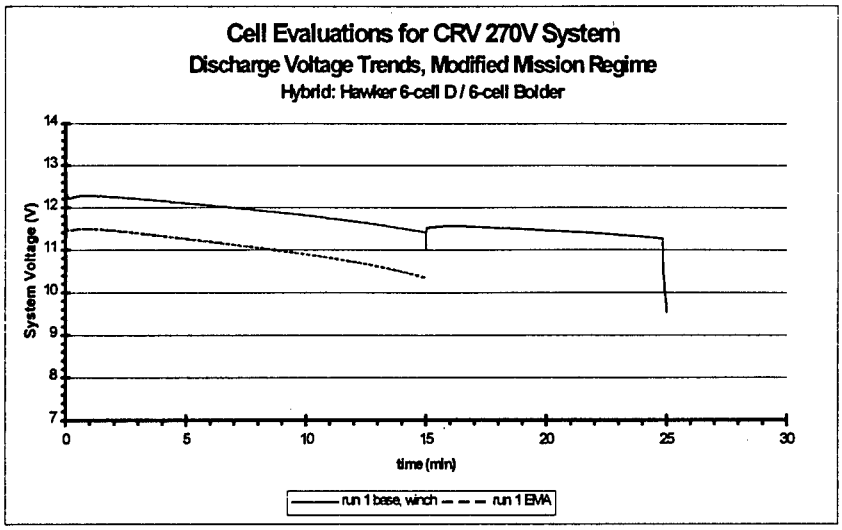

Test Method

- 1 Bolder 6S and 1 Hawker 6S strings were charged independently
- Immediately after, battery strings were paralleled and discharge began
- new power profile was run (81A peak)
- Total Hawker and total hybrid currents were measured throughout run

Results

- Minimum EMA voltage = 10.4V (1.73 V/LA cell)
- Minimum Winch voltage = 9.65V (1.61 V/LA cell)

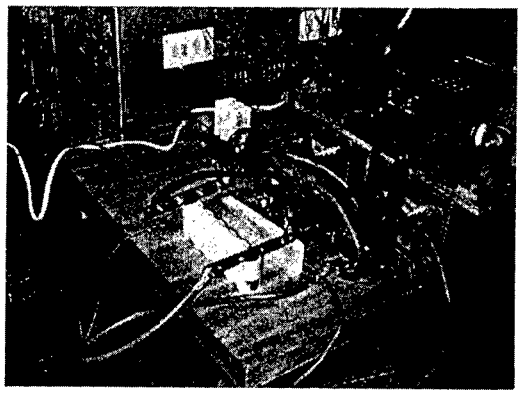

Test set-up at Symmetry Resources, Inc., in Arab, AL

Test set-up at Symmetry Resources, Inc., in Arab, AL

- Bolder LA battery is in background
- Hawker LA D-cell battery is in foreground

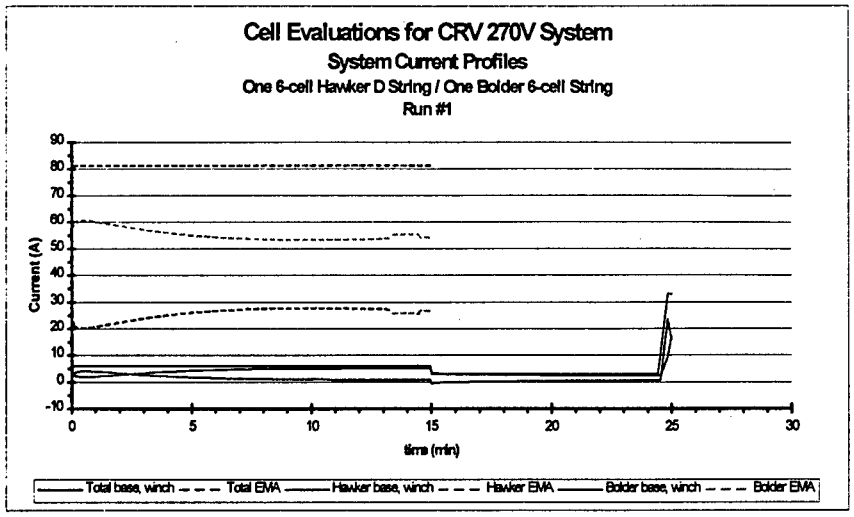

Results

- Bolder current is 75% (61A) of total at first
- Bolder current levels to 66% (53A) after 8 minutes
- Bolder base currents starts at 4A tapers to 1A during EMA phase
- Bolder absorbs only 70% (23A) of Winch pulse at first
- Bolder current fades about 7A at end of 10s Winch pulse
- Bolder does too high a share of EMA base load, little left for winch
- A slightly higher ratio of Hawker to Bolder cells may work better

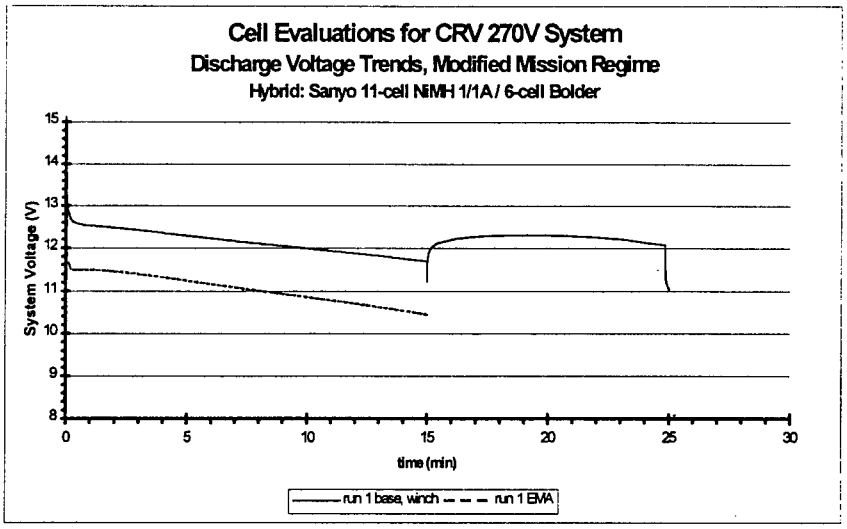

Test Method

- 1 Bolder 6S and 1 Sanyo 11S strings of "A"cells were charged independently
- Immediately after, battery strings were paralleled and discharge began
- new power profile was run (81A peak)
- Total Sanyo and total hybrid currents were measured throughout run

Results

- Minimum EMA voltage = 10.45V (0.95 V/NiMH cell)
- Minimum Winch voltage = 11.06V (1.01 V/NiMH cell)

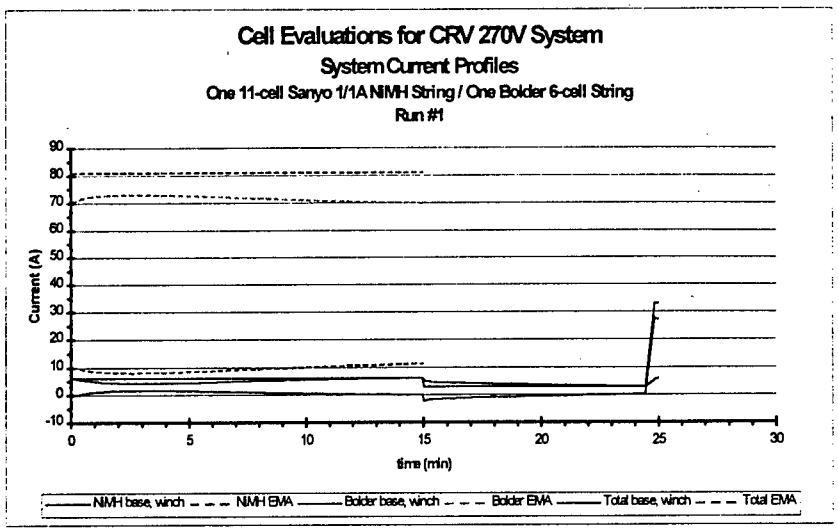

Results

- Bolder current is 88% (71A) of total at first
- Bolder current peaks to 90% (73A) after 2 minutes
- Bolder current ends EMA phase at 86% (70A)
- Bolder base currents starts at 0A, peaks at 2A, and ends at 0A during EMA phase
- Bolder absorbs only 85% (28A) of Winch pulse at first
- Bolder current fades only 1A at end of 10s Winch pulse
- A-size NiMH cells are pushed hard during base loads (6A max)
- Using a NiMH more capable of 2C rates would boost EMA voltage

Observations and Point Design Comparisons

- Observations
  - Bolder only system requires 3 strings and has very little energy margin
  - Parallel 6 Bolder cells with 6 Hawker D-cells
    - 130 cells of each in series
    - 48.8 kg, 23.9 L vs Bolder only system 43.5 kg, 19.9 L
    - A slightly higher ratio of Bolder:Hawker cells may improve peak sharing
  - Parallel 6 Bolder cells with 11 Sanyo NiMH A-cells
    - higher capacity NiMH cell improves winch pulse voltage
    - Cell string ratio = 125 Bolder: 225 Sanyo
    - Hybrid module is 23.1 kg, 12.1 L
    - **47% mass reduction, 39% volume reduction**
    - Using a NiMH cell more capable of 2C rates will boost EMA voltages

Issues with lead acid and conclusions

- Regenerative braking result in voltages above 300V with lead acid
  - Hawker D reached 2.356V when charged at 10A for 60 ms at 98% SOC
  - Bolder 9/5C reached 2.924V when charged at 36.5A for 60ms at 98% SOC
  - Bolder 9/5C reached 2.925V when charged at 36.5A for 60ms at 90% SOC
- 300V maximum is required to prevent corona discharge hazard
  - Energizer subC NiCd reached 1.451V, charged at 20A for 60ms at 98% SOC
- Conclusions for X-38
  - Ultracapacitors are too voluminous when paralleled w/ batts w/o regulation
  - Bolder cell has higher useful power density (W/L) than Ultracaps over entire mission profile
  - 300V Max voltage reqt rules out any lead-acid system
  - NiCd subC only system is baselined

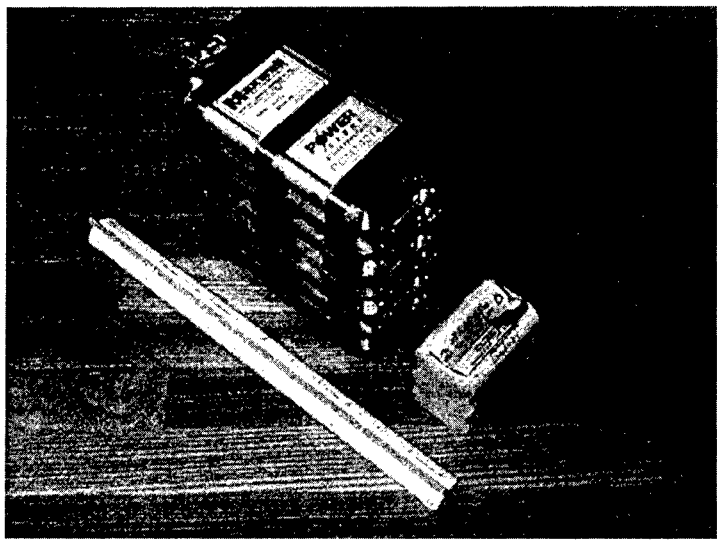

Volume comparison

- Bolder 6-cell battery
- 7S Ultracapacitor Bank

DS-2 MARS MICROPROBE BATTERY

H. FRANK, A. KINDLER, F. DELIGIANNIS, E. DAVIES,
J. BLANKEVOORT, B. V. RATNAKUMAR, AND S. SURAMPUDI

NASA BATTERY WORKSHOP
HUNTSVILLE, AL
OCTOBER 27, 1998

Electrochemical Technologies Group

OUTLINE

- DS-2 MISSION OVERVIEW
- DS-2 BATTERY PERF. REQUIREMENTS
- BATTERY TECHNOLOGY CHALLENGES
- CHEMISTRY SELECTION
- CELL DESIGN OVERVIEW
- PROBLEMS ENCOUNTERED
- PERFORMANCE RESULTS
- CONCULSIONS

NM DS-2 MISSION OVERVIEW

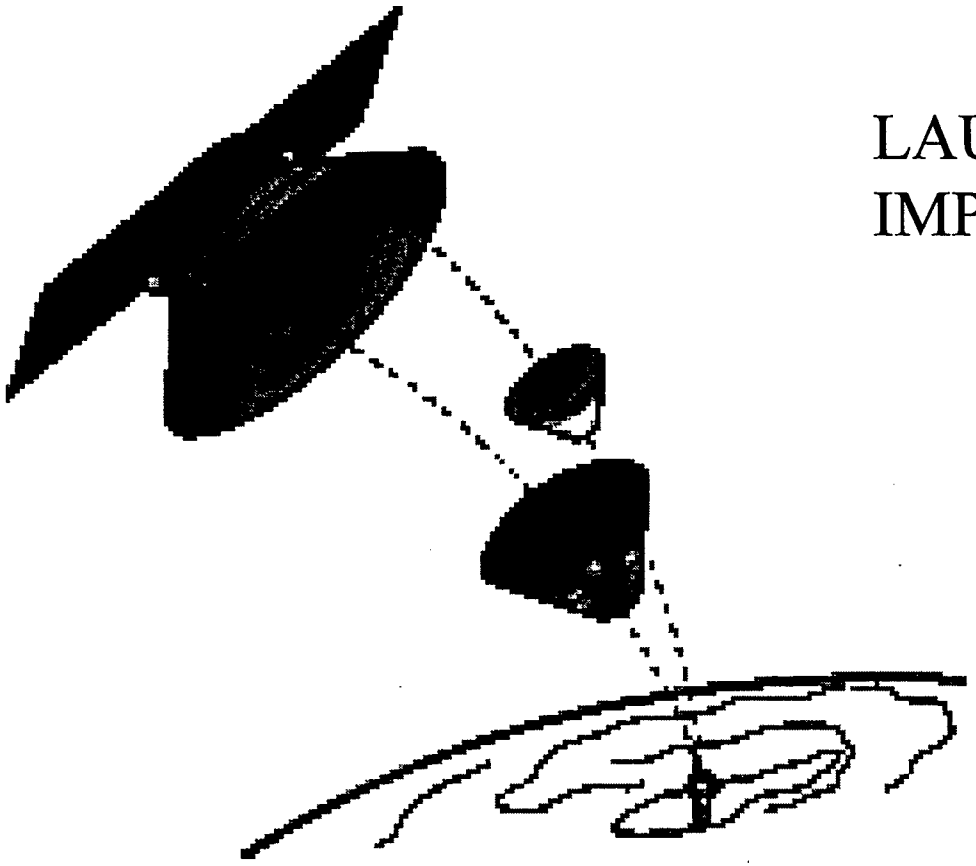

LAUNCH : JAN. 1999
IMPACT MARS: DEC. 1999

Electrochemical Technologies Group

DS2 MISSION OBJECTIVES

TECHNICAL OBJECTIVES

- Demonstrate key technologies which enable future network science missions (e.g., multiple landers, penetrators, or spacecraft)
- Demonstrate a passive atmospheric entry.
- Demonstrate highly integrated microelectronics which can withstand both low temperatures and high decelerations.
- Demonstrate in-situ, surface and subsurface science data acquisition

- **Scientific Objectives**

- Determine if ice is present below the Martian surface
- Measure the local atmospheric pressure
- Characterize the thermal properties of the Martian subsurface soil
- Estimate the vertical temperature gradient of the Martian soil

DS-2 AFTBODY

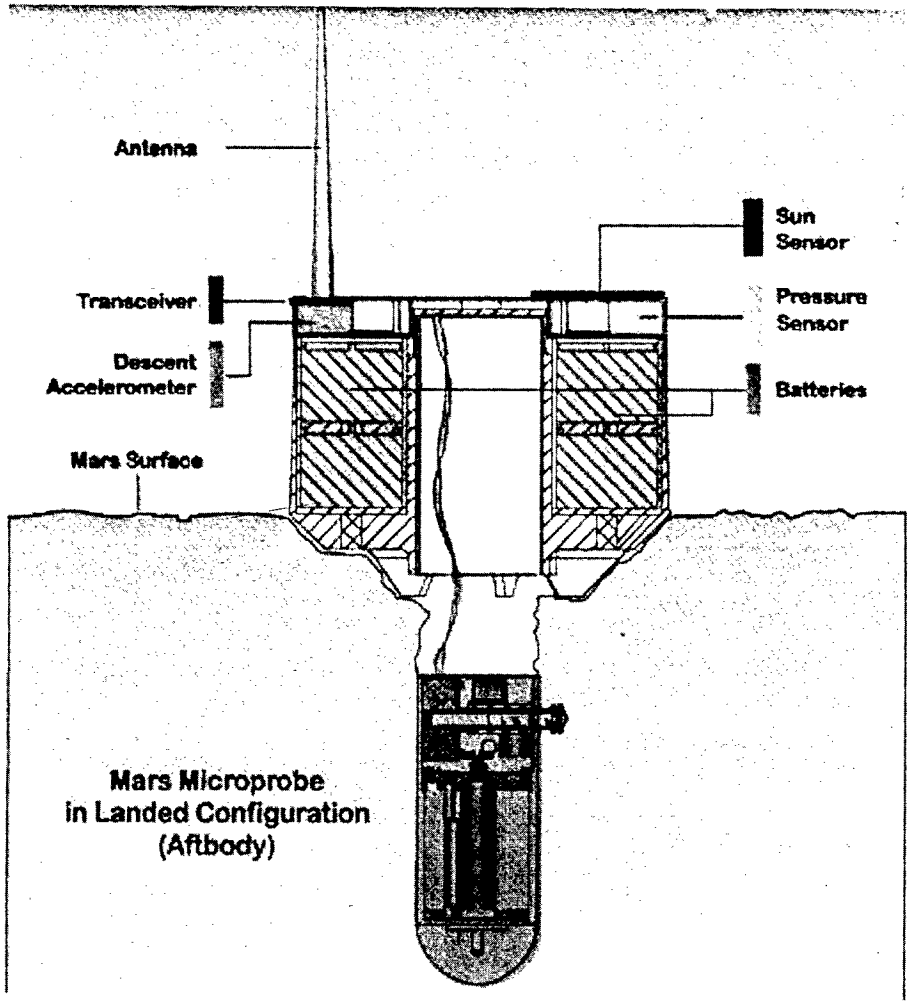
Antenna
Sun Sensor
Transceiver
Pressure Sensor
Descent Accelerometer
Batteries
Mars Surface
Mars Microprobe in Landed Configuration (Aftbody)

DS-2 MARS MICROPROBE BATTERY REQUIREMENTS

- Two 4 cell batteries
- Battery Voltage: 6-14 V
- Battery Capacity: 550 mAh at -80°C
  2 Ah at 25° C
- Shelf Life: 2.5 Years
- Operating Temp.: -60 C and below
- Shock Impact: 80,000 g

Electrochemical Technologies Group

Technology Challenges

- Ultra Low Temperature Operation(-80C)
- High Impact Shock Capability
- Minimal Voltage Delay at -60 C and below
- Three Year Shelf Life

Technical Approach

- **Select Cell Chemistry**
- **Award Contract for Cell Fabrication**
- **Demonstrate Electrical Performance at -80C**
- **Demonstrate Impact Resistance**
- **Demonstrate Life (Microcal)**
- **Demonstrate Safety**
- **Deliver Quality Cells to Project**

DS 2 BATTERY
Li-$SOCL_2$ SYSTEM

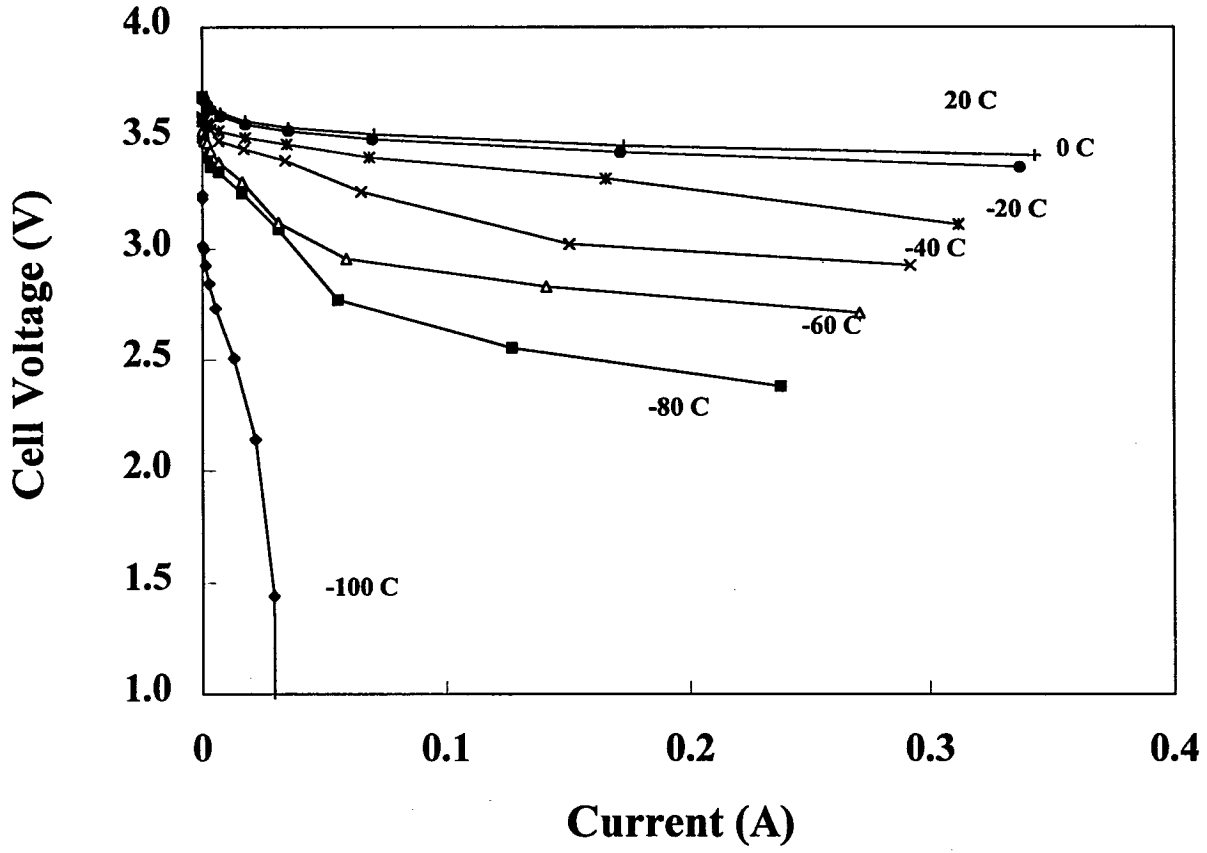

Electrochemical Technologies Group

DS 2 BATTERY
Li-SOCL$_2$ CHEMISTRY DEVELOPMENT

Dsicharge curves of D-size Li-SOCl$_2$ Cell at -80°C at 120 ohm

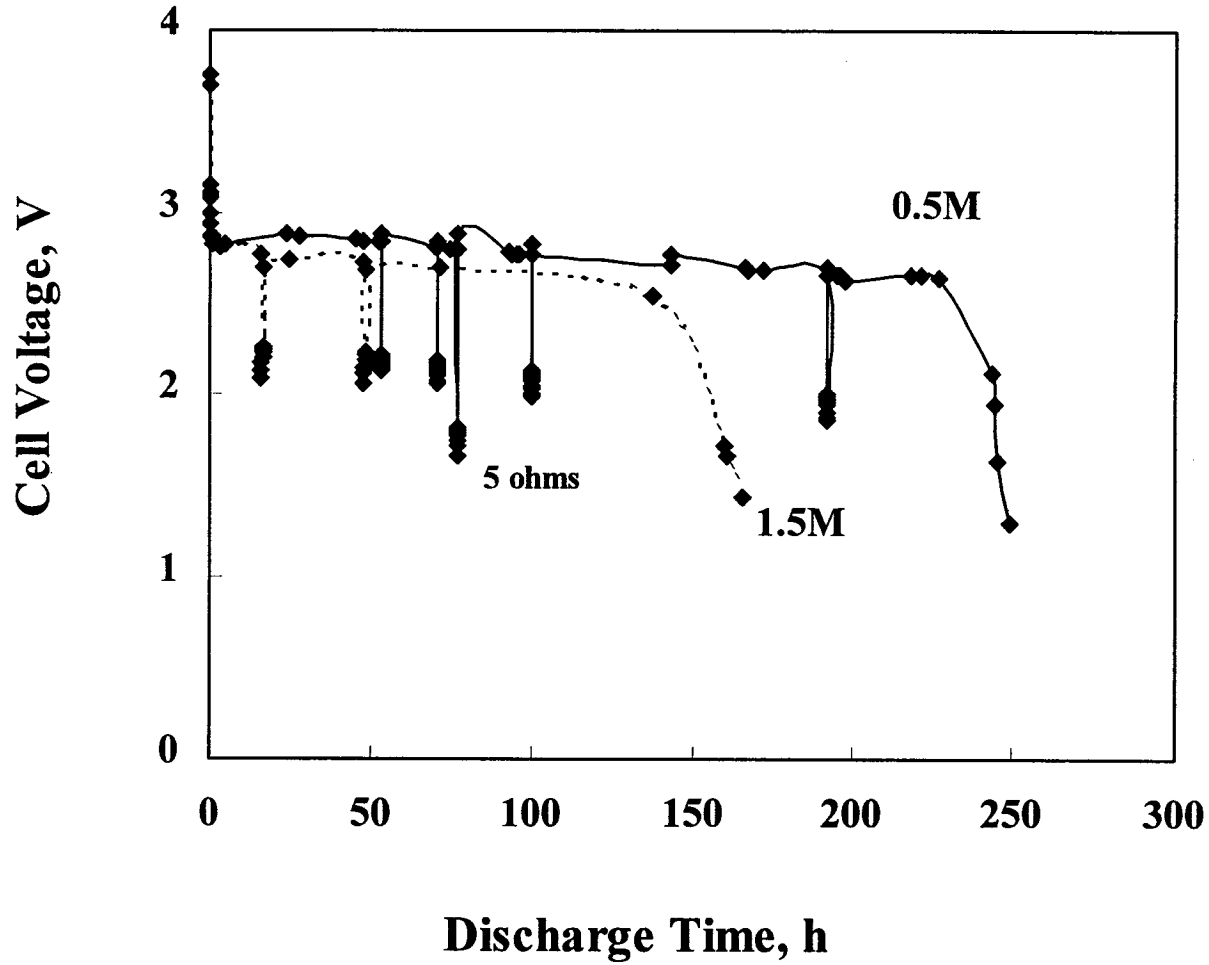

Electrochemical Technologies Group

Ds-2 Microprobe Battery

- Parallel Plate Configuration Perpendicular to to cyl. Axis
- $LiGaCl_4/SOCl_2$ Electrolyte
- Thin Electrodes
- Tefzel Spacer to Provide Stack Compression

INDUSTRIAL PARTNER: YARDNEY TECHNICAL PRODUCTS

Electrochemical Technologies Group

PROFILE TEST

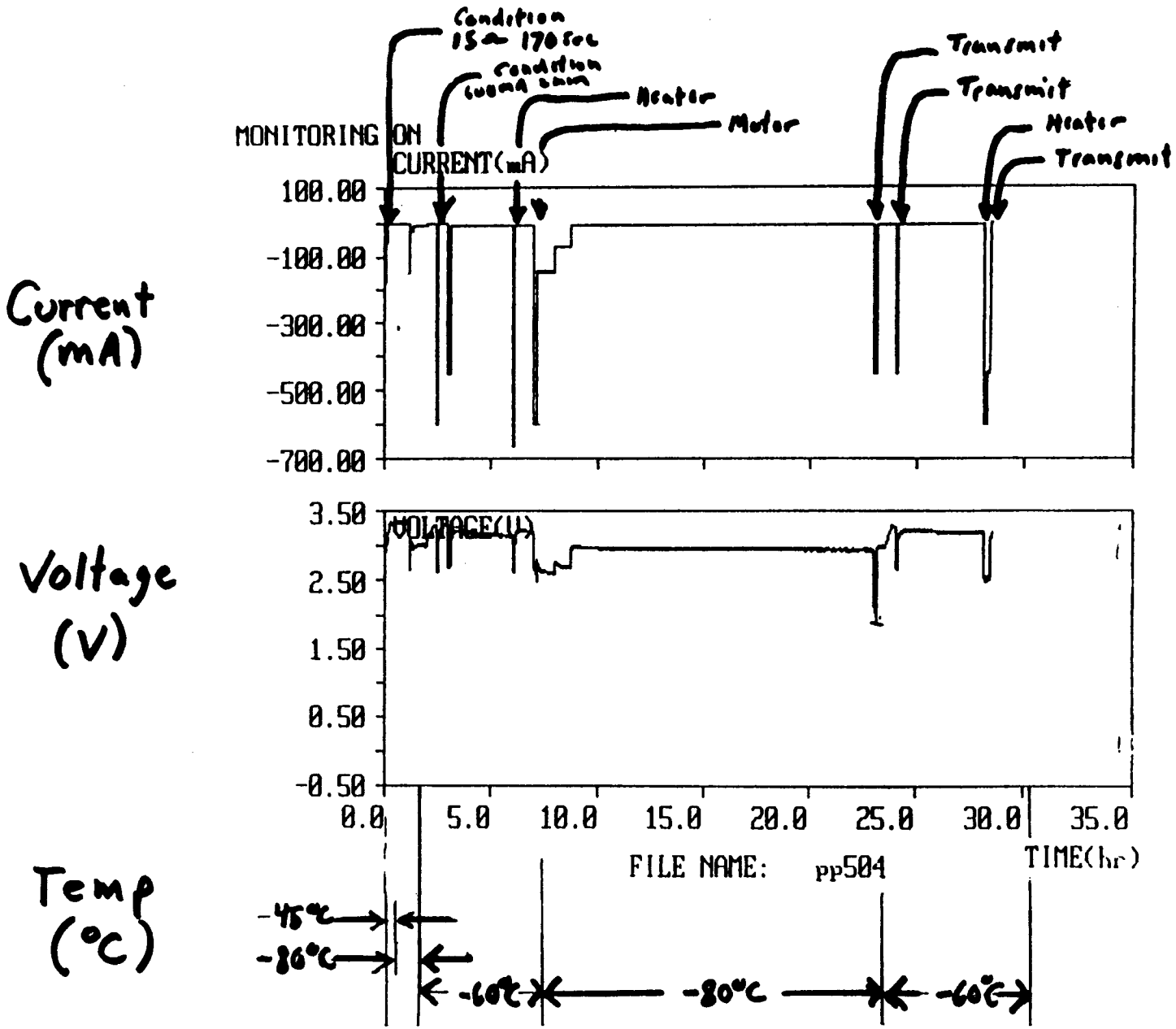

o Meets profile with conditioning

MICROCAL SUMMARY

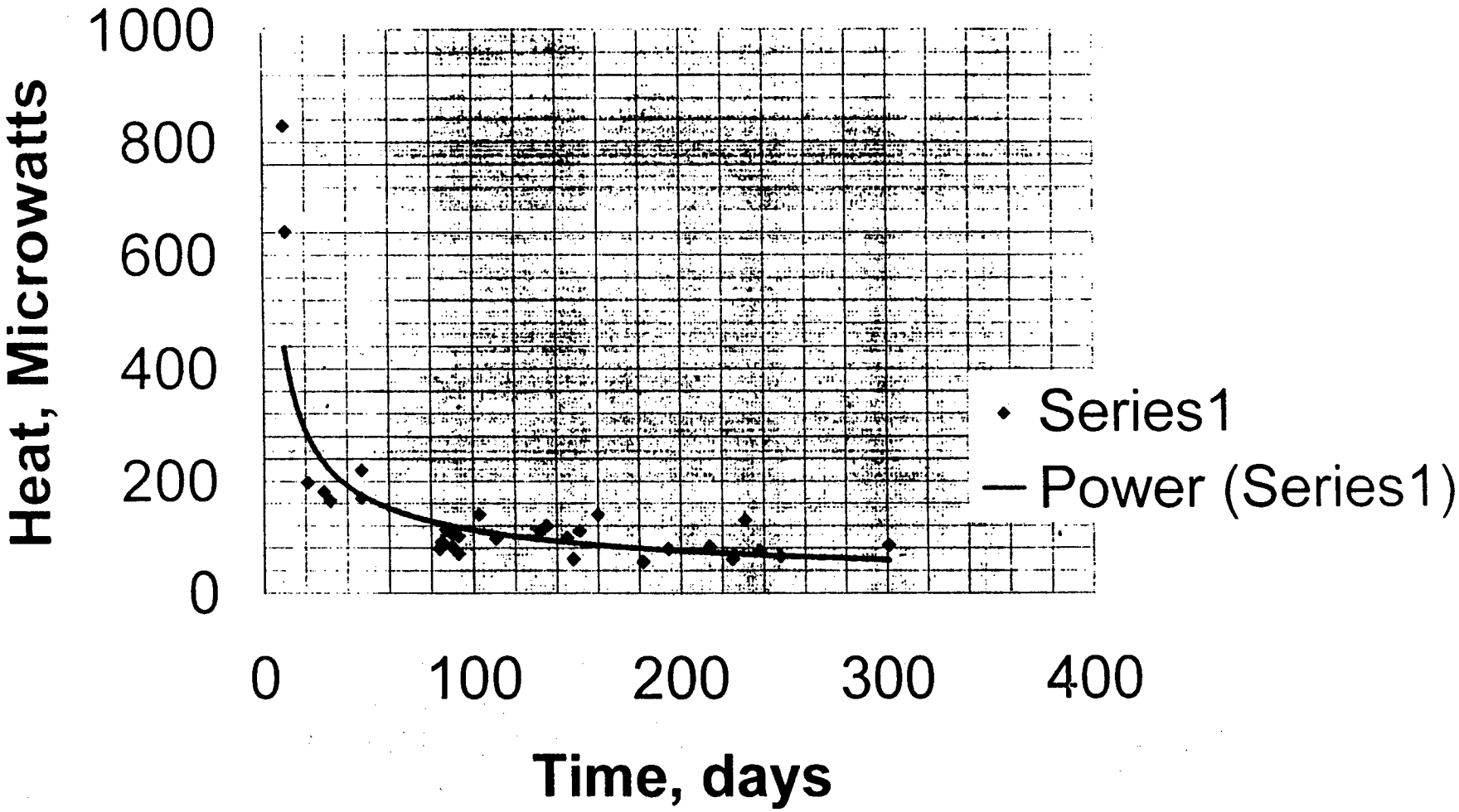

o MAX LOSS RATE ≃ 100 μW = 26.9 μA = 0.2 AH/yr

PROBLEMS ENCOUNTERED

- IMPACT SENSITIVITY
- CRACKING OF SEALS
- VOLTAGE DELAY

IMPACT TESTING
Problems Encountered

TEST	DATE	# Cells	CELL TYPE	PROBLEM
36	3/13/97	4	Old Design	Electrolyte Leak GTM Cracks Three Cells Functioned
38	4/4/97	2	Old Design	Electrolyte Leak GTM Cracks Two Cells Functioned
42	5/29/97	8	Old Design	Electrolyte Leak GTM Cracks Seven Cells Functioned
50	8/28/97	8	New Design	One Cell Vented, One Cell Bulged, Seven Cells Functioned
53	10/29/97	7	New Design	No Problems

Electrochemical Technologies Group

SEAL PROBLEM

PROBLEMS

- RADIAL CRACKS(1-3) WERE OBSERVED IN THE GLASS TO METAL SEALS IN 34 OF 48 CELLS

- FOURTEEN CELLS SHOWED NO CRACKS ON INSPECTION

- CIRCUMFERENTIAL TOOL MARKS OBSERVED IN SOME SEALS

CORRECTIVE ACTIONS

PRE WELD FILL TUBE

IMPROVED HEAT SINKING DURING CASE TO COVER WELD

CHANGE SEAL DIMENSIONS TO REDUCE STRESS

VOLTAGE DELAY PROBLEM

PROBLEM

- Voltage delay in excess of 50 seconds was seen at temperatures lower than -45 C

CORRECTIVE SOLUTION

- Dry the Electrodes to Reduce Water Contamination
- Assemble the Cells within a Week of Electrode Manufacturing
- Ensure Electrolyte Purity (Iron, Water Content)
- Provide second depassivation pulse after landing

DS-2 BATTERY ADDITIONAL TESTS SATIFIED

- **ENVIRONMENTAL**
  - **Thermal cycling, -30 to + 75oC.**
  - **Quasi-static acceleration, 100g for 60 sec.**
  - **Random vibration**
- **SAFETY**
  - **Discharge and Reversal at 114 mA, and at 25 and -80oC.**
  - **Shorting across 0.020 Ohms.**

DS-2 BATTERY ACCOMPLISHMENTS

- Demonstrated low temp (to -80°c) capability.
- Demonstrated capability to withstand shock.
- Demonstrated functionality for mission profile at low temp after shock.
- Demonstrated acceptably low self discharge for 2 year mission life.
- Delivered hardware and documentation.

DS-2 BATTERY CONCLUSIONS

- Can withstand shock (to 80, 000 g).
- Can meet discharge profile post shock at Mars temps.
- Self discharge rate moderate but not excessive (0.2 Ah/year max).
- Can meet environmental requirements and tolerate electrical abuse.

DS-2 BATTERY ACKNOWLEDGMENTS

- This work was carried out at the Jet Propulsion Laboratory, California Institute of Technology under contract with National Aeronautical and Space Administration and in collaboration with Yardney Technical Products, Inc.,.

Design and Flight Performance of NOAA-K Spacecraft Batteries

Gopalakrishna M. Rao, P. R. K. Chetty*, Tom Spitzer, and P. Chilelli**
NASA Goddard Space Flight Center
Greenbelt, Maryland 20771
(301)286-6654

ABSTRACT

The US National Oceanic and Atmospheric Administration (NOAA) operates the Polar Operational Environmental Satellite (POES) spacecraft (among others) to support weather forecasting, severe storm tracking, and meteorological research by the National Weather Service (NWS). The latest in the POES series of spacecraft, named as NOAA-KLMNN', one is in orbit and four more are in various phases of development. The NOAA-K spacecraft was launched on May 13, 1998. Each of these spacecraft carry three Nickel-Cadmium batteries designed and manufactured by Lockheed Martin. The battery, which consists of seventeen 40 Ah cells manufactured by SAFT, provides the spacecraft power during the ascent phase, orbital eclipse and when the power demand is in excess of the solar array capability. The NOAA-K satellite is in a 98 degree inclination, 7:30AM ascending node orbit. In this orbit the satellite experiences earth occultation only 25% of the year. This paper provides a brief overview of the power subsystem, followed by the battery design and qualification, the cell life cycle test data, and the performance during launch and in orbit.

I. INTRODUCTION

The advanced Television Infrared Observation satellite program is a cooperative effort between the National Aeronautics and Space Administration (NASA), the NOAA, the United Kingdom, Canada and France, for providing day and night global environmental and associated data. The NASA is responsible for procurement, launch, and checkout of these spacecraft before transferring them over to NOAA. The Lockheed Martin Missiles and Space (LMMS) Company is the prime contractor responsible for building these spacecraft.

A typical operational system, known as Polar Operational Environmental Satellites (POES), consists of two satellites in sun-synchronous (near polar) orbits, one in a morning (AM) orbit at 833 km, and the other in an afternoon (PM) orbit at 870 km. Figure-1 shows the NOAA-K spacecraft in orbital configuration. The K-Spacecraft of the latest POES series was launched on May 13, 1998 while the other four are in various phases of development and fabrication at LMMS.

To date, the overall Electrical Power Subsystem (EPS) including the batteries has been exhibiting nominal performance per design requirements. Continuous data has been obtained through housekeeping telemetry, and has been analyzed to verify the performance of the power system. This paper provides first a brief

*Kris Engineering, Inc., 14120 Stonecutter Drive, N. Potomac, MD 20878.
** LMMS, Newtown, PA

overview of the overall power subsystem, followed by a description of the battery, design and qualification, the cell life cycle test data, and performance during launch and in orbit.

II. POWER SYSTEM

The NOAA-K EPS, as shown in Figure-2, is based on the principle of Direct Energy Transfer (DET) from the solar cell array. This EPS implements a centralized regulation concept utilizing a partial shunt regulated main power bus approach. Within the power subsystem, three rechargeable batteries are the uninterrupted source of energy for the spacecraft. The EPS consists of a single wing solar array, Solar Array Telemetry Commutator Unit, Solar Array Drive, Array Drive Electronics, Batteries, Battery Current Sensors, Battery Charge Assemblies (BCAs), Power Supply Electronics (PSE), Power Converter, and Controls Power Converter. The batteries supply power to the loads during orbital eclipse and during the periods when the load power demand exceeds the solar array capability.

During normal operation of the power subsystem, satellite load power is supplied by either the solar array or batteries. In sunlight, the solar array supplies the load power directly and provides for battery recharge via the charge regulators. When the spacecraft is in eclipse, the three batteries supply the power for the loads via the discharge diodes and the boost voltage regulator.

Each of these spacecraft carry three conventional nickel-cadmium batteries designed and manufactured by Lockheed Martin. Each battery consists of seventeen 40-Ah capacity cells manufactured by SAFT. Battery cell design has been guided by the life and reliability requirements of 3-years (goal) in orbit performance in addition to a 5-year ground storage.

III Battery Design

The battery system consists of three 40 Ah rated batteries to provide a combined capacity of 120 ampere-hours. Each battery is comprised of 17 series-connected closely matched cells, physically subdivided into two packs: one containing nine cells and the other containing eight (Figure-3). At cell level, all cells in each battery have a) capacities within $\pm$ 3% of the 17 cell average and b) end of charge voltages within $\pm$ 0.008V of the 17 cell average at 21^{0}C and 0^{0}C. Figure-4 shows the details of a cell thermal sleeve whereas Figure-5a shows an assembled 9-cell pack without radiator. A 9-cell pack employs a dummy cell for easy mechanical design. Figure-5b shows the same 9-cell pack with its radiator, connector brackets and spacecraft attaching struts integrated. The same assembly is shown mounted on the spacecraft in Figure-6a. Figure-6b shows a top view of the spacecraft with all six battery packs integrated.

Module Assembly Design

The battery modules are capable of being mounted to the spacecraft, using the predefined interfaces. The 8 and 9 cell packs are designed such that an 8 cell pack can not mechanically mount to the spacecraft in a 9 cell location and viceversa. Battery mechanical interfaces with the spacecraft provide for thermal isolation. The battery is designed such that the thermal control electronics (TCE) connector is easily accessible when the pack is mounted on the spacecraft. The use of dissimilar metals in direct contact with the cells and their modules is avoided. Use of any magnetic material (except energy storage cells) is avoided. The cell assembly is replaceable without degrading the performance or reliability of other battery components. Each battery module is designed to withstand individual cell pressures of up to 65 psig.

The battery module assembly includes the battery module, the module's secondary support structure, and all thermal control components (including the TCE). The maximum weight of a 9-cell module is 52.5 lbs and 8-

cell module is 46.6 lbs.

Thermal Design

Battery packs are designed to achieve orbital average cell temperature from 3^0C to 7^0C during nominal 3-battery operation and from -5^0C to 18^0C during 2-battery operation under worstcase end-of-life conditions. However, under optimum conditions, cell temperature between 0^0C to 7^0C during nominal 3-battery operation and -5^0C to 15^0C during 2 battery operation were achieved. In addition, a maximum gradient within a cell of <5^0C, a maximum cell to cell gradient within a battery of <5^0C and the orbital average battery temperature between 3^0C and 5^0C were achieved. The battery packs are thermally isolated from the spacecraft.

Following are some of the definitions with respect to various temperatures referred in this section. Cell temperature is defined as the average of the temperature of all of the nodes in the cell. Pack temperature is defined as the average of the cell temperatures within the pack. Battery temperature is defined as the average of the 17 cell temperatures within the battery. Maximum gradient within a cell is defined as the maximum temperature difference between any two nodes on the cell. Maximum gradient within the pack is defined as the maximum temperature difference between cells in a pack. Gradient within the battery is defined as the maximum temperature difference between cells in a battery.

The battery temperature control is achieved by active and passive means. Passive temperature control is accomplished by means of a fixed radiative surface, and a multi-layer insulation (MLI) blanket on each module, whereas active temperature control is exercised through a strip heater on each module, controlled by the TCE. Separate strip heaters controlled by two series thermostatic switches serve as back-up to the primary heater circuit.

A functional block diagram for the two packs that make up any one of the three identical 40 Ah batteries is presented in Figure-7. Each pack contains 2 thermistors for the battery voltage/temperature (V/T) limiting reference circuit in the battery charge control electronics. Thermistors bonded to the end surface of cells 6A and 2B provide a combined voltage proportional to temperature for the primary control circuit, and thermistors bonded to the end surface of cells 2A and 5B provide the combined output voltage for the backup control circuit.

A 25% heater margin for the cold case and heater control authority of 25% of the battery average power dissipation during the hot case are incorporated in the thermal design. The battery thermal design allows a continuous trickle charge (0.50 Amps ± 0.20A) operation at any temperature between -5^0C and 30^0C during integration and test. The thermistors are operable over the temperature range of -10^0C to +40^0C. The placement of the V/T telemetry thermistor is optimized such that the temperature sensed by the thermistor is as close to the average pack temperature as possible.

Electrical Design

The electrical harness is designed such that the maximum voltage drop between the battery terminals and input to the battery discharge regulator is <1.0 volt during normal operations and is capable of a maximum charge rate of 15 amps. During ground operations, the battery is capable of being discharged at up to 35 amperes for a minimum of 35 minutes, over the temperature range -5^0C to +30^0C. Each battery provides an output for the Electro Explosive Device bus with a voltage range of 19.5 V to 25.8 V, and up to a 10.0A current under normal operating conditions. A means for electrically grounding the battery structure to the spacecraft structure is provided.

Each module has provisions for connecting individual cells (one wire connection to each cell positive terminal

and one to each cell negative terminal) to the battery reconditioning unit via a separate dedicated connector and to ground reconditioning unit via another separate connector. The battery chassis is electrically double isolated from any cell terminal.

Thermistor circuits bonded to the end surface of cells 3A and 7B provide a separate temperature telemetry signal from each pack for the spacecraft telemetry system. A second set of thermistor circuits, similar to that used for telemetry, are bonded to cells 4A and 4B. These circuits are used only during ground test operations to permit battery pack temperature monitoring while the batteries are charged externally with spacecraft power off. Power for these test thermistor circuits is supplied by the ground support equipment.

In addition to the temperature sensing and control circuits, the battery includes a battery voltage telemetry circuit, test point isolation resistors for monitoring battery voltage during ground testing, and an isolation diode for protection when the battery is charged from a power source external to the satellite during ground checkout.

IV. Battery Qualification/Acceptance Testing

A qualification battery consisting of a 9 cell module and an 8 cell module was constructed and was subjected to the qualification tests as outlined in Figure-8.

All flight batteries were acceptance flight tested following the outline in Figure-9. Each battery is discharged at the 10.0 amperes rate during the random vibration tests. Vibration levels are presented in Table-1.

V. Cell Life Cycle Tests

The intent of the life cycle testing is to evaluate the flight-worthiness of cells from this manufacturer for POES spacecraft batteries. The purpose of the first pack (10 cells) is to simulate the worst-case LEO mission-profile expected for the POES program whereas the second pack (5 cells) reveals performance of these cells under a NASA-Standard stress test LEO mission profile. The test parameters for these tests are summarized in Table-2.

Both the tests were successful. The Mission-Profile test completed 9848 cycles before it was stopped as these batteries were meant for the NOAA-K spacecraft operating in the AM orbit. In this orbit, the spacecraft experiences only about 2100 eclipses per year. The Stress test completed 7106 cycles before it was stopped as this reflects more life than the POES mission requirement.

VI. Battery Charge Control

The three batteries are charged individually by separate charge regulators, but are discharged in parallel through the discharge isolation diodes. Battery charge control is performed by charge regulators which protect the batteries from overcurrent and overvoltage conditions. This function is performed by monitoring battery charge current, voltage, and temperature parameters.

During normal recharge and before the overcharge condition, charge current to each battery is limited to any one of four ground-commandable rates: 12.5, 10.0, 7.5, or 0.5 amperes. The only limitation is that the sum of the three charge rates cannot exceed 30 amperes due to thermal design constraint.

When the battery voltage reaches one of sixteen ground commandable voltage levels (which are a function of battery temperature), the battery current is reduced by a tapering action so that the battery voltage level remains limited to the commanded level. Any one of the sixteen limits, as shown in figure-10a, can be independently selected for each battery.

The sixteen levels have been chosen on the following basis: I) V/T curve 3 is the curve of choice for supporting the maximum satellite load during an 80^0 sun angle orbit (longest eclipse time) after 2 years life; ii) V/T curves 1 and 2 are held in reserve in the event that battery cell charge voltage characteristics increase with age; iii) V/T curves 4 and 5 are available to control battery overcharge and trim C/D ratios with changes in spacecraft loading and sun angle; iv) V/T curves 6, 7, and 8 are available to taper back charge current to safe values (~ 0.5A) during periods of extended overcharge; v) V/T curve levels below level 8 (9-16) are designed to accommodate a variety of conditions which include a possible reduction in cell charge voltage characteristic with aging, development of partial or soft short circuit conditions in some cells, or the actual presence of a full short in one single cell out of the 17 series cells that comprise a battery; and vi) The shape of all 16 voltage limit curves has been purposely depressed at higher battery temperatures to reduce the possibility for thermal runaway.

The specific selection of the V/T curve to be used for charging each battery during any given set of circumstances should have as its goal the achievement of orbital energy balance without excessive battery overcharge. Figure-10b presents a curve showing the minimum charge-to-discharge ratio recommended for ensuring energy balance as a function of battery temperature.

VII. NOAA-K BATTERY OPERATIONS & PERFORMANCE

The NOAA-K spacecraft was launched into an orbit with a period of approximately 102 minutes with eclipse duration varying from 0 to 24 minutes.

A. Operations

Pre-launch recharge controls are set high (charge rate of 10 amps per battery, V/T Level of 4) as a precaution to provide a high recharge level and maintain power balance, in the event of anomalous launch conditions (solar array not tracking the sun or spacecraft attitude error). During the first day in orbit, the V/T level was changed from 4 to 5 for each of the three batteries. On the fifth day, the battery charge rate was reduced from medium rate charge (10 amps) to a low rate charge (7.5 amps). Battery power requirements increased over a two week period as the payload instruments were individually turned-on. Table-3 presents the changes made since launch which influence the performance of the batteries.

The sun angle is expected to decrease with a corresponding decrease in eclipse period, finally towards full sun season with no eclipses. This is a cyclic phenomenon over the life of the mission.

B. Performance

1. Charge Discharge Ratio Control

The charge/discharge trigger was enabled after assuring that batteries have been fully charged-up and this occured about 24 hours after launch. Once this trigger is enabled, power management software computes the charge-discharge ratio and issues commands to lower the charge current from previously selected charge rate (high, medium or low) to trickle charge rate when the charge-discharge ratio reaches preselected value. The

trickle charge rate is indirectly enforced by commanding a V/T level that is 3 or more levels higher than preselected V/T level used at sunrise. For example, the V/T level was changed from 5 to 9. This is illustrated in Figure-11, where the battery voltage, charge current and discharge currents versus time are shown. The charge current of 7.5 amps at sunrise was held constant until the battery voltage reached the V/T limit (corresponding to V/T level 5). Then it started tapering until charge-discharge ratio reached the preselected value of 1.04, where the charge current was reduced to 0.5 amps. A 3 or more levels higher than preselected V/T level reduces the charge current to lower than trickle charge current, however, the hardwired minimum charge current is equal to trickle charge rate of 0.5 amps. Figure-12 is similar to Figure-11 but the C/D control was not enabled yet.

The V/T level is reestablished to normal (predetermined) level at the next sun-return. Ephemeris sun-return is normally a few degrees after the actual orbital sun-rise.

2. Charge Discharge Ratio Control Accuracy

Traces were run to collect data (charge currents, discharge currents, battery voltage, V/T levels, battery temperatures) over an entire orbit sampled at every 8 seconds. Battery charge current and voltage are multiplied and integrated at 8 second integration. The amount of watt-hours of energy taken out during the eclipse and charged during the day are computed.

To compute for the charge to discharge ratio, the amount of energy put into the battery is divided by the amount of energy taken out of the battery. This value is compared with the on-board computer programmed battery recharge ratio and the results are tabulated below:

Battery No.	**AH Discharge**			**C/D Ratio**		**Temperature**
	Ground Computed	On-board Computer	Difference (%)	Ground Computed	On-board Computer Programmed	
Battery-1	3.90 AH	3.91 AH	0.3%	1.04	1.04	3.8^{0}C
Battery-2	4.07 AH	4.08 AH	0.2%	1.04	1.04	3.0^{0}C
Battery-3	3.97 AH	3.97 AH	0.0%	1.04	1.04	3.0^{0}C

The AH discharge and C/D ratios computed by on-board Computer (OBC) are in close match with the ground computed values.

3. Thermal Control of Batteries

Figures-13, 14, & 15 present the battery-1A & 1B temperature and heater status over a time span of two hours for day-of-the-year 135, 155 and 257 respectively. The battery temperature has been maintained between 2.5^{0}C and 4.7^{0}C and heater duty ratio varied over a range. The battery heater is turned-ON by TCE when the lower temperature limit is reached and turned-OFF when the upper temperature limit is reached. In fact, when the heater is turned-ON, it cycles ON and OFF at 14 cycles per second until the upper temperature limit is reached. Due to this cycling nature when it is commanded-ON, it is difficult to predict the duty ratio of the heater due to coincidence/non-coincidence of telemetry sampling with respect to heater cycling as (a) telemetry sampling rate is different from heater cycling rate and (b) both rates are not synchronized. Thus, there is only 50% chance that heater status telemetry gives actual heater duty cycle. The telemetry values are 4.5V for heater OFF indication and is 2.5V for ON indication.

Figure-16 presents the temperature of battery packs 2B and 3A since launch. The temperature of the battery packs should have been maintained above 3^{0}C (based on ground testing) through out the mission life even

though the internal dissipation and external heat fluxes are expected to vary over a wide range depending upon the spacecraft sun angle, eclipse duration, spacecraft eclipse load demands, etc. From the Figure-16, it is clear that at least packs 2B and 3A dipped below 3^0C. This dip may be attributed to the location of the temperature sensor used for thermal control which is different from the location of the temperature sensor used for telemetry (see Figure-7). In addition, a solar array leading offset of $+53^0$ might have created adverse heat fluxes for these battery packs as evidenced from days 139 to 187. On day 187, the offset was changed from $+53^0$ to -45^0 and the battery temperature started increasing even though the eclipse period was gradually diminishing to zero. Preliminary indications are that solar array leading offset might have created external heat fluxes which might have resulted in temperature dip. Also, it is possible that the leading solar array offset might have not been considered in the original analysis. Further analysis to correlate with the flight data is in progress. If determined, the heater size will be increased for NOAA-L and onwards. The current battery pack temperatures will certainly support the mission life goal of 3 years.

4. Load (AH) sharing by Batteries

As explained above, the batteries are ORed using diodes and discharged together. Thus, there is no active effort to force load sharing equally among the three batteries. Table-4 presents the ampere-hour load sharing among three batteries. Their sharing is excellent, each battery supplying about one-third of the total spacecraft load. This reflects on well matched batteries consisting of cells, wiring within each pack, wiring between packs, and wiring to the ORing diodes.

5. Peak Discharge Current.

The battery peak discharge current occurs at the end-of-night. This current is the highest discharge current from the battery because the battery voltage is lowest at the end of this constant power discharge. The peak discharge current observed was in the range of 9 to 10.5 amps, which is about C/4.

VIII. CONCLUSION

With proper in-orbit power system operation, the NOAA-K batteries will continue to perform nominally.

Table-1 Random Vibration Test Levels			
Frequency (Hz)	PSD (G2/Hz)	Duration/Axis	Overall
Qualification Test Levels			
20-70 70-140 140-500 500-1000 1000-2000	0.05 flat +7 dB/octave 0.25 flat -7 dB/octave 0.05 flat	1 minute perpendcular axis	14.5 Grms
20-70 70-140 140-500 500-1000 1000-2000	0.05 flat +7 dB/octave 0.11 flat -7 dB/octave 0.05 flat	1 minute horizontal axis	11.9 Grms
Flight Test Levels			
20-70 70-140 140-500 500-1000 1000-2000	0.05 flat +7 dB/octave 0.11 flat -7 dB/octave 0.05 flat	1 minute perpendcular axis	11.9 Grms
20-70 70-140 140-500 500-1000 1000-2000	0.05 flat +7 dB/octave 0.05 flat -7 dB/octave 0.05 flat	1 minute horizontal axis	7.9 Grms

Table-2 POES NOAA-K, L, M, N, N' Battery Life Test Parameters		
Parameters	Mission-Profile	Stress Test
Temperature	5^0C	20^0C
Orbit duration	102 minutes	90 minutes
Discharge duration	36 minutes	30 minutes
Depth of Discharge	21%	40%
Discharge Rate	14.0 amps constant current	32 amps constant current
Charge rate	10 amps constant current to V/T	32 amps constant current to V/T
V/T level (typical)	NASA V/T Level-5	NASA V/T Level-5
C/D ratio	105% min, 110% max	120% max
Failure Criteria	<4200 cycles for AM orbit <10400 cycles for PM orbit	<5200 cycles
Min Cell Voltage EOD	10 cell pack voltage <11 volts	5 cell pack voltage <5.5 volts
Max Cell Voltage EOC	Any cell >1.56 volts	Any cell >1.56 volts
Cell Voltage Divergence	>100 mV EOC; no limit EOD	>100 mV EOC; no limit EOD

Table-3 Summary of Battery Related Operational Changes		
Day/Time	Command	Description/Function
133:15:50	Spacecraft launched	Spacecraft launched. Charge rate of 10 amps and V/T level of 4 for all batteries
133:16:26	PMCTL BFFF	Monitoring of battery parameters was enabled. State of charge of all three batteries was initialized to 34AH.
133:19:02	CMD B123V05	Enabled sun-return (V/T level-5 for all batteries) and cut back (V/T level-9) V/T levels.
134:15:26	CP POWRC (CMD FIPSI) (CMD CPSTA) (PMTRG 1C00)	Set battery temperature limits to level-1 for on-orbit mode operation (lowered from 28^0C to 14^0C). Enable battery C/D ratio V/T commanding.
	CP ARRAY30LG	Solar array was offset to -30^0 (lag).
134:18:42	PMTRG 1E00	Use patch for state of charge calculations.
135:13:25	CP ARRAY55LG	Solar array offset was changed from -30^0 (lag) to -55^0 (lag).
136:16:17	CP CLMVALU	Set PMS charge state initialization values to 40AH.
137:19:14	CMD BCLLL	Charge Rate was lowered from 10 amps to 7.5 amps.
139:21:48	CP ARRAY53LD	Solar array offset was changed from -55^0 (lag) to $+53.2^0$ (lead).
146:19:22	PMTRG FE7E	Enabled Battery/BCA overtemperature commanding.
169:16:17	CMD B123V06	Changed V/T level from 5 to 6 for all batteries.
187:17:40	CP ARRAY45LG	Solar array offset was changed from $+53.2^0$ (lead) to -45^0 (lag).
197:14:05	CMD B1V07 CMD B3V07	Changed V/T level from 6 to 7 for battery 1. Changed V/T level from 6 to 7 for battery 3.
216:18:44	CMD B2V07	Changed V/T level from 6 to 7 for battery 2.

Table-4 Ampere-Hour Load Sharing Among Three Batteries						
Year/Day/Time	State-of-Charge (AH) during discharge			Load sharing		
	Battery-1	Battery-2	Battery-3	Battery-1	Battery-2	Battery-3
98/139/06:00:47.4	37.05	37.02	37.09	0.33	0.34	0.33
98/141/12:00:47.4	36.41	36.30	36.41	0.33	0.34	0.33
98/143/18:00:47.4	36.31	36.20	36.28	0.33	0.34	0.33
98/147/00:00:47.4	36.25	36.11	36.20	0.33	0.34	0.33
98/150/00:00:47.4	36.33	36.38	36.41	0.34	0.33	0.33
98/152/06:00:47.4	36.19	36.03	36.13	0.33	0.34	0.33
98/154/06:00:47.4	36.14	35.98	36.08	0.33	0.34	0.33
98/157/00:00:47.4	36.11	35.95	36.05	0.33	0.34	0.33
98/160/06:00:47.4	36.11	35.95	36.05	0.33	0.34	0.33
98/163/00:00:47.4	36.13	35.97	35.98	0.32	0.34	0.34
98/164/18:00:47.4	36.06	35.91	36.02	0.33	0.34	0.33

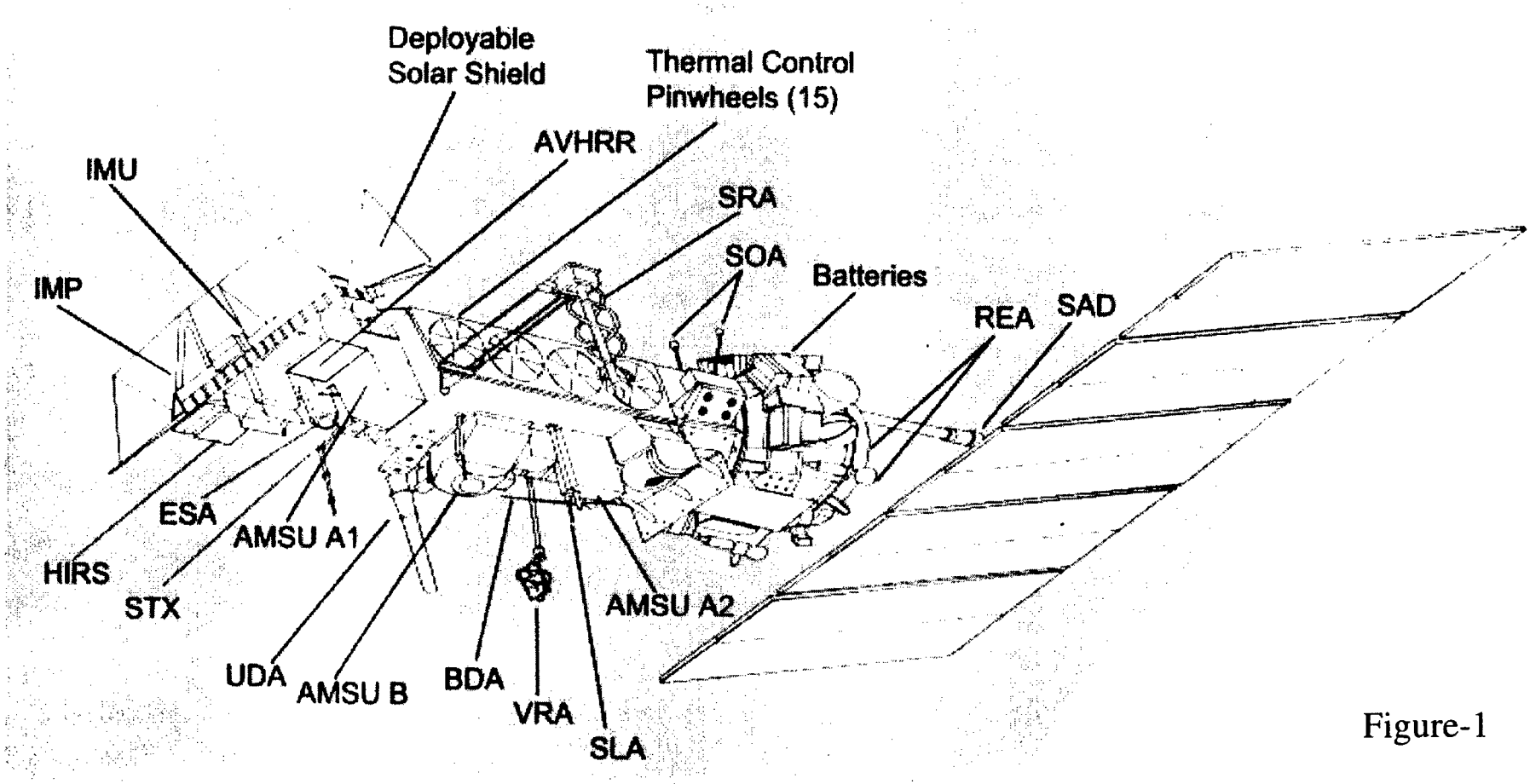
Deployable
Solar Shield
Thermal Control
Pinwheels (15)
AVHRR
IMU
SRA
SOA
Batteries
IMP
REA
SAD
ESA
AMSU A1
HIRS
STX
AMSU A2
UDA
AMSU B
BDA
VRA
SLA

Figure-1

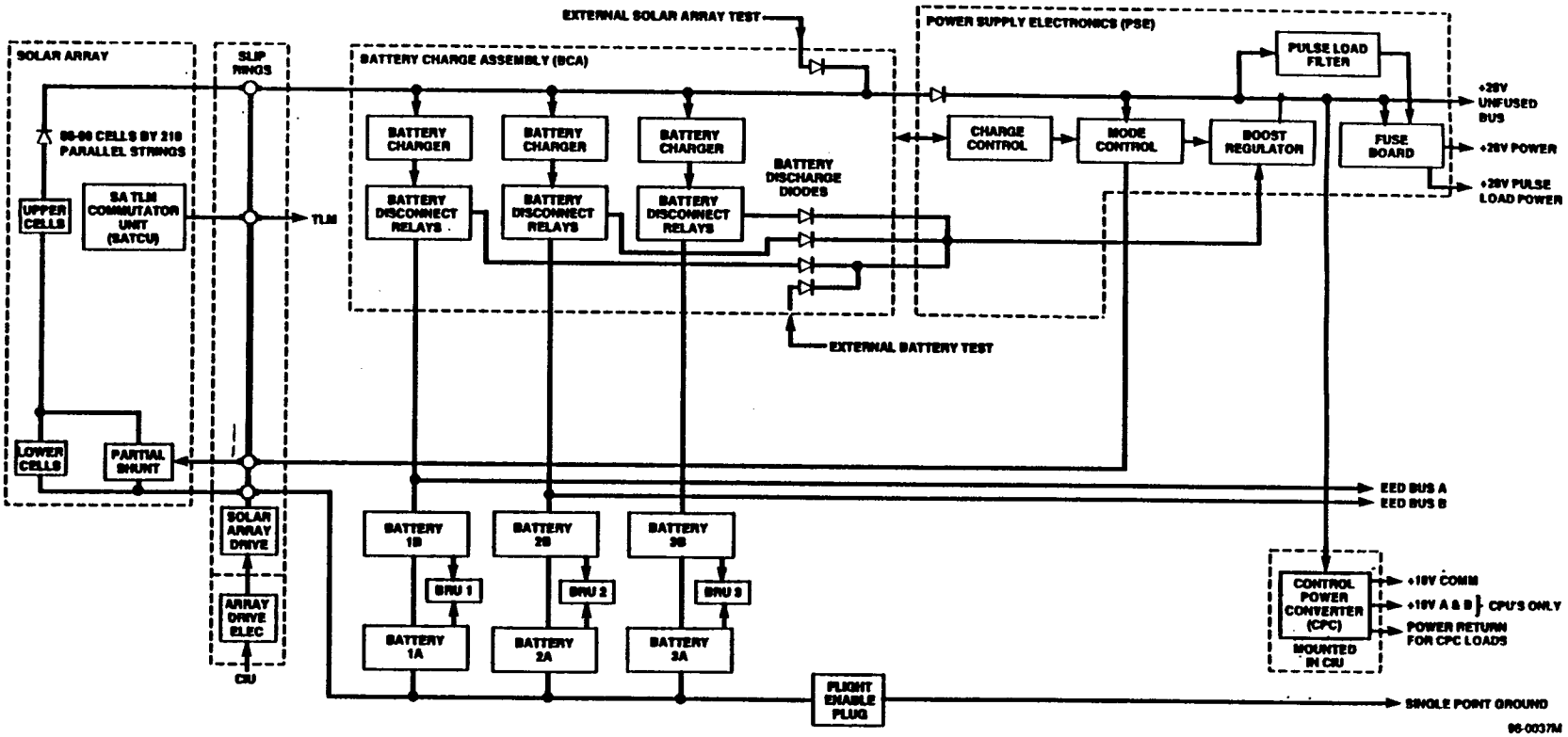

Power Subsystem Functional Block Diagram

Figure-2

"Design and Flight Performance of NOAA-K Spacecraft Batteries" by Gopalakrishna M. Rao et al.

8 CELL

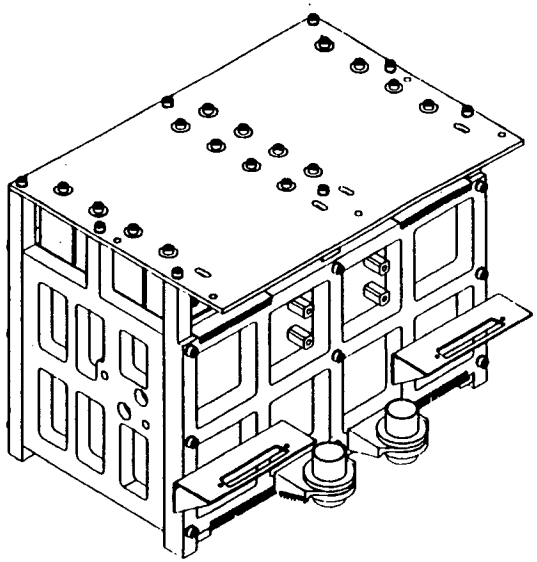

9 CELL

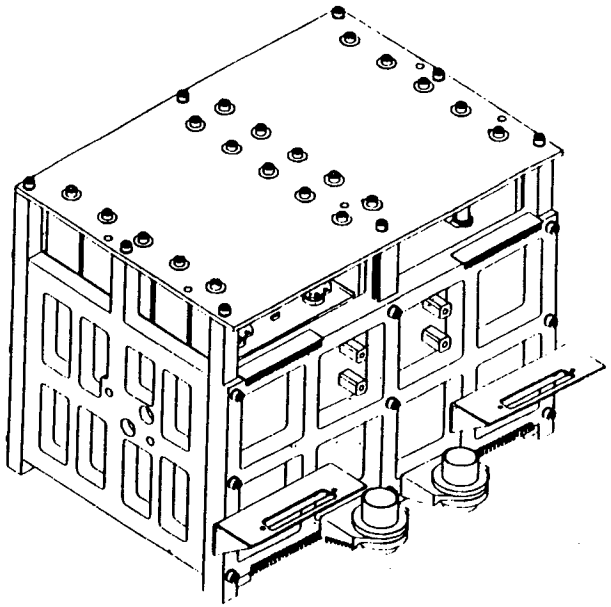

ASSEMBLED CELL PACKS

Figure-3

"Design and Flight Performance of NOAA-K Spacecraft Batteries" by Gopalakrishna M. Rao et al.

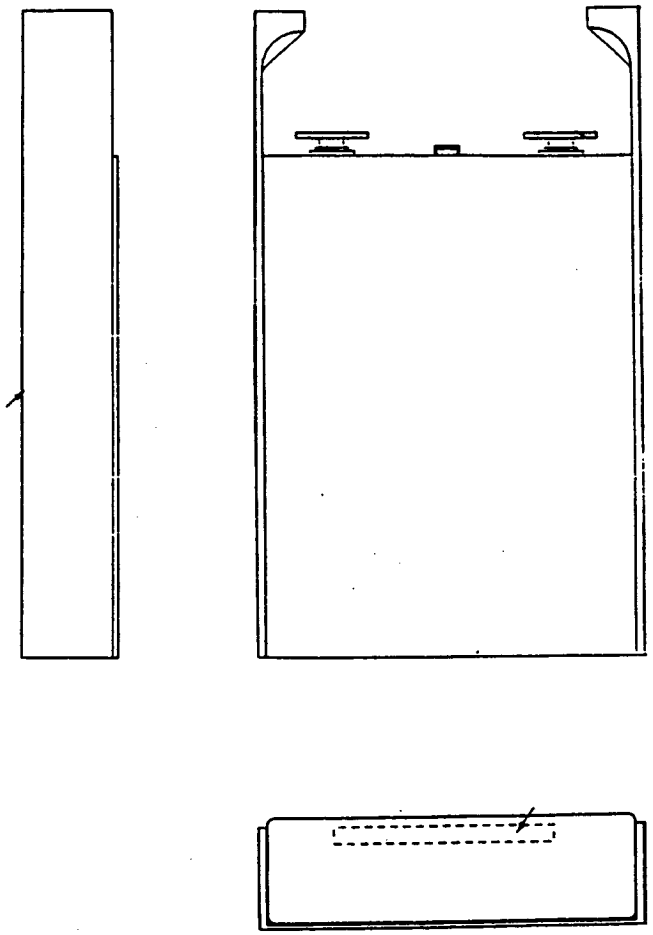

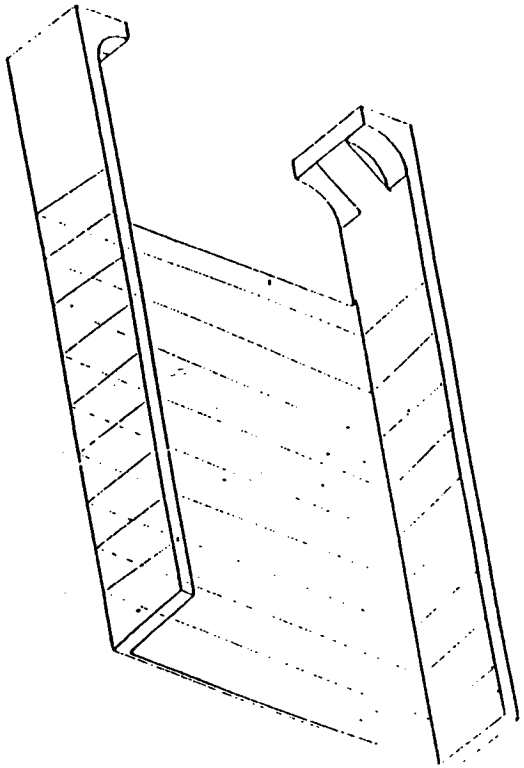

CELL THERMAL SLEEVE
Figure-4

"Design and Flight Performance of NOAA-K Spacecraft Batteries" by Gopalakrishna M. Rao et al.

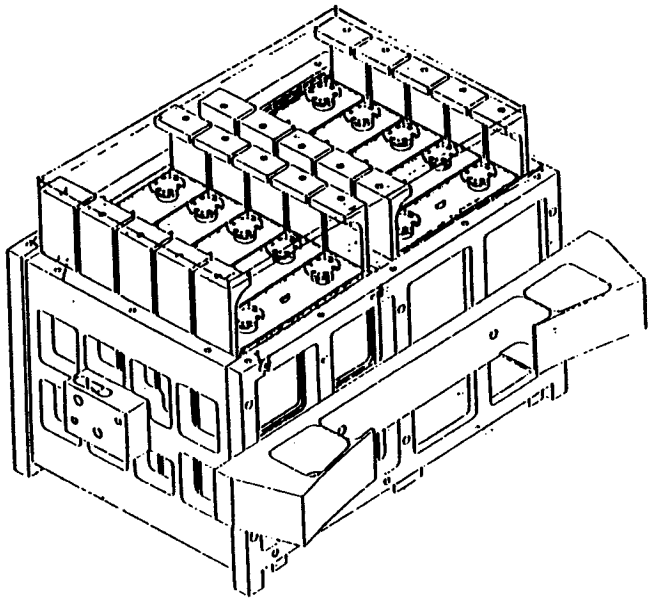

(a)

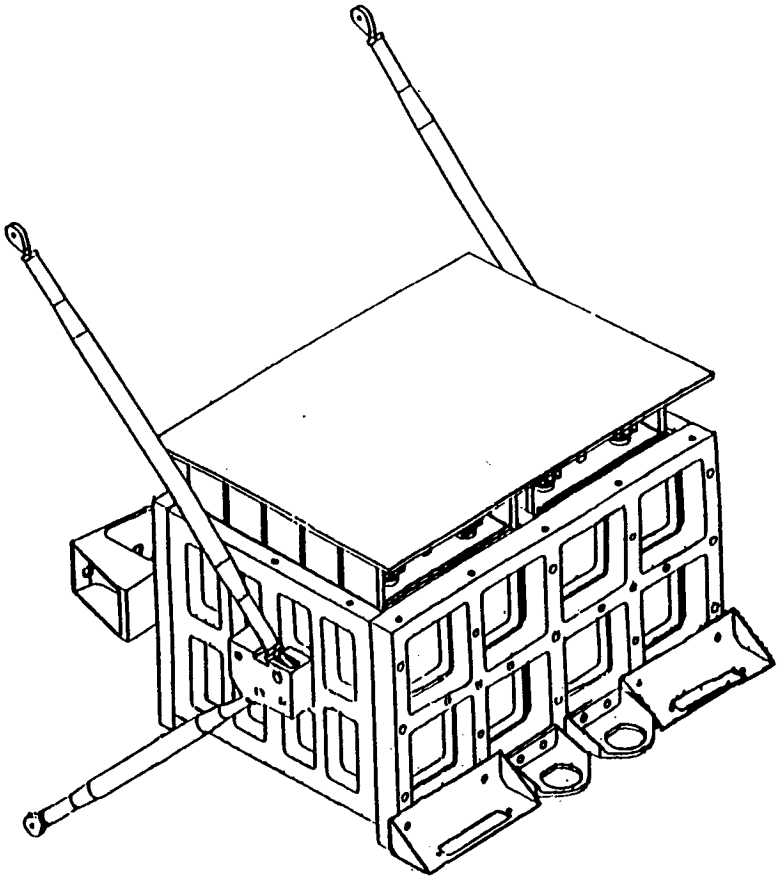

(b)

CELL PACK WITH RADIATOR, CONNECTOR BRACKET & SPACECRAFT ATTACHING STRUTS

Figure-5

"Design and Flight Performance of NOAA-K Spacecraft Batteries" by Gopalakrishna M. Rao et al.

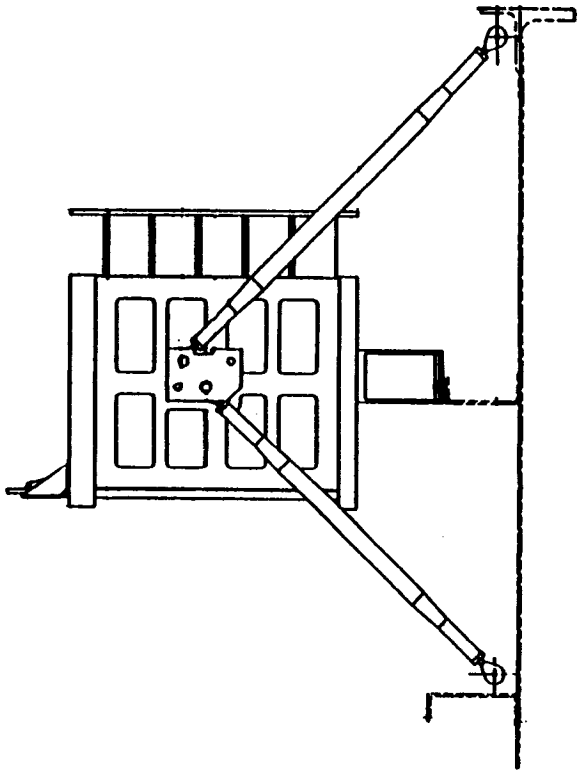

PACK ASSEMBLY MOUNTED ON SPACECRAFT

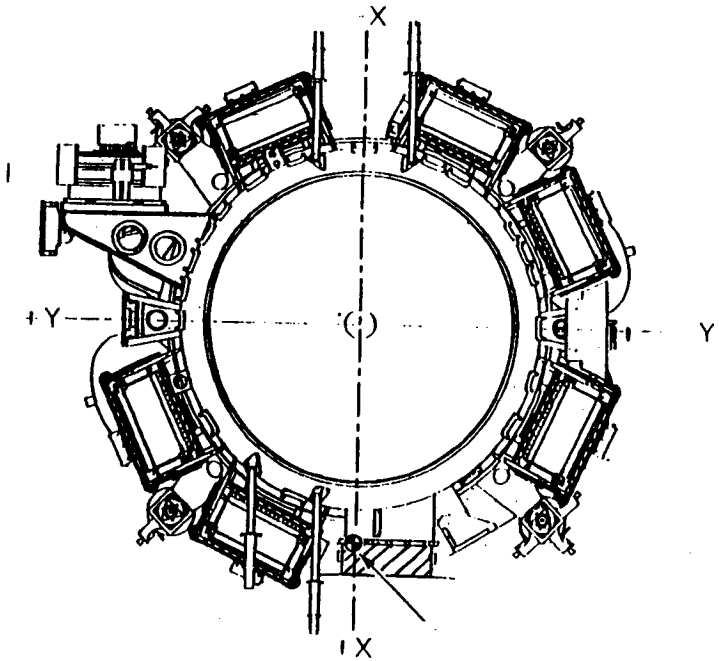

SPACECRAFT WITH ALL SIX BATTERY PACKS INTEGRATED

Figure-6

"Design and Flight Performance of NOAA-K Spacecraft Batteries" by Gopalakrishna M. Rao et al.

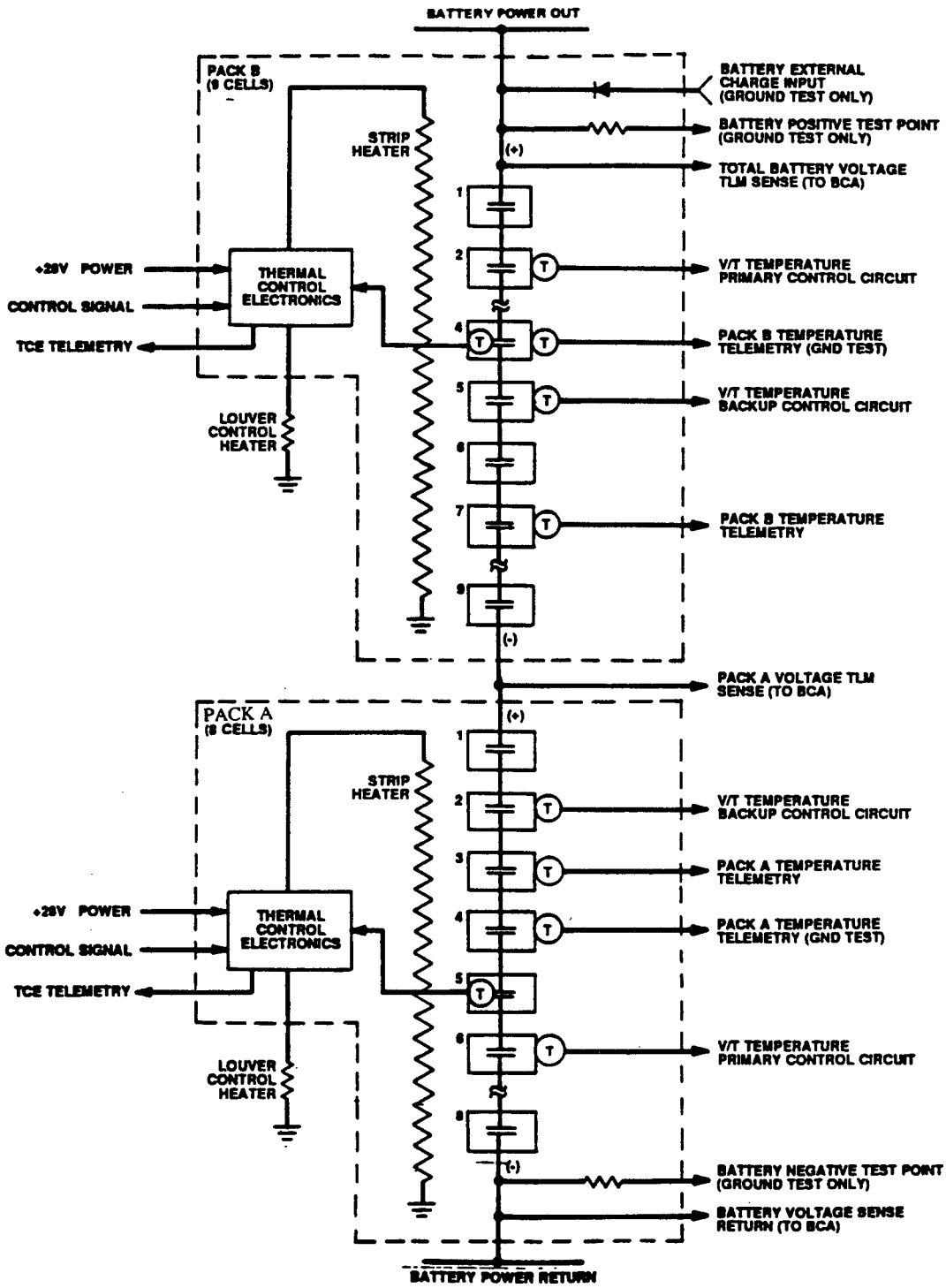
BATTERY POWER OUT
PACK B
(9 CELLS)
STRIP HEATER
THERMAL CONTROL ELECTRONICS
+28V POWER
CONTROL SIGNAL
TCE TELEMETRY
LOUVER CONTROL HEATER
BATTERY EXTERNAL CHARGE INPUT (GROUND TEST ONLY)
BATTERY POSITIVE TEST POINT (GROUND TEST ONLY)
TOTAL BATTERY VOLTAGE TLM SENSE (TO BCA)
V/T TEMPERATURE PRIMARY CONTROL CIRCUIT
PACK B TEMPERATURE TELEMETRY (GND TEST)
V/T TEMPERATURE BACKUP CONTROL CIRCUIT
PACK B TEMPERATURE TELEMETRY
PACK A VOLTAGE TLM SENSE (TO BCA)
PACK A
(8 CELLS)
STRIP HEATER
THERMAL CONTROL ELECTRONICS
+28V POWER
CONTROL SIGNAL
TCE TELEMETRY
LOUVER CONTROL HEATER
V/T TEMPERATURE BACKUP CONTROL CIRCUIT
PACK A TEMPERATURE TELEMETRY
PACK A TEMPERATURE TELEMETRY (GND TEST)
V/T TEMPERATURE PRIMARY CONTROL CIRCUIT
BATTERY NEGATIVE TEST POINT (GROUND TEST ONLY)
BATTERY VOLTAGE SENSE RETURN (TO BCA)
BATTERY POWER RETURN

Figure-7

BATTERY PACK QUALIFICATION TEST FLOW

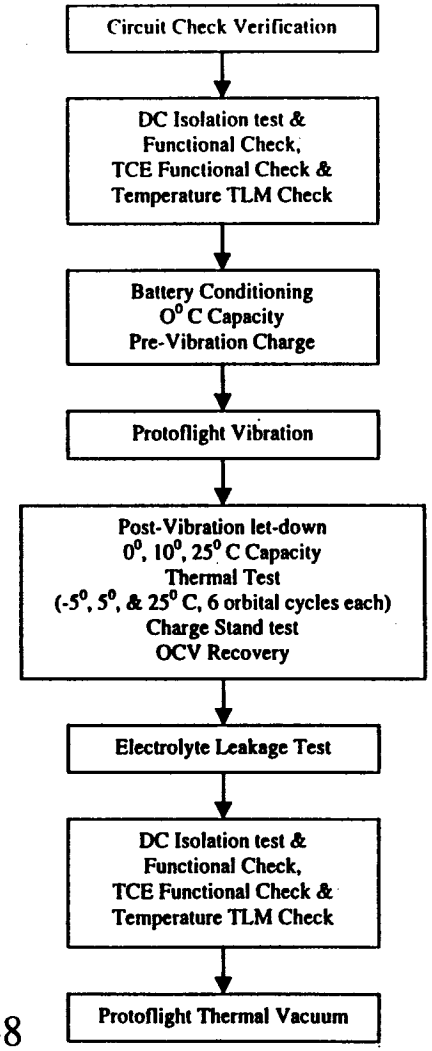

Figure-8

BATTERY PACK ACCEPTANCE TEST FLOW

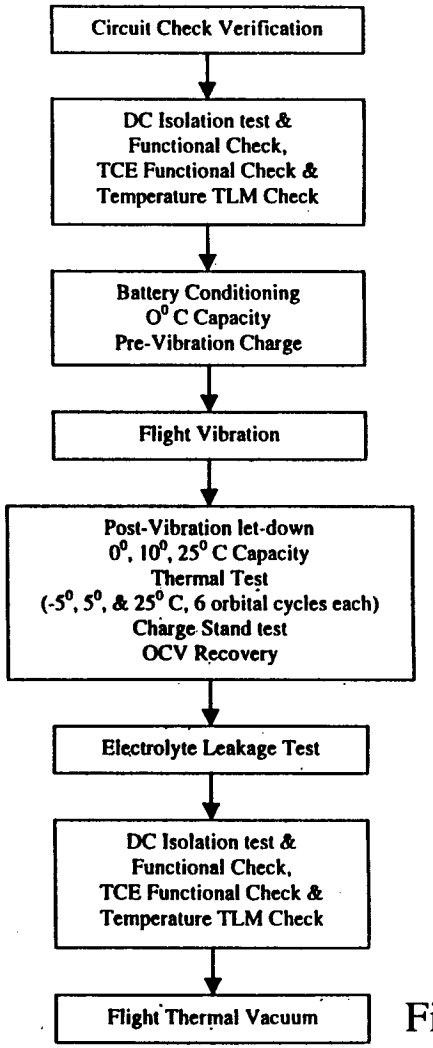

Figure-9

"Design and Flight Performance of NOAA-K Spacecraft Batteries" by Gopalakrishna M. Rao et al.

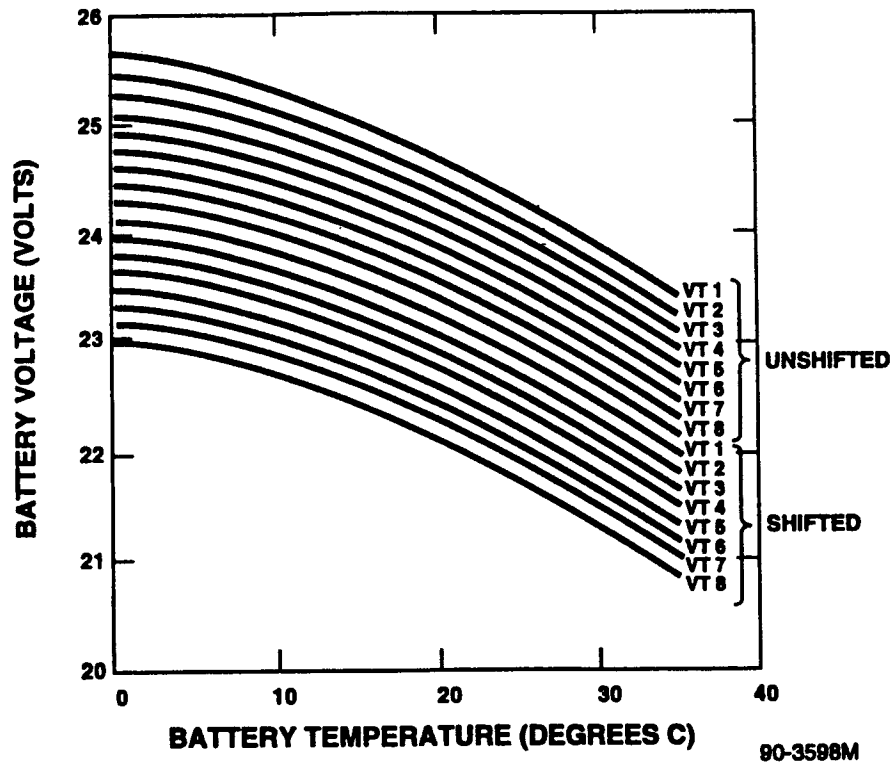

(a)

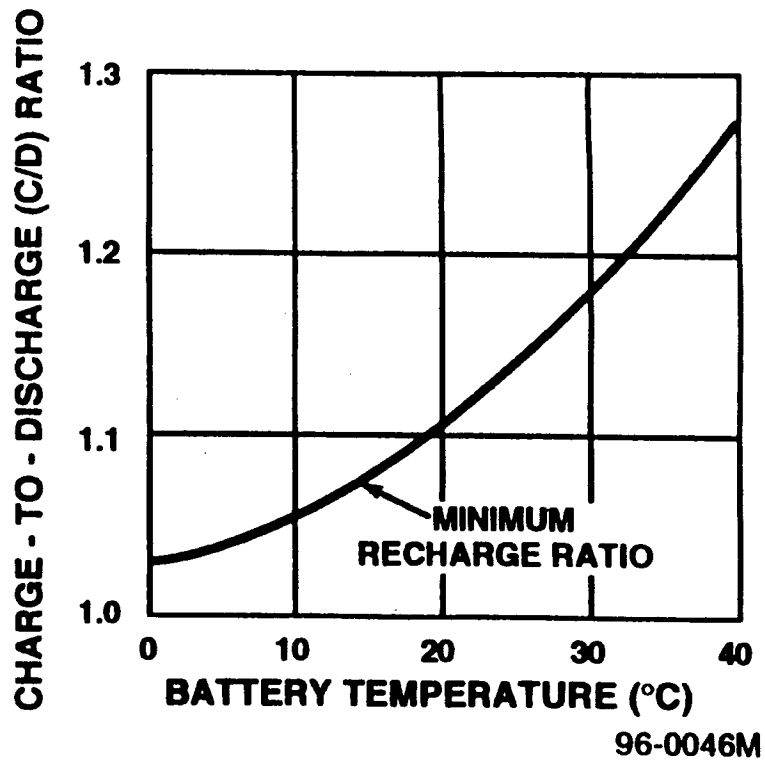

(b)

Figure-10

"Design and Flight Performance of NOAA-K Spacecraft Batteries" by Gopalakrishna M. Rao et al.

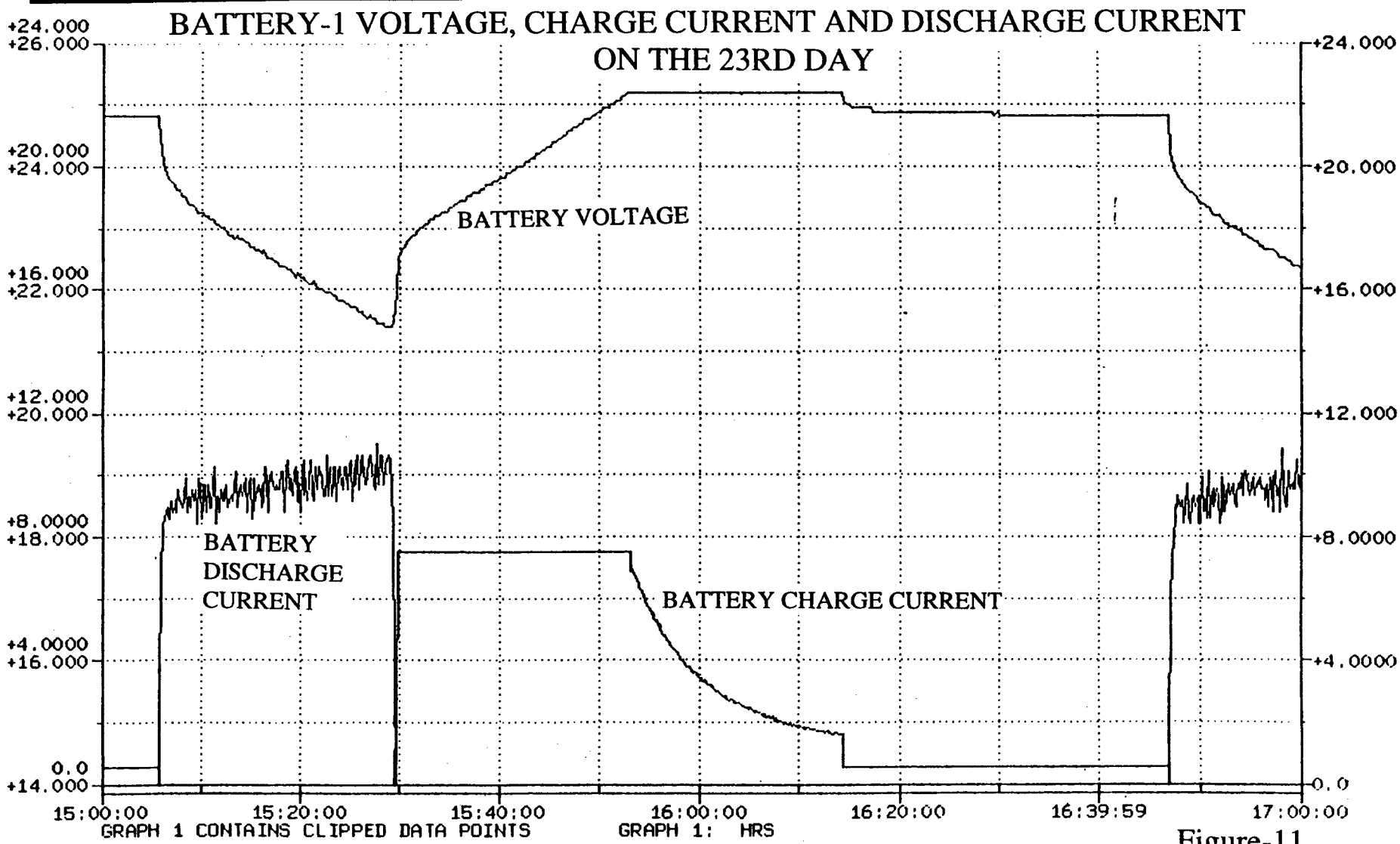

Figure-11

"Design and Flight Performance of NOAA-K Spacecraft Batteries" by Gopalakrishna M. Rao et al.

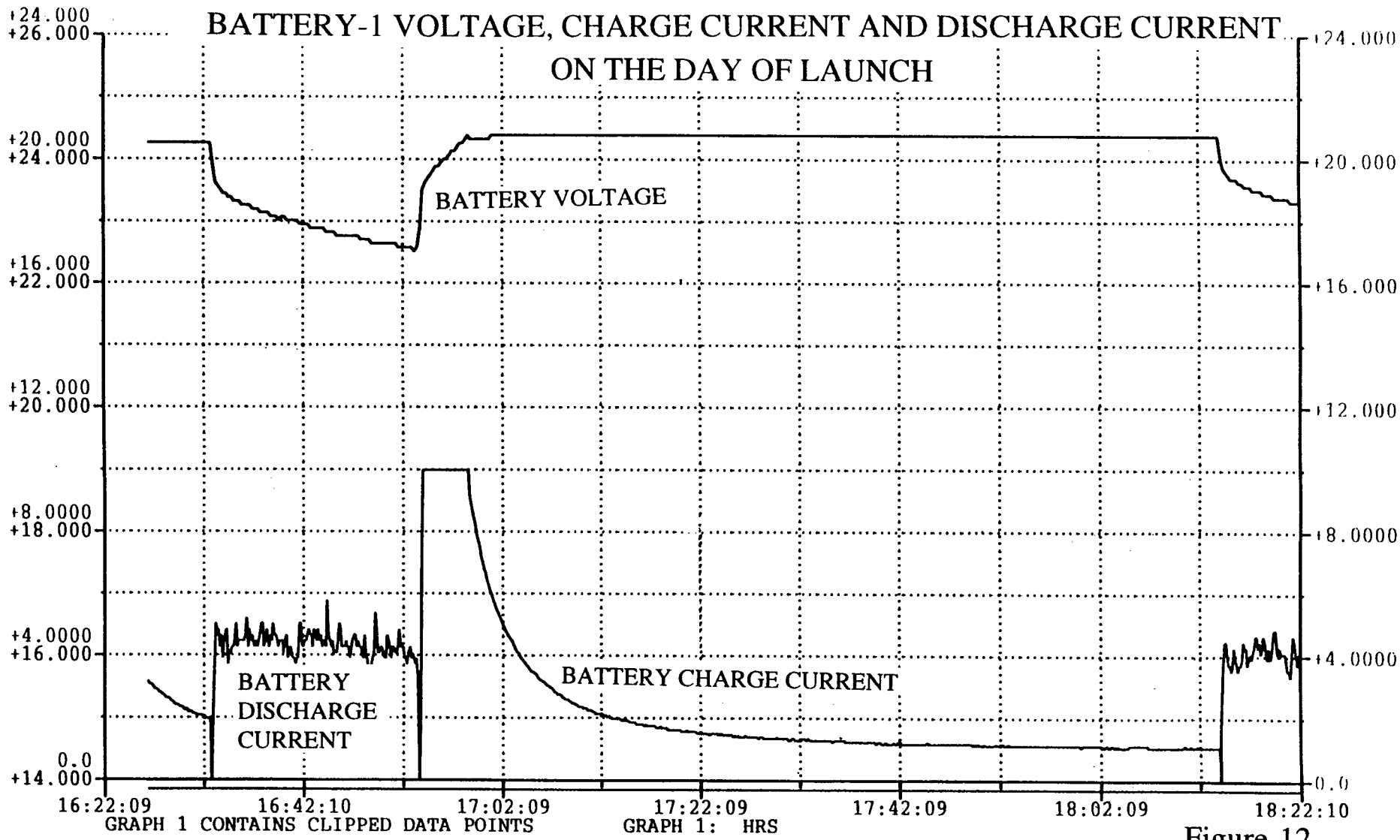

Figure-12

"Design and Flight Performance of NOAA-K Spacecraft Batteries" by Gopalakrishna M. Rao et al.

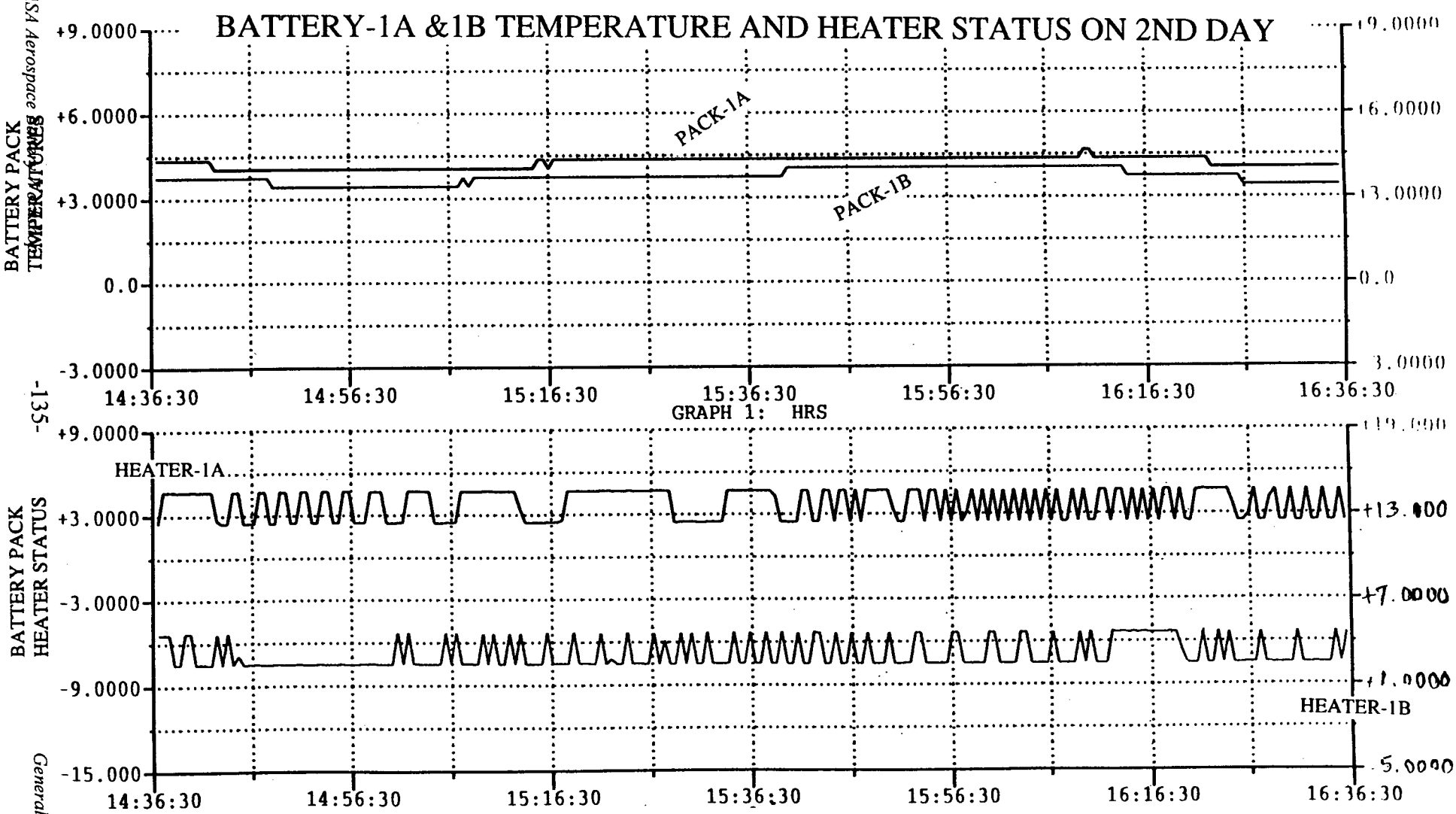

"Design and Flight Performance of NOAA-K Spacecraft Batteries" by Gopalakrishna M. Rao et al.

Figure-13

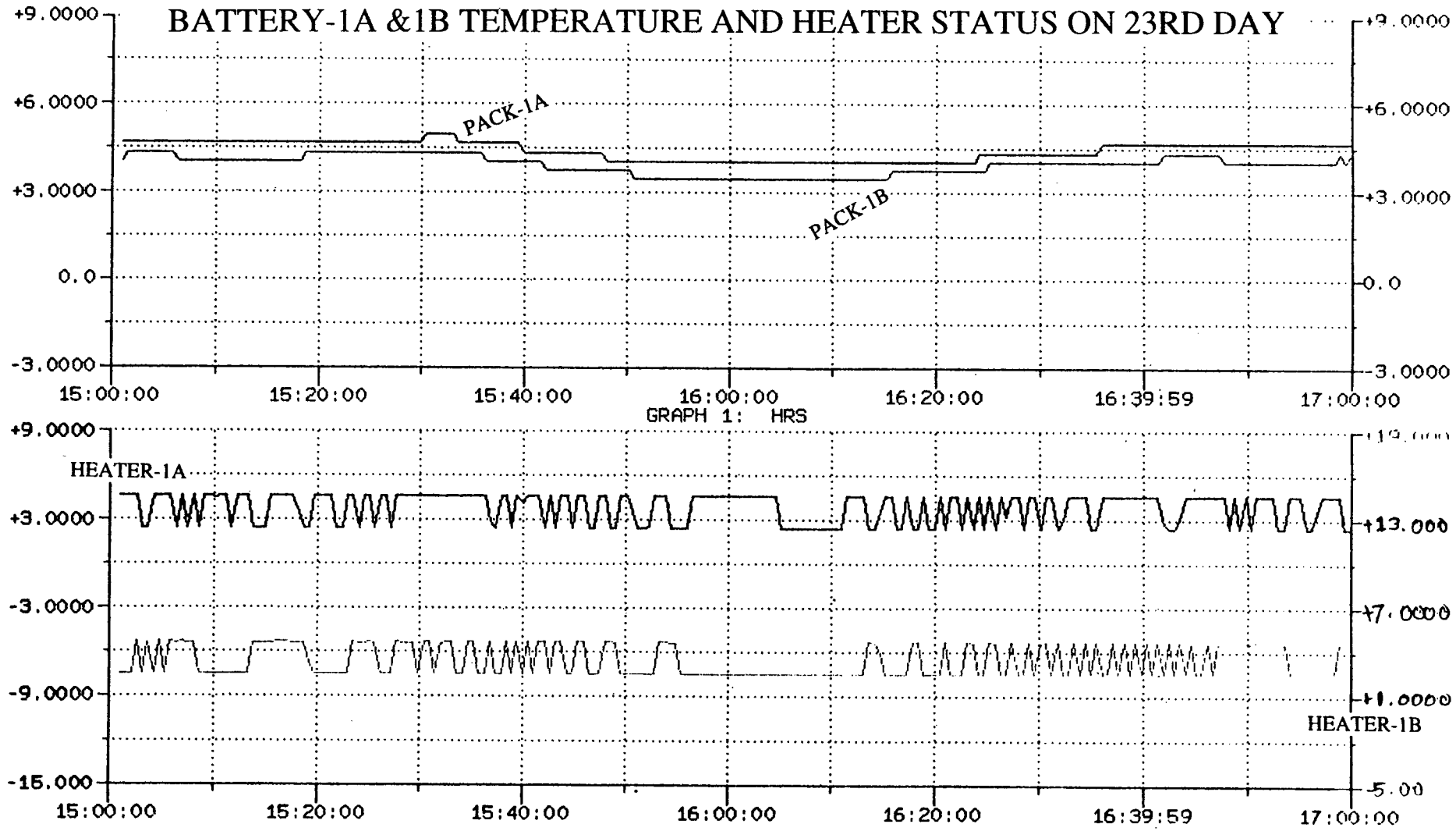

Figure-14

"Design and Flight Performance of NOAA-K Spacecraft Batteries" by Gopalakrishna M. Rao et al.

BATTERY-1A &1B TEMPERATURE AND HEATER STATUS ON 124TH DAY

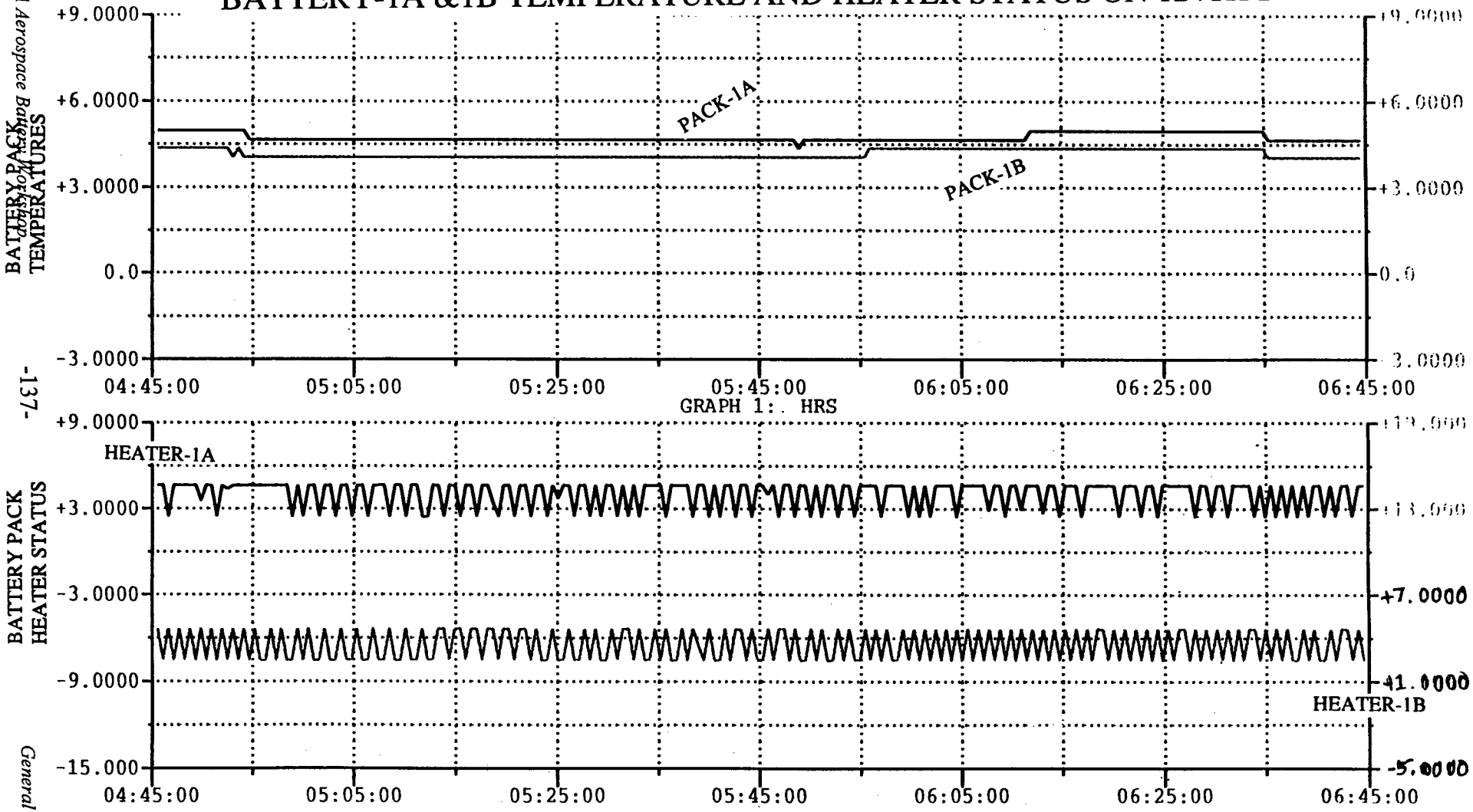

"Design and Flight Performance of NOAA-K Spacecraft Batteries" by Gopalakrishna M. Rao et al.

Figure-15

TEMPERATURES OF BATTERY PACKS-2B & 3A SINCE LAUNCH

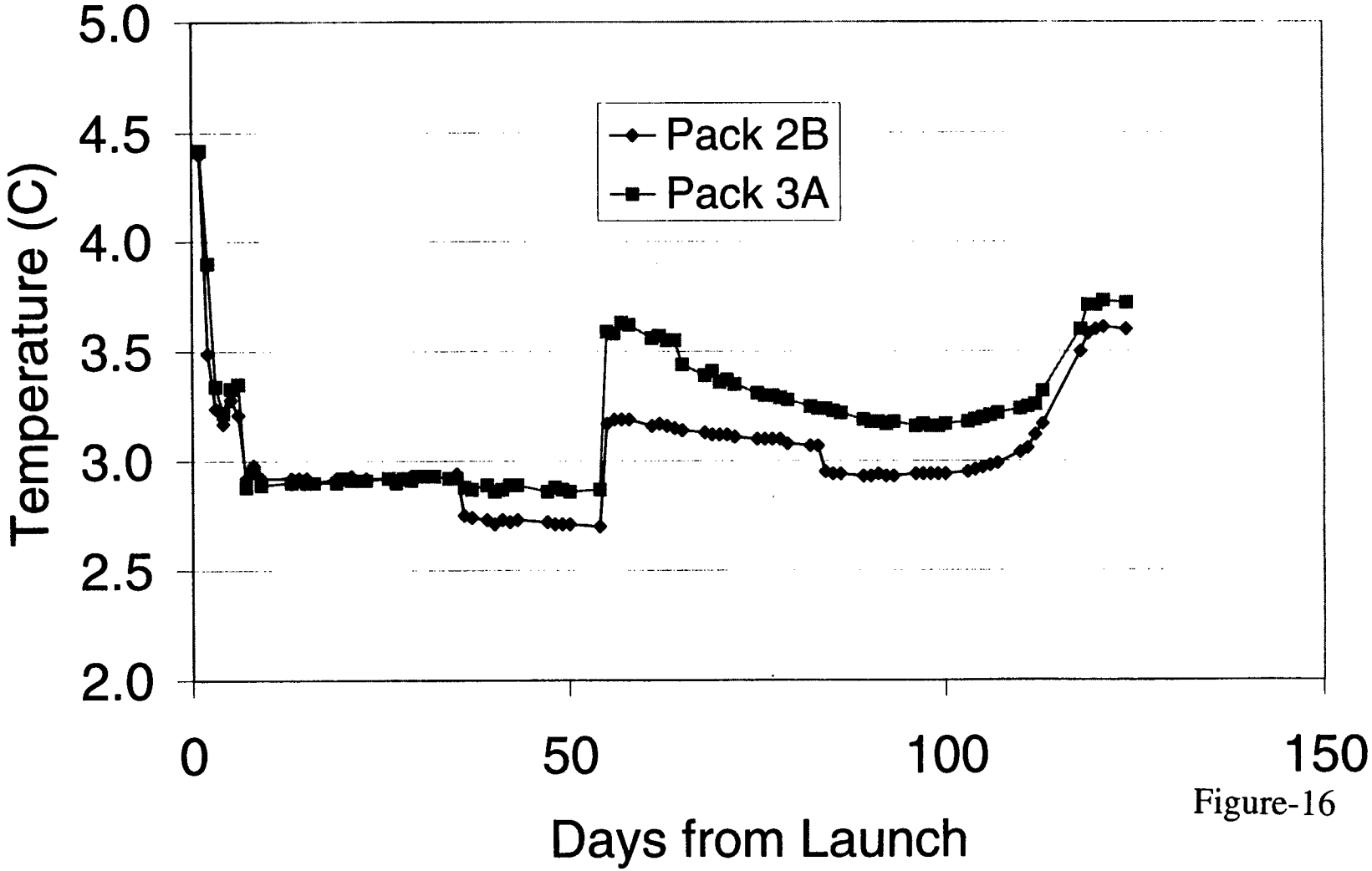

Figure-16

"Design and Flight Performance of NOAA-K Spacecraft Batteries" by Gopalakrishna M. Rao et al.

Lithium-Ion / Nickel-Metal Hydride Session

Lithium-Ion Batteries for Aerospace Applications

S. Surampudi & G. Halpert
Jet Propulsion Laboratory
Pasadena, CA

R. A . Marsh & R. James
U.S. Air Force Research Laboratory
Dayon, OH/Albuquerque NM

NASA BATTERY WORKSHOP

HUNTSVILLE, AL

October 27-29, 1998

OVERVIEW

- Program Goals
- NASA Mission Requirements
- AF Mission Requirements
- Potential Near Term Missions
- Management Approach
- Technical Approach
- Program Road Map

PROGRAM OBJECTIVES

- DEVELOP HIGH SPECIFIC ENERGY AND LONG LIFE LITHIUM ION CELLS AND SMART BATTERIES FOR AEROSPACE AND DOD APPLICATIONS.
- ESTABLISH U.S. PRODUCTION SOURCES
- DEMONSTRATE TECHNOLOGY READINESS FOR
  - ROVERS AND LANDERS BY JANUARY 1999
  - LIBRATION POINT MISSIONS BY 2000
  - GEO MISSIONS BY 2001
  - AIRCRAFT BY 2001
  - UAV BY 2003
  - LEO MISSIONS BY 2003

POTENTIAL NASA APPLICATIONS

Planetary Orbiters

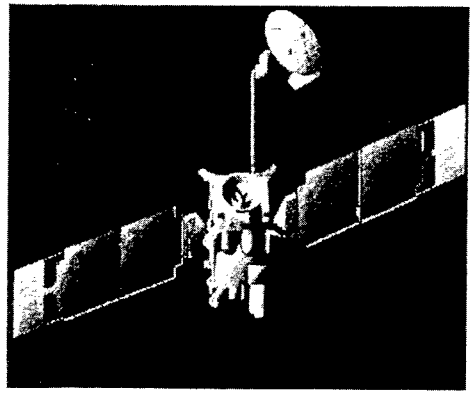

Planetary Lander

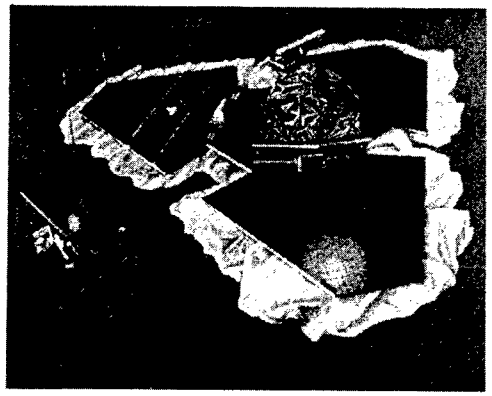

GEO Spacecraft

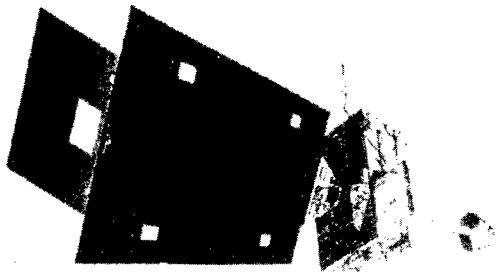

Planetary Rover

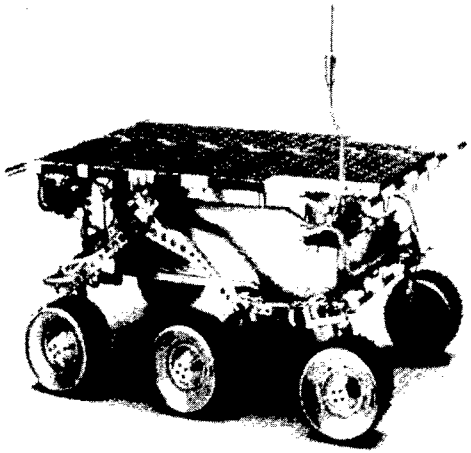

Astronaut Equipment

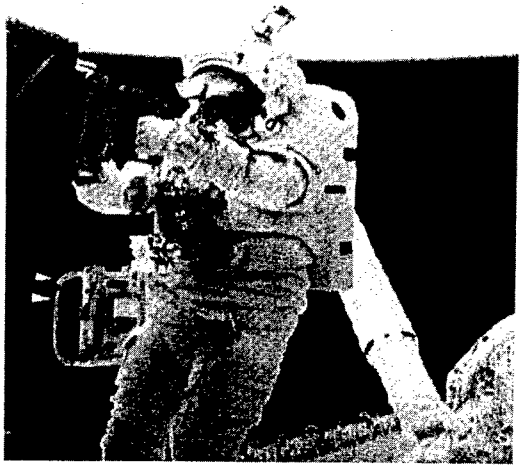

LEO Spacecraft

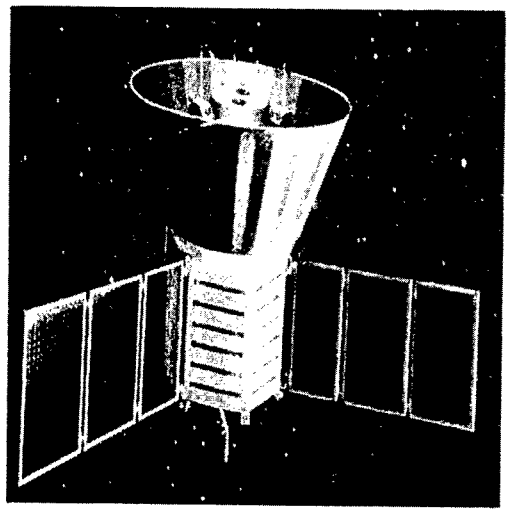

PERFORMANCE REQUIREMENTS

Type	Nominal Voltage (V)	Capacity (Ah)	Temp. Range (°C)	Cycle Life	Dis. Rate Ch. Rate	DOD (%)
Rovers	14	5/7	-30 to +40	>500	C/5-1C C/5-C/3	50
Landers	28	20/25	-20 to +40	>500	C/5 C/2	50
MIDX	28	20	25-30	>100	C/2	50%
GEO	28	20/35	-5 to +30	2000	C/1.6-C/2 C/10-C/20	75
LEO/ ORBITTERS	28	20/35	-5 to +30	30,000	C/2 C/2	>25

POTENTIAL AIR FORCE APPLICATIONS

GEO SPACRAFT

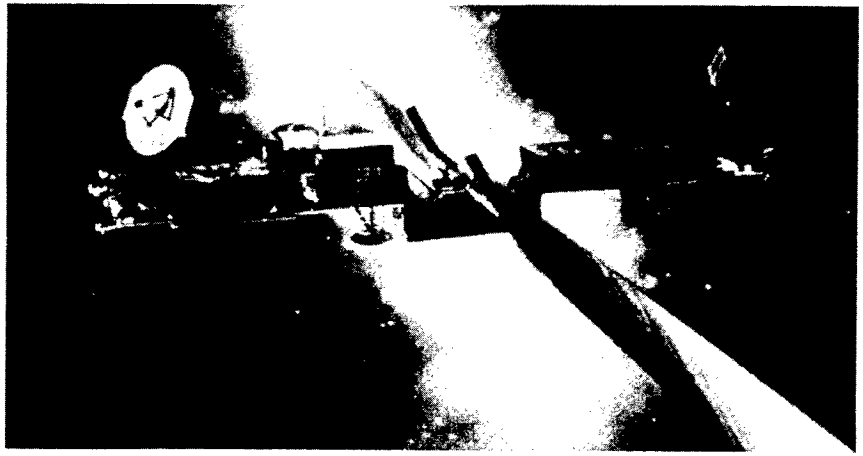

LEO SPACECRAFT

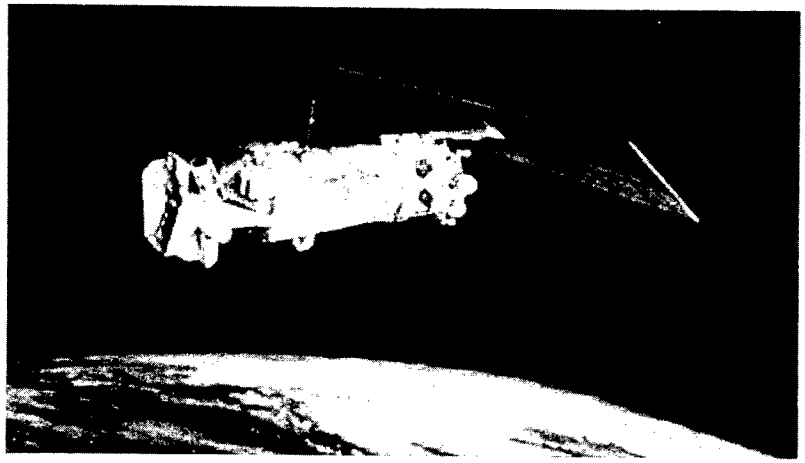

AIR CRAFT

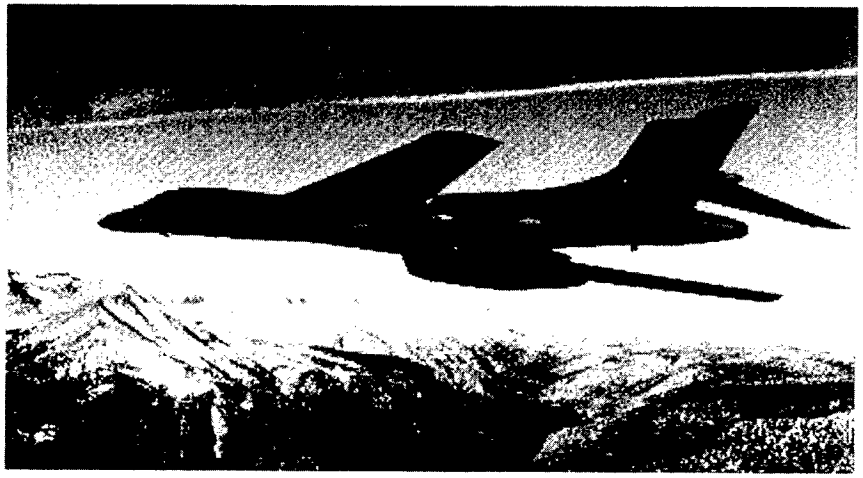

UAV'S

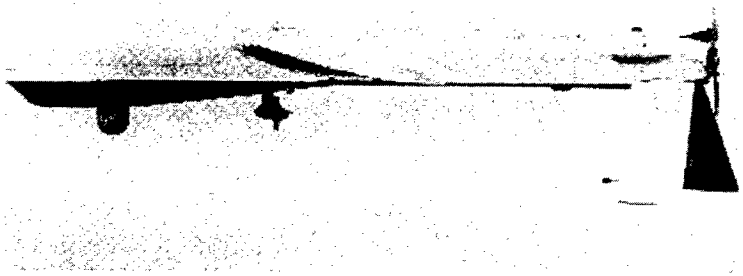

DOD Lithium-Ion Battery Performance Requirements

Type	Operating Voltage	Capacity (Ahr)	Temp. (°C)	Cycle Life	Discharge Rate Charge Rate	% DOD
UAVs	100	200	-40 to +65	1000	C C	50
Aircraft (a)	270	20	-40 to +65	1000	C C	50
Aircraft (b)	270	20	-40 to +65	1000	C C	50
GEO Sats	100	50	-5 to +30	1500	2/3 C C/20	75 (max)
LEO Sats	28	50	-5 to +30	45000	C C/2	25

TECHNOLOGY DRIVERS FOR FOR VARIOUS MISSIONS

MISSION	TECHNOLOGY DRIVER
LANDER/ROVER	LOW TEMP. OPERATION HIGH RATE PULSE CAPABILITY
GEO S/C	TEN-TWENTY YEAR OPERT. LIFE LARGE CAPACITY CELLS (50-200 Ah)
LEO/PLANTERARY S/C	LONG CYCLE LIFE (30,000) MED. CAPACITY CELLS (50 Ah)
AIRCRAFT	LOW TEMP OPERATION HIGH VOLTAGE BATTERIES (270 V)
UAV	LARGE CAPACITY CELLS (200 Ah) HIGH VOLTAGE BATTERIES (100V)

OTHER CHALLENGES: RELIABILITY, SAFETY & COST

POTENTIAL NEAR TERM SPACE MISSIONS/APPLICATIONS

•NASA MISSIONS

•JPL

MARS LANDER AND ROVER -2001

MARS LANDER AND ROVER -2003

MARS SAMPLE RETURN MISSION - 2005

CHAMPOLILON MISSION - 2003

SOLAR PROBE - 2005

•GSFC

SATELITE SERVICING TOOLS

LIBRATION POINT SPACECRAFT (MAP-2000,NGST 2007)

GEO SPACECRAFT(GOES)

LEO SPACECRAFT(EOS)

•AIR FORCE MISSIONS

•GEO

Milsatcom - 2002?

DSP - ?

LEO

SBIRS Low - 2004

NPOESS - 2007

Surveill. Platforms

•AIRCRAFT

AVIATION - 2001

UAVs - 2001

MANAGEMENT APPROACH

PARTICIPATING ORGANIZATIONS/AGENCIES INCLUDE: NASA, AIRFORCE, BMDO, JIST.

DEVELOP TWO SOURCES FOR MANUFACTURING CELLS AND BATTERIES

BUILD ON EXISTING COMMERCIAL TECHNOLOGY AND GOVT TECHNOLOGY DEVELOPMENT EFFORTS/PROGRAMS

TEAMING OF UNIVERSITIES, R&D ORGANIZATIONS AND BATTERY MANUFACTURING COMPANIES IS ENCOURAGED

NASA, AIRFORCE, NAVY LABS AND AEROSPACE PRIMES PARTICIPATE IN TECHNOLOGY EVALUATION FOR VARIOUS MISSIONS

TECHNOLOGY APPROACH

DEVELOPADVANCED ELECTRODE MATERIALS AND ELECTROLYTES TO ACHIEVE IMPROVED LOW TEMPERATURE PERFORMANCE AND LONG CYCLE LIFE

OPTIMIZE CELL DESIGN TO IMPROVE SPECIFIC ENERGY, CYCLE LIFE AND SAFETY

ESTABLISH MANUFACTURING PROCESSES TO ENSURE PREDICTABLE PERFORMANCE

DEVELOP AEROSPACE LITHIUM ION CELLS IN 5, 10, 20, 50, AND 200 AH SIZES

DEVELOP BATTERIES IN 28, 100 AND 270 V CONFIGURATIONS

DEVELOP ELECTRONICS FOR SMART BATTERY MANAGEMENT

DEVELOP A PERFORMANCE DATABASE REQUIRED FOR VARIOUS APPLICATIONS

DEMONSTRATE TECHNOLOGY READINESS FOR VARIOUS NASA AND AIR FORCE MISSIONS

FOR OFFICIAL USE ONLY
LI-ION BATTERY DEVELOPMENT PROGRAM
REQUIREMENTS AND DELIVERABLES

		Design 1		Design 2		Design 3		Design 4	Design 5			
Parameter	Supplier B/L	NASA Rovers	NASA Landers	Aircraft (A)	Aircraft (B)	AF GEO	NASA GEO	AF UAVs	AF LEO	NASA LEO/Pl. Orbiter	Cum Total	Cum Cells
Nominal SystemVoltage	3.5	14	28	270	28	100	28	100	28	28		
EOL Capacity (Ah)	5*	7	20	20	20	50	20	200	50	20		
Temp Range (°C)		-30 to +45	-20 to +45	-40 to +65	-40 to +65	-5 to +30	-5 to +30	-40 to + 65	-5 to +30	-5 to +30		
Life (Cycles)		>500	>500	1,000	1,000	1,500	1,000	1,000	30,000	30,000		
Discharge Rate		C/5 to 1C	C/5 to 1C	C	C	2C/3	2C/3	C	C	C		
Charge Rate		C/5 to C/2	C/5 to C/2	C	C	C/20	C/20	C	C/2	C/2		
DOD (%)		50	50	50	50	75 (max)	75 (max)	50	25	25		
PDR		Feb 99	Oct 98	May 00	May 00	Oct 00	Oct 00	May 00	Oct 00	Oct 00		
1st Generation Cell Del'y (Contract)	Nov 98	May 99	Nov 98	Aug 00	Aug 00	Jan 01	Jan 01	Aug 00	Jan 01	Jan 01		
No. of Cells	30	25	25	20	20	35	25	12	35	40	267	267
CDR		Jun 99	Mar 99	May 01	May 01	Oct 01	Oct 01	May 01	Jun 02	Jun 02		
2nd Generation Cell Del'y (Contract)		Sep 99	Feb 99	Aug 01	Aug 01	Jan 02	Jan 02	Sep 01	Sep 02	Aug 02		
No. of Cells		25	25	20	20	35	25	12	35	40	237	504
"Battery System" Delivery (Contract)		Jul 00	May 99	Apr 02	Apr 02	Jun 02	Jun 02	Jan 02	Feb 03	Feb 03		
No. of Battery Systems		9	2	1	4	2	1	1	2	2	24	
Equivalent Cells		36	16	77	32	58	8	29	16	16	288	792

* Whatever the Company baseline cell is but at least 5 Ah

TECHNOLOGY DEMONSTRATION MILESTONES

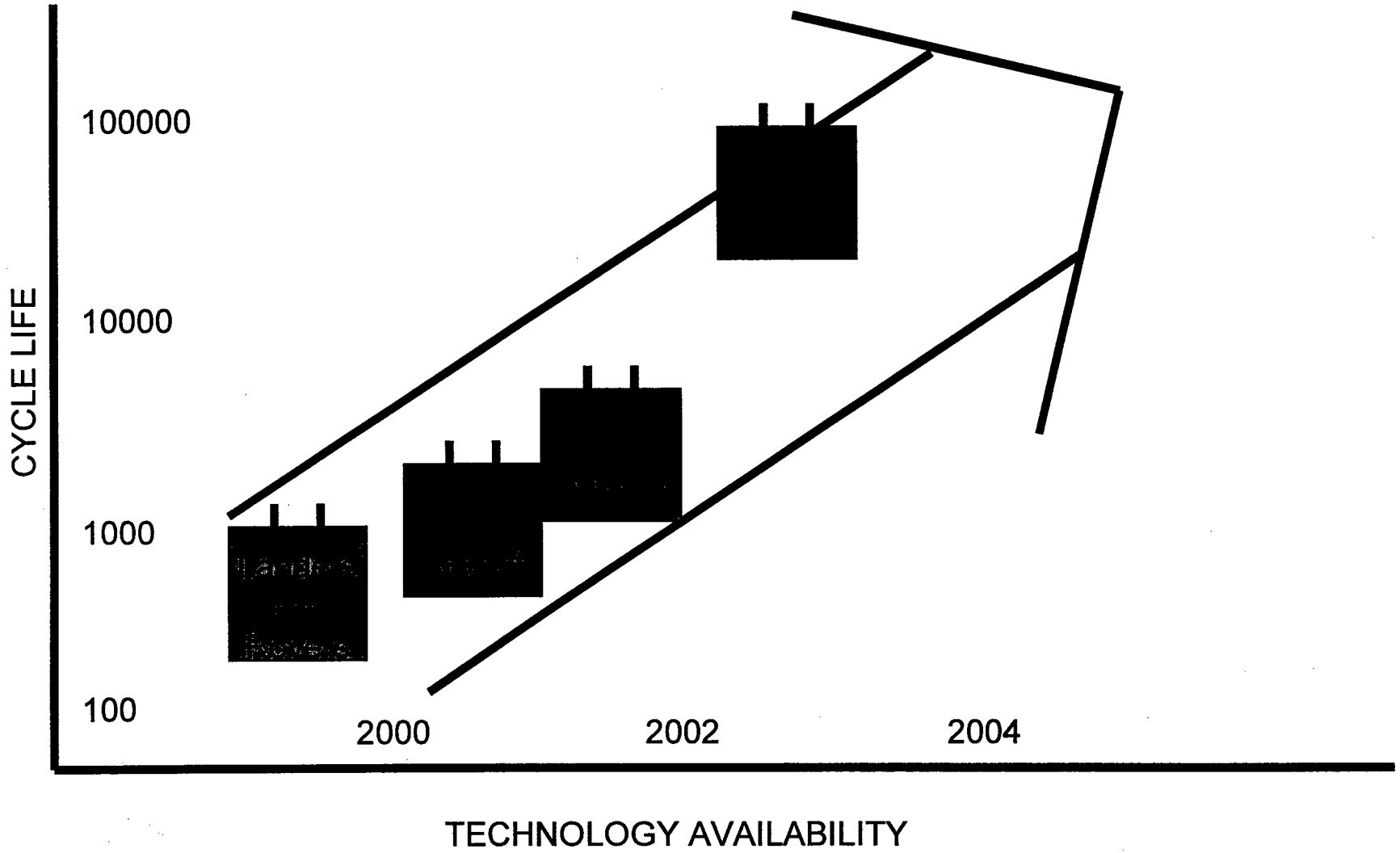

AEROSPACE LITHIUM-ION BATTERY PROGRAM ROADMAP

TASK	98 99 00 01 02 03 04	GOALS
CHEMISTRY & MATERIALS	LOW TEMP. AND STABLE E'LYTE HIGH CAP. & LONG LIFE ELECTRODES SEPARATOR, OC/OD ADDITIVES	IMPROVE - LOW TEMP. PERF. - CYCLE LIFE - OPERATIONAL LIFE
CELL DEVELOPMENT	PROCESS DEV. DESIGN, AND CELL MANUFACTURING 10-20 Ah,500 CYC, LT, HR, 200 Ah 40/50 Ah,2000 CYC, 30000 CYCLE, 20-50 Ah	EST. MANF. PROCESS OPT. CELL DESIGN FAB. 10-200 Ah CELLS
BATTERY DEVELOPMENT	PROCESS DEV. DESIGN & MANF. LANDER/ROV, UAV/AIRCRAFT GEO S/C, LEO, PLANETARY S/C	EST. MANF. PROCESS DEV. SMART BATT. FAB. LANDER, ROVER GEO, LEO S/C, UAV AIRCRAFT BATT.
TESTING & QUALIFICATION	ELECTRICAL PERF., THERMAL, AND SAFETY TESTS 100/50% DOD LEO & GEO LIFE TEST FAILURE MODES & ANALYSIS	EST. DATA BASE DET. FAILURE MODES EST. CHARGE CNTLS DEMON. SAFETY
FLIGHT VALIDATION	LAND/ROVER, S/C TOOLS, UAV/AIRCRAFT, GEO S/C, LEO S/C	DEMON. TECH. FOR LANDER, ROVER GEO, LEO S/C, UAV AIRCRAFT MISSIONS

DELIVERABLES

- FIRST GENERATION CELLS
- SECOND GENERATION CELLS
- ENGINEERING MODEL BATTERIES(EM1)
- MANUFACTURING CONTROL DOCUMENTS
- TEST RESULTS
- DESIGN REVIEW DOCUMENTS
- FLIGHT HARDWARE*

* PROCURED THROUGH SEPARATE CONTRACTS BY RESPECTIVE PROJECTS

MANAGEMENT STRUCTURE

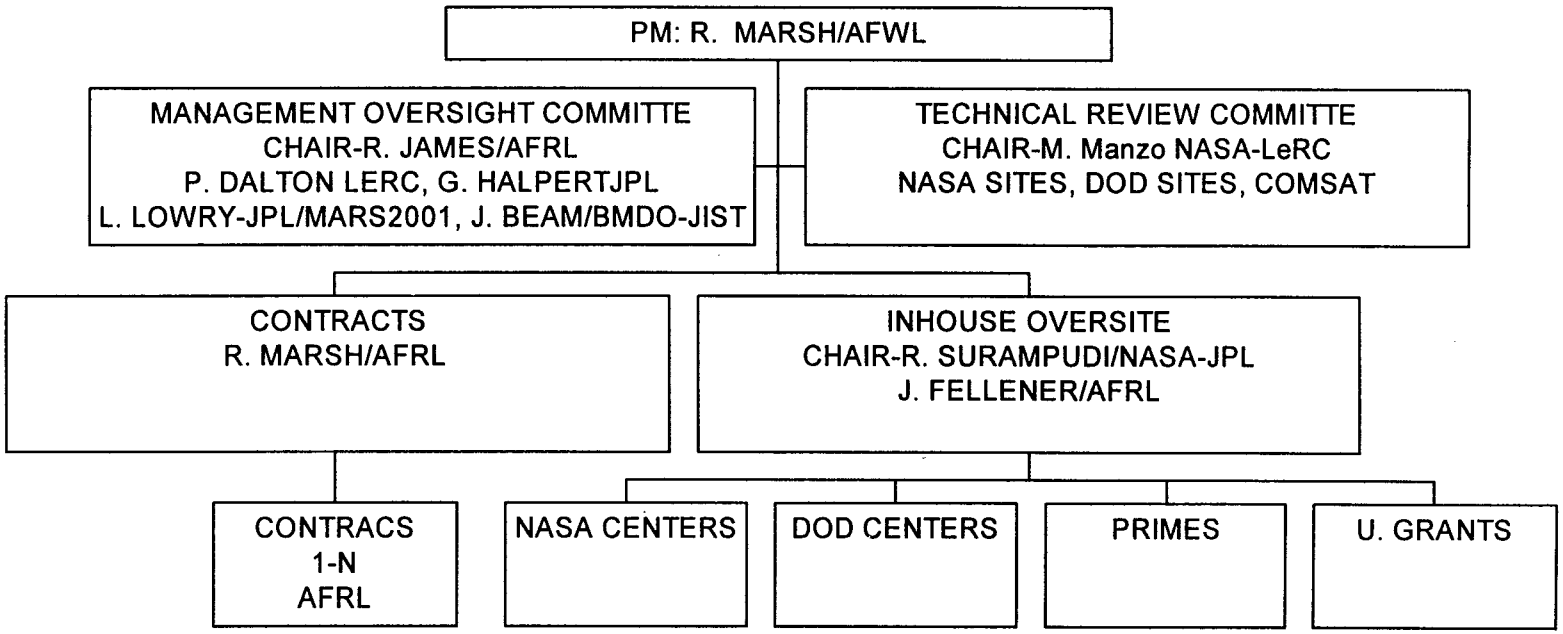

MISSION REQUIREMENTS

	LANDERS	ROVERS	GEO	LEO/ PLA. ORBITER	S/C TOOLS	LIBRATION POINT S/C
CAPACITY (AH)	20-40	5-10	10, 20, 35	10, 20, 35	3-5 AH	20-25 AH
VOLTAGE (V)	28	28	28-100	28	28	28
DIS. RATE	C/5-1C	C/5-C/2	C/2	C/2-C	C/2	C/2
CYCLE LIFE	> 500 (>60%DOD)	>500 (>60% DOD)	2000 (>75% DOD)	>30,000 (>30% DOD)	>100	50
OPER. TEMP (C)	-40 TO 40	-40 TO 40	-5 TO 30	-5 TO 30	0-50C	25-30
SP. ENERGY (Wh/KG)*	>100	>100	>100	>100	>100	100
ENERGY DENSITY (Wh/l)*	120-160	120-160	120-160	120-160	>80	120-160

* 100% DOD BOL

Acknowledgments

Some of the work described in this paper was performed by the Jet propulsion laboratory, California institute of Technology, under a contract with the National Aeronautics and Space Administration.

JPL

MODIFICATIONS TO TASK PLAN

	Revision A	Revision B	Revision C
12/98		150 W System 5 kWh, Nafion Packaged Bat. Charger	
9/99			Generation I 150W,5kWh System USC Membranes 10 kG System Packaged
4/00	150 W System 28V, Packaged 600 Wh	150 W System 5 KwH, 8Kg USC Membrane Packaged	
4/00			Deliver Gen 2 Stack
9/00			Fild Demo Unit with Ball Aerospace

NASA Aerospace Battery Workshop

NASDA
NATIONAL SPACE DEVELOPMENT AGENCY OF JAPAN

The Applicability of Lithium Ion Secondary Battery Cells to Space Programs

Electronic and Information Technology Department
Office of Research and Development
NASDA

Yoshitsugu SONE, Hiroaki KUSAWAKE,
Koichi KANNO, and Saburo KUWAJIMA

Schedule of Space Battery Development

NASDA
NATIONAL SPACE DEVELOPMENT AGENCY OF JAPAN

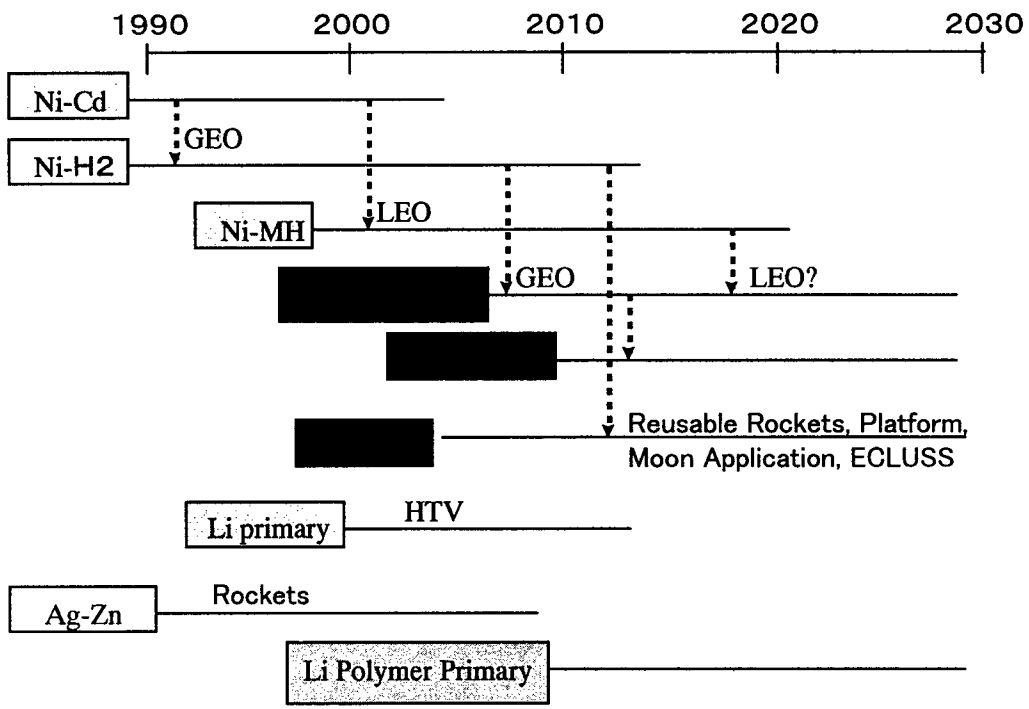

Already and on the way to be developed
Just Started
Studied for the future applications
Developed by Rocket Group

The circuits to control commercial cells

NASDA
NATIONAL SPACE DEVELOPMENT AGENCY OF JAPAN

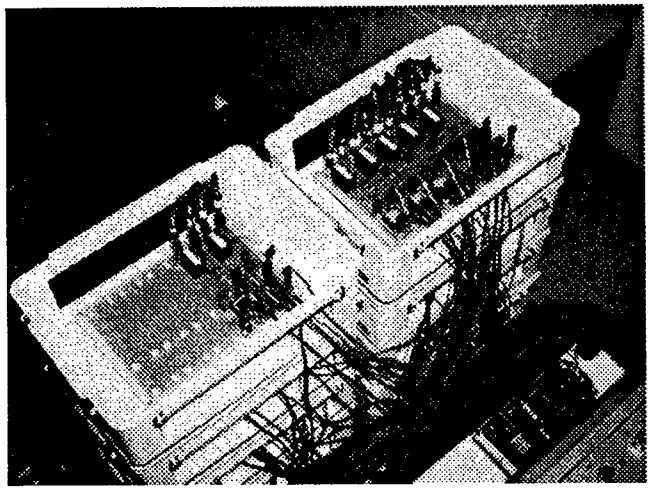

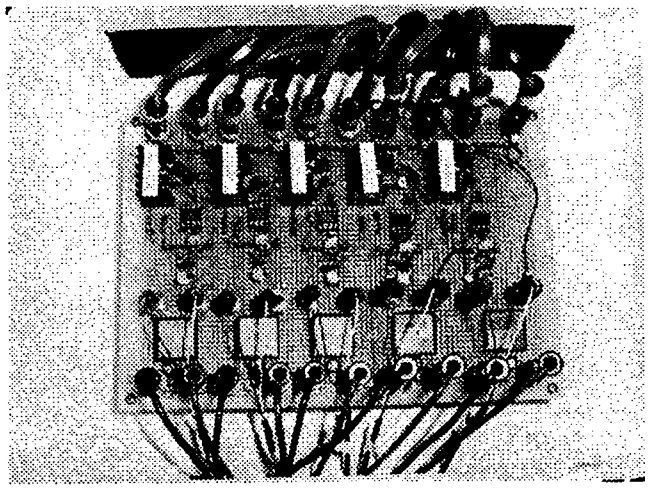

The voltage of each cell was controlled using these circuits. Each cell was charged by CC-CV method. C/D ratio was controlled less than 1.01.

Trend Data of Commercial Cells

NASDA
NATIONAL SPACE DEVELOPMENT AGENCY OF JAPAN

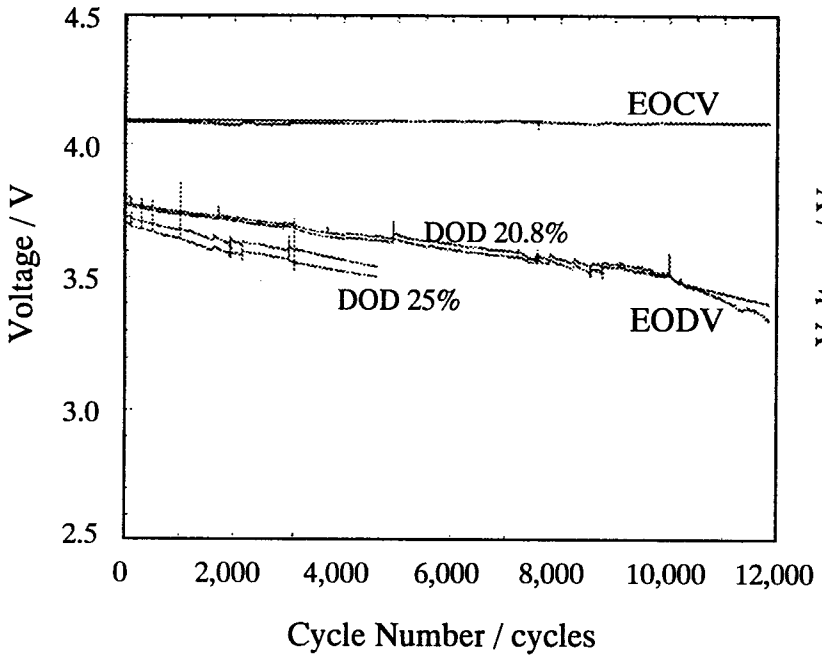

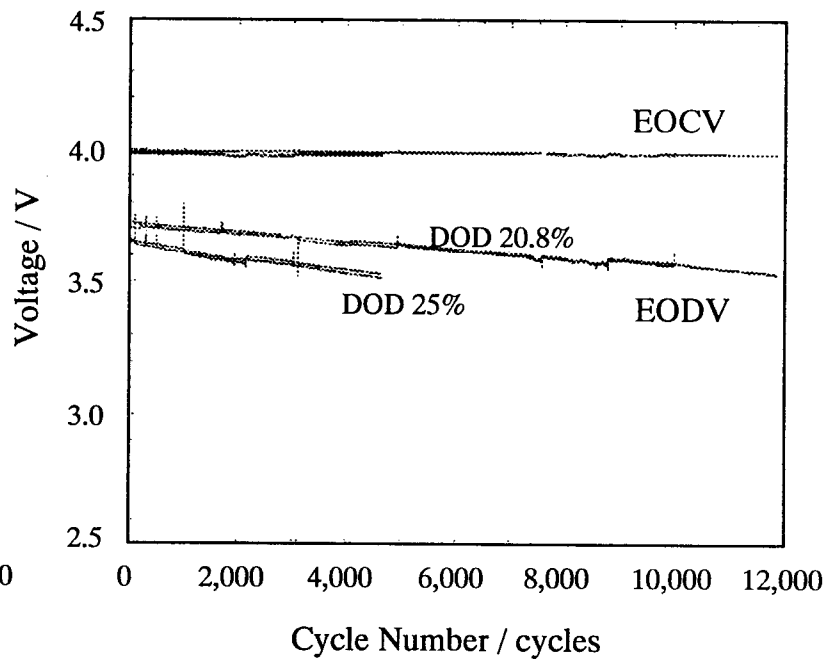

Graphite Type (company A)

The trend data of Graphite type commercial cells are shown. The difference of EODV increased with cycle numbers. It suggests that the deeper DOD may cause the faster degradation of the cell.

Trend Data of Commercial Cells

NASDA
NATIONAL SPACE DEVELOPMENT AGENCY OF JAPAN

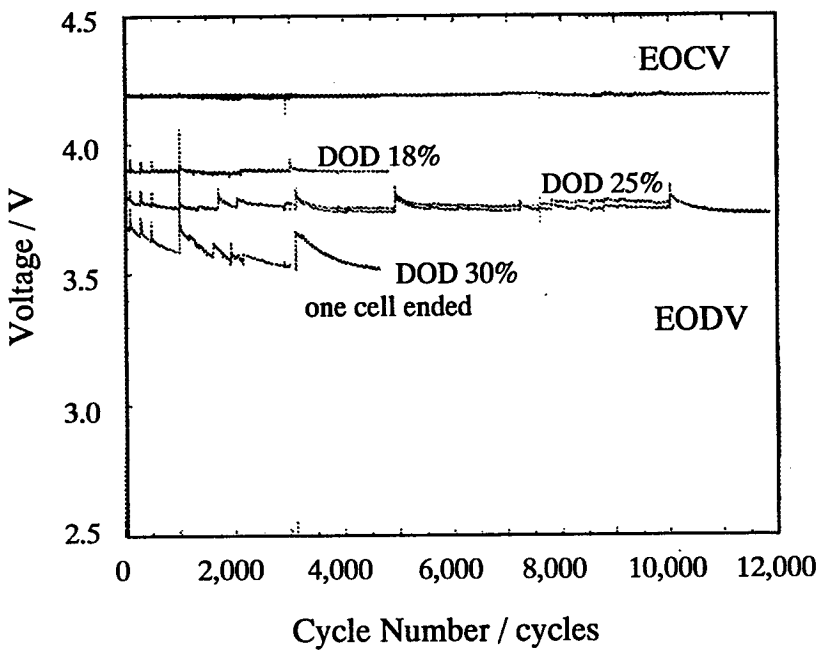

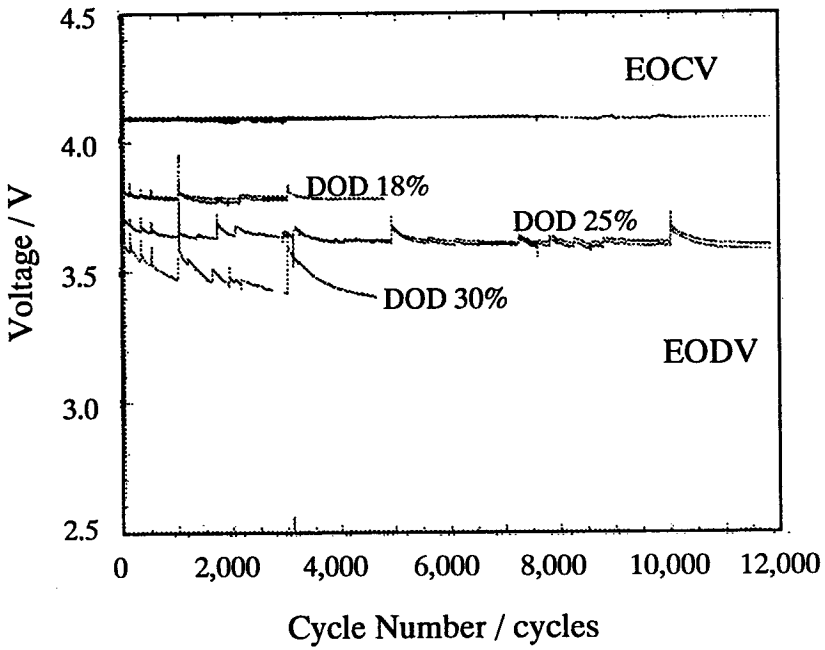

Coke Type (company B)

The trend data of Coke type commercial cells are shown. The EODV of the cells with DOD30% degraded faster than other cells.

Trend Data of Commercial Cells

NASDA
NATIONAL SPACE DEVELOPMENT AGENCY OF JAPAN

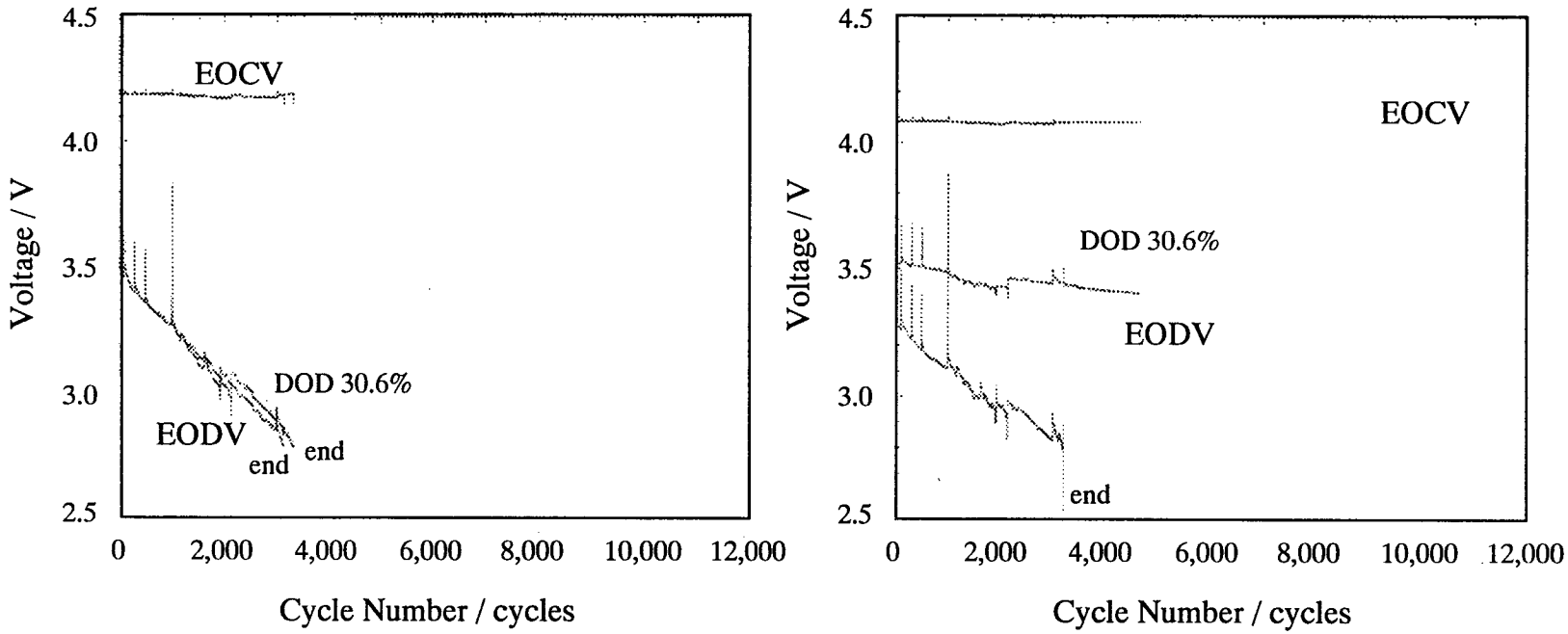

Coke Type (company C)

In the case that we operated the EOCV as to be 4.2V, we observed high degradation of cell performance. One of four cells is still operative.

Trend Data of Commercial Cells

NASDA
NATIONAL SPACE DEVELOPMENT AGENCY OF JAPAN

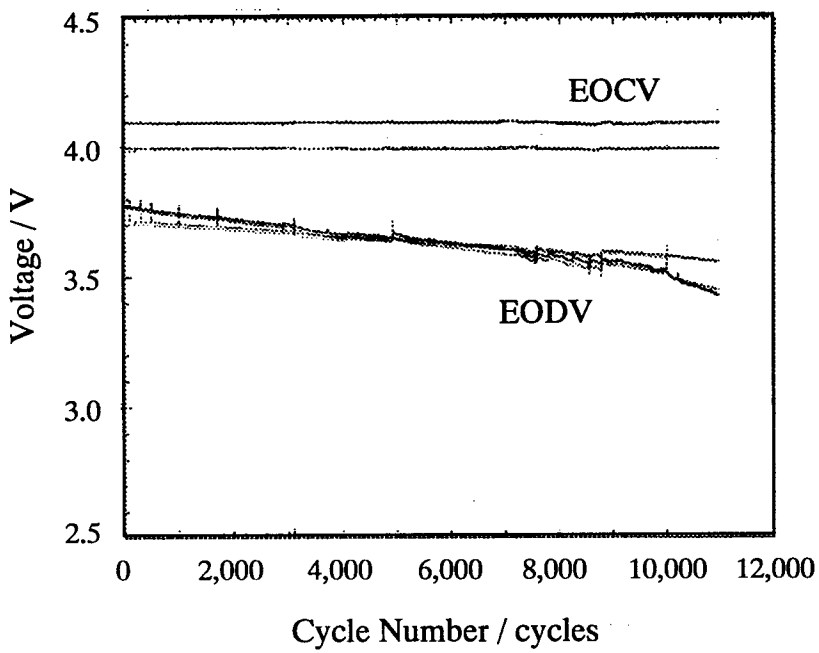

Graphite Type (company A)

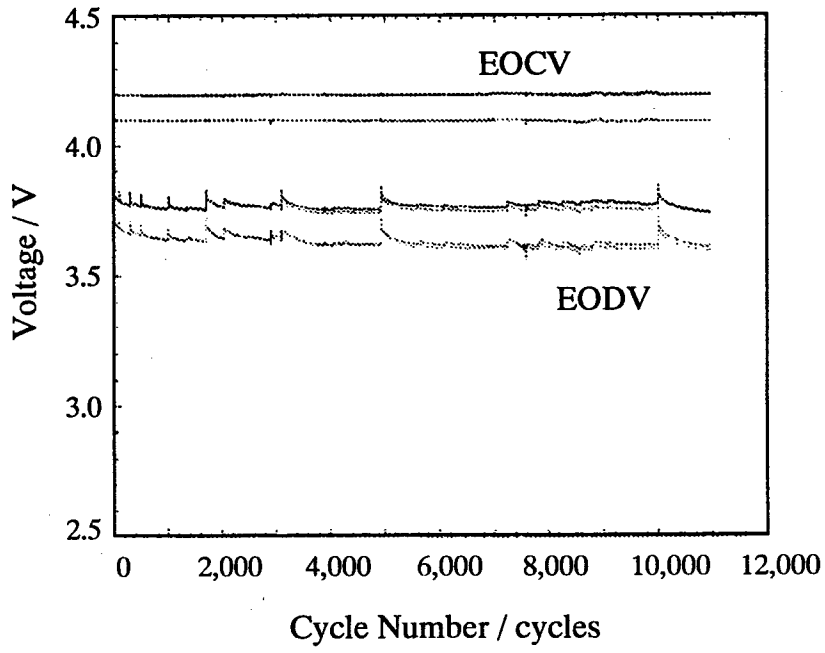

Coke Type (company B)

The degradation of cell performance depended on the EOCV specially in the case of Graphite Type Cell (company A). We didn't find any significant difference of EODV as to Coke Type Cell (company B).

H-II Orbiting Plane-Experimental(HOPE-X)

NASDA
NATIONAL SPACE DEVELOPMENT AGENCY OF JAPAN

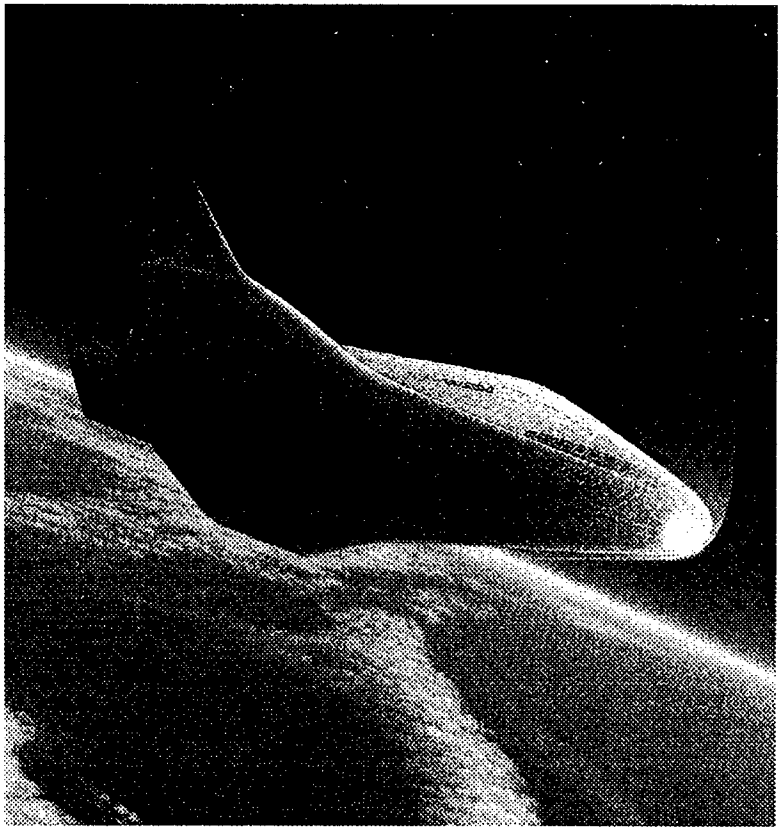

Lithium Ion Secondary Cell for HOPE-X

NASDA
NATIONAL SPACE DEVELOPMENT AGENCY OF JAPAN

Lithium Ion Secondary Cell for HOPE-X

NASDA
NATIONAL SPACE DEVELOPMENT AGENCY OF JAPAN

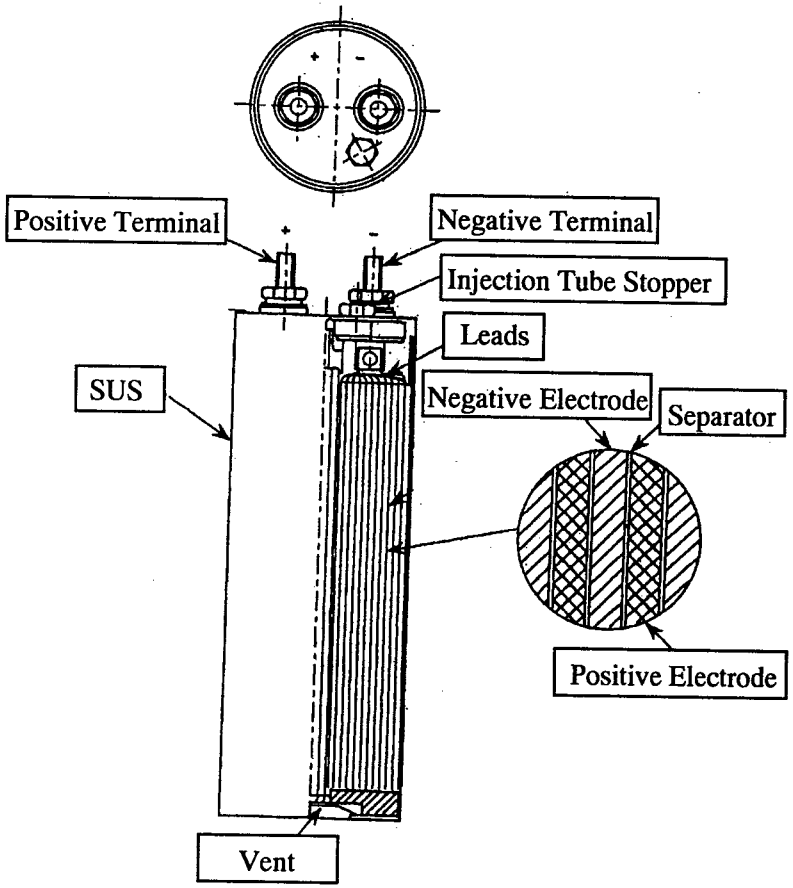

Voltage	3.6 V
Volume	830 m l
Weight	2,030 g
Energy Density (initial)	275 Wh/l, 113 Wh/kg
Approval Current	less than 1C
Applicable Temperature	-10～+60℃
Capacity	50 Ah (nominal) 64 Ah (initial)

Initial Performance of HOPE-X Cells

NASDA
NATIONAL SPACE DEVELOPMENT AGENCY OF JAPAN

We tested the effects of the charge methods on the Capacity. The candidates of the charge method is as follows.

- Constant Current / Constant Voltage (CC-CV) Charge method.

  The maximum capacity of the cell is expected to be realized. This method is comparable to V/T control for the satellite. When we test the life cycle performance of Lithium ion cells, we used this method.

- Constant Current Steps (CC-steps)Charge method.

  The HOPE-X battery is now going to be charged by this method using ground facilities. The battery for HOPE-X will be charged by the following sequence.

  (1)0.5C up to 4.1V
  (2)5 min. interval
  (3)0.2 C up to 4.1 V
  (4)5 min. interval
  (5)0.1 C up to 4.1 V

We measured the capacity using these two methods to reveal which method is approval to charge the battery.

Initial Cell Performance of HOPE-X Lithium Ion Secondary Cells

NASDA
NATIONAL SPACE DEVELOPMENT AGENCY OF JAPAN

-Simulation Test for HOPE-X Operation-

We focused our measurements to check the discharge performance of the cell to see its applicability to HOPE-X.

The points of our test were as follows,

The cells were charged by 0.5C (25 A) at 25℃,
then discharged by
(1) the constant current at 0℃, 25℃, and 60℃, respectively.
(2) the constant current with pulse duration for 30 sec. at 0℃, 25℃, and 60℃, respectively.
(3) the constant current to check the effect of the different experimental history on the discharge curve.
(4) the simulating discharge pattern of HOPE-X operation.

Temperature Dependence of Capacity

NASDA
NATIONAL SPACE DEVELOPMENT AGENCY OF JAPAN

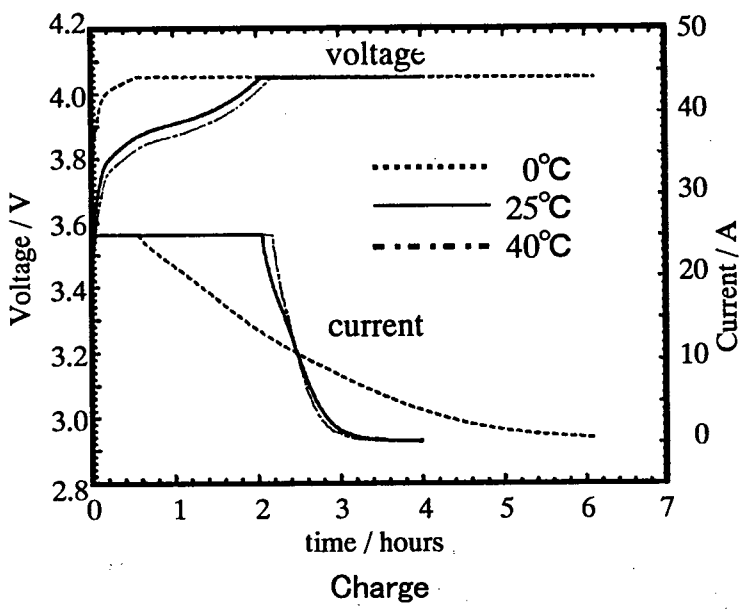

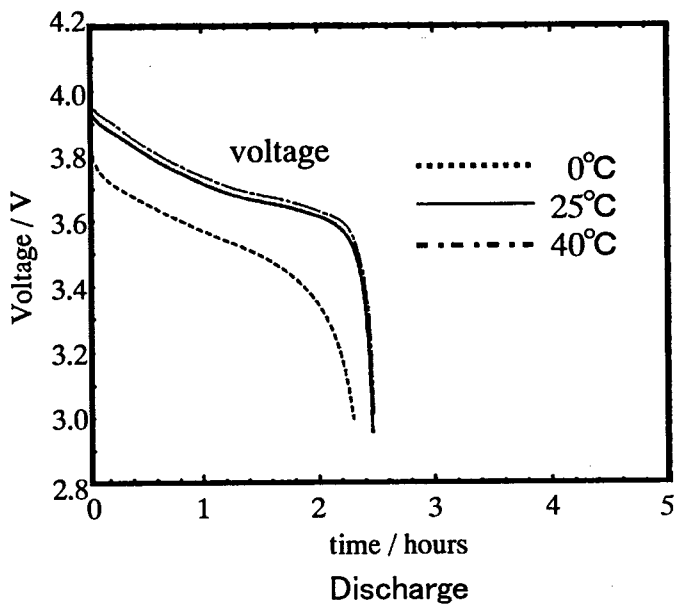

The cell was charged by CC-CV method. This cell was designed to be used between -10 and +60°C. However, the impedance of the cell increased at 0°C, which requested 6 hours to charge the cell. Above 25°C, no significant difference of cell performance was observed.

Temperature Dependence of Capacity

NASDA
NATIONAL SPACE DEVELOPMENT AGENCY OF JAPAN

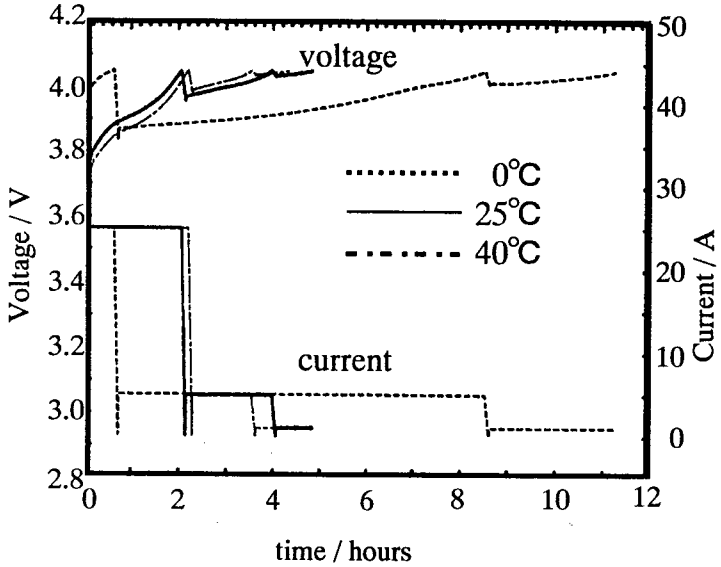

Charge

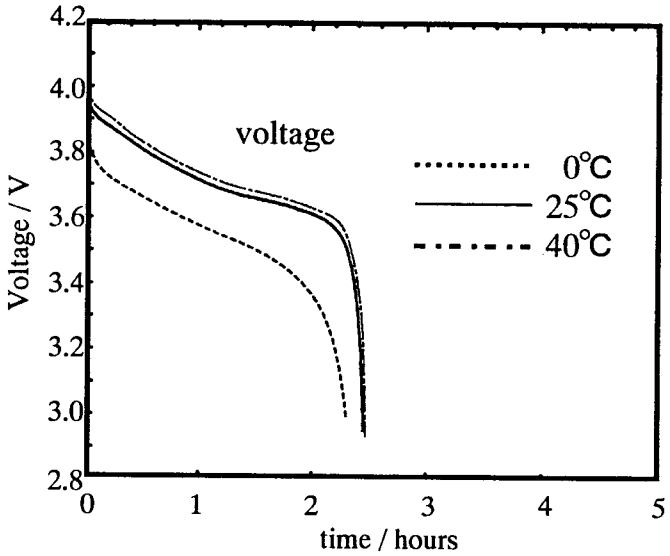

Discharge

A single cell was charged by CC steps. At 0°C, the increased impedance required the charge time for more than 11 hours.

Charge and Discharge Curve at 25℃, Three Cells in Series

NASDA
NATIONAL SPACE DEVELOPMENT AGENCY OF JAPAN

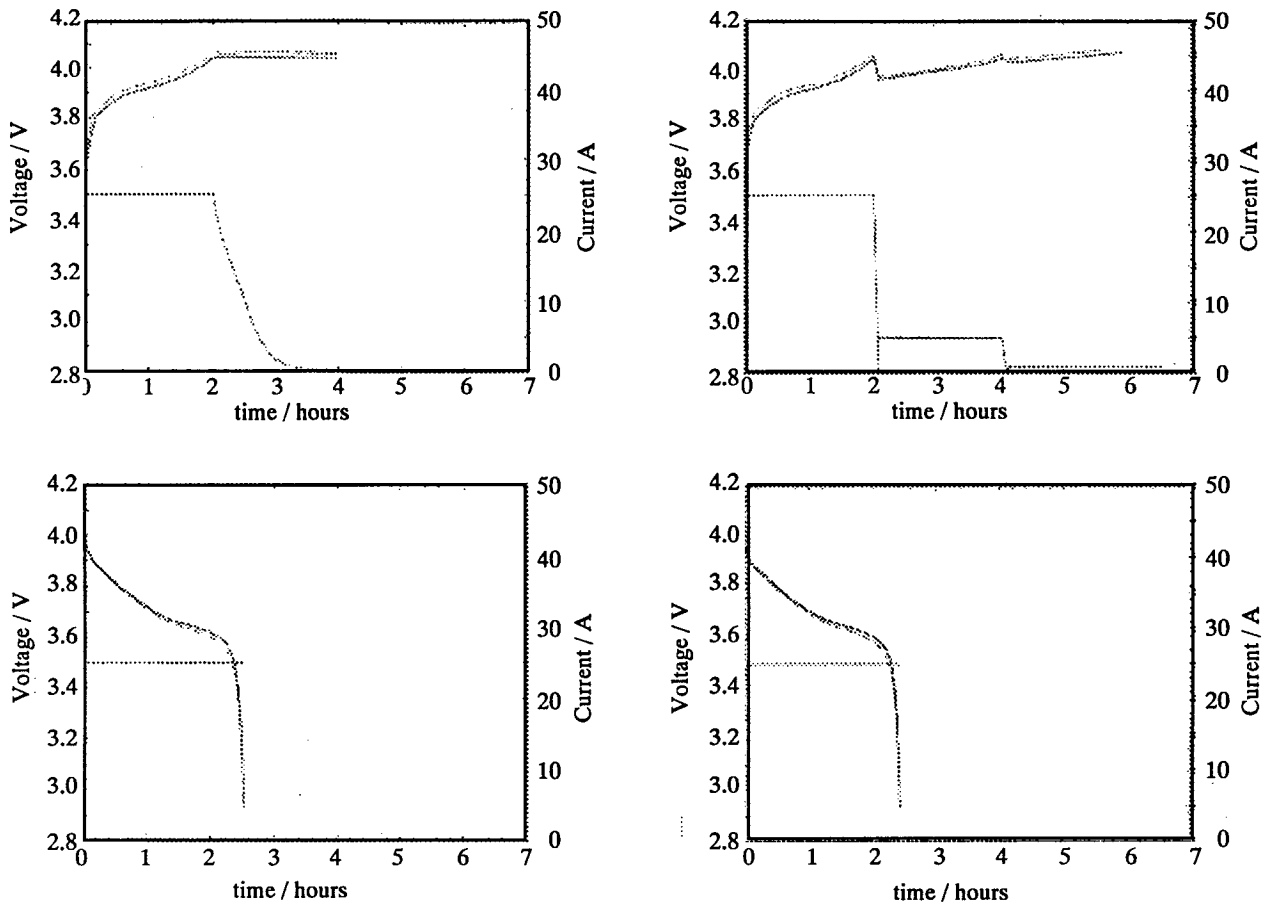

CC-CV Charge

CC multi-step Charge

Three cells were charged and discharged in series. The difference of the experimental history caused a slight difference of the performance of one of three cells, while the curves nearly coincided with each other.

Comparison between CC-CV and CC steps

NASDA
NATIONAL SPACE DEVELOPMENT AGENCY OF JAPAN

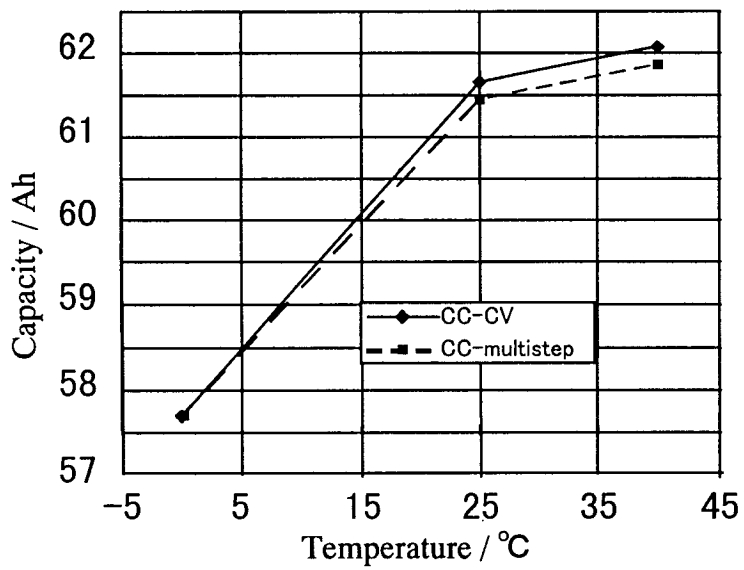

Single cell

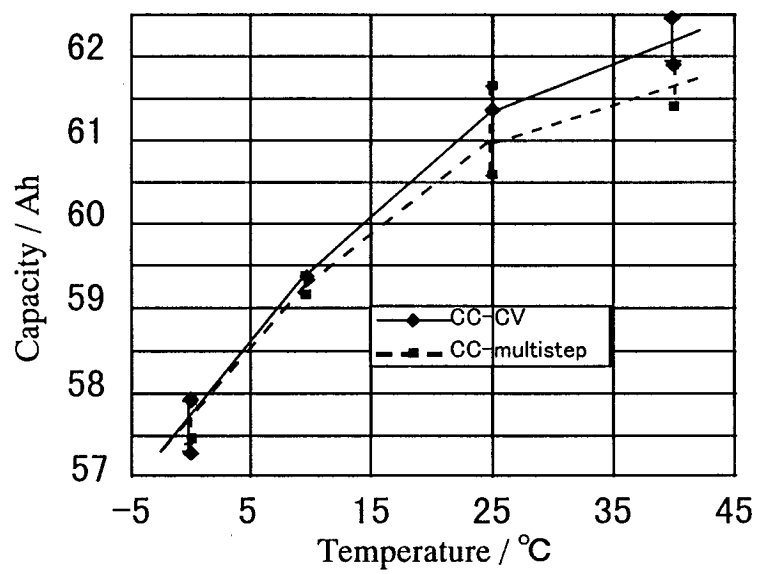

Three cells in series

The capacity acquired by the different charge methods were almost same, where CC-CV method realized a little more capacity than CC steps.
This result was not influenced by the plural number of cells connected in series.

Pulse Duration (at -10℃)

NASDA
NATIONAL SPACE DEVELOPMENT AGENCY OF JAPAN

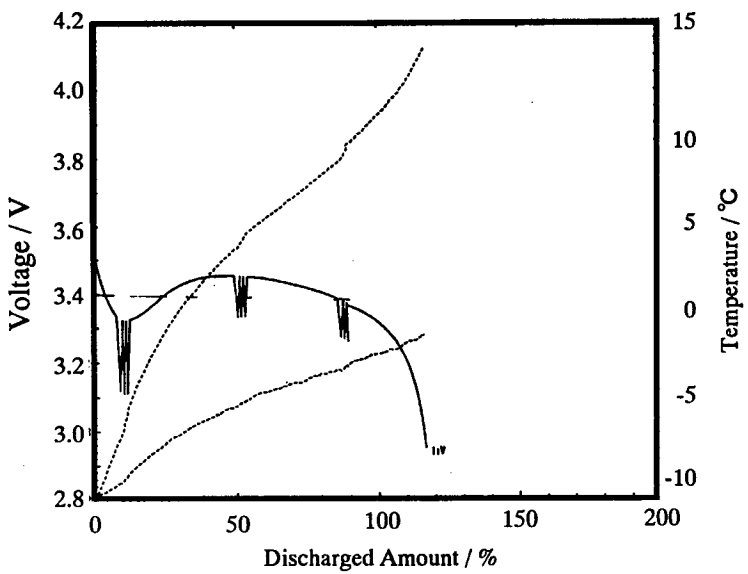

1C+0.5C discharge

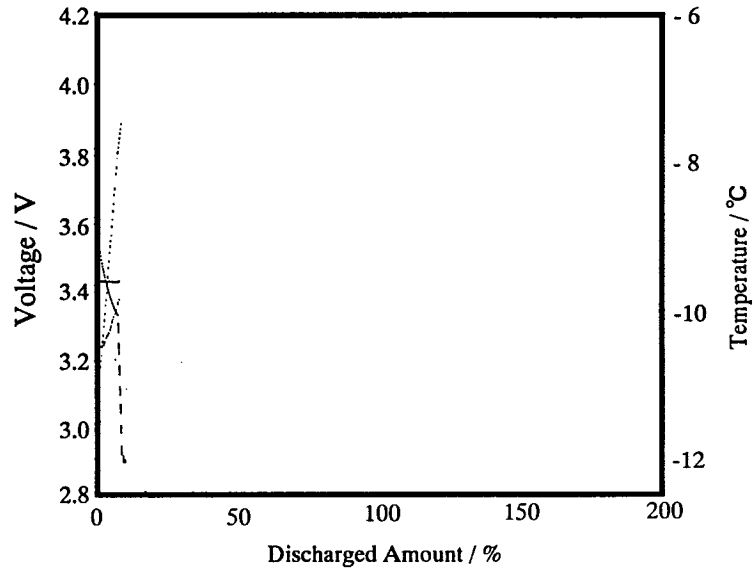

1C+1C discharge

Pulse current was applied to the cell. At -10℃, the impedance of the cell increased. It caused a drastic drop of voltage just after the current was applied. The cell was originally designed so that 1C current can be applied. As a result, the cell voltage was decreased less than 2.9V by the application of 1C pulse current to 1C discharge current, where we discontinued the measurement.

Pulse Duration (at 25, 60°C)

NASDA
NATIONAL SPACE DEVELOPMENT AGENCY OF JAPAN

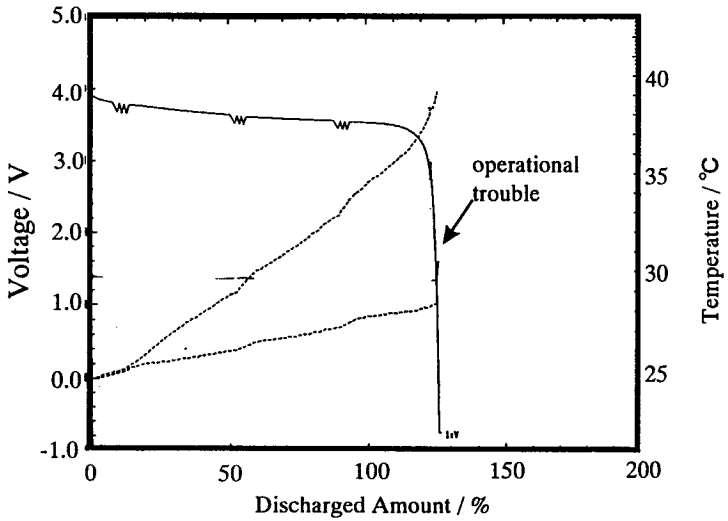

1C+1C discharge at 25°C

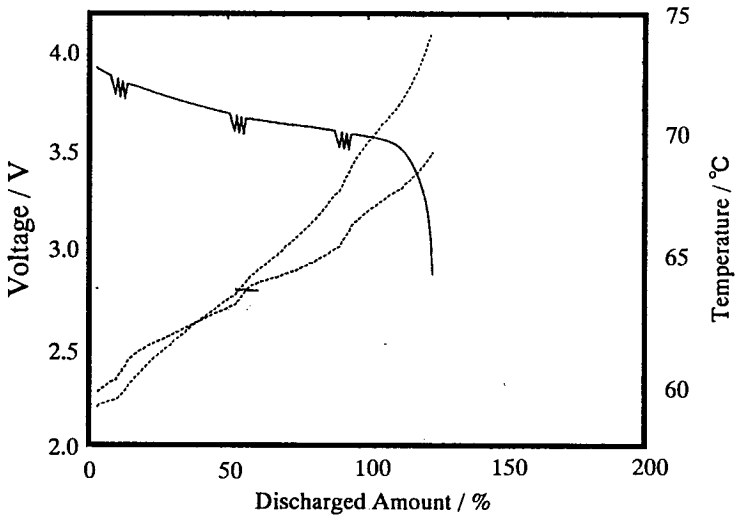

1C+1C discharge at 60°C

Pulse current was applied to the cell at 25°C and 60°C. These temperature does not cause high impedance of the cell. It resulted in the mild drop of discharge voltage during the pulse duration.

HOPE-X Simulation

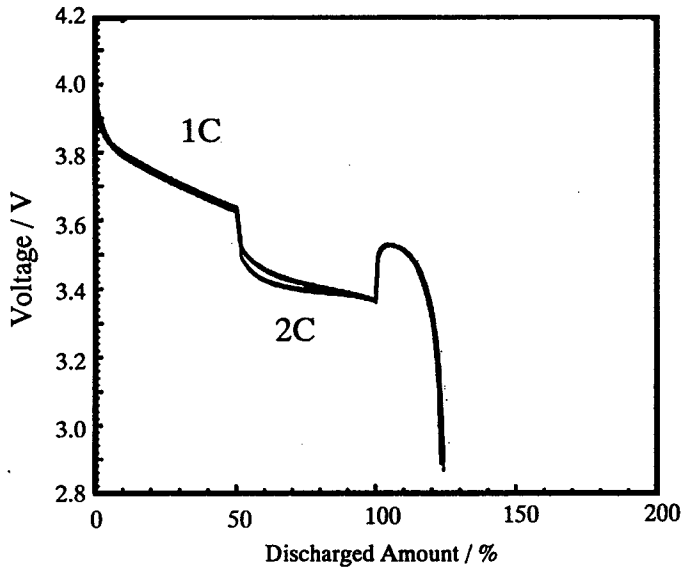

HOPE-X requests 1C discharge for the first 30 min, while it requests 1C discharge for the last 15 min. Though all operations, the cell voltage must be above 3.0V for the operation.

Even during the last 15 min., the voltage was above 3.3V. It suggested us that this cell should be applicable to HOPE-X.

Rectangular Type of Lithium Ion Secondary Cells

NASDA
NATIONAL SPACE DEVELOPMENT AGENCY OF JAPAN

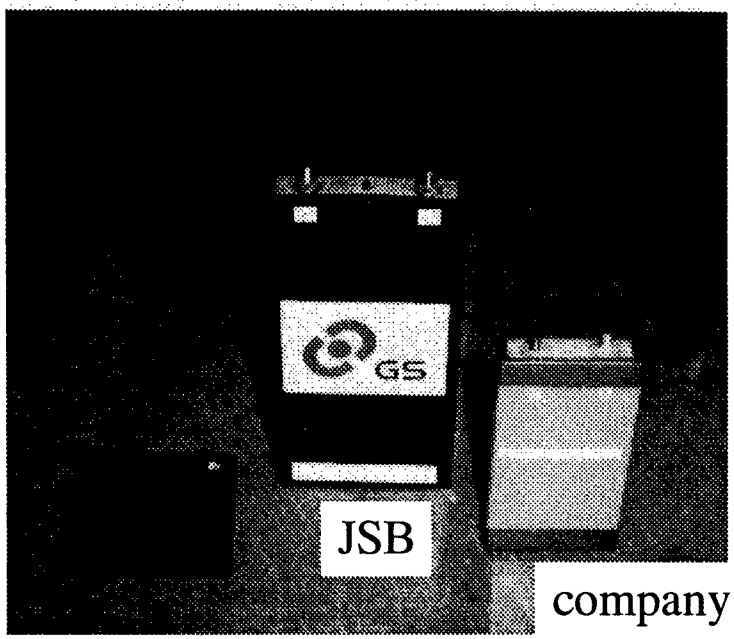

company D

JSB : Japan Storage Battery CO., LTD

Table. The design of Lithium Ion Secondary Cells.
Rectangular type of cells was designed aiming at satellite applications.
Cylindrical cell was prepared for HOPE-X.

	Rectangular A	Rectangular B	Cylindrical cell
Size / mm			
W	98.5	70	ϕ66
D	27	23.5	
H	190	130	244
Weight / g	1300	434	2030
Initial Capacity/ Ah (Nominal)	39 (30)	12 (10)	64 (50)
Initial Energy Density			
Wh/l	278	202	275
Wh/kg	108	100	113

Test Procedure for satellite applications

NASDA
NATIONAL SPACE DEVELOPMENT AGENCY OF JAPAN

Table. Test Procedure of Rectangular Cells
Five cells were connected in series. The temperature for the measurement was 20℃.

			Japan Storage Battery		company D
nominal capacity			30 Ah		10 Ah
capacity measurement	charge	current	3 A (0.1C)		1 A (0.1C)
		constant voltage	20.25 V (4.05 V/cell)		20.25 V (4.05 V/cell)
		time	16 hours		12 hours
	discharge current		15 A (0.5C)		5 A (0.5C)
life cycle test	DOD		25%	40%	40%
	charge	current	9 A(0.3C)	15 A(0.5C)	4.8 A(0.48C)
		constant voltage	20.25 V (4.05 V/cell)		
		time	60 min.		
	discharge	current	15 A (0.5C)	24 A (0.8C)	8 A (0.8C)
		time	30 min.		

We focused our measurements on LEO cycles. Since the GEO cycle is similar to the operational mode of Electric Vehicle, we are paying much attention on the results obtained by the companies.

Charge and Discharge Curve (JSB)

NASDA
NATIONAL SPACE DEVELOPMENT AGENCY OF JAPAN

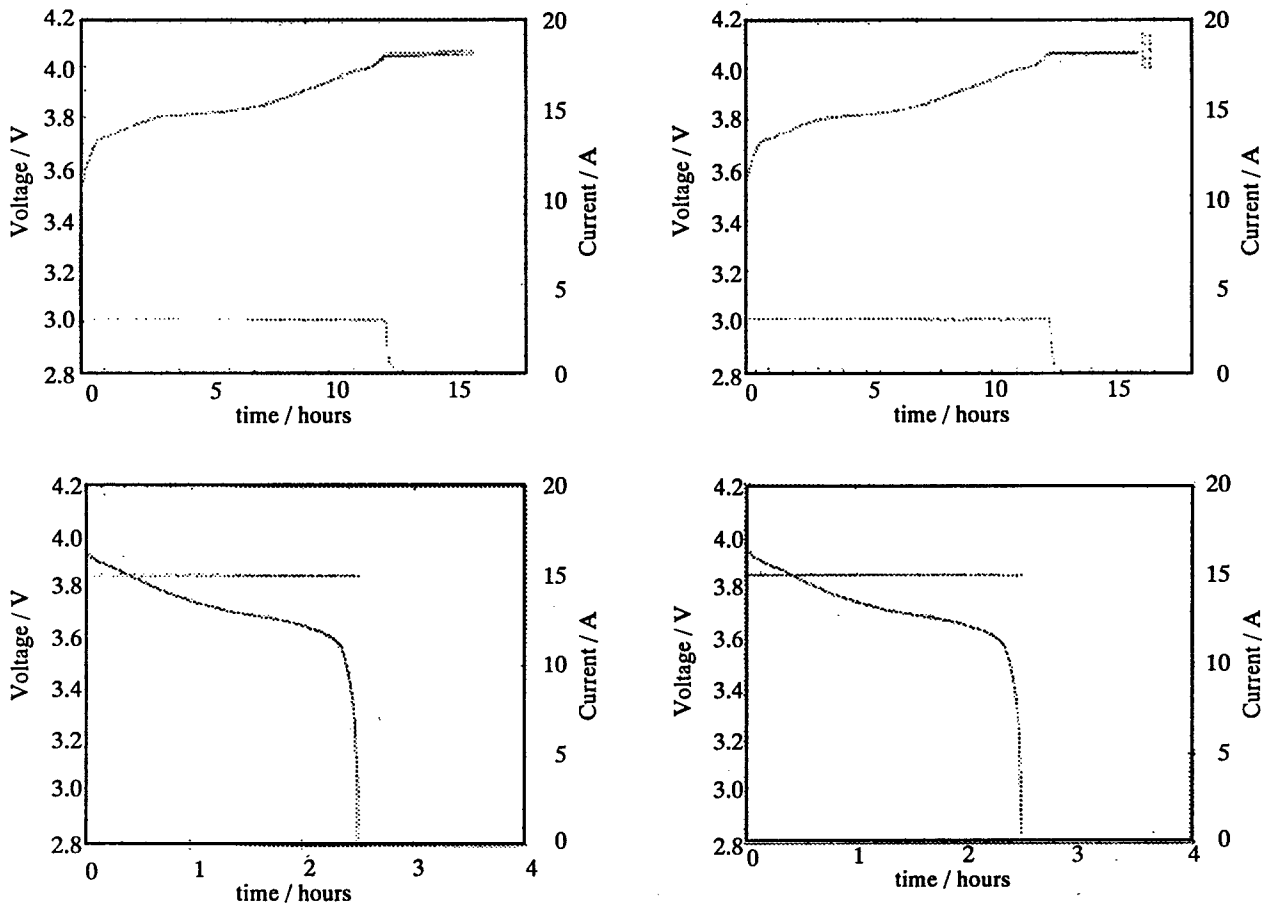

Cells for DOD 25%

Cells for DOD 40%

Charge and Discharge Curve (Company D)

NASDA
NATIONAL SPACE DEVELOPMENT AGENCY OF JAPAN

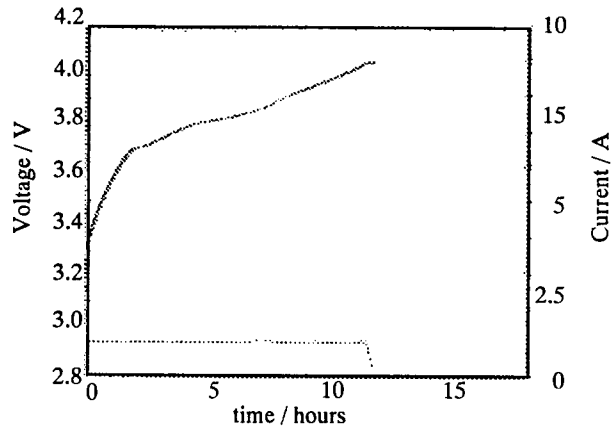

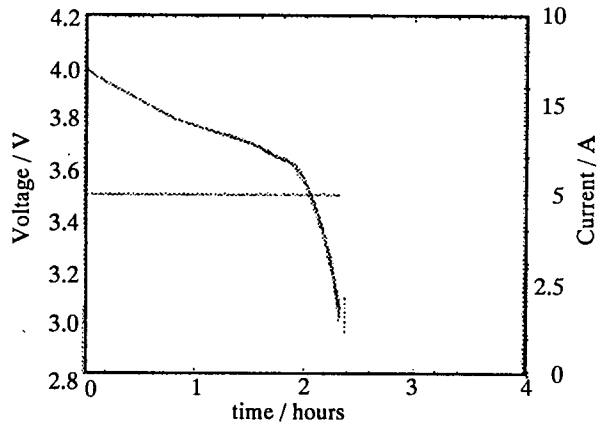

Cells for DOD 40%

Trend Data of Rectangular Cells

NASDA
NATIONAL SPACE DEVELOPMENT AGENCY OF JAPAN

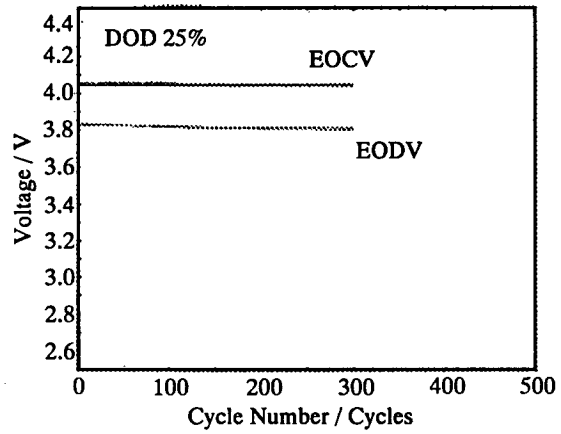

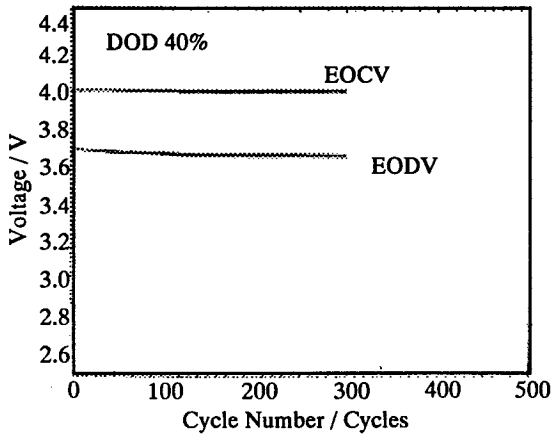

JSB cells

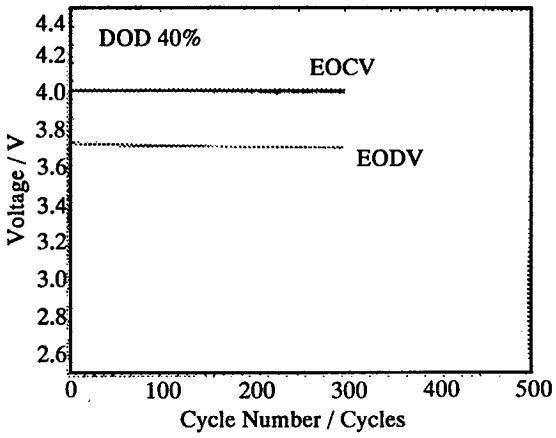

company D

Charge and Discharge Curve after 300 cycles (JSB)

NASDA
NATIONAL SPACE DEVELOPMENT AGENCY OF JAPAN

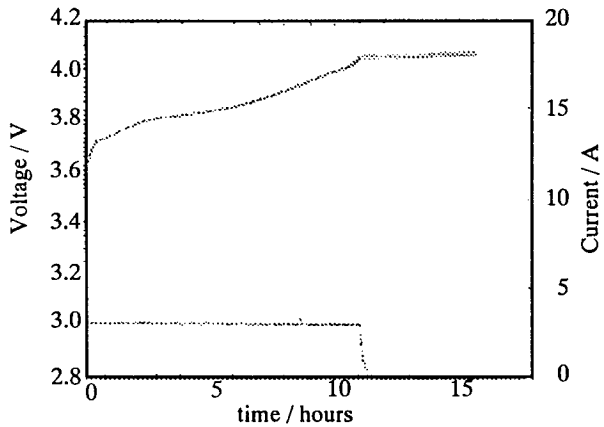

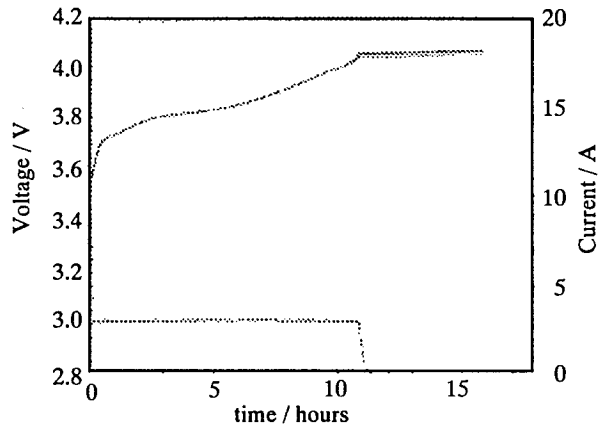

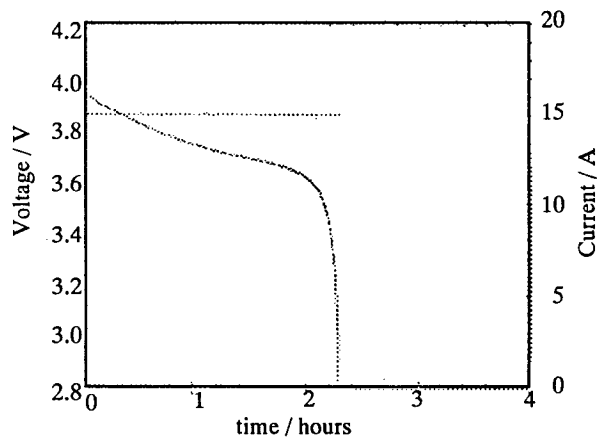

Cells for DOD 25%

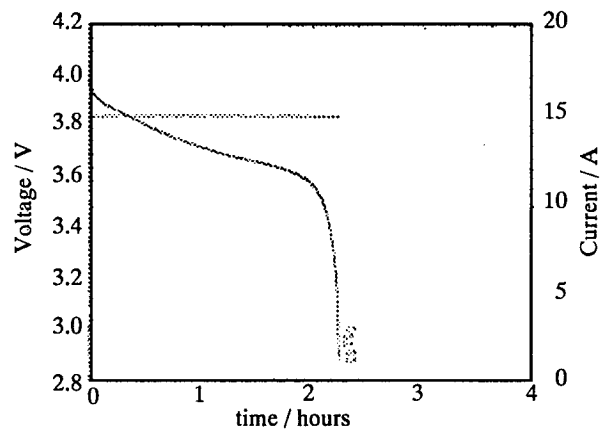

Cells for DOD 40%

Charge and Discharge Curve after 300 cycles (company D)

NASDA
NATIONAL SPACE DEVELOPMENT AGENCY OF JAPAN

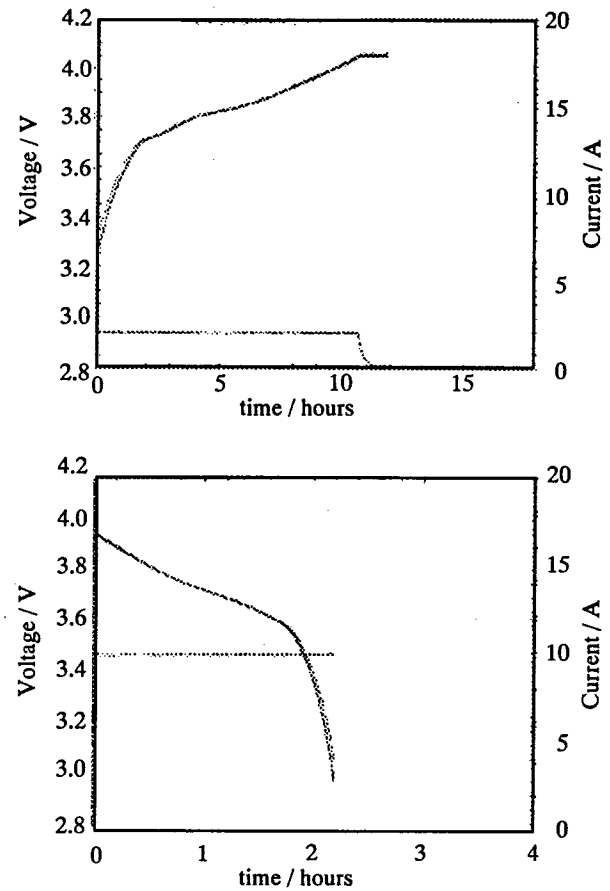

Cells for DOD 40%

Charge and Discharge Curve of 298 cycle, DOD25% (JSB)

NASDA
NATIONAL SPACE DEVELOPMENT AGENCY OF JAPAN

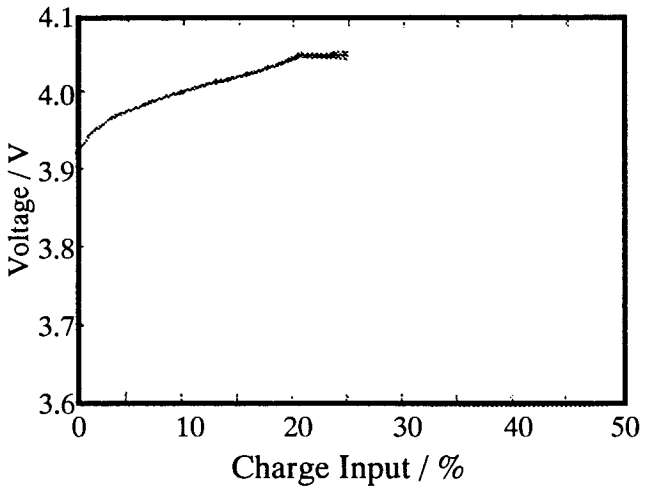

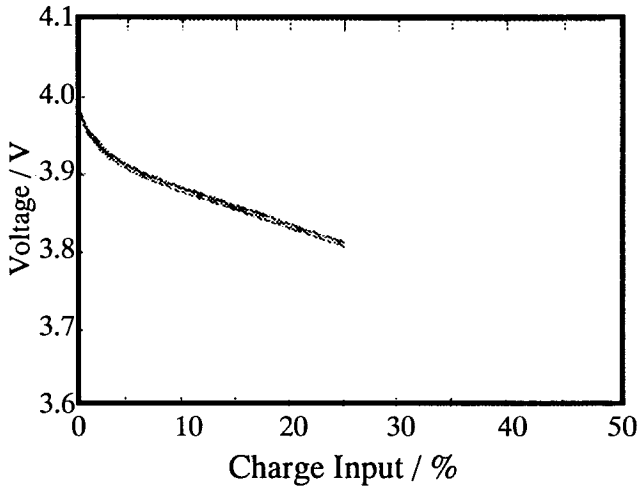

These results are obtained at 298cycle among life cycle test with DOD25%.
C/D ratio is almost 1.01. In the final part of charge, we observed the slight differnce of voltage.

Charge and Discharge Curve of 298 cycle, DOD40% (JSB)

NASDA
NATIONAL SPACE DEVELOPMENT AGENCY OF JAPAN

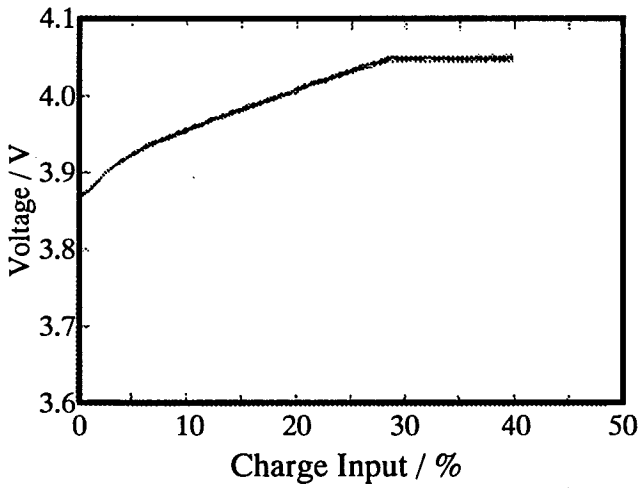

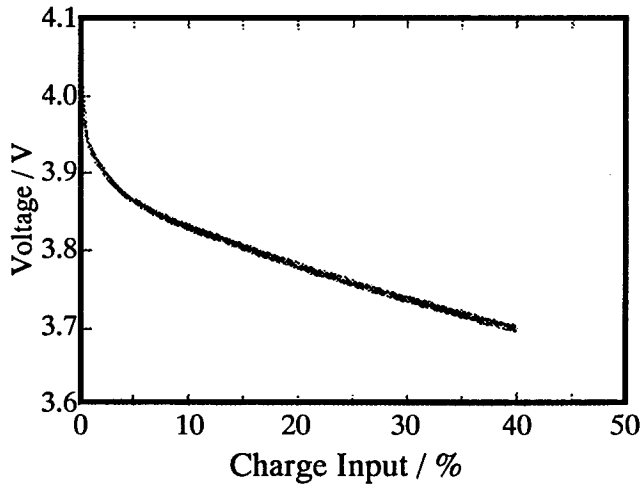

These results are obtained at 298cycle among life cycle test with DOD40%. C/D ratio is almost 1.01. The charge and discharge curves of the five cells are almost coincides with each other.

Charge and Discharge Curve of 298 cycle, DOD40% (company D)

NASDA
NATIONAL SPACE DEVELOPMENT AGENCY OF JAPAN

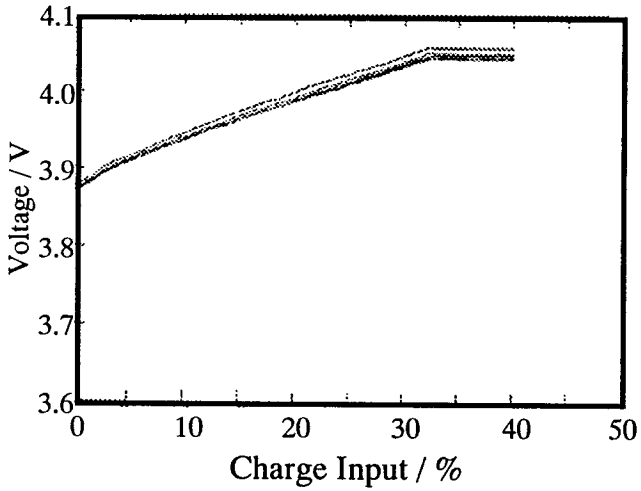

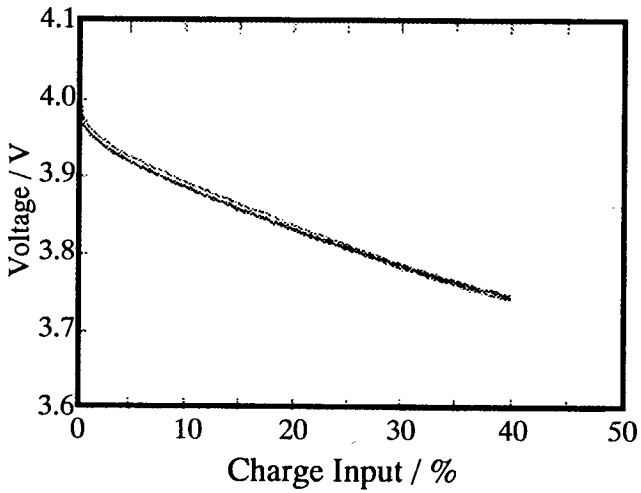

These results are obtained at 298cycle among life cycle test with DOD40%.
C/D ratio is almost 1.01. A slight difference of curves was observed.

Conclusion

NASDA
NATIONAL SPACE DEVELOPMENT AGENCY OF JAPAN

Commercial Cells

- Though the life cycles tests of commercial cells, we confirmed that the cell performance depends on DOD. With Deep DOD, the cell performance degraded faster.
- We also observed the degradation of cell performance affected by EOCV, while the same type of degradation was not always observed through our whole measurements.

Lithium Ion Secondary Cells for HOPE-X

- We compared the capacity obtained by CC-CV and CC steppes. The results suggested that the difference of charge methods do not cause a significant difference of capacity.
- Though HOPE-X simulation tests, we confirmed that this cell is applicable to HOPE-X program.

Rectangular type of Lithium Ion Secondary Cells for Satellite Applications

- The life cycle tests has just started at Tsukuba Space Center.
- We will pay much attention on the performance around EOCV through the cycle tests to find whether we will need a controlling unit for each cell or not.
- We will also consider the controlling methods of Lithium Ion Battery, using the results from our life cycle tests.

EAGLE PICHER Technologies, LLC

TESTING OF THE EAGLE-PICHER LITHIUM-ION SYSTEM

Advanced Electrochemical Systems Operation

Advanced Electrochemical Systems Operation
Federal Systems Department
Eagle-Picher Technologies, LLC
C & Porter Streets
P.O. Box 47
Joplin, Missouri 64802

EAGLE PICHER Technologies, LLC

OUTLINE

- Lithium-Ion Cells
  - Thermal Update
  - Cycle Life Update
  - Shock & Vibration
- Lithium-Ion Battery
  - Cell Uniformity
  - Thermal Testing
  - Electrical Testing
- Summary

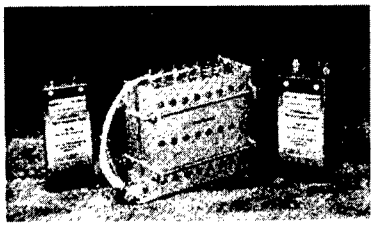

EAGLE PICHER Technologies, LLC

Thermal Model Evaluation

Prismatic Cell

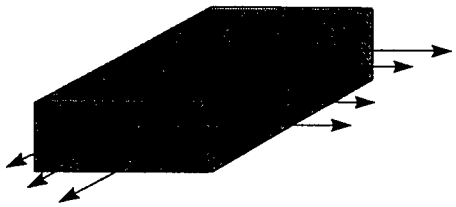

Spiral Cell

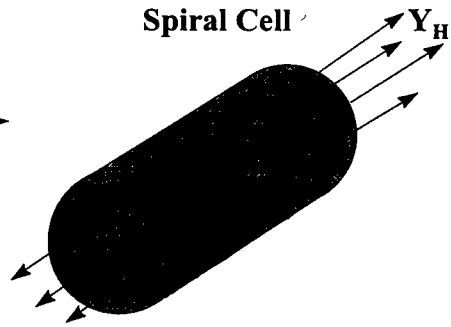

	>C/2	C
ΔT(Z-Y) =	< 3°	< 5°
ΔT(Z-X)=	< 3°	< 5°
ΔT(X-Y)=	< 1°	< 3°

	>C/5	C
ΔT(Z-Y)=	> 5°	> 35°
ΔZ=	~ 1°	> 7°

EAGLE PICHER Technologies, LLC

CYCLE LIFE FOR 15 AH CELLS AT VARIOUS DEPTHS OF DISCHARGE

13,438: 10% DOD @ C

3,664: 14% DOD @ C/5

2,780: 25% DOD @ C/2

1,120: 42% DOD @ C/5 & -4°C

1,043: 50% DOD @ C/2

901: 100% DOD @ C/2

Cycle Life Data

Figures reflect data as of 10/19/98.

EAGLE PICHER Technologies, LLC

CYCLE LIFE TESTING TO DATE

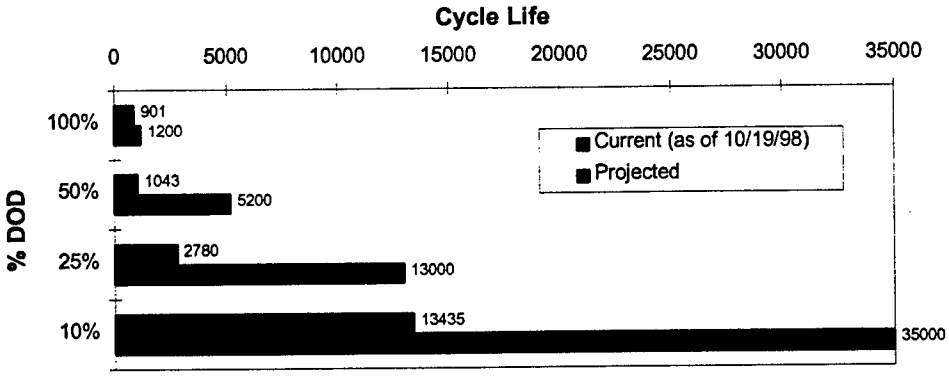

Projected life continues to increase with more testing data.

EAGLE PICHER Technologies, LLC

SHOCK & VIBRATION ENVIRONMENTS

ENVIRONMENT	APPLICATION		
	PRELIMINARY LAUNCH	SATELLITES	EXTENDED LAUNCH
RANDOM VIBRATION			
FREQUENCY (Hz)		20 to 2000	20 to 2000
PSD (G2/Hz)		0.10 to 1.0	.48 to 6.6
DURATION (Min.)		1 Min./Axis	3 Min./axis
G RMS		6 to 35	12 to 80
SHOCK			
ACCELERATION (g)		250 to 24000	100 to 10000
FREQUENCY (Hz)		100 to 10000	100 to 3000

Cells tested to highlighted values.

EAGLE PICHER Technologies, LLC

PERFORMANCE AFTER SHOCK & VIBRATION

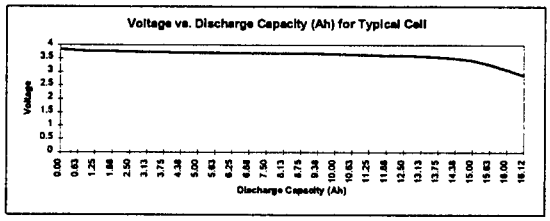

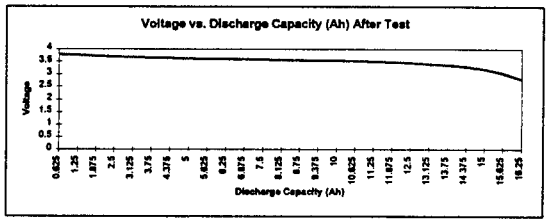

Data from post vibration cells show no abnormal reactions

EAGLE PICHER Technologies, LLC

PROTOTYPE BATTERY DESIGN

- ✦Prototype Satellite Battery Design
  - ◆15 Ah Batteries
  - ◆Built Two 8-Cell Batteries
    - Completed Independent Charge Test
  - ◆Built 28V Battery (Series Charged)
    - Currently Under Test
    - Verified Preliminary Thermal Analysis through Instrumentation
  - ◆Built a 4-Cell Battery
    - Series Charged
    - Completed Life Test (100% DOD)

EAGLE PICHER Technologies, LLC

28 V BATTERY COEFFIENT OF VARIANCE

28 Volt - 15 Ah Battery
Cycle 20 After Completion of Formation Cycling

Cell Number	Discharge Capacity (Ah)
1559802	16.18148
1569801	16.17005
1569802	16.1847
1669801	16.20237
1669802	16.18132
1669803	16.19014
1679802	16.18859
1689801	16.17826
1689803	16.17612
1699802	16.18661

Mean Capacity	16.18396
Standard Deviation (mAh)	11.00107
COV	0.05%

Cell uniformity will lead to longer battery operation.

EAGLE PICHER Technologies, LLC

THERMAL COUPLE LOCATIONS

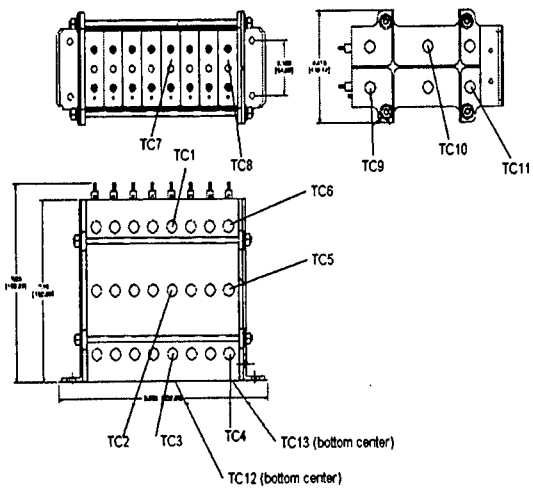

EAGLE PICHER Technologies, LLC

THERMAL CHARACTERISTICS OF BATTERY

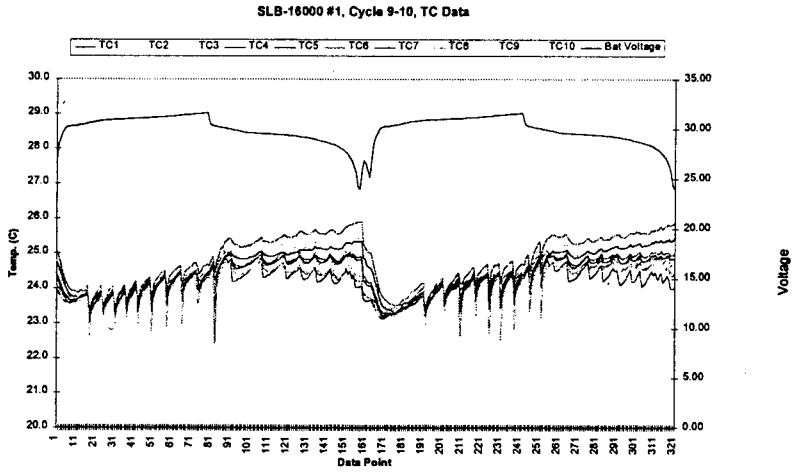

Low Variance in ΔT Leads to Longer Life

EAGLE PICHER Technologies, LLC

4-CELL BATTERY

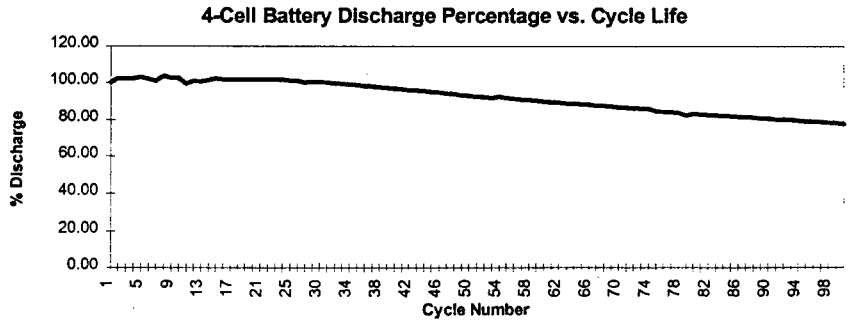

4 Cell Series Battery 100% DOD at C/5 & C/2

EAGLE PICHER Technologies, LLC

CURRENT & FUTURE PROFILES

✦Current Profile (Completed)
- 10 Cycles @ 25° C
- Charge 2.5 A @ 4.1 V for 6.5 hours
- Discharge 2.5 A to 2.8 V
- Discharge 1 A to 2.6 V
- 72 Change Retention

✦Future Profile (Completed)
- 5 Cycles @ 10° C
- Charge 2.5 A @ 4.1 V for 6.5 hours
- Discharge 2.5 A to 2.8 V
- Discharge 1 A to 2.6 V
- 72 Change Retention

✦GEO Season Simulation (On Test)
- 60% DOD
- Charge: C/5
- Discharge: C/2

EAGLE PICHER Technologies, LLC

EAGLE-PICHER GEO SEASON SCHEME

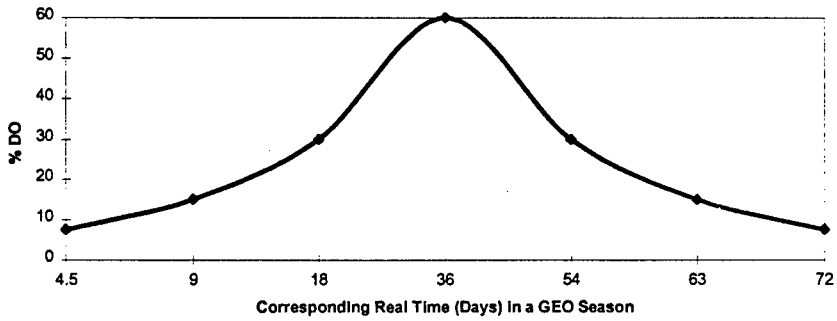

Charge: C/15 Discharge: C/2

Planned operational points for the Eagle-Picher GEO Test Plan.

EAGLE PICHER Technologies, LLC

SUMMARY
1999 DEVELOPMENT PLANS

➔ CELL LEVEL
- ✦ Continued Investigation of Charge Control Methods
- ✦ Develop Improved Analytical Techniques for Screening Cells
- ✦ Revise Accelerated Life Cycle Testing Methods
- ✦ Initiate 100 Ah Cell Level Characterization & Life Cycle Testing
- ✦ LEO Profile Testing

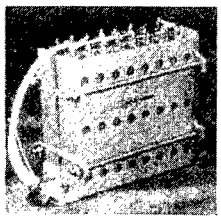

➔ BATTERY LEVEL
- ✦ Develop Battery for Flight Experiment
- ✦ GEO Qualification Testing (15 Ah - 28 V)
- ✦ Finalize Prototype Charger

EAGLE PICHER Technologies, LLC

SUMMARY
1998 ACHIEVEMENTS

- ✦ Completed thermal model
- ✦ Completed preliminary shock & vibration testing
- ✦ Achieved >12,000 cycles @ 10% DOD
  >900 cycles @ 100% DOD
- ✦ Continued battery level testing, including characterization and GEO
  NiH_2 vs. Lithium-Ion Comparison Data Accumulation

EAGLE PICHER Technologies, LLC

FOR MORE INFORMATION CONTACT:

- **Technical**
  - **Chad Kelly**, Asst. Program Manager
  - (417) 623-8000 Ext.436, eplion@aol.com
- **Business**
  - **Doug Wright**, Business Manager
  - (417) 623-8000 Ext.320, dwright@epi-tech.com
- **Other**
  - **Walter McCracken**, Operation Manager
  - (417) 623-8000 Ext.274, wmccracken@epi-tech.com

Evaluation of Safety and Performance of Sony Lithium Ion Cells

Judith A. Jeevarajan
Lockheed Martin, Houston, TX
&
Bobby J. Bragg
NASA/JSC/EP5

Sony Lithium Ion Cells

Physical Characteristics

- **Dimensions (18650)**

Average Weight (g)	Average Height (mm)	Average Diameter (mm)
39.660 ± 0.079	64.91± 0.18	18.12 ± 0.03

Electrochemical Characteristics

- **Open Circuit Voltage**

  3.858 ± 0.015 V

- **Closed Circuit Voltage**

  3.69 ± 0.14 V

Canon Battery (BP-927) Characteristics

- **Weight**: 185 g (approx.)
- **Dimensions**: 38.2 X 39 X 70.5 mm (approx.)
- **Voltage**: 7.2 V
- **Capacity**: 2700 mAh
- **Configuration**: 2P2S
- **Smart Circuit Board**

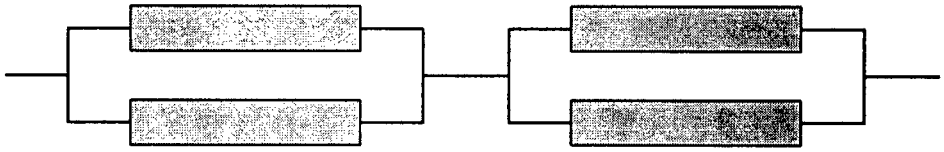

Sony Lithium Ion Cells

Electrochemical Characteristics

- **Capacities at Different Temperatures**

Temperature	Average Capacity (Ah)
40 °C	1.157
25 °C	1.18
10 °C	0.991
-10 °C	0.572

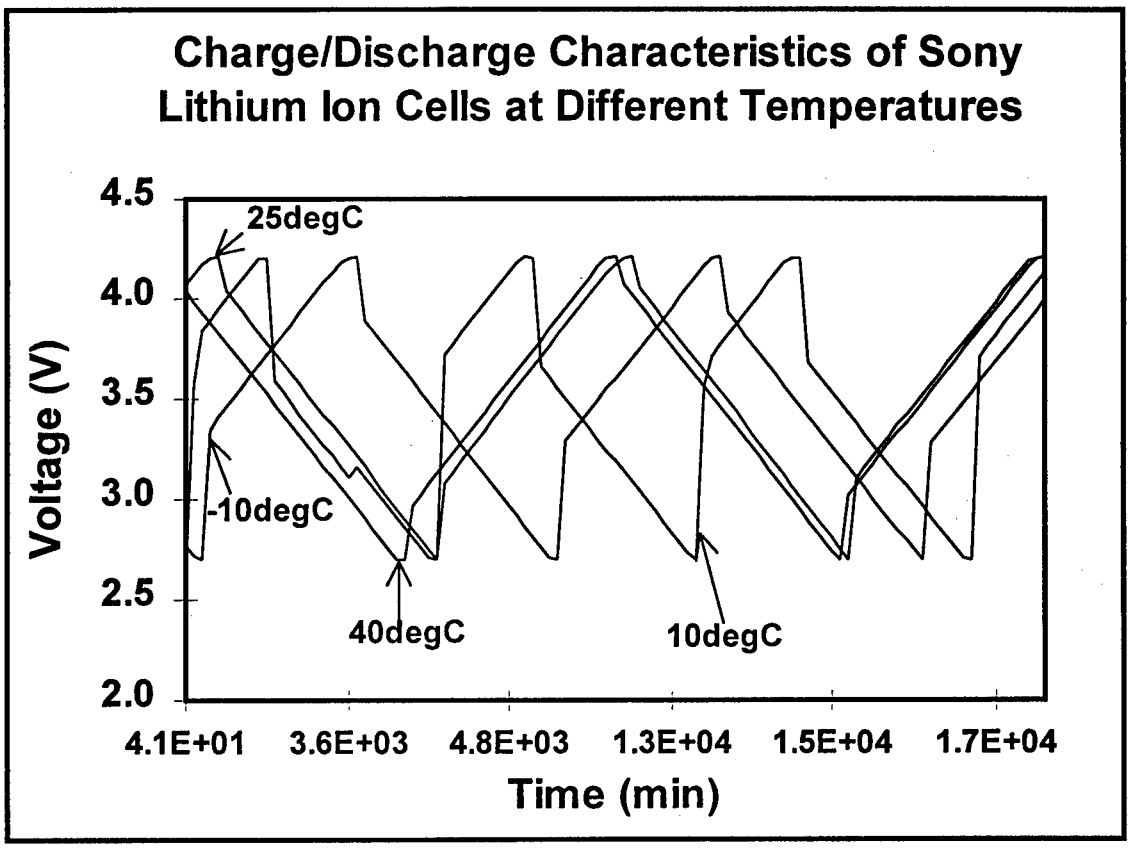

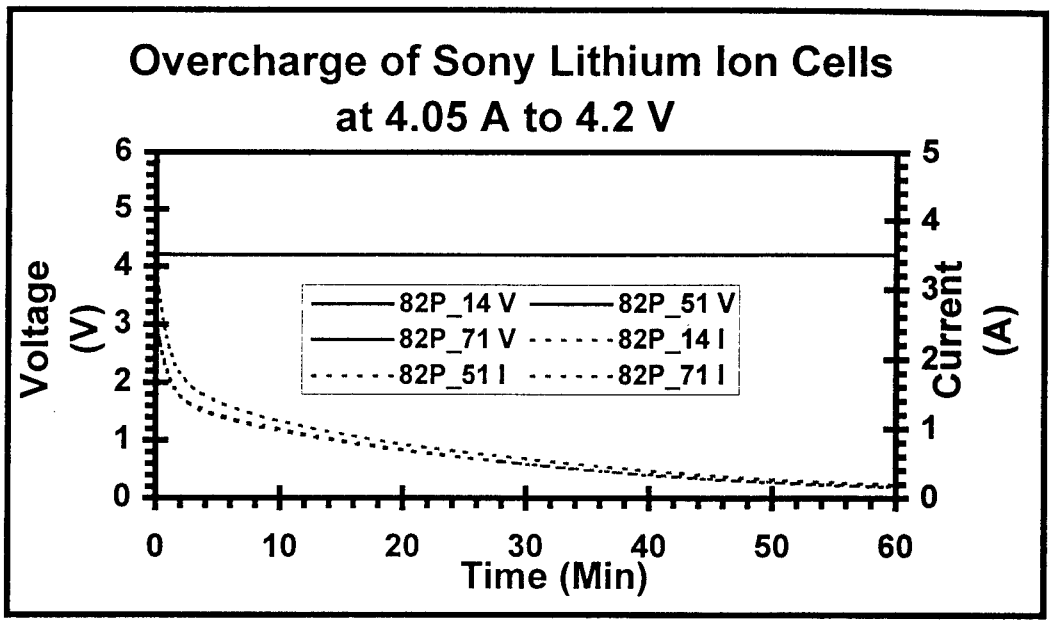

- Attains 4.2 V immediately.
- No venting, fire or explosions due to fast charge.

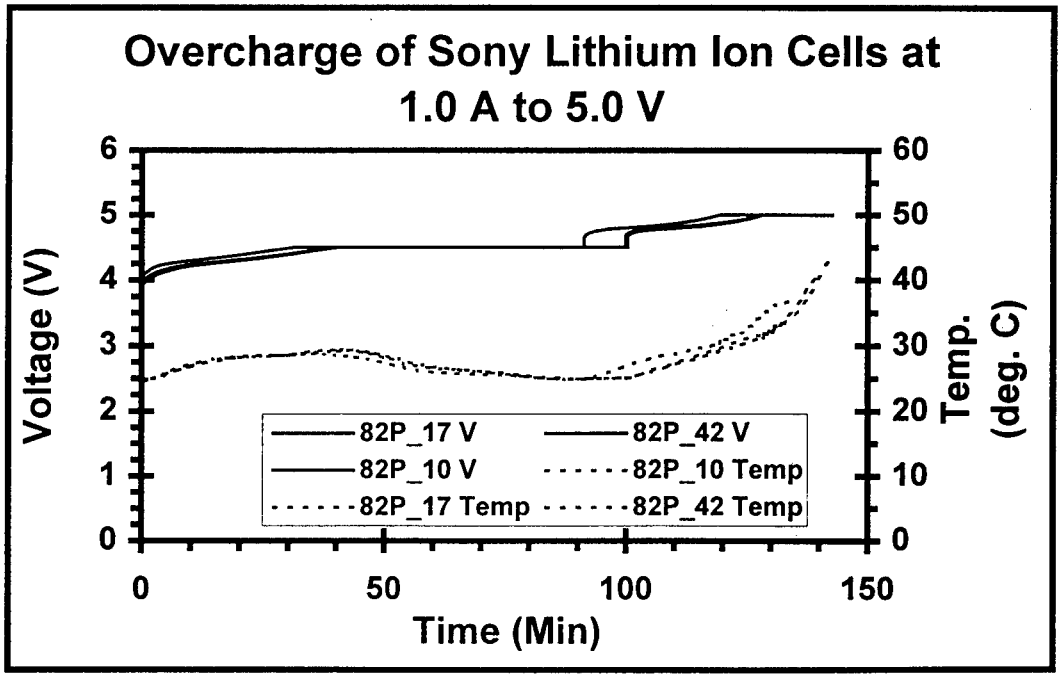

- Current Interrupt Device (CID) is activated when voltage reaches 5.0 V or when maintained at 5.0 V.

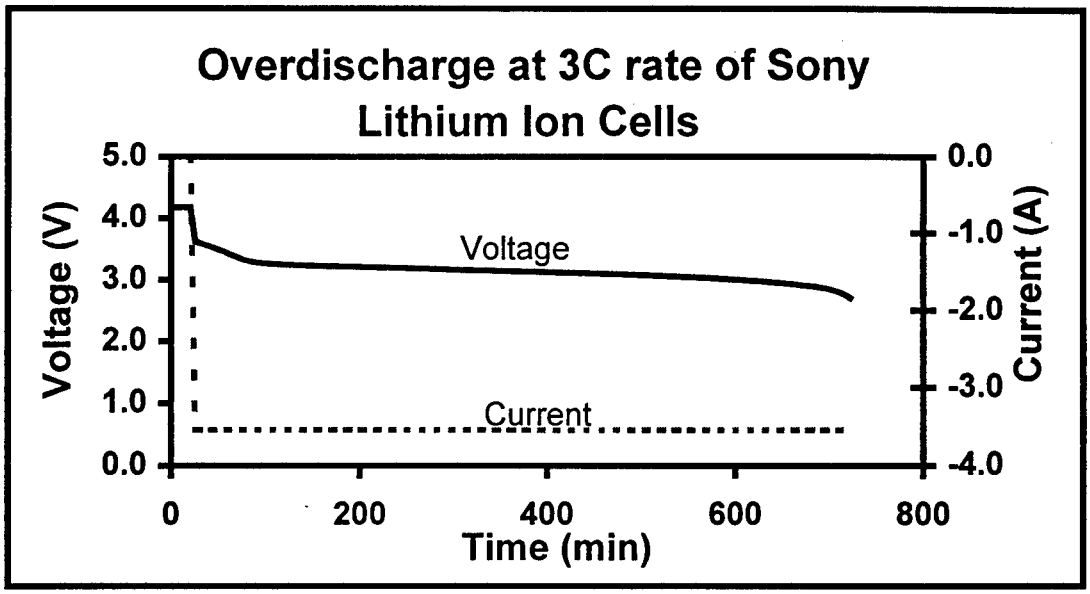

- **Cells performed nominally on charge/discharge cycles.**
- **No venting, fire or explosions**

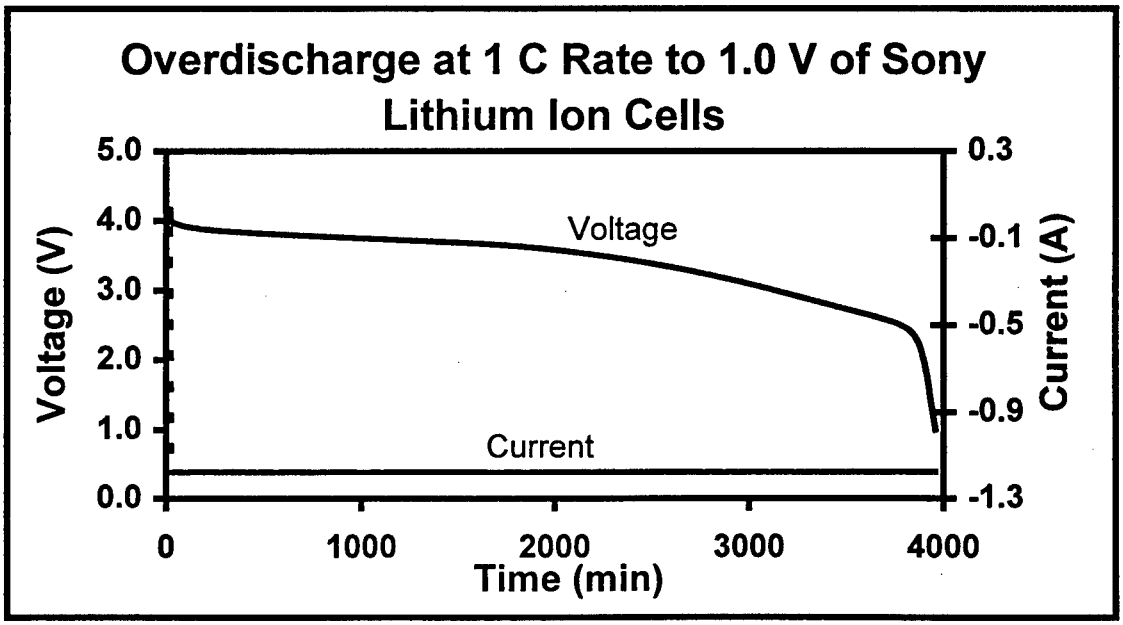

- **Performed nominally on the few charge/discharge cycles carried out after test.**
- **No catastrophic events.**

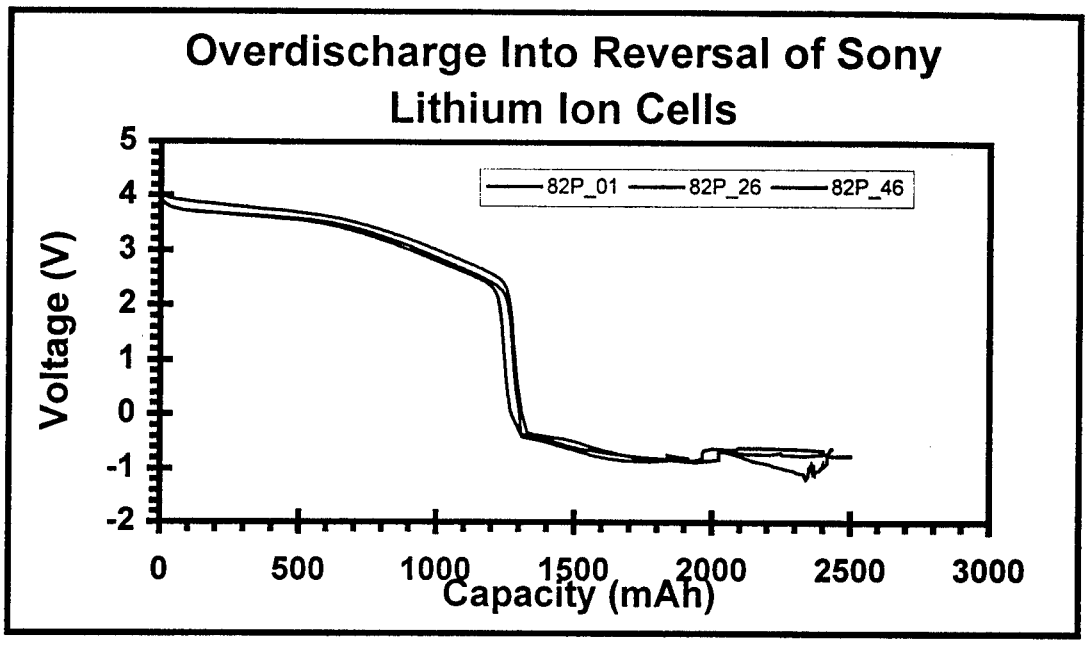

- Cells functional with no changes in capacity for the few cycles performed after test.
- No occurrence of cell venting.

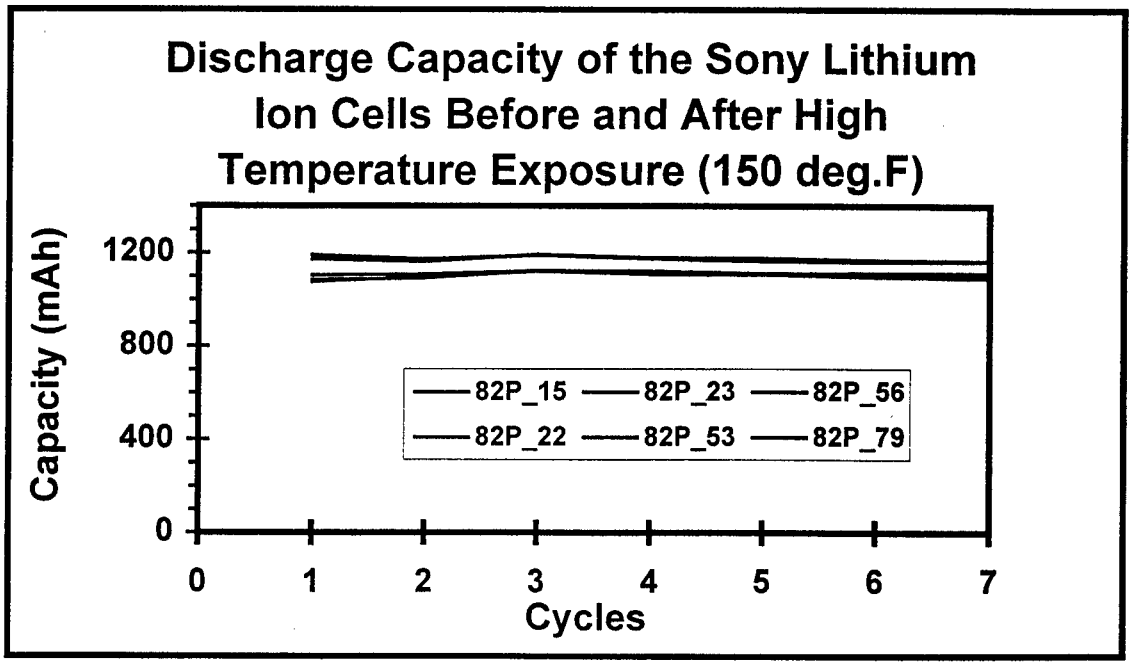

- No changes in functional performance of the cells after exposure to a temperature of 150 °F in an oven.
- No cell venting observed.

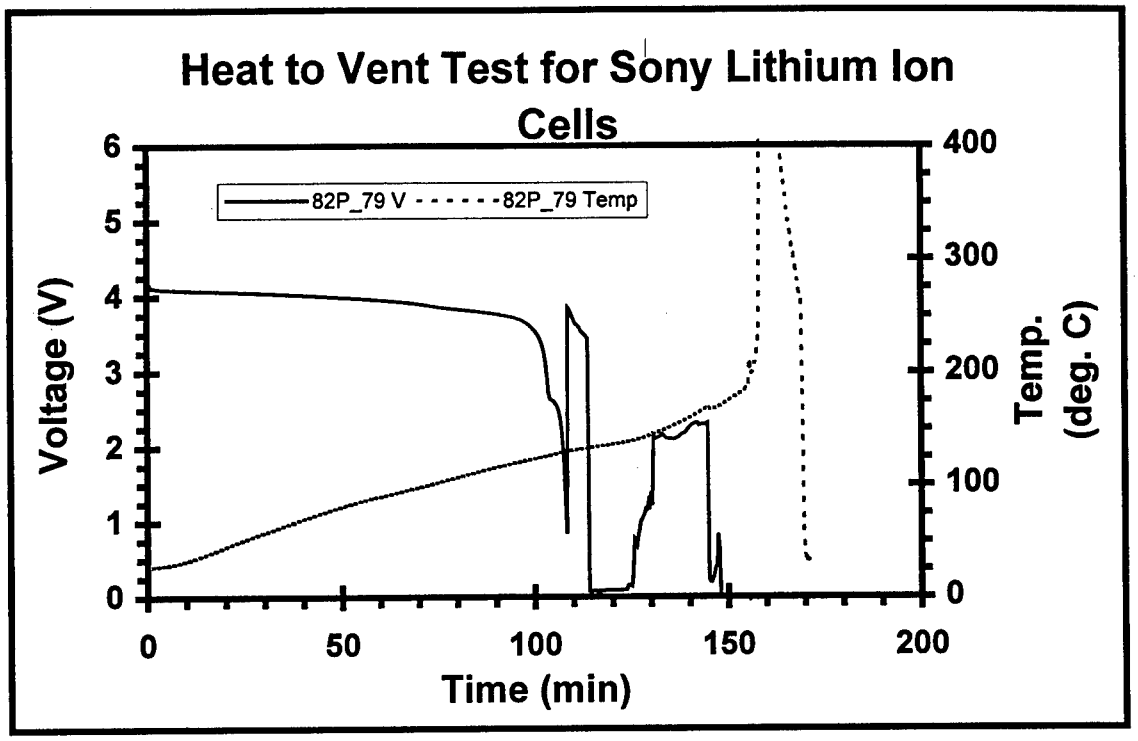

- Venting occurs above 150 °C.

Drop Test on Sony Lithium Ion Cells

- Six cells dropped from a height of 6 ft. and 3 cells from a height of 3 ft.
- Physical damage such as dents around the circumference at the top and bottom.
- No events, no changes in capacity of cells
- No change in weight of cells to indicate occurrence of venting.

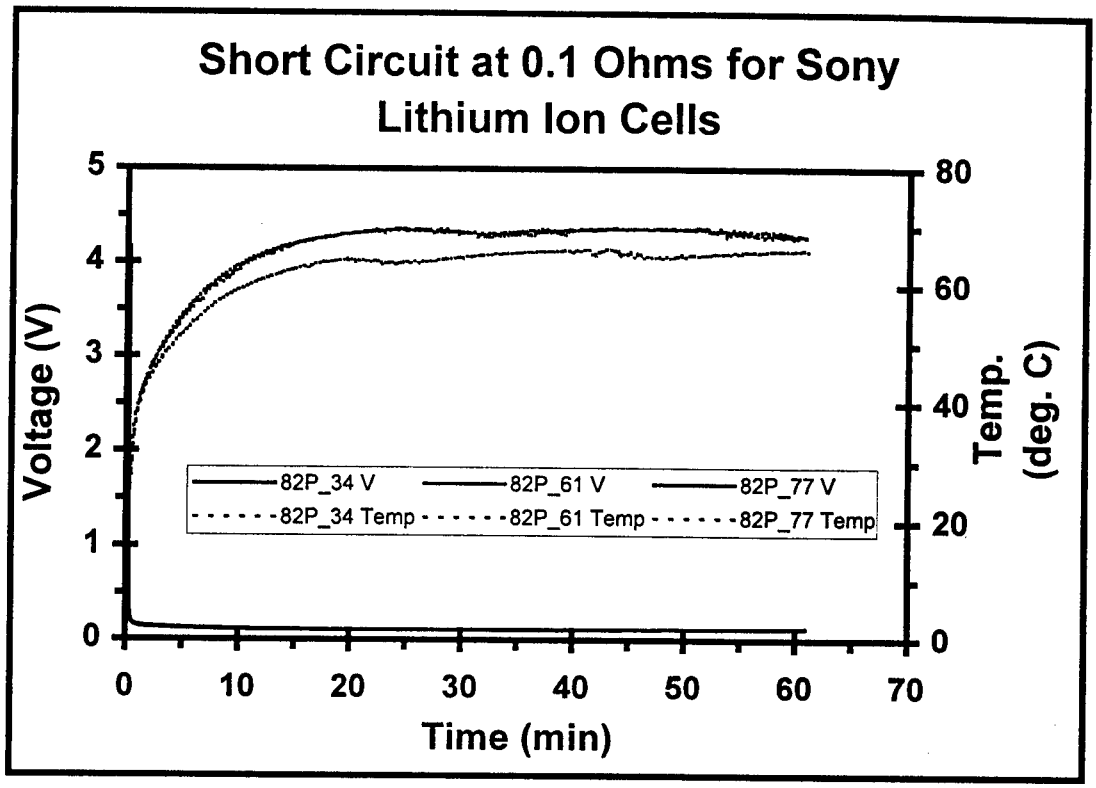

- PTC shuts off any electrical contact immediately.

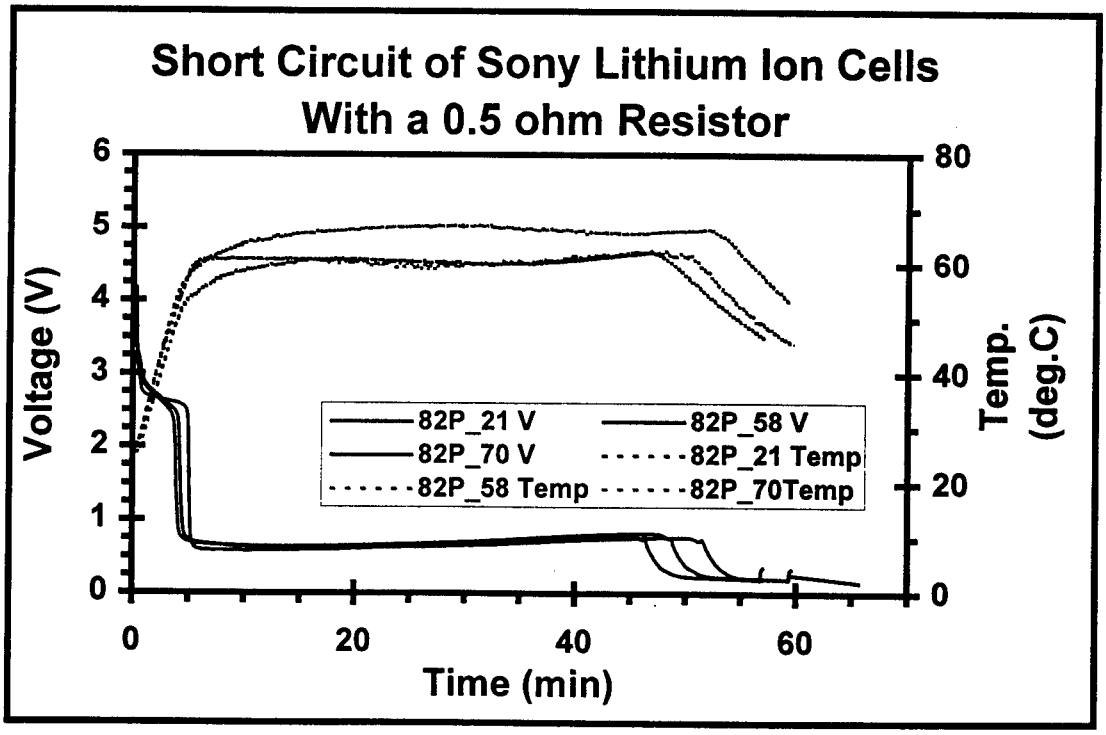

- PTC cuts off electrical contact.
- Electrical contact is reestablished when the PTC stabilizes.

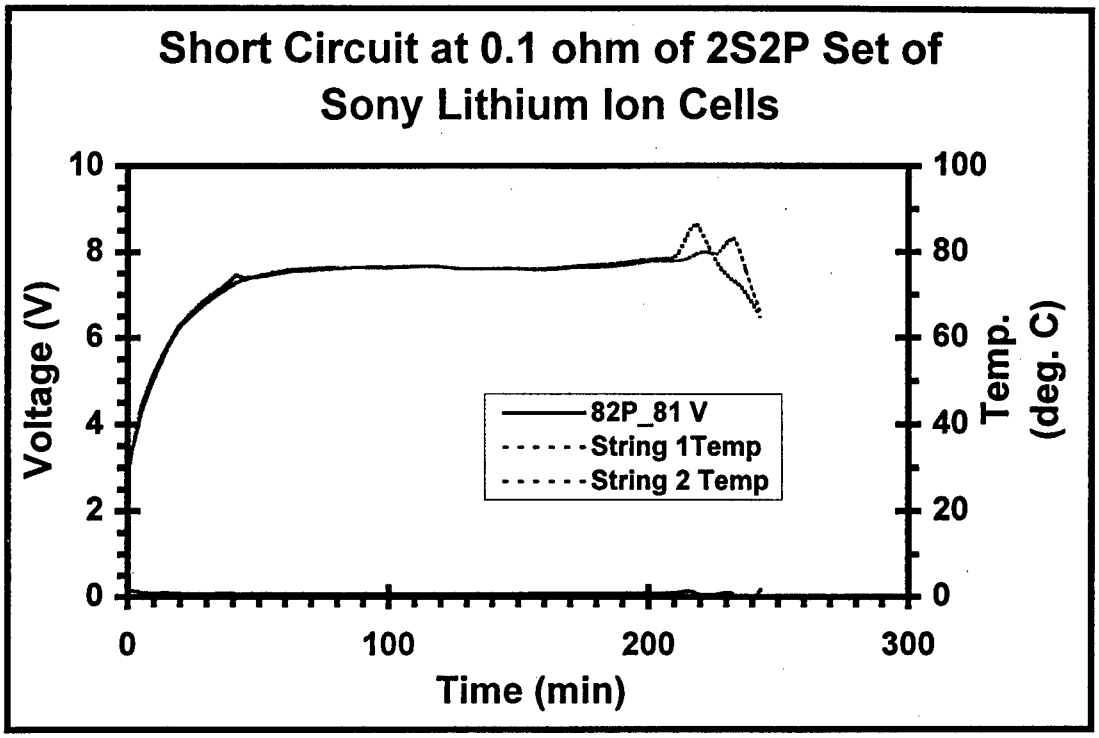

- PTC cuts off electrical contact by an increase in resistance.
- No weight changes in the short circuit tests indicating absence of venting.
- No catastrophic events in the short circuit tests carried out.

Crush Test of Sony Lithium Ion Cells

(a) (b)

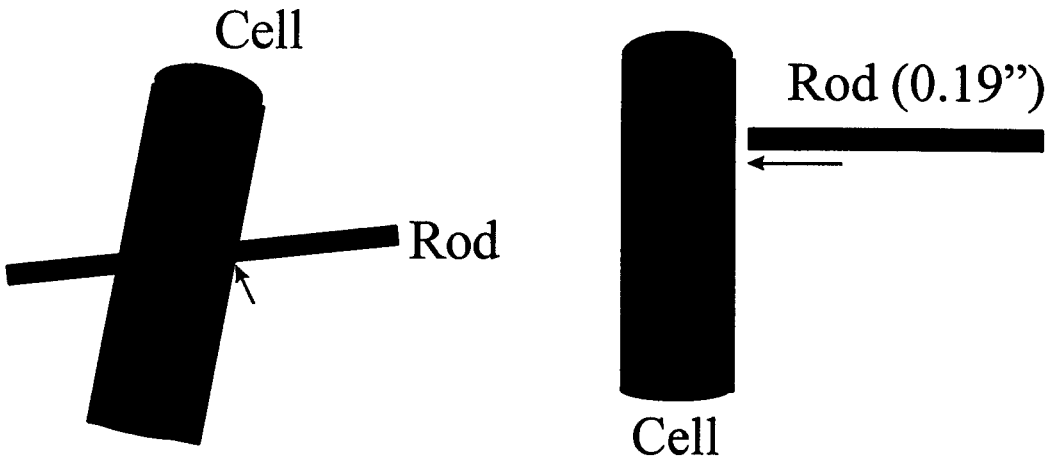

(a) No venting, fire or explosion

(b) Four cells out of six experienced violent venting with thermal runaway, the other two exploded.

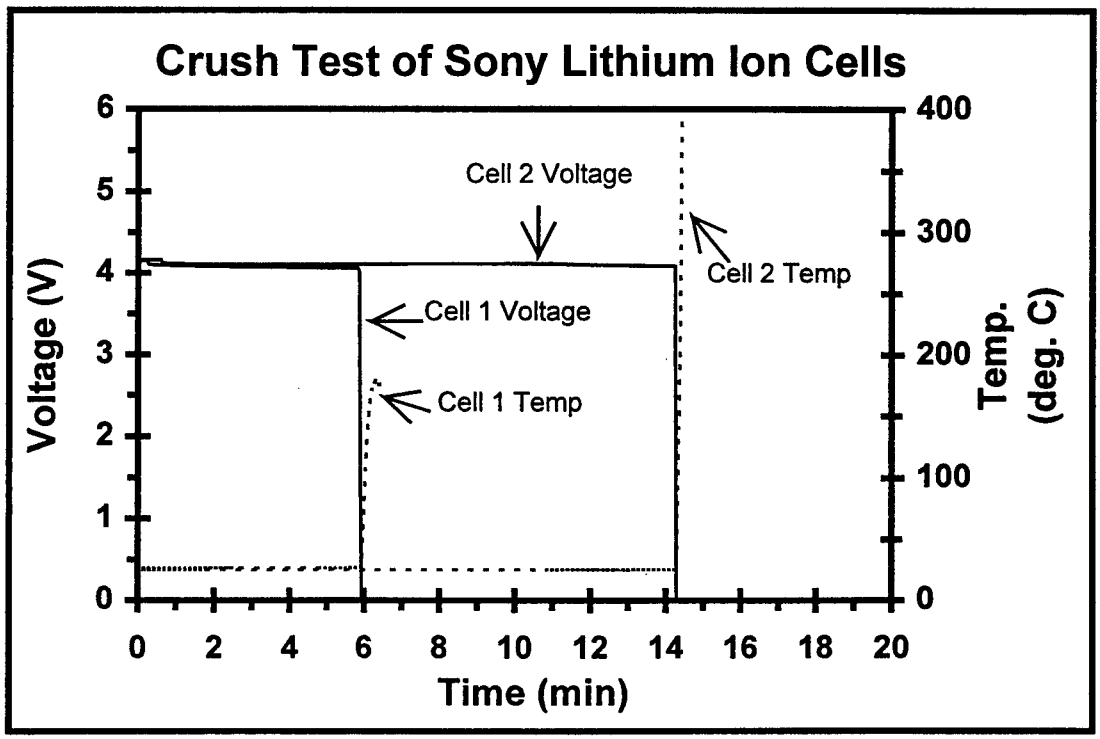

(C)

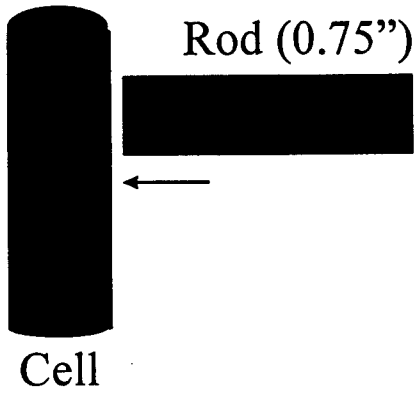

Steel Fixture

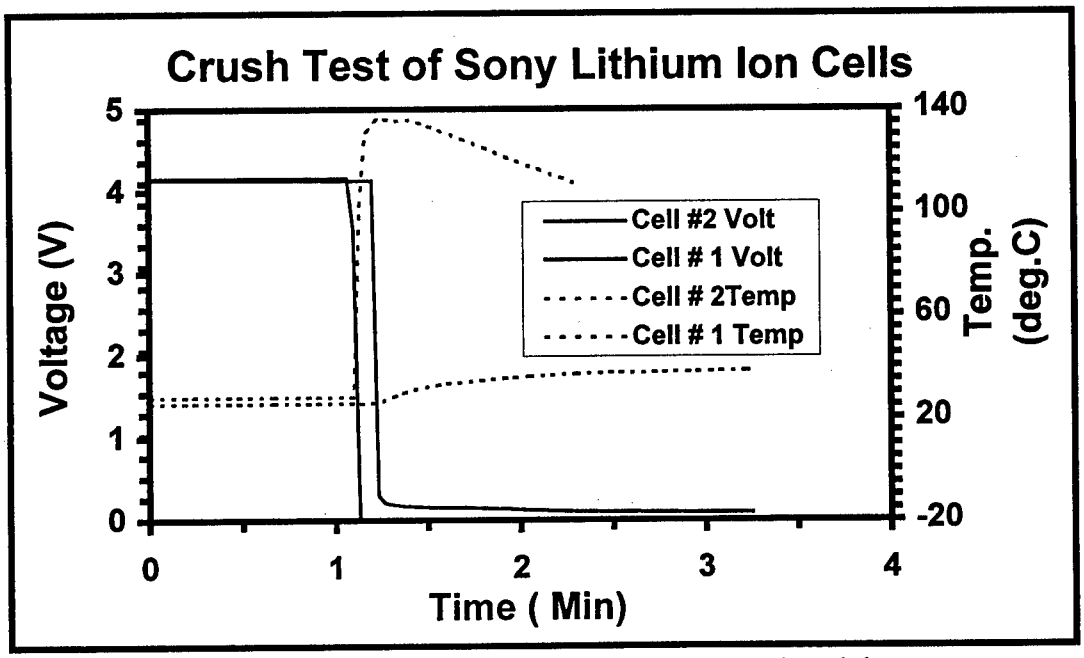

- No explosions. Three of four cells vented with temperatures between 80 °C to 100 °C. Fourth cell vented slowly with temperature around 40 °C.

Teflon Fixture

- No explosions.
- Three of four cells vented with temperatures reaching 400 °C. Split in can wall observed. One cell vented slowly with max. temperature of 100 °C.

Battery Testing

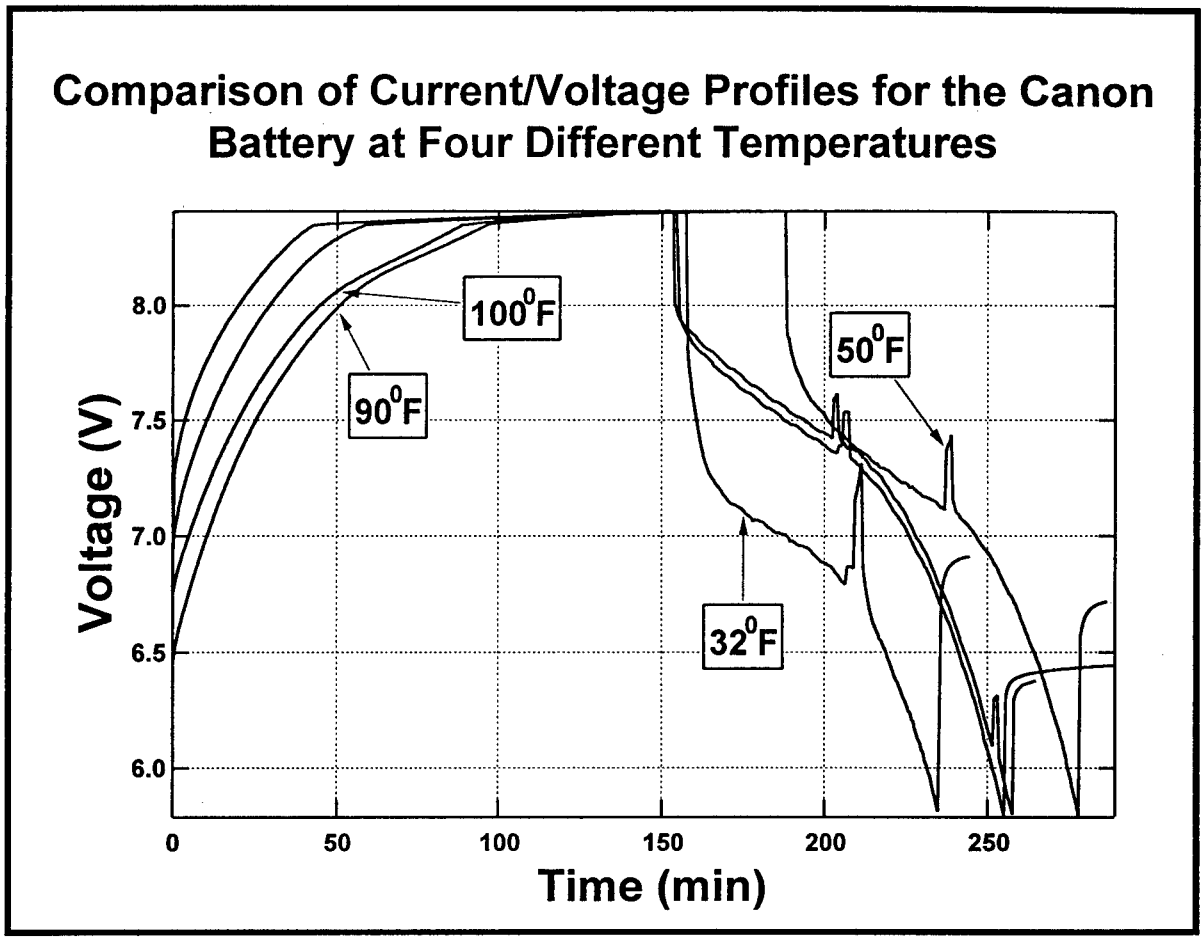

- Longer charging time is required at lower temperatures.
- At 50 °F, the battery required an additional 30 minutes to be fully charged.
- At 32 °F, during the 2½ hour period required for normal charging, only 75 % charging was obtained.
- Battery at room temperature can power the camcorder for 106 minutes. (Manufacturer spec: 90 mins)
- At 90 °F and 110 °F, 100 minutes and 110 minutes respectively of camcorder run time was obtained.
- At 50 °F and 32 °F, 92 minutes and 78 minutes respectively of run time was obtained.

Temperature Profile of Charger Under Different Thermal Conditions

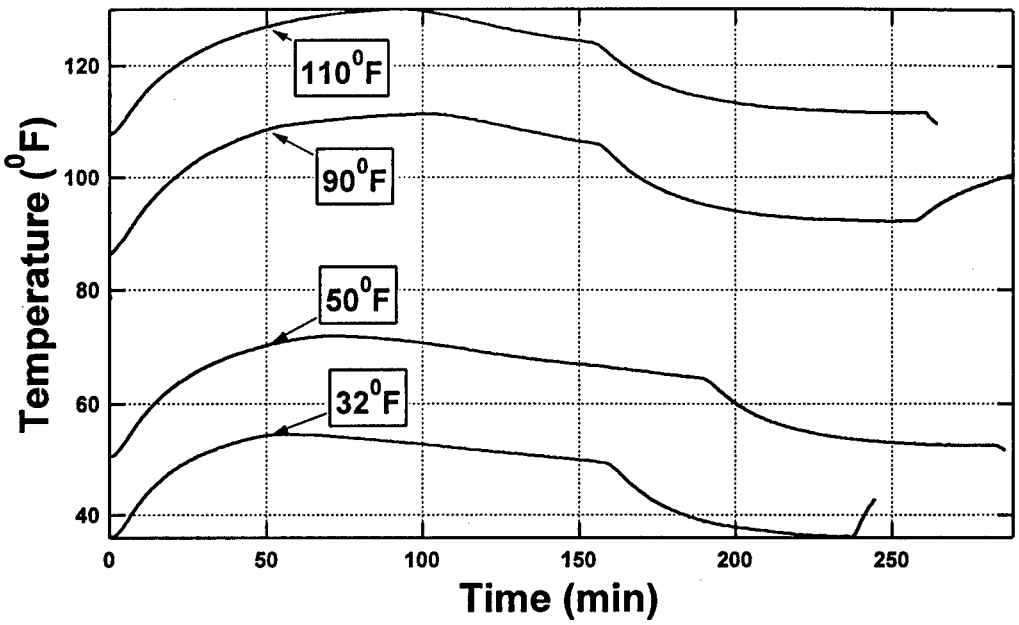

Temperature Profile of Battery Under Different Thermal Conditions

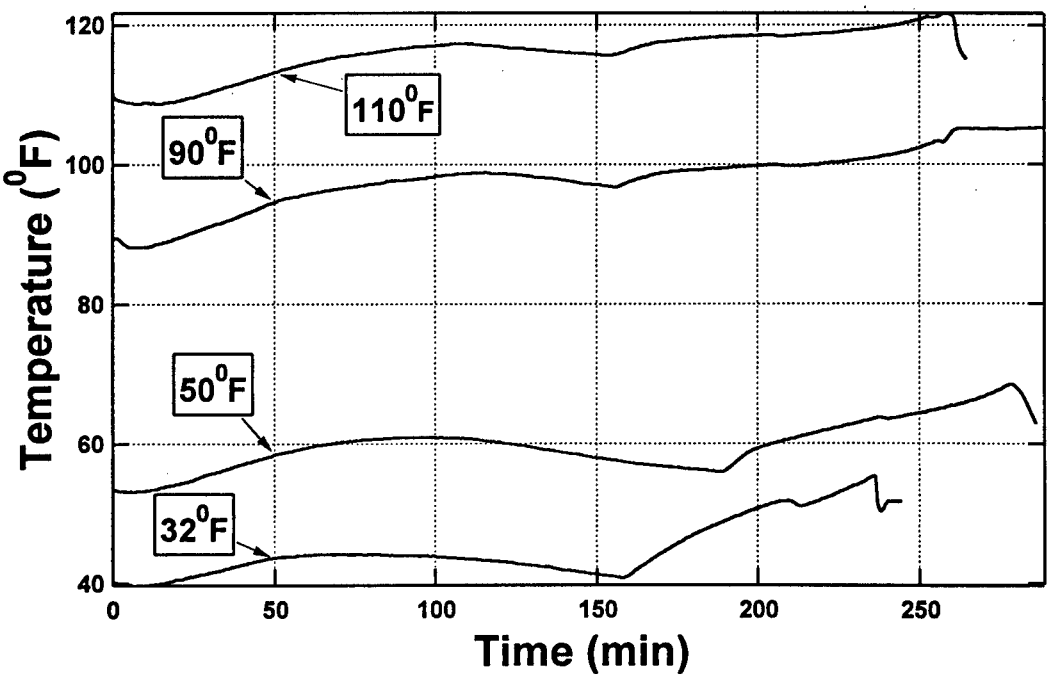

Overcharge of Canon Battery with "Smart" Circuit Board to 10.0 V at 1C Rate

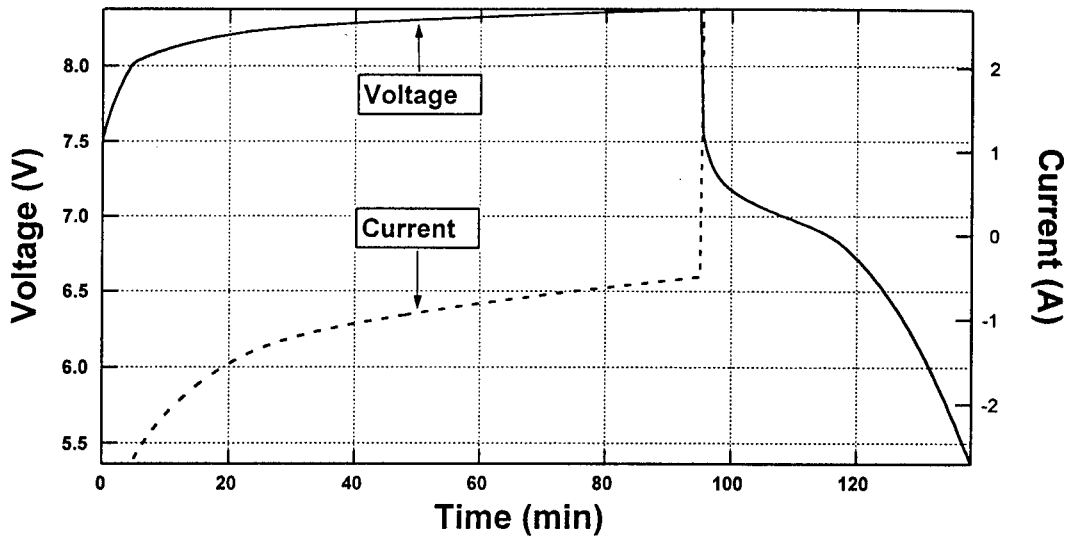

- Voltage does not go above 8.4 V

Overdischarge of Canon Battery to 2.0 V followed by a Charge/Discharge at 1C Rate

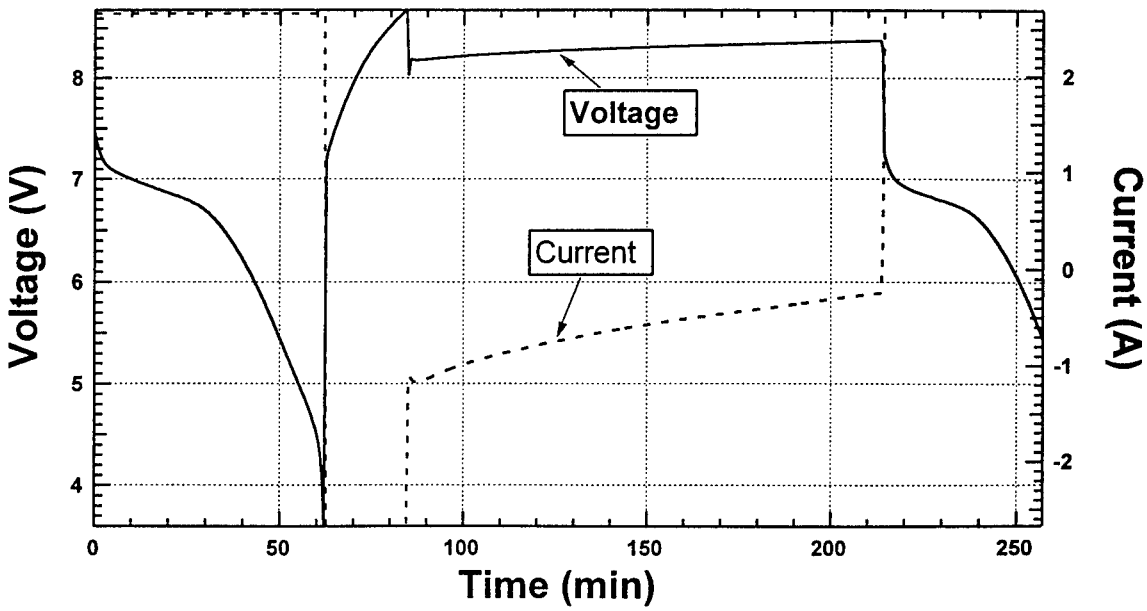

- Voltage does not go below 3.8 V

Charging of Lithium Ion Cells in an Unbalanced Configuration With and Without the Smart Circuit Board

(a)

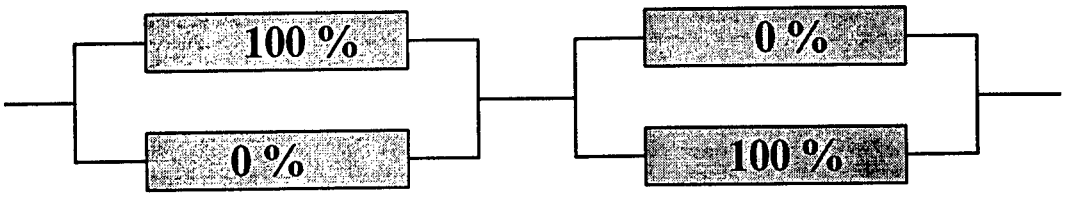

- Cells balance each other even in the absence of circuit board.
- A voltage of 3.8 V at the common nodes was obtained.

Charging of Lithium ion Cells in an Unbalanced Configuration with the Smart Circuit Board

(b)

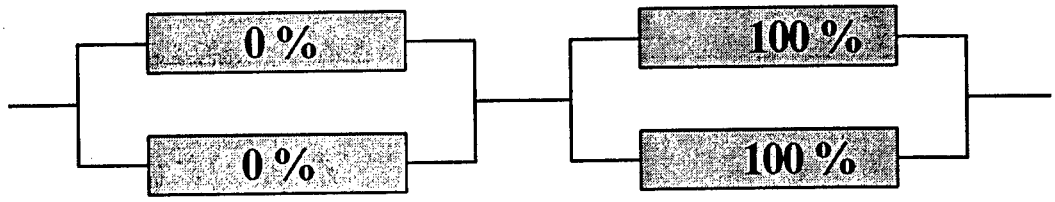

- Very slow charging of cells occurs.
- At the end of six hours the discharged cells (2.7 V) had reached only 3.8 V.
- The charged cells maintained voltage at about 4.4 to 4.5 V.

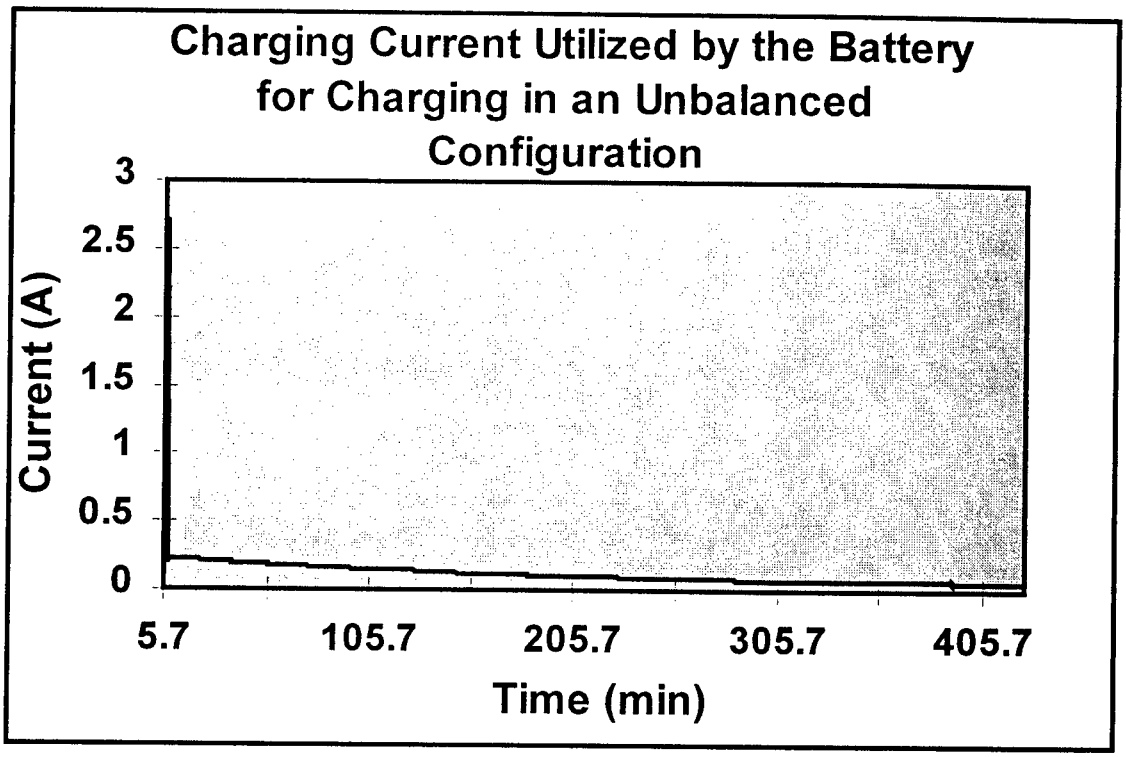

- Current drops to about 0.2 A almost immediately.

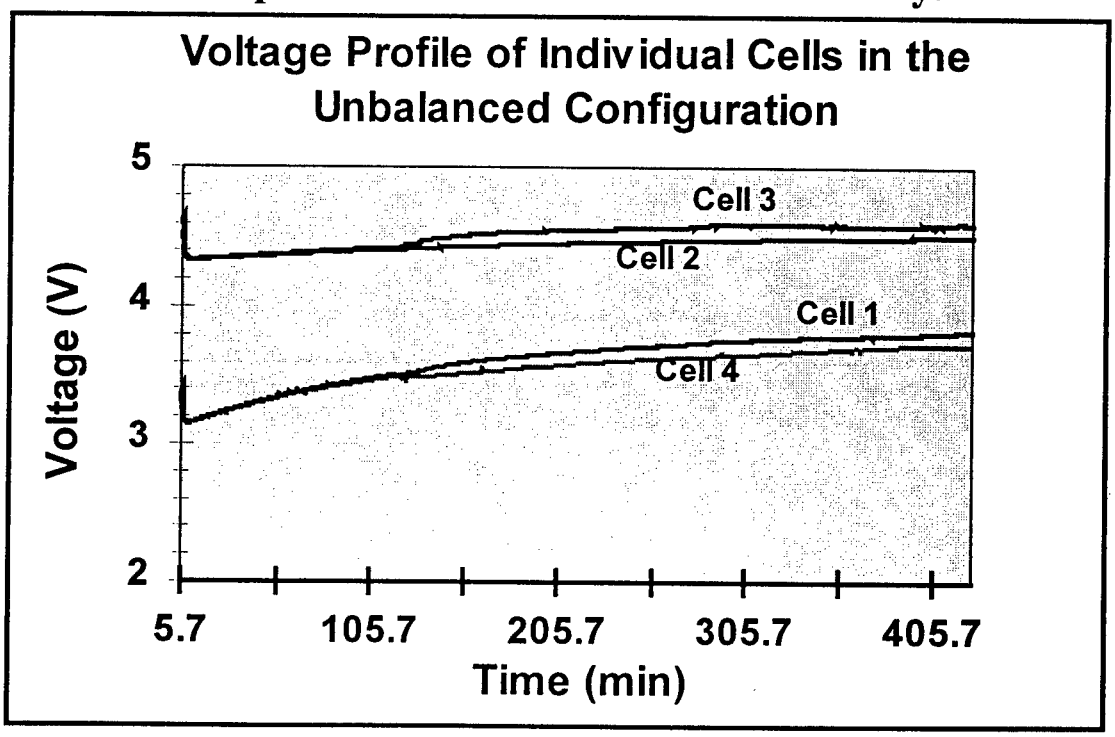

- Voltages rise slowly with the fully charged cells maintaining voltages around 4.5 to 4.6 V. The discharged cells take about 6 hours to reach 3.8 V.

Heat-to-Vent

- Cells thermally abused inside an abuse chamber to cause them to vent.
- Venting occurs above 350 °F, with thermal runaway.
- Vent gases were analyzed using FTIR, GC/MS and compared against standards.

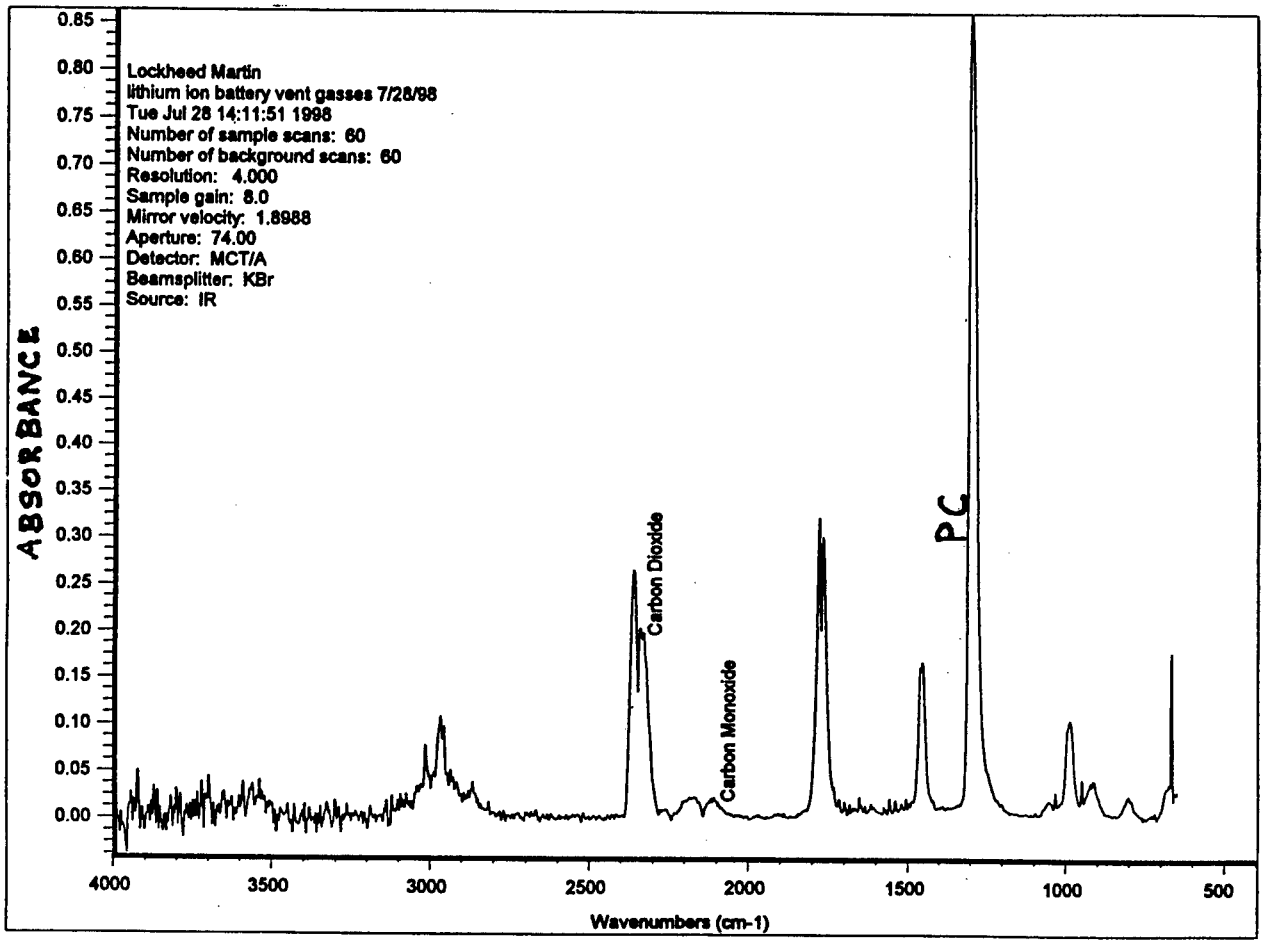

Vibration Test

- The charger, battery pack and cells were subjected to the following vibration spectrum for 15 mins (x, y, z axes)

Frequency	Level
20-80 Hz	+3 dB/octave
80-350 Hz	0.040 g^2/Hz
350-2000 Hz	-3 dB/octave

- Further subjected to the following spectrum for 5 mins (x, y, z axes)

Frequency	Level
20-80 Hz	+3 dB/octave
80-350 Hz	0.1 g^2/Hz
350-2000 Hz	-3 dB/octave

- The battery was subjected to the following spectrum and vibrated for 3 minutes in each of the three mutually perpendicular axes (x, y and z).

Frequency	Level
20-80 Hz	+3 dB/octave
80-350 Hz	0.1 g^2/Hz and 0.2 g^2/Hz
350-2000 Hz	-3 dB/octave

- Finally the battery pack was also shocked 20 times with 11 ms, 20 g^2/Hz sawtooth pulses.

SUMMARY

- **Overcharge:** Tolerant
  CID activated at 5.0 V

- **Overdischarge:** Tolerant

- **High Temperatures:** Tolerant up to about 150 °F (66 °C) (temperature tested). Temperatures >150 °C are required to vent or explode cells. (PTC activated ~130 °C)

- **Drop Test:** Tolerant to drops from 3 ft and 6 ft.

- **External Short circuit:** PTC is activated immediately.

- **Crush Test:** Not consistent. Does not tolerate heavy crush without a heat sink.

- **Thermal tests on battery pack:** Tolerant at all temperatures tested.

- **Overcharging and Overdischarging:** In the battery pack, Smart Circuit board regulates current.

- **Unbalanced Configuration:** In the battery pack, Smart Circuit board regulates current and shunts it around.

- **Heat to vent:** CO, CO_2 gases present. Electrolyte contains DMC, EMC and PC.

- **Vibration test:** Tolerant to five times the level normally used for testing of in-cabin-stowed flight articles.

ACKNOWLEDGEMENTS

Symmetry Resources, Inc. - Sammy Waldrop
Arbin Instruments - Dr. Tracy Piao
NASA-JSC:
ESTA - Jerry Steward
Shane Peck
Brent Hughes
Gwen Gilliam

Chem Lab - Bill Tipton

Bipolar Nickel-Metal Hydride Battery Development Project

prepared by:

John H. Cole

presentation to:

NASA Aerospace Battery Workshop

Contract Agency:

NASA Lewis Research Center

October 27, 1998

Electro Energy Inc.
Shelter Rock Lane
Danbury, CT 06810
203-797-2699
1-800-BIPOLAR
203-797-2697 fax

PROJECT OBJECTIVE: Design of 1 kW Bipolar Ni-MH Battery for LEO-Satellite

Sponsor:	NASA Lewis Research Center
Contractor:	Electro Energy Inc.
Subcontractor:	Eagle-Picher Industries, Inc. Design Automation Associates Rhone-Poulenc, Inc. Rutgers College of Engineering
Duration (Deliverable):	5 Year (Flight-weight Design Package)
Option (Deliverable):	18 Month (3 Flight Quality Batteries)
Technical Requirements:	a. 5-Year Operation in LEO Regime (C:55 min, D: 35 min) b. 40% DOD c. 28 V @ 1kW

Energy Density:	Present SOA	Program Goals
	77 Wh/kg	100 Wh/kg
	175 Wh/l	250 Wh/l
		Challenging-Achievable

PROJECT SUMMARY

Tasks:	Status
Master Work Plan	Complete
Baseline Design	Complete
Component Development	80%
Trade Study	95%
Subscale Bipolar Batteries	66%
Preliminary Design Battery	Complete
Preliminary Boilerplate Hardware	50%
Improved Design Battery	Complete
Improved Design Prototypes	Starts 1998
Optimized Design Battery	Starts 1999
Optimized Design Prototypes	Starts 1999
Final Flight-weight Design	Starts 2000
Prototype Battery Option	Starts 2000

EEI's Stackable Wafer Cell Concept*

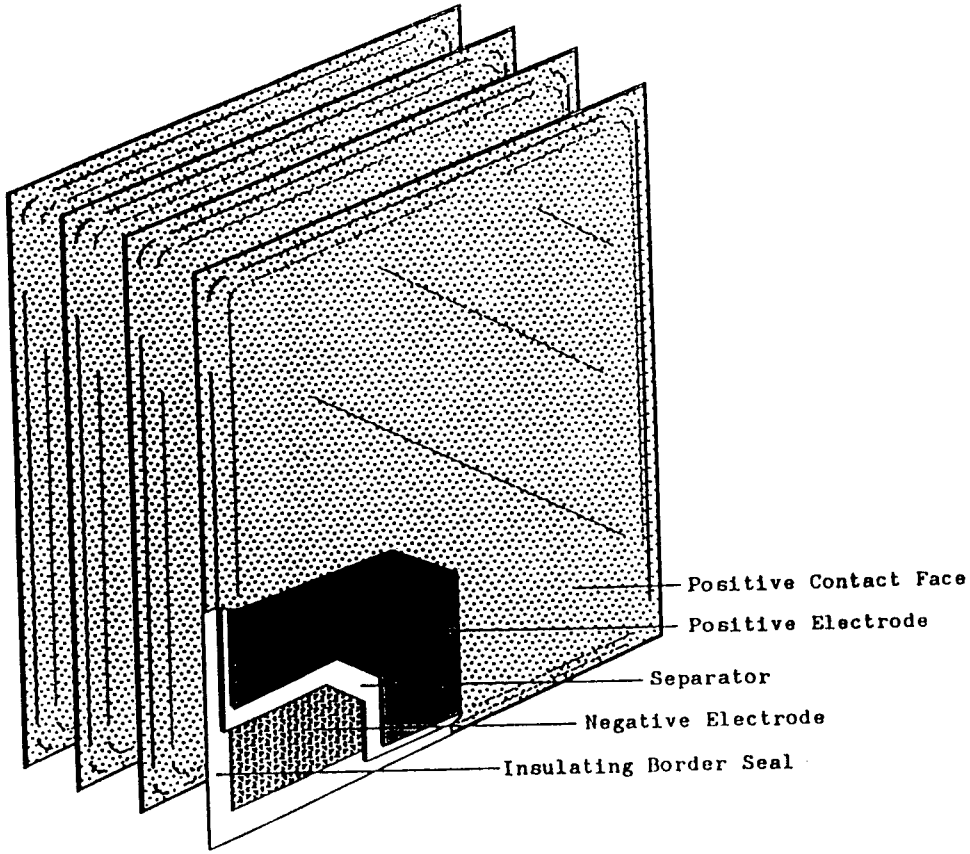

***U.S. Patent #5,393,617**
U.S. Patent #5,552,243

Electro Energy's Bipolar Nickel Metal Hydride Battery

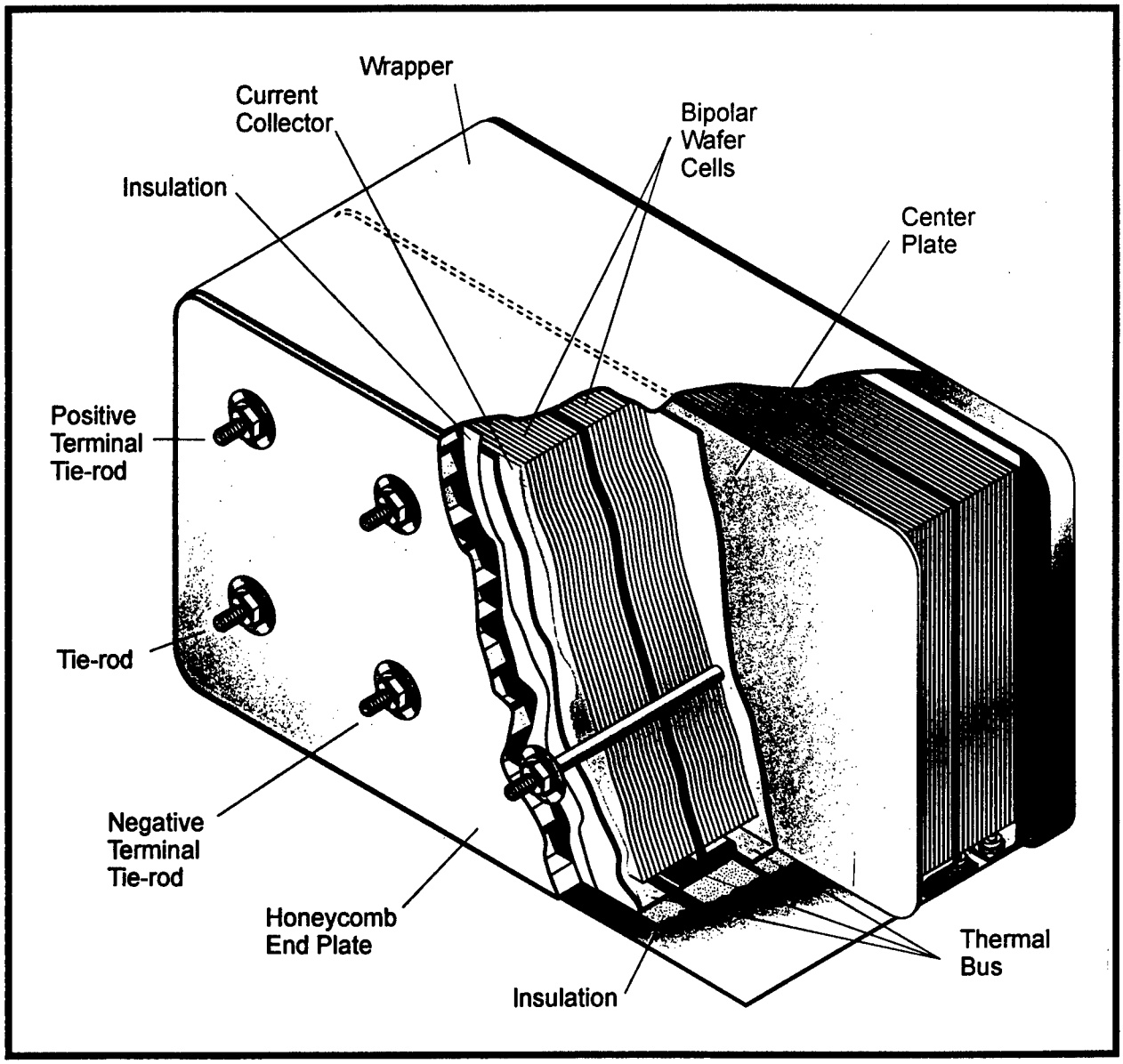

Electro Energy, Inc.

Shelter Rock Lane
Danbury, CT 06810
(203) 797-2699

ADVANTAGES OF EEI WAFER BIPOLAR DESIGN

- Each cell individually sealed
- Allows repair or replacement of individual cells
- No external cell terminals
- No electrode current collectors
- Compatible with plastic bonded electrodes
- Adaptable to heat transfer fins placed in stack
- Scalable to large area, capacity, high voltage
- Automated flexible manufacturing
- Improved energy and power density
- Lower cost

COMPONENT DEVELOPMENT

Component Testing

- Three inch square bipolar wafer cell construction
- Test against baseline Ni or MH electrode with the baseline separator
- Vented, flooded cells
- Sealed starved electrolyte cells
- 50% DOD LEO cycles (55 min. Charge, 35 min. discharge)
- Charge Control:
  - Timed charge & discharge
  - 5% overcharge
- Build & test sample set cells in quadruplicate
- Build & test control cells in duplicate
- DPA Critical Experiments

COMPONENT DEVELOPMENT (cont'd)

Nickel Electrode Development

- Advanced EEI treated nickel compounds:

  Coating Thickness - Suppliers: Tanaka, Skerrit
  Alloying
  NiOH Particle Size
  Microstructure

- EEI plastic bonded nickel construction

- Sintered porous nickel

- Electrochemically impregnated fiber of foam plaque

- Pasted fiber of foam plaque

Resource Allocation

- EEI, EIP, RU

COMPONENT DEVELOPMENT (cont'd)

Metal Hydride Electrode Development

- Incremental Improvements of AB_5:
  - Refractor Metal Substitution Alloys
  - High Stoichiometric Ration Alloy with Mo and/or Si Additions
  - Modified RP40 Grade Alloy
- Radical Improvements of Rechargeable Battery Alloys
  - Mg_2Ni Alloys
  - Li_2Mg_{17} Alloys
- Plastic Bonded & Sintered AB_5 ($LaNi_5$) Construction
- Iron Titanium (FeTi) Doped Magnesium Compounds
- Protective Alloying or Coating

Resource Allocation

- EEI, EPI, Rh-P

COMPONENT DEVELOPMENT (cont'd)

Testing Summary

- **Up to 7000 LEO Cycles @ 50% DOD (Tripled Cycle-Life)**
- Up to 9200 LEO Cycles @ 25% DOD (1.18 volts @ EOD)
- 340 Sets of Cells Built and Tested - About **800** Cells
- Computer Controlled Automated Test Systems
- EEI and EPI Ni Electrodes
- EEI and EPI MH Electrodes

Replanned as a Four Year Task

COMPONENT DEVELOPMENT (cont'd)

Foil Cell Design

- Developed a wafer cell using nickel foil instead of carbon plastic
- Advantages:
  - Lower contact resistance between cells
  - No permeation from sealed cells
  - Stronger wafer package
  - Higher lateral thermal conductivity
  - Long Life
- Disadvantages
  - Increases Cell Assembly Labor
  - Increases Weight (slightly)
- Vented Flooded
  - L175a - 7,400 LEO cycles
  - L142b - 7,000 LEO cycles
- Sealed
  - L225b - 2,600 LEO cycles
  - L229f - 2,120 LEO cycles

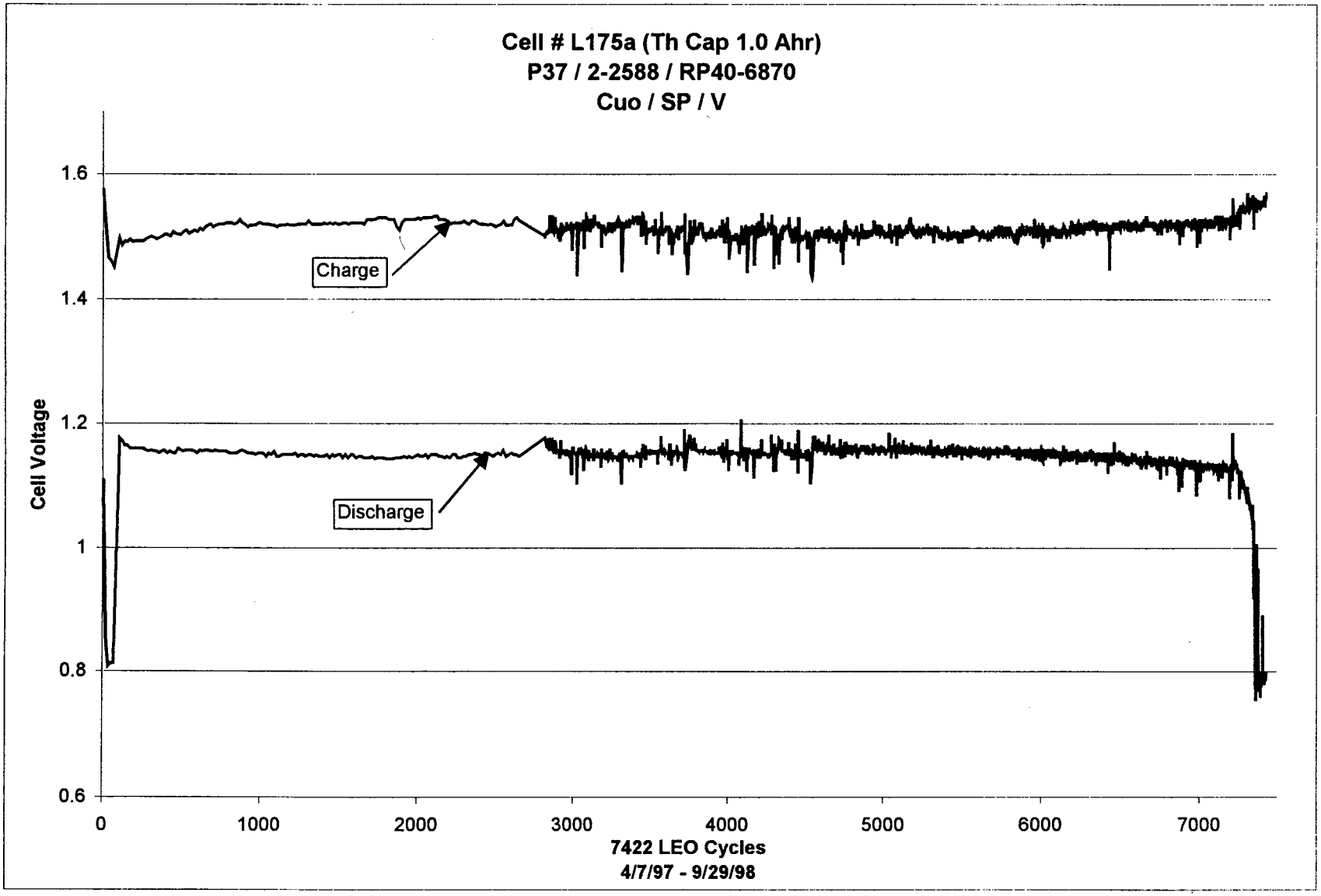
Cell # L175a (Th Cap 1.0 Ahr)
P37 / 2-2588 / RP40-6870
Cuo / SP / V
Cell Voltage
1.6
1.4
1.2
1
0.8
0.6
Charge
Discharge
0
1000
2000
3000
4000
5000
6000
7000
7422 LEO Cycles
4/7/97 - 9/29/98

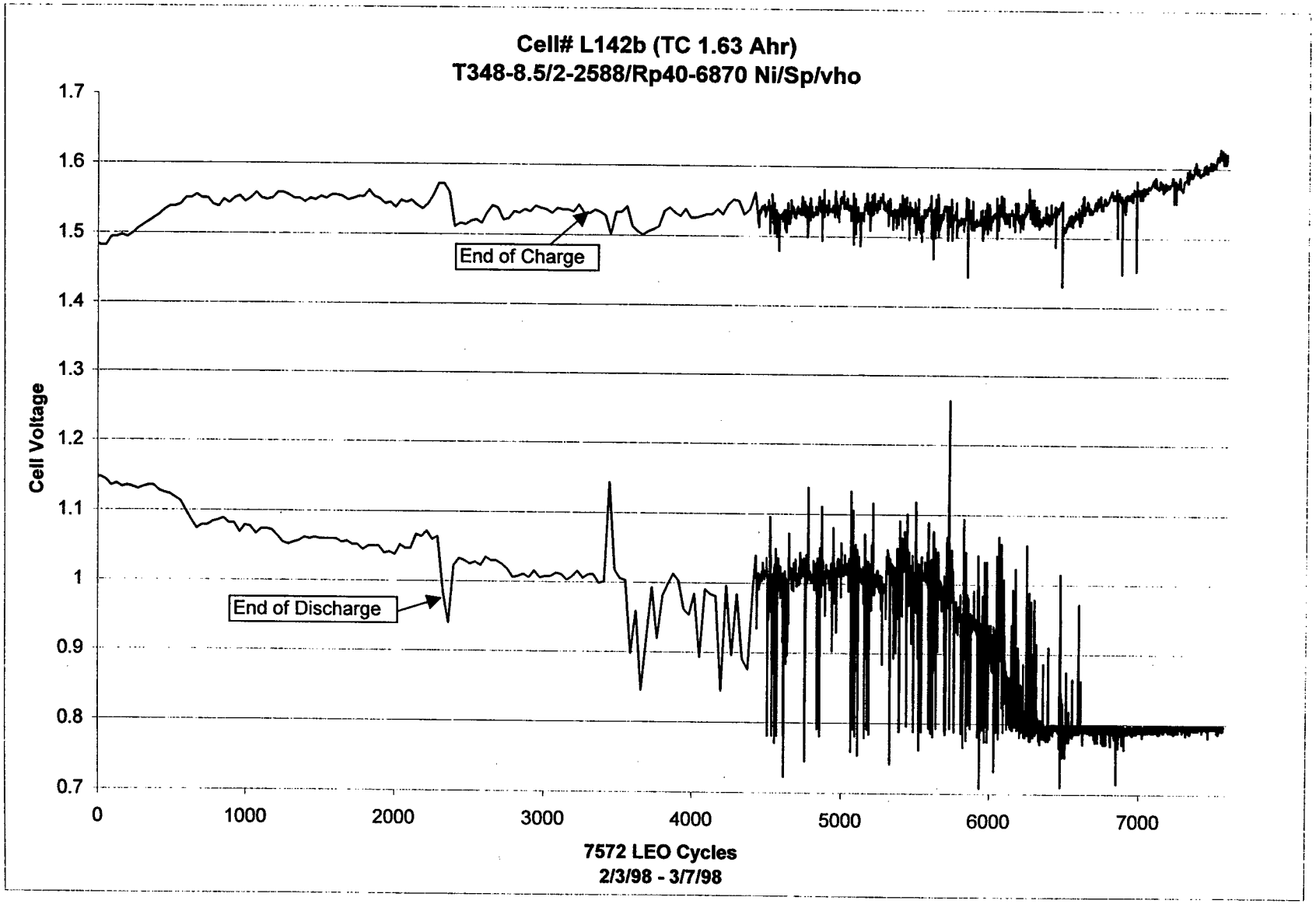
Cell# L142b (TC 1.63 Ahr)
T348-8.5/2-2588/Rp40-6870 Ni/Sp/vho
Cell Voltage
1.7
1.6
1.5
1.4
1.3
1.2
1.1
1
0.9
0.8
0.7
0
1000
2000
3000
4000
5000
6000
7000
End of Charge
End of Discharge
7572 LEO Cycles
2/3/98 - 3/7/98

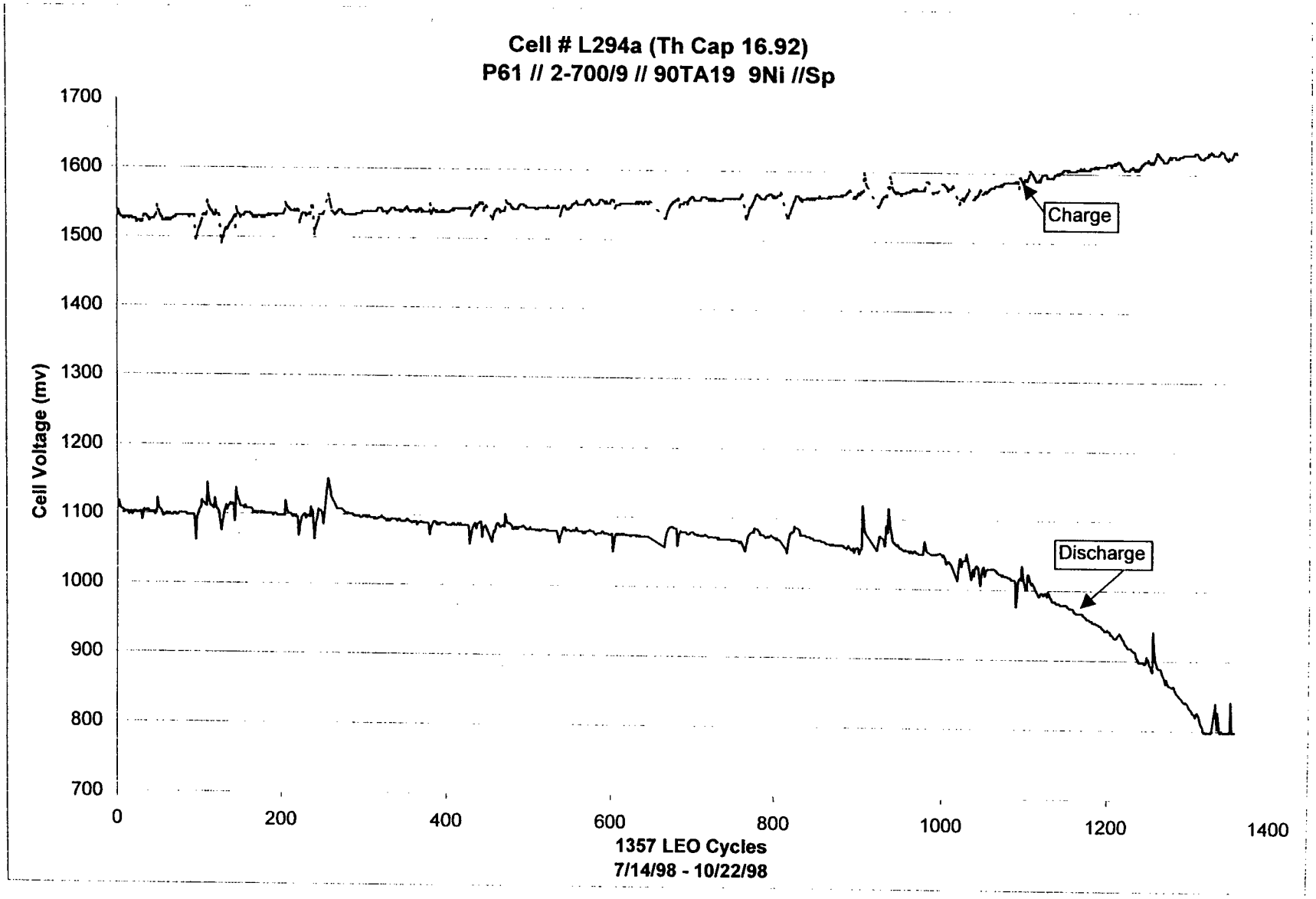
Cell # L294a (Th Cap 16.92)
P61 // 2-700/9 // 90TA19 9Ni //Sp
Cell Voltage (mv)
1700
1600
1500
1400
1300
1200
1100
1000
900
800
700
0
200
400
600
800
1000
1200
1400
Charge
Discharge
1357 LEO Cycles
7/14/98 - 10/22/98

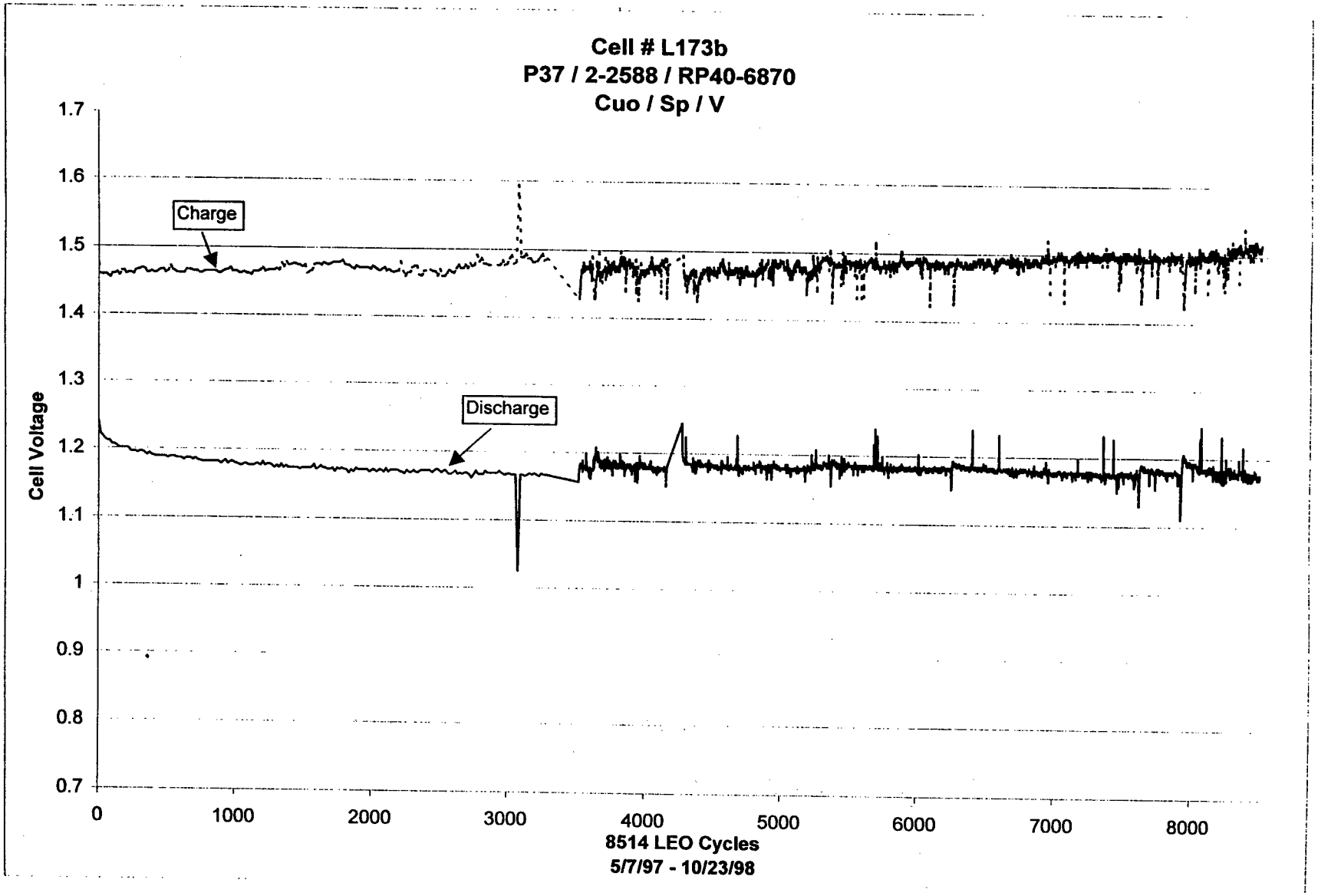
Cell # L173b
P37 / 2-2588 / RP40-6870
Cuo / Sp / V
Charge
Discharge
Cell Voltage
1.7
1.6
1.5
1.4
1.3
1.2
1.1
1
0.9
0.8
0.7
0
1000
2000
3000
4000
5000
6000
7000
8000
8514 LEO Cycles
5/7/97 - 10/23/98

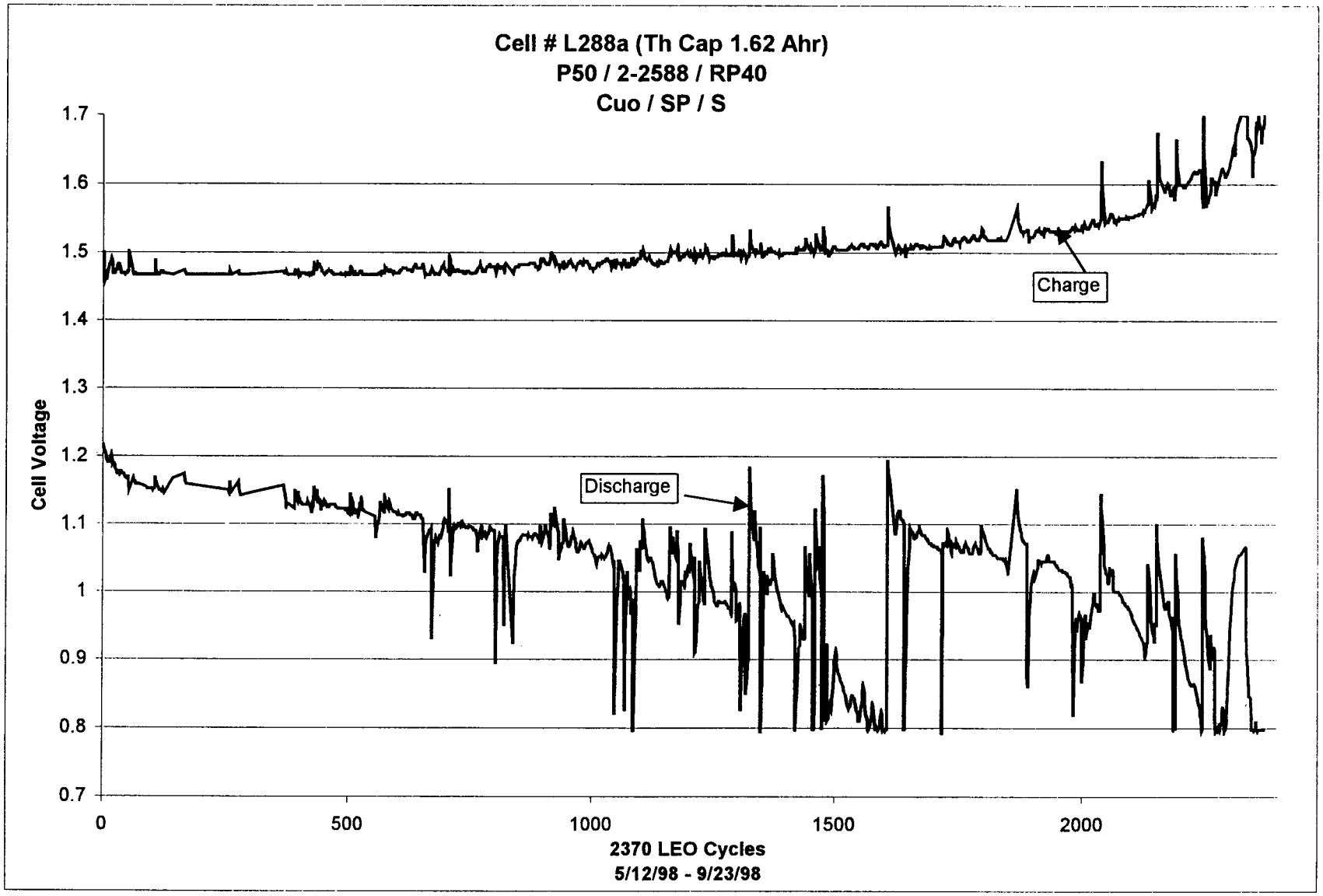
Cell # L288a (Th Cap 1.62 Ahr)
P50 / 2-2588 / RP40
Cuo / SP / S
Cell Voltage
1.7
1.6
1.5
1.4
1.3
1.2
1.1
1
0.9
0.8
0.7
Charge
Discharge
0
500
1000
1500
2000
2370 LEO Cycles
5/12/98 - 9/23/98

COMPONENT EVALUATION IN BIPOLAR CONFIGURATION

Subscale Bipolar Batteries

- Assemble 5-cell Stacks
- Construct Three Inch Square, Sealed, Starved Electrolyte Samples
- Test Three Top Ni Electrodes Against a Baseline MH
- Test Three Top MH Electrodes Against a Baseline NI
- Test for 500 to 1000 LEO Cycles at 50% DOD
- Perform DPA EEI & RU

Test Status:

- On-going: 1,100 LEO Cycles (to date) at 50% DOD; 1.15V @ EOD

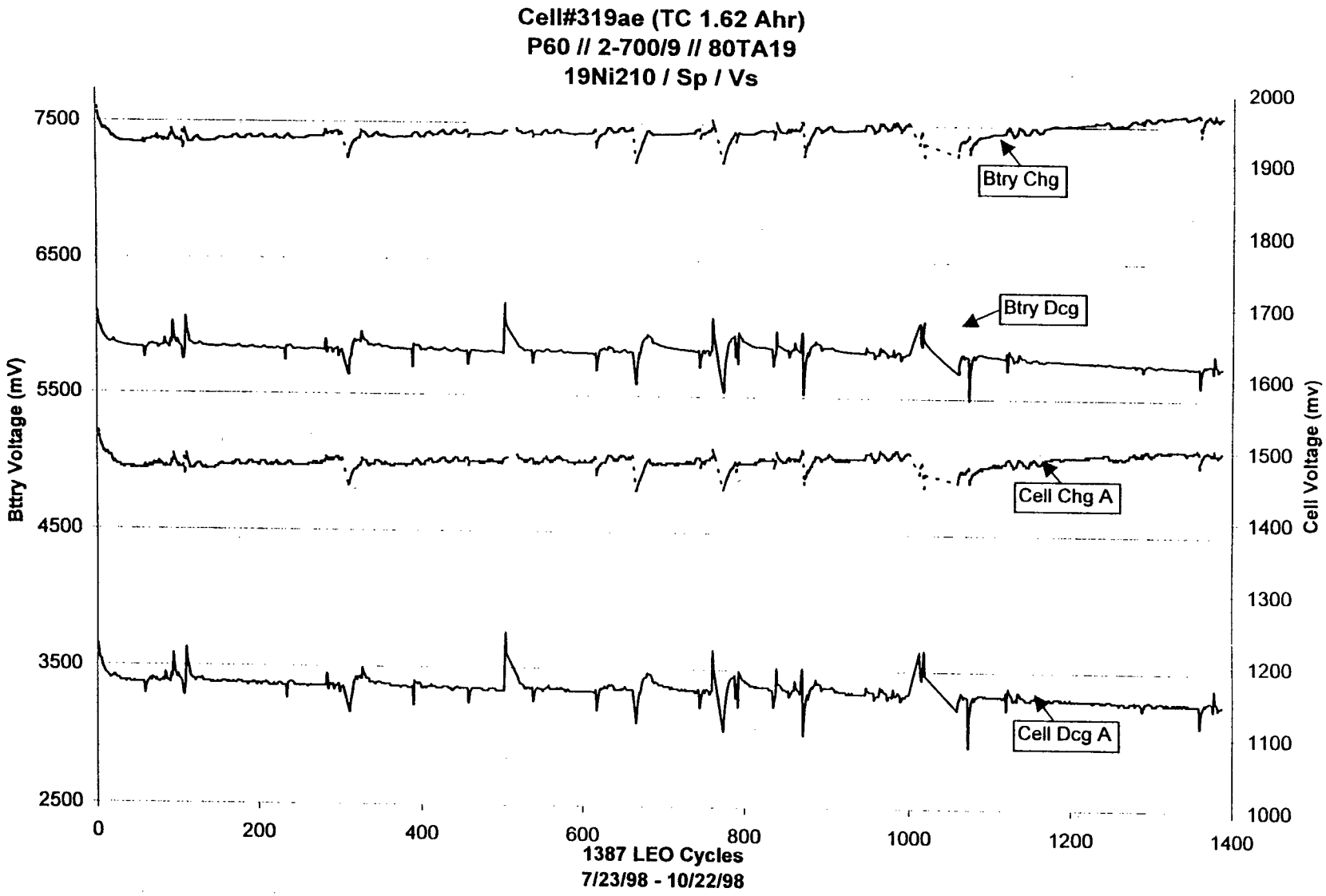
Cell#319ae (TC 1.62 Ahr)
P60 // 2-700/9 // 80TA19
19Ni210 / Sp / Vs
Btry Voltage (mV)
7500
6500
5500
4500
3500
2500
Cell Voltage (mv)
2000
1900
1800
1700
1600
1500
1400
1300
1200
1100
1000
Btry Chg
Btry Dcg
Cell Chg A
Cell Dcg A
0
200
400
600
800
1000
1200
1400
1387 LEO Cycles
7/23/98 - 10/22/98

TRADE STUDY

Rules Based Technology

- Vary all electrode and cell components
- Prismatic vs Cylindrical Configurations
- Single vs Multiple Stack

Output Summary

- Coverpage - Bottom line results and 3D wireframe
- Input/Output Report - I/O by Category
- Weight Summaries - Battery, Cells and Hardware
- Layout - Front View, X-section and details
- Producibility Report
- Costed BOM
- Maintenance Guidelines

Automated Structural Analysis

- Cell Squeeze, Cyclic and Steady State Pressures
- Batch or Interactive
- 3-D wireframe model
- Area Summary
- Goodman Margins
- Contour Plot and Deformation Animation

TRADE STUDY (cont'd)

Automated Thermal Analysis

- Cold plate Location and Temperature, Power Profile
- Batch or Interactive
- 3-D wireframe model
- Area Summary
- Graphs of Max and Min Cell Temp
- Contour Plot of Cells

Trade Study Results		Battery Energy Density
♦ Baseline Flight-weight Design	-	66 Wh/kg 1995
♦ Preliminary Flight-weight Design	-	77 Wh/kg 1997
♦ Optimized Flight-weight Design	-	83 Wh/kg 1998

IMPROVED DESIGN FLIGHT-WEIGHT BATTERY SUMMARY

- Function:
  - The Improved Design Flight-weight Battery is a Flight-weight Battery Design for LEO Satellite applications.
- Description:
  - The battery is prismatic (rectangular) in shape.
  - The outer enclosure serves to contain cell stack pressure and is hermetically sealed.
  - Tie rods are used to maintain cell stack compression.
  - The battery has two (electrically parallel) 24-cell stacks (48 cells). Internal pressure is regulated by a preset relief valve.
  - There are four thermo-couples to monitor internal temperatures.

IMPROVED DESIGN FLIGHT-WEIGHT BATTERY SUMMARY (cont'd)

Design Requirements:

a.	Voltage:	28 V
b.	Current:	22.7 A Charge, 35.7 A Discharge
c.	Power:	1 Kilowatt
d.	Battery Capacity:	52 A-hr (20.8 A-hr at 40% DOD)
e.	Cell Weight (wet):	157 grams
f.	Cell Energy Density:	114 Wh/kg
g.	Cell Capacity:	26 Amp hours
h.	Current Density:	77 mA/cm^2
i.	Cycle Life:	30,000
j.	Operating Temperature:	-10° C to +25° C
k.	Overcharge:	5%
l.	Electrical Insulation Resistance:	> 1 megohm @ 100 VDC
m.	Cooling:	Conductive baseplate
n.	Maximum Temperature Change:	25° C above cold plate
o.	Thermal Generation:	128 Watts Average

IMPROVED DESIGN FLIGHT-WEIGHT BATTERY SUMMARY (cont'd)

Size

- Overall dimensions of the battery case are approximately 12.6" wide by 7.2" high by 4.7" deep
- The Nickel-Metal Hydride cells (12) are approximately: 0.066" thick by 6.56" high by 12.56" wide

Materials

- Enclosure - Titanium
- Thermal Plates - Ni plated aluminum
- Cells:
  - The lightweight Nickel electrode is plastic bonded treated Nickel Hydroxide.
  - The separator consists of one layer of Pellon 2588.
  - The Metal Hydride electrode is EEI plastic bonded RP40.
  - The Electrolyte is 30% by weight Potassium Hydroxide solution with 1% Lithium Hydroxide.
  - Nickel Foil Cell Face.
  - Epoxy Insulating Frame.
- Tie Rods - Titanium
- Current Collectors - Nickel Foil

IMPROVED DESIGN FLIGHT-WEIGHT BATTERY SUMMARY (cont'd)

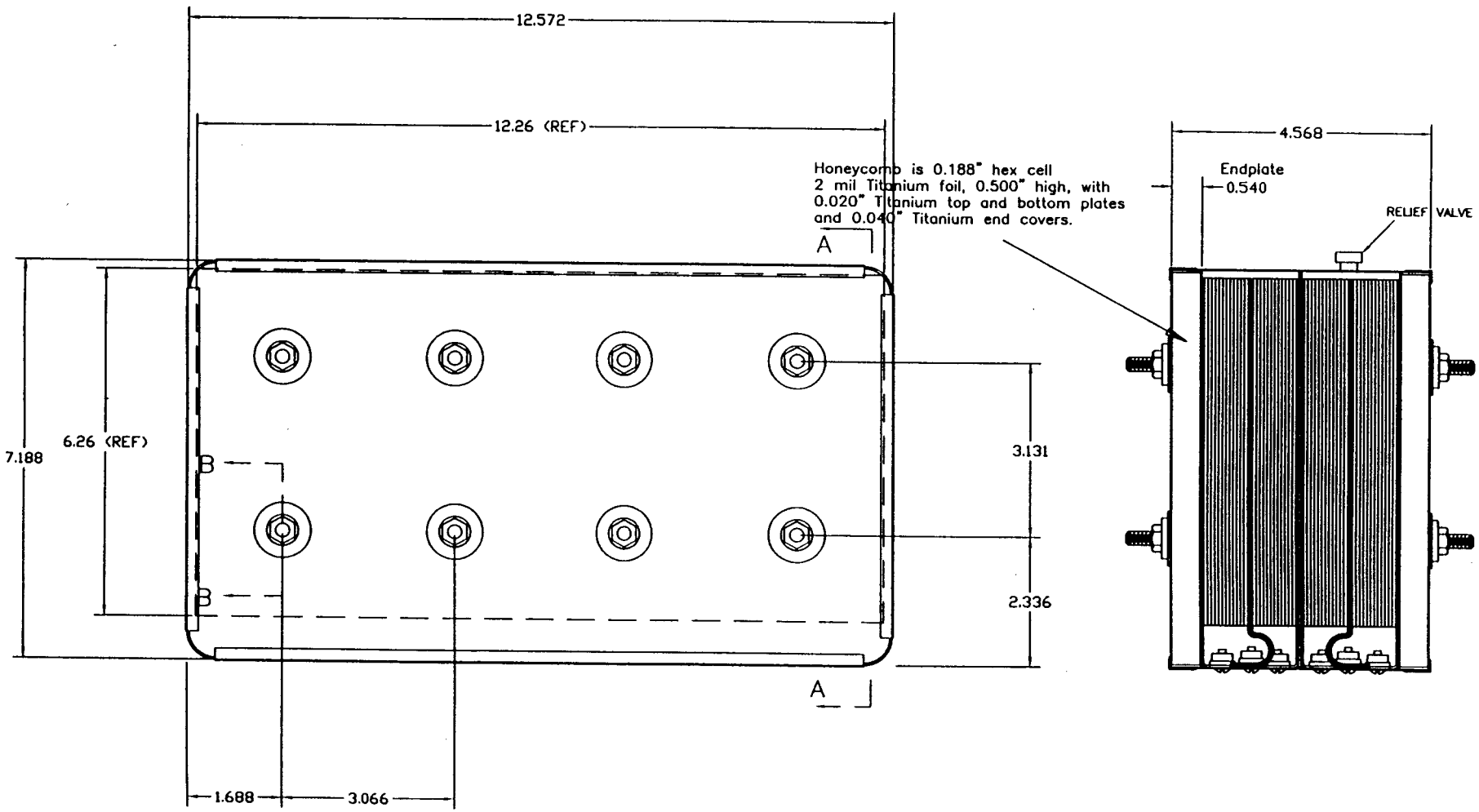

Battery Weight Summary

Battery Weight Table			
Item	Wt.(g)	Wt.(lbs)	Wt.%
Metal–Hydride	5500.0	12.1	31.3
M–H Electrode Additives	27.6	0.1	0.2
Nickel Base & Additives	442.6	1.0	2.5
Active Material Ni Hydroxide	4552.9	10.0	25.9
Electrolyte	2534.1	5.6	14.4
Remainder of Wafer Cell	679.9	1.5	3.9
Thermal Buss	1528.2	3.4	8.7
Stack Hardware	700.2	1.5	4.0
Enclosure and Endplates	1447.6	3.2	8.2
Miscellaneous Items	134.7	0.3	0.8
Total	17548.0	38.7	100

Battery Weight Distribution

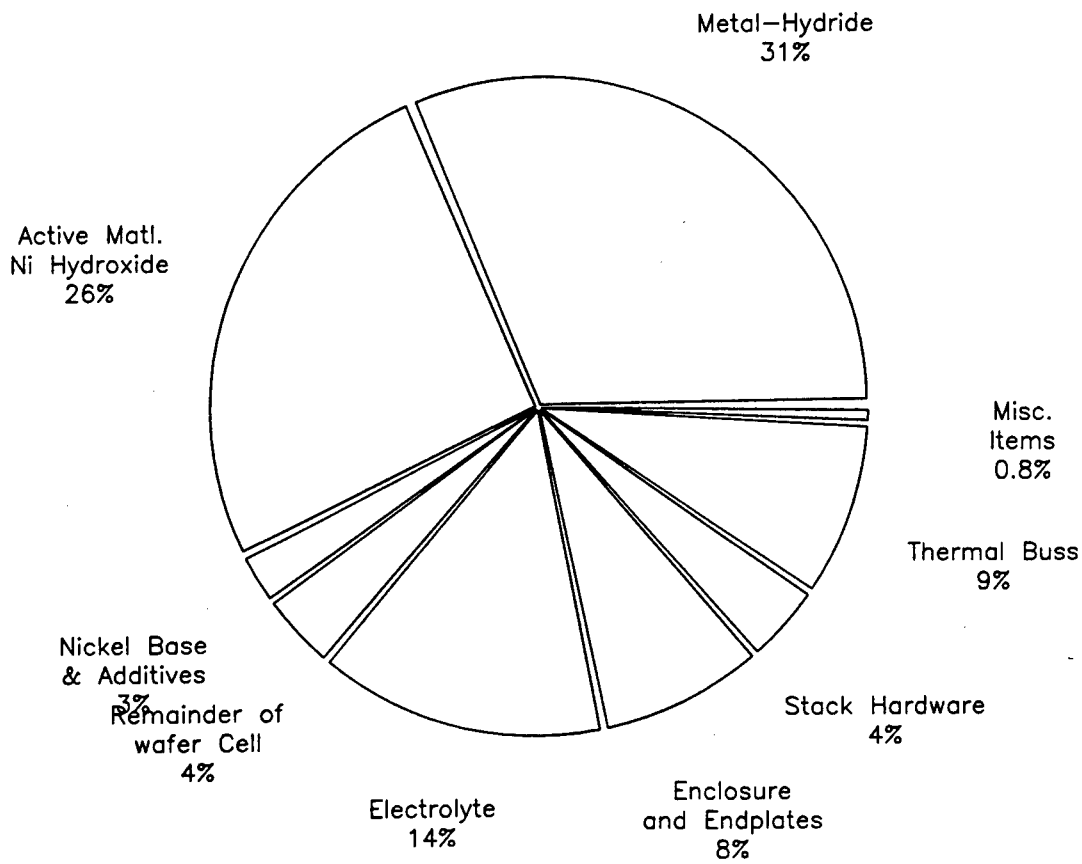

Electro Energy, Inc.
Design Automation Associates
Version: R1.15

Page 6 of 13

NASA Lewis
Research Center
Date: October 20, 1998

Wafer Cell Weight Summary

Wafer Cell Weight Table		
Item	Wt.(g)	Wt.%
Active Material	94.9	33.1
Ni Electrode Additives	9.2	3.2
Metal–Hydride	114.6	40.0
M–H Electrode Additives	0.6	0.2
Washer	0.4	0.1
Separator(s)	2.2	0.8
Electrolyte	52.8	18.4
Insulating Frame	0.8	0.3
Cell Face	10.8	3.8
Total	286.2	100

Wafer Cell Weight Distribution

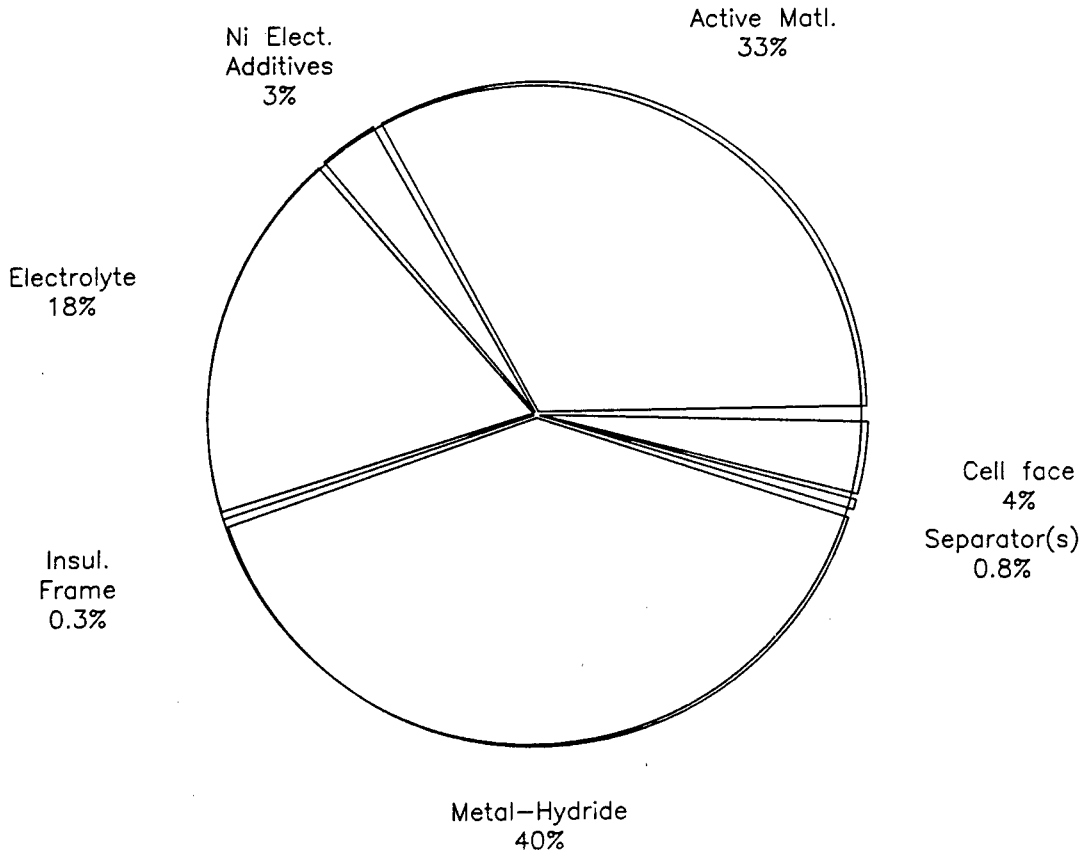

Electro Energy, Inc.
Design Automation Associates
Version: R1.15

Page 7 of 13

NASA Lewis
Research Center
Date: October 20, 1998

PRELIMINARY DESIGN BOILERPLATE BATTERY SUMMARY

- Function:
  - The Preliminary Design Boilerplate Battery is a prototype of the Flightweight Battery Design for Development Testing.
- Description:
  - The battery is prismatic (rectangular) in shape.
  - The outer enclosure serves to contain cell stack pressure and is sealed with o-rings and a gasket.
  - Tie rods are used to maintain cell stack compression.
  - The battery has one 12-cell stack. Internal pressure is regulated by a preset relief valve.
  - There are thermo-couples to monitor internal temperatures.

PRELIMINARY DESIGN BOILERPLATE BATTERY SUMMARY (cont'd)

Size

- Overall dimensions of the battery case are approximately 9.4" wide by 2.5" high by 13.6" long
- The Nickel-Metal Hydride cells (12) are approximately: 0.085" thick by 6.56" high by 12.56" long

Materials

- Enclosure - Ni plated aluminum
- Thermal Plates - Ni plated aluminum
- Cells:
  - The lightweight Nickel electrode is plastic bonded treated Nickel Hydroxide.
  - The separator consists of two layers of Pellon 2588.
  - The Metal Hydride electrode is EEI plastic bonded RP40.
  - The Electrolyte is 30% by weight Potassium Hydroxide solution with 1% Lithium Hydroxide.
  - Nickel Foil Cell Face.
  - Epoxy Insulating Frame.
- Tie Rods - Zinc plated steel
- Current Collectors - Nickel Foil
- Seals - Neoprene

PRELIMINARY DESIGN BOILERPLATE BATTERY SUMMARY (cont'd)

Design Requirements:

a.	Voltage:	14.4 V
b.	Current:	7.9 A Charge, 11.9 A Discharge
c.	Power:	.249 Kilowatt
d.	Battery Capacity:	17.3 A/hr (6.9 A/hr at 40% DOD)
e.	Cell Weight (wet):	313 grams
f.	Cell Energy Density:	63 Wh/kg
g.	Cell Capacity:	17.3 Amp hours
h.	Current Density:	26 mA/cm^2
i.	Cycle Life:	TBD
j.	Operating Temperature:	-10° C to +25° C
k.	Charge Retention:	TBD
l.	Overcharge:	5%
m.	Electrical Insulation Resistance:	> 1 megohm @ 100 VDC
n.	Cooling:	Conductive baseplate
o.	Maximum Temperature Change:	25° C above cold plate
p.	Thermal Generation:	32 Watts Average

PRELIMINARY DESIGN BOILERPLATE BATTERY TASK

- Test Results:
  - Theoretical Capacity: 17.3 A-hrs
  - Formation Capacity: 13.0 A-hrs
  - LEO Test (40% DOD, 5% OC): On-going

- Future Work:
  - Build a second PDBB (Nov. 98)
  - DPA first PDBB (1999)

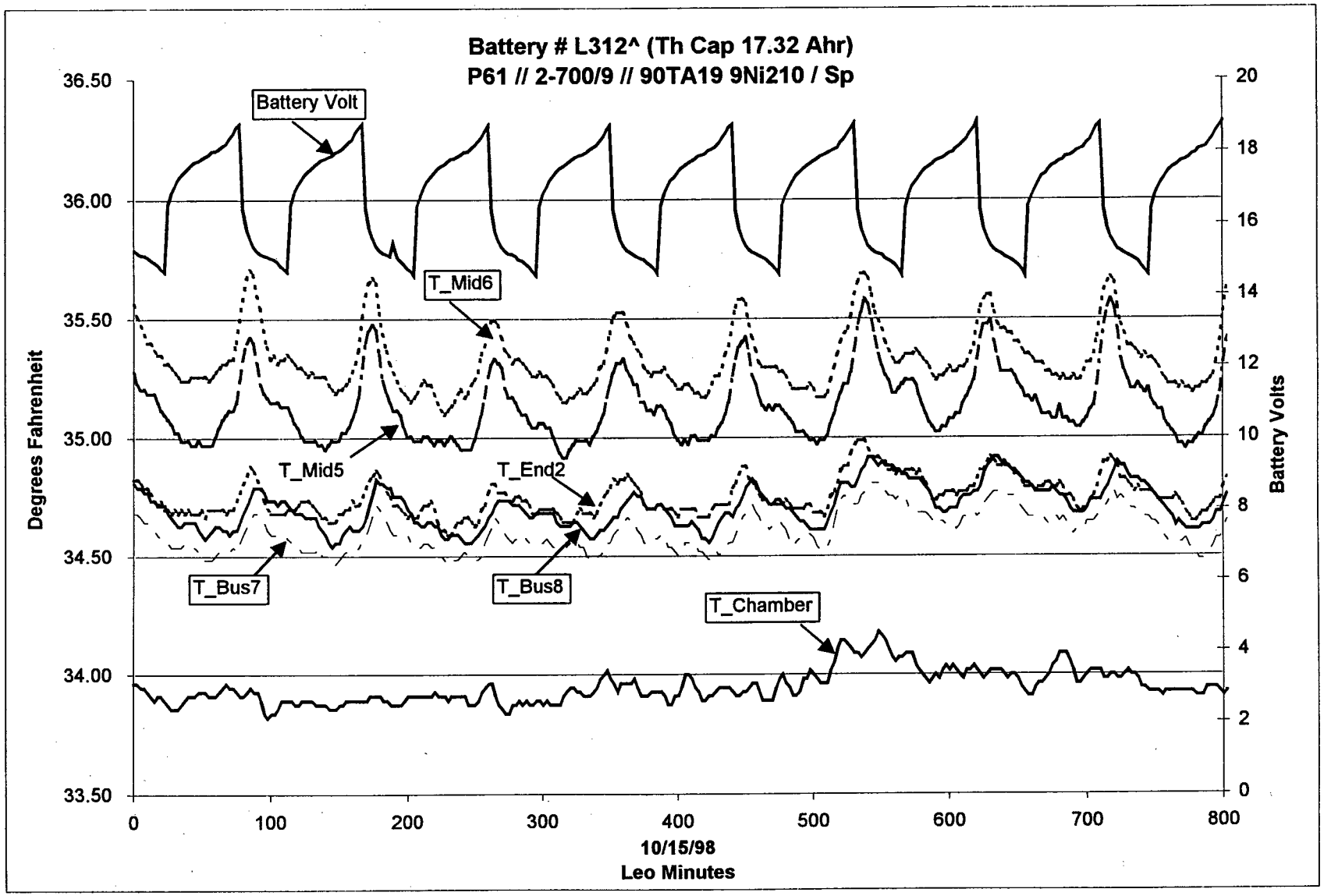
Battery # L312^ (Th Cap 17.32 Ahr)
P61 // 2-700/9 // 90TA19 9Ni210 / Sp
Battery Volt
T_Mid6
T_Mid5
T_End2
T_Bus7
T_Bus8
T_Chamber
Degrees Fahrenheit
Battery Volts
36.50
36.00
35.50
35.00
34.50
34.00
33.50
20
18
16
14
12
10
8
6
4
2
0
0
100
200
300
400
500
600
700
800
10/15/98
Leo Minutes

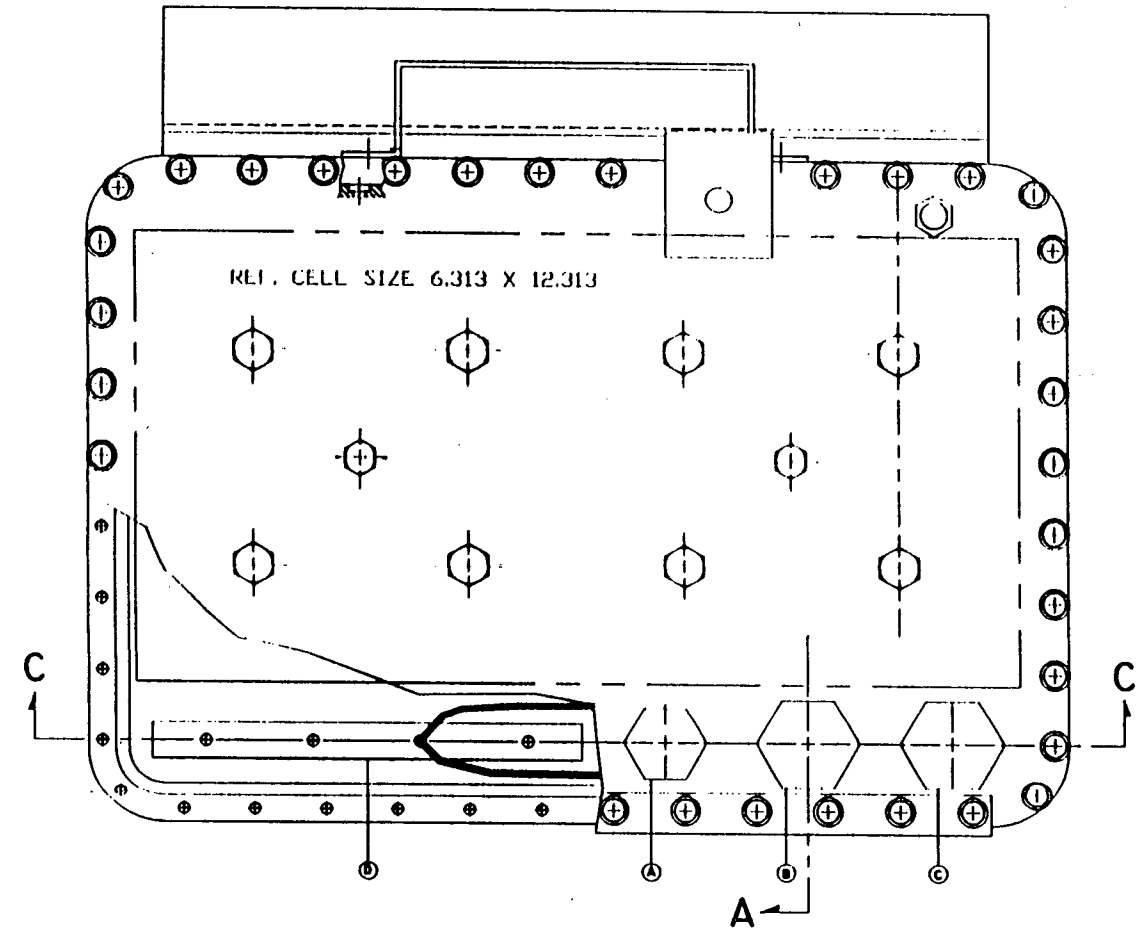

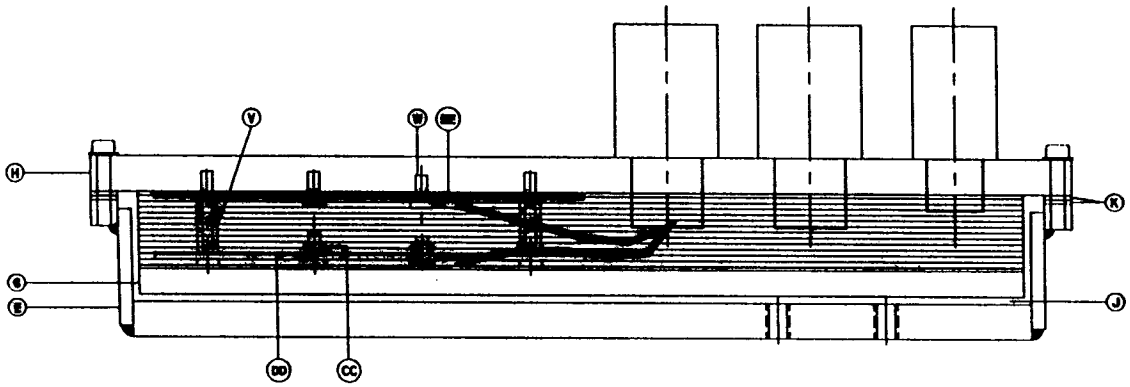

SECTION C-C

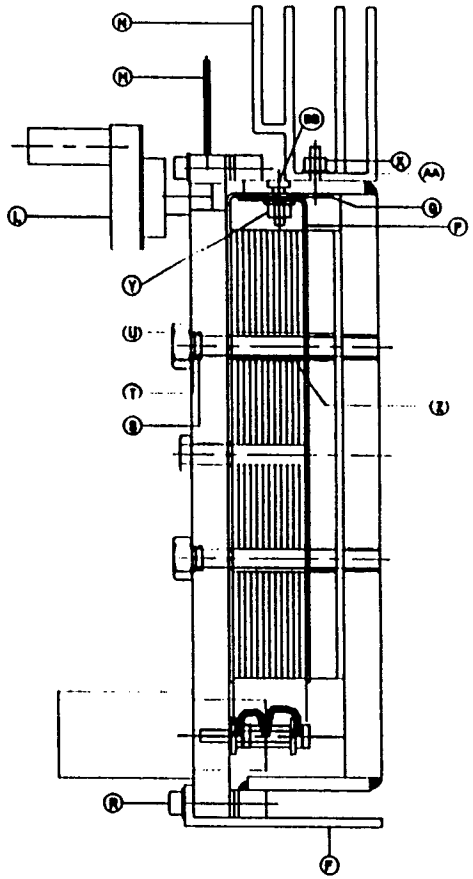

SECTION A-A

PART LIST

ITEM	DESCRIPTION	DWG. OR PART NUMBER	QTY.
A	1/2" SEALED ELECTRICAL FEED	MHCA-040-8	1
B	3/4" SEALED ELECTRICAL FEED	PL-12-2	1
C	3/4" SEALED ELECTRICAL FEED	MHC5-032-16	1
D	BUS BAR	DA-018	1
E	HOUSING WELDMENT	DA-004	1
F	STAND	DA-016	1
G	FLOATING PLAT	DA-011	1
H	COVER	DA-005	1
J	FOAM RUBBER FILL GAP		1
K	GASKETS	DA-019	2
L	OMEGA INDUSTRIAL PRESSURE TRANSDUCER		1
M	HANDLE	MCMASTER CARR P#169A11	1
N	COOLING FAN	DA-015	1
P	THERMAL BUS	DA-013	1
Q	THERMAL BUS, STUD DESIGN	DA-014	1
R	#10-32 SOCKET HEAD SCREW		44
S	O'RING		8
T	BACK UP O'RING		8
U	#1/4-20 BOLT		8
V	#8-32 NYLON STANDOOF 1/4" HEX. X 1"		2
W	#8-32 X .375 SCREW		6
X	#8 NUT		11
Y	#6 SELF LOCKING NUT		11
Z	#1/4-20 TIE RODS		8
AA	#8 WASHER		10
BB	SELF SEALING SCREWS		11
CC	#8 N UT		2
DD	#8 WASHER		2
EE	12 GA. WIRE LUG		2

Preliminary Design Bipolar Ni MHPrototype Battery

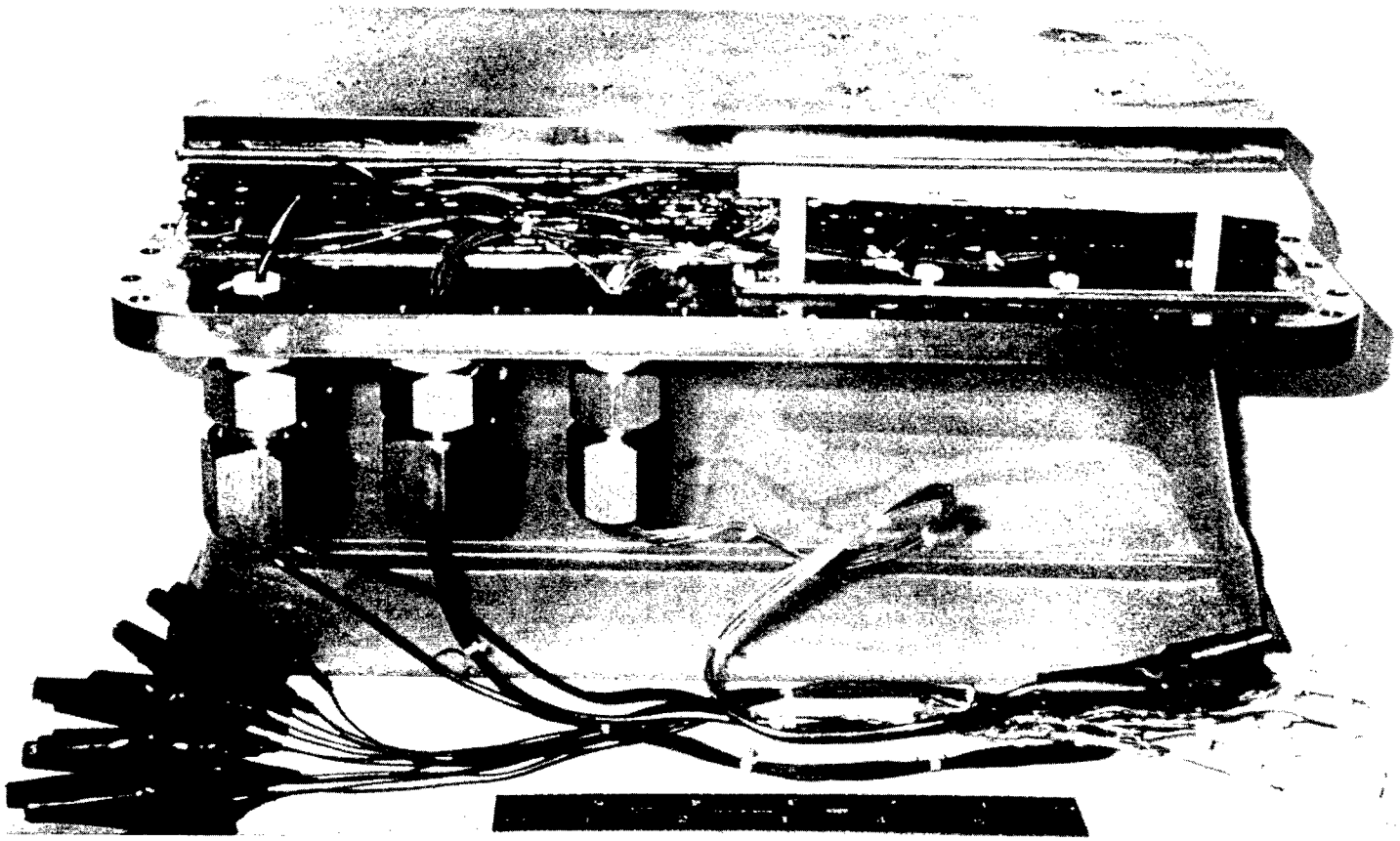

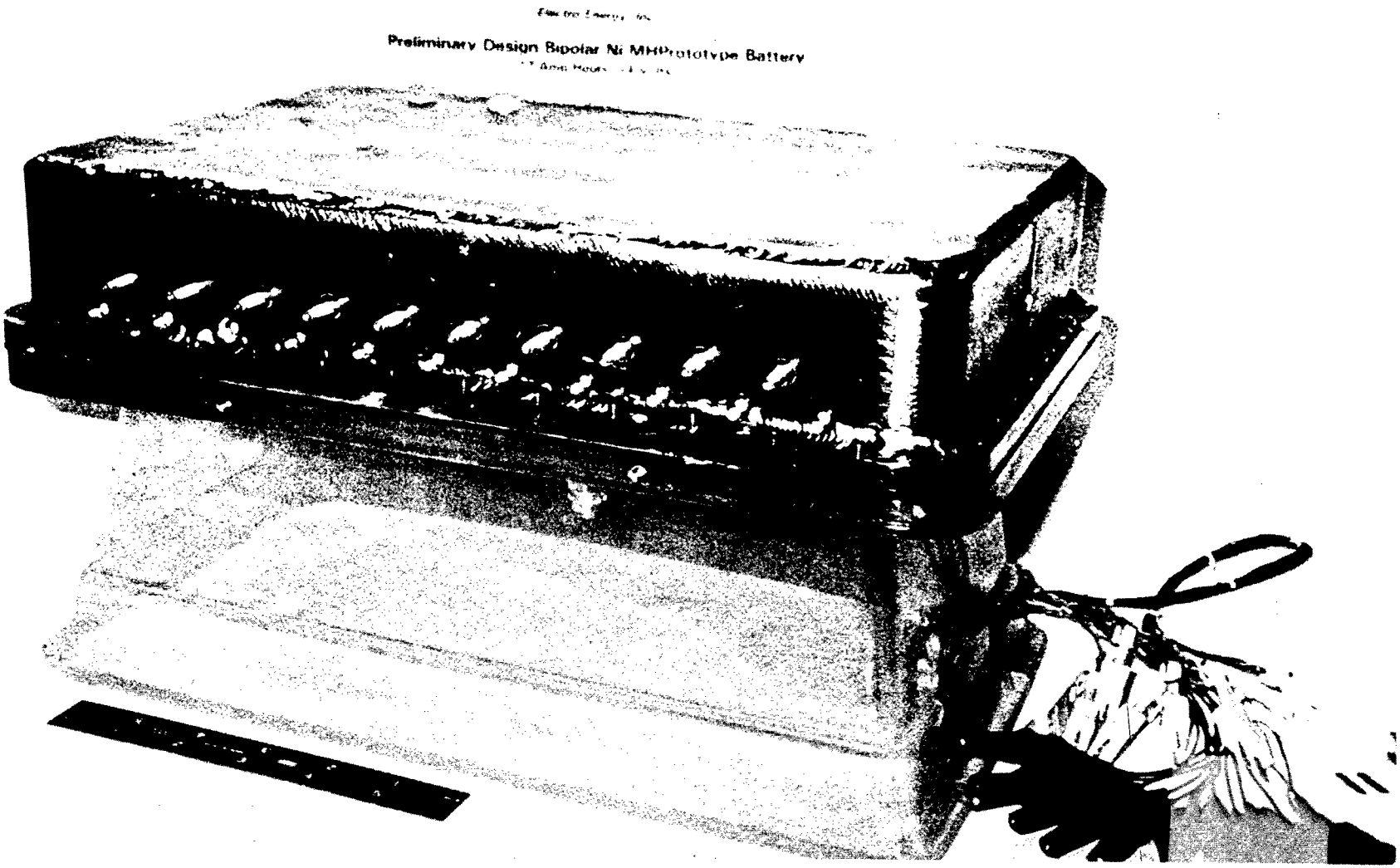
Preliminary Design Bipolar Ni MHPrototype Battery

100 W-HR/kg APPROACHES

(1) Develop a MH Alloy that has 500 mA-hr/g and 5-year LEO Life

- On-going

(2) Develop a Ni Electrode that gives 1.25 electron transfers and a 365 mA-hr/g and 5-year LEO Life

Bipolar Nickel Metal Hydride Battery Design System

User: MnStk+500 mAH/g MH

Power: 1.0 kW
Battery Capacity: 52.1 Ah

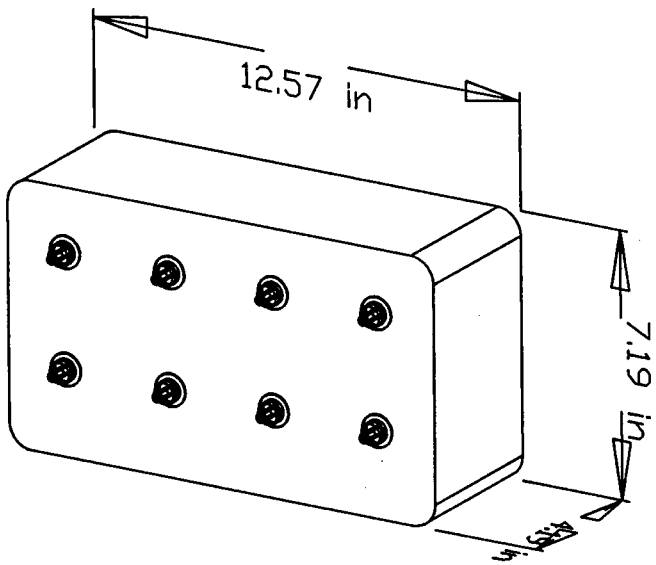

	Metric	SAE
Specific Energy:	99.3 Wh/kg	218.9 Wh/lb
Energy Density:	234.9 Wh/l	8.3 Wh/ft3
Overall Weight:	14.7 kgs	32.4 lbs
Cell Weight:	11.0 kgs	24.3 lbs

Electro Energy, Inc.
Design Automation Associates
Version: R1.15

Page 1 of 13

NASA Lewis
Research Center
Date: October 20, 1998

Bipolar Nickel Metal Hydride Battery Design System

User: Min Stk+125% Theo Ni+365MH

Power: 1.0 kW
Battery Capacity: 52.1 Ah

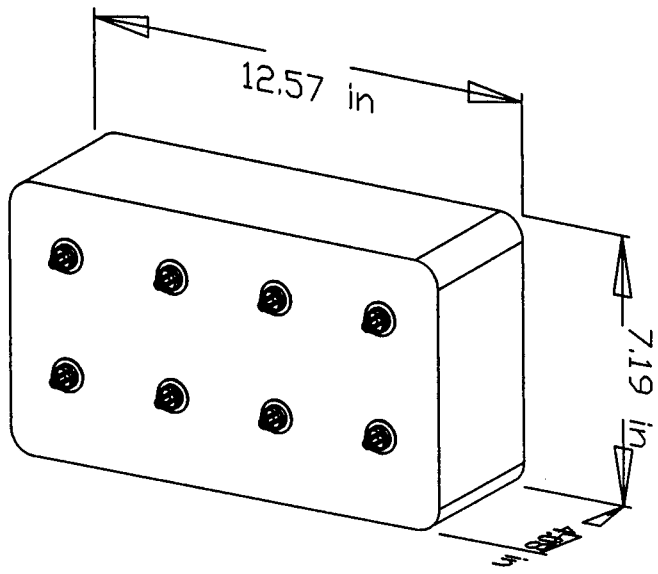

	Metric	SAE
Specific Energy:	100.2 Wh/kg	220.9 Wh/lb
Energy Density:	241.5 Wh/l	8.5 Wh/ft3
Overall Weight:	14.6 kgs	32.1 lbs
Cell Weight:	10.7 kgs	23.7 lbs

Electro Energy, Inc.
Design Automation Associates
Version: R1.15

Page 1 of 13

NASA Lewis
Research Center
Date: October 20, 1998

Status of EEI's Bipolar Ni-MH Battery Project

The Bipolar Ni-MH Battery Project has:

- **Demonstrated the Wafer cell concept in multi-cell stacks on the LEO test regime**

- Demonstrated the advantages of the bipolar wafer cell concept in multi-cell stacks
  - Allows repair or replacement of individual cells
  - No external cell terminals
  - No electrode current collectors
  - Adaptable to heat transfer fins placed in stack
  - Scalable to large area and high capacity
  - Improved energy and power density
  - Lower cost plastic bonded electrodes

- **Tripled the LEO cycle-life of vented-flooded bipolar wafer cells**
  - Vented-flooded cells: 7400 LEO cycles @ 50% DOD
    9200 LEO cycles @ 25% DOD (EODV=1.18 V)

- **Doubled the LEO cycle-life of sealed-starved bipolar wafer cells**
  - Sealed-starved cells: 2400 LEO cycles @ 50% DOD (EODV=1.0 V)

- Completed a very high energy density bipolar battery design
  - 83 Wh/kg (37.8 Wh/lb)
  - 211 Wh/liter (7.4 Wh/ft^3)

Status of EEI's Bipolar Ni-MH Battery Project (cont'd)

The Bipolar Ni-MH Battery Project will:

- Build two .5 kW, 24 cell prototype batteries with lightweight housings and 105 Wh/kg cells in 1999
  - 70 Wh/kg (31.6 Wh/lb)
  - 154 Wh/liter (5.5 Wh/ft^3)
- Build two 1.0 kW, 48 cell prototype batteries with lightweight housings and 114 Wh/kg cells in 2000
  - 82 Wh/kg (37.3 Wh/lb)
  - 204 Wh/liter (7.2 Wh/ft^3)
- Complete a high energy density Flight-weight Bipolar Battery Design and drawing package
  - 100 Wh/kg (45.5 Wh/lb)
  - 235 Wh/liter (8.3 Wh/ft^3)

Conclusions:

- Improved active Ni and/or MH materials a required to increase the battery energy density from 83 Wh/kg to 100 Wh/kg.

Acknowledgments

Thanks and recognition needs to be given to:

- **The NASA Lewis Research Center** for having the vision, and funding the project.
- **Michelle Manzo** and **Tom Miller** for their support, technical expertise, leadership and encouragement.
- **Rhodia** (formerly Rhone-Poulenc), **Rutgers University**, and **Design Automation Associates** for their significant cost sharing contributions.
- **Dr. Bao-Min Ma** (Rh), **Charles Grun** (RU), and **Sean Sullivan** (DAA) for their significant technical contributions and excellent customer support.
- **Eagle-Picher Industries** for their technical guidance and sharing of their extensive design-to-orbit experience.
- **James DeGruson** (EPI) for his project guidance and persistent grappling for EPI resources.

Battery Study For The Shuttle Orbiter EAPU Upgrade

By
B. Otzinger, S. Hwangbo, T. Farkas, G. Schwartz, M. Gajewski,
S. Verzwyvelt, T. Barrera, B. Barrera, C. Johnson
Boeing Defense and Space Group,
12214 Lakewood Boulevard, Downey, California
And B. Irlbeck
NASA/ JSC, Houston, Texas

The NASA Aerospace Battery Workshop
Huntsville, Al
October 27, 1998

Boeing North American, Inc.
Space Systems Division

BOEING

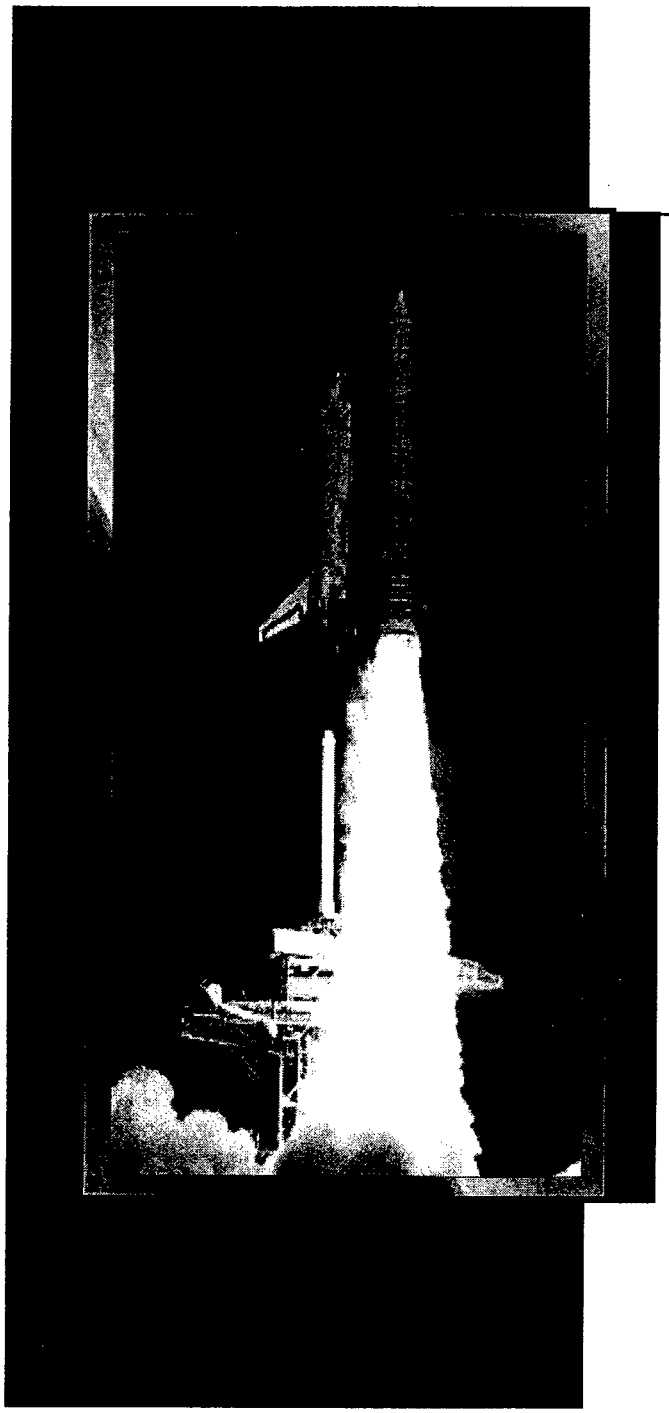

Orbiter Upgrade Electric APU (EAPU) Program

Overview and Status

Sam Hwangbo, BNA
562-922-0252

BOEING

Nissan Electric Minivan

(32 kWh Sony Lithium Battery 360 Vdc Operating Voltage)

Boeing North American, Inc.
Space Systems Division

BOEING

EAPUS Using Mature Commercial Technology

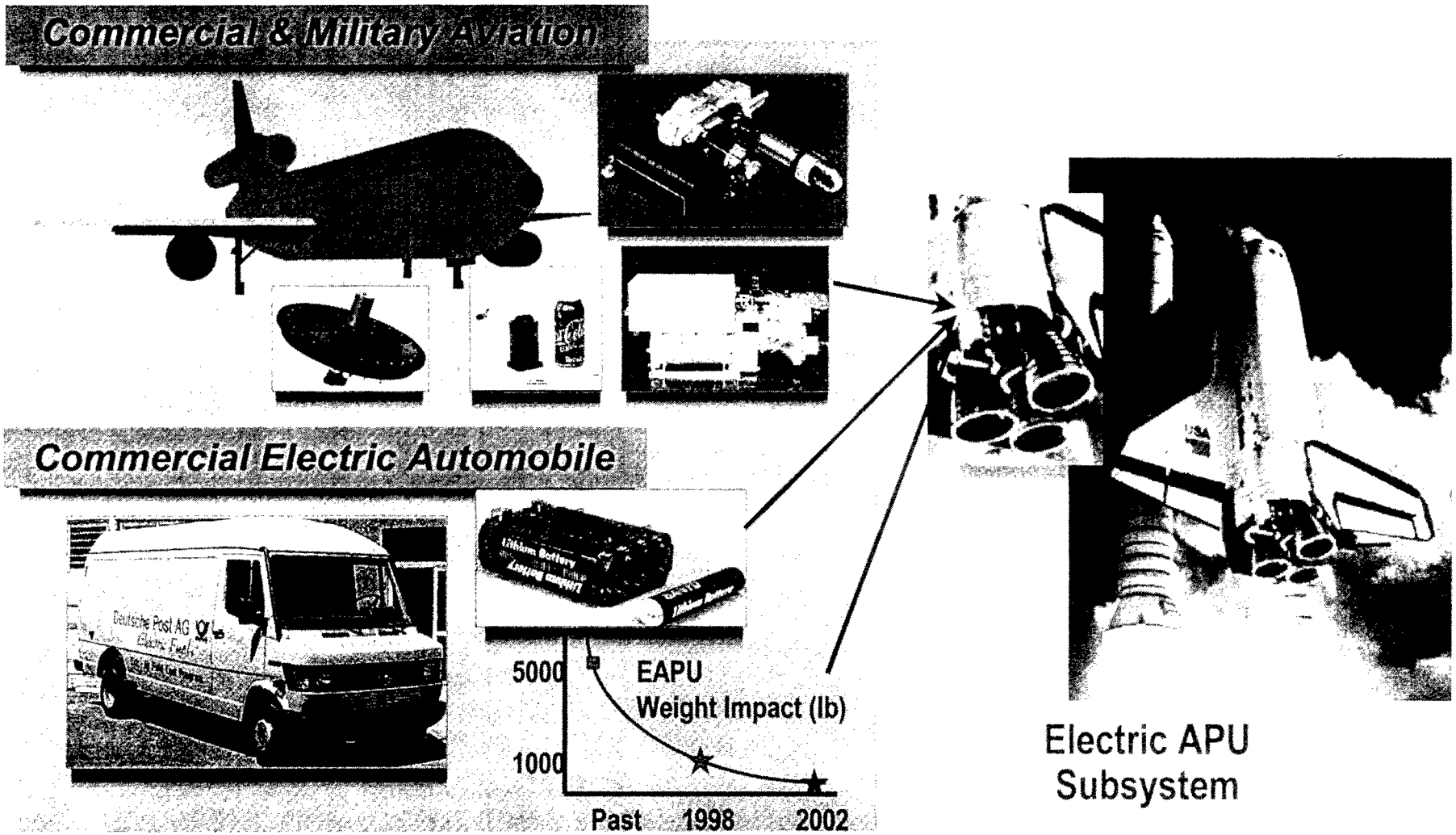

Electric APU Benefits

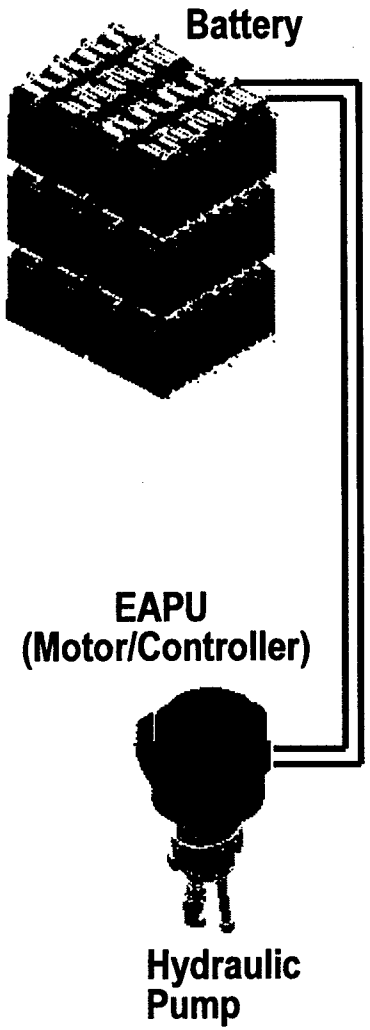

- Improves safety, reliability and restart capability
  - Eliminate toxic & corrosive Hydrazine fuel
  - Eliminate hazards and CRIT 1 failures (turbine overspeed & N2H4 leakage/ignition)
  - Greater than 1000 factor of reliability improvement
  - Eliminate hot restart system and procedures
  - Potential single EAPU landing capability
- Reduces KSC ground turnaround effort
  - Savings > $ 1.2M per year (APU, hydraulics & WSB)
- Reduces long term program cost
- Continuous infusion/application of commercial progress

Boeing North American, Inc.
Space Systems Division

BOEING

Leverage Commercial Investment In Lithium Cells

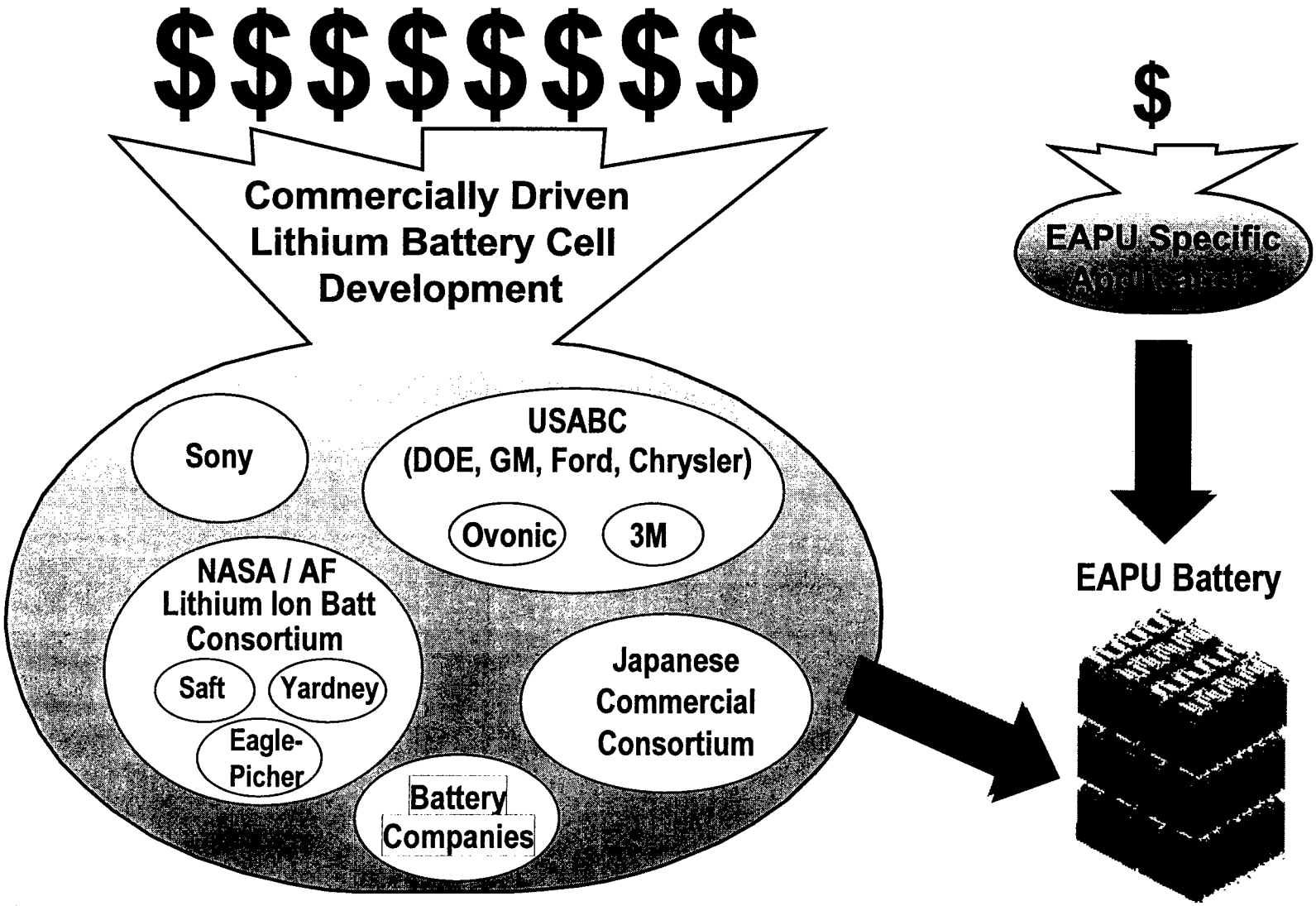

Boeing North American, Inc.
Space Systems Division

BOEING

BNA Prototype EAPU Demonstration Testbed (IR&D)

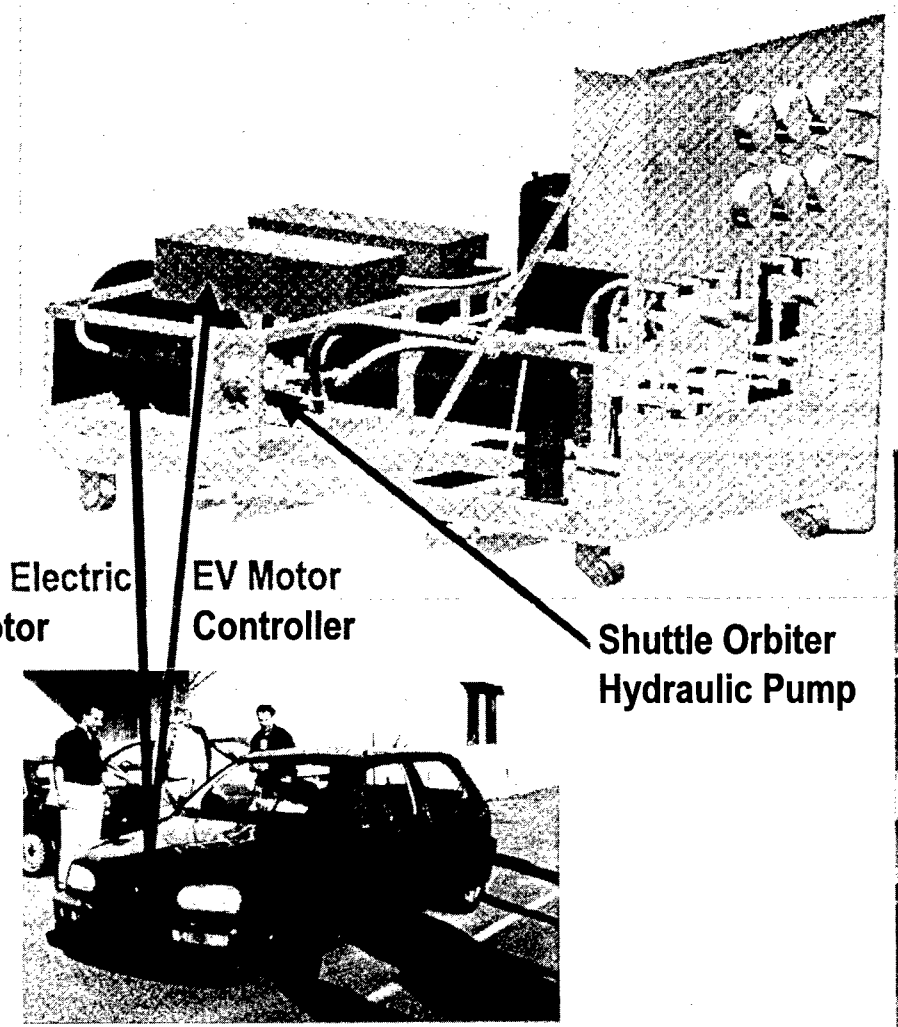

Testbed Under Construction

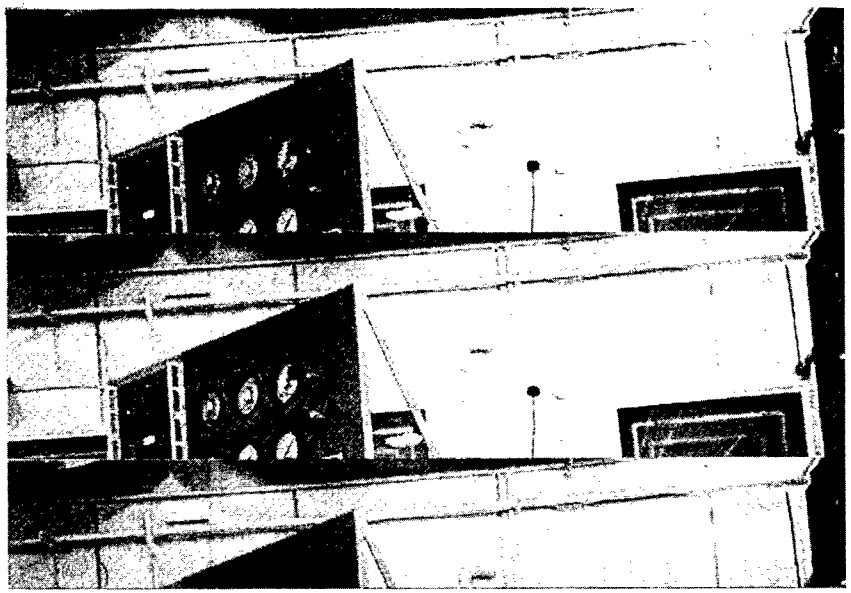

Boeing North American, Inc.
Space Systems Division

BOEING

EAPU Program Plan

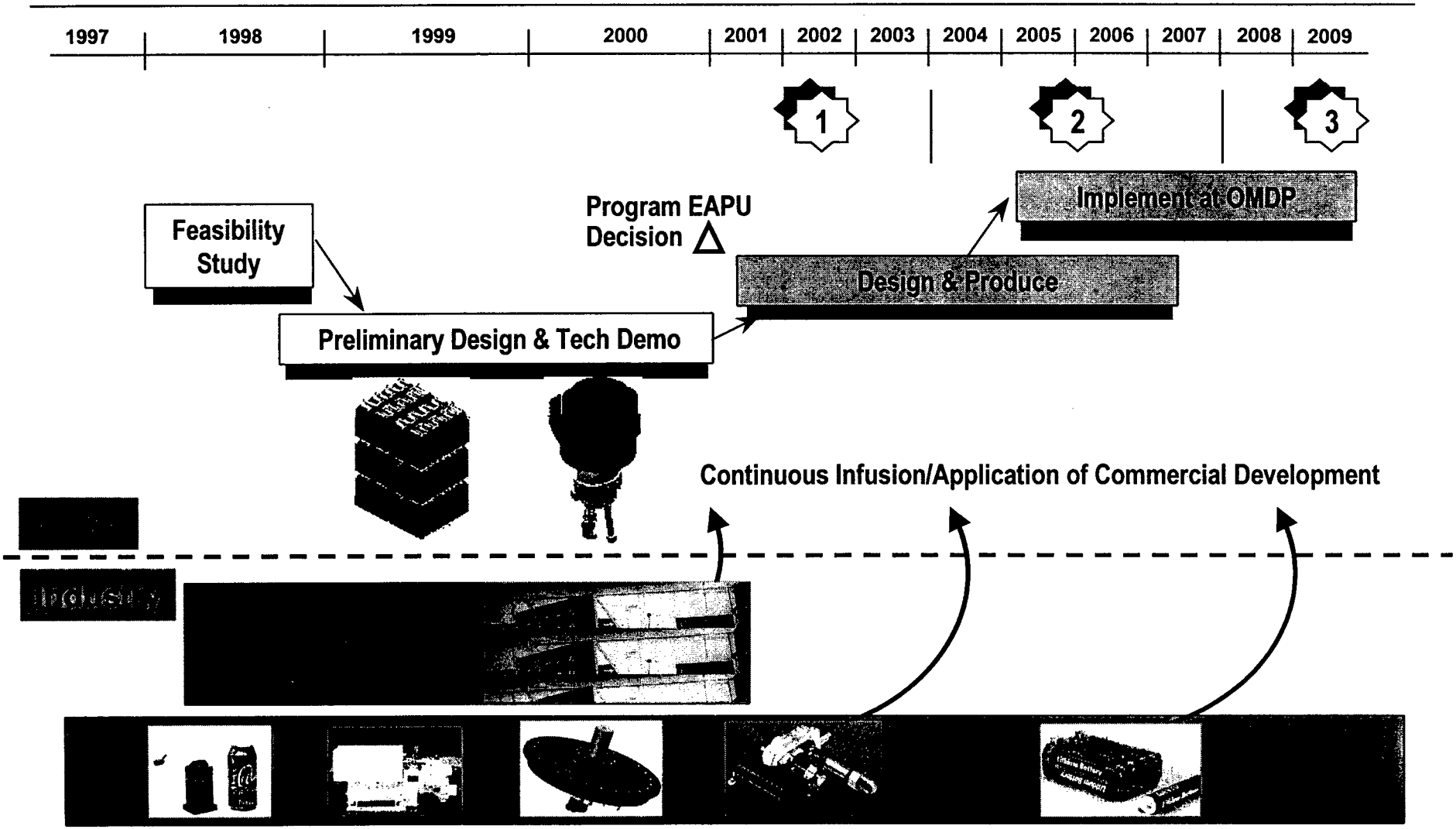

Boeing North American, Inc.
Space Systems Division

BOEING

Working Together

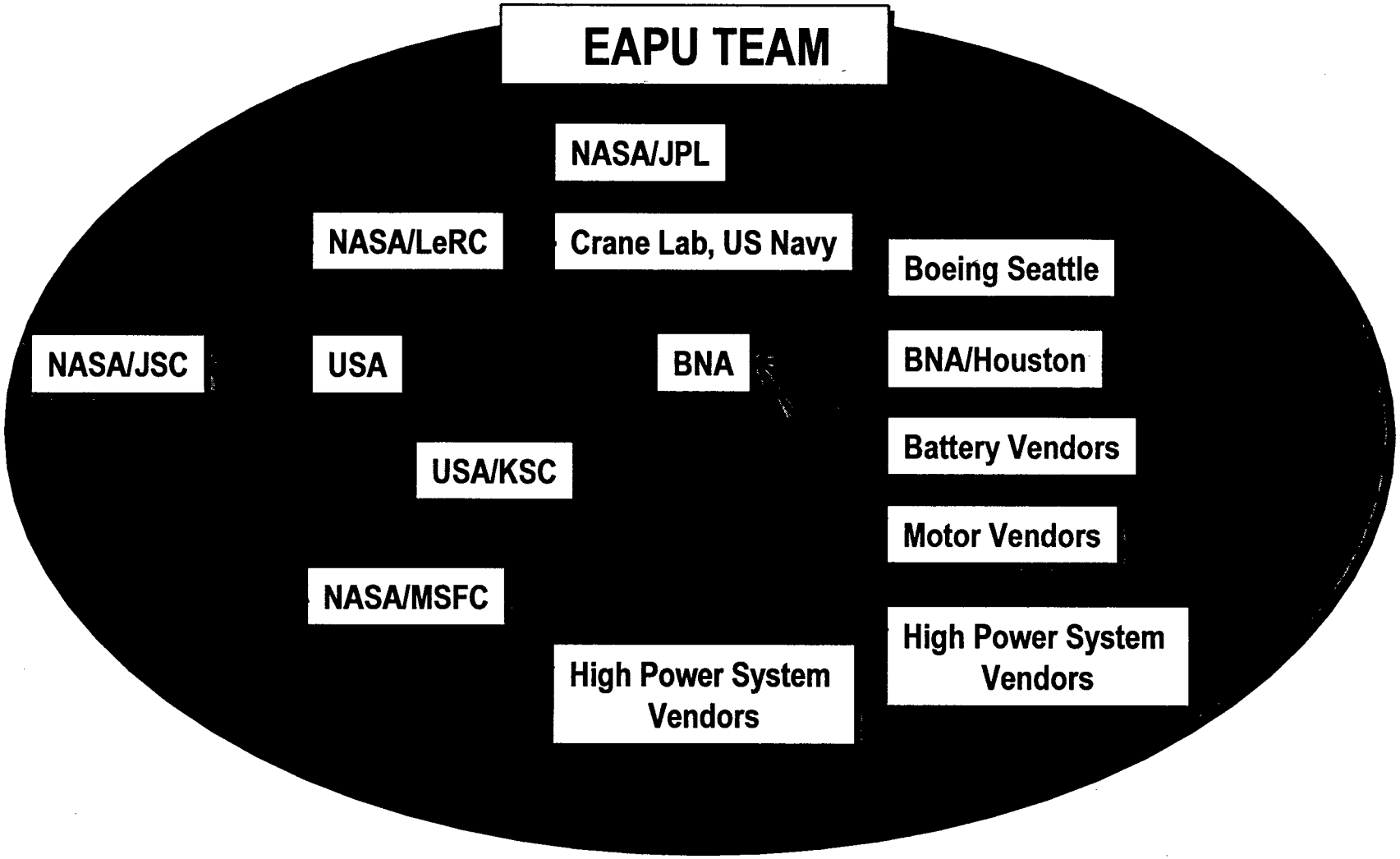

[redacted]

Burton Otzinger, BNA

922-562-5832

Boeing North American, Inc.
Space Systems Division

BOEING

Battery Design Requirement Definition

- DESIGN POINT ANALYSIS CONDUCTED TO EVALUATE FEASIBILITY
- BATTERY SUPPLIER RESPONSE MID-TERM (1 JULY '98)
- REVISED DESIGN DEFINITION :

  LOAD PROFILE
  FLY-SHEET SPECIFICATION

Boeing North American, Inc.
Space Systems Division

BOEING

Battery Weight Estimates by Type (July, 1998)
(37 kW-hr Mission)

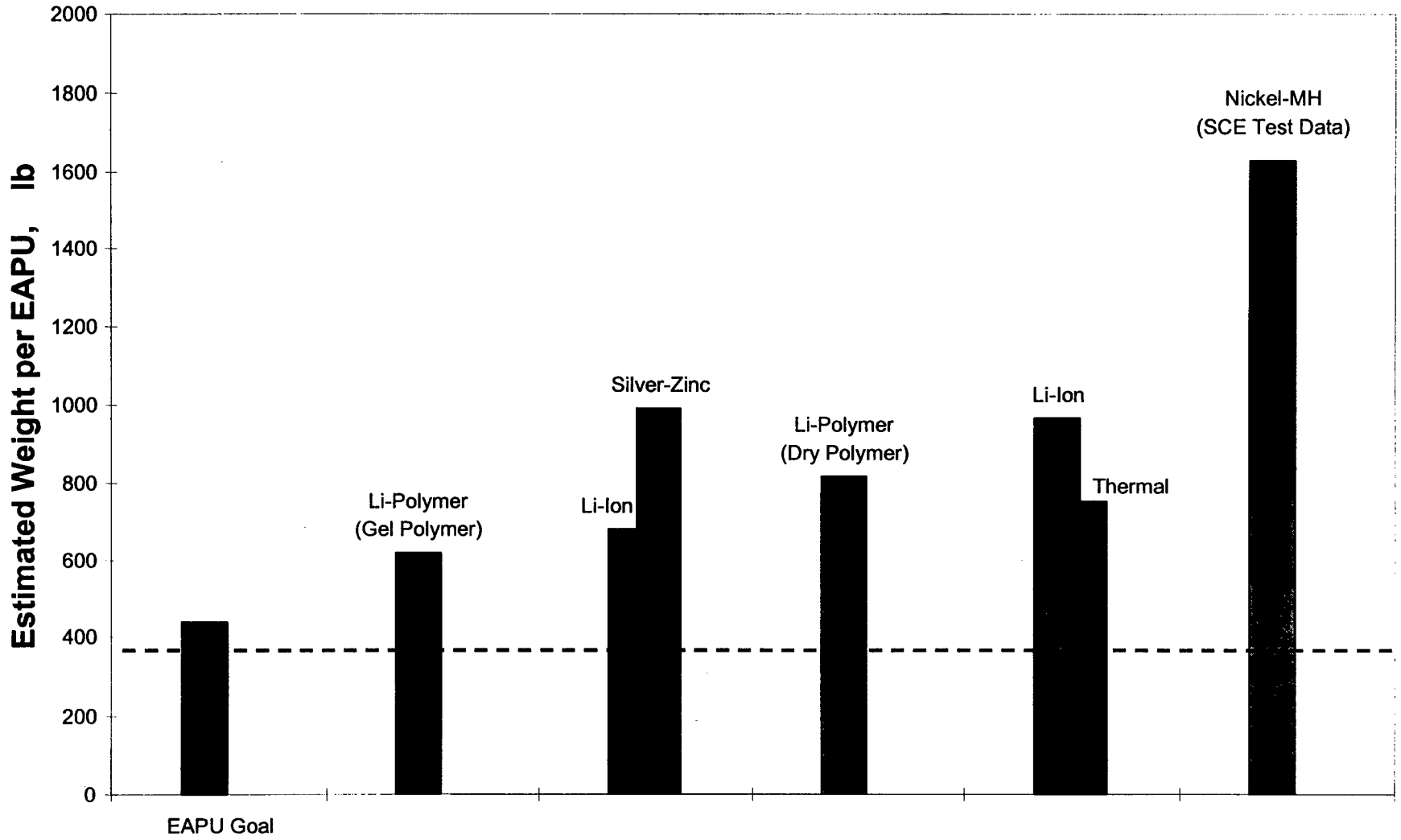

Boeing North American, Inc.
Space Systems Division

BOEING

[redacted] 10AH Cells
Charge-up prior to EAPU Discharge Profile
Temperature: 20.2 Celsius
Charge: Imax=C/2; Vmax=4.1; 5 hours

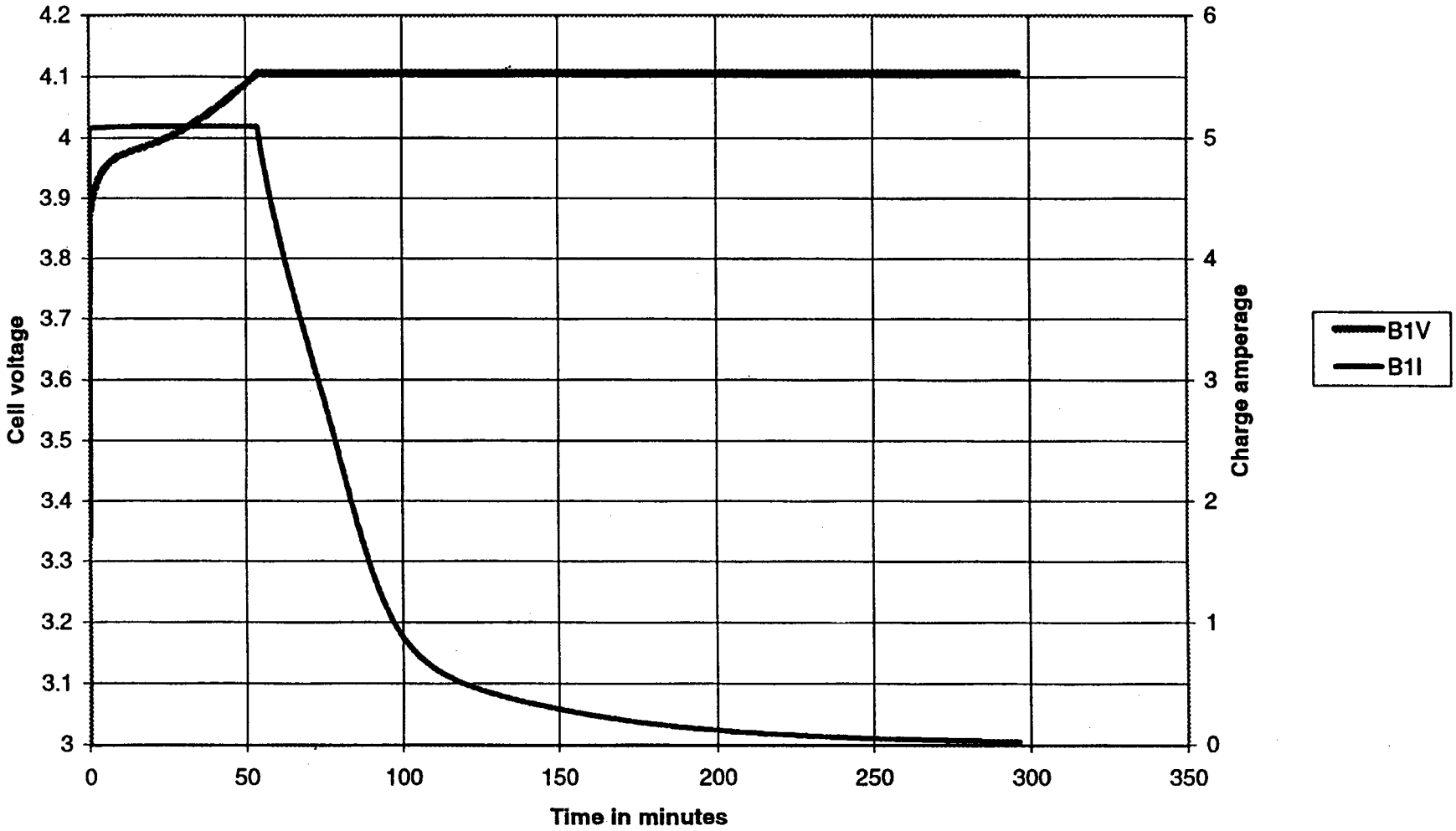

Constant Current Equivalent of Electric APU Power Profile
Discharge Current proportionated to acheive 80% DoD of 10AH Cell Rating

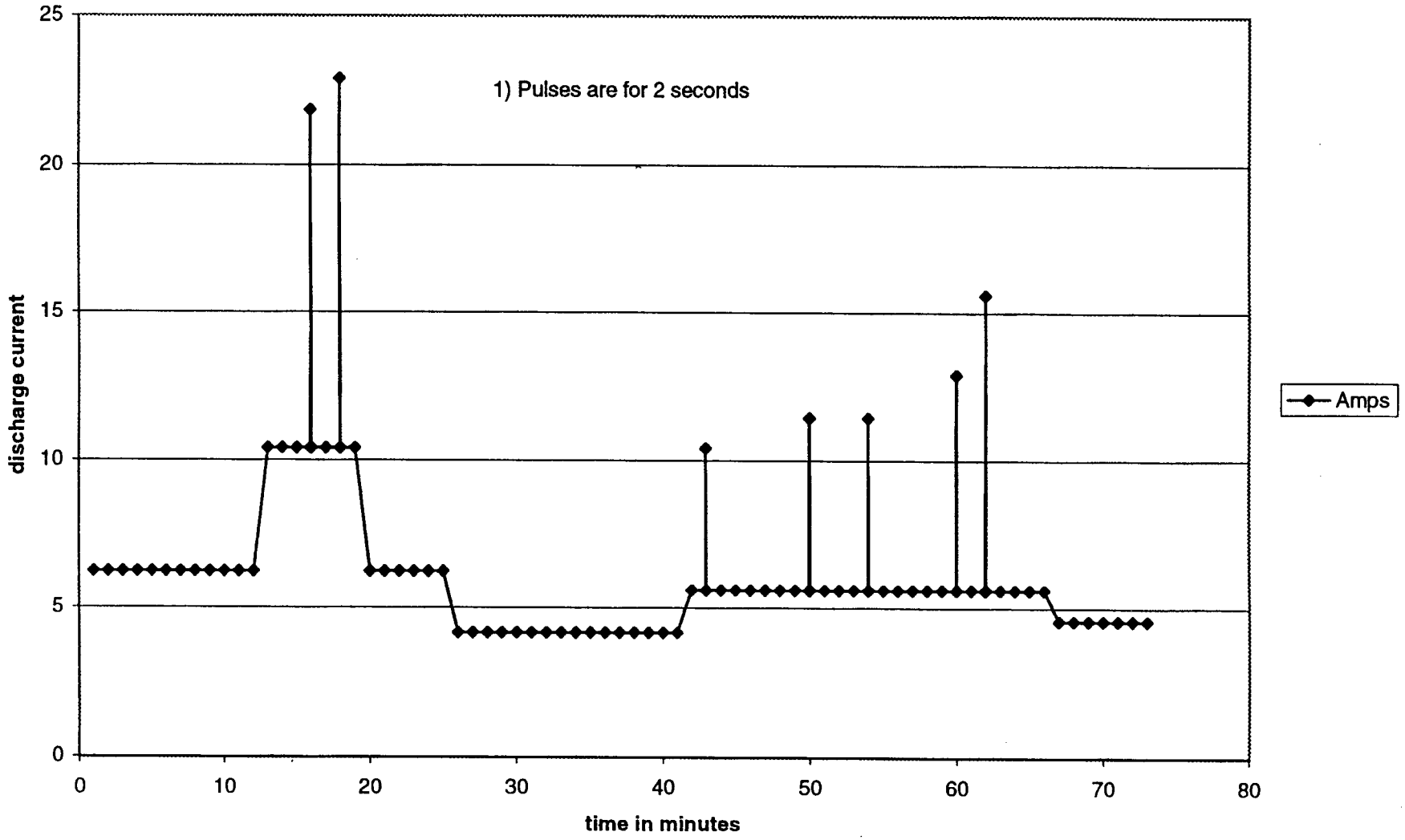

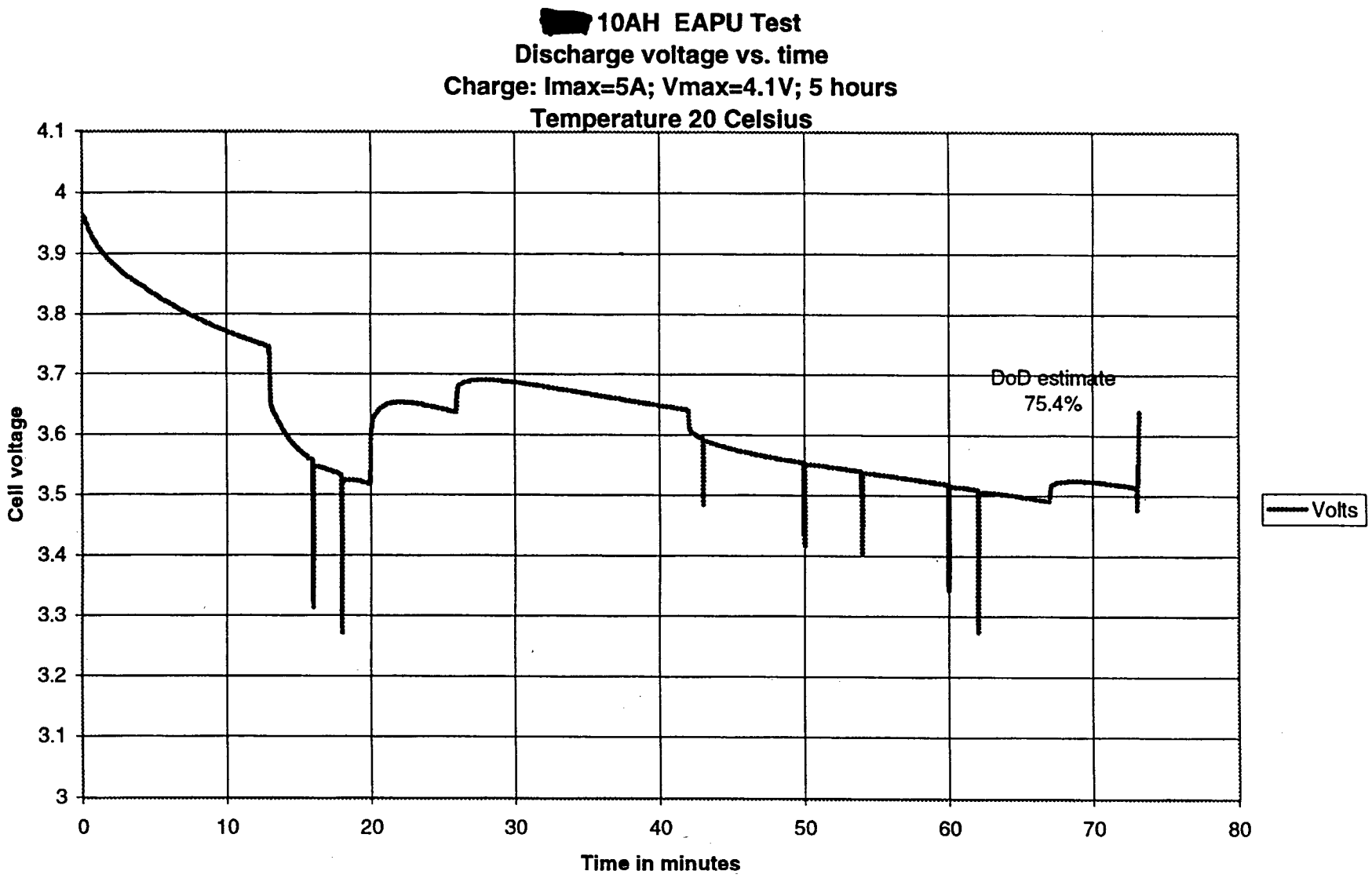
[redacted] 10AH EAPU Test
Discharge voltage vs. time
Charge: Imax=5A; Vmax=4.1V; 5 hours
Temperature 20 Celsius
Cell voltage
4.1
4
3.9
3.8
3.7
3.6
3.5
3.4
3.3
3.2
3.1
3
0
10
20
30
40
50
60
70
80
Time in minutes
DoD estimate
75.4%
Volts

Revised EAPU Power Profile for Battery Vendor Testing

Off-Nominal Flight Condition and Two EAPU Entry Case

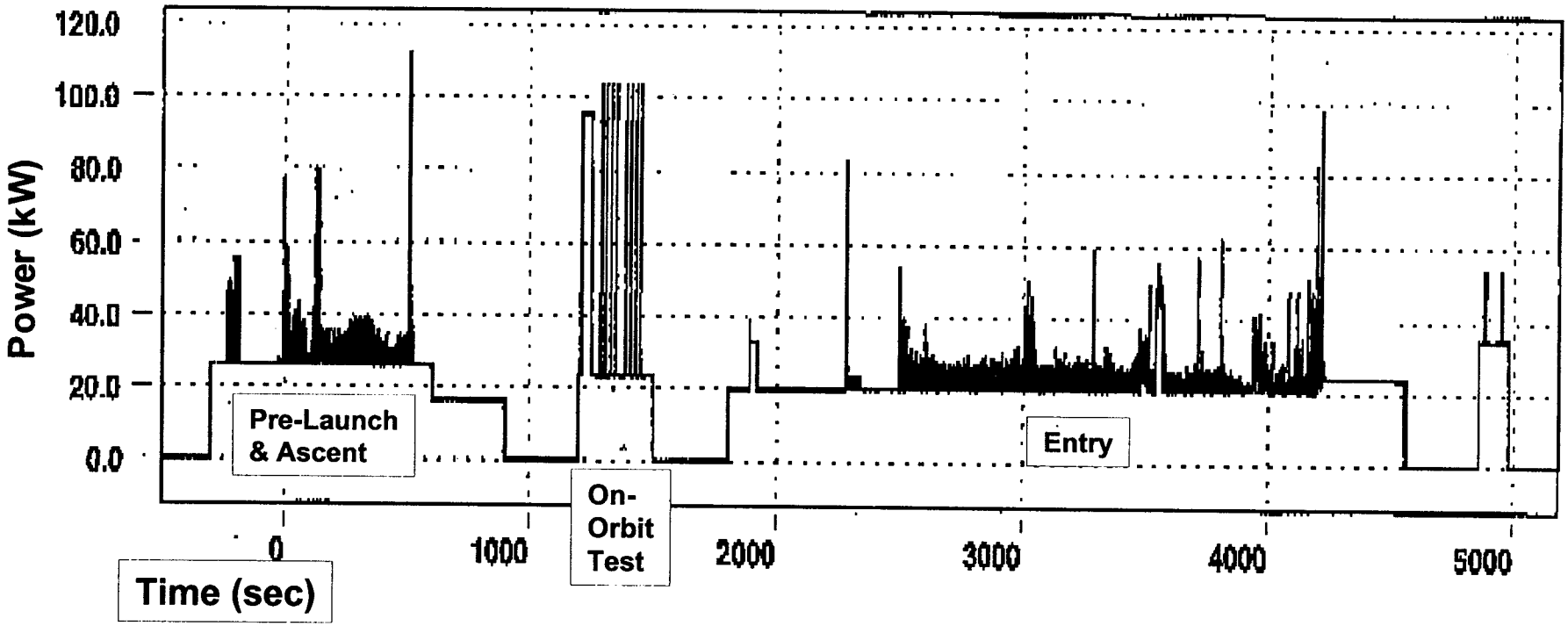

Boeing North American, Inc.
Space Systems Division

BOEING

Battery Design Requirement Fly-Sheet Specification

Battery Type:	**Lithium-Ion** **Lithium-Polymer**
Voltage-	
Nominal:	**270 V.**
Limit:	**250 V Min.**
Discharge-	
Time Line:	**91 Minutes**
Energy (minimum):	**37 kW-h above the 250 Volt. lower limit at 25 °C Min. on the 50th cycle within the 5 year calendar life requirement.**
Delivered Capacity:	**137 A-h (Min.)**
Power Profile:	**See attached chart.**
Peak power capability:	**125 kW with Power spikes 2 Seconds max.**

Boeing North American, Inc.
Space Systems Division

BOEING

Battery Design Requirement Fly-Sheet Specification

Load (Ave.):	**110 Amperes**
Size-	
Envelop (goal):	**0.76m (2.5 ft.) x 0.76m (2.5 ft.) x 0.76m (2.5 ft.)**
Weight (goal):	**200 kg (440 lb.)**
Temperature-	
Operation:	**25 °C to 35 °C**
Non-operational:	**-10 °C to 50 °C**
Heater:	**Maintain 25 °C Min. Temp.**
Life-	
Calendar:	**5 Years**
Cycle:	**50 Charge / Discharge cycles**

Boeing North American, Inc.
Space Systems Division

BOEING

Battery Design Requirement Fly-Sheet Specification

Environment-

Acceleration:	**From 0 to 5 g's, three orthogonal axes**
Random Vibration:	**Constant at 0.70 g^2/Hz from 100 to 400 Hz decreasing at -3 dB/octave from 400 to 2000 Hz.**
Shock:	**TBD**

Other Features-

Cell By-pass Electronics:	**In GSE for charging on ground only. BNA supplied for cell by-pass isolation on discharge.**
Sensors:	**Temperature Thermistors, 2/module.**
Connectors:	**Power, Sensor/heater, Individual cell monitor /charge and Module interconnection.**

Boeing North American, Inc.
Space Systems Division

BOEING

POTENTIAL EAPU BATTERY SUPPLIERS

SUPPLIER	TYPE	STATUS
3M	Li-Ion POLYMER	RFQ, EV BATTERY TEST
ALLIANT	Li-Ion POLYMER	RFQ, 150 AH
SAFT	Li-Ion	EV BATTERY TEST
EAGLE-PICHER	Li-Ion	RFQ, 125 AH
YARDNEY	Li-Ion	25 AH 1ST GENERATION
JAPAN STORAGE BATTERY	Li-Ion	RFQ, 100 AH
BLUE STAR	Li-Ion	RFQ, 100 AH 1ST GENERATION
ULTRALIFE	Li-Ion	10 AH 1ST GENERATION

BATTERY DESIGN AND DEVELOPMENT

- Battery Assembly Concept
- Flight Battery Development Plan
- Battery Test Activity

Construction of Battery Module

- Series Connected String of Li-ion Cells
- Series Redundancy Provided By Cell Isolation Switches
  - Isolation Switch Is Configured to Function As Cell Interconnect
- Thermal Path From the Cell Sides to the Baseplate Provided by Lightweight Aluminum Channels ("Taco Shells")
  - Channel Is Also Provides Structural Support to Cell; Similar to NASA Standard Battery
  - Small Gap Between Bottom of Cell and Channel Allows for Venting
- Endplates Hold Channels Together
- Channels Are Held Down By A Common Bracket To Baseplate
  - Baseplate Provides Thermal Management of Cell

Lithium-Ion Battery Cell Dimension for EAPU

- **Lithium-Ion battery cell for EAPU Rev. 10/19/98**
  - **Shape : Elliptic-Cylindrical or Prismatic**
  - **Rated Capacity : 125 A-h (Minimum)**
  - **Mass : 3.6 kg (Maximum)**
  - **Dimensions (mm) : 197 (H) x 180 (L) (Max.) x 50 (W)**
  - **Can to terminal isolation at both seals**
  - **Storage in inverted orientation for 3 years**
  - **Gas vent feature in bottom of cell can**
  - **Cell can sides flush at top and bottom**

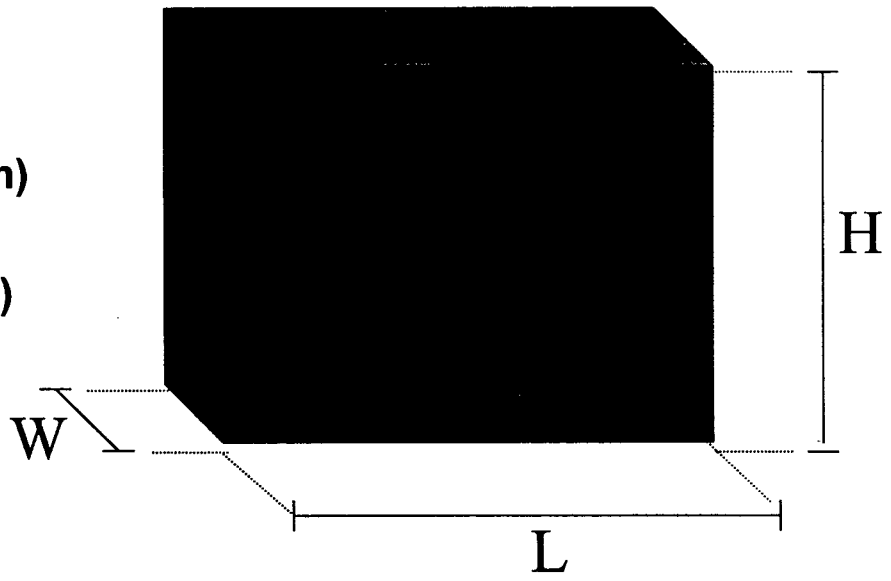

Boeing North American, Inc.
Space Systems Division

BOEING

Battery Module Layout

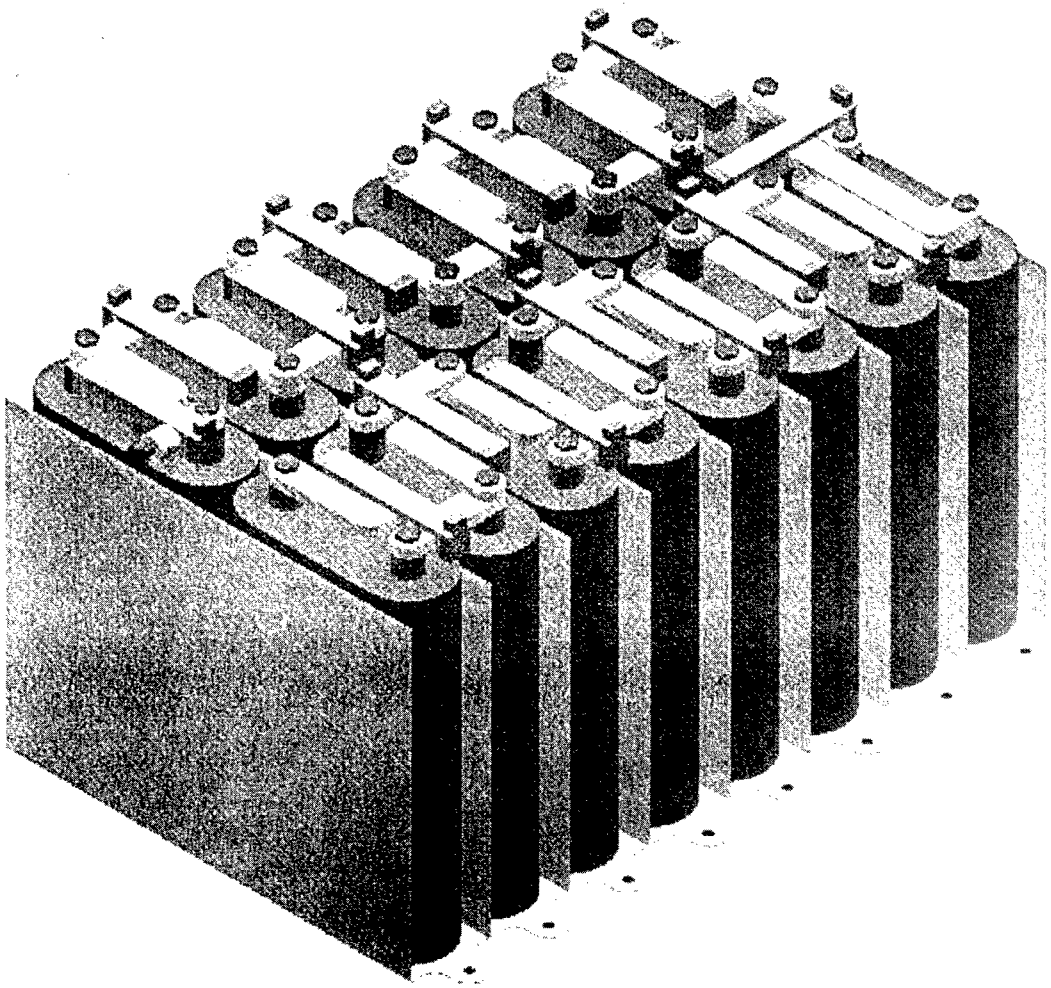

Boeing North American, Inc.
Space Systems Division

BOEING

BATTERY ASSEMBLY CONCEPT

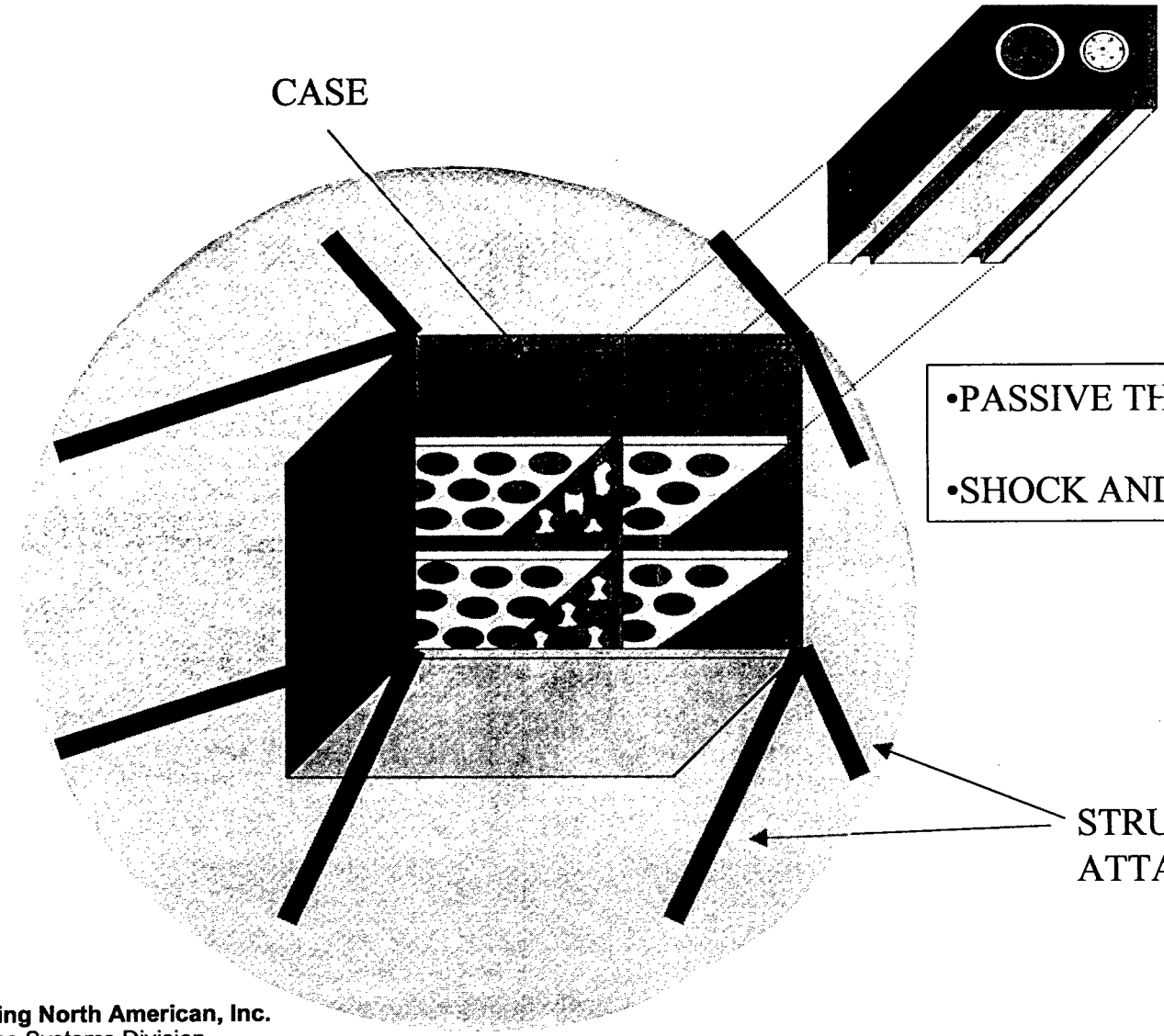

- PASSIVE THERMAL CONTROL
- SHOCK AND VIBRATION ISOLATION

Boeing North American, Inc.
Space Systems Division

BOEING

FLIGHT BATTERY DEVELOPMENT

- **Phase I** **Test Battery (100-150 Ah)**
  - 345 V Battery To Support EAPU System Demonstration
  - Cells Mounted On Three Thermal Control Plates, 32 Li-ion Cells/plate
  - Cells Are Demountable To Facilitate Configuration Changes
  - Plates Can Be Stacked In 2.5 X 2.5 X 2.5 Ft. Configuration
- **Phase II** **Module Configured Battery**
  - Fabricate Cell Modules
  - Complete Inter-cell, Connector And Instrumentation Wiring
  - Demonstrate Operation With Inter-module Connection Concepts
- **Phase III** **Integrated Battery Operated**
  - Assemble Battery Case Mockup
  - Demonstrate Module LRU Feature
  - Demonstrate Completed Battery Operation To EAPU Requirements

BATTERY TEST ACTIVITY

LOCATION	TEST SAMPLE	*TYPE TESTING
PHANTOM BOEING WORKS	CELLS/ MODULES	MISSION ASSURANCE TECHNOLOGY ASSESSMENT
BNA	CELLS	BATTERY/MODULE FABRICATION
BOEING WASH.	CELLS	THERMAL PROPERTIES
SOUTHERN CALIF. EDISON	BATTERY	EAPU SYSTEM TEST BED
JPL	CELLS	SELECTED 50 AH CELL TESTS
LEWIS RESERARCH LABORATORY AT CRANE TEST FACILITY	CELLS	SAFETY ASSESSMENT

*CELL TESTING LIMITED TO SUPPLIERS THAT WILL PRODUCE LARGE CAPACITY CELLS SUITABLE FOR EAPU APPLICATION

Battery Reliability And Safety Features

- Flight Energy Margin Confirmation.
- Battery Cells Are Series Redundant.
- Battery Cell By-pass Isolation During Discharge For Short And Open-circuit Conditions.
- Battery Cell Charge Current By-pass Provided In GSE Non- Flight Hardware.
- Shock And Vibration Isolation
- Passive Battery Heat Rejection With Heater Maintaining 25 ^{o} C Minimum Operating Temperature.

Acknowledgment

The work described here was carried out at the Boeing North American, Inc. under contract with the National Aeronautics and Space Administration/ Johnson Space Center and Boeing Research and Development (IR&D)

DPA Findings Focused Session

Expert System for Nickel Hydrogen Battery Cell Diagnostics

A. Zimmerman and L. Thaller
Electronics Technology Center
The Aerospace Corporation
El Segundo, California 90245

Introduction

The diagnosis of the root-cause or causes for performance problems in battery cells is often a difficult task because each of the component characteristics, physical processes, or chemical processes in most battery cells typically has a strong interaction with many other variables in the cell. In nickel hydrogen battery cells this is particularly true because of the co-existence of solid, liquid, and gaseous active phases, each of which can provide coupling between the components and processes that occur within the cell. In nickel hydrogen cells, as is the case for most battery cells, diagnostic procedures in the event of performance problems typically involve the combination of some electrical tests (hopefully perceptive), cell disassembly and inspection, and physical/chemical analysis of the cell components. All laboratories that perform such DPA (Destructive Physical Analysis) procedures have a somewhat different set of procedures and analyses that are followed. Some analyses may be either more or less appropriate for any given cell, depending on the performance signatures of that cell. However, typically a standard DPA regimen is utilized by any given laboratory, with the expectation that a broad range of analysis procedures will yield the key information needed to diagnose the root cause for the cell problems.

A more efficient approach to the DPA of battery cells in general (and nickel hydrogen cells as discussed herein) has been developed at The Aerospace Corporation. This approach defines a DPA in terms applying the correct diagnostic procedures from a large toolbox of procedures, performing only those analyses that are most appropriate for the observed behavior of the battery cell. Thus, with this approach, the details of each DPA procedure are generally different from all other DPA procedures. The most appropriate procedures to be used for a given DPA are those that have the greatest likelihood of yielding the root cause for the cell performance problems or degradation modes. Determination of the most appropriate analysis associated with each root cause (and its performance signatures) is based on a combination of performance modeling, experience, and the known symptoms exhibited by the cell. This approach to the perceptive DPA of nickel hydrogen battery cells has been codified into an expert system for nickel hydrogen battery cell DPA, which will be described here along with examples to both validate the system and illustrate its use.

Description of Expert System

The Expert System for Battery Cell Analysis (ESBCA) provides a software package that allows a user to interactively design a DPA procedure to best fit the observed behavior of a battery cell, or to determine the most likely root-cause for any collection of observed battery cell symptoms. This software system, which was developed with support from NASA (MSFC), is presently at Version 1.1, which is described here. It is designed to operate on a PC in a Windows 95/98/NT environment, and can be installed from a set of four floppy disks at present. Version 1.1 of ESBCA considers 32 different root-causes for nickel hydrogen battery problems or degradation, and has a toolbox of 52 different analysis procedures at its disposal to

differentiate between these root causes. The ESBCA system, when installed on the user's computer, is run by selecting the program entitled CellAnly, which should be automatically added to the Start/Programs menu during the installation procedure.

The ESBCA system saves each DPA in an analysis file, which contains the cell design characteristics, DPA analysis results, and electrical or chemical analysis symptoms. The File menu in the ESBCA system enables the user to either open a new analysis file by selecting File/New, or open an existing analysis file by selecting File/Open. When an analysis file is opened, a summary window appears that contains a title, the cell design, and sections describing the positives, separator, negatives, electrolyte, and a list of electrical, physical, and chemical analysis symptoms for the cell. Parameters that may be directly edited are highlighted in blue. These parameters are changed by clicking the mouse cursor on them, then either selecting a new option from the pop-up list or typing the new parameter in the box that appears (note: before any parameter may be edited, the Edit/Activate menu item must be selected). After any parameter is changed, selecting the Edit/Undo menu item will reverse the change. A description of each field on the summary window is provided in the following list.

1. Title: A description of the cell and its key features.
2. Capacity: The nameplate capacity may be changed to any desired value. The actual capacity is calculated based on one stored electron per nickel atom in the active material, and thus will vary with number of positives and positive characteristics.
3. Cell diameter: Any standard cell size or design may be selected from the popup list.
4. Stack type: Back-to-back, Recirculating, or Double-anode stack types may be selected from the popup list.
5. Positives: Substrate types of sinter, fiber, or foam nickel may be selected from the popup list. Total number of positives may be specified. The plaque porosity, thickness, loading level, and cobalt additive levels may all be specified in the positive data table. This table has three columns. The first column provides the initial positive electrode characteristics (i.e. when new), the second column allows the user to enter any desired degraded characteristics to from which swelling, corrosion and degraded electrolyte characteristics and distributions are calculated. The third column allows values measured during DPA to be entered.
6. Separator: The type of separator may be selected from the popup list. The total thickness of the separator may also be entered.
7. Negatives: The thickness of the negative may be entered.
8. Electrolyte: The electrolyte weight, concentration (wt %), grams per Ah actual capacity, and the percentage of the separator void volume filled with electrolyte appear in the electrolyte data table. The last two lines in this table are all calculated values, and cannot be edited. The data in the first two lines may be edited and correspond to measured (or nominal) electrolyte fill and concentration at cell activation and at the time of cell DPA. In the column labeled "degraded", these parameters are all calculated based on the specified degradation from the initial state of the positives.
9. Symptom list: In each analysis file a list of cell symptoms is maintained that provides a detailed enumeration of all results (or symptoms) from electrical, physical, and chemical analyses associated with the cell testing or DPA. These symptoms may be edited by clicking the mouse cursor on the desired symptom to highlight it, then selecting the Edit/Symptoms/Add, Change, or Delete menu item. If Add or Change is selected, a dialog box will appear to allow the desired symptom and its value to be changed or added to the list. Delete will simply eliminate the highlighted symptom or symptoms from the list.

An additional electrical performance summary window can be viewed by selecting the Edit/Electrical Performance menu item. This form simply allows capacity, voltage, and pressure

behavior signatures to be maintained in the analysis file. It is not linked into the expert system in any other way.

For the cell design specified in each analysis file, default electrode and separator parameters are provided that are appropriate for most cells. However, selecting the menu items under the Edit/Design Details menu selection allows the user to alter the area of the separator, positive and negative plates as well as the separator porosity.

In the Tools menu there are three analysis tools that allow this system to be effectively used to help in the DPA of a nickel hydrogen cell. The symptom list on the analysis summary window serves as the basis for evaluating the most likely root causes for the cell performance. The Tools/Root Causes menu selection activates a tool that translates the symptom list into the most likely root causes, which are displayed in the Root Cause Window. The 15 highest probability root causes are displayed, with the most likely at the top of the list. Typically, this tool is used to obtain the most likely explanations for cell behavior, and then using the additional Preferred Analysis Tool, the DPA analysis procedure best suited to either confirm or reject any possible root cause may be easily determined.

The normal course of a cell DPA involves three phases. During the initial phase, during which only very general symptoms are known (such as the capacity is low by 30%), numerous root causes are likely with nearly equal probability. The second phase of a DPA involves collecting data from a number of analysis procedures to eliminate (or confirm) the most likely root causes. During this intermediate phase the user strives to eliminate all but one particular root cause scenario. The final phase of the DPA is reached when all but one root cause have been eliminated to a satisfactory probability.

The analysis that is most likely to either confirm or eliminate a particular root cause displayed in the Root Cause Window may be obtained by first highlighting the pertinent root cause by clicking the mouse cursor on it. Selecting the Tools/Preferred Analysis menu item will open a Preferred Analysis Window that provides a detailed description of the highlighted root cause, a list of DPA analyses that relate to the highlighted root cause (most appropriate analyses listed first), and a detailed description of any DPA analysis procedure that is selected from this list. Performing the chemical, electrical, or physical analyses listed first by this tool will maximize the probability that the results will either eliminate or confirm the selected root cause, and most probably minimize DPA time and effort. It should be noted that the Root Cause and Preferred Analysis Windows function in concert with each other. Highlighting a new root cause will shift the focus of the Preferred Analysis Window to the new root cause that was selected.

Selecting the Tools/Procedures menu item will access an additional tool that is quite useful. A Procedures Window is opened that displays a list of all DPA procedures and symptoms known to the ESBCA system, along with the procedures for carrying out these analyses and literature references.

The following sections will illustrate the use of this expert system by using it to guide the reader through seven DPA scenarios taken from actual cell situations. In each case it will be demonstrated how the user can quickly get to a highly certain root cause for the cell problems with a minimal amount of analysis effort.

Example 1. Well Performing Cell from Long-Term Life-Test

This particular cell is not a typical candidate cell for a DPA, since it was performing well after 42,000 cycles in a life test. Normally, well performing cells are not considered sufficiently interesting to warrant a DPA. However, in this case there was significant interest in our laboratory in determining why this cell had performed quite well, and what modes and degrees of degradation had accumulated in the cell components. The cell had a capacity that was about 98% of the original capacity, charge retention that was good, and exhibited relatively normal

charge and discharge voltages. Initially, these relatively vague symptoms were all that were known about the cell, with the exception of the fact that it was filled with a large excess of electrolyte, approximately 6.6 g of 31% electrolyte per ampere-hour (assuming 98.77 Ah).

Figure 1 shows the expert system evaluation of this cell. Cycle life completed by the cell is specified to the expert system based on "equivalent" 100% DOD cycles, which equal the actual number of cycles times the fractional DOD for each cycle. The expert system indicates that the largest potential problem with this cell is the very large excess amount of electrolyte at beginning of life, which is likely to have led to premature cell problems if operated in a zero-G environment with any significant overcharge. The stack in this cell was totally flooded at beginning of life, with an additional amount of free electrolyte (about 150% of the separator void volume) probably gathering in a pool in the bottom of the cell as it was cycled. Of course in a ground-based life-test, this pool of excess electrolyte simply acts as a reservoir to supply electrolyte to the stack as the plates swell over life (through the wall wick). While a reservoir of free electrolyte in a ground test may improve life and performance in some cell designs, it is unlikely to have had a large impact on this cell, because two layers of zircar typically provide a sufficiently large electrolyte reservoir internal to the stack to preclude stack dryout during life. This situation is exemplified by Figure 2, which shows the same cell, but with the pool of free electrolyte hypothetically removed at beginning of life, i.e. hypothetical draining of free electrolyte during activation. In Fig. 2 electrolyte has been removed until the percentage of the stack volume filled is just below 100%.

DPA analysis of this cell indicated an average of 20.7% corrosion of the sinter in the nickel electrode giving about a 600 psi hydrogen precharge at end-of-life, as well as about 10.5% swelling of the positives. With these basic physical characteristics, the expert system (see Fig. 2) indicates that positive plate expansion and corrosion, along with the resultant precharge change are the most likely issues in this cell. The remaining 13 possible issues enumerated in Fig. 2 can only be rejected or confirmed based on the appropriate DPA analyses, as suggested by the Preferred Analysis Tool. For example, in Fig. 2 the appropriate procedure to evaluate the possible role played by iron contamination is displayed by the Preferred Analysis Tool.

A complete DPA for this cell is indicated in Fig. 3. Here the results of all analyses suggested as appropriate for this cell have been performed, and the results tabulated in the symptom list. These analyses included a spectrographic analysis of positive active material for iron and calcium, X-ray diffraction of positive active material for Ni_2O_3H, positive loading distribution analysis, electrolyte distribution analysis, spectrographic analysis of electrolyte for silicon, impedance monitoring during a charge retention stand test, positive plaque pore size analysis, positive plate stress test, organic analysis in positive plates, and cobalt uniformity analysis. This complete DPA has confirmed the initial evaluation that positive plate expansion and corrosion were the primary issues likely to limit the life and performance of this cell. If this high level of certainty was not required, the DPA analysis could have been limited to simply measurement of corrosion (by residual gas analysis) and positive plate expansion.

Example 2. Failed Cell from 60% DOD Life-Test

Example 2 draws on experience from a 81 ampere-hour MANTECH cell with a composite separator consisting of one layer of zircar and 1 layer of asbestos. The cell failed after about 10,000 cycles at 60% DOD in a ground life-test. Tests after failure indicated a cell capacity that was about 45% low, and good charge retention capacity. Providing this relatively basic information along with the swelling of the positives and the positive corrosion to the expert system provided the evaluation shown in Figure 4. The expert system indicates that to a very high probability, the cell has problems caused by separator dryout. When the fact that the

discharge voltage plateau had dropped more than 100 mv at end of life was added to the list of symptoms in the expert system, the probability of cell dryout increased to over 97%. At present this analysis provides the most reliable evaluation available for the root cause for the failure of this cell. While the additional possible root causes listed in Figure 4 could be eliminated with further analysis effort, such effort probably is not warranted in this situation simply to increase our confidence from 97% to 100%. This example shows how a large amount of DPA analysis on cell components can be eliminated when this expert system is correctly applied, with little loss in the confidence that the correct root cause has been established.

Example 3. Failed Cell from 75% DOD Life-Test

A 48 ampere-hour cell failed after about 1000 cycles in a 75% DOD life test at 20 deg C. The cell exhibited about a 30% capacity loss, good charge retention behavior, only 8% swelling of the positive plates, and 5.5% corrosion of the nickel sinter in the positive plates (from pressure growth in the cell). This cell was quite puzzling because none of the traditional failure modes for nickel hydrogen cells seemed to account for the behavior of this cell. It should be pointed out that all cells in this test pack had appeared to degrade in the same way, thus this was no special behavior associated with an outlying cell. When this information was supplied to the expert system, the evaluation shown in Figure 5 was obtained. Plate expansion due to high stress was listed as the most likely root cause for cell failure, with hydrogen precharge being a possible problem if the cells were stored as another possibility. Since the plate expansion was not very great, and the cells had not been stored but had failed during cycling, both these root causes were not given a high probability. More interestingly, the third root cause listed was some process that could de-activate nickel electrode active material so that it could no longer be charged or discharged. At the time of this DPA, no such process had been identified, but deactivation has long been recognized as a possible scenario for capacity loss.

After extensive evaluation of electrodes from this cell, it was discovered that active material had in fact been converted from the normal nickel hydroxide to a new material Ni_2O_3H, which was electrochemically inert. A technique was developed that utilized x-ray diffraction to assay the amount of this compound in active material taken from nickel electrodes, as is described in Fig. 5. This assay indicated that about 30% of the active material had undergone this conversion to inactive material. When this analysis result was added to the list of symptoms for this cell, the expert system evaluation in Figure 6 was obtained, which indicated a 100% probability that Ni_2O_3H formation was the root cause. This provided a quite definitive root cause for the failure of this cell, in spite of the fact that the process whereby active material is deactivated is not clearly understood.

Example 4. Cell with Capacity Fading after Storage (Hydrogen precharged)

Example 4 is drawn from experience with a 76 ampere-hour cell with two layers of zircar separator and a hydrogen precharge of about 15 psi. This cell was found to fade in capacity after extended periods of passive discharged storage. While today we recognize this condition as due to the reaction of the excess hydrogen gas with the nickel electrode and the resultant degradation in the active material, at the time of this DPA this root cause was not yet widely accepted. The accepted fix today for this problem is to utilize a nickel precharge. Of more interest however, is assuring that when provided with the pertinent symptoms, this expert system can clearly recognize this root cause for capacity fading.

Figure 7 indicates the initial evaluation provided by the expert system when given a 30% reduction in capacity at beginning of life and good charge retention test performance for this cell. The most likely root cause when provided this rather limited information is indeed given as the loss or absence of nickel precharge, assuming the cell had been subjected to storage. However, due to the lack of more specific data the certainty is not very high that this is the correct verdict. Additional certainty in the root cause may be obtained by carrying out further analyses, as indicated by the Preferred Analysis Tool, for the most likely root causes.

The positive and negative precharge measurements are the best analyses for eliminating loss of nickel precharge as a root cause. For this cell essentially zero positive precharge was found, and about 3% hydrogen precharge was found, based on flooded nickel electrode tests and analysis of residual gas in the cell. When this information is put into the symptom list for this cell, the expert system indicates 100% likelihood that lack of nickel precharge was responsible for the capacity fade, assuming that the cell was exposed to some storage time, which was true in this case. This result is indicated in Figure 8. Thus, this expert system is clearly capable of determining if capacity fading is due to storage in a hydrogen-precharged state. Furthermore, this root cause was pinpointed simply based on a gas analysis for the cell and a simple residual capacity measurement for the nickel electrodes from the cell. Utilization of the expert system in this instance could have saved a tremendous amount of DPA effort, since this cell was subjected to an extensive DPA that examined all significant degradation and failure modes.

Example 5. Early-Life Failure of Single-layer Zircar Cell

A cell with a single layer of zircar separator was activated with 38% KOH electrolyte, then placed into a life test. After about 100 cycles this cell was found to have degraded performance due to significant capacity loss to a 1.0 volt discharge limit. Charge retention capacity was found to be good. Initial DPA results based on plate thickness measurements and residual gas analysis indicated 1.3% corrosion of the positive sinter and about 12% swelling. The relatively large amount of swelling is likely to have been the result of the high electrolyte concentration in the cell. When the expert system was provided this information, its evaluation concluded that the cell had failed due to dryout of the separator, largely as a result of the plate swelling, as indicated in Figure 9. Based on the approximately 83% confidence for this verdict, no additional DPA testing would be typically needed to eliminate the remaining remotely possible root causes listed in Fig. 9. This example provides another situation where the expert system allows the user to evaluate when a DPA process has arrived at a point of reasonable closure.

Example 6. Early-Life Failure of a Cell Containing Excess Electrolyte

One of the most common sources of problems causing early-life failures in nickel hydrogen cells is the presence of more electrolyte than can be readily contained in the electrode stack. This example analyzes a 76 ampere-hour cell with two layers of zircar separator that was filled with about 20 cc more electrolyte than could be contained within the electrode stack. The cell gave slightly lower capacity than was expected (up to 20% low) and had relatively poor (~70-75%) charge retention test results at beginning of life. DPA revealed some discoloration around the edges of the stack, but did not clearly locate any shorting paths. Little corrosion or swelling of the positive plaque was found, based on positive plate thickness measurements and residual gas analysis for the cell.

When this information was provided to the expert system, the evaluation showed in Figure 10 was obtained. This evaluation gave a 90+% confidence that the cell problems came from low-level short circuits due to oxygen evolution and popping during cell overcharge, and furthermore that the root cause for these problems was an excessive electrolyte fill. At this confidence level it would be perfectly reasonable to stop the DPA and declare a successful diagnosis. However, further extensive DPA analyses were performed in this case to rule out all other possibilities, making popping and excessive electrolyte the only viable root cause for the problems with this cell. The expert system can efficiently guide the user through the process of maximizing confidence in the diagnosis by choosing the most appropriate additional tests to perform on the cell components.

Example 7. Failure of a Cell with Asbestos Separator

This cell is a 76 ampere-hour COMSAT design cell, having asbestos separator and a back to back design, with no wall wick. After about 1000 40% DOD cycles in a life test, this cell was removed because of a low end of discharge voltage. Initial DPA results indicated minimal corrosion or swelling of the positives. However the charge retention capacity was somewhat low, and the standard capacity was about 40% low. When given these symptoms, the expert system provided the evaluation in Figure 11. This evaluation suggests that the most likely root cause is some kind of short-circuit, perhaps caused by popping, excessive overcharge, or localized overcharge. However, the confidence in this diagnosis is not extremely high. Given these symptoms, this is a very reasonable evaluation. However, measurement of residual capacity after a C/2 capacity discharge revealed that the 40% low capacity was due to large amounts of residual capacity that could only be discharged at voltages below 1 volt. Similarly, the charge retention test gave low results because appreciable residual capacity was not being counted. Clearly these results are not consistent with a short circuit.

If the symptoms are modified so that the charge retention capacity includes all charge retained following the 72-hr open circuit stand (based on cell pressure), the retention increases to 85%. When this modified symptom is provided to the expert system, all possibilities of short-circuiting are eliminated. The most likely degradation mode then becomes capacity loss due to storage with a hydrogen precharge. Since this cell did not experience any storage, this root need not be pursued in any further detail. The next most likely root cause is active material deactivation by Ni_2O_3H formation. X-ray diffraction analysis of active material did not reveal any of this compound. When this added symptom is added to the symptom list, the most likely root cause becomes a non-uniform distribution of electrolyte through the cell. However, an electrolyte distribution analysis revealed an electrolyte uniformity factor of 0.92. When this information is added to the symptom list, the next most likely root cause is silicon contamination. A spectrographic analysis of the electrolyte for silicon contamination revealed 4.3% silicate by weight in the electrolyte, which is a very high level and has presumably come about due to exchange between the silicates in the asbestos separator and the hydroxides in the electrolyte. Addition of the silicate level to the expert system symptom list provides the evaluation shown in Figure 12, which indicates silicon contamination as the sole cause for poor cell performance.

This example illustrates how the user can use the expert system to screen all the possible root causes for a problem that initially does not have a very clear diagnosis. In this case only three specialized analyses were required on cell components to arrive at a conclusion with a very high confidence level. In contrast, with no guidance as to the most appropriate analyses, it is very likely that 10-20 specialized chemical or electrical analyses could be performed before stumbling on one that was relatively definitive.

Conclusions

An Expert System for Battery Cell Analysis (ESBCA) has been developed for the purpose of guiding the diagnosis of performance problems or degradation in nickel hydrogen battery cells. Applying it to seven different cell DPA efforts that have occurred over the years has validated the ESBCA system. In all cases the ESBCA system was capable of rapidly guiding a user to a very conclusive root cause for the observed cell symptoms. In each case the interactive combination of the ESBCA system with the DPA results resulted in a major reduction in the DPA analysis and test effort. In several of the examples an order of magnitude reduction in effort was realized relative to the actual DPA testing that was ultimately required to confidently identify a root cause. To maximize the probability of rapidly arriving at the cause of cell issues, we recommend that an expert system such as this be utilized to guide all future nickel hydrogen cell DPA efforts.

Figure 1. Example 1 Cell
Beginning of Life Expert-System Evaluation

Expert System for Battery Cell Analysis

File Edit Tools Help Windows

Validation NiH2 Cell Analysis File – Very wet cell with good performance after 42,000 cycles

90.00 AH Nickel Hydrogen Cell with diameter of 4.5 inches Back-to-Back Stack

Actual Capacity(100% util.): 98.77

Positives: Total Number: 34 Substrate: Sinter

Swelling(%): 10.82 Corrosion(%): 20.70

	Initial	Degraded	Analysis
Plaque Porosity(%)	82.00	87.12	87.23
Thickness(mils)	34.00	37.68	37.63
Loading Level(g/ccv)	1.70	1.977	1.97
Co Additive(%)	5.00	5.00	5.00

Symptom List

Low Capacity (C/2 rate), 2.00 %
Equiv. 100% DOD Cycles, 16.80 Kcyc
Charge retention capacity, 85.00 %

Separator: Zircar(2 layer) 24.00 mils thick

Negative: 6.00 mils thick

Electrolyte:

	Initial	Degraded	Analysis
Fill Weight (g)	656.00	606.09	606.00
Weight Percent	31.00	33.55	33.51
g/AH(actual)	6.64	6.14	6.14
% sep. void filled	250.34	215.07	214.87

Evaluation of Most Likely Root Causes

3 Symptoms Listed for C:\CellAnly\ValCase1.dat

Root Cause	Probability(%)
Excessive Electrolyte Fill in Cell	100.00

Selected Root Cause:
Excessive Electrolyte Fill in Cell

Describe Cause

Show Procedure

Analysis/Symptom

Uniform Electrolyte factor
Electrolyte Concentration

Description of Root Cause

Excessive electrolyte results when more than 100% of the stack volume (not counting the gas screen volume) is filled with electrolyte. This condition can result in popping and cell short-circuits, particularly in a zero-G operating environment or if the cell is tested on its side in a gravitational field. Better draining of the cell during activation can fix this problem.

Figure 2. Example 1 Cell
Expert System Evaluation without Pool of Free Electrolyte

Expert System for Battery Cell Analysis

File Edit Tools Help Windows

Validation NiH2 Cell Analysis File – Very wet cell with good performance after 42,000 cycles

90.00 AH Nickel Hydrogen Cell with diameter of 4.5 inches Back-to-Back Stack

Positives: Total Number: 34 Substrate: Sinter Actual Capacity(100% util.): 98.77

Swelling(%): 10.82 Corrosion(%): 20.70

	Initial	Degraded	Analysis
Plaque Porosity(%)	82.00	87.12	87.23
Thickness(mils)	34.00	37.68	37.63
Loading Level(g/ccv)	1.70	1.977	1.97
Co Additive(%)	5.00	5.00	5.00

Symptom List

Low Capacity (C/2 rate), 2.00 %
Equiv. 100% DOD Cycles, 16.80 Kcyc
Charge retention capacity, 85.00 %

Separator: Zircar(2 layer) 24.00 mils thick

Negative: 6.00 mils thick

Electrolyte:

	Initial	Degraded	Analysis
Fill Weight (g)	363.00	313.09	313.00
Weight Percent	31.00	35.94	35.91
g/AH(actual)	3.68	3.17	3.17
% sep. void filled	99.38	64.22	63.96

Evaluation of Most Likely Root Causes

3 Symptoms Listed for C:\CellAnly\ValCase1.dat

Root Cause	Probability(%)
Plate expansion(high stress)	37.50
Positive plate corrosion	34.35
Loss of Ni Precharge/storage	9.77
Contamination: Iron	6.17
Deactivation via Ni2O3H formation	3.75
Plate expansion(nonuniform loading)	2.03
Non-uniform electrolyte distribution	1.41
Contamination: Silicon	0.94
Abnormal Plaque Pore Size Distribution	0.90
Non-uniform loading	0.90
Separator Contact loss with plates	0.90
Contamination: Organics	0.60
Weak positive plaque	0.44
Poorly Distributed Co Additive	0.29
Contamination: Calcium	0.06

Selected Root Cause:
Contamination: Iron

Describe Cause | Show Procedure

Analysis/Symptom

Iron Level in the Positive
Negative Polarization
Capacity loss at High Temp
Low End-Of-Charge Voltage
Low Capacity (C/2 rate)
Charge retention capacity
Capacity loss at Low Temp

Description of Root Cause

Iron contamination increases the rate of oxygen evolution on the positive, making cells less efficient and decreasing the capacity achievable from the nickel electrode. Negative overpotentials are increased by iron contamination.

Figure 3. Example 1 Cell
Expert System Evaluation after All Recommended Analyses

Expert System for Battery Cell Analysis

File Edit Tools Help Windows

Validation NiH2 Cell Analysis File – Very wet cell with good performance after 42,000 cycles

90.00 AH Nickel Hydrogen Cell with diameter of 4.5 inches Back-to-Back Stack

Positives: Total Number: 34 Substrate: Sinter Actual Capacity(100% util.): 98.77

Swelling(%): 10.82 Corrosion(%): 20.70

	Initial	Degraded	Analysis
Plaque Porosity(%)	82.00	87.12	87.23
Thickness(mils)	34.00	37.68	37.63
Loading Level(g/ccv)	1.70	1.977	1.97
Co Additive(%)	5.00	5.00	5.00

Separator: Zircar(2 layer) 24.00 mils thick

Negative: 6.00 mils thick

Electrolyte:

	Initial	Degraded	Analysis
Fill Weight (g)	363.00	313.09	313.00
Weight Percent	31.00	35.94	35.91
g/AH(actual)	3.68	3.17	3.17
% sep. void filled	99.38	64.22	63.96

Symptom List

Low Capacity (C/2 rate), 2.00 %
Equiv. 100% DOD Cycles, 16.80 Kcyc
Charge retention capacity, 85.00 %
Iron Level in the Positive, 10.00 ppm
Ni2O3H level by x-ray Diff, 0.00 %
+ Uniform Loading Factor, 0.91
Uniform Electrolyte factor, 0.95
Si Level in Electrolyte, 8.00 ppm
Impedance Change, 72 Ch. OC, 5.00 %
Positive Pore Size(average), 24.00 u
Organic Level in Positive, 20.00 ppm
Positive Stress swelling, 2.00 %
+ Cobalt Uniformity Factor, 0.87
Calcium level in positive, 6.00 ppm

Evaluation of Most Likely Root Causes

14 Symptoms Listed for C:\CellAnly\ValCase1.dat

Root Cause	Probability(%)
Plate expansion(high stress)	51.35
Positive plate corrosion	33.51
Loss of Ni Precharge/storage	15.14

Selected Root Cause:
Plate expansion(high stress)

Describe Cause | Show Procedure

Analysis/Symptom

Positive Plate Swelling
Equiv. 100% DOD Cycles
Loading Level(average)
Plaque Porosity(average)
Capacity loss at Low Temp
Low Capacity (C/2 rate)
Capacity loss at High Temp
Plaque Corrosion Level
Decrease in Flooded + Util
Increased EOC Pressure
Increased EOD Pressure
Capacity below 1.0 volt
Low mid-discharge Voltage

Description of Root Cause

Nickel electrodes expand over life in response to active material expansion and contraction during cycling, as well as hydrodynamic forces associated with overcharge.

Figure 4. Expert System Evaluation for Example 2 Cell

Expert System for Battery Cell Analysis

File Edit Tools Help Windows

Validation NiH2 Cell Analysis File – AZ cell with capacity loss from 60% DOD cycling

81.00 AH Nickel Hydrogen Cell with diameter of 3.5 inches Back-to-Back Stack

Positives: Total Number: 64 Substrate: Sinter

Swelling(%): 30.00 Corrosion(%): 16.85

Actual Capacity(100% util.): 86.28

	Initial	Degraded	Analysis
Plaque Porosity(%)	76.00	84.65	84.30
Thickness(mils)	30.00	39.00	39.00
Loading Level(g/ccv)	1.70	1.575	1.57
Co Additive(%)	5.00	5.00	5.00

Separator: Zircar(2 layer) 24.00 mils thick

Negative: 6.00 mils thick

Electrolyte:

	Initial	Degraded	Analysis
Fill Weight (g)	374.00	322.94	322.50
Weight Percent	31.00	35.90	35.77
g/AH(actual)	4.33	3.74	3.74
% sep. void filled	99.42	39.90	40.05

Symptom List

Low Capacity (C/2 rate), 45.00 %
Equiv. 100% DOD Cycles, 6.00 Kcyc
Charge retention capacity, 85.00 %

Evaluation of Most Likely Root Causes

3 Symptoms Listed for C:\CellAnly\ValCase2.dat

Root Cause	Probability(%)
Cell has dried out	81.59
Plate expansion(high stress)	4.42
Loss of Ni Precharge/storage	3.77
Positive plate corrosion	3.20
Deactivation via Ni2O3H formation	2.43
Non-uniform electrolyte distribution	0.91
Contamination: Silicon	0.61
Abnormal Plaque Pore Size Distribution	0.58
Non-uniform loading	0.58
Separator Contact loss with plates	0.58
Contamination: Organics	0.39
Contamination: Iron	0.30
Plate expansion(nonuniform loading)	0.22
Poorly Distributed Co Additive	0.19
Weak positive plaque	0.18

Selected Root Cause:
Cell has dried out

Describe Cause | Show Procedure

Analysis/Symptom

- Capacity below 1.0 volt
- Residual Positive Capacity
- Positive Plate Swelling
- Low mid-discharge Voltage
- High End-Of-Charge Voltage
- Capacity loss at Low Temp
- Uniform Electrolyte factor
- Electrolyte Concentration

Description of Root Cause

Cell dryout results when there is insufficient electrolyte in the separator to support ionic current flow at the C/2 rate. This typically occurs when less than 50% of the separator pore volume is filled with electrolyte, and is largely driven by plate expansion. The key signature for this root cause is high cell impedance, particularly at high discharge rates.

Figure 5. Initial Expert System Evaluation of Example Cell 3

Expert System for Battery Cell Analysis

File Edit Tools Help Windows

Validation NiH2 Cell Analysis File – Double zircar cell with capacity loss from 75% DOD cycling

48.00 AH Nickel Hydrogen Cell with diameter of 3.5 inches Back-to-Back Stack

Positives: Total Number: 32 Substrate: Sinter

Actual Capacity(100% util.): 55.85

Swelling(%): 8.33 Corrosion(%): 5.51

	Initial	Degraded	Analysis
Plaque Porosity(%)	82.00	84.30	84.30
Thickness(mils)	36.00	39.00	39.00
Loading Level(g/ccv)	1.70	1.628	1.63
Co Additive(%)	5.00	5.00	5.00

Symptom List

Low Capacity (C/2 rate), 30.00 %
Equiv. 100% DOD Cycles, 1.00 Kcyc
Charge retention capacity, 85.00 %

Separator: Zircar(2 layer) 24.00 mils thick

Negative: 6.00 mils thick

Electrolyte:

	Initial	Degraded	Analysis
Fill Weight (g)	202.00	194.49	201.00
Weight Percent	31.00	32.20	31.36
g/AH(actual)	3.62	3.48	3.60
% sep. void filled	95.15	75.42	82.42

Evaluation of Most Likely Root Causes

3 Symptoms Listed for C:\CellAnly\ValCase3.dat

Root Cause	Probability(%)
Plate expansion(high stress)	28.39
Loss of Ni Precharge/storage	24.91
Deactivation via Ni2O3H formation	16.07
Non-uniform electrolyte distribution	6.03
Contamination: Silicon	4.02
Abnormal Plaque Pore Size Distribution	3.86
Non-uniform loading	3.86
Separator Contact loss with plates	3.86
Contamination: Organics	2.57
Contamination: Iron	2.53
Poorly Distributed Co Additive	1.25
Weak positive plaque	1.21
Plate expansion(nonuniform loading)	1.21
Contamination: Calcium	0.24

Selected Root Cause:
Deactivation via Ni2O3H formation

Describe Cause | Show Procedure

Analysis/Symptom

- Ni2O3H level by x-ray Diff
- Inactive Positive Capacity
- Decrease in Flooded + Util
- Low Capacity (C/2 rate)
- Cycle overcharge(% of C)
- Residual Hydrogen Pressure
- Increased EOD Pressure
- Capacity loss at Low Temp
- Capacity loss at High Temp
- High Mid-Charge Voltage
- Low mid-discharge Voltage

Description of Root Cause

Some conditions of cell operation (high temperature and voltage) or electrode storage (dry with some residual charge) can result in conversion of nickel hydroxide into Ni2O3H, which is electrochemically inert, thus producing a permanent capacity degradation.

Figure 6. Expert System Evaluation of Example Cell 3 Including Assay for Active Material Deactivation

Expert System for Battery Cell Analysis

File Edit Tools Help Windows

Validation NiH2 Cell Analysis File – Double zircar cell with capacity loss from 75% DOD cycling

48.00 AH Nickel Hydrogen Cell with diameter of 3.5 inches Back-to-Back Stack

Positives: Total Number: 32 Substrate: Sinter Actual Capacity(100% util.): 55.85

Swelling(%): 8.33 Corrosion(%): 5.51

	Initial	Degraded	Analysis
Plaque Porosity(%)	82.00	84.30	84.30
Thickness(mils)	36.00	39.00	39.00
Loading Level(g/ccv)	1.70	1.628	1.63
Co Additive(%)	5.00	5.00	5.00

Symptom List

Low Capacity (C/2 rate), 30.00 %
Equiv. 100% DOD Cycles, 1.00 Kcyc
Charge retention capacity, 85.00 %
Ni2O3H level by x-ray Diff, 30.00 %

Separator: Zircar(2 layer) 24.00 mils thick

Negative: 6.00 mils thick

Electrolyte:

	Initial	Degraded	Analysis
Fill Weight (g)	202.00	194.49	201.00
Weight Percent	31.00	32.20	31.36
g/AH(actual)	3.62	3.48	3.60
% sep. void filled	95.15	75.42	82.42

Evaluation of Most Likely Root Causes

4 Symptoms Listed for C:\CellAnly\ValCase3.dat

Root Cause	Probability(%)
Deactivation via Ni2O3H formation	100.00

Selected Root Cause:
Deactivation via Ni2O3H formation

Describe Cause | Show Procedure

Analysis/Symptom:

- Ni2O3H level by x-ray Diff
- Inactive Positive Capacity
- Decrease in Flooded + Util
- Low Capacity (C/2 rate)
- Cycle overcharge(% of C)
- Residual Hydrogen Pressure
- Increased EOD Pressure
- Capacity loss at Low Temp
- Capacity loss at High Temp
- High Mid-Charge Voltage
- Low mid-discharge Voltage

Description of Root Cause:

Some conditions of cell operation (high temperature and voltage) or electrode storage (dry with some residual charge) can result in conversion of nickel hydroxide into Ni2O3H, which is electrochemically inert, thus producing a permanent capacity degradation.

Figure 7. Initial Expert System for Example 4 Cell

Expert System for Battery Cell Analysis

File Edit Tools Help Windows

Validation NiH2 Cell Analysis File – Double zircar cell with capacity fade from storage

76.00 AH Nickel Hydrogen Cell with diameter of 3.5 inches Back-to-Back Stack

Positives: Total Number: 48 Substrate: Sinter Actual Capacity(100% util.): 83.78

Swelling(%): 0.83 Corrosion(%): 0.29

	Initial	Degraded	Analysis
Plaque Porosity(%)	82.00	82.20	82.27
Thickness(mils)	36.00	36.30	36.20
Loading Level(g/ccv)	1.70	1.682	1.72
Co Additive(%)	5.00	5.00	5.00

Separator: Zircar(2 layer) 24.00 mils thick

Negative: 6.00 mils thick

Electrolyte:

	Initial	Degraded	Analysis
Fill Weight(g)	305.00	304.41	304.00
Weight Percent	31.00	31.06	31.56
g/AH(actual)	3.64	3.63	3.63
% sep. void filled	96.34	94.48	94.91

Symptom List

Low Capacity (C/2 rate), 30.00 %
Equiv. 100% DOD Cycles, 0.00 Kcyc
Charge retention capacity, 87.00 %

Evaluation of Most Likely Root Causes

3 Symptoms Listed for C:\CellAnly\ValCase4.dat

Root Cause	Probability(%)
Loss of Ni Precharge/storage	34.77
Deactivation via Ni2O3H formation	22.43
Non-uniform electrolyte distribution	8.41
Contamination: Silicon	5.61
Abnormal Plaque Pore Size Distribution	5.38
Non-uniform loading	5.38
Separator Contact loss with plates	5.38
Contamination: Iron	3.59
Contamination: Organics	3.59
Poorly Distributed Co Additive	1.74
Plate expansion(nonuniform loading)	1.68
Weak positive plaque	1.68
Contamination: Calcium	0.34

Selected Root Cause

Loss of Ni Precharge/storage

Describe Cause Show Procedure

Analysis/Symptom

Residual Positive Capacity
+ Cobalt Uniformity Factor
H2 or Negative Precharge
Residual Hydrogen Pressure
Insoluble Cobalt Material
Decrease in Flooded + Util
High Mid-Charge Voltage
High mid-discharge Voltage
Low Capacity (C/2 rate)
Capacity below 1.0 volt
Decreased EOC Pressure
Capacity loss at Low Temp
Capacity loss at High Temp

Description of Root Cause

Nickel precharged cells tend to lose their active precharge during extended storage (i.e. about 5% of cell capacity per year). This, or any of a number of other processes that can inactivate precharge, can give a hydrogen precharged condition that can result in permanent capacity degradation during subsequent passive storage.

Figure 8. Example 4 Evaluation with Precharge Levels Specified

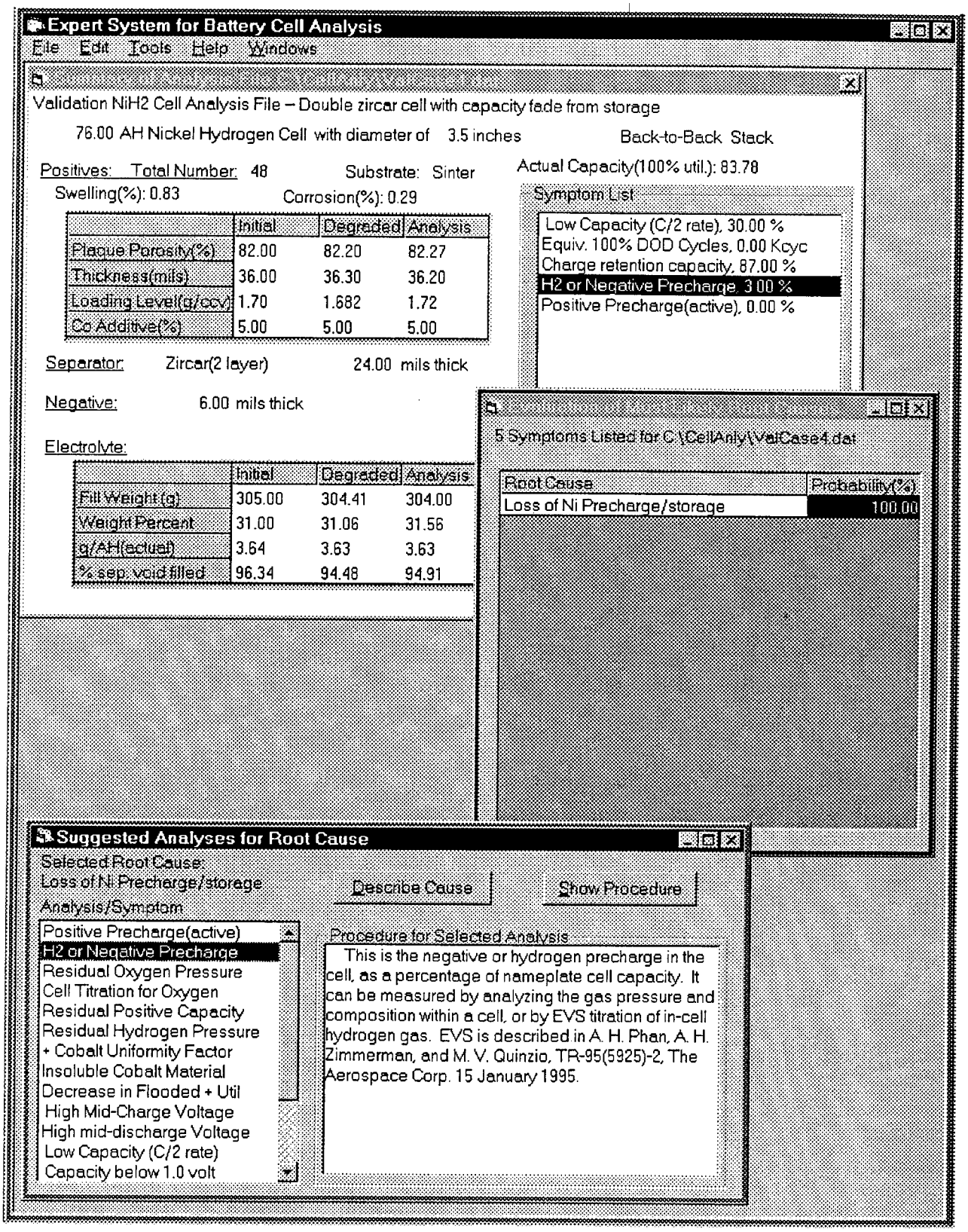

Figure 9. Expert System Evaluation for Example 5 Cell

Expert System for Battery Cell Analysis

File Edit Tools Help Windows

Validation NiH2 Cell Analysis File – Single zircar cell with electrolyte dryout due to plate expansion

65.00 AH Nickel Hydrogen Cell with diameter of 3.5 inches Back-to-Back Stack

Positives: Total Number: 48 Substrate: Sinter

Actual Capacity(100% util.): 69.82

Swelling(%): 12.00 Corrosion(%): 1.32

	Initial	Degraded	Analysis
Plaque Porosity(%)	82.00	84.14	84.10
Thickness(mils)	30.00	33.60	33.60
Loading Level(g/ccv)	1.70	1.404	1.41
Co Additive(%)	5.00	5.00	5.00

Separator: Zircar(1 layer) 12.00 mils thick

Negative: 6.00 mils thick

Electrolyte:

	Initial	Degraded	Analysis
Fill Weight (g)	200.00	197.76	197.20
Weight Percent	31.00	31.35	31.36
g/AH(actual)	2.86	2.83	2.82
% sep. void filled	93.17	52.51	52.26

Symptom List

- Low Capacity (C/2 rate), 20.00 %
- Equiv. 100% DOD Cycles, 0.10 Kcyc
- Charge retention capacity, 84.00 %

3 Symptoms Listed for C:\CellAnly\ValCase5.dat

Root Cause	Probability(%)
Cell has dried out	73.64
Loss of Ni Precharge/storage	9.17
Deactivation via Ni2O3H formation	5.91
Non-uniform electrolyte distribution	2.22
Contamination: Silicon	1.48
Abnormal Plaque Pore Size Distribution	1.42
Non-uniform loading	1.42
Separator Contact loss with plates	1.42
Contamination: Iron	1.23
Contamination: Organics	0.95
Poorly Distributed Co Additive	0.46
Weak positive plaque	0.44
Plate expansion(high stress)	0.15
Contamination: Calcium	0.09
Plate expansion(nonuniform loading)	0.01

Suggested Analyses for Root Cause

Selected Root Cause:
Cell has dried out

Describe Cause | Show Procedure

Analysis/Symptom

- Capacity below 1.0 volt
- Residual Positive Capacity
- Positive Plate Swelling
- Low mid-discharge Voltage
- High End-Of-Charge Voltage
- Capacity loss at Low Temp
- Uniform Electrolyte factor
- Electrolyte Concentration

Procedure for Selected Analysis

This is the percent of total capacity discharged below 1.0 volts after C/2 discharge to 1.0 volts, and includes all residual capacity dischargeable at a C/100 rate. Temperature is 10 deg C, and charging is at a C/10 rate for 16 hr.

Figure 10. Expert System Evaluation for Example 6 Cell

Expert System for Battery Cell Analysis

File Edit Tools Help Windows

Validation NiH2 Cell Analysis File – Cell with popping problems

76.00 AH Nickel Hydrogen Cell with diameter of 3.5 inches Back-to-Back Stack

Positives: Total Number: 48 Substrate: Sinter Actual Capacity(100% util.): 81.45

Swelling(%): 0.00 Corrosion(%): 0.56

	Initial	Degraded	Analysis
Plaque Porosity(%)	82.00	82.10	82.00
Thickness(mils)	35.00	35.00	35.00
Loading Level(g/ccv)	1.70	1.721	1.70
Co Additive(%)	5.00	5.00	5.00

Separator: Zircar(2 layer) 24.00 mils thick

Negative: 6.00 mils thick

Electrolyte:

	Initial	Degraded	Analysis
Fill Weight (g)	320.00	318.90	320.00
Weight Percent	31.00	31.11	31.00
g/AH(actual)	3.93	3.92	3.93
% sep. void filled	107.46	107.19	107.46

Symptom List

Low Capacity (C/2 rate), 20.00 %
Equiv. 100% DOD Cycles, 0.01 Kcyc
Charge retention capacity, 74.00 %

3 Symptoms Listed for C:\CellAnly\ValCase6.dat

Root Cause	Probability(%)
Excessive Electrolyte Fill in Cell	51.05
Short Circuit(popping)	39.93
Short Circuit(excessive O2)	2.88
Loss of Ni Precharge/storage	1.87
Deactivation via Ni2O3H formation	1.21
Short Circuit(localized O2)	0.72
Non-uniform electrolyte distribution	0.45
Contamination: Silicon	0.30
Abnormal Plaque Pore Size Distribution	0.29
Non-uniform loading	0.29
Separator Contact loss with plates	0.29
Contamination: Iron	0.23
Contamination: Organics	0.19
Poorly Distributed Co Additive	0.09
Weak positive plaque	0.09

Suggested Analyses for Root Cause

Selected Root Cause:
Excessive Electrolyte Fill in Cell

Describe Cause | Show Procedure

Analysis/Symptom:
Uniform Electrolyte factor
Electrolyte Concentration

Description of Root Cause:
Excessive electrolyte results when more than 100% of the stack volume (not counting the gas screen volume) is filled with electrolyte. This condition can result in popping and cell short-circuits, particularly in a zero-G operating environment or if the cell is tested on its side in a gravitational field. Better draining of the cell during activation can fix this problem.

Figure 11. Initial Expert System Evaluation for Example 7 Cell

Expert System for Battery Cell Analysis

File Edit Tools Help Windows

Validation NiH2 Cell Analysis File – COMSAT cell with low capacity

76.00 AH Nickel Hydrogen Cell with diameter of 3.5" COMSAT Back-to-Back Stack

Positives: Total Number: 62 Substrate: Sinter

Actual Capacity(100% util.): 88.20

Swelling(%): 3.33 Corrosion(%): 1.40

	Initial	Degraded	Analysis
Plaque Porosity(%)	76.00	77.10	77.00
Thickness(mils)	30.00	31.00	31.00
Loading Level(g/ccv)	1.70	1.653	1.65
Co Additive(%)	5.00	5.00	5.00

Symptom List

Low Capacity (C/2 rate), 40.00 %
Equiv. 100% DOD Cycles, 0.50 Kcyc
Charge retention capacity, 78.00 %

Separator: Asbestos 12.00 mils thick

Negative: 6.00 mils thick

Electrolyte:

	Initial	Degraded	Analysis
Fill Weight (g)	255.00	250.88	252.00
Weight Percent	38.00	38.62	38.50
g/AH(actual)	3.05	3.00	3.02
% sep. void filled	91.19	77.81	79.04

Evaluation of Most Likely Root Causes

3 Symptoms Listed for C:\CellAnly\ValCase7.dat

Root Cause	Probability(%)
Short Circuit(popping)	54.30
Loss of Ni Precharge/storage	11.26
Short Circuit(excessive O2)	10.86
Deactivation via Ni2O3H formation	7.27
Non-uniform electrolyte distribution	2.72
Short Circuit(localized O2)	2.71
Contamination: Silicon	1.82
Abnormal Plaque Pore Size Distribution	1.74
Non-uniform loading	1.74
Separator Contact loss with plates	1.74
Contamination: Organics	1.16
Contamination: Iron	0.90
Poorly Distributed Co Additive	0.56
Weak positive plaque	0.55
Plate expansion(nonuniform loading)	0.55

Selected Root Cause:
Short Circuit(popping)

Describe Cause

Show Procedure

Analysis/Symptom

Charge retention capacity
Leakage Current at 1.0 volt
Low Capacity (C/2 rate)
Cycle overcharge(% of C)
Decreased EOC Pressure
Capacity loss at High Temp
Capacity loss at Low Temp
Low mid-discharge Voltage
Low Mid-Charge Voltage
Low End-Of-Charge Voltage

Procedure for Selected Analysis

This is the percentage of capacity retained after open-circuit stand for 72 hr at 10 deg C, following recharge at C/10 for 16 hr. Capacity is discharged at a C/2 rate to 1.0 volts.

Figure 12. Final Expert System Evaluation for Example 7 Cell

Expert System for Battery Cell Analysis

File Edit Tools Help Windows

Validation NiH2 Cell Analysis File – COMSAT cell with low capacity

76.00 AH Nickel Hydrogen Cell with diameter of 3.5" COMSAT Back-to-Back Stack

Positives: Total Number: 62 Substrate: Sinter

Actual Capacity(100% util.): 88.20

Swelling(%): 3.33 Corrosion(%): 1.40

	Initial	Degraded	Analysis
Plaque Porosity(%)	76.00	77.10	77.00
Thickness(mils)	30.00	31.00	31.00
Loading Level(g/ccv)	1.70	1.653	1.65
Co Additive(%)	5.00	5.00	5.00

Symptom List

Low Capacity (C/2 rate), 40.00 %
Equiv. 100% DOD Cycles, 0.50 Kcyc
Charge retention capacity, 85.00 %
Ni2O3H level by x-ray Diff, 0.00 %
Uniform Electrolyte factor, 0.89
Si Level in Electrolyte, 43000.00 ppm

Separator: Asbestos 12.00 mils thick

Negative: 6.00 mils thick

Electrolyte:

	Initial	Degraded	Analysis
Fill Weight (g)	255.00	250.88	252.00
Weight Percent	38.00	38.62	38.50
g/AH(actual)	3.05	3.00	3.02
% sep. void filled	91.19	77.81	79.04

Evaluation of Most Likely Root Causes

6 Symptoms Listed for C:\CellAnly\ValCase7.dat

Root Cause	Probability(%)
Contamination: Silicon	100.00

Selected Root Cause:
Contamination: Silicon

Describe Cause | Show Procedure

Analysis/Symptom

Si Level in Electrolyte
Low mid-discharge Voltage
Capacity loss at Low Temp
Capacity below 1.0 volt
Low Capacity (C/2 rate)
High End-Of-Charge Voltage
Capacity loss at High Temp
Residual Positive Capacity
High Mid-Charge Voltage

Description of Root Cause

Silicate contamination can significantly increase the impedance of the nickel hydrogen cell. Often high silicate levels can shift significant capacity down to a discharge plateau below 1.0 volts.

Nickel Electrode Failure by Chemical De-activation of Active Material

A. Zimmerman, M. Quinzio, G. To, P. Adams, and L. Thaller
The Aerospace Corporation
El Segundo, California

Abstract

A nickel hydrogen battery cell that had experienced early life failure in an accelerated life-test was disassembled and analyzed to determine the underlying cause for the failure. Cell failure was clearly the result of a large loss of usable capacity in the sintered nickel electrodes. This failure was not associated with electrode swelling, sinter corrosion, loss of cobalt additives, poor active material conductivity, or poor charge efficiency, all of which are known degradation processes in nickel electrodes. The failure of these electrodes was linked directly to the formation of a nickel oxide-hydroxide phase Ni_2O_3H that has not been previously linked to failure in nickel electrodes. This material appears to be electrochemically inert, resulting in up to 50% loss of usable active material in these electrodes. The formation of this material was highly non-uniform through the cell, being concentrated in regions where the electrode temperature was expected to be greatest. Ongoing study is evaluating the specific conditions in the nickel electrode that accelerate failure due to formation of Ni_2O_3H.

Nickel electrodes have served as the positive electrode in a wide range of rechargeable battery cells, such as nickel cadmium, nickel zinc, nickel hydrogen, and nickel metal-hydride, over the years. The principal attraction of the nickel electrode has been its ability to provide an extremely large number of charge-discharge cycles, thus potentially providing very long cycle life and high battery reliability. For example, performance goals in nickel hydrogen battery cells have approached 60,000 cycles at 60% depth-of-discharge (DOD). The key to attaining long cycle life is to understand the failure modes that can arise in the cells, and to control the principal degradation processes by either special design features or modified cell operating conditions. Typically, in the nickel hydrogen cells widely used for battery power in modern satellites, degradation of the nickel electrode limits the battery life. For this reason analysis of failure modes, processes, and mechanisms in nickel electrodes is a key step in further extending the life and performance of nickel hydrogen cells.

Modern nickel hydrogen cells often provide cycle life spanning 5 to 15 years of operation or more, depending on the operating conditions. For this reason, the performance of particular cells or cell designs is often based on accelerated life testing. The key issue in such testing is establishing the acceleration factors in the test, and making sure that the appropriate degradation and failure modes are the ones that are accelerated. For these reasons, analysis of a group of nickel hydrogen cells that had been tested and had failed quite early in life under accelerated conditions was of great interest. One of these cells (S/N 7), which were 48 Ah

cells (~60 Ah actual capacity) of the RNH 48-1 design produced by Eagle-Picher Industries, was obtained for detailed analysis to determine the cause for failure.

The life test data for the cell that was analyzed has been described in detail elsewhere (Ref. 1). The points that were felt to be significant in this life test were the high DOD (60%), the high test temperature (20 degrees C), and the high peak charge voltages that were allowed (nearly 1.7 volts/cell near the end of the test). All of these points were felt to constitute significant stress accelerators for various degradation modes, as will be discussed later. At the end of the life test, the failure symptom was an end-of-discharge voltage below 1.0 volt. At this point, standard capacity checks indicated that the cells had lost nearly 40% of their capacity. Charge retention tests gave no indication whatsoever that even low level internal shorts had contributed to cell failure. The analysis reported here was done to determine the degradation processes responsible for failure of these cells after only about 1200 charge-discharge cycles.

Before disassembly, the gas within the fully discharged cell was sampled and analyzed. The discharged cell was found to contain 42.4 psia of gas, having the composition: hydrogen 94.2 mole %, water vapor 4.6%, nitrogen 1.1%, oxygen 0.05% and methane 0.04%. Assuming that the state of charge of the nickel electrode was 15% for the fully discharged cell when first built, this hydrogen pressure implies that approximately 8% of the nickel metal in the sintered plaque used in the positive plates had undergone corrosion during cycling. This is not generally enough corrosion in itself to result in significant degradation in performance or failure of the positive electrodes.

The cell was disassembled by removing the stack of electrodes from the pressure vessel, and dividing the stack into positive, negative (with gas screen), and separator groups that were each weighed to determine the electrolyte distribution through the cell. No unusual damage to the edges of the stack, plates or separators was found that might have contributed to failure. The plate stack appeared to be reasonably wet with electrolyte throughout, suggesting that separator dryout was not likely to be the cause of failure. After rinsing each group of components free of electrolyte, the thickness of the electrodes were measured, giving the results reported in Table 1. The average initial thickness of these electrodes is about 36 mils, which gives an average swelling of 13.4%. A swelling of less than 15-20% is very unlikely to have resulted in failure for a cell with two layers of zircar separator.

Table 1. Measured Nickel Electrode Thicknesses for Cell S/N 7

Upper Stack		Lower Stack	
Plate Pair	Thickness (mil)	Plate Pair	Thickness (mil)
1(Top)	41.45, 44.40	9(Top)	42.32, 39.32
2	40.82, 42.92	10	41.00, 40.85
3	42.98, 39.12	11	42.62, 36.98
4	40.00, 41.28	12	41.82, 40.62
5	41.32, 41.45	13	39.72, 42.05
6	41.02, 40.08	14	37.52, 40.85
7	42.00, 42.28	15	38.40, 39.52
8(bottom)	40.98, 39.65	16(bottom)	38.90, 42.32

Samples of the nickel electrodes were subjected to a flooded utilization test that was designed to determine capacity and performance. This test involved cycling in a 31% KOH

electrolyte flooded cell that was equipped with a Hg/HgO reference electrode and a nickel sheet counter-electrode, and which was sealed in an airtight assembly to prevent contamination from atmospheric gases. These tests were done at room temperature, 22-25 degrees C. The cycling involved an initial discharge at 0.2 ma/cm^2 to -0.5 volts, then charge for 16 hr at 2 ma/cm^2, a standard discharge, charge for 32 hr at 2 ma/cm^2, then a final standard discharge. The standard discharge involved discharge at 10 ma/cm^2 to -0.4 volts, followed by discharge at 2 ma/cm^2 to -0.45 volts, and finally by discharge at 0.2 ma/cm^2 to -0.5 volts. Figures 1 and 2 indicate how selected electrodes from the cell performed in this test. The electrodes from the cell are not only much lower in capacity than a new electrode, which typically provides 110% utilization, but they also show a wide variation in capacity for different locations within the cell stack. In addition, the low capacity electrodes show little tendency to recharge to a normal capacity as they are subjected to increased charge input, behavior that is commonly seen for new or normal electrodes. These results strongly suggest that degradation of the nickel electrodes was responsible for the failure of this cell.

Physical degradation of sintered nickel electrodes is one of the most common degradation modes seen in nickel hydrogen cells. This type of degradation typically leads to significant expansion and/or corrosion of the sinter structure. Very little corrosion was seen for these electrodes. Figure 3 shows cross sections of (a) an electrode from another cell that had failed after more than 30,000 charge-discharge cycles as a result of physical degradation, (b) an electrode with about 10% swelling from failed cell S/N 7, and (c) a new electrode. Sample (a) had experienced swelling greater than 30%, along with significant internal fracturing and blistering. No internal or external physical degradation is seen for the sample from failed cell S/N 7 (Fig. 3b) that can explain why the nickel electrode performance has become severely degraded.

Chemical deloading of all the active material from the plate samples that were subjected to flooded utilization testing (Figs. 1 and 2) revealed that all these plates contained about the same amount of active material per unit area. Thus, the low capacity could not be explained by loss of active material from some electrodes, or from certain areas of electrodes. In addition the amount and composition of cobalt additive in the active material from all plates were very similar to the levels in a new plate sample. The results from the chemical analysis of loading levels were combined with the capacity measurements to provide nickel electrode utilization, which are summarized in Table 2. The plate numbering in Table 2 assigns plate 1 to the upper plate in the cell (top plate, top pair, and upper stack). A normal utilization for a new electrode is on the order of 110%, meaning that 1.1 electrons can be cycled for each nickel atom in the active material. These results suggest that the active material either could not be charged normally, or could not be discharged normally, and that the effect was greatest in the middle regions of the stacks where the highest temperatures would be expected.

Table 2. Measured Utilization Levels for Nickel Electrodes from Cell S/N 7

Electrode ID	Utilization(%)
Plate 1 (top of stack)	93.35
Plate 7 (middle of stack)	61.53
Plate 11 (near bottom of stack)	70.87

Two tests were done to determine whether the low capacities were due to an inability to discharge some charged material that was well isolated in the sintered plaque structure. The first of these tests involved magnetically separating active material from the plaque nickel

metal for well ground up samples. The separated active material powder was then mixed with carbon black (30% by weight) and a thin film was pressed between two coupons of nickel sinter. This assembly is normally capable of very effectively discharging any residual charge that is physically isolated in nickel electrode active material. For samples from the failed cell, no added discharge capacity was obtained, indicating that there was very little charged active material that was physically isolated from the current collecting surfaces in this cell. The second test was a chemical analysis for the average oxidation-state of the separated active material powder. This test involved reaction of the active material with ferrous ammonium sulfate, followed by back-titration of the remaining ferrous ions with a standard permanganate solution. This analysis indicated the active material to have an oxidation state of about 2.21 when averaged over four plates from the top stack. These results clearly indicated that the active material was not fully discharged to nickel hydroxide, and also could not be electrochemically discharged any further than some oxidation state that was intermediate between nickel (II) and nickel (III).

The chemical phases present in isolated active material were evaluated using x-ray diffraction (Ref. 2). Figure 4 compares the x-ray pattern for separated active material powder from plate 7 (a very poorly performing plate), with that of normal active material that was fully discharged. Clearly, the plate 7 material contains an additional phase. Figure 5 compares the x-ray pattern for the plate 7 material with published patterns for nickel hydroxide, γ-NiOOH, and Ni_2O_3H (Refs. 3,4), the three compounds that were most likely to be present in the sample. The active material from plate 7 appears to contain a roughly equal mix of nickel hydroxide and Ni_2O_3H. While Ni_2O_3H shares many diffraction peaks with γ-NiOOH, it has some additional peaks that clearly show up in the measured pattern, while several γ-NiOOH peaks are absent. In addition, γ-NiOOH is unlikely to be present in significant quantities because it normally is electrochemically quite active when discharge is attempted. These results suggest that some of the normal active material has undergone a conversion to Ni_2O_3H, and that the Ni_2O_3H is electrochemically inert to further charge or discharge. In fact, for the active material that was analyzed from cell S/N 7, the average oxidation state of 2.21 that was measured as well as the x-ray peak intensities indicate that 42% of the active material is Ni_2O_3H. This average amount of deactivated active material is consistent with the approximately 40% capacity loss experienced by cell S/N 7.

The FTIR spectrum of isolated active material may also be compared to that of nickel hydroxide and that of Ni_2O_3H. Since we have been unable to completely isolate Ni_2O_3H from nickel hydroxide, a differential FTIR spectrum (relative to pure $Ni(OH)_2$) for a sample of active material isolated from plate 7 of cell S/N 6 is shown in Figure 6. Also shown in Fig. 6 are the peak locations and intensities from the published infrared spectrum of Ni_2O_3H (Refs. 3,4). The result is fully consistent with the active material from cell S/N 7 containing a mixture of nickel hydroxide and Ni_2O_3H.

The formation of Ni_2O_3H in nickel electrodes as a result of electrochemical cycling has not been previously established, nor has the role of this material in cell failure been identified. One previous study of well-cycled nickel electrodes that had low capacity found an unknown phase having x-ray diffraction peaks consistent with Ni_2O_3H (Ref. 5), however the history and chemical state of those electrodes was not well documented. The formation of Ni_2O_3H thus presents a new degradation mode for the nickel electrode, assuming that a correlation exists between measured electrode capacity and the level of Ni_2O_3H that each electrode contains. Figure 7 provides such a correlation based on utilization measurements and x-ray diffraction

assays of the amount of Ni_2O_3H in electrodes from cell S/N 7. The solid line is the theoretical correlation, assuming zero electrochemical activity for Ni_2O_3H and 110% utilization for active material containing no Ni_2O_3H, which is consistent with the utilization of new electrodes of this design. The points show the utilization and amounts of Ni_2O_3H found in samples of plates throughout the failed cell. It was discovered that the amount of Ni_2O_3H could vary by a factor of two over different regions of a single plate, but that the utilization paralleled these variations. Therefore, it was critical to measure both utilization and x-ray patterns for small samples that were adjacent to each other on the individual nickel electrodes. Figure 7 shows an excellent correlation between the quantity of Ni_2O_3H in the active material and the utilization. This correlation confirms that formation of Ni_2O_3H from active material in nickel electrodes is indeed a performance degrading mechanism in nickel hydrogen cells that has not been previously recognized.

The mechanism responsible for the formation of Ni_2O_3H is not well established at present. Clearly, this compound represents a dehydrated form of nickel oxyhydroxide that could form either electrochemically or by dehydration. We have previously seen evidence that this compound can form during the dry storage of partially charged nickel electrodes, although the key factors enabling this apparent dehydration process have not yet been identified. In the cycling nickel hydrogen cell, where water activity is quite high, it is unexpected that dehydration is responsible for formation of Ni_2O_3H. The data reported here thus suggest that an electrochemical or catalytic process may be responsible for the formation of Ni_2O_3H in cycling nickel hydrogen cells. Work is continuing to identify the mechanism by which Ni_2O_3H forms in nickel electrodes during dry storage of electrodes, as well as during the long-term cycling of activated nickel hydrogen cells.

Conclusions

The conclusion that can be drawn from this study is that active material in nickel electrodes can be deactivated to an electrochemically inactive phase, which has been identified as Ni_2O_3H. This deactivation can occur during cycling of a nickel hydrogen cell, and may be accelerated by the high temperatures and high overcharge voltages experienced by the cell analyzed in this study. The same deactivated material may also be formed during dessicated storage of partially charged nickel electrodes. At present the mechanisms that can lead to deactivation of nickel electrode active material, and the conditions that accelerate deactivation are the subject of further study. The role that has been played by nickel electrode deactivation in life-test failures reported throughout the battery industry over the years remains to be established.

References

1. J. Brewer, NASA MSFC, private communication.
2. All x-ray diffraction patterns reported here were obtained using chromium radiation.
3. C. Greaves, A. Malsbury, and M. Thomas, *Solid State Ionics* **18 & 19**, 763 (1986).
4. A. Malsbury and C. Greaves, *J. Solid State Chem.* **71**, 418 (1987).
5. R. McEwan, *J. Phys. Chem.* **75**, 1782 (1971).

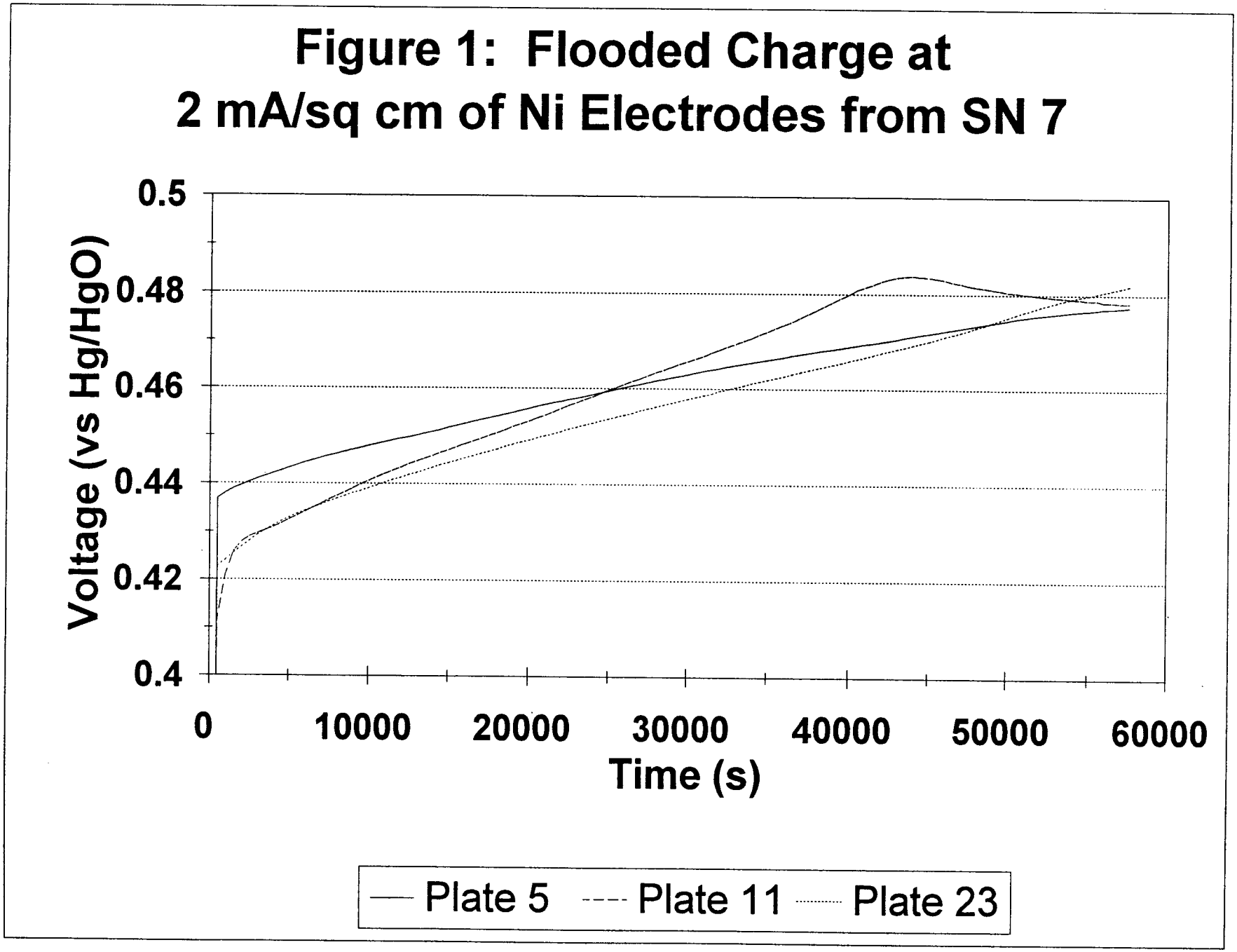
Figure 1: Flooded Charge at
2 mA/sq cm of Ni Electrodes from SN 7
Voltage (vs Hg/HgO)
0.5
0.48
0.46
0.44
0.42
0.4
0
10000
20000
30000
40000
50000
60000
Time (s)
Plate 5
Plate 11
Plate 23

Figure 2: Flooded Discharge at 10 mA/sq cm of Ni Electrodes from SN 7

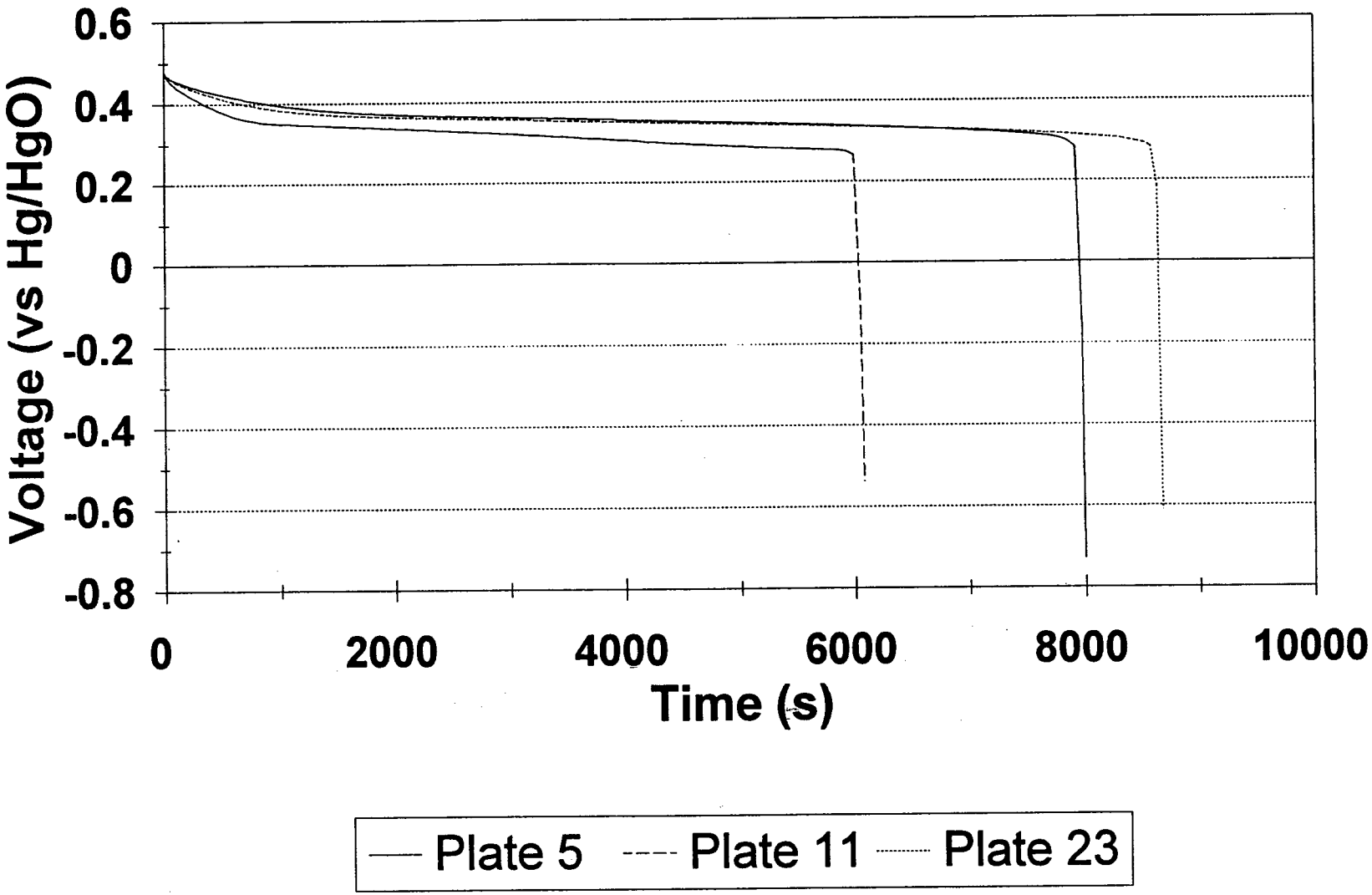

Figure 3. Cross Sections of Nickel Electrodes

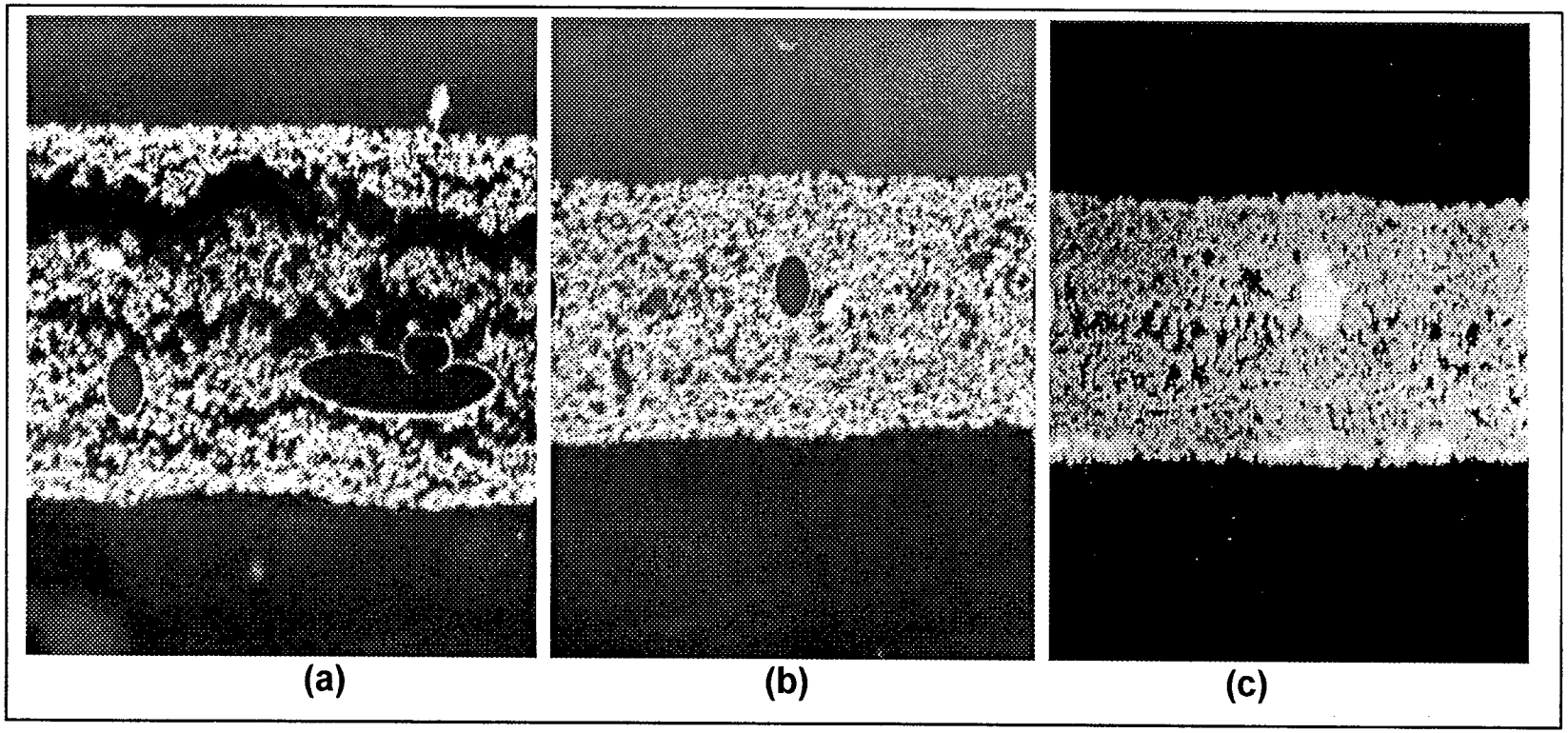

Cycled to Failure | From S/N 7 | New Electrode

Figure 4. X-ray Diffraction for S/N 7 and Normal Discharged Active Material

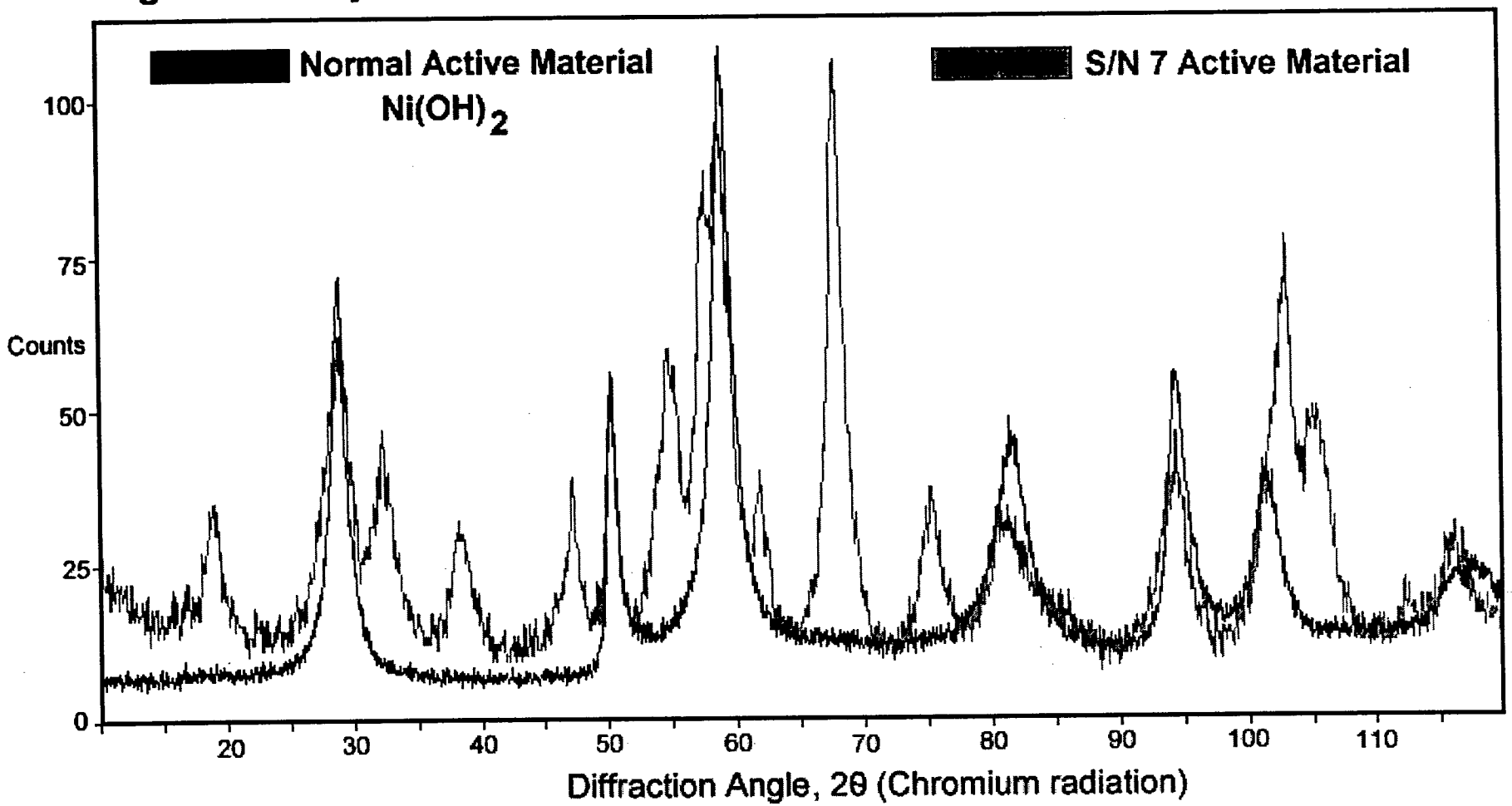

Figure 5. X-ray Diffraction for Active Material (Cell S/N 7)

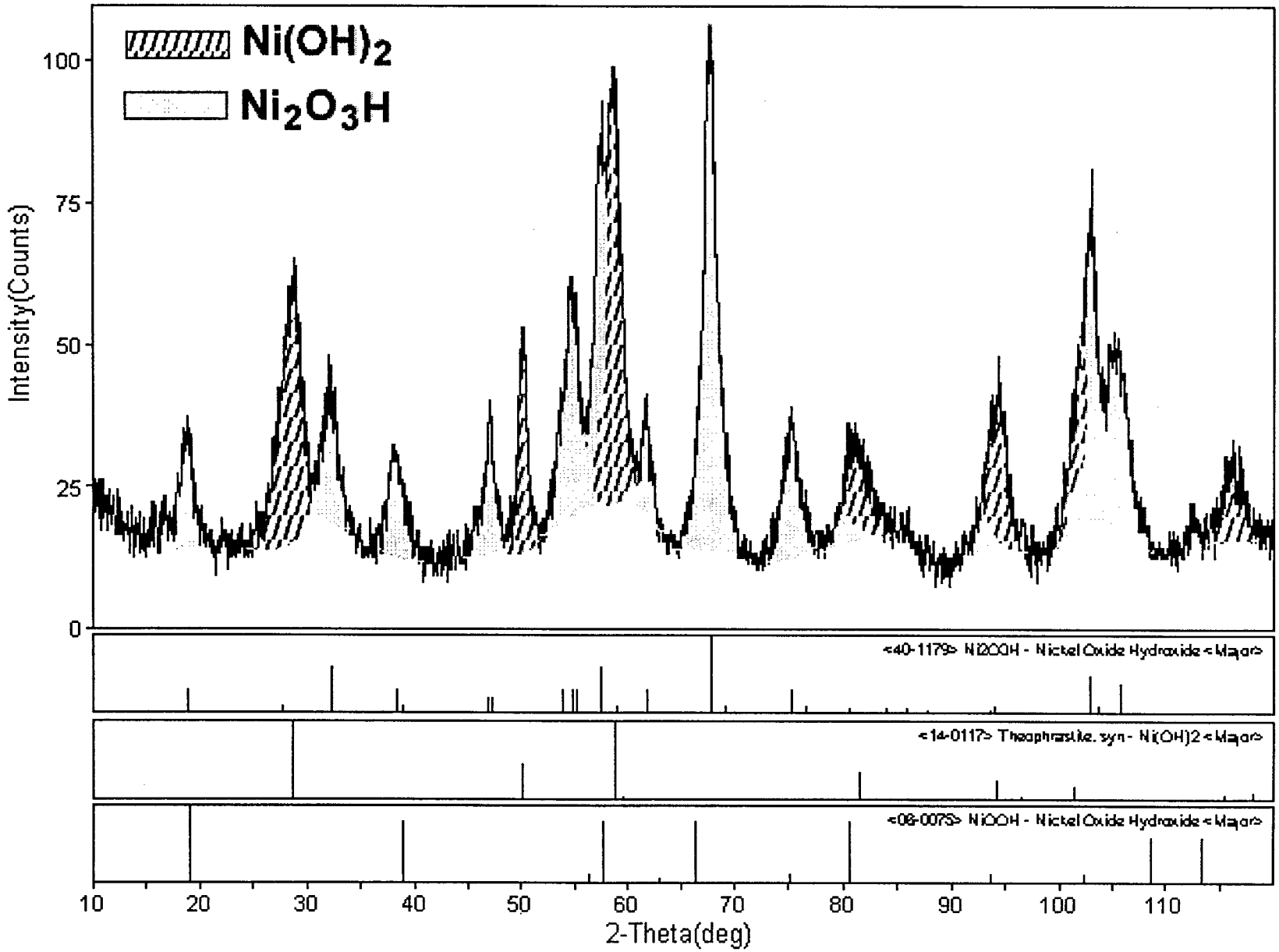

Figure 6. Difference FTIR of S/N 7 Active Material (vs. $Ni(OH)_2$)

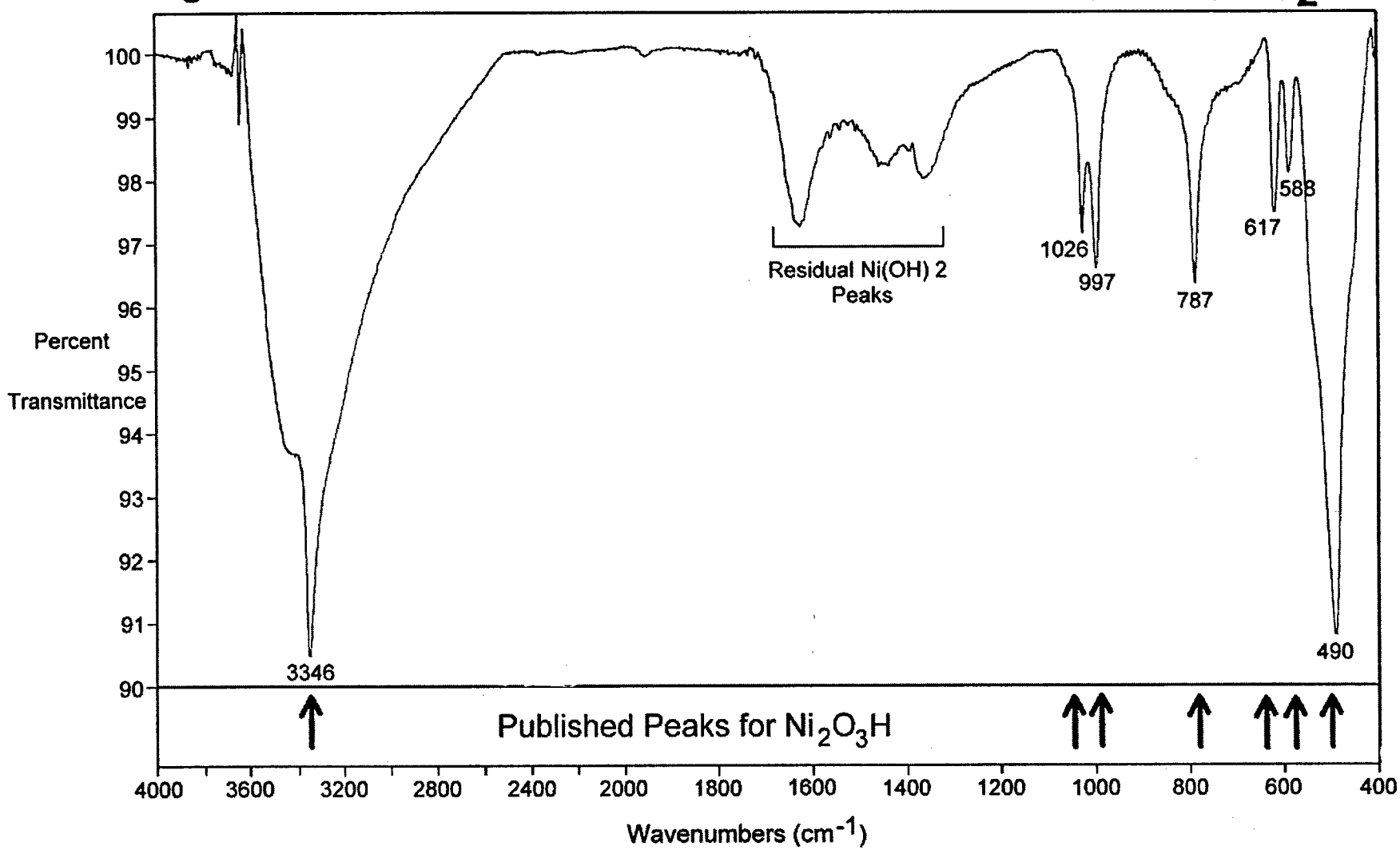

Figure 7.

% Ni_2O_3H vs Utilization

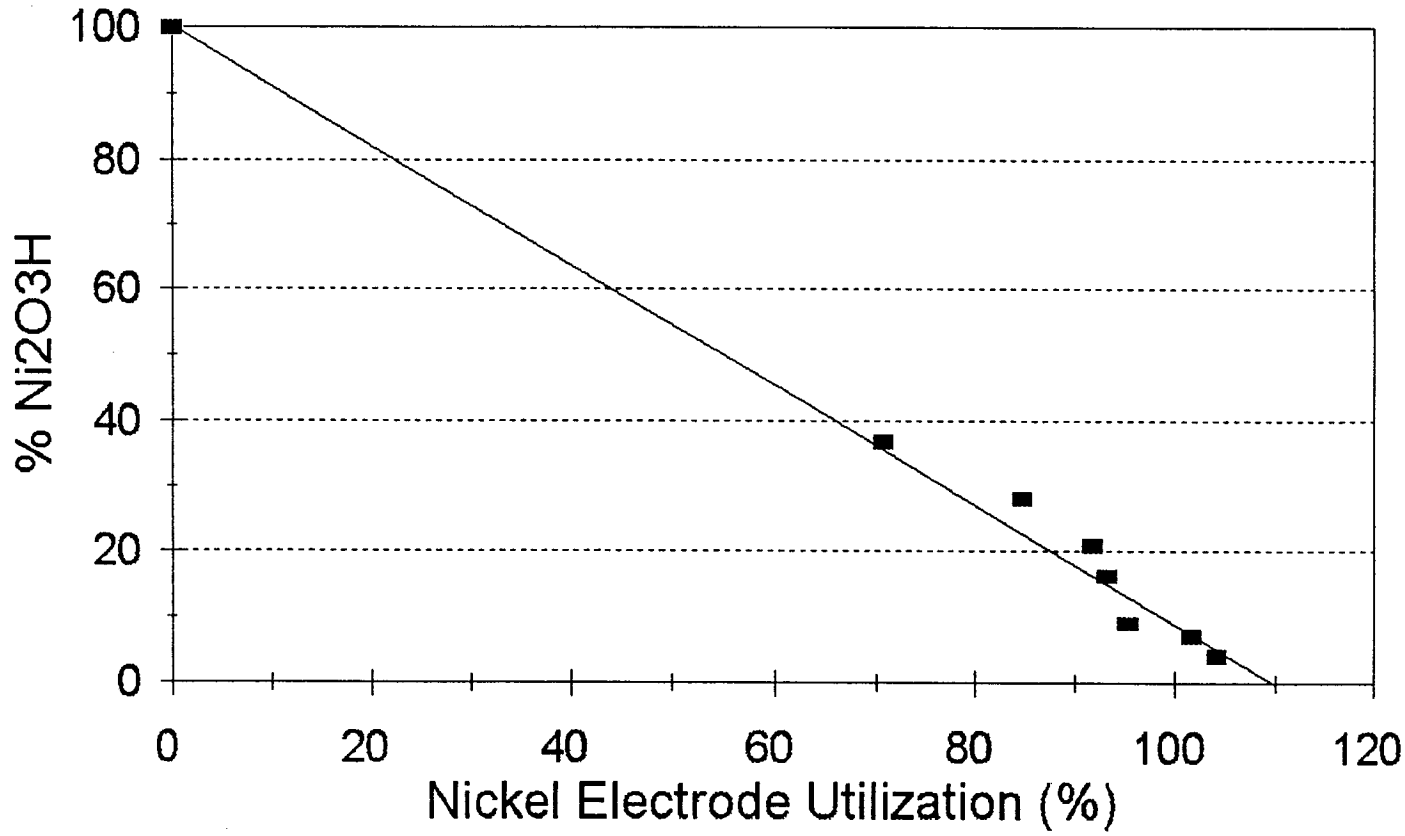

Design Performance Analysis

Studies of Component Degradation and Silver Migration in Experimental Silver-Zinc Cells

NAVAL SEA SYSTEMS COMMAND

NSWC

Naval Surface Warfare Center

CRANE DIVISION

Harlan L. Lewis
Senior Scientist
Naval Surface Warfare Center
Crane, IN 47522

1998 NASA Aerospace Battery Workshop
October 27-29 1998
Huntsville Al Hilton Hotel

NAVAL SEA SYSTEMS COMMAND

NSWC

Naval Surface Warfare Center

CRANE DIVISION

DESIGN PERFORMANCE ANALYSIS

* **Concept of Design Performance Analysis (DPA)**

  - **An attempt to evaluate the influence of each of the components of a particular electrochemical cell chemistry on the performance characteristics of that chemistry**

NAVAL SEA SYSTEMS COMMAND

NSWC

Naval Surface Warfare Center

CRANE DIVISION

DESIGN PERFORMANCE ANALYSIS

* Approach to Experimental Design

- Importance of rigorous control for each parameter selected for study
- All elements except one must be kept constant
- Need to assure that data are representative in each experiment by using statistical reliability
- Use model systems to reduce experimental costs and the quantity of support equipment
- Need to incorporate a control standard in every experimental design

NAVAL SEA SYSTEMS COMMAND

NSWC

Naval Surface Warfare Center

CRANE DIVISION

DESIGN PERFORMANCE ANALYSIS

* **An Example - Standard AgZn Separation**

  - Role of plate separation in cell performance - cycle life and wet life, to failure
  - Select a set of physical properties for measurement which relate to cell performance
  - Select a set of separators with a common material base which represent what industry is likely to USE, based on cost and availability
  - Use reproducible model cells for experimentation
  - Choose a Fleet-standard specification for cell performance

NAVAL SEA SYSTEMS COMMAND

NSWC

Naval Surface Warfare Center

CRANE DIVISION

DESIGN PERFORMANCE ANALYSIS

* **An Example - Standard AgZn Separation**

  - Perform periodic cell dissection and analysis to chart cell degradation processes
  - Perform post-mortem cell dissection and analysis on cells which fail performance specifications
  - Validate model cell performance for selected separations from model cells, in full-size Fleet hardware using an actual Fleet Lot Acceptance specification
  - Confirm degradation processes with periodic cell dissection and analysis
  - Rewrite Lot Acceptance performance specification to incorporate cell life improvement found in studies

NAVAL SEA SYSTEMS COMMAND

NSWC

Naval Surface Warfare Center

CRANE DIVISION

DESIGN PERFORMANCE ANALYSIS

* Current Component Characterization

- Cellulosic separation for rechargeable silver-zinc chemistry
- Clear Flexel cellophane (1 mil) vs silver-treated Flexel cellophane (1 mil)
- All other parameters constant, including number of layers and internal stack pressure
- Both are widely used in battery industry
- Competing claims on performance use and Navy "need to know"
- Draft a performance specification for consistent performance expectations for Navy applications

NAVAL SEA SYSTEMS COMMAND

NSWC

Naval Surface Warfare Center

CRANE DIVISION

DESIGN PERFORMANCE ANALYSIS

* **Approach to Experimental Design**

  - Importance of rigorous control for each parameter selected for study
  - All elements except one must be kept constant
  - Need to assure that data are representative in each experiment by using statistical reliability
  - Use model systems to reduce experimental costs and the quantity of support equipment
  - Need to incorporate a control standard in every experimental design

NAVAL SEA SYSTEMS COMMAND

NSWC

Naval Surface Warfare Center

CRANE DIVISION

DESIGN PERFORMANCE ANALYSIS

* Selection of Evaluation Properties

- Set S1 - Clear cellophane, Set S2 - Silver-treated cellophane
- Physical properties of separation to include dry and wet tensile strength, x-ray crystallinity, and degree of polymerization dry and after degradation experiments under conditions of alkaline hydrolysis and oxidative deterioration
- Discharge performance during repeated cycling and after 30-day wet stands (failure testing based on MK89 performance specification)
- Silver migration rates from a layer-by-layer analysis of separation in dissected cells at intervals during cell performance studies

NAVAL SEA SYSTEMS COMMAND
NSWC
Naval Surface Warfare Center
CRANE DIVISION

DESIGN PERFORMANCE ANALYSIS

Cellophane Physical Properties*

Type	Tensile Strength (lbs)				Crystallinity
	Dry		24 hr Soak - 45% KOH		Dry
	MD	TD	MD	TD	$R = I_{22}/I_{12}$
Clear	5.35±0.21	3.44±0.19	0.80±0.06	0.42±0.05	0.46
Silvered	8.48±0.55	4.50±0.39	0.63±0.12	0.30±0.06	0.41
DuPont '77	5.68±0.28	3.08±0.10	0.71±0.11	0.25±0.04	0.54
DuPont '80	5.04±0.26	3.10±0.17	0.81±0.08	0.38±0.05	0.50

* The tensile strength measurements are an average of six samples; the crystallinity is taken from x-ray diffraction data, a ratio of two peak intensities, based on a method of H. Yokota, J. Polym. Sci., Polym. Lett., 21, 285 (1983).

Interpretation: Tensile strength and crystallinity data suggest that silver coating of cellophane reduces wet strength but does not affect crystallinity.

NAVAL SEA SYSTEMS COMMAND

NSWC

Naval Surface Warfare Center

CRANE DIVISION

DESIGN PERFORMANCE ANALYSIS

Cellophane Degree of Polymerization During Chemical Degradation at 50C*

Type	Dry	45 % KOH under Nitrogen			45% KOH under Oxygen			45% KOH under Argon w 0.05M AgO		
		4 hr	24 hr	48 hr	4 hr	24 hr	48 hr	4 hr	24 hr	48 hr
Clear	268	269	248	n/a	183	154	83	179	78	58
Silvered	277	259	200	161	188	182	153	214	108	83
DuPont '77	261	221	181	151	249	224	210	199	106	98
DuPont '80	265	229	230	218	251	165	125	190	132	74

* The gas atmospheres were maintained by bubbling the appropriate gas through a fritted disk in the bottom of the vessels.

Interpretation: Degree of polymerization data indicate that silver-coated cellophane film degrades less in alkaline hydrolysis and Ag(II) oxidizing conditions.

NAVAL SEA SYSTEMS COMMAND

NSWC

Naval Surface Warfare Center

CRANE DIVISION

DESIGN PERFORMANCE ANALYSIS

Silver Content of Separation by Layer in mg/cm^2

Cell	Fiber Layer	Layer 1	Layer 2	Layer 3	Layer 4	Layer 5	Layer 6	Total
S!-Baseline	0.143	0.766	0.138	0.016	4 E-4	0	0	1.062
S2-Baseline	0.068	0.878	0.318	0.056	0.011	9.4 E-3	6 E-4	1.341
S1-50 Cycle	0.186	3.652	1.369	0.282	8.0 E-3	0	0	5.489
S2-50 Cycle	0.034	0.904	0.890	0.628	0.019	6.0 E-3	4.1 E-3	2.475
S1-88 Cycle	0.408	5.377	2.564	1.100	0.309	0.0314	0.020	9.810
S2-109 Cycle	0.170	1.466	1.577	1.480	0.189	0.011	1.7 E-3	4.895
S2-153 Cycle	0.239	1.877	2.043	2.562	0.420	0.029	5.4 E-3	7.176
S1-7 Month	0.302	6.600	3.716	2.334	0.935	6.7 E-3	6 E-4	13.827
S2-7 Month	0.200	3.420	2.383	1.625	0.146	0.015	9.0 E-3	7.775
S1-12 Month	0.317	3.389	2.846	1.847	0.409	n/a	n/a	8.807
S2-13 Month	0.177	3.390	3.893	2.018	0.408	n/a	n/a	9.886
S1-21 Month	0.526	6.539	5.305	3.530	0.386	1.5 E-3	n/a	16.304
S2-21 Month	0.123	3.226	2.996	4.139	1.059	0.126	0.019	11.689

1. The data for 21 months are averaged for two cells for S1 and for three cells for S2.
2. The 12 month data for S1 show the anomalous behavior typical of short failure cells, which has been noted in short failure cycle life cells also.

Interpretation: Layer-by-layer silver content analysis shows that the silver accumulation in each separation layer is less when silver-treated cellophane is used.

NAVAL SEA SYSTEMS COMMAND

NSWC

Naval Surface Warfare Center

CRANE DIVISION

DESIGN PERFORMANCE ANALYSIS

Silver Content form Cycle Life Cell Study (total mg)

Cycles	S1 - Silver	S2 - Silver	Comment
Baseline (6)	171	255	Baseline property dissection, formation complete
50	925	469	50 Cycle dissection
63	492		Short failure, overcharge 1 cycle
64	423		Short failure, overcharge 8 cycles
78	696		Short failure, no overcharge cycles
80		768	Short failure, no overcharge cycles
83	812		Short failure, overcharge 3 cycles
86	1404		Capacity failure (10.7 Ah on discharge)
88	1677		Capacity failure (11.5 Ah on discharge)
109		928	100 Cycle dissection (14.1 Ah)
153		1330 (2)	Capacity failure (two cells, 12.4 and 11.1 Ah)

1. The short failure cells in S1 gave data which were consistent among those cells, but anomalous with respect to the non-shorted cells.

Interpretation: Silver migration through separation layers is definitely slowed during cycling, by silver treatment of cellophane.

NAVAL SEA SYSTEMS COMMAND

NSWC

Naval Surface Warfare Center

CRANE DIVISION

DESIGN PERFORMANCE ANALYSIS

Silver Content form Wet Life Cell Study (total mg)

Months	S1 - Silver	S2 - Silver	Comment
7	1550	1350	6 Month dissection (overran 1 month)
12	1700		Short failure, no overcharge cycles
13		1740	12 Month dissection (overran 1 month)
21	2942 (2)	2161 (3)	End of testing for wet life (20.5 and 22.5 Ah resp.)

1. Repetition of anomalous data for S1 - short failure cell.
2. At 21 months, two cells were analyzed for S1 and three cells for S2.

Interpretation: Silver migration through separation layers is slowed by silver treatment of cellophane in wet life testing.

NAVAL SEA SYSTEMS COMMAND

NSWC

Naval Surface Warfare Center

CRANE DIVISION

DESIGN PERFORMANCE ANALYSIS

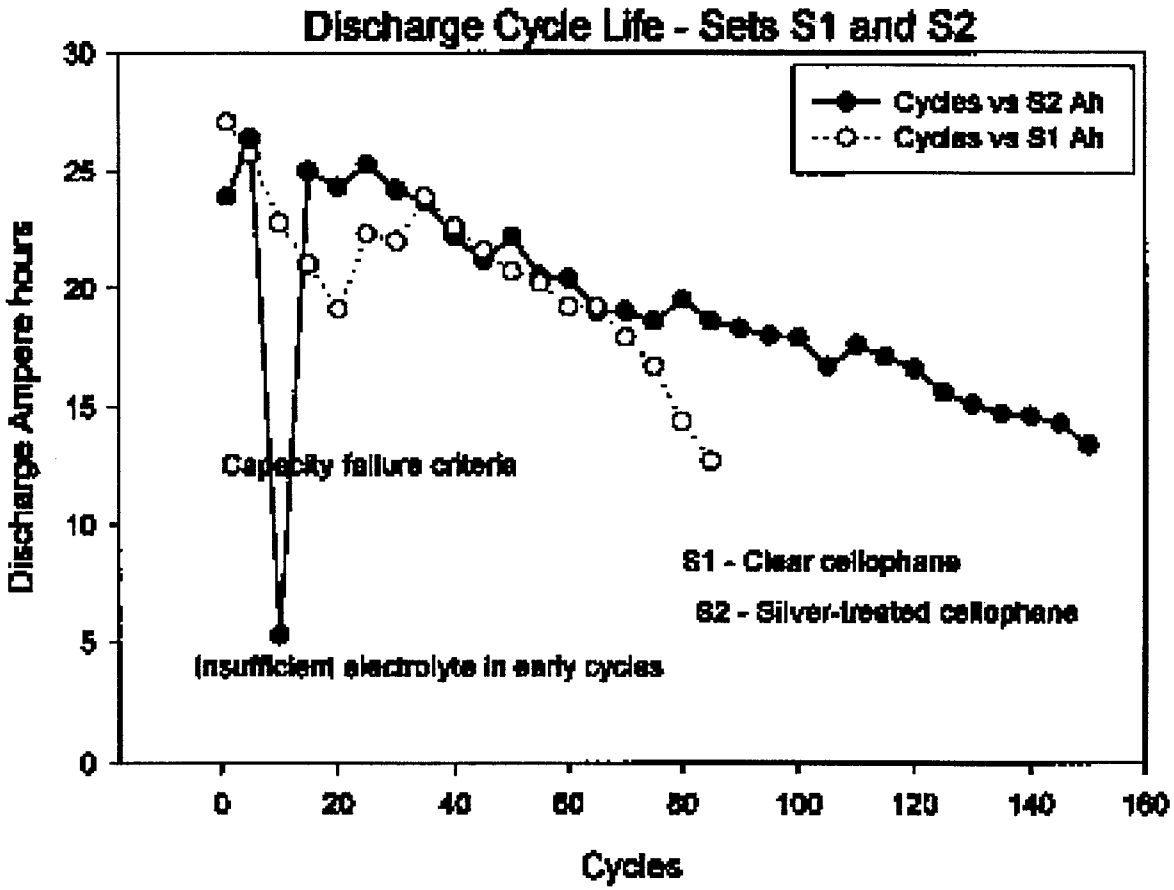

Interpretation: Cell Set S2 showed superior discharge capacity with fewer short failures

NAVAL SEA SYSTEMS COMMAND

NSWC

Naval Surface Warfare Center

CRANE DIVISION

DESIGN PERFORMANCE ANALYSIS

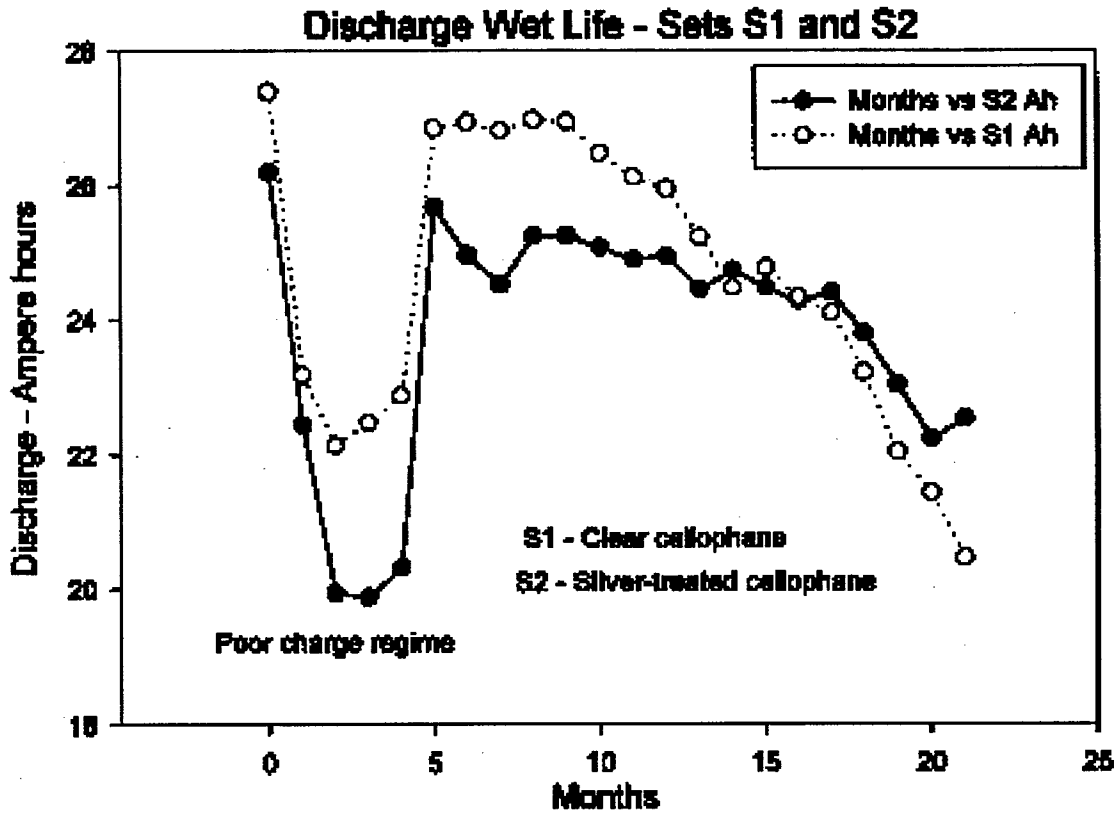

Interpretation: No significant difference in discharge capacity until 18 months

NAVAL SEA SYSTEMS COMMAND

NSWC

Naval Surface Warfare Center

CRANE DIVISION

DESIGN PERFORMANCE ANALYSIS

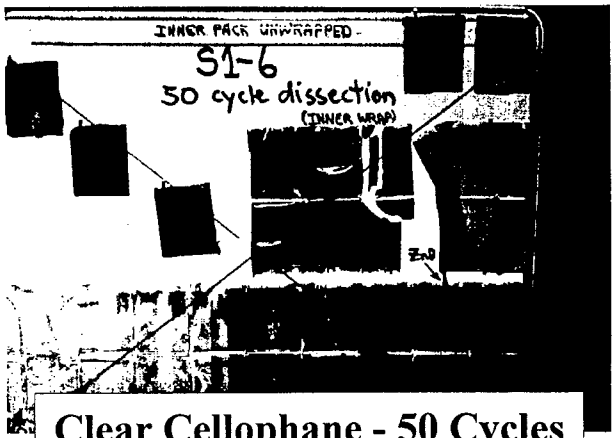

Clear Cellophane - 50 Cycles

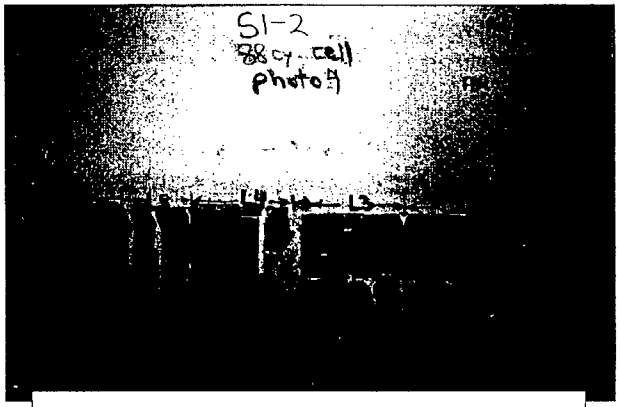

Clear Cellophane - 88 Cycles

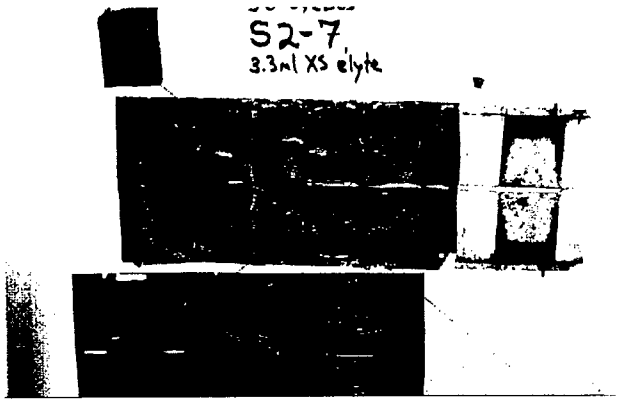

Silver-Treated Cellophane - 50 Cycles

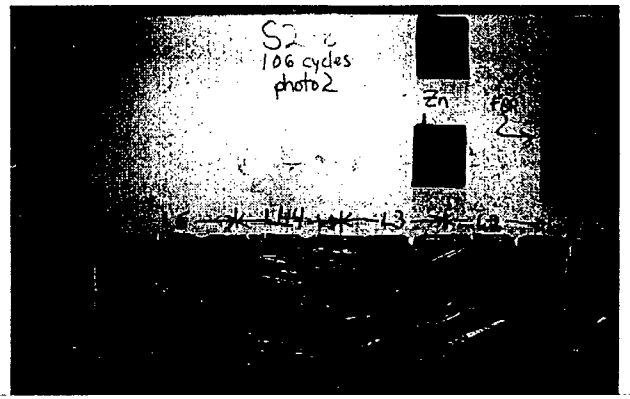

Silver-Treated Cellophane - 106 Cycles

NAVAL SEA SYSTEMS COMMAND

NSWC

Naval Surface Warfare Center

CRANE DIVISION

DESIGN PERFORMANCE ANALYSIS

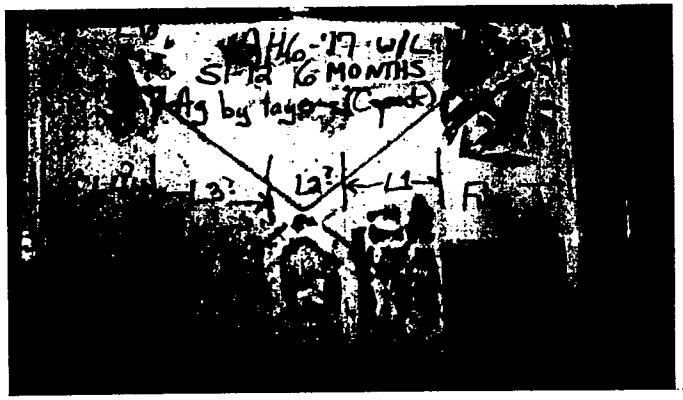

Clear Cellophane - 7 months wet stand

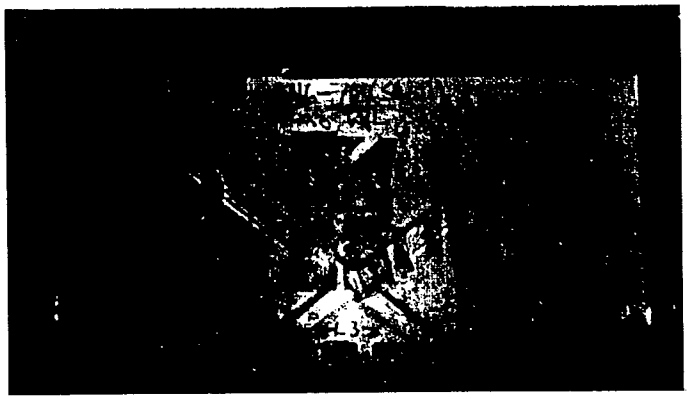

Clear Cellophane - 12 months wet stand

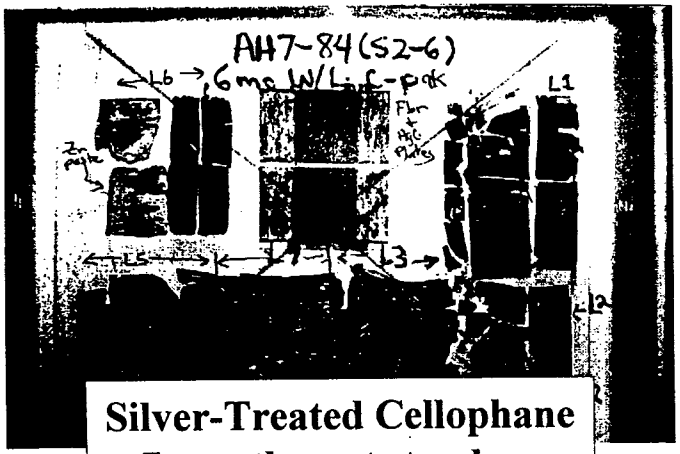

Silver-Treated Cellophane - 7 months wet stand

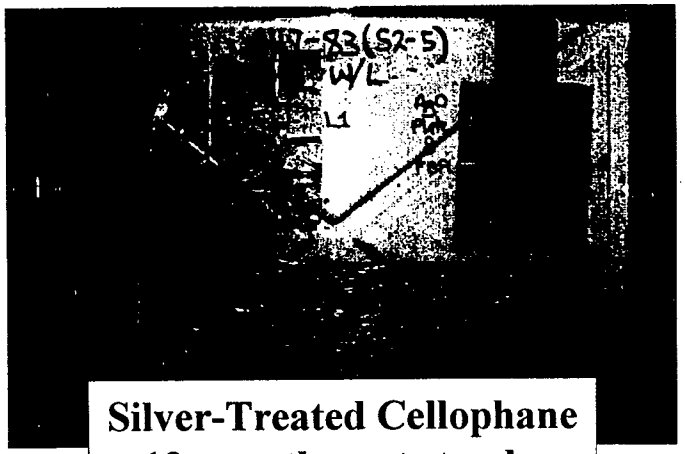

Silver-Treated Cellophane - 13 months wet stand

NAVAL SEA SYSTEMS COMMAND

NSWC

Naval Surface Warfare Center

CRANE DIVISION

DESIGN PERFORMANCE ANALYSIS

* Evaluation of Data

- Degree of polymerization data indicate that silver-coated cellophane film degrades less in alkaline hydrolysis and Ag(II) oxidizing conditions
- Tensile strength data suggest that silver treatment of cellophane film reduces wet strength
- Cycle life data show extended cell life and higher discharge capacities for cells built with silver-treated cellophane
- Wet life data are ambiguous
- Silver migration through separation layers is definitely slowed by silver treatment
- Photographic evidence shows that silver-treated cellophane is more robust and less subject to degradation under cell operating conditions

NAVAL SEA SYSTEMS COMMAND

NSWC

Naval Surface Warfare Center

CRANE DIVISION

DESIGN PERFORMANCE ANALYSIS

* **Conclusion**

  - **Silver treatment of cellophane film for separator applications in rechargeable silver-zinc cells appears, from physical property and model cell data, to result in improved resistance to electrolyte degradation, longer cell cycle life, less tendency to short development, and lower silver migration rates**

N.B. ***All results on cell performance must be verified and validated in Fleet hardware***

NAVAL SEA SYSTEMS COMMAND

NSWC

Naval Surface Warfare Center

CRANE DIVISION

DESIGN PERFORMANCE ANALYSIS

* Remaining Questions

- Can physical property data with respect to cellulose-based separation be used as a predictor of cell performance?
- What should be the future direction of cellophane development?

  Amorphous content important - *reduce*

  X-ray crystallinity important - *increase*

  Dry and wet tensile strength important - *increase*

  Degree of polymerization important - *increase (but must also maintain flexibility)*

  "Skin" thickness important - *poorly understood*

  Electrical resistivity important - *relation to other properties poorly understood*

Studies of Component Degradation
During Testing of
Nickel-Hydrogen Cells

NAVAL SEA SYSTEMS COMMAND

NSWC
Naval Surface Warfare Center
CRANE DIVISION

Authors: Steve Wharton & Harry Brown

1998 NASA AEROSPACE BATTERY
WORKSHOP
October 27-29 1998 Huntsville AL.

1

OUTLINE

I. Introduction *p.2.*

II. Cell Design *p.3.*

III. Destructive Physical Analysis *p.4.*

IV. General Findings *p.10.*

V. Less Obvious Findings *p.21.*

VI. Conclusions, Recommendations, and Future Work *p.26.*

NAVAL SEA SYSTEMS COMMAND

NSWC
Naval Surface Warfare Center
CRANE DIVISION

Studies of Component Degradation in Nickel Hydrogen Cells

I. INTRODUCTION

The Naval Surface Warfare Center, Crane Division, in Crane, IN, Aerospace Battery Branch (Code 6095) has been involved in the test and evaluation (T&E) of nickel-hydrogen (Ni/H_2) electro-chemical power sources for almost fourteen years.

One test-pack of Ni/H_2 Independent Pressure Vessel (IPV), 125Ah, 1.2VDC cells has been on-test for almost ten years, and five of the six total cells have finally failed. The last three, longest-lived cells have all completed over 46,640 simulated 90minute low earth-orbit (LEO) cycles--an equivalent of almost eight years or more of continuous service. The one remaining cell has completed over 53,735 cycles, and is still cycling. These three long-lived cells all contain a catalyzed wall-wick (CWW) as an advanced design-feature being evaluated to extend cell service life.

The CWW is designed for two main purposes including: to aid in uniform electrolyte distribution (through wall-wicking), and to act as an alternate (catalytic) surface upon which hydrogen and oxygen gases can recombine to minimize negative (NEG) electrode degradation from this destructive, "popping," recombination.

The design features of the cells are summarized in the Cell Design slide (p.3). It is important to note that the only difference between these two groups of three cells is the CWW, and that the **tops** of the cells are the POS-end **up** during all of the lifecycle testing.

This paper presents some of the significant observations of destructive physical analysis (DPA) of the five failed cells and discusses these findings. It is presented in the format of 21 color photographs and numerous other written observations of the condition of key internal components of these test cells.

NAVAL SEA SYSTEMS COMMAND

NSWC Naval Surface Warfare Center CRANE DIVISION

Studies of Component Degradation in Nickel Hydrogen Cells

II. Cell Design

NASA LeRC Pack 5001L

Manuf. &p/n: Eagle Picher
RNH 125-1 CWW
RNH 125-3 Non-CWW

125 Ahr, 4.5 in. Dia, IPV

Separator: Asbestos/Serrated edges
Wall thickness: 40 mils
Electrolyte: 26% KOH
Terminals: Axial (opposed)

Test Conditions:

Depth of Discharge 60%
Temperature 10°C
LEO orbit 90 Min/cycle
Discharge 36 Min.
Charge 54 Min.
Recharge 104%

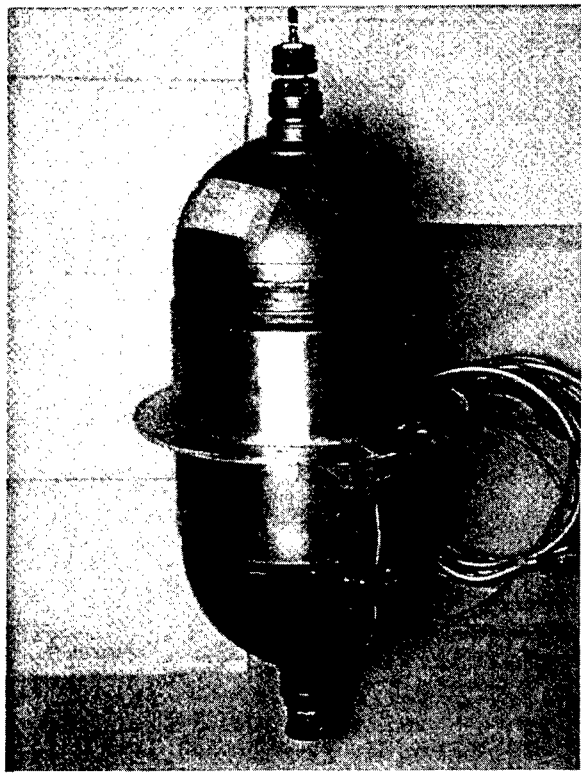

Cell Serial No:	Cell Type	Cycles To 1.0 volt
1	CWW	49,689
2	CWW	*53,300
3	CWW	46,645
4	Non-CWW	20,590
5	Non-CWW	14,308
6	Non-CWW	9,588

*** Still cycling and still on-test**

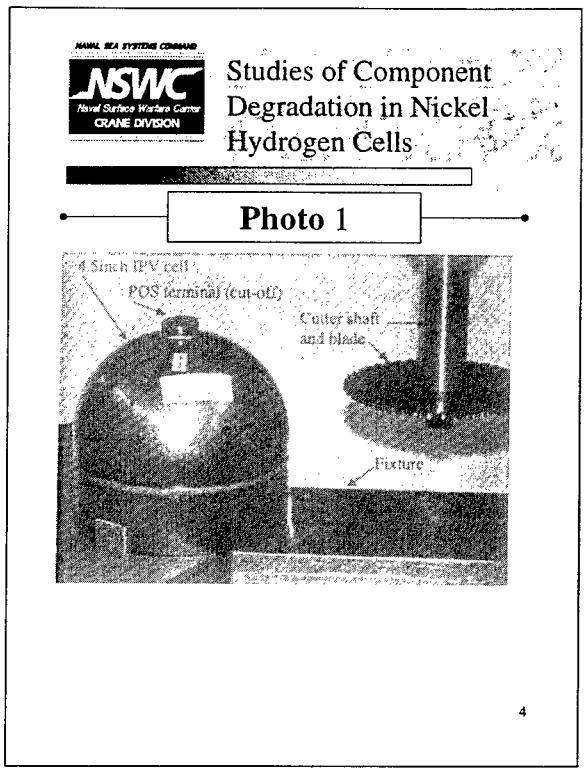

III. DESTRUCTIVE PHYSICAL ANALYSIS (DPA)

Stepwise DPA Procedure

This Section presents the simplified DPA process in photographs and discussion.

Step 1: Discharge and Depressurization.

Once the cell fails lifecycle testing, it is removed from the test pack electrically. However, it remains in the test chamber environment until just before DPA, at which time it is removed from the chamber and allowed to warm to room ambient temperature. The cell is then shorted through a low-resistance load for several days and then the fill tube is snipped off with sidecutters (no photographs) to allow any remaining gasses to escape.

Step 2: Opening the Vessel:

Photograph (Photo) 1: The 4.5inch diameter cell is held in the fixture ready to begin the cutting operation. The cutter moves around the fixed cell. Up to four cuts are made through the cell walls and both terminals are cut-off close to the dome ends. The wall cuts include: three circumferencial (girth) cuts around the cylinder and one longitudinal cut along the side of the cylinder.

Studies of Component Degradation in Nickel Hydrogen Cells

Photo 2

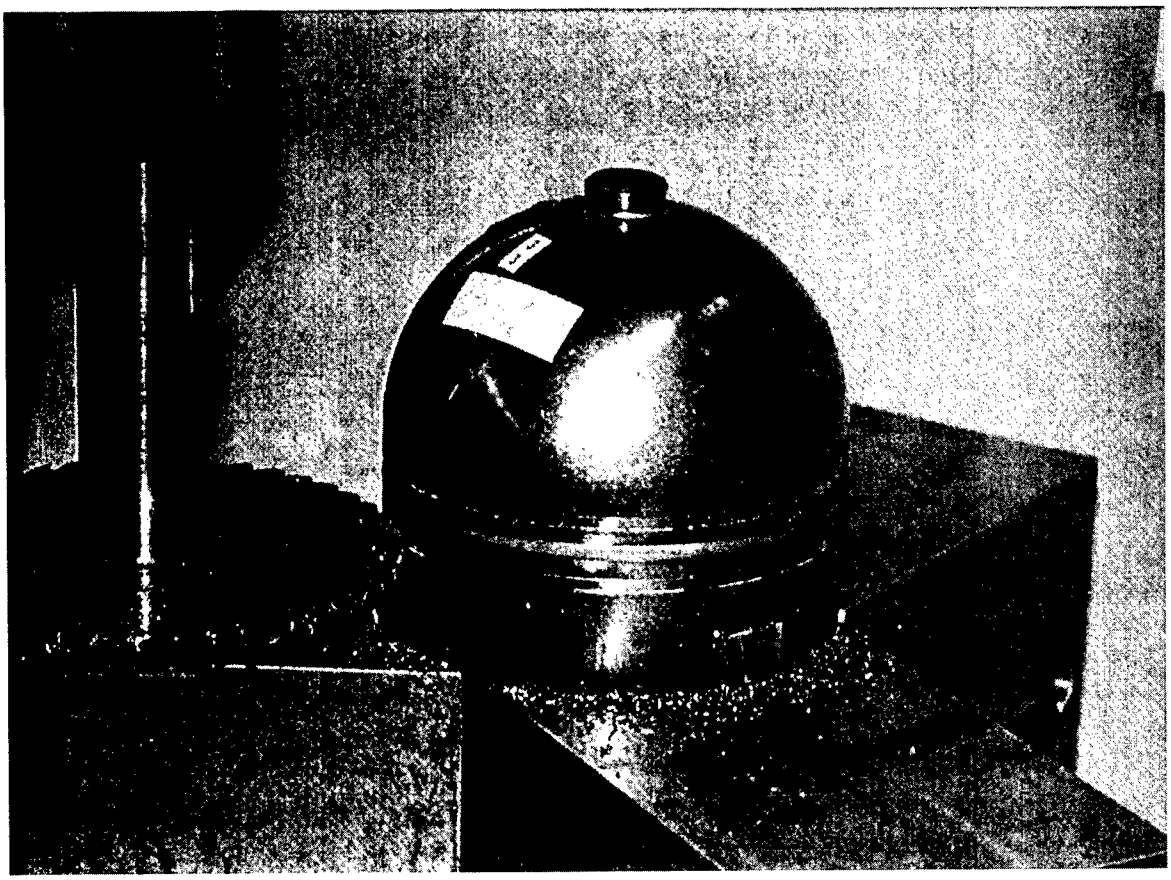

Photo 2: The two top cuts are made at the positive (POS) end of the IPV cylinder; one on either side of, and close to the weld ring. The cuts are made all of the way through the wall carefully to avoid cutting into the cell stack. A third cut (not shown) is made at the bottom negative (NEG) end of the cylinder to facilitate pushing the cell stack assembly out of the vessel.

NAVAL SEA SYSTEMS COMMAND

NSWC
Naval Surface Warfare Center
CRANE DIVISION

Studies of Component Degradation in Nickel Hydrogen Cells

Photo 3

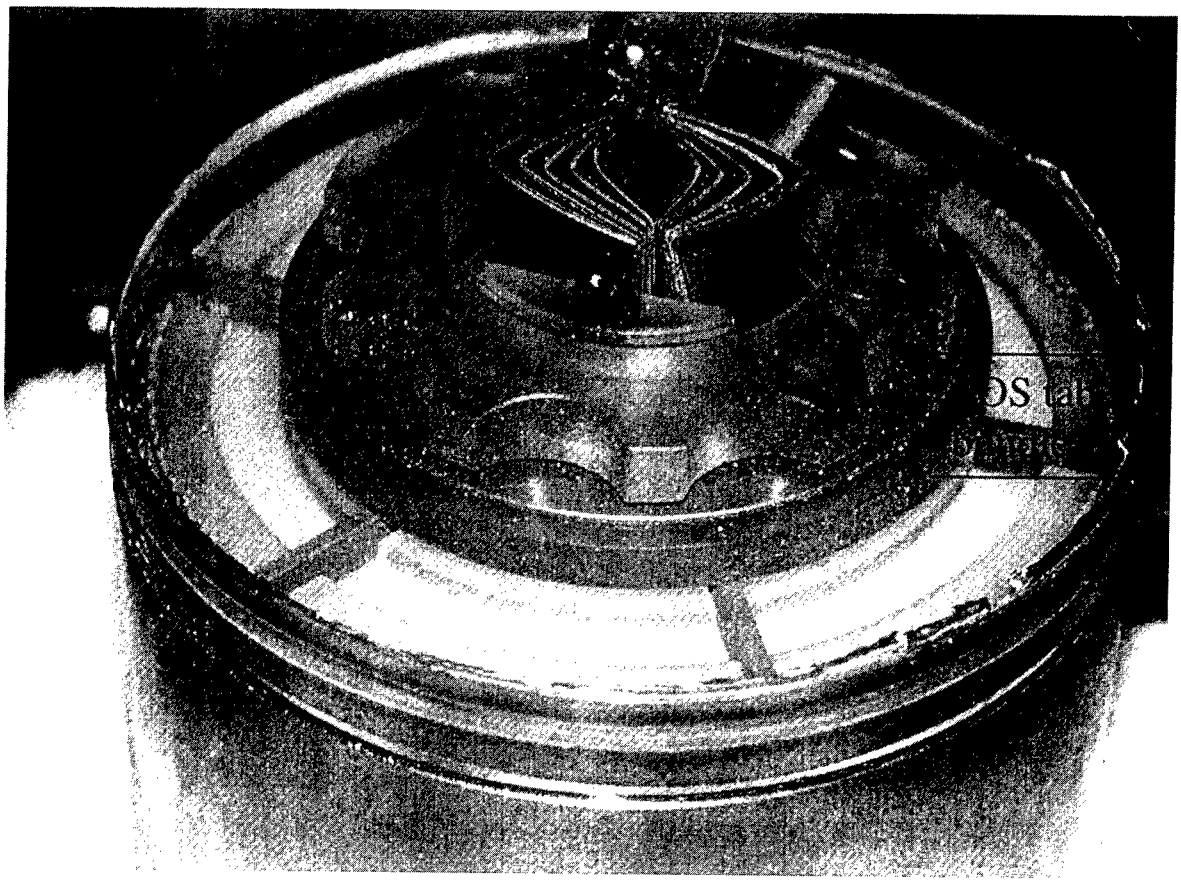

Photo 3: The POS tab bundle and terminal are cut off and the inert top-parts including the weld ring are removed and examined to allow the cell stack to be pulled out through the cylinder top. All of these inert parts are shown and identified in Photo 6.

Studies of Component Degradation in Nickel Hydrogen Cells

Photo 4

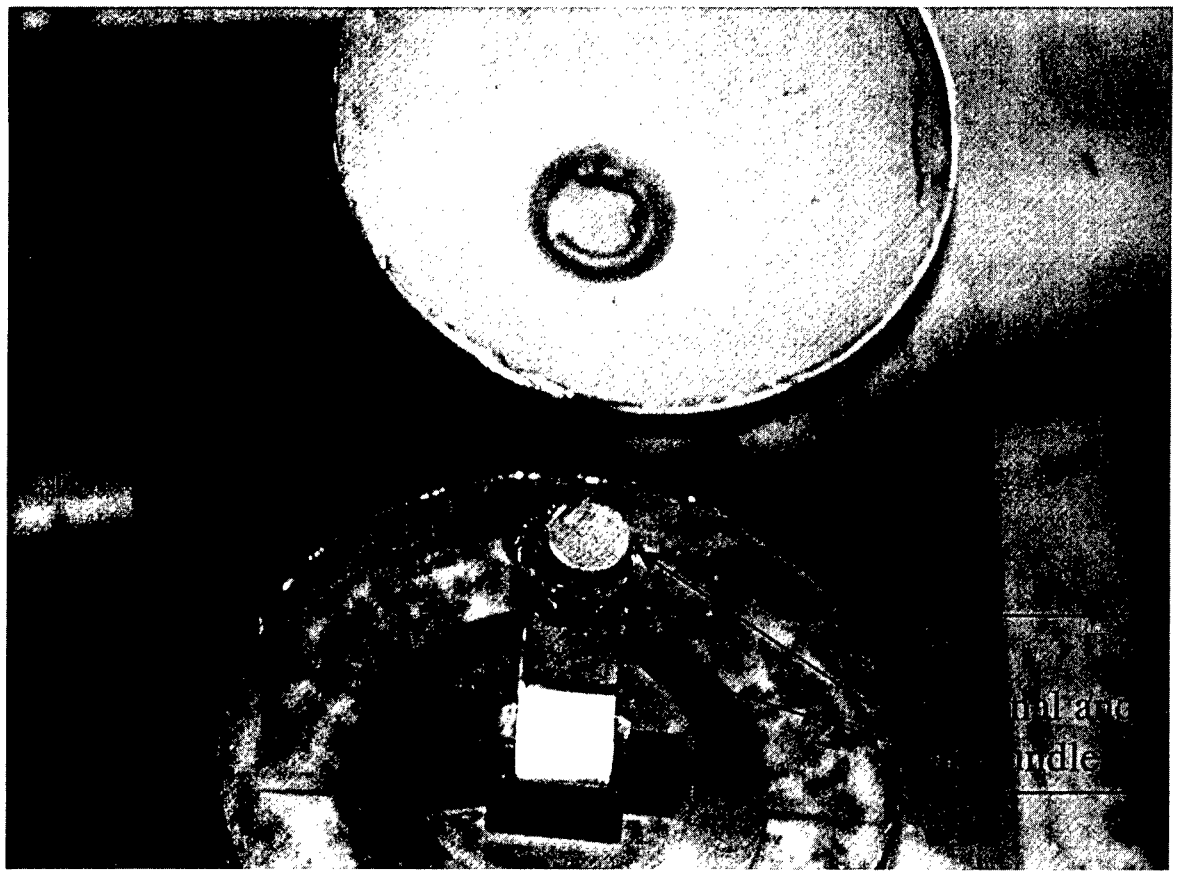

Photo 4: The cell is inverted in the fixture, the one bottom circumferential cut is made, and the dome bottom is removed and examined to allow pushing on the inert bottom-parts to facilitate cell stack removal. The NEG terminal and tab bundle are cut off to allow the cell stack to be disassembled.

NAVAL SEA SYSTEMS COMMAND

NSWC
Naval Surface Warfare Center
CRANE DIVISION

Studies of Component Degradation in Nickel Hydrogen Cells

Photo 5

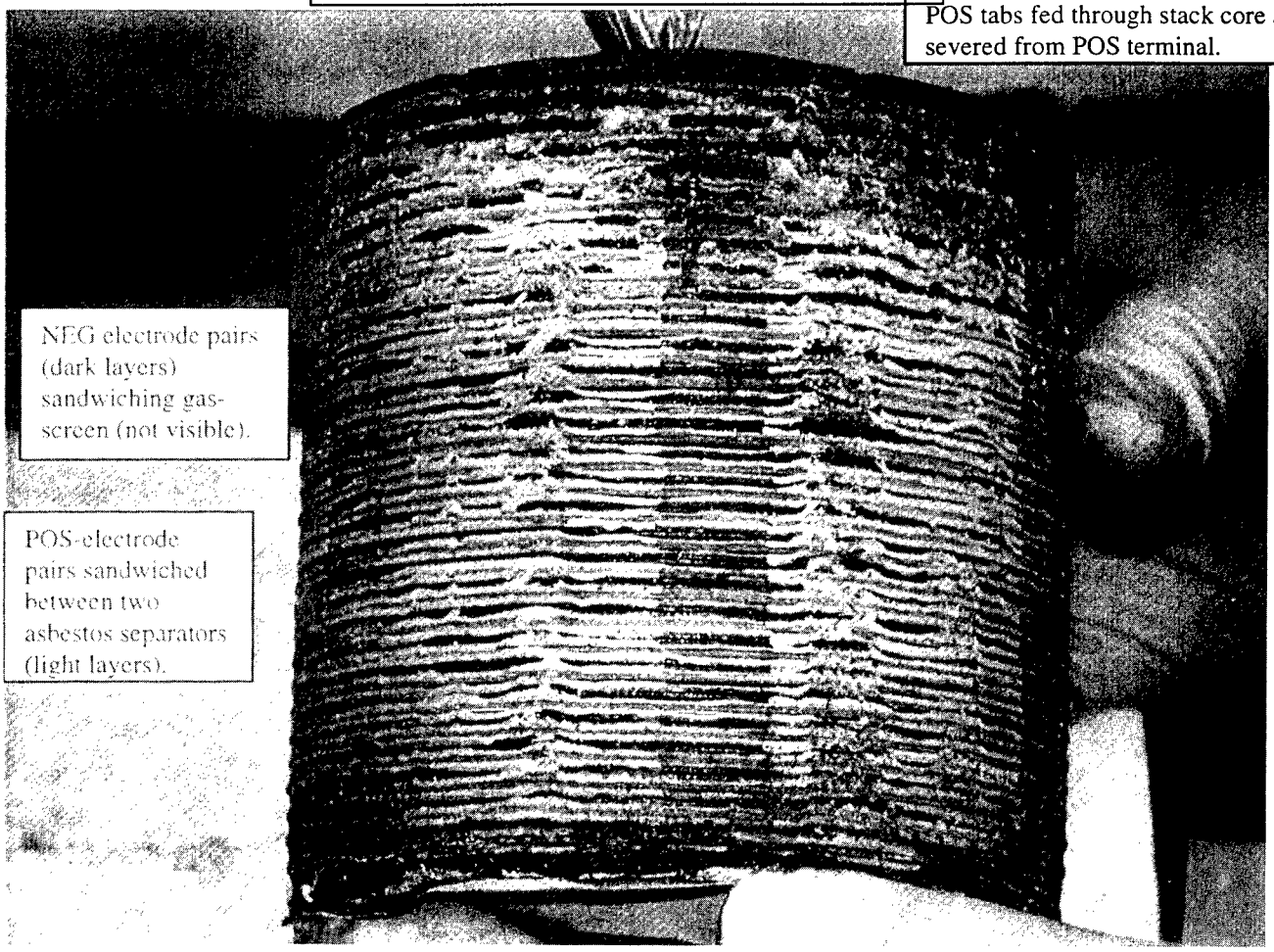

Steps 3 and 4: Cell Stack Removal and Stack Disassembly:
Photo 5: Once the cell stack has been pushed out of the vessel, the stack is disassembled, one component at a time through all of the alternating layers of electrodes and separators. Physical measurements and observations are made and recorded at this time.

Studies of Component Degradation in Nickel Hydrogen Cells

Photo 6

Photo 6: Expanded view of all inert support parts. Note: that only the Core Nut is fixed onto the flanged Core Support, that the Weld Ring is fixed to the vessel Cylinder Wall, and that ALL parts are made to allow stack expansion downward on the Core Support.

Studies of Component Degradation in Nickel Hydrogen Cells

Photo 7

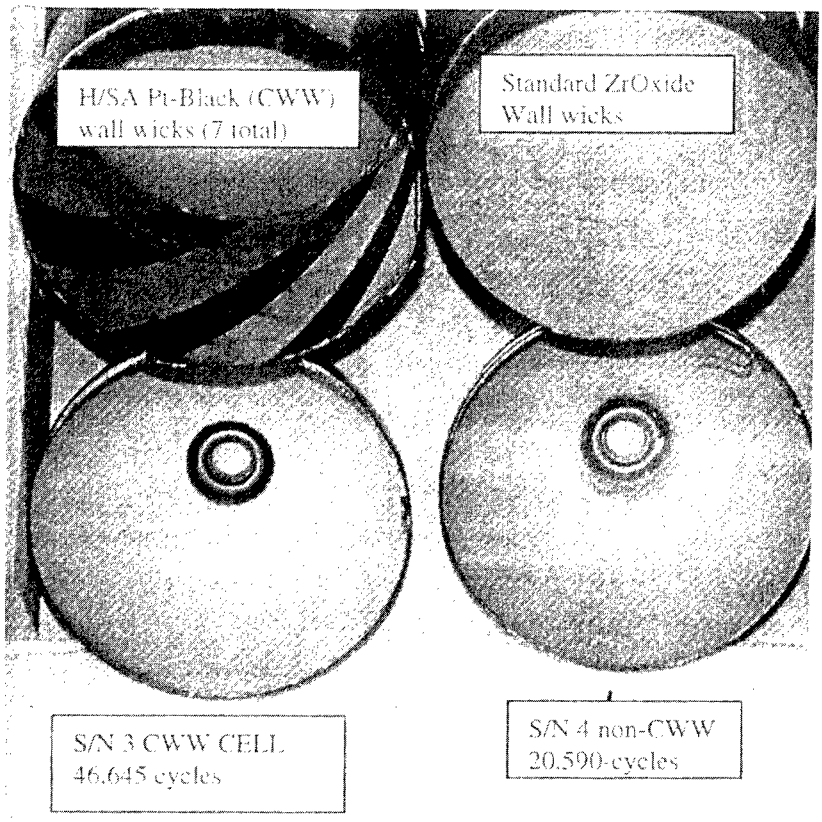

IV. General Findings: CWW /vs/ non-CWW Cells.

This Section presents some of the general findings in comparing CWW and non-CWW IPV cells in photographs and discussion.

Photo 7: Inside the CWW (left) and the non-CWW (right) vessels. The CWW consists of seven diagonal stripes that cover approximately one-third of the inside cylinder surface. Their composition is mainly high surface-area (HSA) platinum black. The white coating is zirconium-oxide.

NAVAL SEA SYSTEMS COMMAND

NSWC
Naval Surface Warfare Center
CRANE DIVISION

Studies of Component Degradation in Nickel Hydrogen Cells

Photo 8

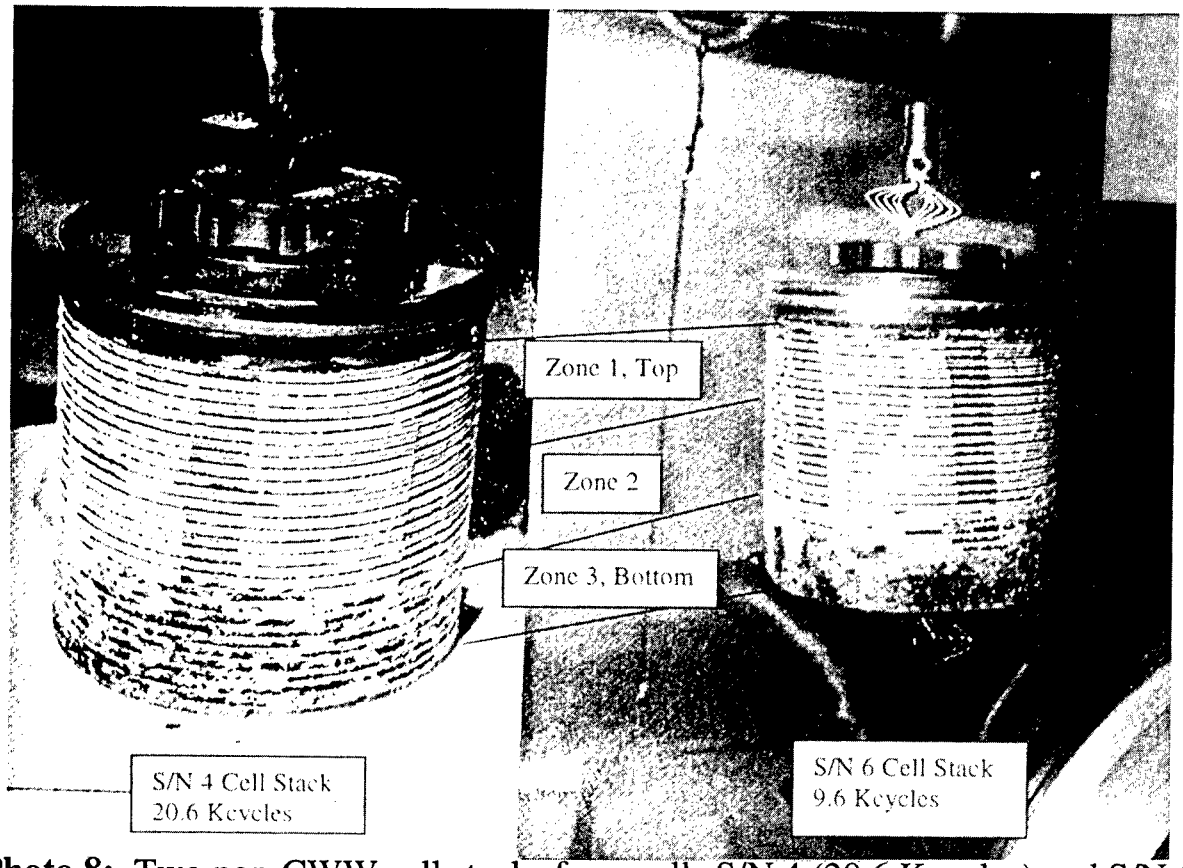

Photo 8: Two non-CWW cell stacks from cells S/N 4 (20.6 Kcycles) and S/N 6 (9.6), to compare to CWW cell S/N 3 (46.6 Kcycles, Photo 5). Note disintegration of separator edges in bottom (Zone 3) of S/N's 4 and 6. This occurrence is most notable in non-CWW cells (which completed only 9.6, 14.3, 20.6Kcycles). The separators appear to swell or extrude into stack-to-wall gap and and mechanical disintegration results from swell-cycling. Increased moisture in Zone 3 (test-bottom in gravity environment) may exacerbate this problem.

NAVAL SEA SYSTEMS COMMAND

NSWC
Naval Surface Warfare Center
CRANE DIVISION

Studies of Component Degradation in Nickel Hydrogen Cells

Photo 9

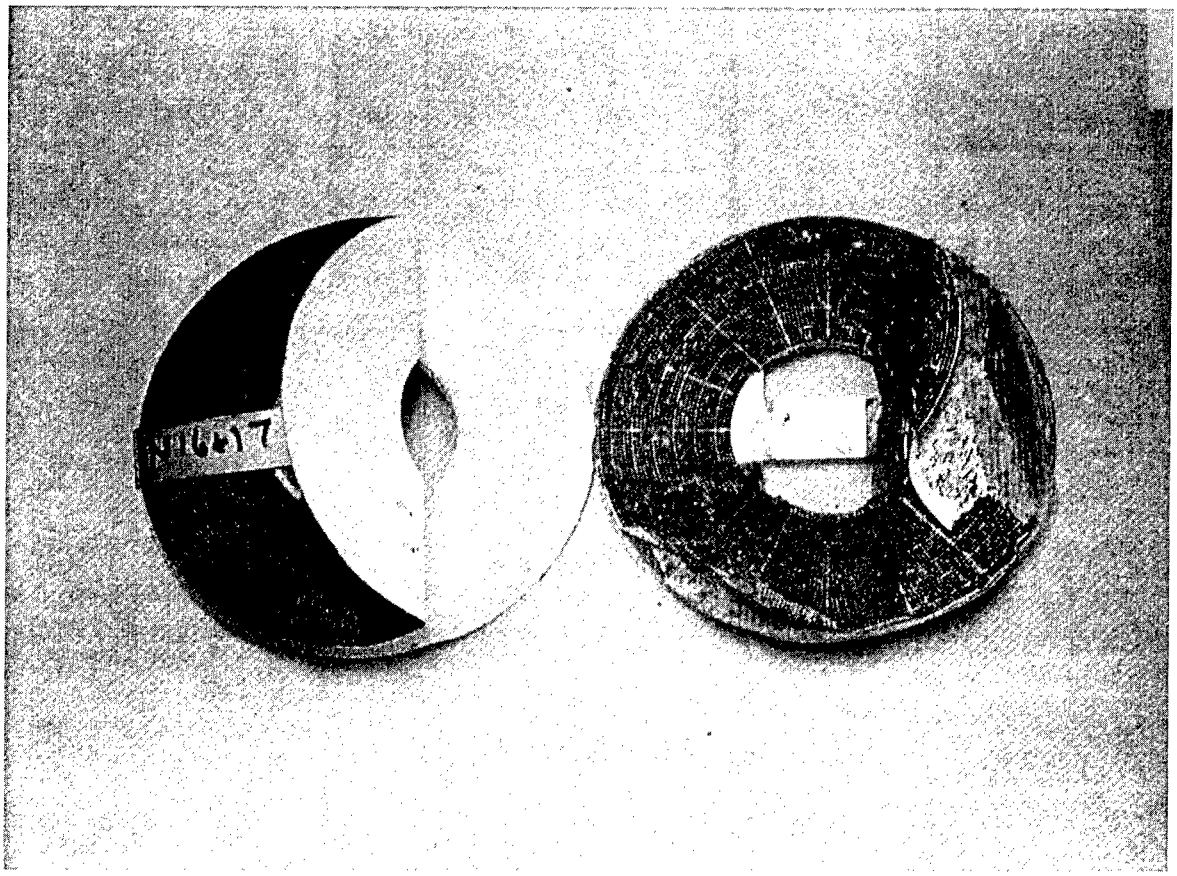

Photo 9: Comparing NEG electrodes from top (Zone 1) of cell stack to NEG electrodes from Zone 3. Note that: Zone 1 NEG electrodes (left) are in pristine condition: **no/few** popping holes, **no** active material loss, **no** teflon-backing debonding, and **no** teflon-backing rivetted to the gas screen, but that Zone 3 NEG electrodes (right) are in very poor condition with: hundreds of large and small popping holes, considerable active material loss, teflon backing debonding, and teflon rivetting to the gas screen.

NAVAL SEA SYSTEMS COMMAND

NSWC
Naval Surface Warfare Center
CRANE DIVISION

Studies of Component Degradation in Nickel Hydrogen Cells

Photo 10

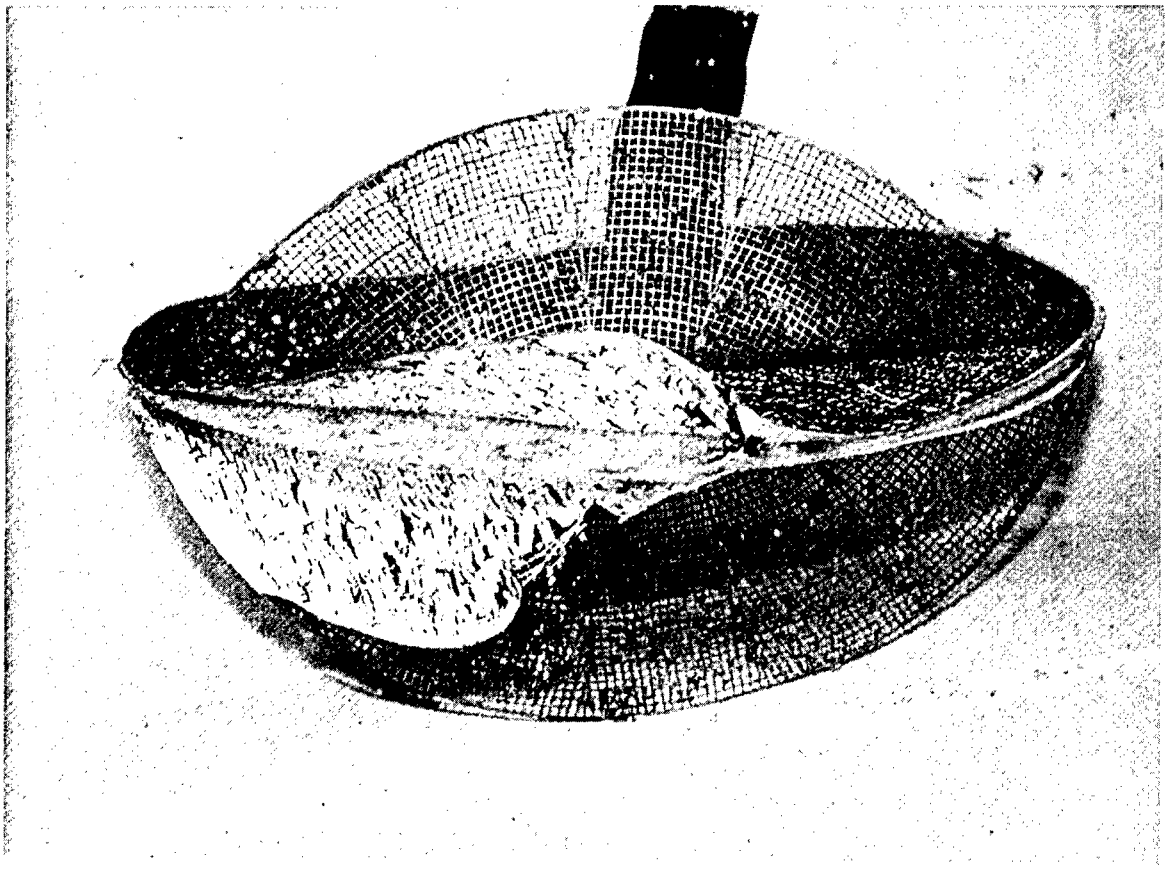

Photo 10: A Zone 3 NEG electrode pair close-up showing just how badly deteriorated the NEG electrode is: **hundreds of large and small popping holes**, considerable **active material loss** (almost 100%), teflon backing **debonding**, and teflon **riveting** to the gas screen. The disintegrated active material may be acting as the preferred popping-gas recombination site over the CWW, and popping may become a run-away problem.

NAVAL SEA SYSTEMS COMMAND

NSWC
Naval Surface Warfare Center
CRANE DIVISION

Studies of Component Degradation in Nickel Hydrogen Cells

Photo 11

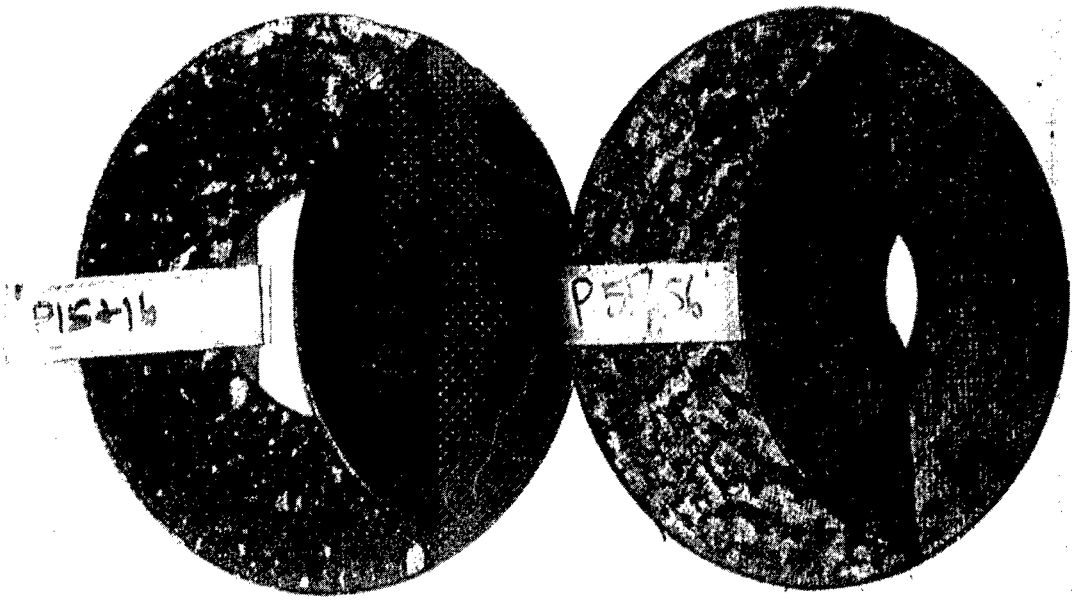

Photo 11: Comparing POS electrodes from Zones 1 and 3. Zone 1 POS electrode pairs (left) are only about 50% swollen in surface area (mottled appearance) and less swollen in thickness, drier, less stuck (hammered) onto separators with less active material disintegrated from their faces, and more uniform in coloration inside (between POS electrode pairs). But, Zone 3 POS electrode pairs (right) are **85% or more swollen in surface area** and **more swollen in thickness, wetter, more hammered** onto separators with **more active material disintegrated** from surface, and **less uniform in coloration inside** (more yellowish, green colored spots). ***Note: The "lighter" material in between the Zone 3 POS pairs may be charged nickel (NiOOH), which is consistent considering the condition of the NEG electrodes in the bottom of the stack (Photo 10) which probably cannot discharge (add H_2 gas) to the POS electrodes.***

NAVAL SEA SYSTEMS COMMAND

NSWC
Naval Surface Warfare Center
CRANE DIVISION

Studies of Component Degradation in Nickel Hydrogen Cells

Photo 12

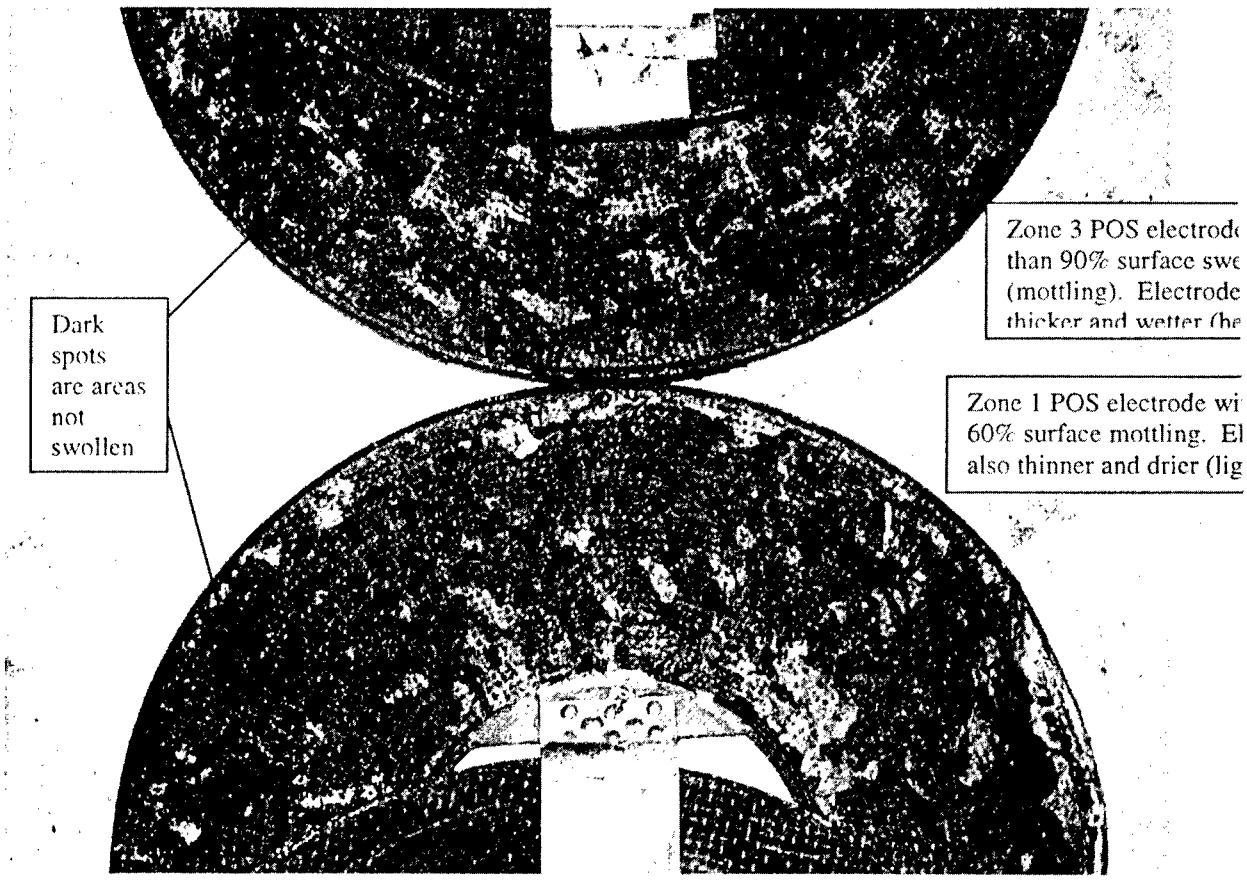

Photo 12: Zone 1 and Zone 3 POS electrode pairs close-up (from S/N 1, 49.7 Kcycles) showing more swollen surface area (mottled) on the outside surfaces on Zone 3 (top) and more lighter colored spots inside (topmost, and Photo14). Zone 3 POS electrodes may still be charged because they cannot be discharged when opposite disintegrated NEG electrodes.

NAVAL SEA SYSTEMS COMMAND

NSWC
Naval Surface Warfare Center
CRANE DIVISION

Studies of Component Degradation in Nickel Hydrogen Cells

Photo 13

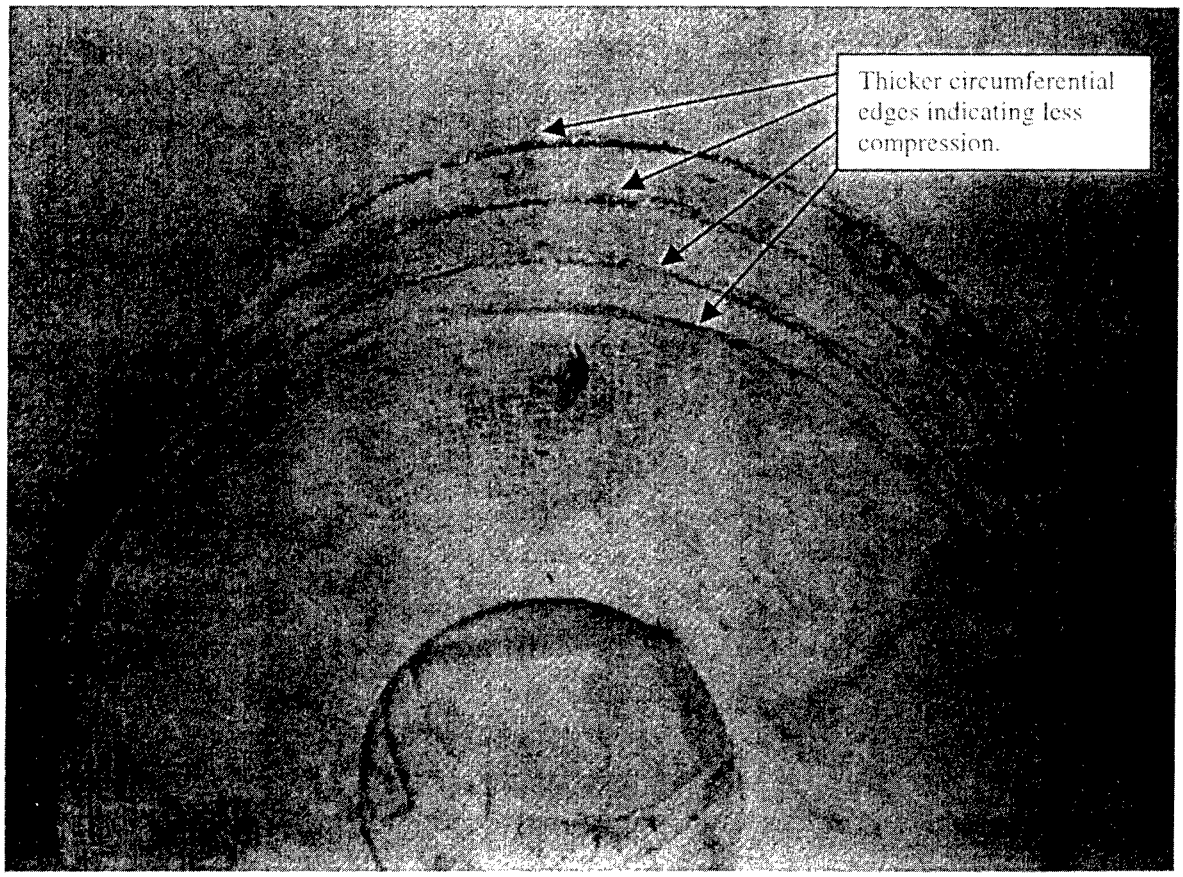

Photo 13: Separators from Zone 1 (S/N 1, 48.6 Kcycles) showing no grid imprint/material transfer and swollen edges where separators appear to have been worked (squeezed, or extruded) out into the stack-to-wall clearance gap.

NAVAL SEA SYSTEMS COMMAND

NSWC
Naval Surface Warfare Center
CRANE DIVISION

Studies of Component Degradation in Nickel Hydrogen Cells

Photo 14

Photo 14: Separators from the middle of the cell stack (Zone 2), where some popping holes in NEG electrodes and some hammering in POS electrodes begin to appear. This photo shows that both NEG grid material transfer and POS material transfer occur back-to-back on opposite faces of the separator surfaces suggesting that popping hammers both NEG and POS electrode material into the separators and may cause the observed extrusion into the wall gap lower in the stack (Zone 3) where the occurrence is worse.

Photo 15

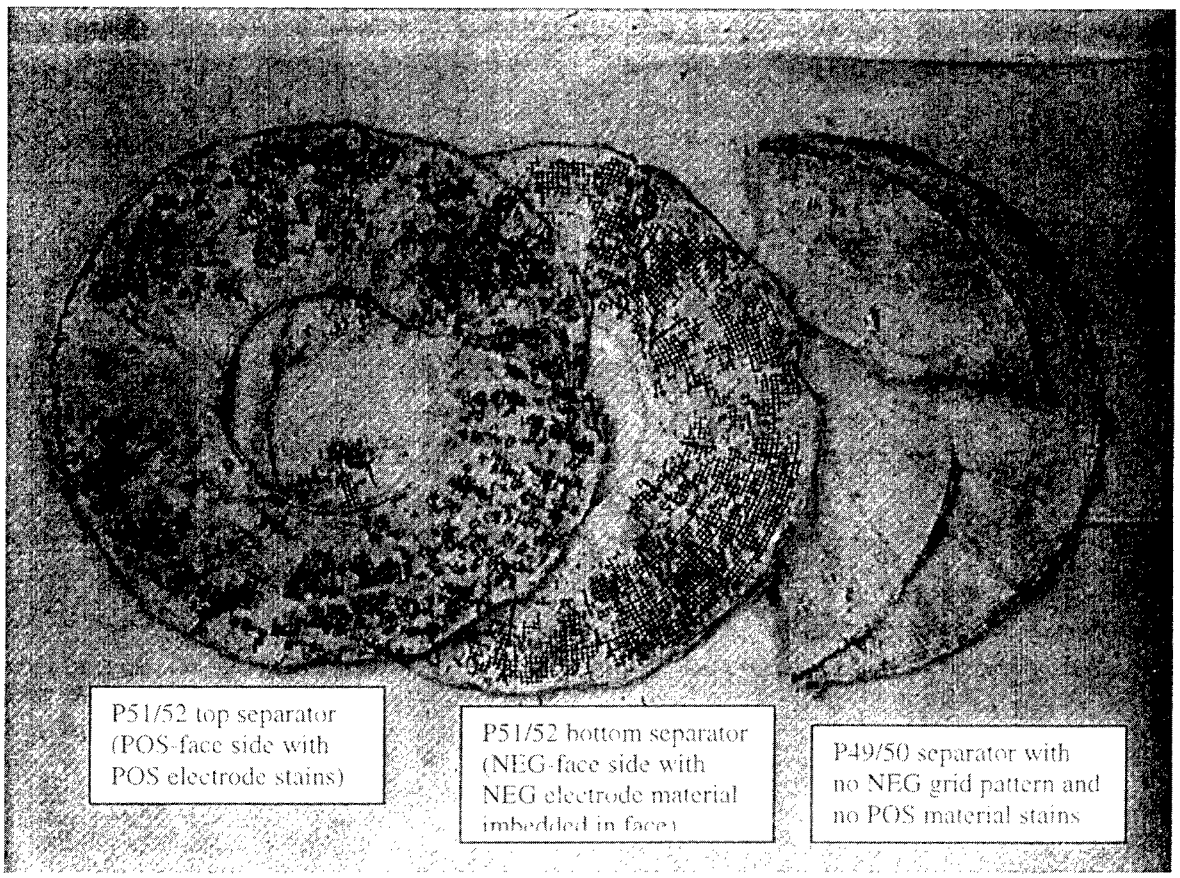

Photo 15: Comparing two hammered separators from Zone 3 (left) to one not-hammered separator also from Zone 3 (right). Some Zone 3 separators in the longer-lived (CWW) cells were in the same condition as Zone 1 and 2 separators, but these were found **only** opposite NEG electrodes that were in similarly good (Zone 1) condition (with few popping holes and little material disintegration).

Studies of Component Degradation in Nickel Hydrogen Cells

Photo 16

Photo 16: Comparing NEG and POS electrode pairs and separators from the three cell-stack zones (Zone 1 on top, etc...). This photo summarizes the most obvious findings from the five-cell DPA's. This summary is given below and Photo 16 is shown full-size on p.20:

19

FOR NEGATIVE ELECTRODES:

1. Increased number and size of popping holes from top-to-bottom of cell stack (Zone 1-to-3),

2. Increased loss of active (HSA platinum-black) material from the NEG grid,

3. Increased: debonding of teflon-backing , rivetting to the gas screen, and grid pattern (and active material) transfer to the surface of the teflon-backing;

FOR POSITIVE ELECTRODES:

1. Increased weight from stack top-to-bottom,

2. Increased swelling, surface mottling, and surface disintegration from top-to-bottom,

3. Increased color variation on the faces between POS electrode pairs from top-to-bottom;

AND FOR SEPARATORS:

1. Increased wetness from top-to-bottom,

2. Increased hammering (sticking) onto POS electrode faces from top-to-bottom,

3..Increased disintegration of outside edges and working into the stack-to-wall space from top-to-bottom,

4. And increased NEG and POS electrode material transfer and embedding into the separator faces from top-to-bottom of the cell stack.

NAVAL SEA SYSTEMS COMMAND

NSWC
Naval Surface Warfare Center
CRANE DIVISION

Studies of Component Degradation in Nickel Hydrogen Cells

Photo 16

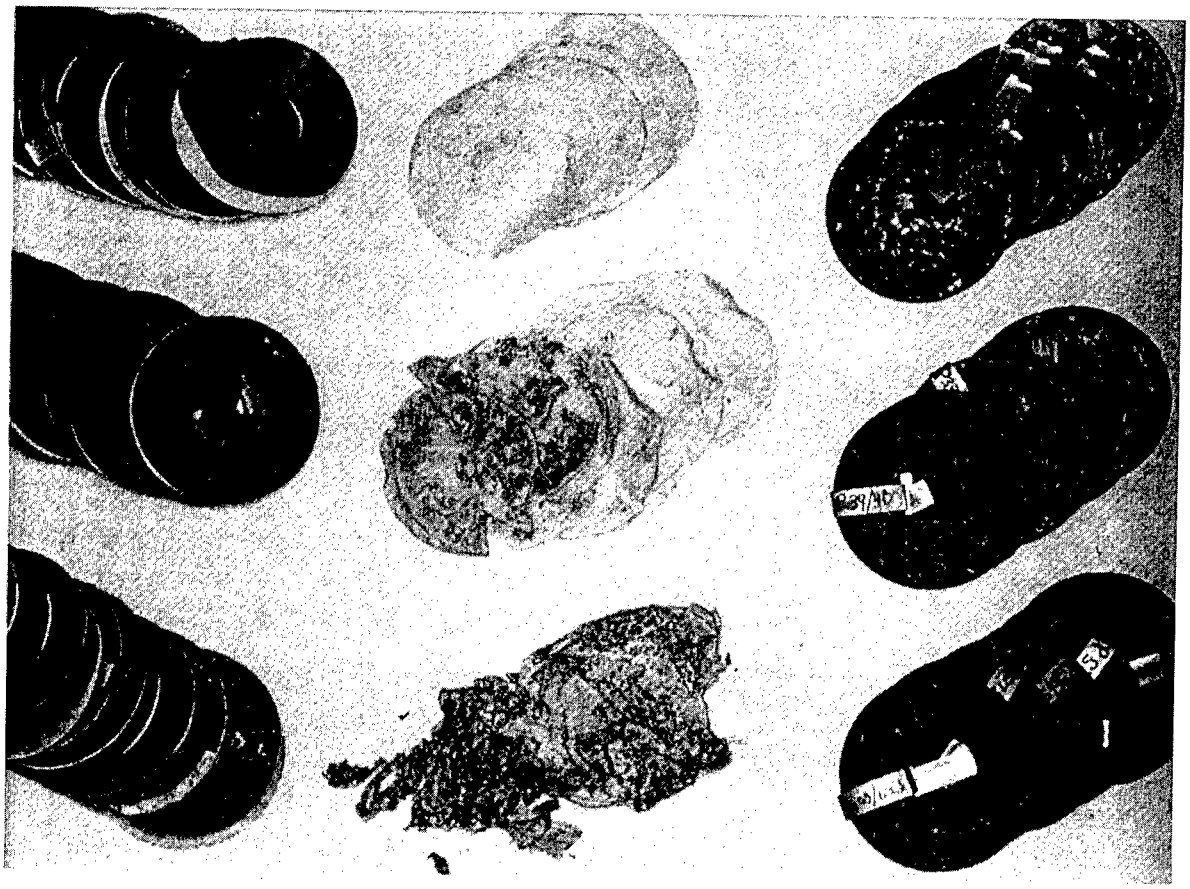

Photo 16: Comparing NEG and POS electrode pairs and separators from the three cell-stack zones (Zone 1 on top; Zone 2, middle; and Zone 3, bottom: NEG electrodes on left; separators, middle; POS, right). A more comprehensive summary is given on p.19.

Photo 17

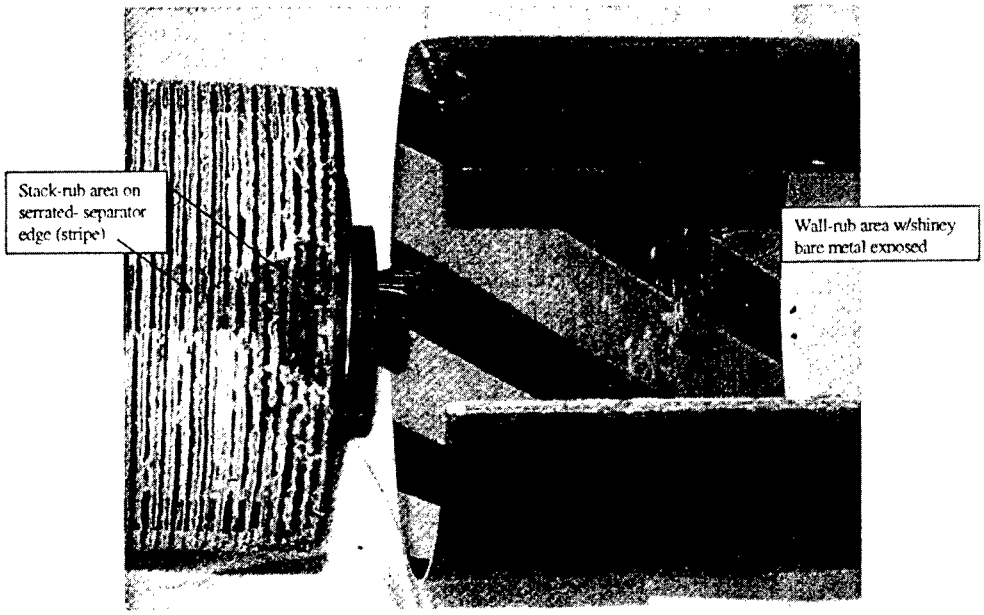

V. Less Obvious Findings.

This Section presents some findings about the mechanical, swell-cycling which appears to accompany electrical cycling in photographs and discussion.

Photo 17: Shows both: worn spots on the inside vessel walls and rubbed-off separators at the **bottom** of the cell stack (CWW Cell S/N 1, 49.7 Kcycles), and **both in exactly the same area of significant hard shorting.**

NAVAL SEA SYSTEMS COMMAND

NSWC
Naval Surface Warfare Center
CRANE DIVISION

Studies of Component Degradation in Nickel Hydrogen Cells

Photo 18

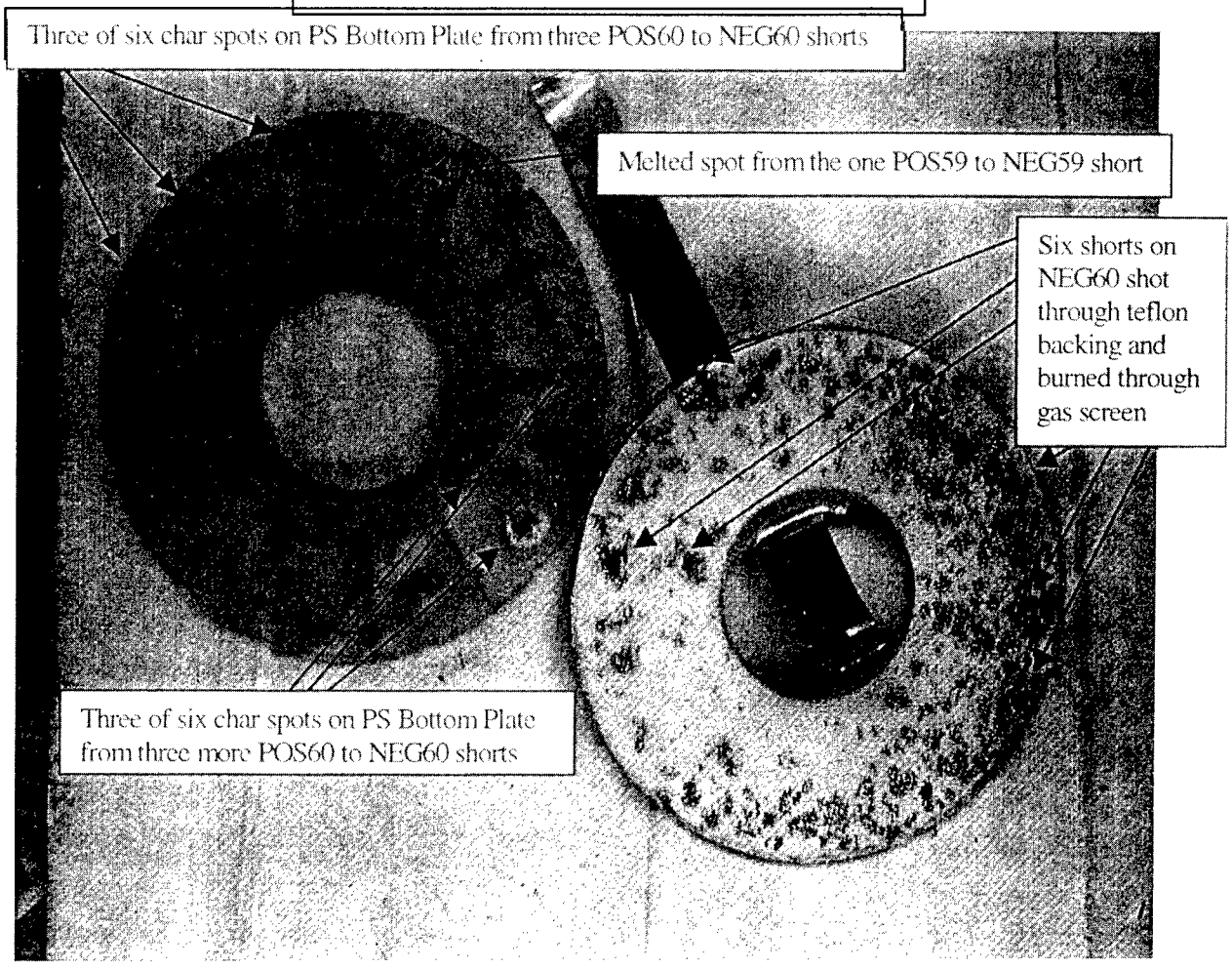

Photo 18: Six charred spots on the same polysulfone (PS) Bottom Plate shown in Photo 17 (Cell S/N 1) where the cell-stack had rubbed against the vessel wall. These six hard, hot shorts were discovered in NEG/POS electrode pair 60 (the last, and bottom most electrode pair in the cell stack). One short was so hot that it melted the NEG electrode grid-wire.

Photo 19

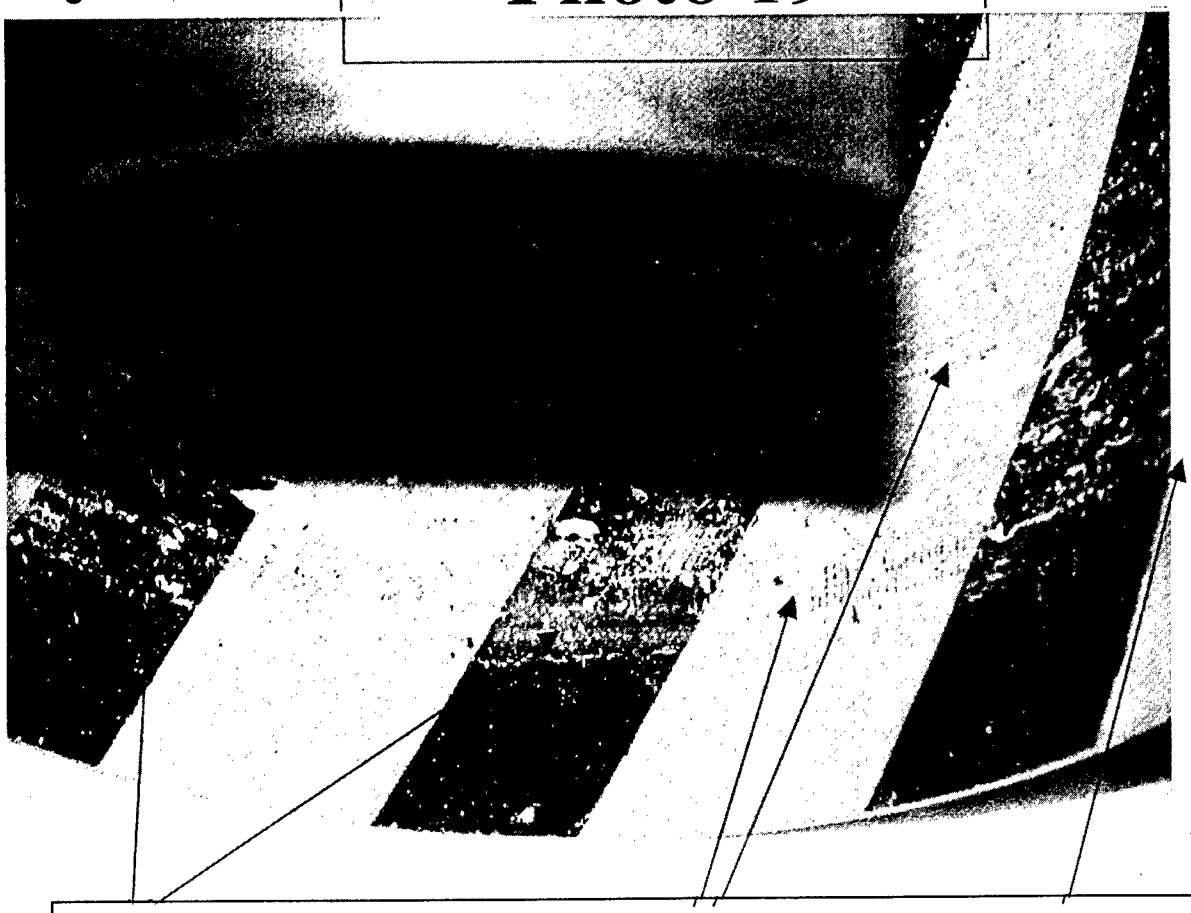

The two wall-rub areas just above PS Bottom Plate, and two grid tracks, the longer continuing off photo to right

Photo 19: Close-up of two worn-to-bare-metal areas and grid tracks (series of short parallel scratches) on vessel wall corresponding to dead-bottom of the cell stack (Cell S/N 1, 48.7Kcycles, NEG/POS electrode pair 60). This is the place on the stack where the **most** stack expansion takes place. As the cell swell-cycles during electrical (charge and discharge) cycling, the top of the stack is fixed to the top of the cylinder by the weld-ring and the stack-bottom is where the sum of all swelling has its greatest, additive effect.

NAVAL SEA SYSTEMS COMMAND

NSWC
Naval Surface Warfare Center
CRANE DIVISION

Studies of Component Degradation in Nickel Hydrogen Cells

Photo 20

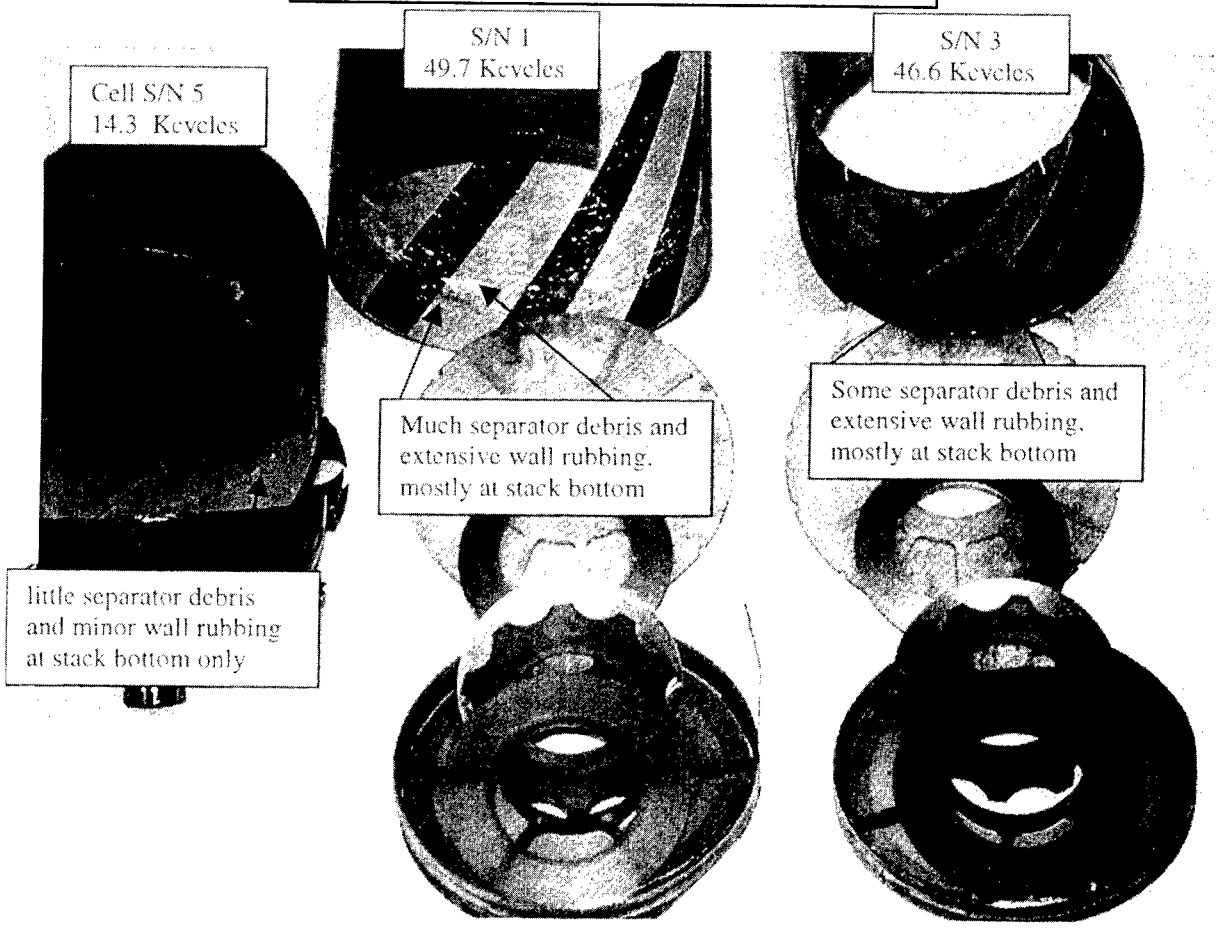

Photo 20: Comparing rubbing at the cell stack bottoms (PS Bottom Plate) in three different IPV vessels: Cell S/N 5 (14.3Kcycles) has only a little at the bottom, Cells S/N 1 and 3 have three-times the number of cycles and have considerably more rubbing evidence. The internal component assemblies also show evidence of swell-cycling (See Photo 21).

Studies of Component Degradation in Nickel Hydrogen Cells

Photo 21

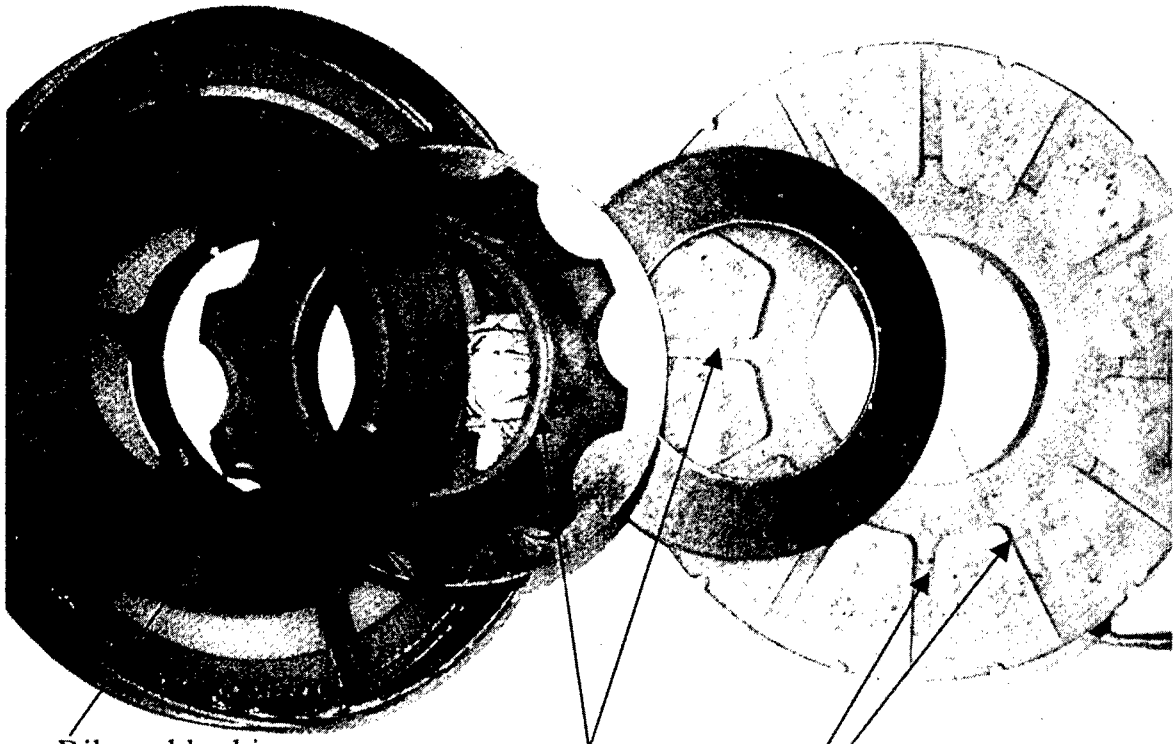

Photo 21: Comparing swell-cycling evidence on other PS inert parts and Belleville (metal) washers. The six weld-ring ribs are rubbed into the top PS washer (left), the bottom metal washer has rubbed a dark wear-ring into the ribs of the PS bottom plate and the same ribs on the bottom plate are polished (shiney) from wearing against the metal bottom washer.

NAVAL SEA SYSTEMS COMMAND

NSWC
Naval Surface Warfare Center
CRANE DIVISION

Studies of Component Degradation in Nickel Hydrogen Cells

CONCLUSIONS

VI. Conclusions, Recommendations, and Future Work.

The following is summarized from the photographs, observations, and measurements made during the five-cell DPA's:

1. The CWW functions well in both of its designed properties to: facilitate more uniform electrolyte distribution in the cell stack, and provide a remote surface for popping gas recombination;

2. Degradation of Zone 3 NEG electrodes appears to be the **main** cause of capacity loss in all five cells examined;

3. There is strong evidence of mechanical cycling (a consequence of electrical cycling) in the longer-lived CWW cells which appears to be the **main** cause of shorting in these failed cells.

Further Discussion:

Uniform electrolyte distribution is important in Ni/H_2 cells. However, the problem of non-uniform distribution may be more a problem of the test environment, than the service environment which is the micro-gravity of orbit.

Non-destructive popping-gas recombination is critically important to the long-life of NEG electrodes. But, when popping disintegrates the NEG electrodes, then the disintegrated active material becomes the preferred recombination site, and popping becomes a run-away problem.

Mechanical cycling combined with wetter bottom (Zone 3) separators appears to squeeze (extrude) wet separator material out into the wall-gap early in the cycle-life of non-CWW cells and later in CWW cells. Mechanical cycling also appears to be responsible for the observed wear on bearing surfaces of inert internal components and vessel walls.

RECOMMENDATIONS

1. The CWW should become a standard design feature of all Ni/H_2 cells to achieve more passive gas-recombination and uniform electrolyte distribution. If micro-gravity demands that a still-more-perfect electrolyte distribution be achieved, then a different, more mechanically durable separator may have to be adopted or developed.

2. Since Zone 3 NEG electrodes appeared to have been destroyed by popping, then a method to reduce or eliminate popping should be devised. Perhaps the percent (excess) recharge should be reconsidered, or reevaluated to periodic overcharge, but not every cycle.

3. Since the longer-lived CWW cells showed signs of mechanical cycling wear, then design or manufacturing, or both will have to be re-evaluated to reduce this mechanical wear, especially that which leads to shorting to the vessel walls.

Further Discussion:

NWSC, Crane's role in the NASA-team is primarily one of Test and Evaluation. However, NSWC, Crane should perform DPA's whenever affordable to derive valuable information to feed-back into the design and manufacturing processes; and DPA's should be considered the all-important final step in the evaluation of design and manufacturing changes.

All test cells appear to have been well built, and the three CWW cells performed extremely well compared to the number of other test-design iterations tested since they were built.

DESTRUCTIVE PHYSICAL ANALYSIS OF FLIGHT- AND GROUND-TESTED SODIUM-SULFUR CELLS

Margot L. Wasz and Boyd J. Carter
The Aerospace Corporation

Lt. Charles M. Donet
Air Force Research Laboratory

Richard S. Baldwin
NASA Lewis Research Center

1998 NASA Aerospace Battery Workshop
Huntsville, Alabama, October 27-29

Destructive physical analysis (DPA) was used to study the effects of microgravity on the sulfur electrode in sodium-sulfur cells. The cells examined in this work were provided by the Air Force Research Laboratory (AFRL) from their program on sodium-sulfur technology. The Naval Research Laboratory (NRL) provided electrical characterization of the flight-tested and ground-tested cells. The DPA was conducted by The Aerospace Corporation at the Technology Operations Division in El Segundo, California. This study was sponsored by the NASA-Lewis Research Center.

BACKGROUND

- The sodium-sulfur battery experiment (NaSBE) flew last November on Space Shuttle Columbia Mission, STS-87.
- Cells were heated to 350°C, cycled to verify capacity and simulate GEO and LEO profiles, then cooled down to ambient temperature from various states of charge (SOC)
- Ground tests duplicating the flight experiment were performed on four other sodium-sulfur cells from the same production lot last May

Last November, four sodium-sulfur cells were flown as a flight experiment on the Space Shuttle Columbia Mission, STS-87. This experiment was the third phase of an AFRL program (NaSTEC) to qualify sodium-sulfur cells for use in space. Earlier phases demonstrated cycle life and safe response under abuse conditions in ground tests.

The flight experiment, designed and executed by NRL, began by heating the cells to 350°C at a rate of about 18°C/hour. Two capacity verification cycles were performed, then two cycles at a simulated geosynchronus orbit (GEO) operation, and finally, 16 cycles at a simulated low earth orbit (LEO) operation. During the final discharge, individual cells were taken off line at different times, trapping them at nominal states of charge (SOC) of 100%, 80%, 60%, and 40%. Afterwards, the cells were cooled down to ambient temperature at a rate of about 14°C/hour. The same duty cycles were duplicated on four other cells on the ground to provide a direct comparison for better understanding the effects of microgravity on cell performance.

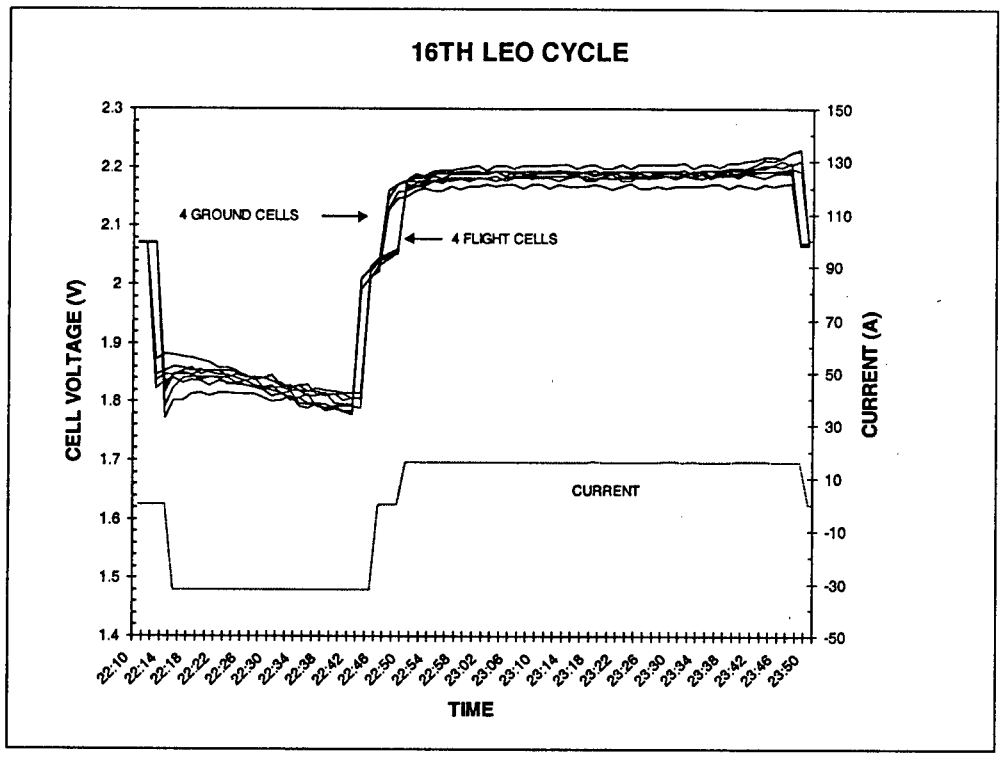

The above plot is an overlay of cell voltages from both the flight and ground-tested cells during the 16th LEO cycle. The simulated LEO orbit consisted of a thirty minute discharge at 32A (C/1.25) followed by a sixty minute charge at 16A (C/2.5). The total depth of discharge per cycle was about 40%. The cells were also maintained at open circuit for several minutes between charge and discharge and between each cycle.

Comparisons of the electrical performance from the tests show good agreement. For the cycle shown above, cell temperatures are lower in the flight cells (329-347°C) than in the ground cells (343-355°C).

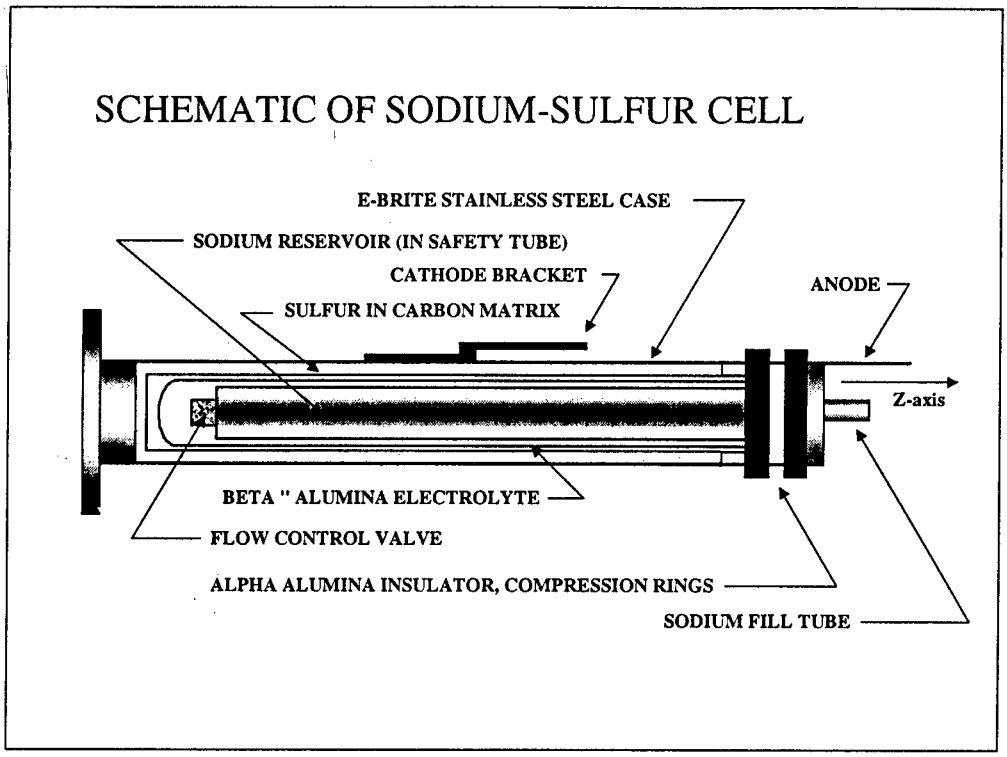

Twenty, 40 ampere-hour, sodium-sulfur cells were built by Eagle-Picher (EP) for the program in June, 1996. Each cell had a stainless steel safety tube which contained the sodium. A flow control valve made of porous nickel frit placed at the bottom of the safety tube moderated the flow of sodium to the inner diameter of the β" alumina electrolyte. The sulfur active material surrounded the ceramic electrolyte and was itself embedded in a carbon fiber matrix for conductivity. The cell case, whose inside surface was plated with chromium, was in electrical contact with the sulfur. The cathode terminal was welded on the outside of the case. The anode terminal, which passed through the top of the cell, was in electrical contact with the safety tube. The cathode and the anode were electrically isolated by an α-alumina insulator which was diffusion-bonded to an aluminum piece which was, in turn, diffusion -bonded to the stainless steel. Two compression rings protected the diffusion-bonded areas against external stresses. The length of each cell was about 9.44 inches. The average cell weight, including a flange piece welded to the bottom of the cell for connecting to an external support, was 580 grams.

During acceptance testing and in the ground experiment, cells were placed in an "anodes up" orientation.

TEST PLAN

- The program goals were to determine the effects of microgravity and to look for any signs of wear-out modes that could shorten life
- Preliminary work utilized visual inspection, ac impedance testing, and radiographic analysis to look for signs of electrolyte failure and to examine the structure of the sulfur electrode
- The core DPA effort focused on the sulfur electrode including composition analysis and elemental mapping
- Additional analysis examined the case and seals when signs of corrosion were found

The purpose of this study was to search for differences between the flight and ground-tested cells that could affect electrical performance or reveal any unanticipated response to the microgravity environment. In particular, the sulfur electrode would be analyzed to look for the effect of microgravity on mass transport and interfacial reactions at the β'' alumina interface. Also, signs of electrolyte cracking and any wear-out mode such as corrosion that would threaten cycle life would be investigated.

Post flight analysis began with nondestructive evaluation by visual and radiographic inspection of all cells. Based on these results, DPA activities were selected with primary focus on the characterization of the sulfur electrode to determine the composition of phases present and their distribution throughout the cell.

TEST METHODS

- Fein Focus Radiography
- Optical Microscopy
- X-ray Diffraction (XRD)
- Raman Spectroscopy
- Scanning Electron Microscopy
- Energy Dispersive X-ray Analysis (EDX)

NOTE: Because of the reactivity of the active material to air, DPA was performed in a dry box, and all of the above methods were done using environmental cells

A variety of analytical techniques were used to examine material from the cells in this program. Nondestructive analysis utilized impedance measurements, stereo and x-ray microscopes to search for signs of leakage, thermal anomalies ("hot spots"), and electrolyte cracking, as well as to begin examination of the cathode material.

Sodium and sulfur are reactive in air, therefore all DPA activities were performed in an inert environment. Cell were dissected in an argon-filled glove box monitored with a residual gas analyzer and an oxygen sensor. Water concentration was typically less than 1 ppm. Environmental cells held powder samples permitting the collection of x-ray diffraction (XRD) patterns without exposure to air. Similarly, a transfer container was used to carry samples from the glove box to the JEOL JSM-840 scanning electron microscope (SEM) without exposure to air. Optical images and Raman spectra were also collected through the glass lid of an environmental cell. Of the material analyzed, only the cell cases were exposed to air prior to imaging and SEM/EDX.

RADIOGRAPHY

- Fein Focus and still x-ray radiography were used to look for signs of cracking in the electrolyte and to examine the structure of the sulfur electrode
- Results
  - No signs of electrolyte cracking
  - More change along the z-axis in the ground-tested cell at 100% SOC
  - Low density region identified under the sodium flow control valve

Real time x-ray radiography was performed on all four flight and ground cells using a Fein Focus model 160.52 x-ray camera. Seals at the top of the cell were examined closely for signs of leakage. Next, the sulfur-electrolyte interface was examined while slowly rotating the cell, beginning at the top, to look for signs of cracking. None were found.

X-ray radiography generates images where light and dark contrast correspond to relative changes in the type and density of material present. Contrary to expectation, the bottom of the sulfur region of ground-tested cell at 100% SOC was lighter than the top suggesting voids or low density material at the bottom of the cell. The flight-tested cell at 100% SOC was more homogeneous, and showed signs of a higher density phase along its entire length. The structure of the sulfur electrode at 40% SOC was about the same between flight and ground cells with signs of mixed low and high density material along the length of the cell. In all eight cells, a round light area directly under the flow control valve was observed.

The largest differences between flight and ground-tested cells were found for the nominal 100% SOC condition. Therefore, these cells were selected for DPA. Flight and ground cells at 40% SOC were also selected for DPA to bracket the range of possible effects.

MACROSCOPIC OBSERVATIONS

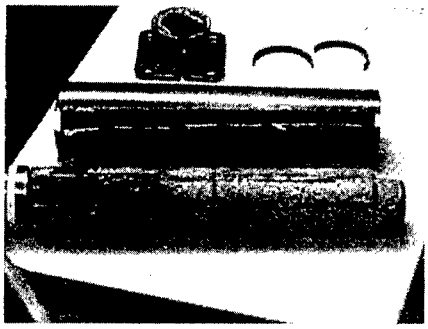

FLIGHT CELL #1

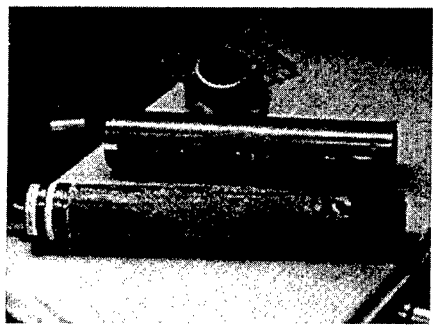

GROUND CELL #1

- Flight Cell - Voids concentrated at top
- Ground Cell - Voids concentrated at bottom

The above images of the sulfur electrode were taken through the window of the glove box within minutes of removal of the cell case during the DPA process and show the flight and ground-tested cells at 100% SOC. The top of the flight cell was composed of mostly voids in the carbon matrix. A small amount of sulfur was found in the top area at the surface of the electrolyte. This trend was reversed in the ground cell where the low density, low sulfur, region was concentrated at the bottom of the cell. This finding was unexpected because two cells from the same lot which had passed acceptance testing in the same "anodes up" orientation had large voids concentrated at the top, similar to the flight cell. Therefore, it is likely that some other factor than gravity is responsible for where the voids are concentrated.

The flat, gray material located on the surface of the active material on some of the areas is $CrNaS_2$ that has separated from the case.

MACROSCOPIC OBSERVATIONS

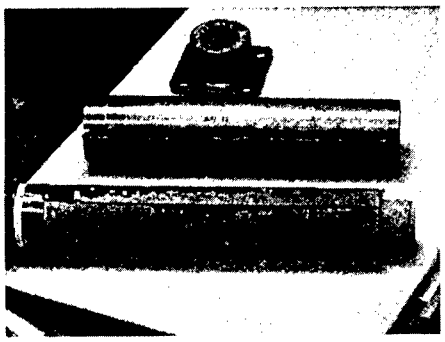

FLIGHT CELL #4

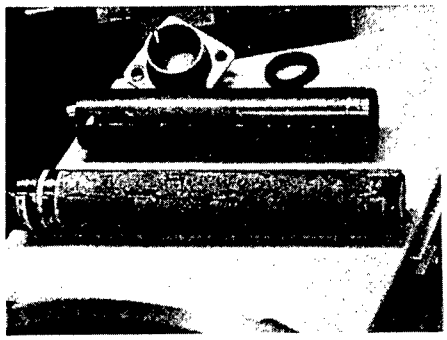

GROUND CELL #4

- Flight Cell - Voids concentrated along edges of carbon mats
- Ground Cell - Voids concentrated at bottom

The images above show the flight and ground cells at the nominal 40% SOC condition. Voids, along with orange and rich yellow regions are evident. Voids in the flight cell concentrated along the length of the cell at the interface between carbon mats. This trend was less evident in the ground cell where voids also concentrated at the bottom of the cell. A large amount of the orange phase was found on top of the carbon mat at the top of the ground cell.

Again, as seen in the other two cells at 100% SOC, $CrNaS_2$ adhered to some parts of the the sulfur electrode in both cells.

MACROSCOPIC OBSERVATIONS

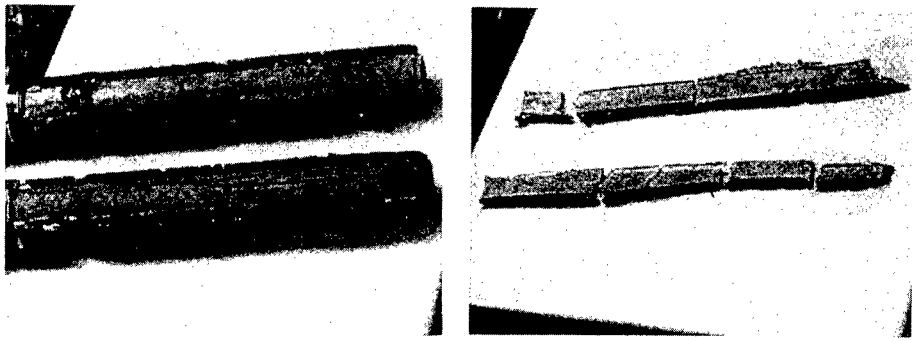

CELLS AT 100% SOC (FLIGHT CELL ON TOP)

- Orange phase found at the sulfur/electrolyte interface on both cells (Na_2S_5)

These images show the interface of the sulfur electrode and the electrolyte after the sulfur matrix was peeled away on cells at 100% SOC. Removal of the active material was difficult in both cells. The flight cell (top) showed an orange phase at the interface along 70% of its length. At the top, the interface was light yellow, characteristic of sulfur. In the ground cell (bottom), the orange phase was found along the entire length of the cell. In both cells, the orange phase appeared to be situated only at the electrolyte interface, and the region on the outer diameter of the active material appeared only gray or yellow.

MACROSCOPIC OBSERVATIONS

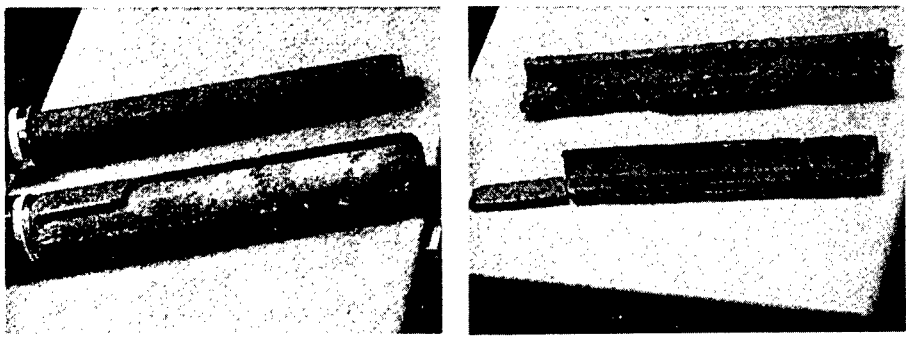

CELLS AT 40% SOC (FLIGHT CELL ON TOP)

- Flight cell - Uniformly orange throughout cathode material (Na_2S_5)
- Ground cell - Orange and yellow (Na_2S_5 and Na_2S_4)

The above images show the interface of the sulfur electrode and the electrolyte after the sulfur matrix was peeled away on cells at 40% SOC. Removal of the active material was much easier, particularly in the flight cell (top). The interface on the flight cell was uniformly orange along its entire length. However, the interface on the ground cells (bottom) showed both orange and yellow regions. The white patches on the electrolyte correspond with the orange and region in the sulfur electrode. Note that, unlike cells at 100% SOC, the colored regions found at the electrolyte interface extend to the outer diameter of the sulfur electrode.

MACROSCOPIC OBSERVATIONS

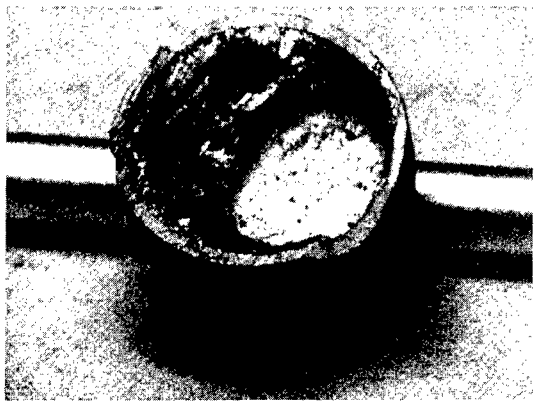

CROSS SECTION OF BOTTOM OF FLIGHT CELL #4

- Large void found directly under the flow control valve inside the electrolyte

The bottom of the ceramic electrolyte on flight cell #4 (40% SOC) was removed using a diamond wafering saw. The low density region under the flow control valve identified with the x-ray camera was found to be a large void. Although this feature was found on all flight and ground cells, it could represent non-optimal performance for the cell design.

XRD RESULTS

- Three samples per cell
- Flight and ground cells at 100% SOC indexed to sulfur, although other minor peaks were recorded
- Both cells at 40% SOC contained unidentifiable peaks which relaxed to either Na_2S_5 or Na_2S_4
  - Flight cells showed mostly Na_2S_5 (relaxed)
  - Ground cells showed Na_2S_5 and Na_2S_4 (relaxed)

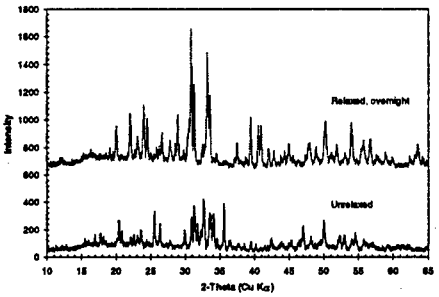

Relaxation in a powder sample from the bottom of ground cell #4. Peaks in the upper spectra index to Na_2S_5.

Three powder diffraction samples were prepared in the glove box from the cathode material located at 20%, 50% and 80% along the axis of the cell. Care was taken to insure that all of the active material from the inner diameter to the outer diameter would be present. The sample was then ground to a fine powder with a mortar and pestle and placed in an environmental XRD sample holder. XRD spectra were collected using a Philips diffractometer and Cu K_α generator operating at 45kV/30mA. A monochromator was used to suppress Cu K_β peaks.

XRD spectra for both flight and ground cells at 100% SOC indexed to sulfur for all three regions. Minor peaks belonging to a metastable sodium polysulfide phase were also found in all samples. These peaks were strongest in the middle sample of the flight cell and the bottom sample of the ground cell.

XRD spectra from the cells at 40% SOC contained metastable peaks which relaxed to Na_2S_5 and Na_2S_4 upon repeated exposure to the x-rays. Relaxation only occurred with exposure to the x-ray radiation. The flight cells relaxed to mostly Na_2S_5 with little change along the length of the cell, whereas the ground cells relaxed to both Na_2S_5 and Na_2S_4 phases. A higher concentration of Na_2S_4 was found at the middle and bottom of the ground cell.

RAMAN SPECTROSCOPY

- Orange and yellow regions seen during DPA on ground cell #4 identified
  - Deep yellow region is mostly Na_2S_4
  - Orange region is mostly different phases of Na_2S_5
  - Crystallites of both Na_2S_5 and Na_2S_4 could be found in either region
- Other findings from Raman analysis
  - Three phases of Na_2S_5 found, β- and γ-phases seemed to be less stable than the α-phase
  - No free sulfur in samples from ground cell #4
  - Possible preferred orientation of phases

Quantification of the sodium and sulfur present in the sulfur electrode by SEM/EDX was unable to identify the source of the yellow and orange phases seen macroscopically. Therefore, Raman spectroscopy was used to analyze the material.

Reference Raman spectra for Na_2S_2, Na_2S_3, Na_2S_4, α-Na_2S_5, β-Na_2S_5, γ-Na_2S_5 and sulfur were found from a review of the published literature. A sample containing both the orange and yellow regions from the ground cell left at 40% SOC was examined. Spectra from all three phases of Na_2S_5 were found in the orange grains in the orange region. Yellow grains in the orange region were Na_2S_4. Likewise, orange grains in the yellow region were found to be Na_2S_5 and the yellow grains Na_2S_4. The β and γ-phases found, however, seemed to be less stable than the α-phase of Na_2S_5. Also, the peak intensities recorded suggest possible preferred crystal orientation for the Na_2S_5 phases.

SEM/EDX - SULFUR ELECTRODE

- Three samples from each cell examined
- Na, S, Cr, Al, C and O mapped from the inner to the outer diameter of the active material
- Quantification - the table below shows the ratio of atomic % Na to atomic %S found in the sodium-rich phases of the sulfur electrode

Flight #1	Region	Ground #1
0.086	top	0.072
0.123	middle	0.146
0.117	bottom	0.092
Flight #4	**Region**	**Ground #4**
0.142	top	0.140
0.117	middle	0.155
0.114	bottom	0.206

Three samples from each cell were examined by SEM/EDX. The samples were cut from cathode material located at 20%, 50%, and 80% along the cell axis. Care was taken to insure that material from both the electrolyte interface and the case interface was included in each sample. After cutting, the samples were smoothed with fine grit sandpaper to remove contamination and to create a flat surface for analysis. Debris from the sanding process was removed with a brush. Samples were transferred from the glovebox to the SEM in an airtight holder preventing exposure to air. During the SEM/EDX analysis, regions were imaged and mapped for the x-ray spectra of Na, S, Cr, Al, C and O from the inner to outer diameter. When a sodium-rich phase was found, a ZAF quantification routine was used to calculate the atomic percents of sodium to sulfur present.

The cells at the nominal 100% SOC showed separate phases of sulfur and sodium polysulfide. The distribution of the phases was similar, and the concentration of sodium in each cell was highest at the middle of the cell. The sodium distribution of the cells at 40% SOC appeared homogeneous and little difference was found between the two cells. Overall, the sodium concentration was higher in the ground cell, particularly in the bottom sample. The following two pages show the sodium maps of the three samples for each cell. The white areas evident in the cells at 40% SOC are voids in the material.

EDX MAPPING OF FLIGHT (LEFT) AND GROUND (RIGHT) CELLS AT 100% SOC (NOMINAL)

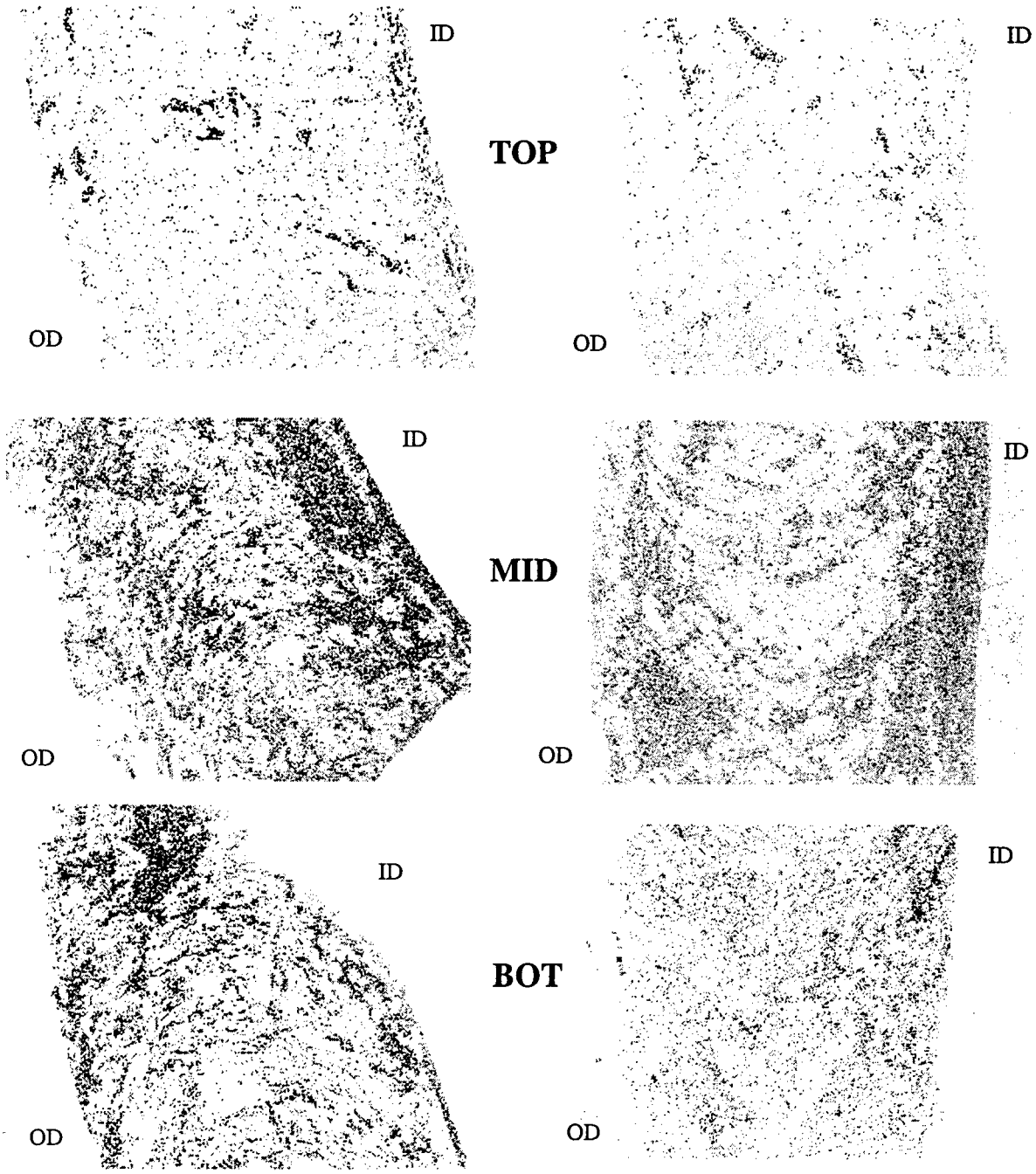

Bands of sodium-rich phases were found in the middle samples of each cell

EDX MAPPING OF FLIGHT (LEFT) AND GROUND (RIGHT) CELLS AT 40% SOC (NOMINAL)

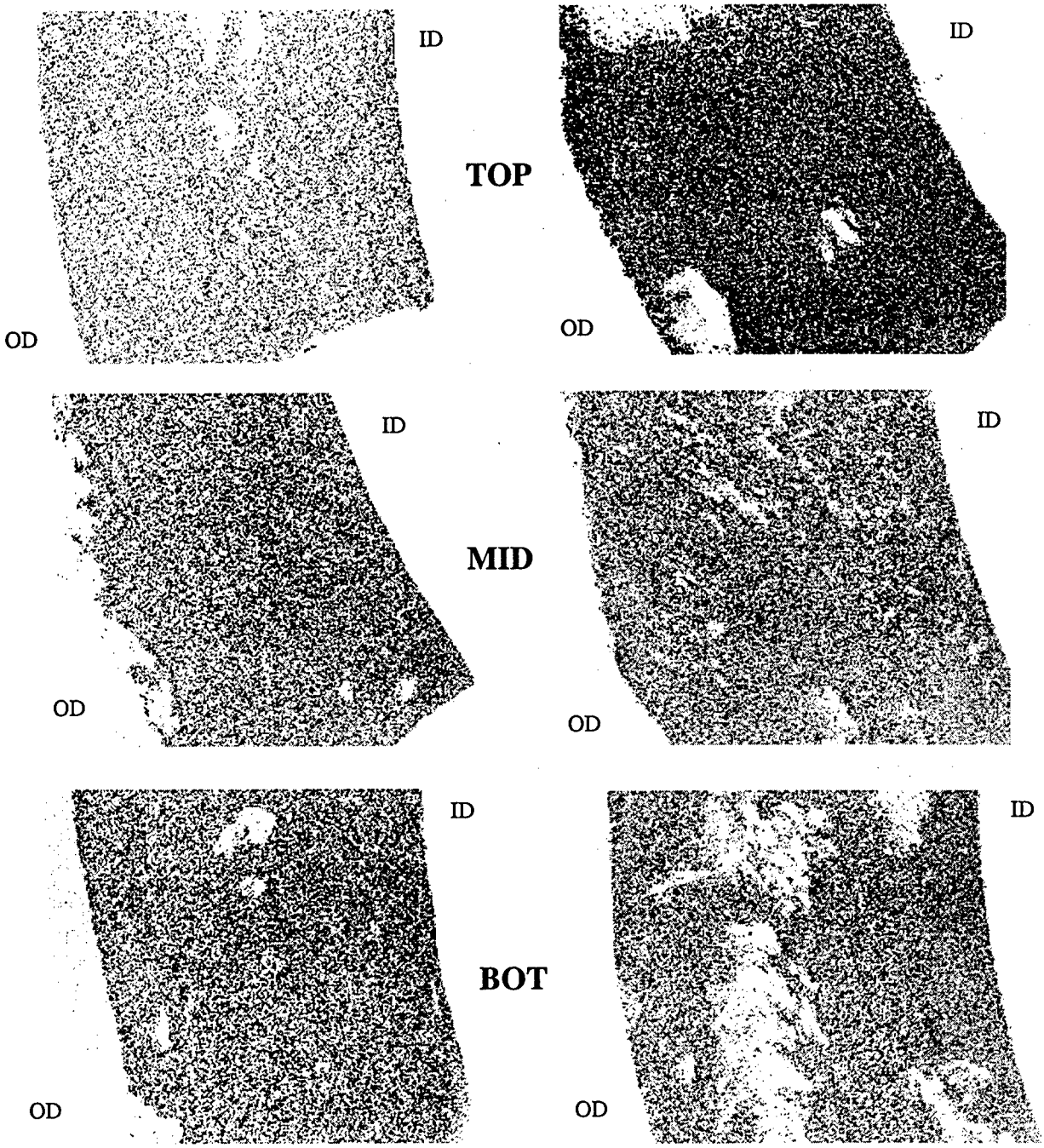

Sodium concentration is homogeneous along each cell (the white areas in the samples are voids)

CELL CASE ANALYSIS

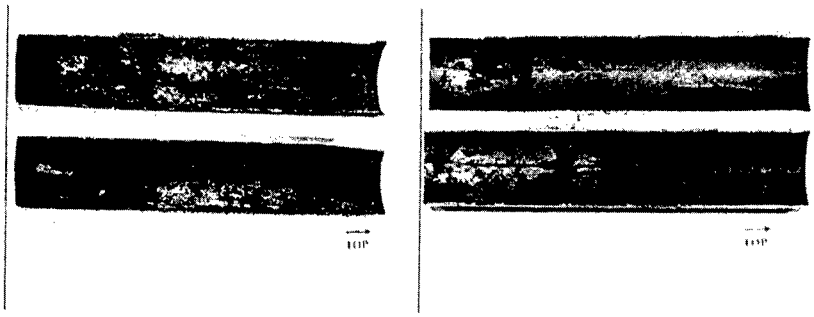

- The inside surface of the case from cells at 100% SOC (left) differed from cases from cells at 40% SOC (right)
- Both flight and ground cell cases looked about the same

Any corrosion of the cell case would have important implications for long duration use of the cell design. Therefore, the condition of the interior of the cell cases was examined. The general appearance of the cell cases varied with SOC, however, both flight and ground-tested cells appeared the same at the same SOC. The above images show the appearance of the inside of the cell cases for cells at 100% SOC (left) and 40% SOC (right). Cells at 100% SOC contained metallic bright areas and areas of gray/green black. The cells at 40% SOC also had some bright, metallic regions as well red and dark shiny black deposits.

The cell cases were cleaned in acetone and dried in air prior to imaging.

SEM/EDX - CELL CASE, INNER DIAMETER

- EDX of the different phases identified the following
  - metallic = Cr
  - gray/green phase, $CrNaS_2$
  - shiny black phase, $(Cr,Na)_2S_2$
  - red phase, 1.0Cr:2.3Na:2.8S
- No iron found in the EDX spectra

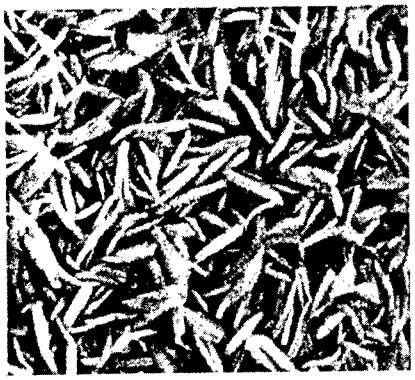

$CrNaS_2$ crystals found on case

The four different phases found on the cell cases were analyzed by SEM/EDX. The shiny metallic phase was chromium, and the other phases were all combinations of Cr, Na, and S. Quantification of the gray/green phase indicated that it was stoichiometric $CrNaS_2$.

No iron was found in any of the EDX spectra and no sign of corrosion past the chromium layer was found in this portion of the analysis.

SEM/EDX - CELL CASE, CROSS-SECTION

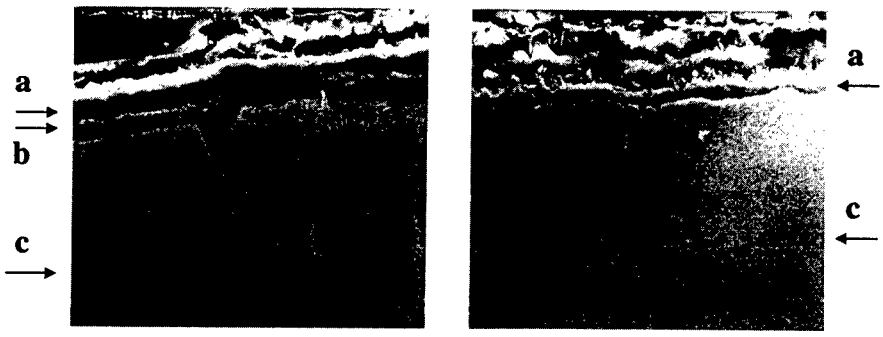

Pitting and cracks found on the inner diameter of the cell case. a) $CrNaS_2$ layer, b) chromium oxide (black spots), and c) chromium/stainless steel interface

The cell case of the ground cell left at 40% SOC was sectioned with a diamond wafering saw, mounted in metallographic epoxy resin, and polished.

Optical and SEM imaging found cracks in the chromium layer and signs of pitting attack. The above images show examples of these features, including cracks which appear to initiate from the $CrNaS_2$ layer. The region above the $CrNaS_2$ layer is the epoxy resin which has also reacted with the $CrNaS_2$. The darks spots at the chromium-$CrNaS_2$ interface on the image at the left are chromium oxide.

SUMMARY OF OBSERVATIONS

- Distribution of voids in the sulfur electrode was different between flight and ground cells at 100% and 40% SOC, different sodium polysulfide phases were found in flight and ground cells at 40% SOC
- No evidence for electrolyte cracking or leakage at seals, possible evidence for the non-passive formation of $CrNaS_2$

CONCLUSIONS

- Cell design appears to have worked well in microgravity
- The chemical composition of the sulfur electrodes in the flight cells were at least as uniform, if not more so, than the sulfur electrodes in the ground cells
- The ground test data base should provide a conservative life estimate for on-orbit life and performance

To summarize, some features were found in the sulfur electrode which could be the result of differing gravity environments. The distribution of voids was different between cells at both 100% and 40% SOC. Also, the sodium polysulfide phases found at 40% SOC were not the same between the flight and ground cells. No signs of sulfur leakage were found on any of the cells, nor were there any signs of cracking of the electrolyte in either the electrical or radiographic data. However, analysis of the cell case suggest that the $CrNaS_2$ compounds formed on the chromium liner are not passive. This could have implications for long term use of this design feature.

In conclusion, the cell design as a whole worked well in the microgravity environment. The chemical composition of the sulfur electrodes in the flight cells were at least as uniform, if not more so, than the sulfur electrodes in the ground cells. This finding implies that the ground test data base should provide a conservative life estimate for on-orbit life and performance for this chemistry.

ACKNOWLEDGEMENTS

- Paul Adams (XRD, still radiography, Aerospace)
- Jim Barrie (Raman spectroscopy, Aerospace)
- Jim Degruson (Technical advice, EP)
- Chris Garner (Technical advice, NRL)
- Carole Hill (Technical advice, Aerospace)
- Martin Leung (Fein Focus radiography, Aerospace)
- Marc Marcus, Dennis Smith (Technical Support, Aerospace)
- Joe Uht, Michael Tueling (SEM/EDX, Aerospace)

The authors would like to thank the above individuals for their expertise and advice throughout the course of this work.

USING DPA RESULTS FROM BOILER PLATE NiH2 CELLS TO HELP UNDERSTAND DESIGN LIMITATIONS AND VALIDATE NEW CELL COMPONENTS

Presented to 1998 NASA BATTERY WORKSHOP

Thierry Jamin French Space Agency CNES Toulouse

Max Schautz European Space Agency Noordwijk

October 28

1. SCOPE

- Research is continuously underway to promote the use of new materials in aerospace cells
- Mass saving and economical target may preferentially lead to alternate separator and positive material at NiH2 Aerospace Technology level
- CNES has been envolved for years with SORAPEC in developping lightweight positive design and in evaluating different Zirfon separator materials (Z1, Z2)
- ESA / VITO developmental activity of new Zirfon (Z28) specifically designed as an alternate to SOA Zircar for NiH2 technology
- A large characterization program with different labs (SAFT Research, LRCS Amiens , LTVP Paris) is still undergoing on these components

2. INTRODUCTION

- **Boiler plate testing as a preliminary step is helpfull to run an almost representative evaluation under cycling**
- **EOL/BOL functionnal features comparison helps to understand their behavior evolution with ageing**
- **Accelerated GEO cycling (rapide cycle or wear out) were performed on BP incorporating Z2 / foam based or Z28 / dry sinter at 10°C and 80% maxi dod**

3. LIGHTWEIGHT POSITIVE ELECTRODES

- **Thin (1.2 mm) electrodes made from foam substrate were preliminary selected**
- **Active material is a commercial grade high density ternary β Nickel Hydroxide**
- **Adapted formulation with corresponding additives enhances activation, efficiency and stability**
- **Compression post processing insures an optimised loading level (125 - 145 mg Ni(OH)2) to limit swelling**

4.ZIRFON SEPARATOR MATERIAL FEATURES

- It is a composite material family made by casting technique of a mixture of PSO solvated in NMP solution and zircone powder
- Pore former is added to achieve the desired porous spectrum
- The 3D structure film is revealed when inmersed in a non solvant
- High wettability is linked with high developped BET surface of ZrO2
- Various types were sequentially studied Z1, Z2 and more recently Z28
- Z2 material is made of 82%w ZrO2 and 18% PSO while Z28 exhibits 75%/15% composition

ZIRFON 2 / ZIRFON 28 COMPARATIVE PHYSICAL FEATURES

Type of separator	ZIRFON 2	ZIRFON 28
Weight (g/m*2)	270	180
Resistivity (m Ω.cm*2)	90	70
Electrolyte retention (mg/cm*2)	30	35
Bubble pressure (bars)	1.5	0.3
Porosity (%)	75	81
Average pore size (μ)	1.3	6

ZIRFON SEPARATOR MATERIAL - Cont 'd

- Comparing Z28 with Z2 former material shows there is some mass decrease (180 / 270 g/m*2) partially because of a slightly lower density of the bulk (2.8 / 3.1) , due to the difference in composition, but also and essentially because of an increase in porosity (81 / 75 %)
- For roughly the same thickness (ie 330 μ) the electrolyte resistivity is lower (90 / 70 mΩ .cm*2) because of an improved retention (35 / 30 mg KOH / cm*2)
- Bubble pressure is lower (0.3 / 1.5 bars) because of the average pore size increase (6 μ / 1.3 μ)

ZIRFON 2 SURFACE MEB PICTURE

ZIRFON 2 Neuf

Provenance SOKAPEC

Lot N°02-538-549

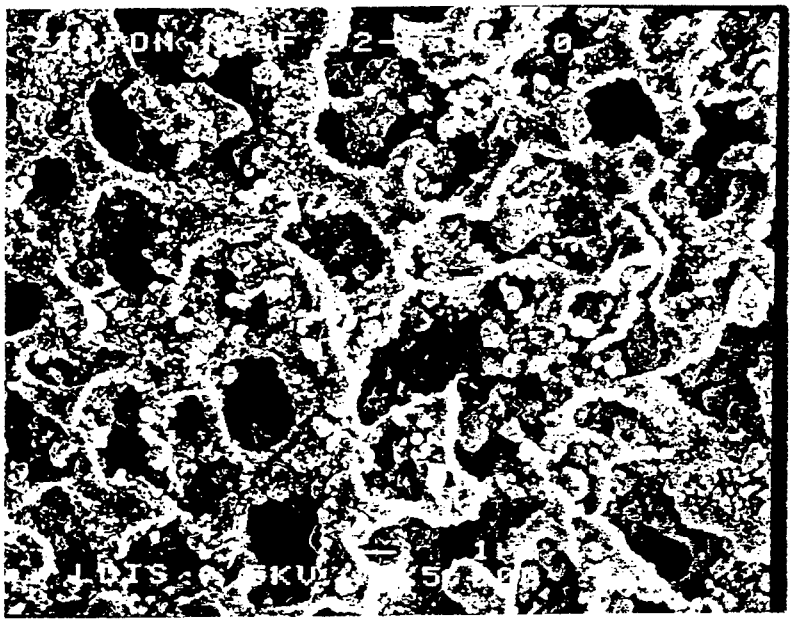

ZIRFON 2 Neuf

Provenance VITO

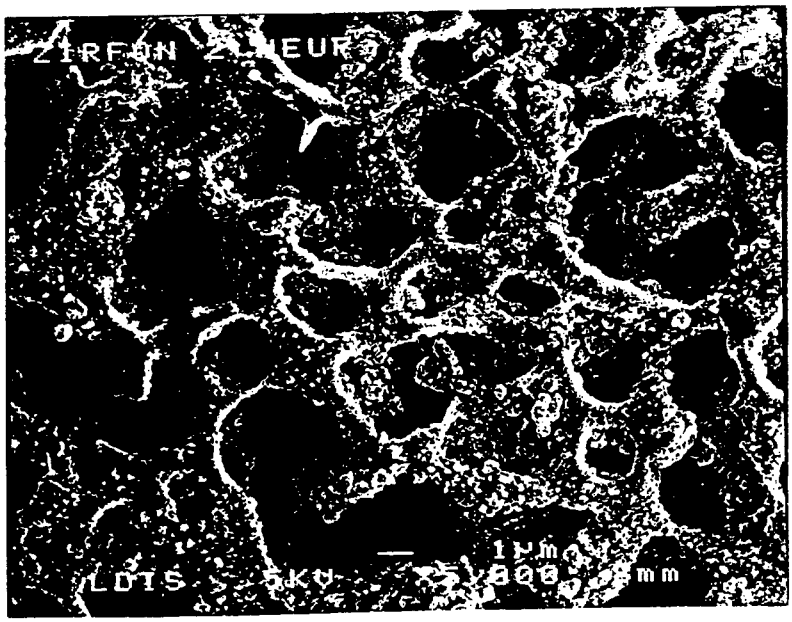

Nasa Aerospace Battery Workshop, October 27-29, 1998

ZIRFON 28 SURFACE MEB PICTURE

ZIRFON 3 NEUF EN SURFACE

SURFACE 1

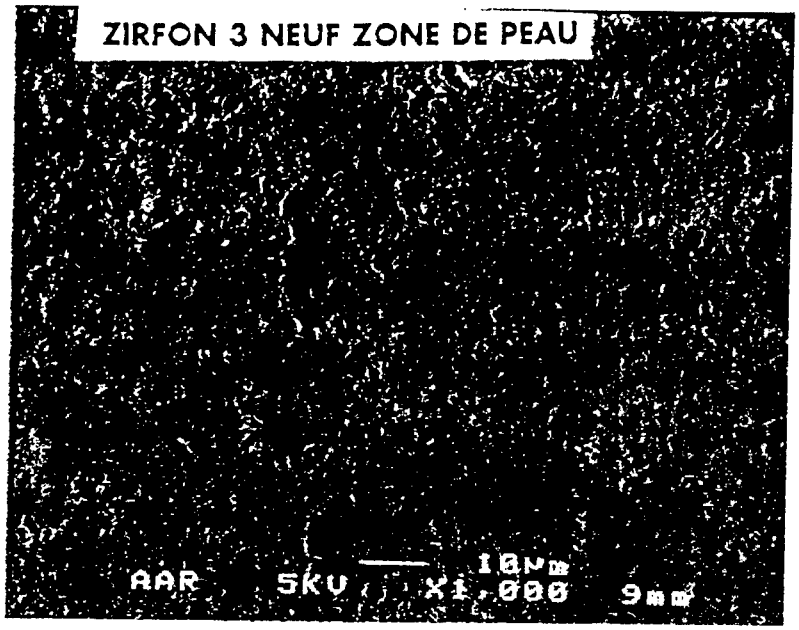

SURFACE 2

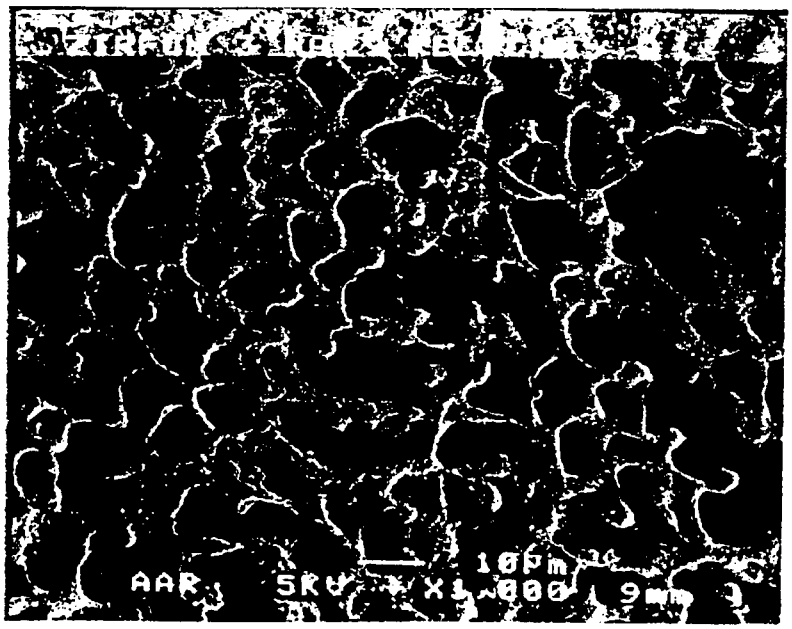

Nasa Aerospace Battery Workshop, October 27-29, 1998

COMPARATIF ZIRFON 2 ET ZIRFON 3 DANS L'EPAISSEUR
(CRYOFRACTURE ALCOOL)

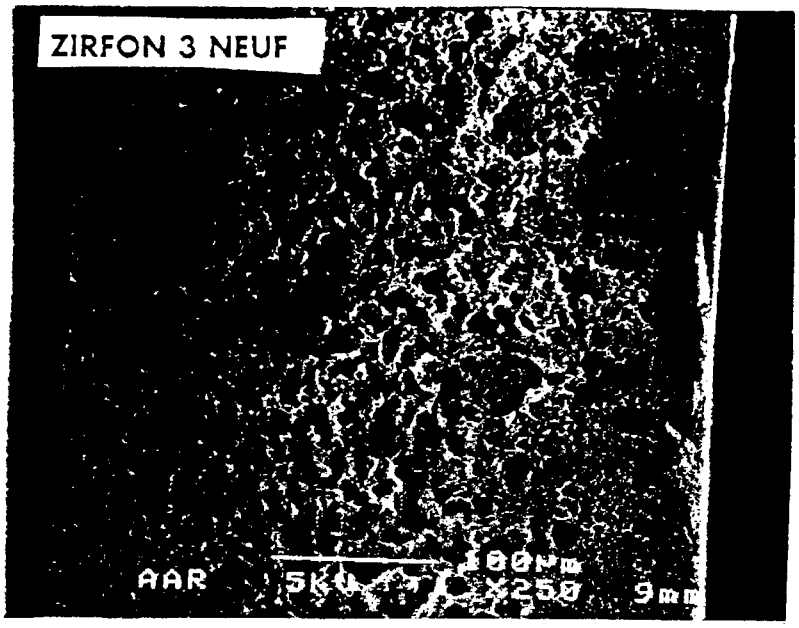

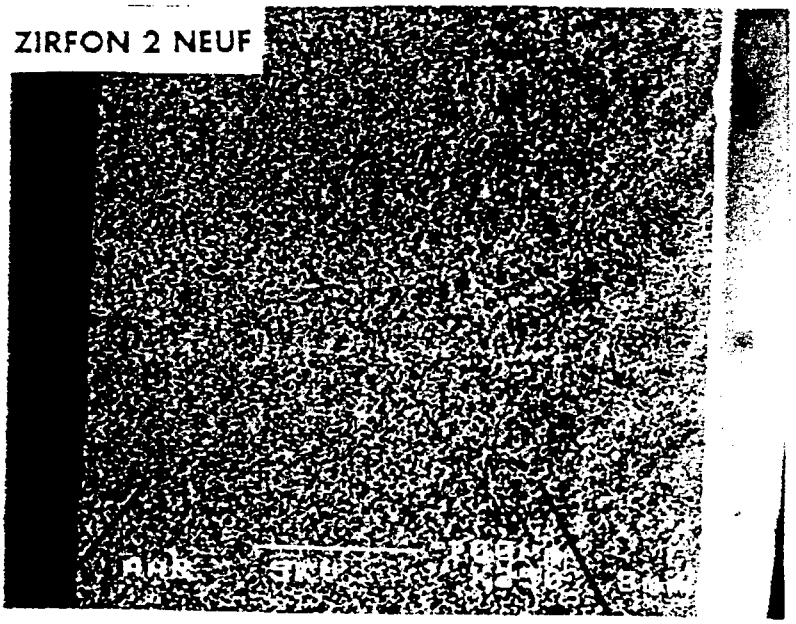

5. STACK DESIGN

- Two different stacks size were mounted to study Z2 and Z28 (15 Ah and 30Ah)
- In both cases whatever the positive type is (foam based or dry sinter) a back to back design is used
- Stack expansion allowed with spring device
- Z2 separator mounted as a mono layer while Z28 is a double layer

6. EXPERIMENTAL APPARATUS - CYCLING CONDITIONS

- BP are equipped with temperature and pressure transducers
- Cyclic K factor: 1.15 with 4 cycles a day for Z2 BP (rapid cycle)
- Cyclic K factor: ranging from 1.06 to 1.15 with 12 cycles a day for Z28 BP (wear out cycle)

EXPERIMENTAL THICKNESS AND RESISTIVITY MEASUREMENT APPARATUS

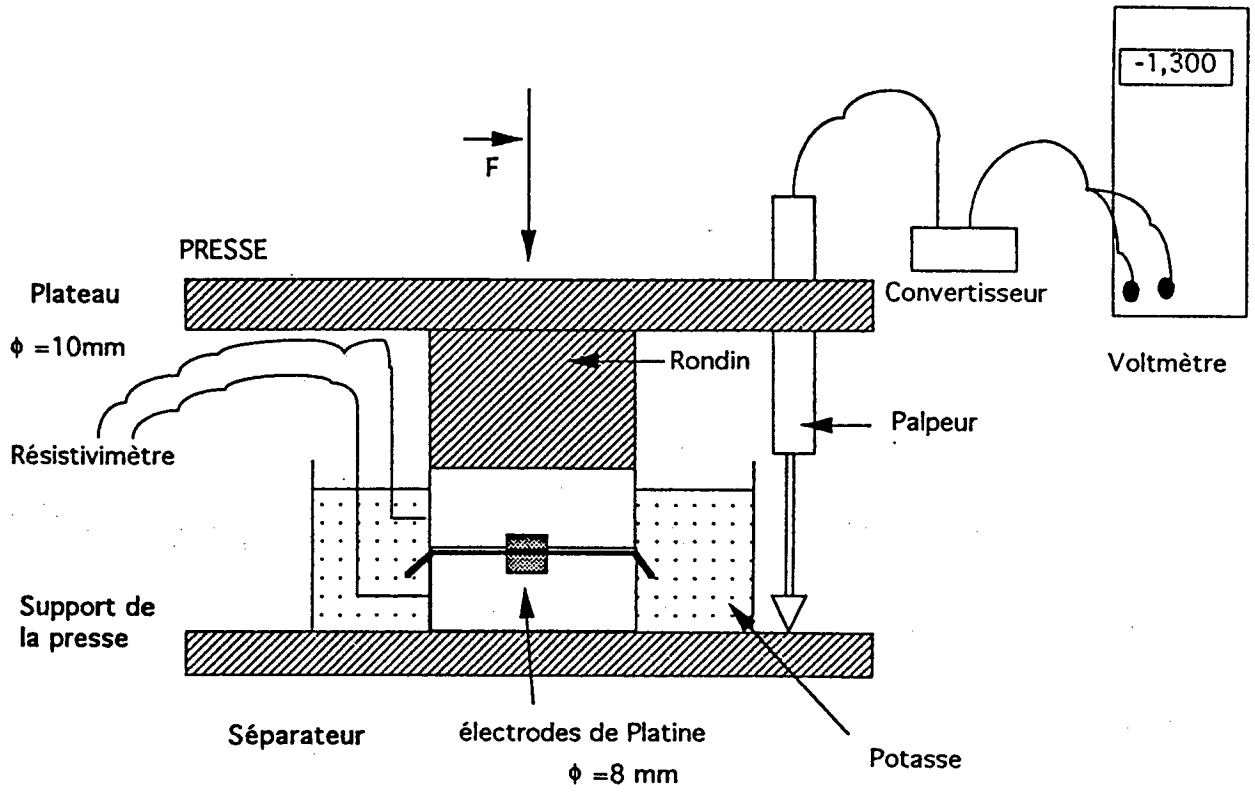

Nasa Aerospace Battery Workshop, October 27-29, 1998

7. COMPONENTS CHARACTERIZATION TECHNIQUES

- **7.1 SEPARATOR**
- **Focus on compression effect on thickness, retention and resistivity**
- **Porosity measurements + capillary ascent**
- **O2 permeation kinetic**
- **MEB pictures for superfacial aspect**

- **7.2 POSITIVES**
- **Swelling**
- **Porosity**
- **Structural analysis with X ray pattern**
- **Textural analysis with FEG and TEM pictures**
- **Micro dosing of active material**

8. EXPERIMENTAL RESULTS
8.1 Z2 ELECTRICAL - CYCLING

- Z2 BP stopped after 1200 cycles (Z13) and after 2320 cycles (Z6 ')
- Same evolution with slight decrease of V EOD with time (1.18 V BOL / 1.12 V EOL)
- 10% capacity fading under std conditions (kinetic limitations because almost full recovery under low rate discharge) confirmed by FEL measurements (-5 to -17 %)
- No short from charge retention testing
- Electrolyte distribution changes with net transfer from separatór (31% BOL / 22.4 EOL) to positive
- Minor changes in separator (-7%) and negative (-2%) thickness

ZIRFON 2 BOILER PLATES VOLTAGE EVOLUTION UNDER RAPID CYCLE TESTING

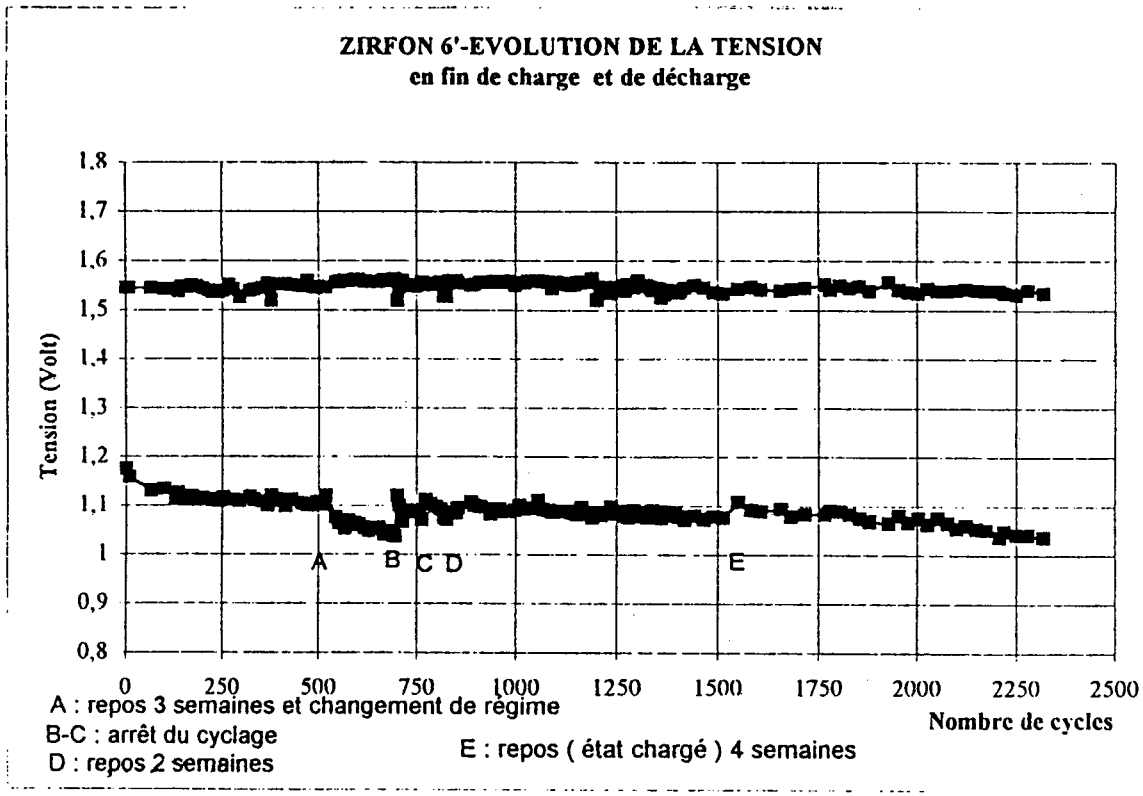

Nasa Aerospace Battery Workshop, October 27-29, 1998

Z2 STACK COMPONENTS ELECTROLYTE REPARTITION EOL / BOL

CONTENT %	BOL	EOL
POSITIVE	54	63.2
NEGATIVE	15	14.4
SEPARATOR	31	22.4

ZIRFON 2 main features evolution with cycling

Reference state	New	After 2320 cycles
Weight (g/m*2)	269	259
Thickness (μ)	327	305
Porosity (%)	76	68
Drop test (sec)	1	36

COMPARATIF ZIRFON 2 NEUF ET ZIRFON 2 CYCLE
(Répartition de zircone dans l'épaisseur des séparateurs)

Z2 fresh and cycled cross section

ZIRFON 2 NEUF

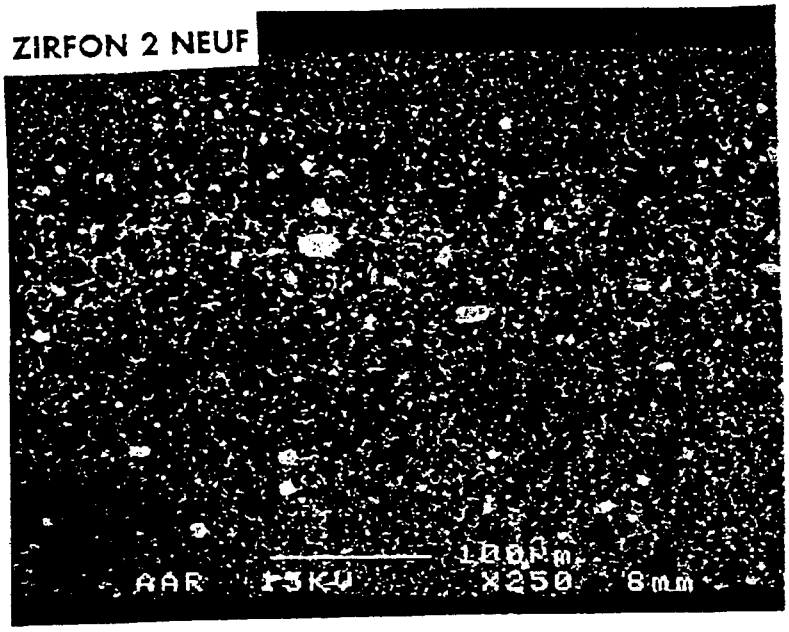

ZIRFON 2 CYCLE

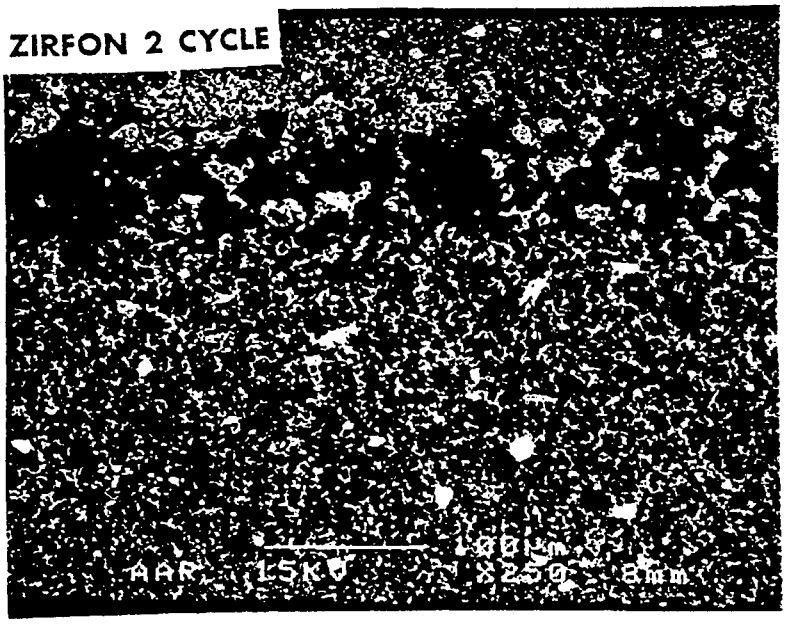

Nasa Aerospace Battery Workshop, October 27-29, 1998

ZIRFON 2 Hg POROUS SPECTRUM EVOLUTION WITH AGEING

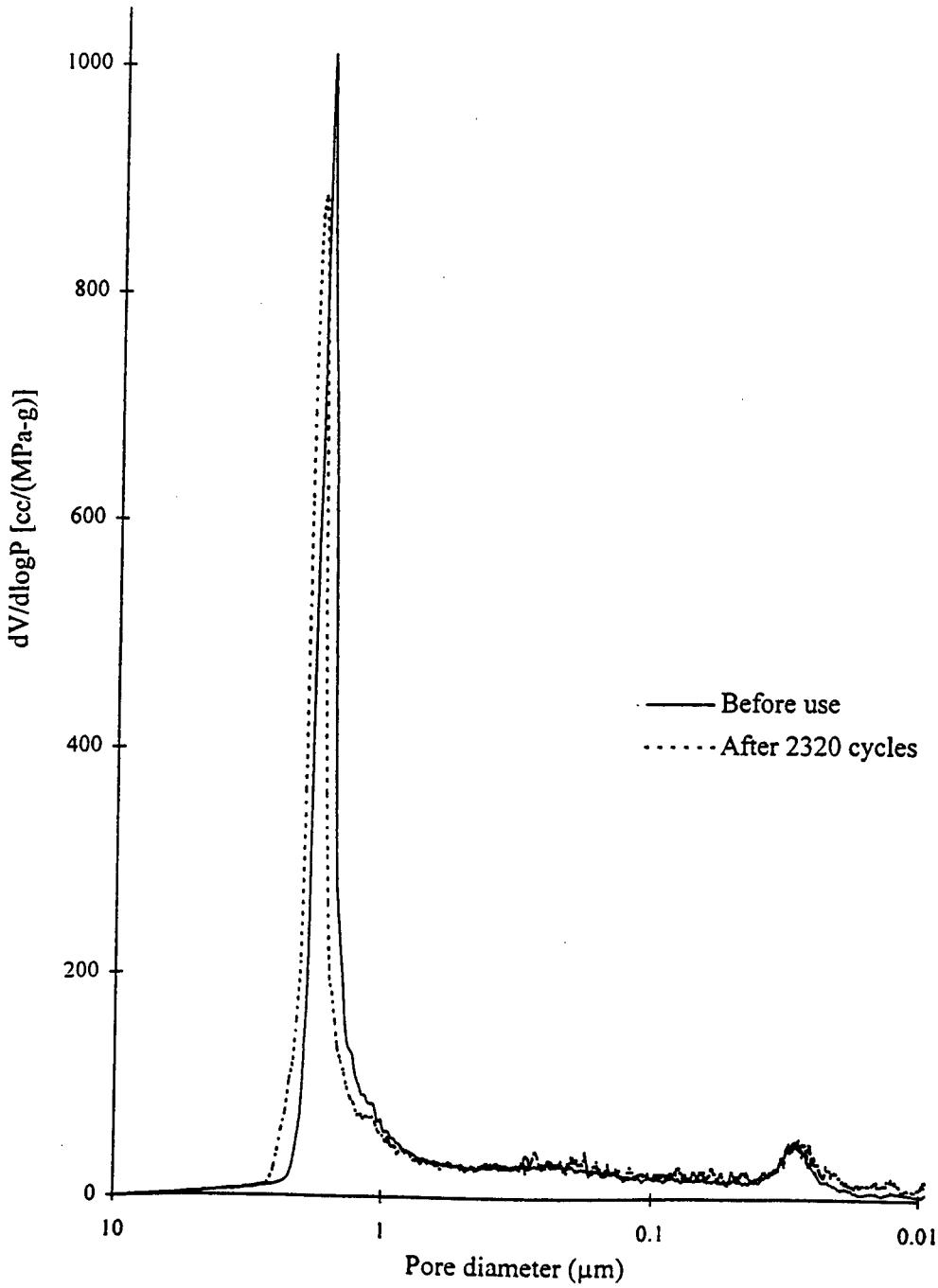

FRESH ZIRFON 1 / 2
O2 PERMEATION KINETIC
= f (electrolyte saturation)

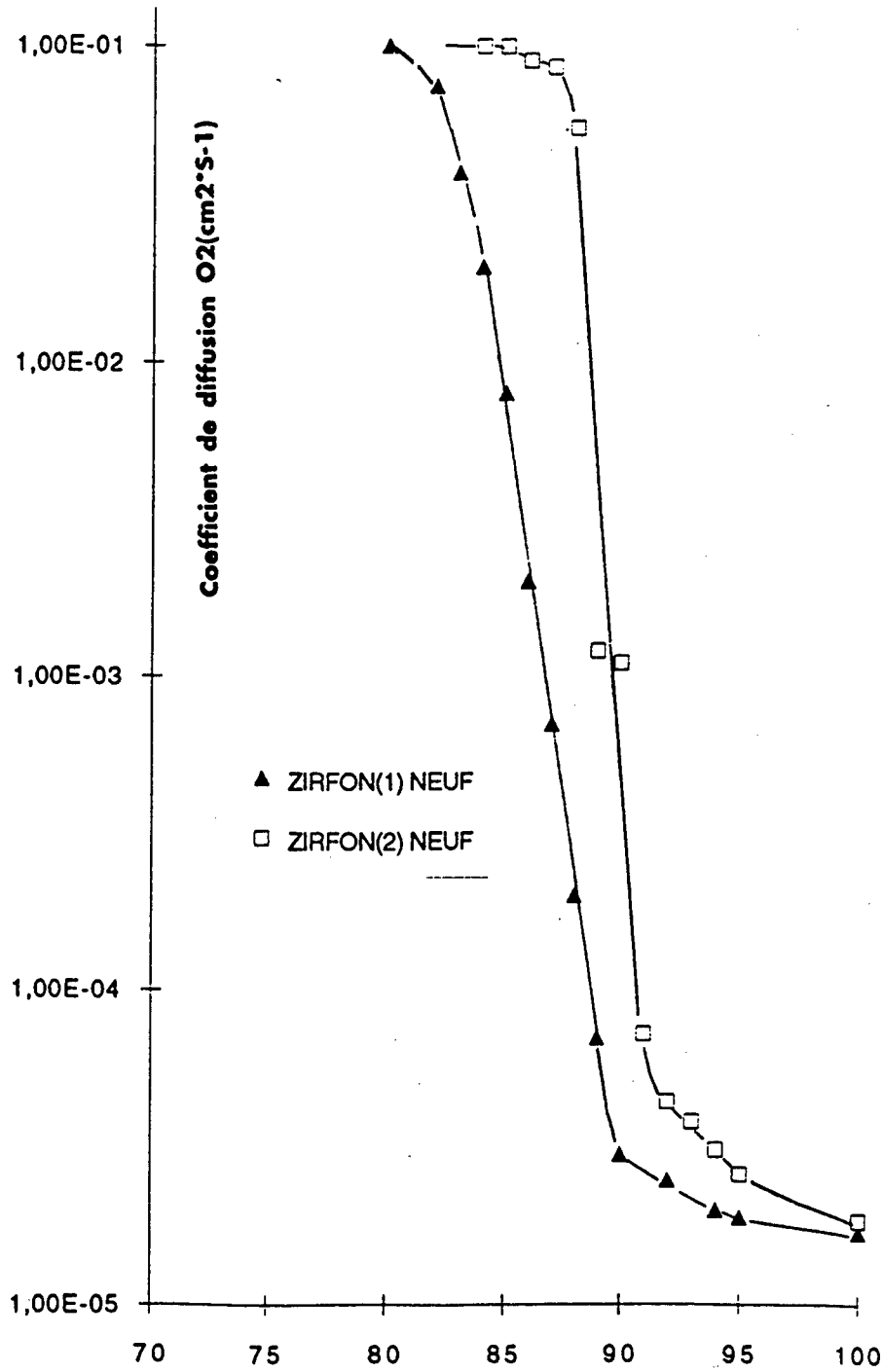

8.1 Z28 ELECTRICAL - CYCLING Cont 'd

- **Among 2 Z28 BP one has done more than 1400 cycles before reaching 0.9V limit**
- **Mid discharge V evolution over time from 1,21V down to 1,13V**
- **C/2 capacity almost identical between BOL and EOL**
- **Second plateau increases at 0.5 V**

ZIRFON 28 BOILER PLATES VOLTAGE EVOLUTION UNDER WEAR OUT CYCLING

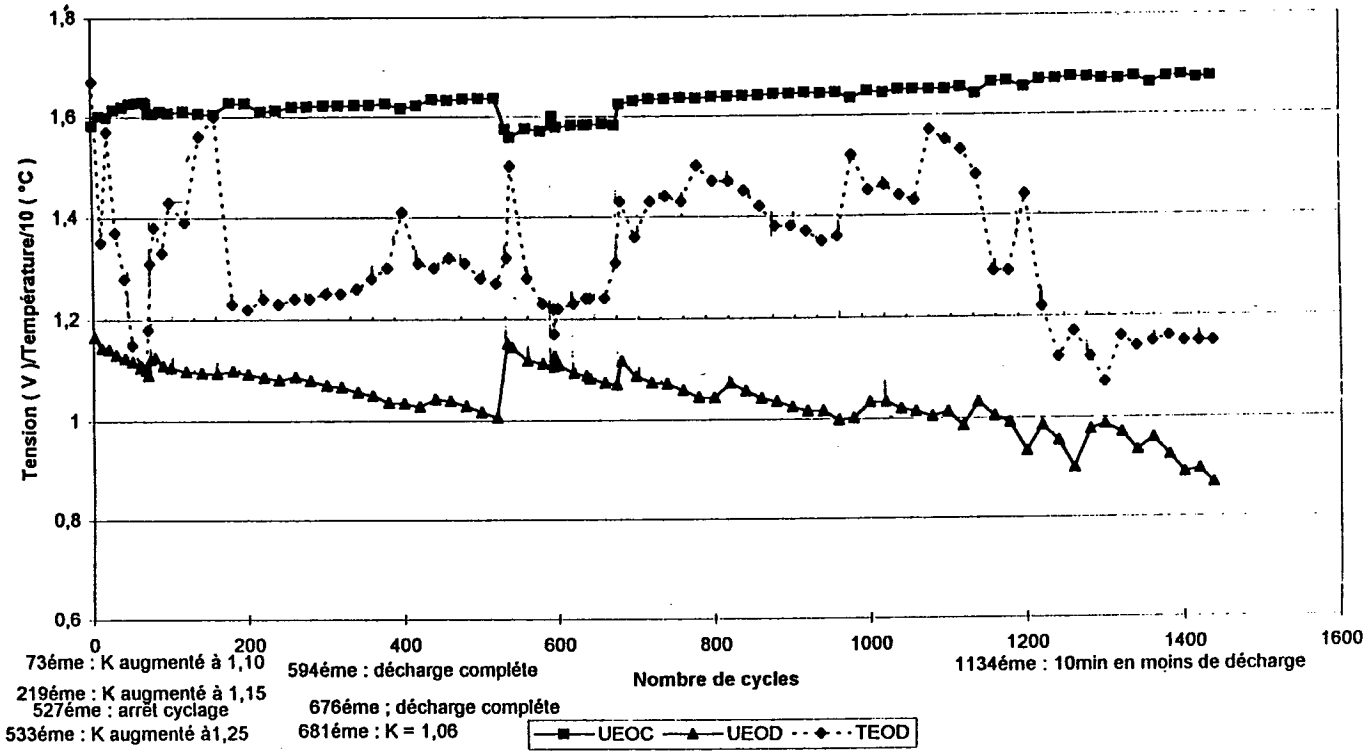

Nasa Aerospace Battery Workshop, October 27-29, 1998

8.2 ZIRFON RESULTS

- **Fresh samples hysteresis with estimate compression threshold at 10Kg/cm*2**
- **Within 25Kg/cm*2 range non linear modulated thickness decrease (18% for Z2 and 36% for Z28)**
- **Fresh Z2 and Z28 compression reduce porosity, retention and resistivity**
- **Z2 aged samples average pore size slihtly changes while porosity decreases, weight too by 4% and drop test reveals a lower wettability**
- **Cycled Z2 resistivity increase correlated with active material transport onto separator material surface with cork effect (2mg/cm*2)**

ZIRFON 28 / ZIRFON 2 COMPRESSION CHARACTERISTICS

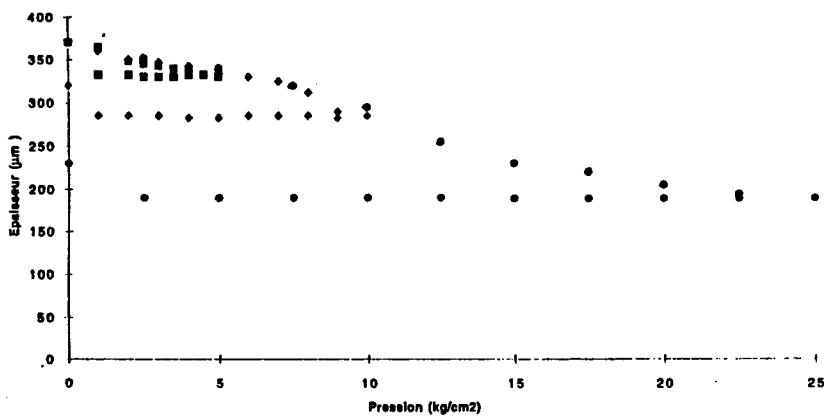

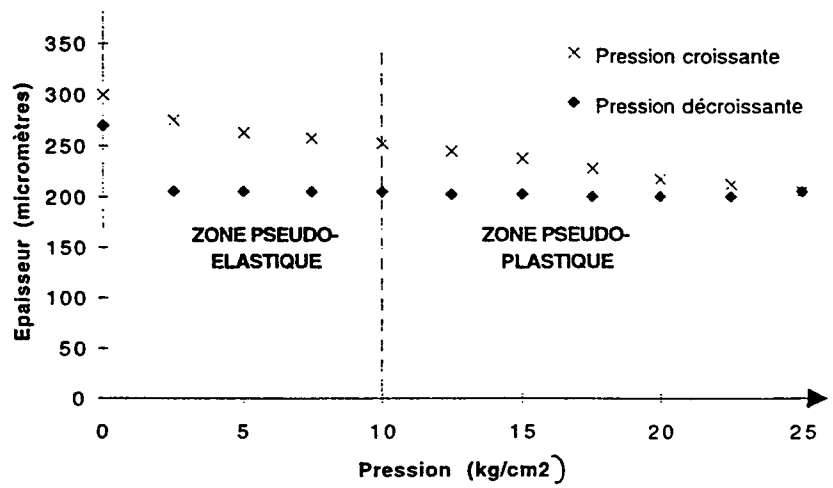

Z28/ Z2 THICKNESS EVOLUTION WITH COMPRESSSION (24h then 12h rest)

Compression (Kg/ cm*2)	5	25
Zirfon 2 fresh Thickness (330 μ)	330 μ (Δ 0%)	270 μ (Δ - 18%)
Zirfon 2 cycled (2320 cycles) Thickness (310 μ)	307 μ (Δ - 1 %)	245 μ (Δ - 19.5 %)
Zirfon 28 fresh Thickness (365 μ)	360 μ (Δ - 1.4 %)	230 μ (Δ - 36 %)

ZIRFON 28 / ZIRFON 2 COMPARISON - RESISTIVITY AND AGEING EFFECTS (mΩ cm*2)

Electrolyte	KOH 26%	KOH 31 %
Fresh Z 2	80	90
Fresh Z2 after compression at 25 Kg / cm*2 24 h and 12h rest	80	90
Z2 cycled 2320 cyles	160	150
Fresh Z 28	70	70
Fresh Z28 after compression	70	70

8.2 ZIRFON RESULTS Cont 'd

- **Z2 material has a bi modal porous spectrum while Z28 has a tri modal repartition: in addition to micro and meso porosity featured by zircone powder Z28 exhibits a macro porosity network**
- **Z28 compression under high yield (25Kg/cm*2) promotes a switch from macro to meso pore size**

8.3 FOAMY POSITIVE ELECTRODES RESULTS

- At BOL Co stabilizes βIII phase inhibiting γIII phase formation
- Highest capacity electrodes exhibit lower average cristallites size
- Gamma phase oxidised material is quantitatively measured in low capacity electrodes and absent in high capacity ones
- This phase seems to be linked with second plateau promoting capacity decrease at 1V and transfer
- Local active material depletion on substrate could explain that
- HNi2O3 phase very minoritary on rear surface of low capacity plates after 1200 cycles
- After 2320 cycles all plates charged or discharged are non symetric with HNi2O3 phase on rear face (other positive side)

POSITIVE CHARGED SAMPLES AFTER 1200 CYCLES 001 X RAY PATTERNS CORRELATION WITH CAPACITY VARIATION

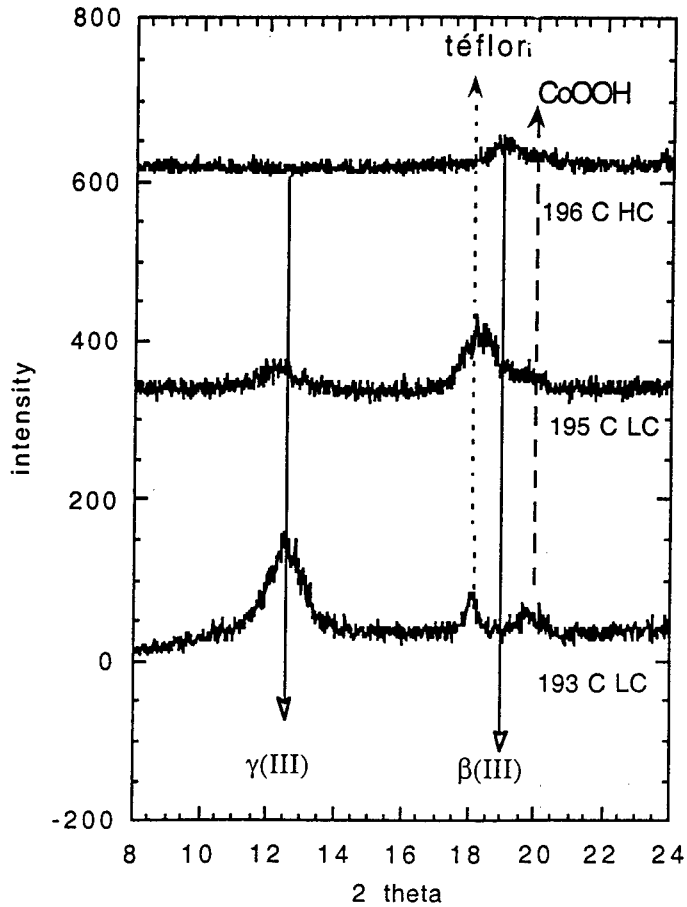

POSITIVE DISCHARGED SAMPLES AFTER 1200 CYCLES AVERAGE CRISTALLITES SIZE

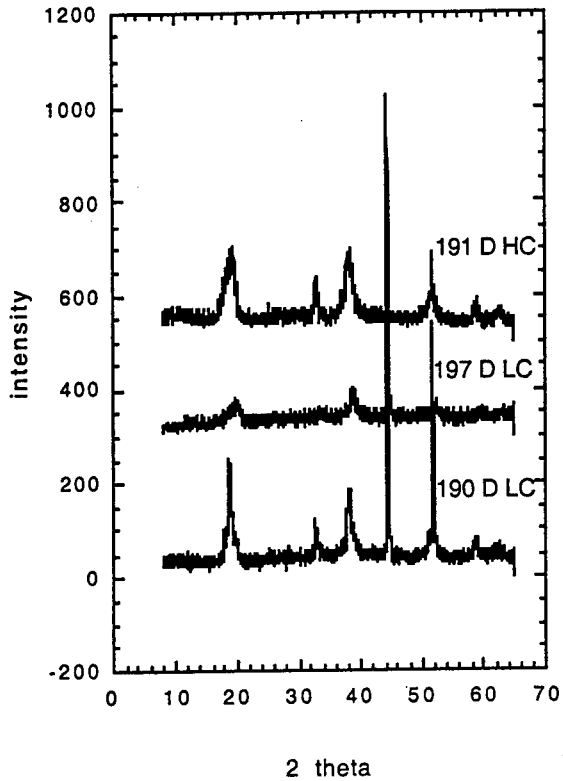

Comparaison des tailles de cristallites dans les états déchargés

Raies hkl	Elec 191- Tc(Å)	Elec 190- Tc(Å)
001Ni	47.575	125.71
001Co	110.10	101.40
100	135.68	182.67
101	59.303	90.583
110	101.76	108.39
111	76.577	91.089

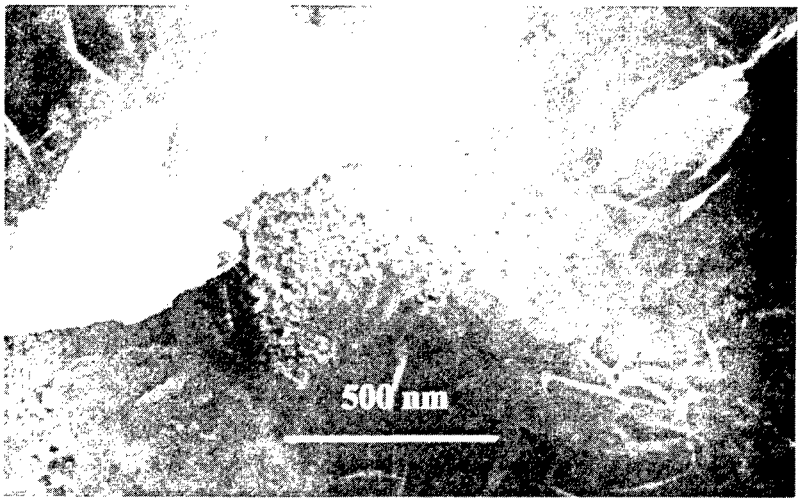

Electrode 196C- 1200 cycles- HC photo196tr2

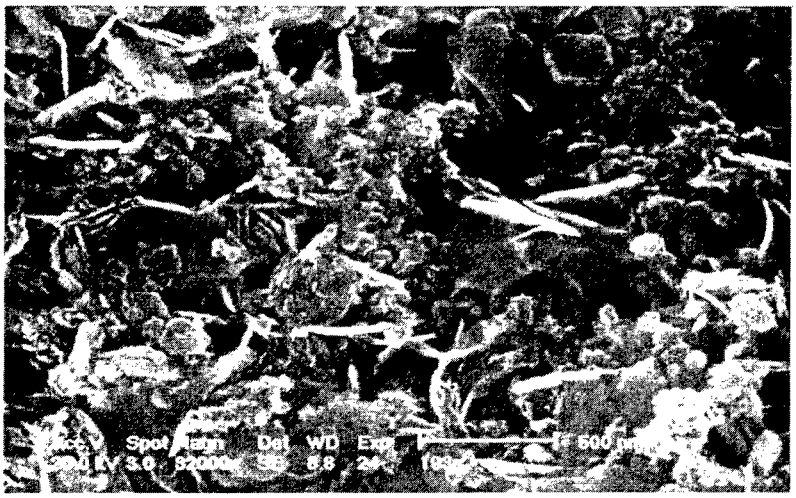

Electrode 193C- 1200 cycles- LC - photo193s1 - texture typique

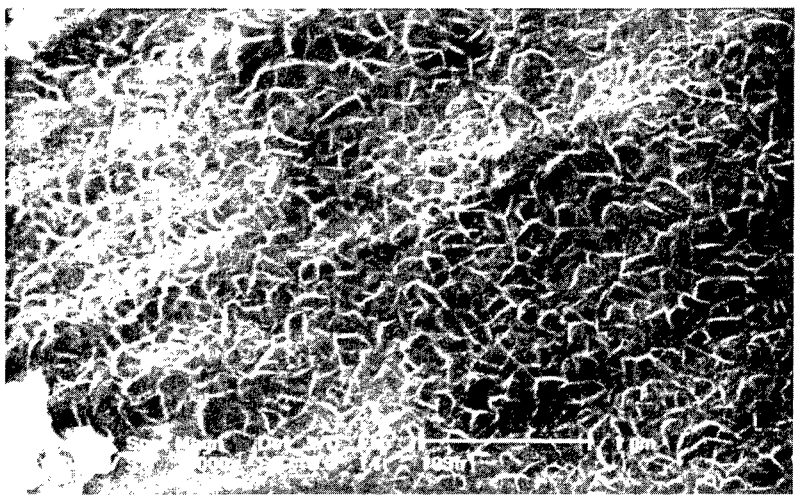

Electrode 193C- 1200 cycles- LC - photo193tr1- texture +rare (γ ?)

Etats chargés, 1200 cycles, à fort grossissement

POSITIVE SURFACE FEG PICTURES DISCHARGED STATE 1200 CYCLES

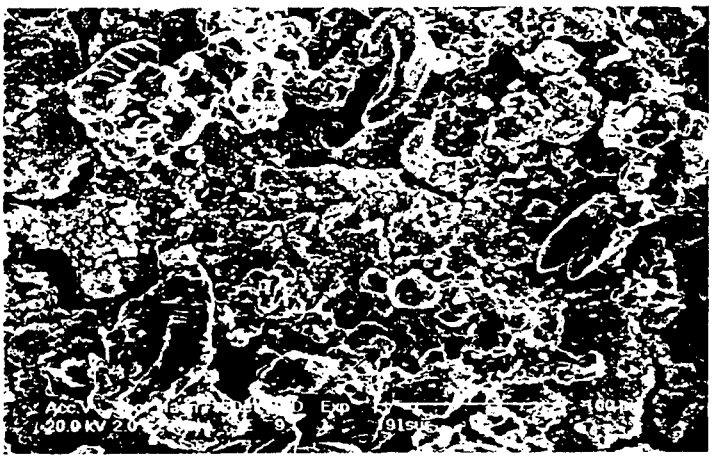

Electrode 191- 1200 cycles- HC photo191sur1

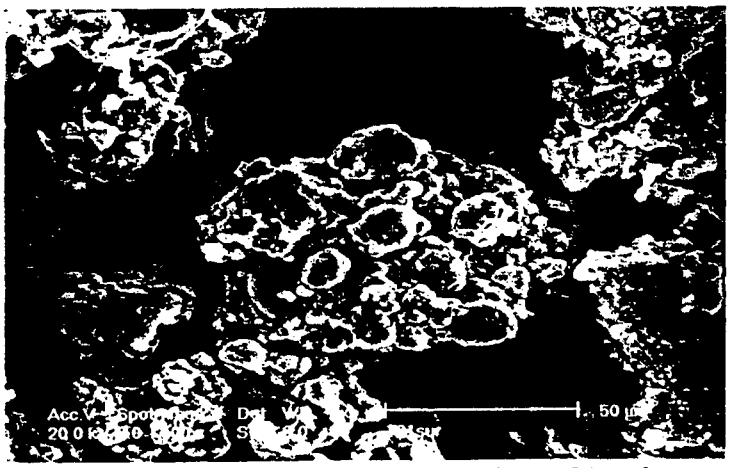

Electrode 191 1200 cycles HC photo191sur3

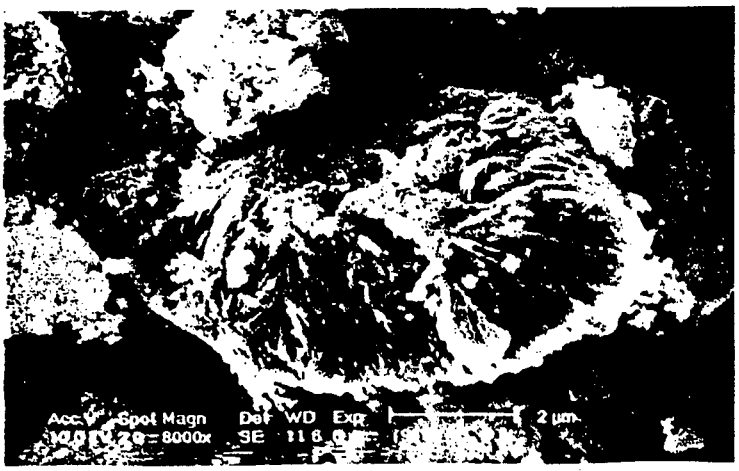

Electrode 191 1200 cycles HC photo191tr

DISCHARGED POSITIVE COLLECTOR INTERFACE 1200 CYCLES CAPACITY CORRELATION

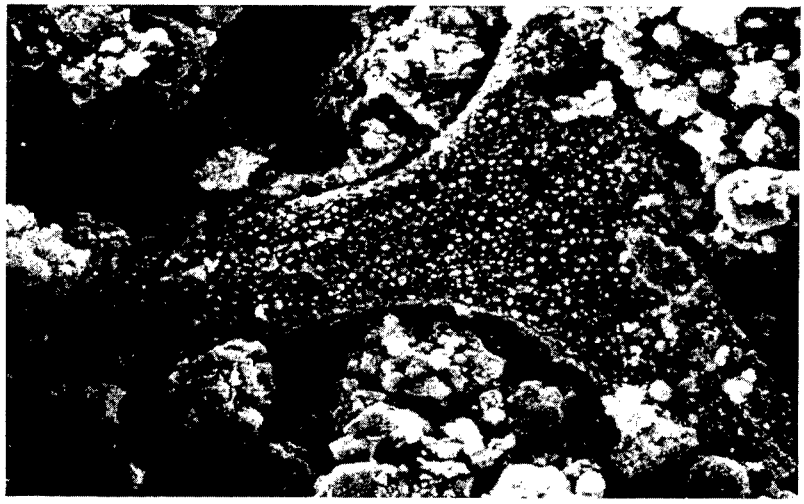

Electrode 190 1200 cycles LC photo190surf
interface de mauvaise qualité

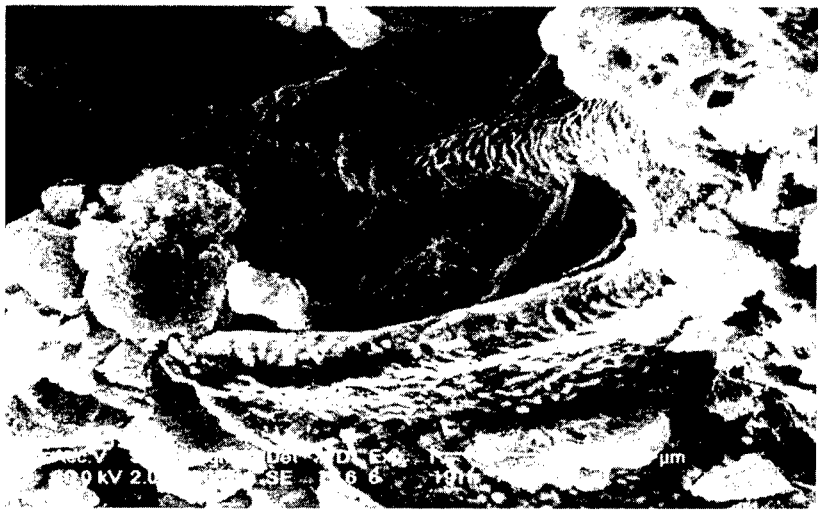

Electrode 191 -1200 cycles HC - photo191tr06-
l'interface matière active/collecteur semble de bonne qualité
(zones dénudées très rares)

8.3 FOAMY POSITIVE ELECTRODES RESULTS Cont 'd

- Spherical shaped Tanaka texture is kept along with cycling
- Platelets with non homogeneous shape and size are typical
- Rear face exhibit dense acicular particles in some area (HNi2O3 ?)
- Small lost of active material and high stability of positives are associated with good EOL electrical data probably due to good charging efficiency and low k factor

POSITIVE CHARGED SAMPLES
X RAY PATTERNS AFTER 2320 CYCLES
HNi2O3 on rear face

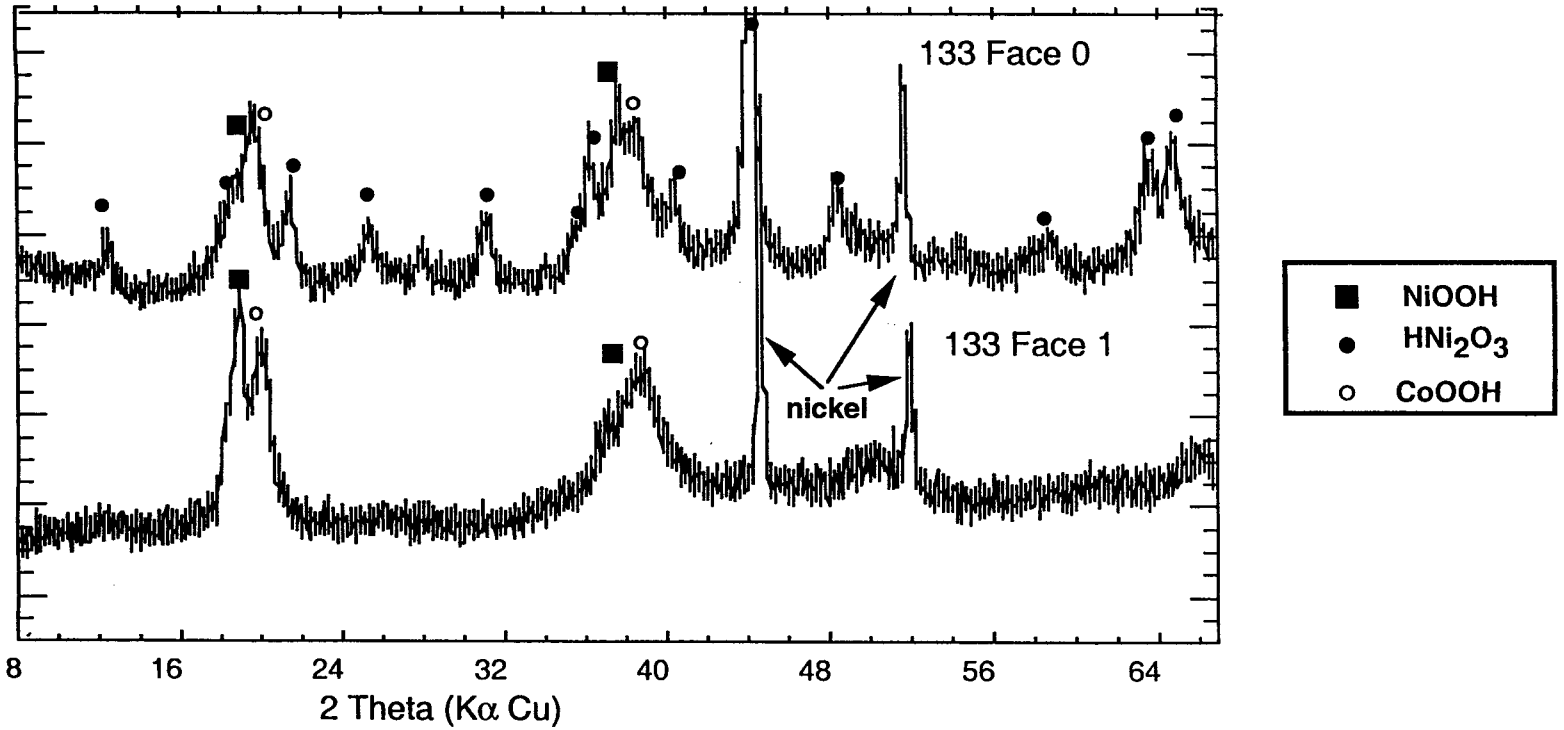

2320 CYCLES POSITIVE SAMPLE
MEDIUM MAGNIFICATION FEG PICTURE

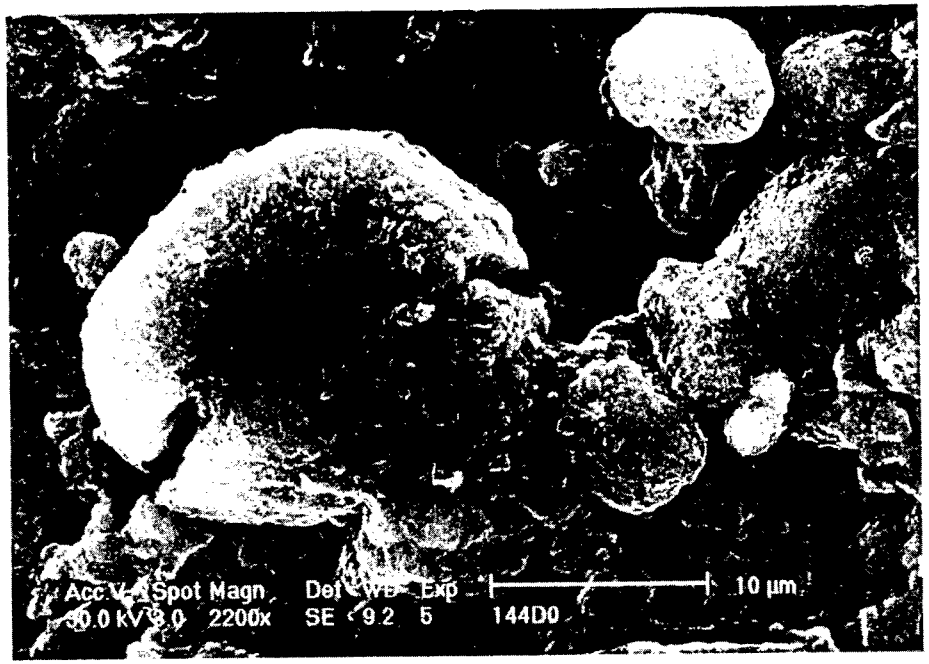

Electrode 144 Découpe D- face 0 - photo5

SURFACE POSITIVE SAMPLE 2320 CYCLES
TYPICAL ACICULAR CRISTALS ON REAR FACE

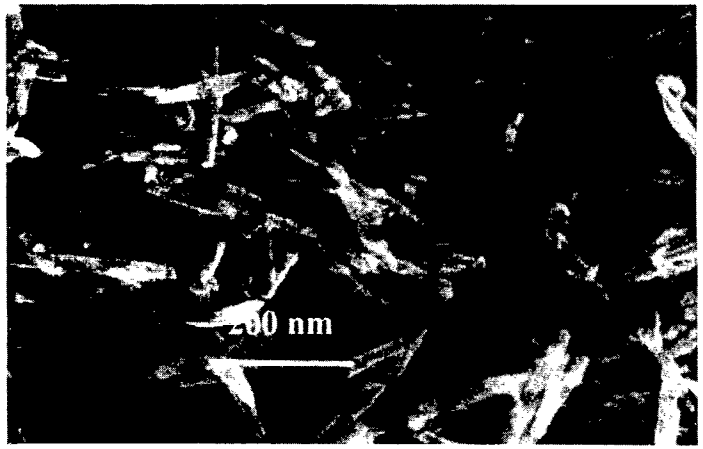

Electrode 144 Découpe A- face 1 - photo 7
Présence de batonnets en grande quantité (phase HNi2O3 ?)

9. DISCUSSION

- ZIRFON 2 material have a plastic behavior because of high stength applied at stack level
- Z2 has a wide elasticity range and recovers partially its thickness
- Continuous compression along 1.5 years of testing has substancially modified internal surface and wettability
- Limited weight loss proves there is no chemical degradation at room temperature
- Lightweight electrode implies light collector with reduced stiffness with a compromise at loading level
- Adjusted design plus appropiate stack compression achieves low swelling goal

9. DISCUSSION CONT 'd

- Positive swelling induces electrolyte transfer from separator to positive through a capillary sucking effect
- Even with a limited KOH amount associated with one layer there were still margins
- Microscopic examination demonstrates that original texture does still exist that survive milling effect due to gas evolution and phase changes
- Excellent efficiency is observed along the cycling with a limited K factor while capacity recovery is still high and voltage decrease low

10. CONCLUSIONS

- DPA activities are helpfull to support BOL/EOL comparison on many functionnal aspects and to characterize ageing
- Main issue of replacing critical components can be satisfactorily adress with innovative tested items
- ESA/VITO development was successfull and Z28 cycling data confirm our long term interest that must lead soon to a further evaluation step
- Total updating of Z2 / Z28 results is awaited soon
- interdisciplinary specialists federation gives a good level of understanding on these new components
- Next step is to perform large capacity cells testing and qualification before to offer the market this evolved design

"Destructive Physical Analysis of Lithium–Ion Cells."

Presented by Nathan "Ned" Isaacs
Co-authored by John Baker, Joseph Bytella, Ken Richardson, and Brian Stein
Mine Safety Appliances Company, Sparks, Maryland

Abstract

The preparation of effective Destructive Physical Analysis (DPA) procedures is an important element of MSA's Li–Ion development program. New methods are needed for analysis of organic components and other materials not being used in Ni–H_2 and Ni–Cd cells. Likewise, physical structures are different, requiring new DPA methods. Several examples of DPA procedures are presented. Data are presented on the DPA of a prototype, prismatic, 15-Ah, Li–ion cell currently under development at MSA. Plate-to-plate resistance buildup, vibration results, and gas sampling data are presented. DPAs were also performed on 1991-vintage, SONY 20500 Li–ion cells and on 1996-vintage, SONY 18650 Li–ion cells. Anode and cathode materials in both cell sets are compared. The anodes and cathodes were studied (using ICP) for lithium content in both charged and discharged states. Other analytical studies were conducted using SEM–EDS, GC, GC–MS, TGA, TGA–MS, DSC, and laser light-scattering particle analysis. FTIR was used to analyze residues on current collector foils.

Slide 2: Outline of Presentation

During this presentation, I will present: an MSA, preliminary DPA procedure, a DPA requirement from a NASA statement of work for a Li–ion cell, and a TBTC DPA protocol for an 18650-type, wound, Li–ion cell.

Data are presented on the DPA of a prototype, prismatic, 15-Ah, Li–Ion cell currently under development at MSA. Plate-to-plate resistance buildup, vibration results, and gas sampling data are presented.

DPAs were also performed on 1991-vintage, SONY 20500 Li–ion cells and on 1996-vintage, SONY 18650 Li–ion cells. Anode and cathode materials in both cell sets are compared.

Anodes and cathodes were studied (using ICP) for lithium content in both charged and discharged states. Other analytical studies were conducted using SEM–EDS, GC, GC–MS, TGA, TGA–MS, DSC, and laser light-scattering particle analysis. FTIR was used to analyze residues on current collector foils.

I will finish this presentation with a summary and some conclusions.

Slide 3: MSA Preliminary Li–Ion Metal-cell DPA Procedure

A preliminary procedure for Li–Ion, metal-cell destructive physical analyses is shown on the next two overheads. This slide covers the general areas of:

- Safety
- Report Format
- Cell Measurements
- Cell Condition
- Cell Disassembly
- Visual Observations
- Hardware Preparation

The cell disassembly steps should be performed in a glove box in a dry room.

Slide 4: MSA DPA Procedure Continued

On this slide, there is a continuation of the hardware-preparation steps. Also shown are:

- Physical Measurements
- Chemical Analysis
- Other Analysis

It is important to mention that many of the findings of a DPA have less meaning without a thorough "before" analysis. Therefore, it is recommended that a "before" analysis be performed prior to, or in concert with, the DPA.

Also note that there are several analytical procedures that need to be prepared. These are not trivial procedures. They will take time and the commitment of an experienced analytical chemist.

Slide 5: NASA DPA Requirement (from a Statement of Work)

These requirements were taken from a Statement of Work for a Li–ion cell. However, many of the steps are carried over from aqueous-cell DPAs. For example, capacity determination in electrolyte and separator absorbency may not be appropriate for Li–ion cells.

Slide 6: Tracor Battery Technology Center DPA Protocol

This DPA Protocol was prepared by P. H. Regato, E. Kebede, J. C. Massingill, and Dr. N. Margalit of TBTC for DPA of wound Li–Ion cells.

The protocol shown is a composite of four separate blocks. Blocks two through four are intended to be performed in a glove box.

Slide 7: TBTC DPA Block 1

Block 1 first deals with cell-identification information. Preliminary cell examinations and non-destructive tests are performed. Then, leads are examined and tested. Finally, the labels are removed and the bare cell is examined.

Slide 8: TBTC DPA Block 2

The disassembly steps in this block are intended to be performed in a glove box. Steps are shown for the positive plate, separator, various insulators, and the header.

Slide 9: TBTC DPA Block 3

These disassembly steps should also be performed in a glove box. Shown on this block are negative plate, cell can, tabs, connectors and miscellaneous items. The binder analysis was inadvertently omitted from the negative-plate steps.

Slide 10: TBTC DPA Block 4

These disassembly steps should also be performed in a glove box. The safety features are examined, and the electrolyte is analyzed.

Slide 11: 15-Ah Prototype Cell

MSA's 15-Ah prototype cell was assembled in the 50-Ah cell case. There are 40 positive and 39 negative electrodes, plus two negative half-electrodes. The electrodes were bolted to the terminals since welding procedures had not been developed at the time the cells were built.

Slide 12: 15-Ah Prototype Cell—Electrode Stack Assembly

The electrode stacks are bolted to the underside of the terminal posts as shown. One-half of the electrode tabs are connected to each side of the individual terminals.

Slide 13: 15-Ah Prototype Cell—Cell Stack Assembly

The prototype cell has two aluminum spacers, one on each side of the cell stack. Also shown are the terminal attachments.

Slide 14: LEO 15-Ah Prototype—Prototype Cycling

Shortly after cycling began on the 15-Ah cell, the specific capacity dropped to 60 mAh/g of Li_xCoO_2. Analyses were initiated to determine the causes for the capacity fade.

Slide 15: LEO 15-Ah Prototype—Tab Resistance Data

Tab resistance data showed an impedance buildup between the electrodes in the stack. For the copper negatives, impedance and resistance for tab 1, the innermost tab, were 1.8 and 1.5 ohms, respectively. The buildup for the whole stack was 4.3 and 3.5 ohms respectively. When the individual tabs were welded together, the stack impedance and resistance were only 1.2 and 1.7 ohms.

The resistance buildup was worse for the aluminum tabs on the positive electrodes. Impedance and resistance rose from 4 and 5 to 52 and 56 ohms, respectively. When the electrodes were welded together, the stack impedance and resistance were 4.1 and 4.0 ohms.

Slide 16: 15-Ah Prototype—Vibration Testing

The 15-Ah cell was vibration tested in the fully charged condition. The three axes are illustrated on the cell schematic.

Slide 17: 15-Ah Prototype—Vibration Test Protocol

Random vibration tests (in Y, X, and Z axes) were performed at 0.01, 0.04, and 0.08 G^2/Hz. Open circuit voltage, AC resistance, and Electronic Impedance Spectroscopy (EIS) readings were taken before and after each vibration sequence. During vibration, the cell was under a 1.3-ohm resistive load.

The vibration was equivalent to acceleration levels of 3.79, 7.57, and 10.71 g-rms. For future tests, the vibration acceleration level will be increased to 26.9 g-rms.

Slide 18: 15-Ah Prototype—Vibration (0.08 G^2/Hz, X-axis)

There was no resonance associated with the cell. However, at 0.08 G^2/Hz, there was some ringing of the accelerometer that was attributed to the vibration fixture.

Slide 19: 15-Ah Prototype Vibration—X-ray & Electrical

The X-rays taken after the vibration sequences showed no changes in the cell. Both open circuit voltage and AC resistance showed slight declines during the test.

Slide 20: 15-Ah Prototype Vibration—EIS Data

The results of the EIS scans are pictured on this slide. There was a lowering of Z' between the first and second semi-circle from 0.063 to 0.050 at 0.04 G^2/Hz. However, Z' remained unchanged after vibrations above that level.

Slide 21: 15-Ah Prototype—Gas Sampling Experiment

Headspace gases were sampled from cells after the second full charge. The gases were collected in stainless steel containers. They were analyzed on an HP 5890 gas chromatograph equipped with a 5971 mass detector.

The data obtained were only qualitative. This is because calibration curves had not been developed for standard gases, and volume and pressures had not been measured for the samples. During the determinations, there was column leakage as evidenced by an abundance of CO_2 and H_2O in the Total Ion Chromatographs (TIC).

Slide 22: 15-Ah Prototype—Typical GC–MS TIC

This is a typical TIC from one of the GC–MS runs.

Slide 23: 15-Ah Prototype—GC–MS Results

The following gases were detected from the three cells that were sampled.

- Cell 1: CO_2, H_2O, O_2, $H_2C{=}CH_2$, C_2H_6 and $H_3CHC{=}CH_2$
- Cell 2a: CO_2, H_2O, N_2, O_2, $H_2C{=}CH_2$ and $H_3CHC{=}CH_2$
- Cell 2b: CO_2, H_2O, O_2, $H_2C{=}CH_2$, $H_3CHC{=}CH_2$, and $(C_2H_5O)_2CO$ (i.e., DEC, which is one of the electrolyte solvents.)

These gases were in general agreement with the headspace gases discussed in a poster by Dr. Kazuma Kumai, et al, at the 9th International Meeting on Lithium Batteries in Edinburgh, Scotland last summer.

Slide 24: 15-Ah Prototype—GC–MS Results Comparison

This slide shows the headspace gases found by Kumai, et al. Their tests used an electrolyte of 1 M $LiPF_6$ dissolved in a mixture of PC, EMC, DEC, and DMC. The MSA cells contained 1.0 M $LiPF_6$ dissolved in PC:EC:DEC 1:1:2.

The MSA results are compared to the Kumai results. It is interesting to note that most of the hydrocarbons found in the MSA cells are unsaturated.

Slide 25: 15-Ah Prototype—Kumai Gas-Generation Model

This slide contains overcharge and overdischarge profiles for Li–ion cells and a chart that outlines Kumai's gas-generation model.

Slide 26: DPA Studies on SONY Li–ion Cells

DPAs were performed on 1991-vintage, 20500 cells and on 1996-vintage, 18650 cells. Anodes and cathodes were studied (using ICP) in both charged and discharged states. The ratio of $M_{Li(anode + cathode)}/M_{Co}$ ranged from 1.130 to 1.182 for the 1991 cells and 1.003 to 1.088 for the 1996 cells.

Gravimetric analysis And Thermal Gravimetric Analysis (TGA) were also performed, and data are shown. SEM comparison of anodes and cathodes of SONY and MSA cells are presented.

Slide 27: DPA Studies on SONY Cells—Analysis Steps

This slide gives the DPA procedural steps and the reasons for these steps.

Slide 28: ICP Analysis of 1991-Vintage, SONY 20500 Cells

These cells were analyzed while in the charged state. The distribution of lithium between the positive and negative electrodes was determined. The ratio of lithium in the anode and cathode to cobalt ranged from 1.130 to 1.182.

Slide 29: ICP Analysis of 1996-Vintage, SONY 18650 Cells

Some of these cells were discharged and others charged when they were analyzed. Again, the distribution of lithium between the positive and negative electrodes was determined. The ratio of lithium in the anode and cathode to cobalt ranged from 1.003 to 1.088. One of the cells was aged (after being charged) for a year at room temperature.

Slide 30: Thermal Gravimetric Analysis (TGA) of 1991-Vintage, 20500 Cells

This slide tabulates gravimetric and TGA studies on 20500 cells.

Slide 31: Thermal Gravimetric Analysis (TGA) of 1996-Vintage, 18650 Cells

This slide tabulates gravimetric and TGA studies on 18650 cells.

Slide 32: SEM Comparison of SONY and MSA Electrodes

This slide compares SEM photographs of positive and negative electrodes from SONY and MSA Cells. The magnifications of the photographs have been adjusted so that they are at an equivalent scale.

SONY's hard carbon negatives are significantly more planar that the MCMB negatives used by MSA. However, the appearance of the positive electrodes is similar.

Slide 33: Summary and Conclusions

The Li–ion DPA procedures differ from those used for Ni–Cd or Ni–H_2. Dry rooms or glove boxes are needed for many of the steps.

Resistance buildup is an important issue in Li–ion cells, which have many very thin aluminum and copper electrodes, connected in parallel.

Preliminary vibration results are encouraging.

Models exist for the prediction of headspace gases. However, the analysis of such gases requires very rigorous procedures.

A procedure exists for ICP and TGA of electrodes.

SEM is useful for electrode comparisons.

Acknowledgements

Although I am presenting this paper, all of the physical work was performed by my co-authors. I want to acknowledge the help of Dr. Pinakin Shah, who is the Principal Investigator of MSA's Li–Ion program, and Dr. Cheryl Matthias, who manages MSA's Analytical Chemistry Staff. In addition, I want to thank "Toti" Recato and Dr. Nehemiah Margalit of Tracor Battery Technology Center for their contributions to this paper.

Destructive Physical Analysis (DPA) of Lithium–Ion Cells

Presented at the 1998
NASA Aerospace Battery Workshop
Huntsville, AL
October 28, 1998

Presented by Nathan "Ned" Isaacs
Co-authored by John Baker, Joseph Bytella,
Ken Richardson, and Brian Stein

Mine Safety Appliances Company
38 Loveton Circle
Sparks, MD 21152
(410) 472-7700

Outline of Presentation

- Presentation of 3 DPA Guidelines or Procedures
  - MSA Preliminary Procedure
  - NASA, from Statement of Work for Li–Ion Cell
  - Tracor Battery Technology Center, Rockville, MD
- Physical Findings on a 15-Ah Prismatic Prototype Cell
  - Plate-to-plate Resistance Buildup
  - Vibration Results
  - Gas Sampling Data
- DPA Results on 1991- and 1996-vintage SONY Li–Ion Cells
- Anode and Cathode Studies using Various Analytical Procedures
- Summary and Conclusions

Mine Safety Appliances Company
38 Loveton Circle • Sparks, MD 21152 • (410) 472-7700

MSA Preliminary Li–Ion Metal-cell DPA Procedure

1. General Safety

1.1. Sections 3 through 5 should be conducted under a hood in the dry room.
1.2. Rubber gloves and lab coat should be worn at all times.

2. Report Format

2.1. The report should follow the outline per form DPA 002 (Li–Ion DPA Format).

3. Cell Measurements

3.1. Record the force required to return the broad face to a flat condition.
3.2. Perform EIS, OCV, weight, dimensions, AC impedance measurements and visual observations.

4. Cell Condition

4.1. Complete a summary description of the previous electrical cycling of the cell. Attach reference data if applicable.
4.2. The cell shall be fully discharged to 2.75 volts.

5. Cell Disassembly

(Note: Even in a dry room, the use of a glove box is an important consideration.)

5.1. Cut open fill tube and drain all electrolyte into a clean and dry 250 mL beaker.
5.2. Record the weight of the drained electrolyte.
5.3. Collect a 30 mL sample in a clean and dry 30 mL Teflon bottle for chemical analysis.
5.4. Cap fill tube.
5.5. Submerge cell in liquid nitrogen for 2 hours.
5.6. With cell in a vice, use Dremel tool to cut the case on all four faces just below the cover weld bead. Make an additional two cuts along the full length of the case sides.
5.7. Remove the cover and cell stack from the case and make visual observations.
5.8. Cut the comb/tab connections.
5.9. Remove one electrode at a time and make visual observations.
5.10. Remove the separators from the negative electrodes.

6. Visual Observations

6.1. Look for any unusual items on all of the component parts. Inspect the weld joints at 10X magnification. Record pertinent information on form DPA 001.

7. Hardware Preparation

7.1. Weigh and measure each of the electrodes in the step 7.2. Measure the thickness at the four corners and the center plus the length and width.

Mine Safety Appliances Company
38 Loveton Circle • Sparks, MD 21152 • (410) 472-7700

October 28, 1998

MSA DPA Procedure Continued

7.2. Clean the following parts in by agitating in glass jar filled with DEC. Repeat 3 times.
- 7.2.1. The two outside positive electrodes on each broad face
- 7.2.2. The two middle positive electrodes
- 7.2.3. The two outside negative electrodes on each broad face not including the very outside ones
- 7.2.4. The two middle negative electrodes.
- 7.2.5. The six separators associated with the above negative electrodes.

7.3. Air dry for 8 hours minimum.

7.4. Oven dry the electrodes at 100 degrees C for 8 hours minimum.

8. Physical Measurements

8.1. Weigh and measure each of the electrodes cleaned in Step 7.2 in accordance with Step 7.1.

9. Chemical Analysis

9.1. Electrolyte
- 9.1.1. HF per QCIP TBD
- 9.1.2. Moisture per QCIP TBD
- 9.1.3. Cobalt per QCIP TBD
- 9.1.4. Copper per QCIP TBD
- 9.1.5. Aluminum per QCIP TBD

9.2. Positive Electrode
- 9.2.1. Lithium per QCIP TBD
- 9.2.2. Cobalt per QCIP TBD
- 9.2.3. Copper per QCIP TBD
- 9.2.4. Aluminum per QCIP TBD

9.3. Negative Electrode
- 9.3.1. Lithium per QCIP TBD
- 9.3.2. Copper per QCIP TBD
- 9.3.3. Aluminum per QCIP TBD

9.4 Head Space Gas Analysis

10. Other Analysis

10.1. Separator
- 10.1.1. SEM at 30,000 X

10.2. Electrodes
- 10.2.1. SEM at 1,000 X (45 degree tilt)

NASA DPA Requirement (from a Statement of Work)

- A tear-down analysis of cells shall be performed on any failed cell to explain anomalous behavior such as suppressed voltage, low capacity, bulging and leakage.
- The cell vendor shall prepare a DPA procedure.
- The DPA shall be performed in a dry room due to the sensitivity of the components to moisture and air.
- The procedure shall consists of the following steps at minimum:
  - Physical measurements, mass and leakage
  - Electrochemical capacity and self-discharge
  - Cell case puncture and gas collection in a glove box and gas analysis
  - Cell dissection and examination of the stack
  - Examination of the cell can for corrosion
  - Examination of the terminal feedthru
  - Extraction of the electrolyte from the stack
  - Analysis of the electrolyte for the components and impurities such as Cu, Co, Ni, and Al
  - Infrared spectra of the electrolyte to determine oxidation/reduction and polymerization
  - Stack disassembly and examination of the anodes, cathodes and the separator
  - Capacity determination of positive and negative plate in EC/DMC/LiPF6 electrolyte
  - Chemical analysis of the positive and negative plates
  - Calculation of theoretical capacity and capacity balance
  - Analysis of Al grid and Cu grid for corrosion
  - Absorbency of the separator
  - Tensile strength of the separator
  - Analysis of Li dendrites in the separator
- The DPA shall be extended to include special testing using EXAF for trace metals, SEM analysis of damaged electrodes and X-ray diffraction of the active material under extraordinary situations such as capacity fade and low voltage.

Mine Safety Appliances Company
38 Loveton Circle • Sparks, MD 21152 • (410) 472-7700

Tracor Battery Technology Center DPA Protocol

- This DPA Protocol was prepared by P. H. Recato, E. Kebede, J. C. Massingill, and Dr. N. Margalit of TBTC for DPA of wound Li–Ion cells.

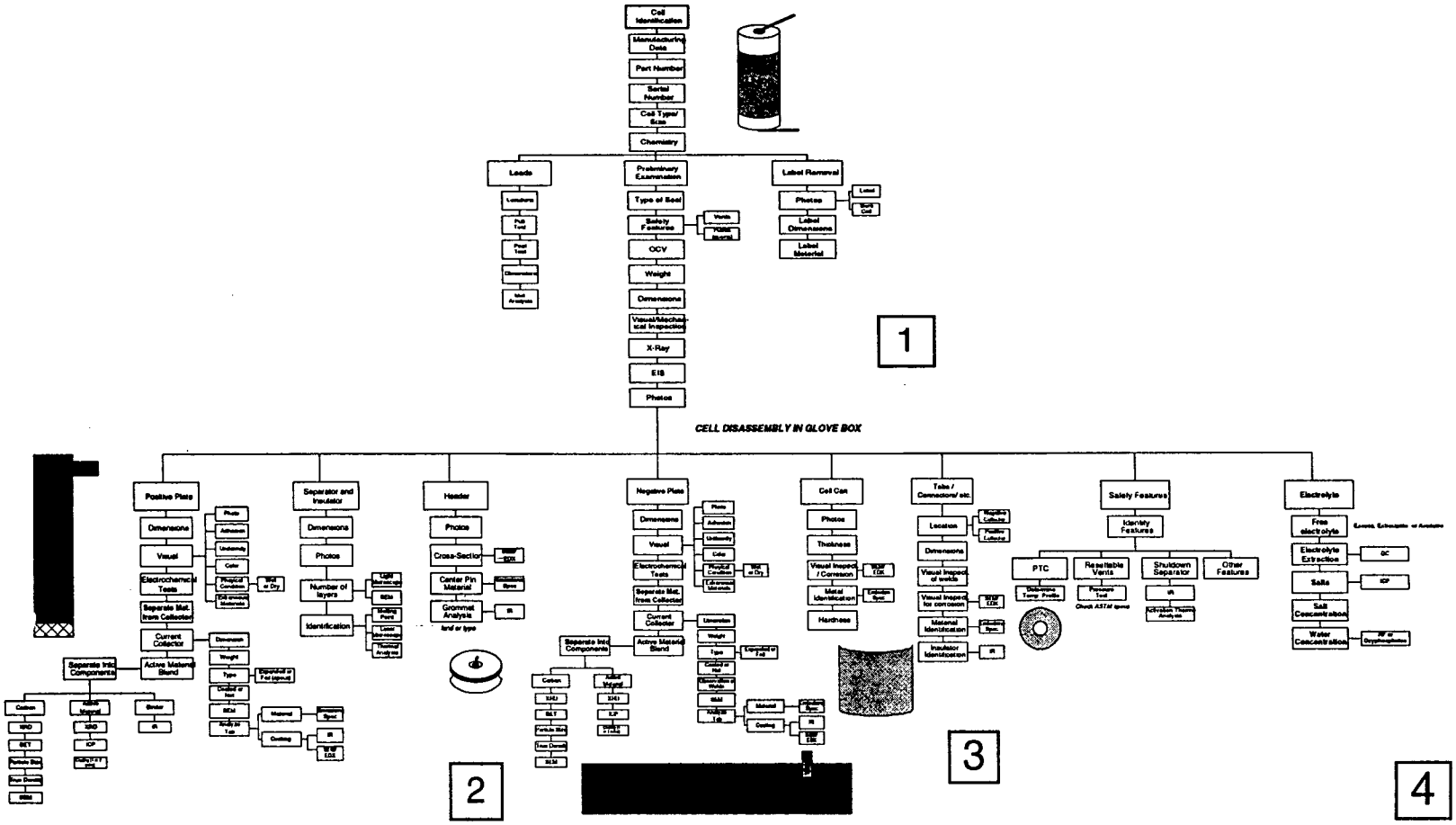

Mine Safety Appliances Company
38 Loveton Circle • Sparks, MD 21152 • (410) 472-7700

October 28, 1998

TBTC DPA Block 1

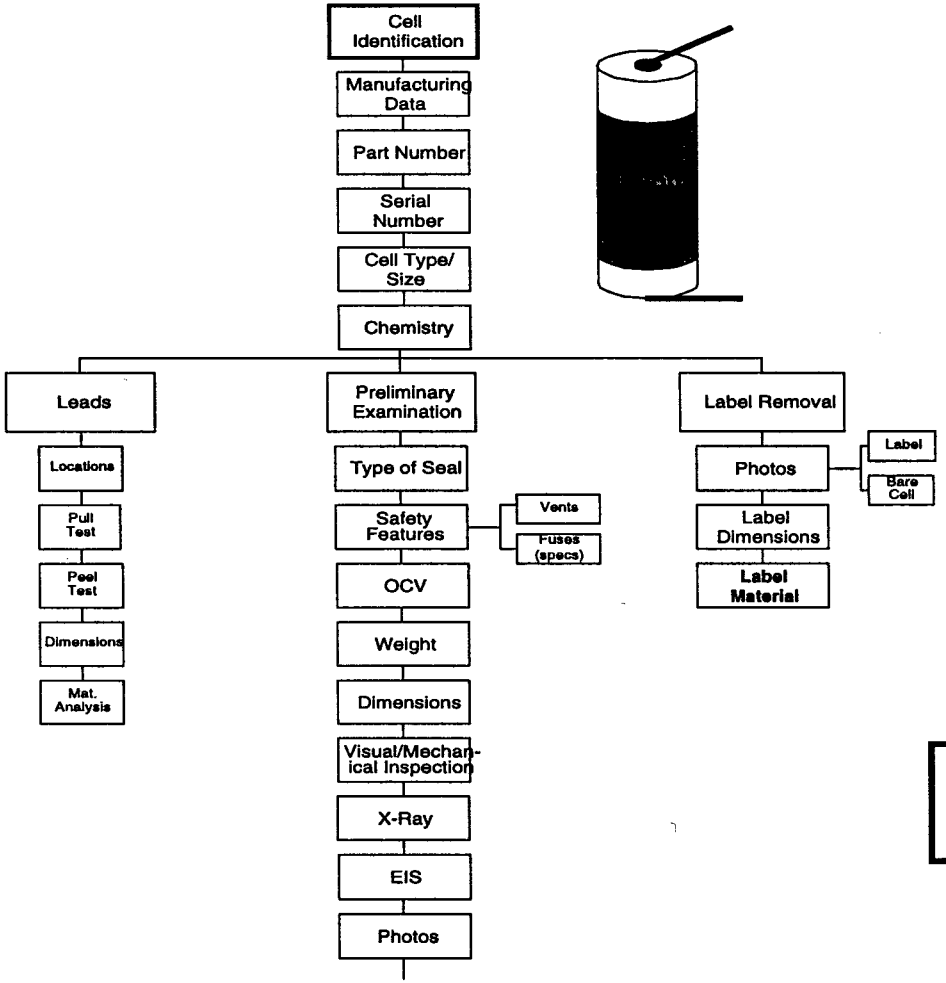

1

Mine Safety Appliances Company
38 Loveton Circle • Sparks, MD 21152 • (410) 472-7700

October 28, 1998

TBTC DPA Block 2

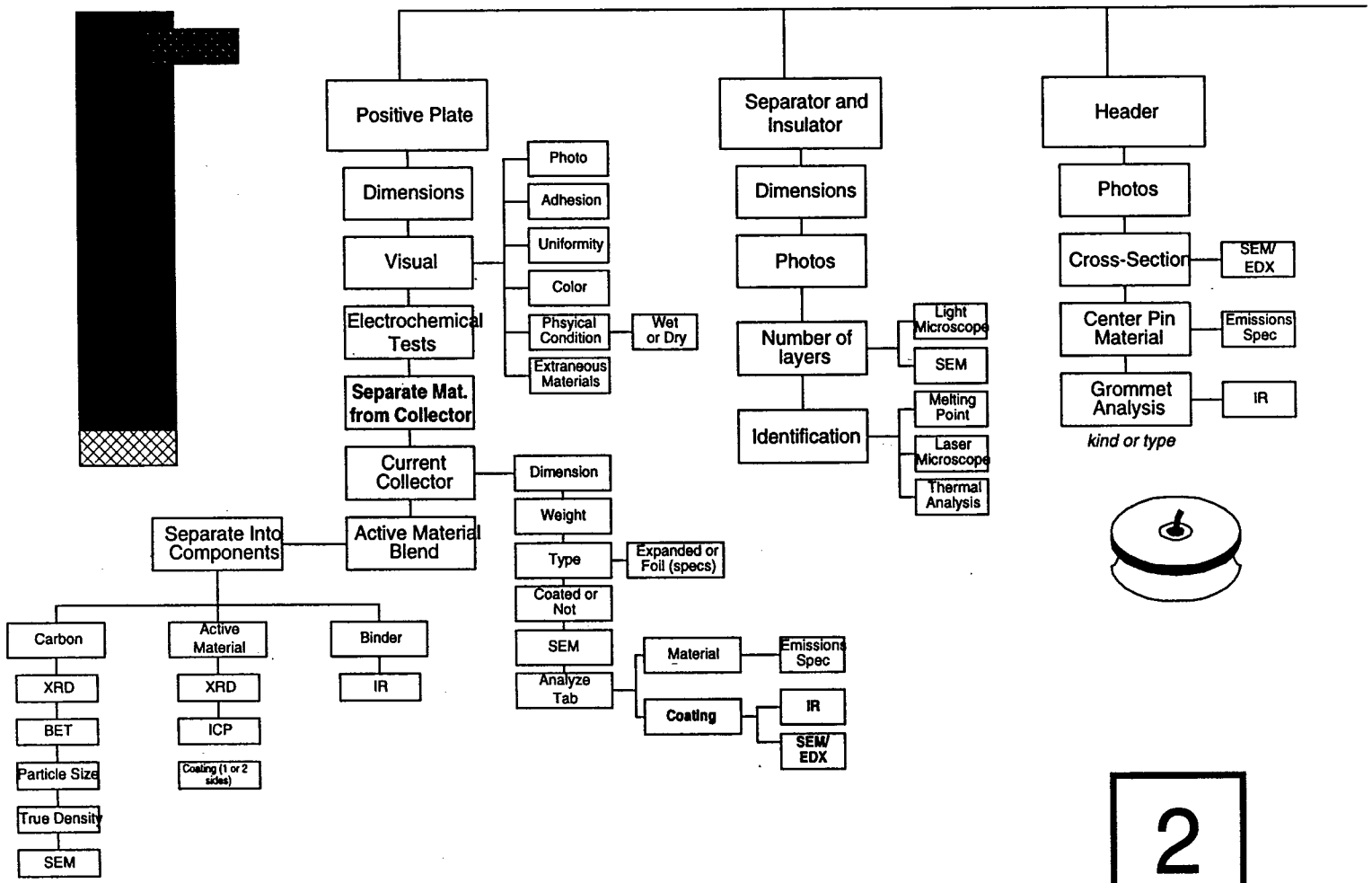

Mine Safety Appliances Company
38 Loveton Circle • Sparks, MD 21152 • (410) 472-7700

TBTC DPA Block 3

CELL DISASSEMBLY IN GLOVE BOX

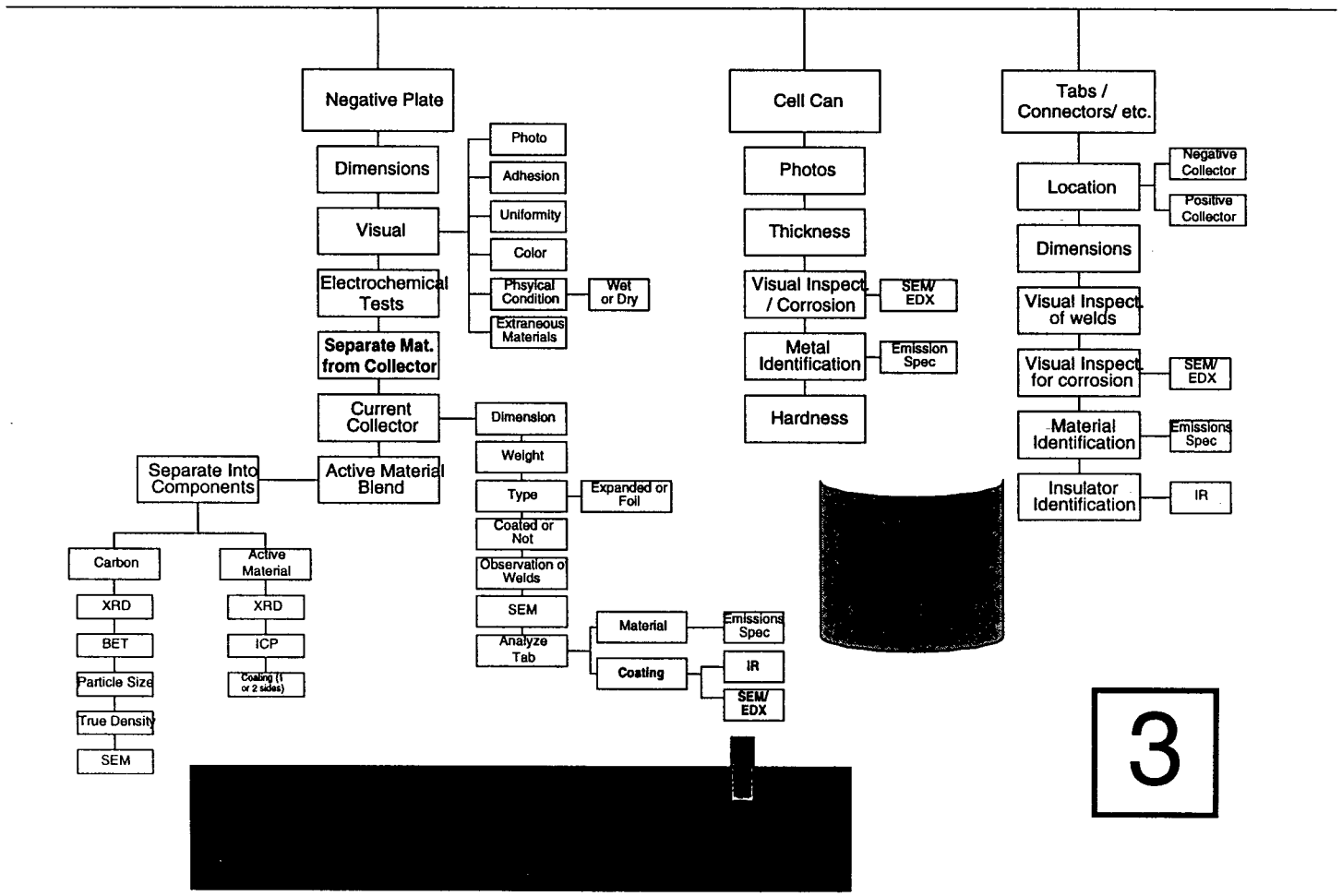

Mine Safety Appliances Company
38 Loveton Circle • Sparks, MD 21152 • (410) 472-7700

October 28, 1998

TBTC DPA Block 4

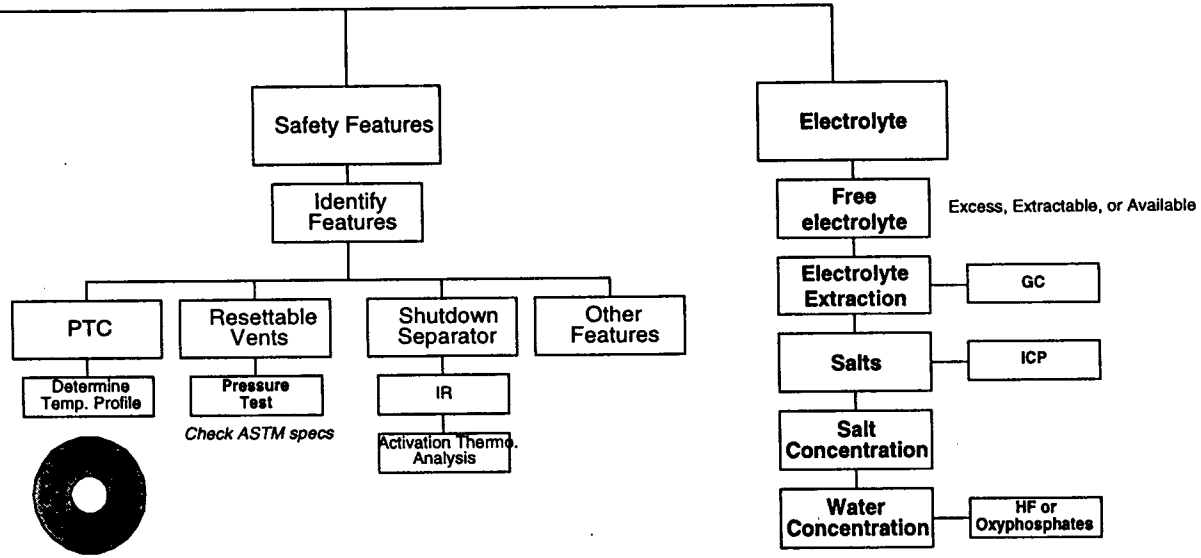

4

Mine Safety Appliances Company
38 Loveton Circle • Sparks, MD 21152 • (410) 472-7700

October 28, 1998

15-Ah Prototype Cell

- Objectives
  - Develop Assembly Processes
  - Baseline for (3) LM 1 Cells
- Design Summary
  - Enclosed in 50 Ah Hardware
  - 40 Positive Electrode
  - 39 Negative Electrodes
  - 2 One-half Negative Electrodes
  - Bagged Negative Electrodes
  - 2 Aluminum Spacers
  - Bolted Configuration
  - Tefzel Insulators
  - Lithium Reference Electrode

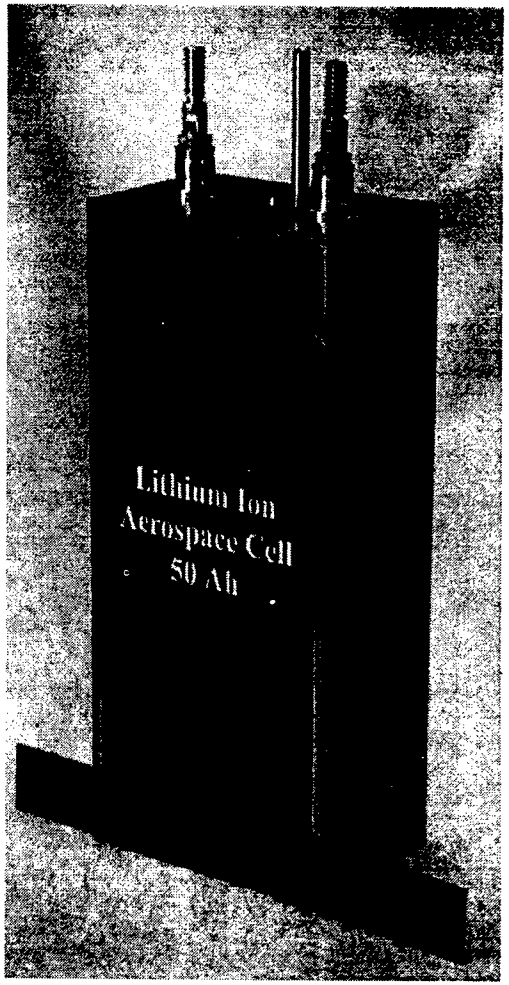

Mine Safety Appliances Company
38 Loveton Circle • Sparks, MD 21152 • (410) 472-7700

15-Ah Prototype Cell — Electrode Stack Assembly

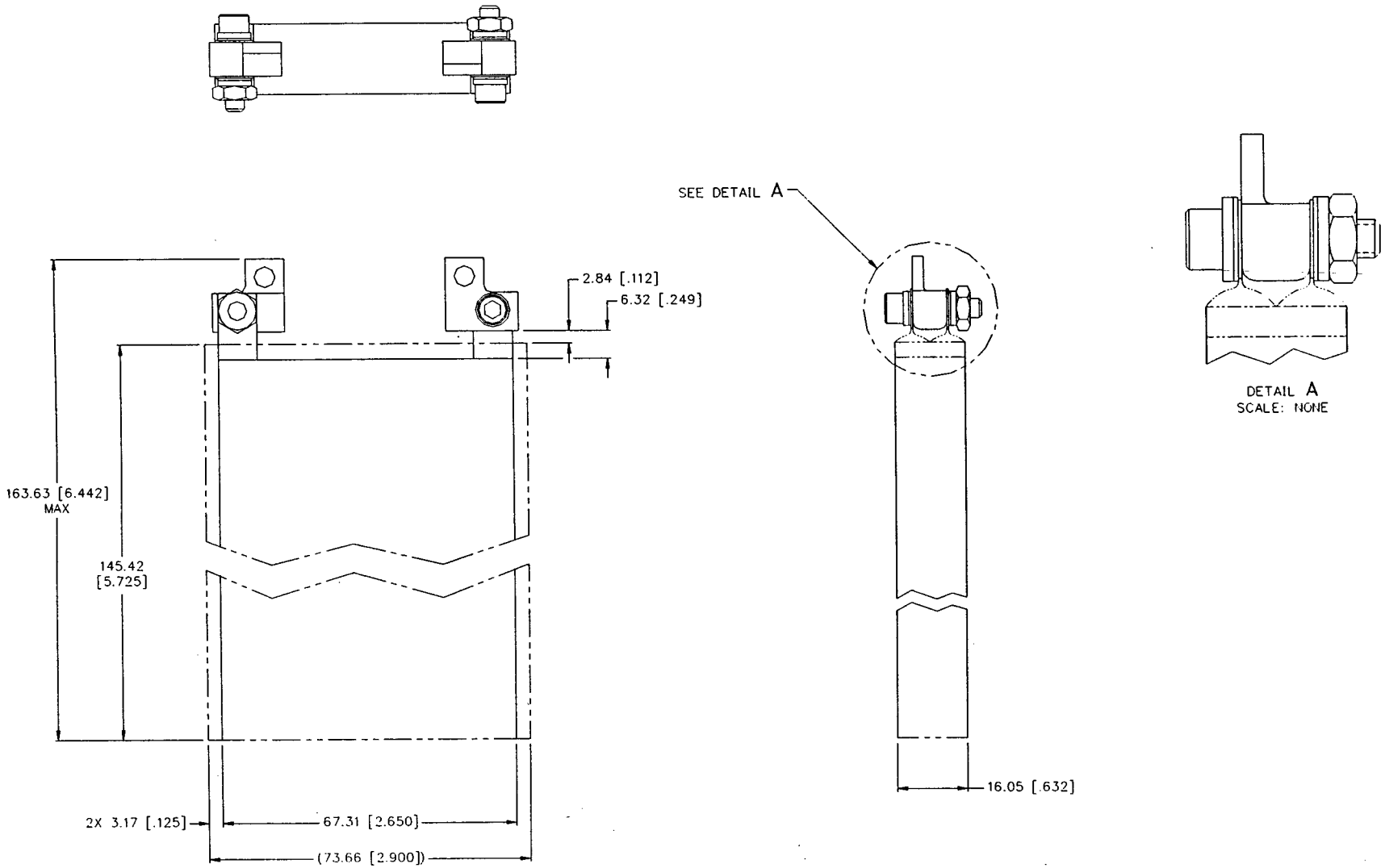

October 28, 1998

Mine Safety Appliances Company
38 Loveton Circle • Sparks, MD 21152 • (410) 472-7700

15-Ah Prototype Cell — Cell Stack Assembly

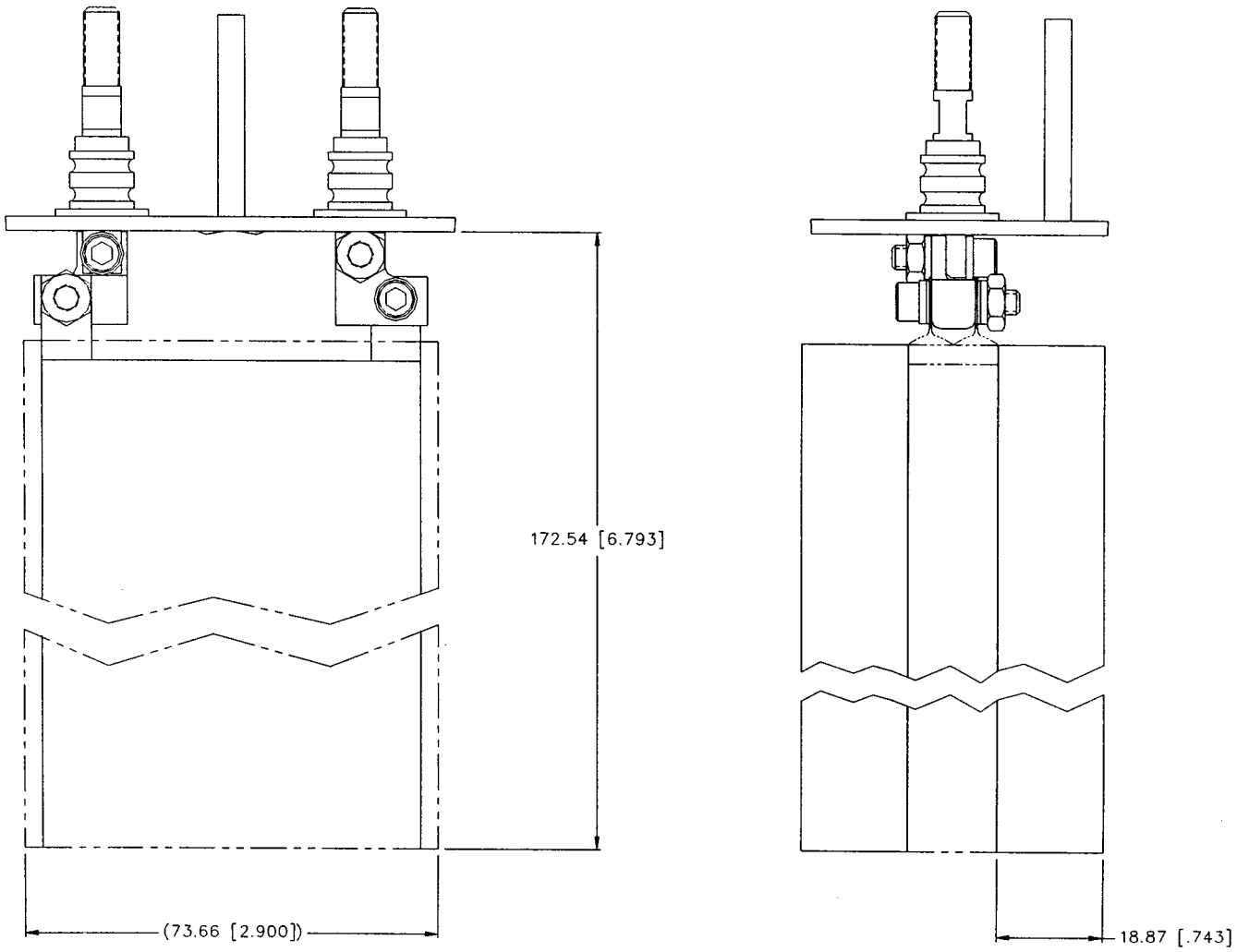

October 28, 1998

Mine Safety Appliances Company
38 Loveton Circle • Sparks, MD 21152 • (410) 472-7700

LEO 15-Ah Prototype — Prototype Cycling

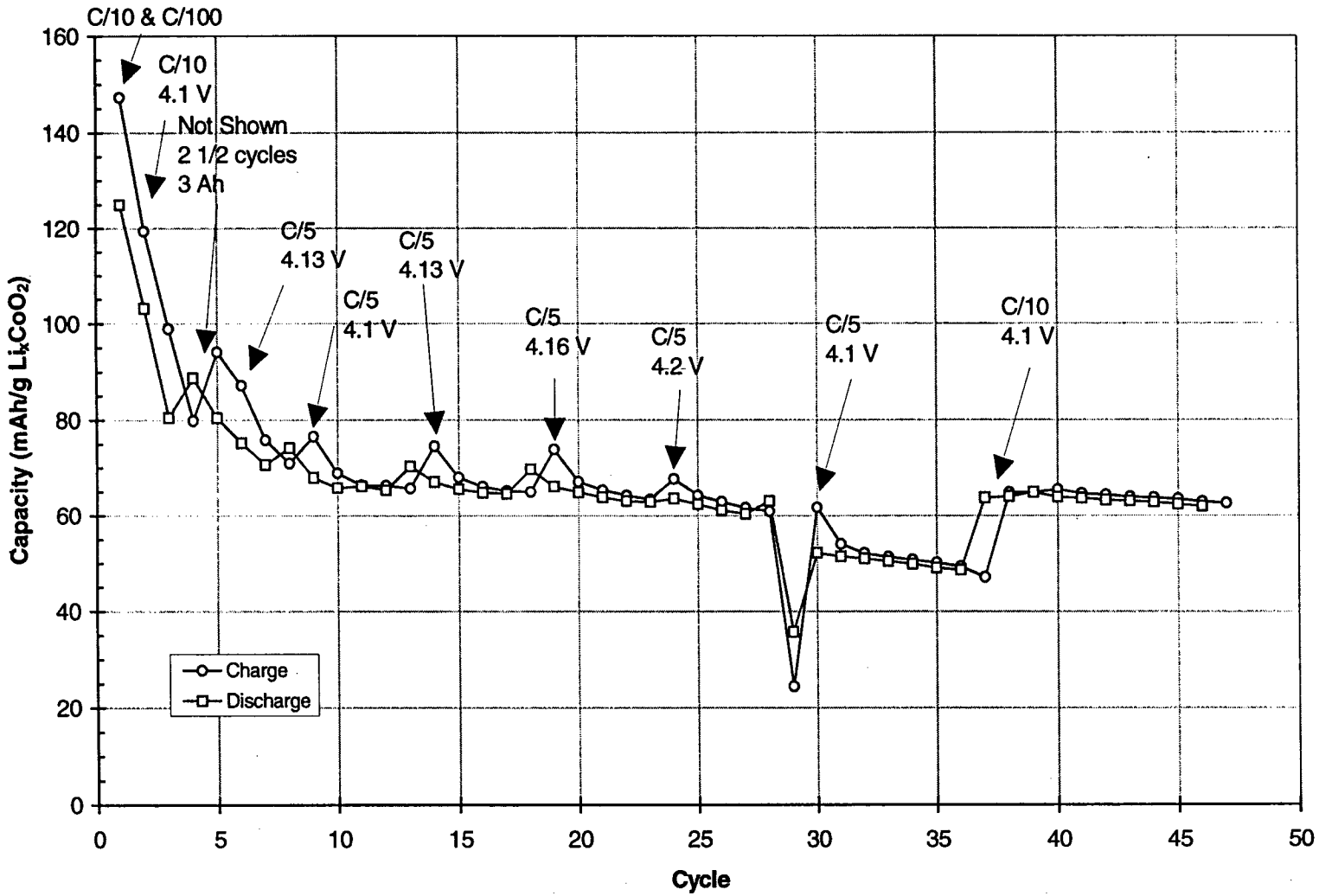

Mine Safety Appliances Company
38 Loveton Circle • Sparks, MD 21152 • (410) 472-7700

LEO 15-Ah Prototype — Tab Resistance Data

	Tab / Terminal Resistance (milli-Ohms)								
	Aluminum					Copper			
	Welded		Bolted			Welded		Bolted	
Location	AC Imped	DC Resist	AC Imped	DC Resist		AC Imped	DC Resist	AC Imped	DC Resist
1	3.7	3.4	4	5		1.6	1.6	1.8	1.5
2	3.9		5			1.3		2.0	
3	3.8		8			1.3		2.1	
4	4.0		15			1.5		2.0	
5	4.0		16			1.6		2.5	
6	3.9		21			1.7		2.2	
7	3.8		23			1.4		2.6	
8	3.9		29			1.3		2.7	
9	3.8		32			1.2		2.8	
10	3.9		34			1.6		2.9	
11	3.8	3.9	35	43		1.7	1.7	3.0	2.5
12	3.9		39			1.5		3.0	
13	3.8		42			1.3		3.0	
14	3.8		43			1.7		3.2	
15	3.9		46			1.5		3.2	
16	3.9		47			1.7		3.3	
17	4.0		49			1.5		3.3	
18	3.9		50			1.8		3.7	
19	3.9		51			1.8		4.0	
20	4.1	4.0	52	56		1.2	1.7	4.3	3.5

Note: Tab 1 is the innermost tab

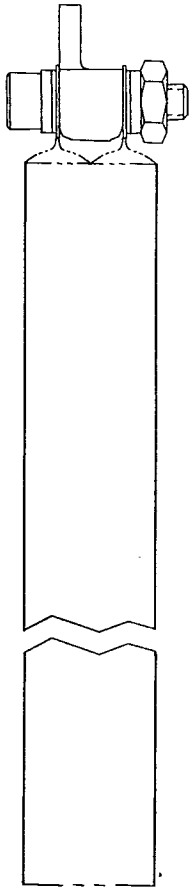

Mine Safety Appliances Company
38 Loveton Circle • Sparks, MD 21152 • (410) 472-7700

15-Ah Prototype — Vibration Testing

- Cell Initially in Fully Charged Condition
- Fill Tube Pinched and Welded

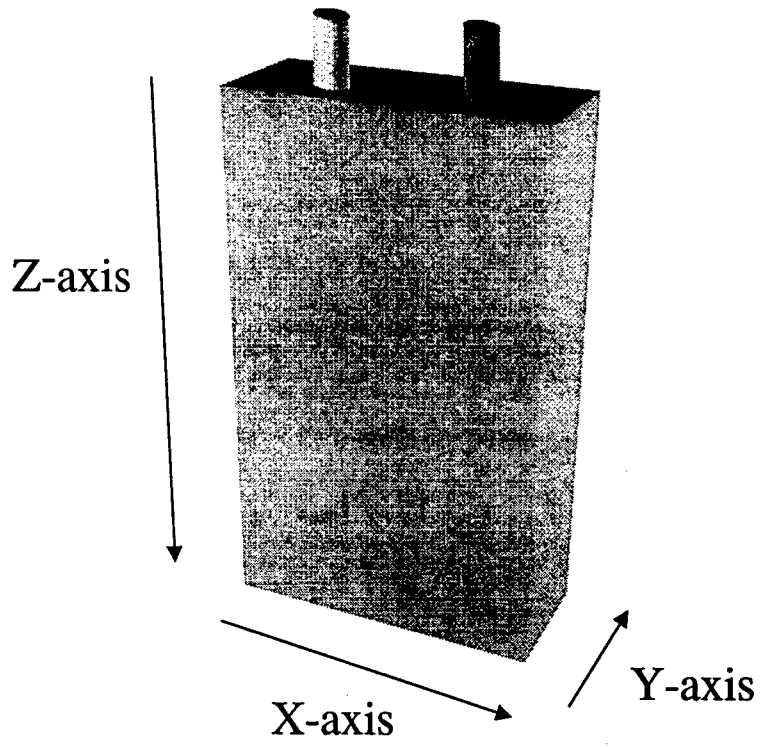

October 28, 1998

Mine Safety Appliances Company
38 Loveton Circle • Sparks, MD 21152 • (410) 472-7700

15-Ah Prototype — Vibration Test Protocol

- Electrical Readings: OCV, AC Resistance, EIS
- Random Vibration in Y, X, and Z axis at 0.01, 0.04, and 0.08 G^2/Hz
  - Cell was under resistive load (C/5 - 1.3 Ω) during vibration.
  - Electrical data were recorded between each axis change.
  - X-ray images were recorded before vibration, after Y-axis 0.01 G^2/Hz, and after all vibration completed.

Level (G^2/Hz)	Acceleration (g - rms)
0.01	3.79
0.04	7.57
0.08	10.71

Note: Future vibration test levels will be increased to 26.9 g-rms

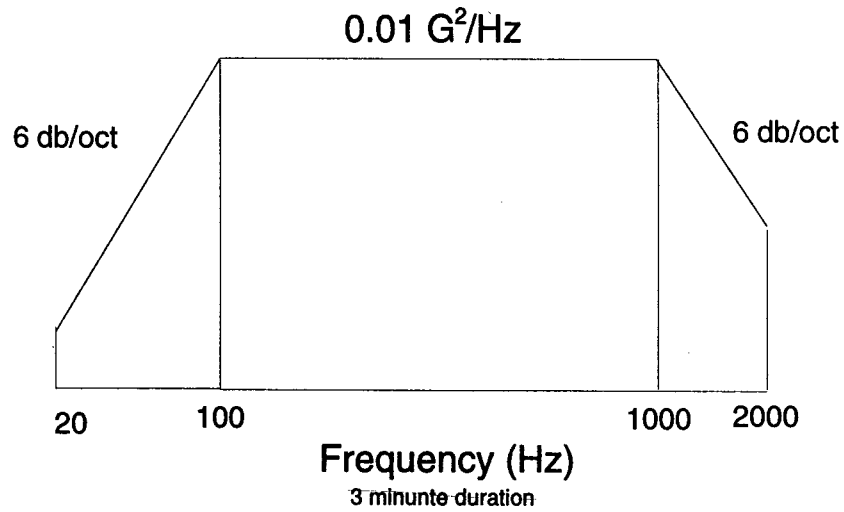

Mine Safety Appliances Company
38 Loveton Circle • Sparks, MD 21152 • (410) 472-7700

15-Ah Prototype — Vibration (0.08 G^2/Hz, X-axis)

Accelerometer Ringing Attributed to Fixture

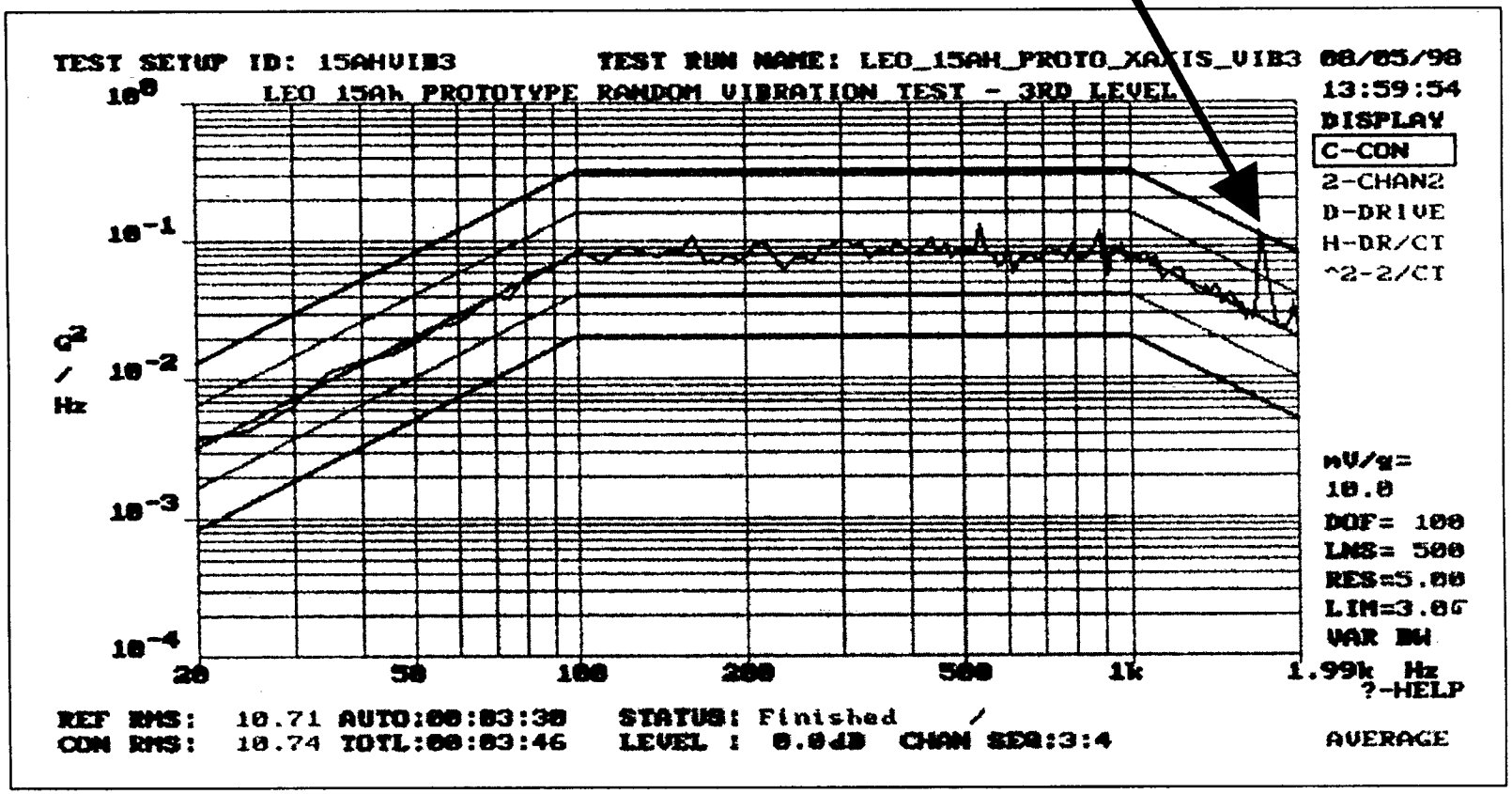

October 28, 1998

Mine Safety Appliances Company
38 Loveton Circle • Sparks, MD 21152 • (410) 472-7700

15-Ah Prototype Vibration — X-ray & Electrical

- X-rays showed no differences
- Open Circuit Voltage & AC Resistance @ 1,000 Hz

Test Time	OCV (V)	AC Resistance (mΩ)
Before Weld	4.0814	43
After Weld/Before Vib.	4.0739	43
After 0.01, Y	4.0563	44
After 0.01, X	4.0489	44
After 0.01, Z	4.0387	40
After 0.04, Y	4.0305	37
After 0.04, X	4.0418	37
After 0.04, Z	4.0185	38
After 0.08, Y	4.0122	37
After 0.08, X	4.0046	36
After 0.08, Z	3.9983	36

Mine Safety Appliances Company
38 Loveton Circle • Sparks, MD 21152 • (410) 472-7700

15-Ah Prototype Vibration — EIS Data

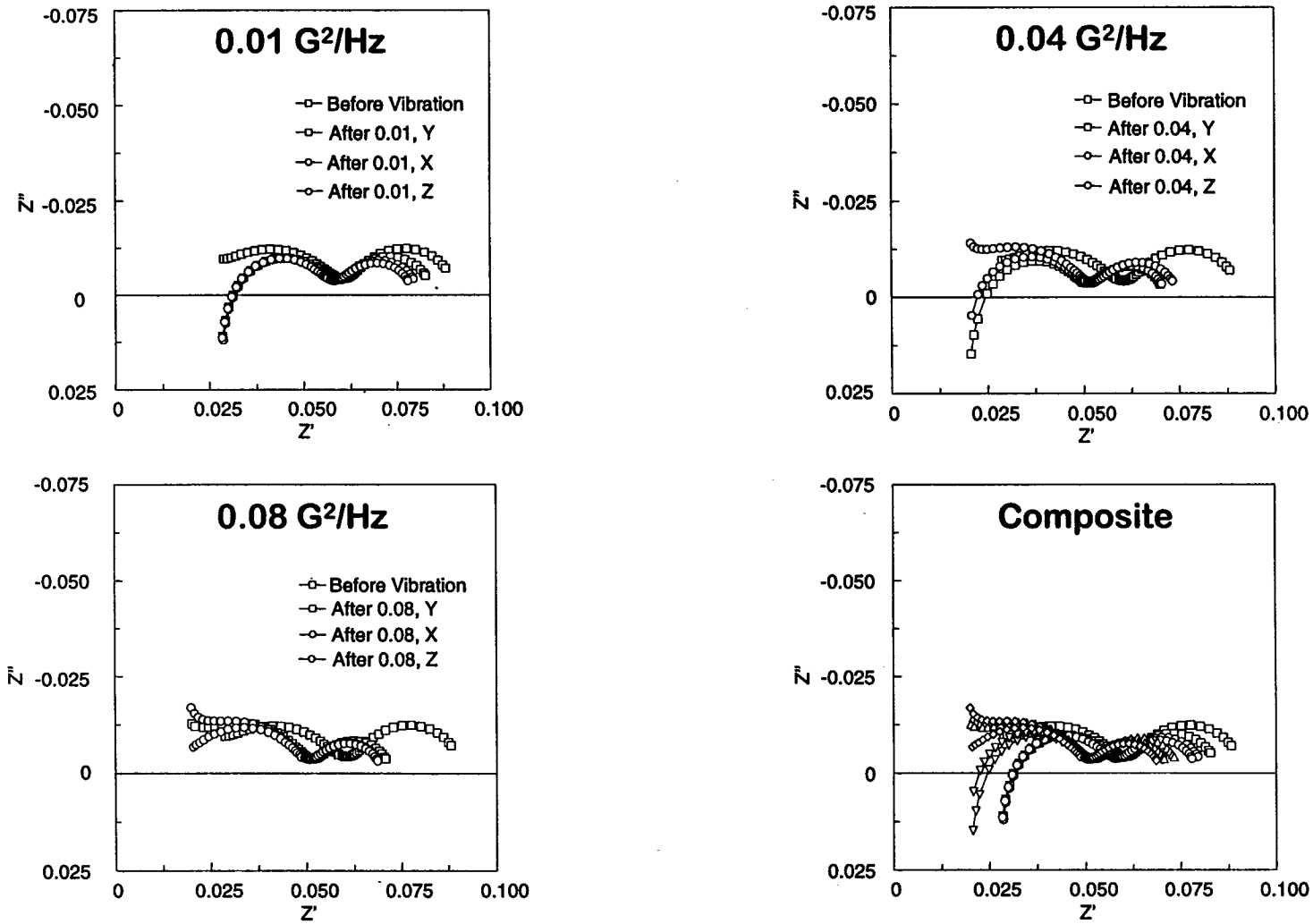

15-Ah Prototype — Gas Sampling Experiment

- Gas Samples Collected in Stn. Steel Containers.
- Cells Were Sampled after the Second Full Charge.
- Samples Were Analyzed with a Hewlett Packard 5890 Gas Chromatograph Equipped with a 5971 Mass Detector (M/Z range of 12 to 550 AMU).
- Qualitative Data Were Collected.
  - Calibration curves had not been developed for standard gases.
  - Volumes and pressures had not been measured for the samples.
- Abundance of CO_2 and H_2O in the Total Ion Chromatographs (TIC) Indicates Column Leakage.

Mine Safety Appliances Company
38 Loveton Circle • Sparks, MD 21152 • (410) 472-7700

15-Ah Prototype — Typical GC–MS TIC

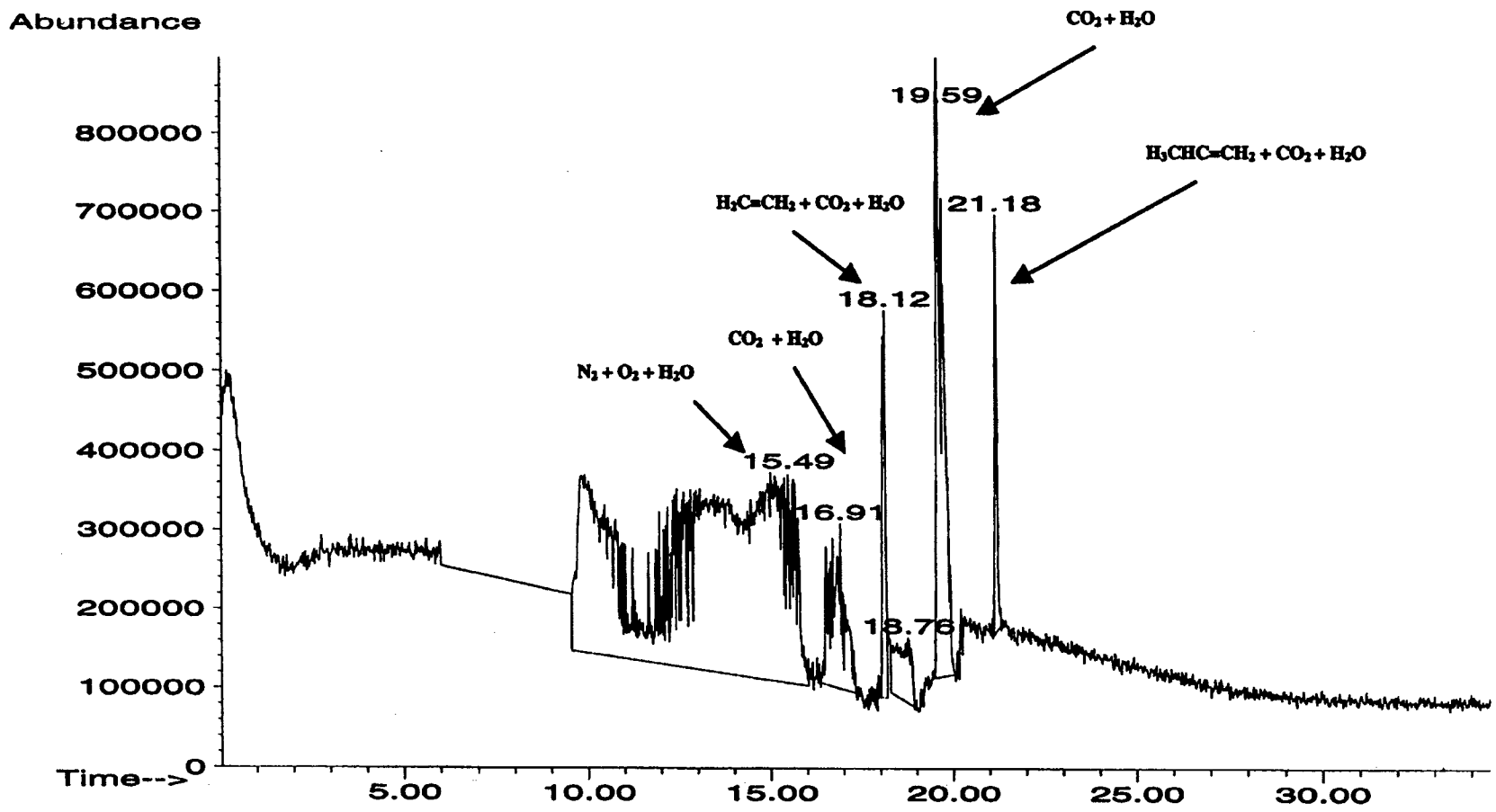

October 28, 1998

Mine Safety Appliances Company
38 Loveton Circle • Sparks, MD 21152 • (410) 472-7700

15-Ah Prototype — GC–MS Results

- The Following Gases Were Detected from the Three Cells That Were Sampled.
  - Cell 1: CO_2, H_2O, O_2, $H_2C{=}CH_2$, C_2H_6 and $H_3CHC{=}CH_2$
  - Cell 2a: CO_2, H_2O, N_2, O_2, $H_2C{=}CH_2$ and $H_3CHC{=}CH_2$
  - Cell 2b: CO_2, H_2O, O_2, $H_2C{=}CH_2$, $H_3CHC{=}CH_2$, and $(C_2H_5O)_2CO$ (i.e., DEC, which is one of the electrolyte solvents.)
- This Is in General Agreement with a Poster Presented by Dr. Kazuma Kumai, et al, at the 9th IMLB in Edinburgh, Scotland.
  - " Mechanism of Electrolyte Decomposition in Commercial Lithium–Ion Cell after Long Charge and Discharge Cycles," Kazuma Kumai, Hajime Miyashiro, Yo Kobayashi, Katsuhito Takei, and Rikio Ishikawa, CRIEPI, Tokyo, Japan

Mine Safety Appliances Company
38 Loveton Circle • Sparks, MD 21152 • (410) 472-7700

15-Ah Prototype — GC–MS Results Comparison

- The table below was presented by Kumai, et al. Their electrolyte was 1 M $LiPF_6$ dissolved in a mixture of PC, EMC, DEC, and DMC.
- The qualitative, MSA GC–MS results are shown (in red) below the Kumai table. MSA's electrolyte was 1.0 M $LiPF_6$ in PC:EC:DEC 1:1:2.

Composition of generated gases in the nominal operating voltage range (4.2V/2.5V), and during overcharging and overdischarging.

Test No.	Test conditions: Charge current	Test conditions: Discharge current	Cycle number	Capacity at end cycle	Composition of detected gases (%): O_2	N_2	CO_2	CO	CH_4	C_2H_6	C_3H_8	C_3H_6	Total volume (mℓ)
R1	Before cycle test				5.3	43	1.7		40	4.2	0.4		0.95
R2	200mA	100mA	2043	0.6Ah	2.7	8.5	2.2		72	6.7	7.2	0.4	2.23
R3		125mA	2397	0.6Ah	1.7	5.9	4.1		73	7.0	7.9	0.4	2.42
R4		200mA	2331	0.5Ah	1.5	6.5	7.2		61	7.6	15.6	0.8	2.63
R5		500mA	2301	0.5Ah	2.3	11.0	4.0		62	9.2	10.4	0.6	1.73
R6	125mA	125mA	1915	0.6Ah	2.1	7.7	1.3		75	7.8	6.2	0.2	2.01
R7	200mA		2570	0.5Ah	3.2	6.6	3.2		72	8.3	7.2	0.4	2.78
R8	500mA		3111	0.6Ah	6.1	25	2.5		51	6.2	8.5	0.4	1.75
R9	200/200mA, overcharge		880	0.6Ah	1.3	5.3	76		12	2.6	2.7		10.57
R10	200/200mA, overdischarge		880	0.0Ah	0.3	1.5	71	0.6	21	3.2	0.8	1.0	40.21

	O_2	N_2	CO_2	CO	CH_4	C_2H_6	C_3H_8	C_3H_6	
Cell 1	×		×			×		×	H_2O, C_2H_4
Cell 2a	×	×	×					×	H_2O, C_2H_4
Cell 2b	×		×					×	H_2O, C_2H_4, DEC

Mine Safety Appliances Company
38 Loveton Circle • Sparks, MD 21152 • (410) 472-7700

15-Ah Prototype — Kumai Gas-Generation Model

- Below are overcharge and overdischarge profiles of Li–ion cells and Kumai's gas-generation model.

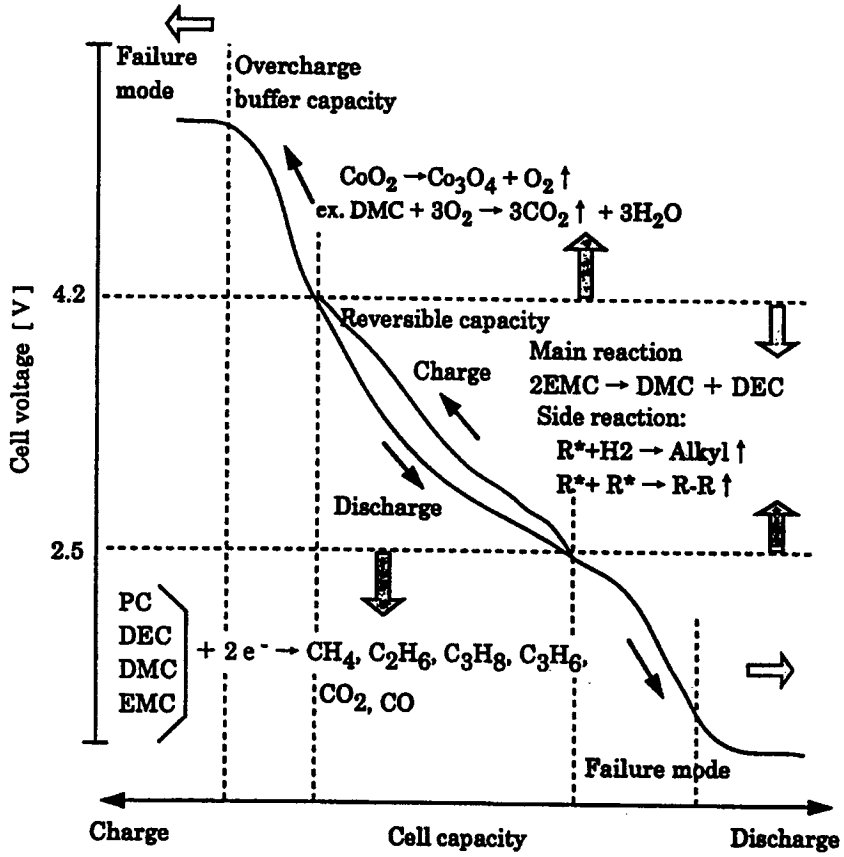

DPA Studies on SONY Li–ion Cells

- DPAs Were Performed on 1991-vintage, 20500 Cells and on 1996-vintage, 18650 Cells.
- Anodes and Cathodes Were Studied (Using ICP) in Both Charged and Discharged States.
- The Ratio of $M_{Li(anode + cathode)}/M_{Co}$ Ranged from 1.130 to 1.182 for the 1991 Cells and 1.003 to 1.088 for the 1996 Cells.
- Gravimetric Analysis and Thermal Gravimetric Analysis (TGA) Were Also Performed, and Data Are Shown.
- SEM Comparison of Anodes and Cathodes of SONY and MSA Cells Are Presented.

Mine Safety Appliances Company
38 Loveton Circle • Sparks, MD 21152 • (410) 472-7700

DPA Studies on SONY Cells — Analysis Steps

Step	Procedure	Reason
1	Wash anodes and cathodes with propylene carbonate then decant off excess propylene carbonate.	Remove the electrolytes from electrodes.
2	Boil or reflux (soxhlet) electrodes in acetone. Positives: 100% acetone, Negatives: 100% acetone or 75% acetone/25% water (vol/vol).	Delaminate positive active material (Li_xCoO_2 + polymer + carbon) from Al and soften negative active material (polymer + carbon) from Cu.
3	Scrap active materials from electrodes' current collector substrates with Teflon-coated spatula.	Separate electrodes' active materials from substrates.
4	Vacuum dry active materials at 120 °C for 24 hours.	Determine weights of electrodes' active materials.
5	Digest active materials in concentrated HCl for 4 hours.	Remove Li/L^+ from anode and Li_xCoO_2 from positive electrodes.
6	Filter digested electrodes' slurries through filter discs then wash with deionized water.	Separate negative active materials (polymer + carbon) from Li/Li^+ and positive active materials (polymer + carbon) from Li_xCoO_2.
7	Vacuum dry electrodes' active materials at 110 to 120 °C for 24 h; then weigh.	Determine weights of polymer + carbon in anode and Li_xCoO_2 in cathode. Weight of Li_xCoO_2 determined by difference in the positive electrode weight before and after HCl digestion.
8	Analyze electrodes' acetone and HCl digestion extracts by ICP for Li and Co.	Determine total Li in anode and total Li, total Co and x in Li_xCoO_2 in positive electrodes.
9	Analyze electrodes' active materials (polymer + carbon) by DSC.	Determine melting points of polymers in electrodes.
10	Analyze electrodes' active materials (polymer + carbon) by TGA.	Determine concentrations of polymers in electrodes by gravimetric factors determined from fluoropolymers.

Mine Safety Appliances Company
38 Loveton Circle • Sparks, MD 21152 • (410) 472-7700

ICP Analysis of 1991-Vintage, SONY 20500 Cells

Cell Identification	*Cell L53XXX-01*		*Cell L53XXX-02*		*Cell L53XXX-04*		*Cell L53XXX-06*	
Cell Condition	*Charged from 2.5 to 4.2 V @ 135 mA max*		*Charged from 2.8 to 4.1 V @ 100 mA max*		*Charged from 2.8 to 4.1 V @ 100 mA max*		*Charged from 2.5 to 4.2 V @ 135 mA max*	
Analytical Results	**Neg.*****	**Pos.**	**Neg.*****	**Pos.**	**Neg.*****	**Pos.**	**Neg.*****	**Pos.**
Wt Li_xCoO_2 (g)*	-	9.6897g	-	9.7393g	-	9.6890g	-	9.6576g
Wt Total P (g)/ Wt %	0.0667g	0.0388g/ 0.400%	0.0244g	0.0425g/ 0.436%	0.0674g	0.0261g	0.0654g	0.0249g
Li as $LiPF_6$ (g)/ Wt %	0.0149g	0.0087g/ 0.090%	0.0055g	0.0095g/ 0.098%	0.0151g	0.00585g	0.0147g	0.00558g
Wt Total Co (g)/ Wt %	0.0000g	5.8979g/ 60.868%	0.0000g	5.7588g/ 59.130%	0.0g	6.634g 58.15%	0.0g	5.693g 58.95%
Wt Total Li (g)/ Wt %	0.3872g	0.4578g/ 4.725%	0.3472g	0.4672/g 4.797%	0.3373g	0.4489g 4.633%	0.3564g	0.4217g 4.366%
Wt Total Li (g) – Li (as $LiPF_6$(g))/wt %	0.3723g	0.4491g/ 4.635%	0.3417g	0.4577g/ 4.700%	0.3222g	0.4430g 4.572%	0.3417g	0.4161g 4.309%
Wt O By Differ. (g)/wt %	-	3.3427g/ 34.497%	-	3.5228g/ 36.170%	-	3.612g 37.28%	-	3.548g 36.74%
O (moles)	-	2.156	-	2.261	-	0.2258	-	0.2218
O Excess (moles)	-	0.156	-	0.261	-	0.0346	-	0.0286
X in Li_xCoO_2	**0.535**	**0.647**	**0.504**	**0.675**	**0.485**	**0.668**	**0.509**	**0.621**
Total Li, Anode + Cathode (g) (corrected For Li in $LiPF_6$ (g))	0.8214		0.7994		0.7652		0.7578	
$M_{Li\ (anode+cathode)}/M_{Co}$	1.182		1.179		1.153		1.130	

*** Wt Li_xCoO_2 (g) determined by the weight change of Li-ion positives by dissolution of Li_xCoO_2 in HCl;**
***** Negative electrodes washed with 75% acetone/25% water (vol/vol).**

October 28, 1998

Mine Safety Appliances Company
38 Loveton Circle • Sparks, MD 21152 • (410) 472-7700

ICP Analysis of 1996-Vintage, SONY 18650 Cells

Cell Identification	*Cell L53P1-01*		*Cell L53P1-02*		*Cell L53P1-04*		*Cell L53P1-06*		*Cell L53P1-03*	
Cell Condition	1100 mAh discharge at 100 mA to 2.8 V		1075 mAh charge to 4.1 V from 2.8 V		1334 mAh discharge at 135 mA to 2.5 V		1360 mAh charge to 4.2 V from 2.5 V		1140 mAh charge to 4.1 V from 2.8 V; 1 year before DPA	
Analytical Results	**Neg.****	**Pos.**	**Neg.****	**Pos.**	**Neg.****	**Pos.**	**Neg.****	**Pos.**	**Neg.*****	**Pos.**
Wt Li_xCoO_2 (g)*	-	11.8083g	-	11.4315g	-	12.0783g	-	11.3038g	-	11.4488g
Wt Total P (g)/ Wt %	0.0021g	0.0000g/ 0.000%	0.0027g	0.0000g/ 0.000%	0.0357g	0.0000g/ 0.000%	0.0363g	0.0000g/ 0.000%	0.0057g	0.0016g/ 0.0140%
Li as $LiPF_6$ (g)/ Wt %	0.0005g	0.0000g/ 0.000%	0.0006g	0.0000g/ 0.000%	0.0084g	0.0000g/ 0.000%	0.0100g	0.0000g/ 0.000%	0.0013g	0.0004g/ 0.003%
Wt Total Co (g)/ Wt %	0.0000g	6.6641g/ 56.436%	0.0000g	6.6825g/ 58.457%	0.0000g	6.7767g/ 56.106%	0.0000g	6.5546g/ 57.986%	0.0000g	7.0066g/ 61.199%
Wt Total Li (g)/ Wt %	0.0764g	0.7782g/ 6.590%	0.3209g	0.4969g/ 4.347%	0.0784g	0.7900g/ 6.541%	0.4091g	0.4329g/ 3.830%	0.3181g	0.5120g/ 4.472%
Wt Total Li (g) - Li (as $LiPF_6$(g))/wt %	0.0759g	0.7782g/ 6.590%	0.3203g	0.4969g/ 4.347%	0.0700g	0.7900g/ 6.541%	0.3991g	0.4329g/ 3.830%	0.3168g	0.5116g/ 4.469%
Wt O By Differ. (g)/wt %	-	4.3660g/ 36.974%	-	4.2521g/ 37.196%	-	4.5116g/ 37.353%	-	4.3163g/ 38.185%	-	3.9306g/ 34.332%
O (g Attached)	-	2.413	-	2.344	-	2.453	-	2.426	-	2.146
O Excess	-	0.413	-	0.344	-	0.453	-	0.426	-	0.146
X in Li_xCoO_2	**0.097**	**0.991**	**0.407**	**0.631**	**0.088**	**0.989**	**0.517**	**0.561**	**0.383**	**0.620**
Total Li, Anode + Cathode (g) (corrected for Li in $LiPF_6$ (g))	0.8541g		0.8172g		0.8600g		0.8300g		0.8284g	
$M_{Li\ (anode+cathode)}/M_{Co}$	1.088		1.038		1.077		1.078		1.003	

*** Wt Li_xCoO_2 (g) determined by the weight change of Li-ion cathodes (Polymer/Li_xCoO_2/C) by dissolution of Li_xCoO_2 in HCl.**
**** Negative electrodes washed with 100% acetone; *** Negative electrodes washed with 75% acetone/25% water (vol/vol).**

October 28, 1998

Mine Safety Appliances Company
38 Loveton Circle • Sparks, MD 21152 • (410) 472-7700

Thermal Gravimetric Analysis (TGA) of 1991-Vintage, 20500 Cells

Cell Identification	*L53XXX-01*		*L53XXX-02*		*L53XXX-04*		*L53XXX-06*	
Components	**Neg.*** **	**Pos.**	**Neg.*** **	**Pos.**	**Neg.*** **	**Pos.**	**Neg.*** **	**Pos.**
Al Current Collector (g)	-	1.2920g	-	1.3291g	-	1.3378g	-	1.3218g
Cu Current Collector (g)	2.3192g	-	2.3498g	-	2.3395g[a]	-	2.3526g[a]	-
Tab Weight (appears to be Ni) (g)	-	-	-	-	0.0682g	Did not attach	0.6760g	Did not attach
Positive Active Materials (PVdF + Li_xCoO_2 + Carbon) (g)	-	10.7421g	-	10.7998g	-	10.7404g	-	10.7345g
Positive Active Material (residue)(g) (PVdF + Carbon)	-	1.0524g	-	1.0605g	-	1.0514g	-	1.0769g
Li_xCoO_2 in Positive (positive active materials (g) – Positive Residue (g)) (g/%)	-	9.6897g (90.20%)	-	9.7393g (90.18%)	-	9.6890g (90.21%)	-	9.6576g (89.97%)
Polymer (PVdF) in Positive Residue (TGA analysis of positive residue) (g/%)	-	0.2865g (2.67%)	-	0.3079g (2.85%)	-	0.3203g (2.98%)	-	0.3126g (2.92%)
Carbon in Positive by TGA (Positive residue (g)-polymer in residue) (g/%)	-	0.7659g (7.13%)	-	0.7527 (6.97%)	-	0.7314g (6.81%)	-	0.7632g (7.11%)
Negative Active Materials (g)	-	-	-	-	8.4680g	-	8.5240g	-
Negative Active Materials (res.) (PVdF and Carbon) (g)	6.5735g	-	6.5679g	-	6.5180g	-	6.4524g	-
HCl Soluble Negative Active Materials (by difference)	-	-	-	-	1.9500g	-	2.0716g	-
Polymer (PVdF) in Negative (TGA analysis of negative) (g/%)	0.5561g (8.46%)	-	0.5478g (8.34%)	-	0.5371g (8.24%)	-	0.4853g (7.52%)	-
Carbon in Negative by TGA (Negative residue (g) – polymer in residue) (g/%)	6.0174g (91.54%)	-	6.0201g (91.66%)	-	5.9809g (91.76%)	-	5.9672g (92.48%)	-

*** Components dried at 110°C for 24 hours under vacuum.**
***** Negative electrodes washed with 75% acetone/25% water (vol/vol).**

October 28, 1998

Mine Safety Appliances Company
38 Loveton Circle • Sparks, MD 21152 • (410) 472-7700

Thermal Gravimetric Analysis (TGA) of 1996-Vintage, 18650 Cells

Cell Identification	*L53P1-01*		*L53P1-02*		*L53P1-04*		*L53P1-06*		*L53P1-03*	
Components	**Neg.****	**Pos.**	**Neg.****	**Pos.**	**Neg.****	**Pos.**	**Neg.****	**Pos.**	**Neg.*****	**Pos.**
Al Current Collector (g)	-	1.5649	-	1.5205	-	1.4270	-	1.5268	-	1.4746
Cu Current Collector (g)	-	-	-	-	-	-	-	-	2.5192	-
Positive Active Materials ($PVdF + Li_xCoO_2 +$ Carbon) (g)	-	12.9944	-	12.6440	-	13.3032	-	12.5571	-	12.6708
Positive Active Material (residue) (PVdF + Carbon) (g)	-	1.1861	-	1.2125	-	1.2249	-	1.2488	-	1.2220
Li_xCoO_2 in Positive (Positive active materials (g) - Positive Residue (g)) (g/%)	-	11.8083 (90.87)	-	11.4315 (90.41)	-	12.0783 (90.79)	-	11.3083 (90.06)	-	11.4488 (90.36)
Polymer (PVdF) in Positive Residue (TGA analysis of positive residue) (g/%)	-	0.3607 (2.78)	-	0.4045 (3.20)	-	0.3633 (2.73)	-	0.3505 (2.79)	-	0.3408 (2.69)
Carbon in Positive by TGA (Positive residue (g)-polymer in residue) (g/%)	-	0.8254 (6.35)	-	0.8080 (6.39)	-	0.8620 (6.48)	-	0.8978 (7.15)	-	0.8806 (6.95)
Negative Active Materials (residue) (PVdF and Carbon) (g)	4.9598	-	4.8126	-	4.9763	-	4.9727	-	4.9846	-
Polymer (PVdF) in Negative (TGA analysis of negative) (g/%)	0.3490 (7.04)	-	0.3706 (7.70)	-	0.3913 (7.86)	-	0.4482 (9.01)	-	0.3813 (7.65)	-
Carbon in Negative by TGA (Negative residue (g) – polymer in residue) (g/%)	4.6108 (92.96)	-	4.4420 (92.30)	-	4.5850 (92.14)	-	4.5247 (90.99)	-	4.6033 (92.35)	-

Components dried at 110 – 120 °C for 24 hours.
**** Negative electrodes washed with 100% acetone; *** Negative electrodes washed with 75% acetone/25% water (vol/vol).**

Mine Safety Appliances Company
38 Loveton Circle • Sparks, MD 21152 • (410) 472-7700

SEM Comparison of SONY and MSA Electrodes

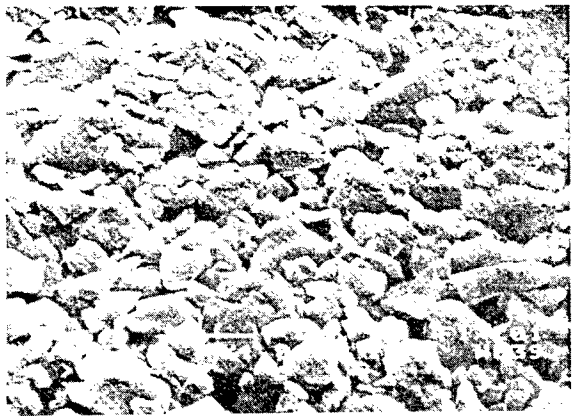

SONY 20500 Negative (1991)

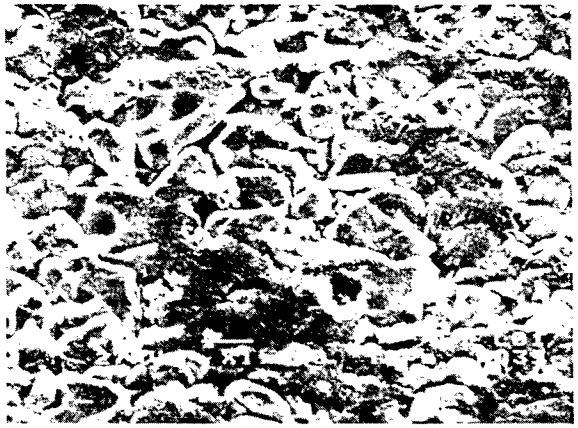

SONY 20500 Positive (1991)

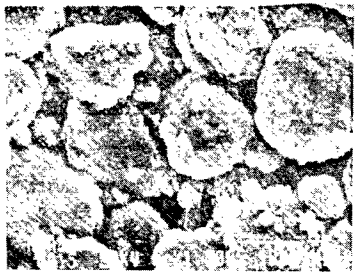

MSA Negative Electrode

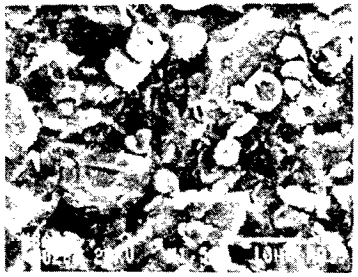

MSA Positive Electrode

Mine Safety Appliances Company
38 Loveton Circle • Sparks, MD 21152 • (410) 472-7700

October 28, 1998

Summary and Conclusions

- The Li–ion DPA procedures differ from those used for Ni–Cd or Ni–H_2. Dry rooms or glove boxes are needed for many of the steps.
- Resistance buildup is an important issue in Li–ion cells, which have many very thin aluminum and copper electrodes, connected in parallel.
- Preliminary vibration results are encouraging.
- Models exist for the prediction of headspace gases. However, the analysis of such gases requires very rigorous procedures.
- A procedure exists for ICP and TGA of electrodes.
- SEM is useful for electrode comparisons.

Mine Safety Appliances Company
38 Loveton Circle • Sparks, MD 21152 • (410) 472-7700

Acknowledgments

- Although I am presenting this paper, all of the physical work was performed by my co-authors.
- I want to acknowledge the help of Dr. Pinakin Shah, who is the Principal Investigator of MSA's Li-Ion program, and Dr. Cheryl Matthias, who manages MSA's Analytical Chemistry Staff.
- In addition, I want to thank "Toti" Recato and Dr. Nehemiah Margalit of Tracor Battery Technology Center for their contributions to this paper.

Mine Safety Appliances Company
38 Loveton Circle • Sparks, MD 21152 • (410) 472-7700

Nickel-Hydrogen Session

EAGLE PICHER
Eagle-Picher Technologies, LLC

POWER Subsystems

Proposed Convention for Assigning NiH_2 Cell Capacity

"A cell by any other name . . . "

Convention for Cell Capacity

- NOMINAL CAPACITY VALUES FOR CELLS ARE ASSIGNED BY THE MANUFACTURER

- NO STANDARD CONVENTION EXISTS TO DEFINE "NOMINAL" CAPACITY

Convention for Cell Capacity

PROPOSED DEFINITION OF THE NOMINAL CAPACITY OF A NiH2 CELL:

...is equal to the theoretical capacity, rounded to the nearest whole number, of the active material in its positive electrodes, if they were of nominal loading, thickness and porosity.

Convention for Cell Capacity

- **The theoretical capacity of Ni(OH)2 and Co(OH)2 is 0.289 Ah/g.**

- **Typical values for positive electrodes include:**
  - 0.030 in. thickness
  - 80% porosity
  - 1.65 g/ccv loading

Convention for Cell Capacity

- **Assumed Conditions for Standardized Capacity Measurement:**
  - FULL CHARGE AT 10°C
  - CONSTANT TEMPERATURE CONTINUED DURING DISCHARGE
  - END VOLTAGE OF 1.0 VOLTS
  - CAPACITY NOT LIMITED BY CURRENT DENSITY

EAGLE PICHER
Eagle-Picher Technologies, LLC

POWER Subsystems

Convention for Cell Capacity

EXTREMES

	Actual Ah	Present Nom. Ah	Proposed Nom. Ah	Error	Utilization at Cell Level
RNH 86-1	93.3	86	84	-2%	111.1%
RNH 50-61	68.6	50	62	+24%	111.1%

Note: DOD IS AFFECTED TO THE SAME PERCENTAGE ERROR, e. g:

RNH 50-61	Ah out (as 50Ah)	Ah out (as 62 Ah)	Error
50% DOD	25	31	(31 - 25) / 25 = 24%

Convention for Cell Capacity

Case No.	Cell Desig.	Actual Avg. Cap. (Ah)	Present Nominal (Ah)	Proposed Nominal (Ah)	% Error in DOD	Disch. Rate (a.)	C-rate Difference (amps)	% Util. at Cell Level
1	RNH 86-1	93.3	86	84	-2	43.0	-2	111.1
2	RNH 60-5	67.1	60	59	-2	30.0	-1	114.1
3	RNH 76-11	83.5	76	75	-1	38.0	-1	110.7
4	RNH 16-1	18.8	16	16	0	8.0	0	117.8
5	RNH 131-1	140.0	131	131	0	97.4	0	106.5
6	RNH 76-15	86.3	76	78	3	38.0	2	110.1
7	RNH 65-15	73.3	65	67	3	32.5	2	109.1
8	RNH 100-7	109.7	100	105	5	74.5	5	104.9
9	RNH 64-3	74.5	64	69	8	42.3	5	108.6
10	RNH 50-57	61.7	50	56	12	30.0	6	110.2
11	RNH 40-23	47.4	40	45	13	20.0	5	105.8
12	RNH 30-1	37.2	30	34	13	15.0	4	110.7
13	RNH 76-3	98.0	76	87	14	38.0	11	112.9
14	RNH 50-59	61.7	50	59	18	30.0	9	104.9
15	RNH 50-61	68.6	50	62	24	25.0	12	111.1

EAGLE PICHER
Eagle-Picher Technologies, LLC

POWER Subsystems

Convention for Cell Capacity

Impact on DOD of Using Actual Cell Capacities

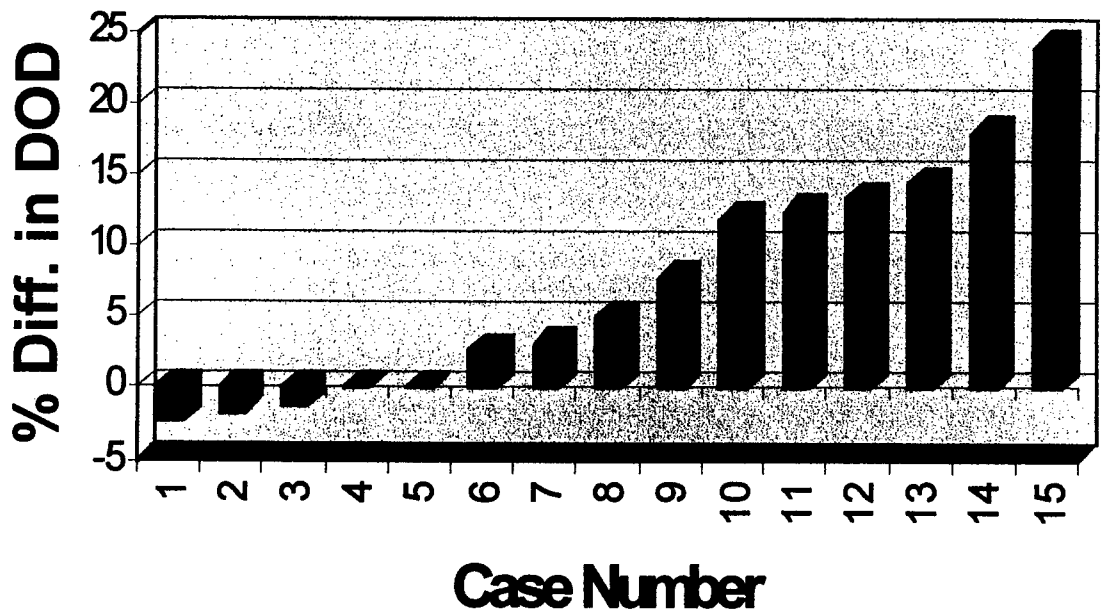

Convention for Cell Capacity

- SOME INFLUENCES ON THE CHOICE OF NOMINAL CAPACITIES:

- MODIFY CAPACITY BUT RETAIN HERITAGE
- SUPPORT A HIGHER EODV
- SUPPORT A HIGHER DISCHARGE CURRENT
- MINIMIZE PAPERWORK AFTER A DESIGN CHANGE (e.g., adding electrodes)
- CUSTOMER PREFERENCE

Convention for Cell Capacity

- "UTILIZATION" IN THE TABLE OF CELL DESIGNS ASSUMES NOMINAL ELECTRODES - ACTUAL UTILIZATION MAY VARY

- TRUE UTILIZATIONS AT THE ELECTRODE LEVEL HAVE A SIMILAR RANGE - 105% TO 118 % IS TYPICAL

EAGLE PICHER
Eagle-Picher Technologies, LLC

POWER Subsystems

Convention for Cell Capacity

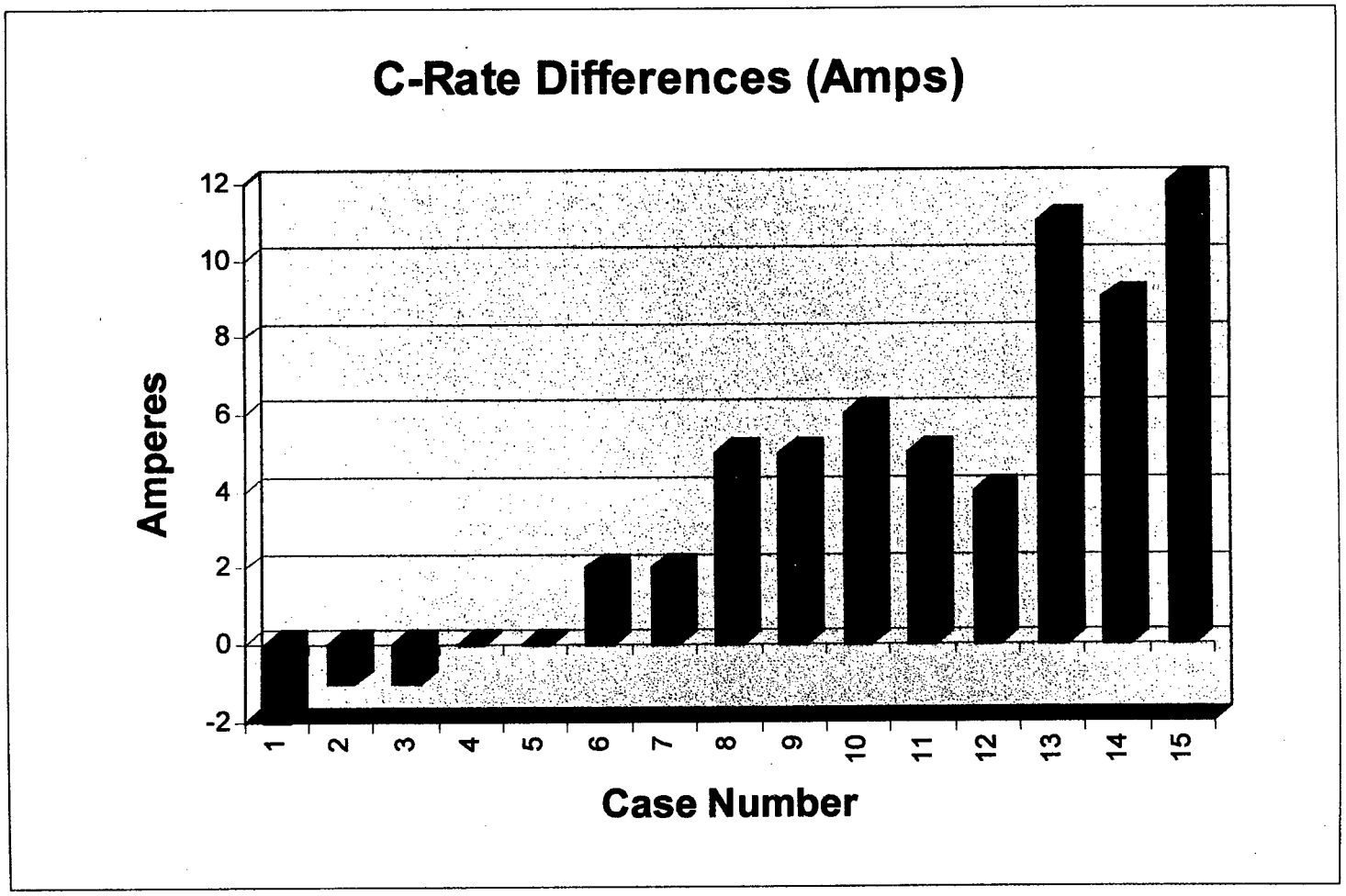

Convention for Cell Capacity

- FOR A DISCHARGE RATE CHANGE OF -2 TO +12 AMPS, CAPACITY TO 1.0 VOLT CHANGES $\leq$ 1 Ah

- WHY LOW IMPACT? -CELL DESIGN ANTICIPATES AMPERAGE REQUIREMENTS

EAGLE PICHER
Eagle-Picher Technologies, LLC

POWER Subsystems

Convention for Cell Capacity

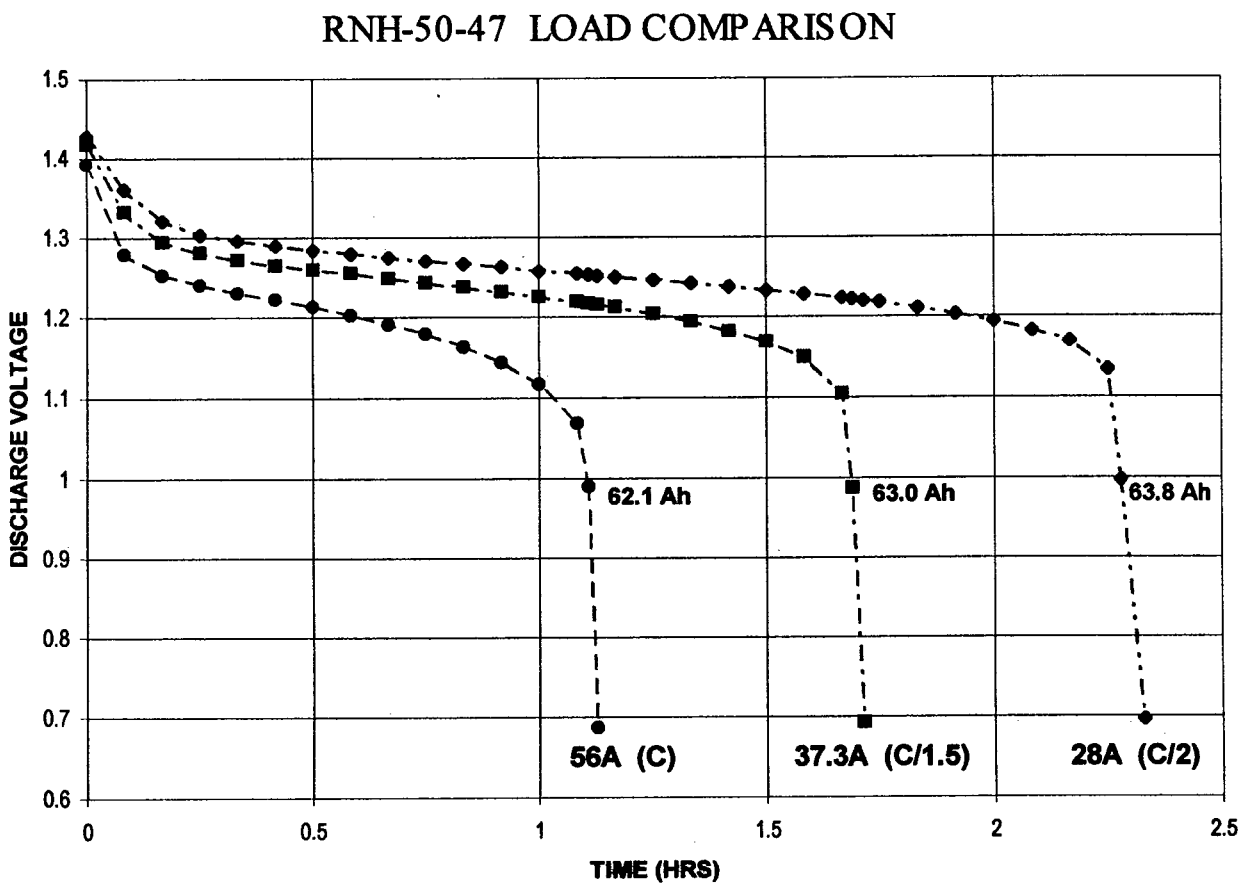

Convention for Cell Capacity

- WHAT ABOUT THE "WARM ON DISCHARGE" EFFECT?

- TO 1.0 VOLTS, CHANGE IS ONLY ~2.5%
- TO 1.1 VOLTS, CHANGE CAN BE ~10%

Convention for Cell Capacity

HOW MUCH DOES THE DEFINITION OF "NOMINAL" AFFECT THE SETTING OF A CELL'S PRECHARGE?

IT DEPENDS ON HOW YOU DO IT:

- **Method 1: VENT AFTER DISCHARGE**
- **Method 2: VENT DURING CHARGE**

Convention for Cell Capacity

Method 1: VENT AFTER DISCHARGE

precharge = C_{Total} - $C_{(0.7v)}$ - X psig H_2

THERE IS NO EFFECT - THIS METHOD ADJUSTS THE PRECHARGE IN PROPORTION TO THE INDIVIDUAL CELL'S ACTUAL CAPACITY.

Convention for Cell Capacity

Method 2: VENT DURING CHARGE

- C = 50 Ah (present nominal)
- C = 56 Ah (proposed convention)

- 5.0 amps X 1.5 hours = 7.5 Ah precharge (13.4%)
- 5.6 amps X 1.5 hours = 8.4 Ah precharge (15.0%)

CONCLUSIONS

- NO STANDARD FOR RATING EXISTS
- EVALUATING CYCLE-LIFE IS MISLEADING IF NOMINAL IS BIASED
- AN INCREASE IN DOD OF ONLY 20% CAN DECREASE CYCLE LIFE BY ABOUT HALF

CONCLUSIONS

A CONSISTENT BASIS FOR COMPARISON IS NEEDED TO:

- COMPARE CELL DESIGN FEATURES
- COMPARE EFFECTS OF TESTING METHODS
- COMPARE CURRENT FLIGHT PERFORMANCE

CONCLUSIONS

- CONTROL PRECHARGE
- PROJECT BATTERY CYCLE LIFE
- COMPARE NiH2 TO Li-ION, NiCd, etc.
- BETTER EXPLOIT EXISTING DOD CAPABILITIES, WHICH ARE UNDER-USED

LOCKHEED MARTIN
Missiles & Space

NiH_2 BATTERY RELIABILITY UPDATE

Douglas P. Hafen
Lockheed Martin Missiles & Space

Presented at

The 1998 NASA Aerospace Battery Workshop

October 27-29, 1998

LOCKHEED MARTIN
Missiles & Space

NiH_2 Battery Reliability Update

INTRODUCTION

- A NiH2 RELIABILITY EQUATION WAS PUBLISHED AT THE 1992 IECEC.
- SIGNIFICANT LIFE DATA HAS BEEN GENERATED SINCE THAT TIME FRAME.
- IT WAS DESIRED TO UPDATE THE 1992 HAFEN RELIABILITY EQUATION FOR APPLICATIONS SUCH AS THE HUBBLE SPACE TELESCOPE (HST) BATTERIES.
- THIS EQUATION RELATES OPERATING DEPTH-OF-DISCHARGE (DOD), CYCLES EXPERIENCED, BATTERY RELIABILITY, NUMBER OF BATTERIES AND CELLS AND ALLOWABLE FAILURES.
- TYPICALLY THE SOLUTION BEING SOUGHT IS THE UNKNOWN VALUE OF EITHER BATTERY RELIABILITY, MAXIMUM ALLOWABLE DOD OR CYCLE LIFE WITH FOUR QUANTITIES KNOWN FOR THAT CASE.

LOCKHEED MARTIN
Missiles & Space

NiH_2 Battery Reliability Update

DATABASE DESCRIPTION

- UTILIZED DATA FROM TWO SOURCES
  - 1997 BATTERY WORKSHOP PAPER BY C. FOX et al, DESCRIBING EAGLE-PICHER DATA
  - 1997 IECEC PAPER BY B.A. MOORE et al, DESCRIBING NAVSURFWARCENDIV DATA
- CELL DATA BASE INCLUDED
  - BOTH GEO AND LEO
  - VARIOUS IPV CELL DESIGNS
  - TESTS CONDUCTED AT TEMPERATURE OF 5-10°C
- EXCLUDED FROM THE DATABASE
  - CPV AND SPV
  - TESTS CONDUCTED OUTSIDE OF RANGE OF 5-10°C
- CYCLES REPORTED MAY BE ONE OF THREE TYPES
  - FAILURE / TEST DISCONTINUED / CYCLE LIFE REPORTED WITH TEST CONTINUED

LOCKHEED MARTIN
Missiles & Space

NiH_2 Battery Reliability Update

TYPICAL SET OF DATA

- FOR EACH PACK THE DATA IS DOD AND CYCLES EXPERIENCED. THE CYCLES REPORTED MAY BE ONE OF THREE TYPES (FAILURE / TEST DISCONTINUED / CYCLE LIFE REPORTED WITH TEST CONTINUED).
- ADDITIONAL DATA FOR EAGLE-PICHER DATABASE
  - NUMBER OF CELLS
  - PART NUMBER
  - TYPE OF TESTING (REALTIME GEO, ACCEL LEO, ETC.)
- FOR NAVSURFWARCENDIV DATA
  - TEMPERATURE
  - PACK DESIGNATION
  - MANY DESIGN DETAILS SUCH AS SEPARATOR AND STACK CONFIGURATION
  - TYPE OF TESTING (REALTIME GEO, ACCEL LEO, ETC.)

LOCKHEED MARTIN
Missiles & Space

NiH_2 Battery Reliability Update

EAGLE-PICHER DATA (1997 BATTERY WORKSHOP PAPER, C. FOX et al)

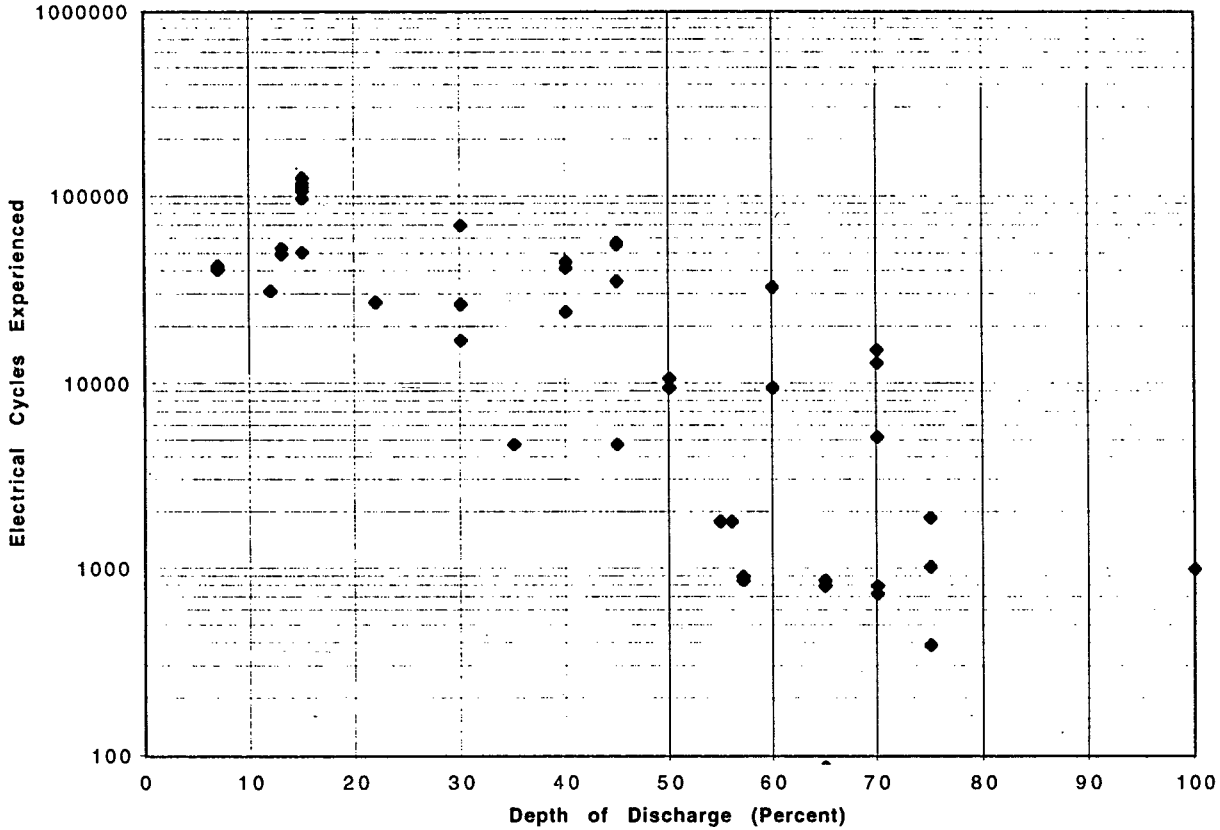

October 27- 29, 1998

LOCKHEED MARTIN
Missiles & Space

NiH_2 Battery Reliability Update

NAVSURFWARCENDIV DATA (1997 IECEC PAPER, B.A. MOORE et al)

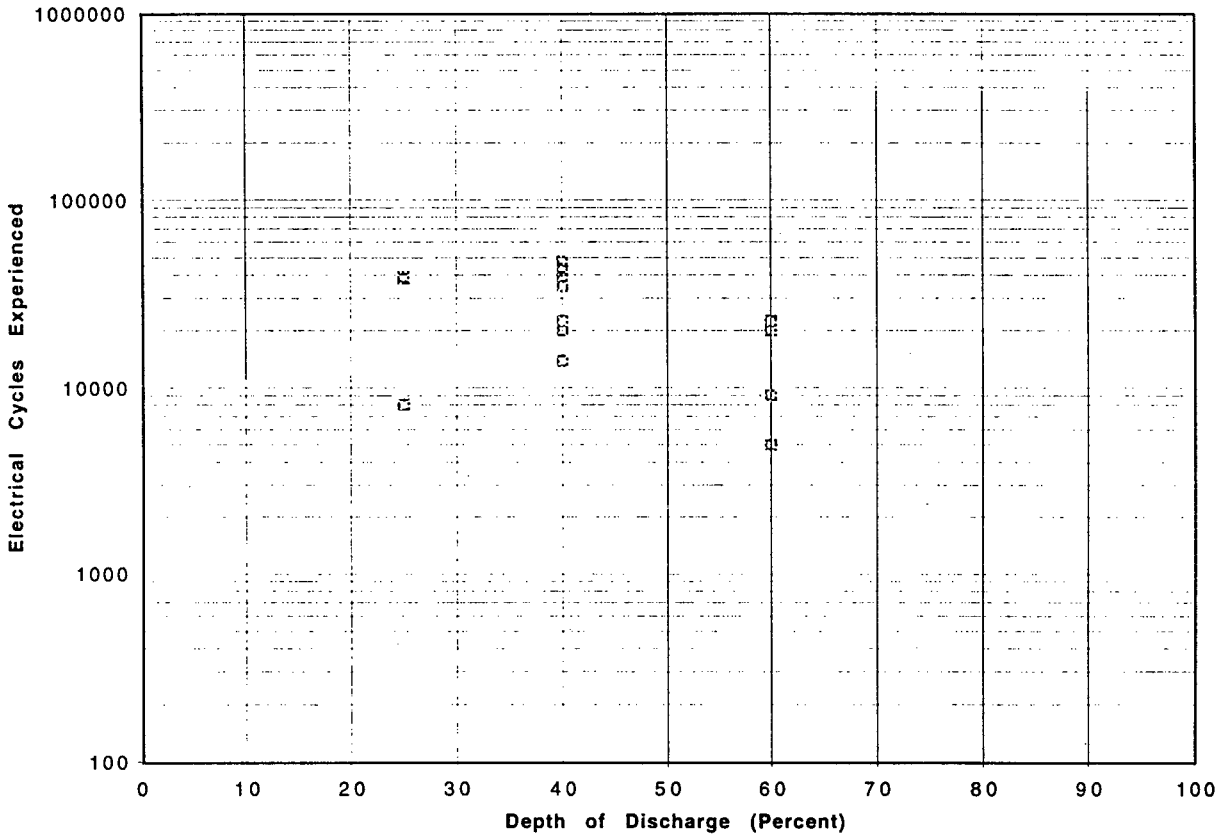

October 27- 29, 1998

LOCKHEED MARTIN
Missiles & Space

NiH_2 Battery Reliability Update

GOAL OF RELIABILITY EQUATION

- THE EQUATION IS A RELATIONSHIP BETWEEN OPERATING DOD, CYCLES EXPERIENCED, BATTERY RELIABILITY, NUMBER OF BATTERIES/CELLS AND ALLOWABLE FAILURES.
- THE EQUATION IS A GENERAL EQUATION APPLYING TO STATE-OF-THE-ART NICKEL-HYDROGEN CELLS.
  - THE EQUATION FALLS CONSERVATIVELY WITHIN THE UPPER ENVELOPE OF DATA
  - THE EQUATION SET WILL NOT APPLY IF A LESS THAN OPTIMUM DESIGN IS USED. THALLER'S 1998 IECEC PAPER HAS A DISCUSSION OF CELL DESIGNS WHICH ARE EXPECTED TO HAVE LESS THAN OPTIMUM LIFE

LOCKHEED MARTIN
Missiles & Space

NiH_2 Battery Reliability Update

THALLER EQUATION

- REFERENCE:1993 NASA BATTERY WORKSHOP
- LIFE IS PROPORTIONAL TO THE CAPACITY MARGIN
  - CAPACITY MARGIN IS (1 + f -DOD)
  - f IS THE FRACTION OF THE CAPACITY DESIGNED INTO THE CELL REPRESENTING ACTUAL CAPACITY ABOVE NOMINAL CAPACITY
- LIFE IS INVERSELY PROPORTIONAL TO DOD
  - A IS THE PROPORTIONALITY CONSTANT AND APPEARS IN THE DENOMINATOR
- LIFE = (1 + f - DOD) / (A * DOD)

LOCKHEED MARTIN
Missiles & Space

NiH_2 Battery Reliability Update

Shape of Curves from Thaller Equation

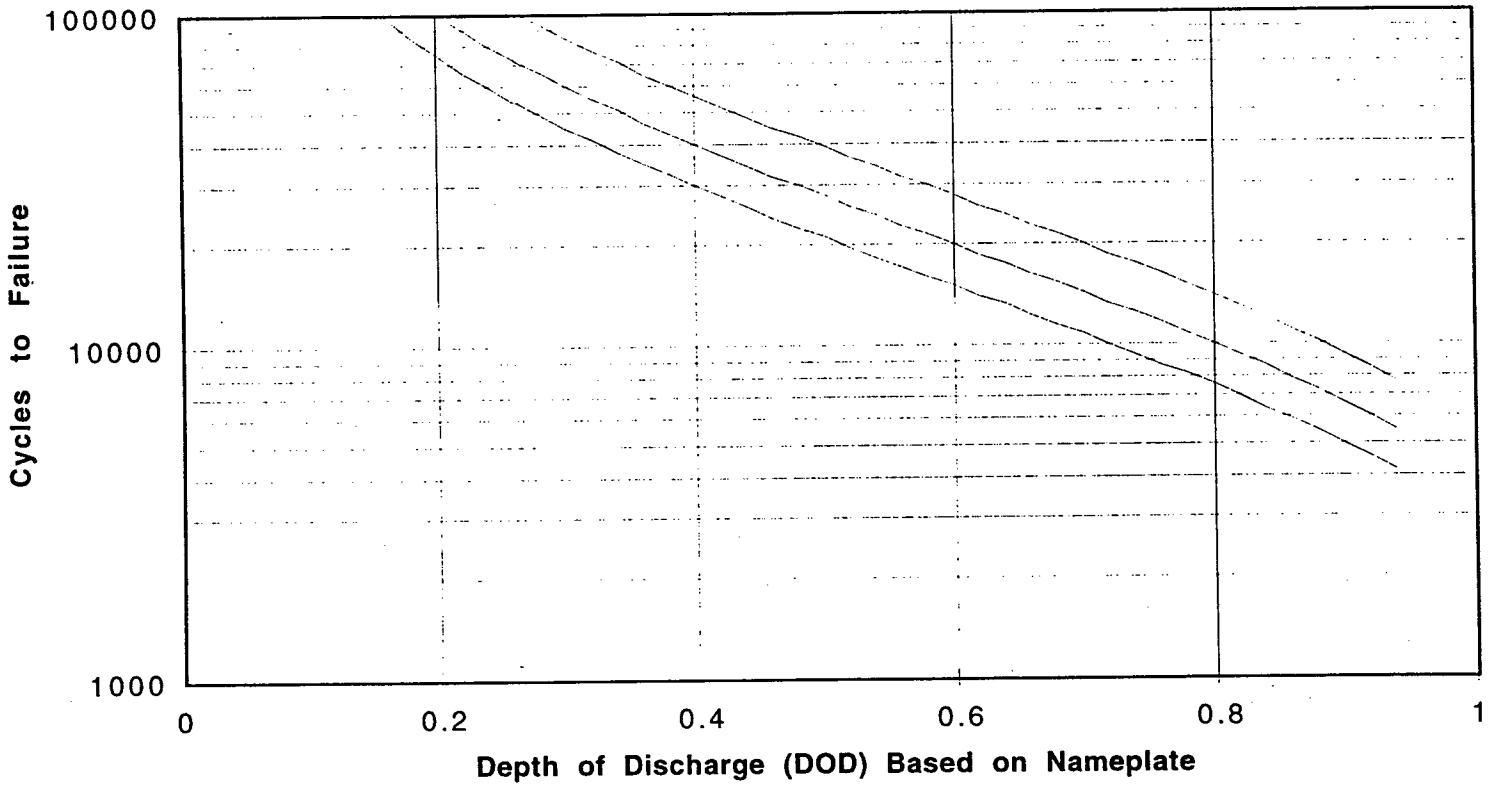

October 27- 29, 1998

NiH_2 Battery Reliability Update

MODIFIED EQUATION

- THE FORM OF THALLER'S EQUATION IS LIFE = (1 + f - DOD) / (A * DOD)
- CHANGE IN DENOMINATOR (THE RATE AT WHICH LIFE IS EXPENDED)
  - NOW MODELED TO BE LINEAR WITH DOD INSTEAD OF PROPORTIONAL
  - THE CONSTANT A IS MOVED TO THE NUMERATOR AND LABELED A'
- LIFE = A' * (1+ f - DOD) / (B + DOD)
- MODIFIED EQUATION SAYS LIFE IS LIMITED EVEN AT ZERO DOD
  - THE CONSTANT B MODELS THE REACTION RATE AT ZERO DOD

LOCKHEED MARTIN
Missiles & Space

NiH_2 Battery Reliability Update

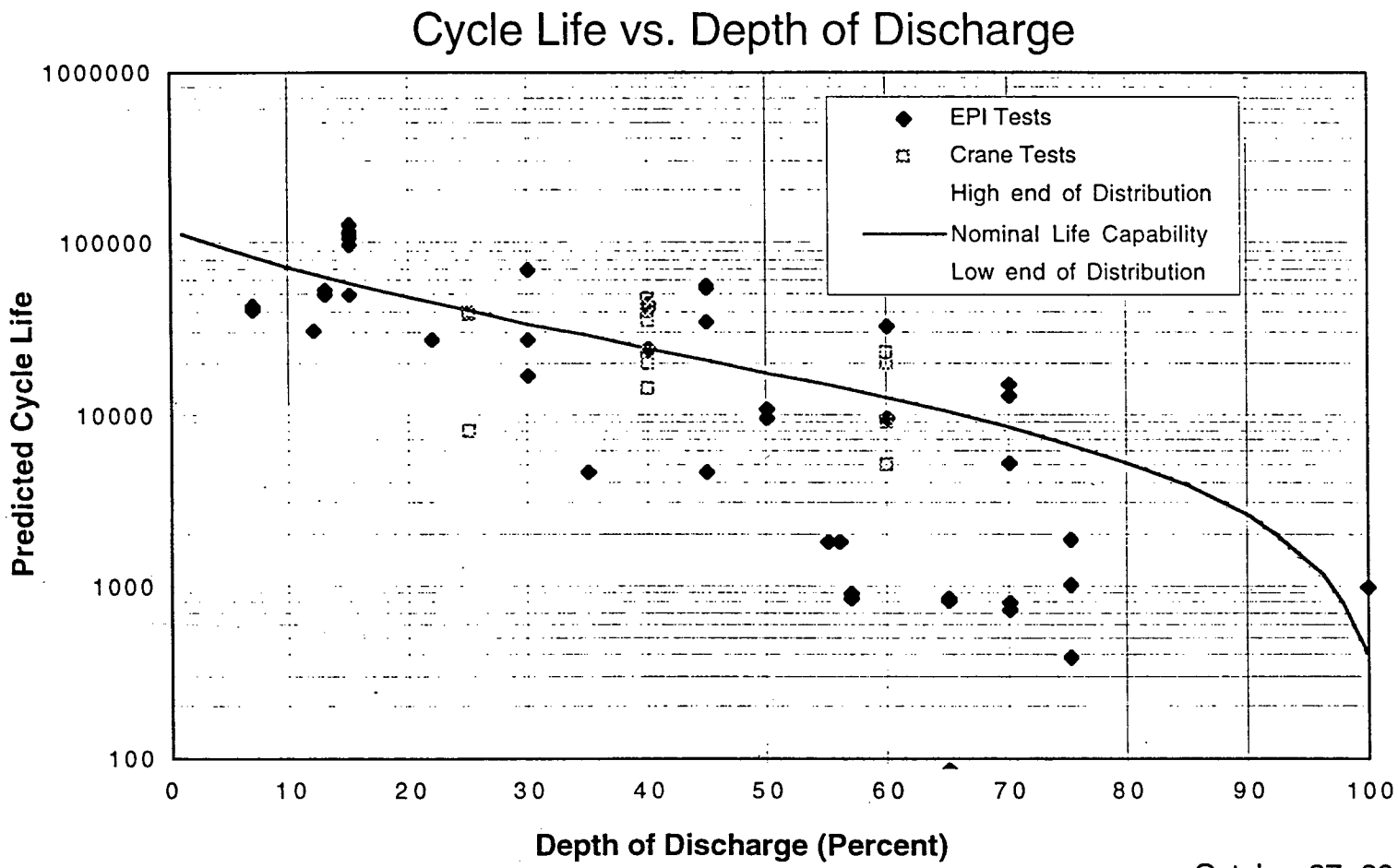

October 27- 29, 1998

LOCKHEED MARTIN
Missiles & Space

NiH_2 Battery Reliability Update

EXPLANATION OF WEIBULL PARAMETERS ALPHA AND BETA

- ALPHA IS THE SCALE PARAMETER FOR THE WEIBULL EQUATION.
  - CHARACTERISTIC TIME CORRESPONDING TO 63.2 PERCENTILE

- BETA IS THE SHAPE PARAMETER.
  - DESCRIBES BROADNESS OF DISTRIBUTION (LIKE STD DEV. IN A BELL CURVE)
  - HIGH BETA INDICATES A TIGHT DISTRIBUTION
  - LOW BETA INDICATES A BROAD DISTRIBUTION
  - SLOPE OF CUMULATIVE HAZARD VS. TIME-TO-FAILURE ON LOG-LOG PAPER

October 27- 29, 1998

LOCKHEED MARTIN
Missiles & Space

NiH_2 Battery Reliability Update

COMPLETE EQUATION SET

- CONSTANTS

  $A' = 35{,}000$
  $B = 0.2$
  $f = 0.02$
  $\beta = 13.7$ (value at 40% DOD from Hafen 1992 IECEC paper)

- EQUATIONS FOR RELIABILITY

  Dependence of α on DOD (DOD expressed as a fraction)

  $$\alpha = A' * (1 + f - DOD) / (B + DOD)$$

  Weibull model for relationship between cycle life and cell reliability

  $$\text{cycle life} = \alpha * (-\ln(R_{cell}))^{1/\beta}$$

- EQUATIONS RELATING CELL AND BATTERY RELIABILITY

  For no cell failures allowed

  $$R_{batt} = R_{cell}^{N}$$

  For one cell failure allowed

  $$R_{batt} = R_{cell}^{N} + N * (1 - R_{cell}) * R_{cell}^{N-1}$$

October 27- 29, 1998

LOCKHEED MARTIN
Missiles & Space

NiH_2 Battery Reliability Update

RELIABILITY VS. CYCLE LIFE

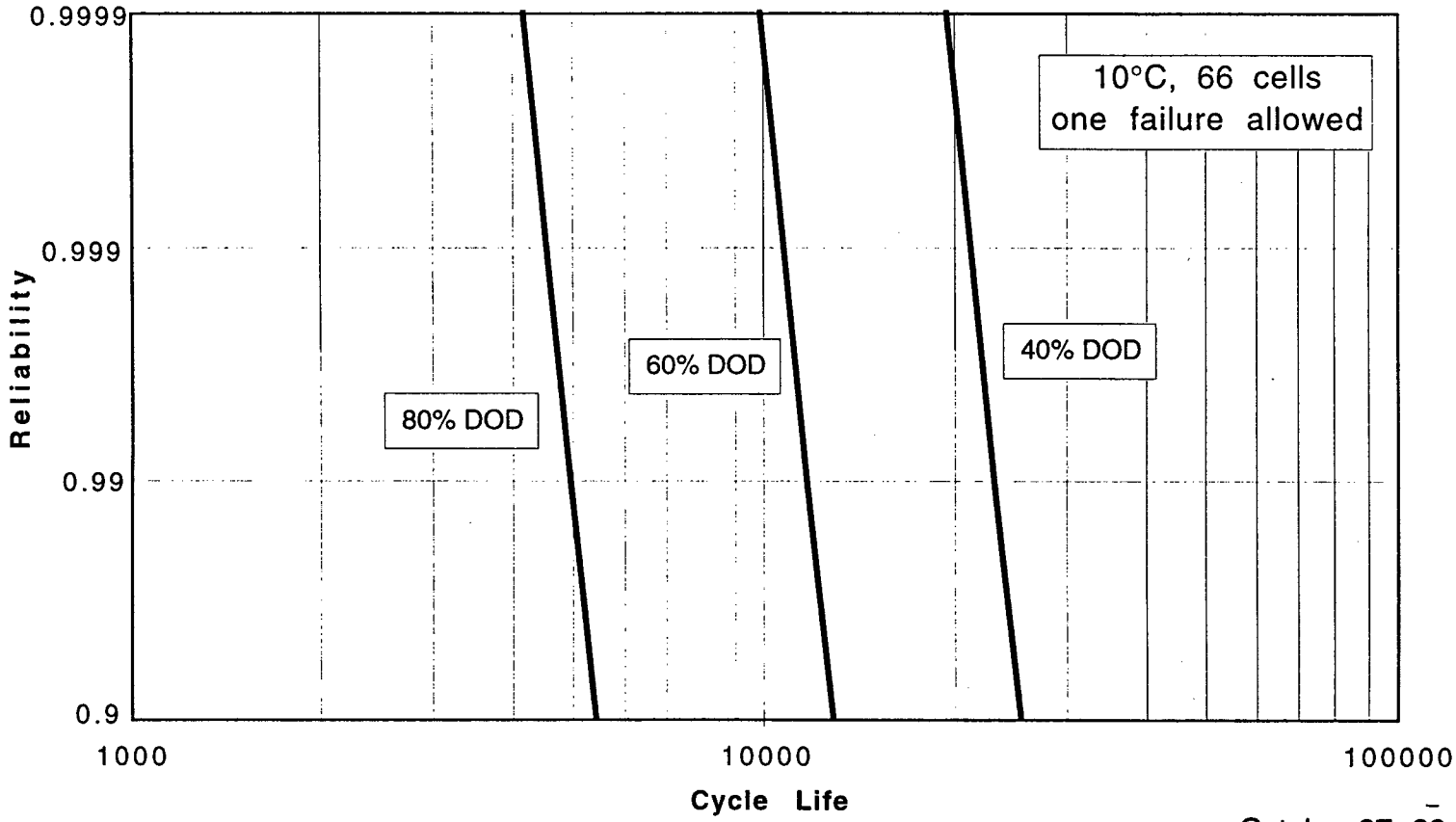

October 27- 29, 1998

LOCKHEED MARTIN
Missiles & Space

NiH_2 Battery Reliability Update

COMPARISON WITH PRIOR EQUATION

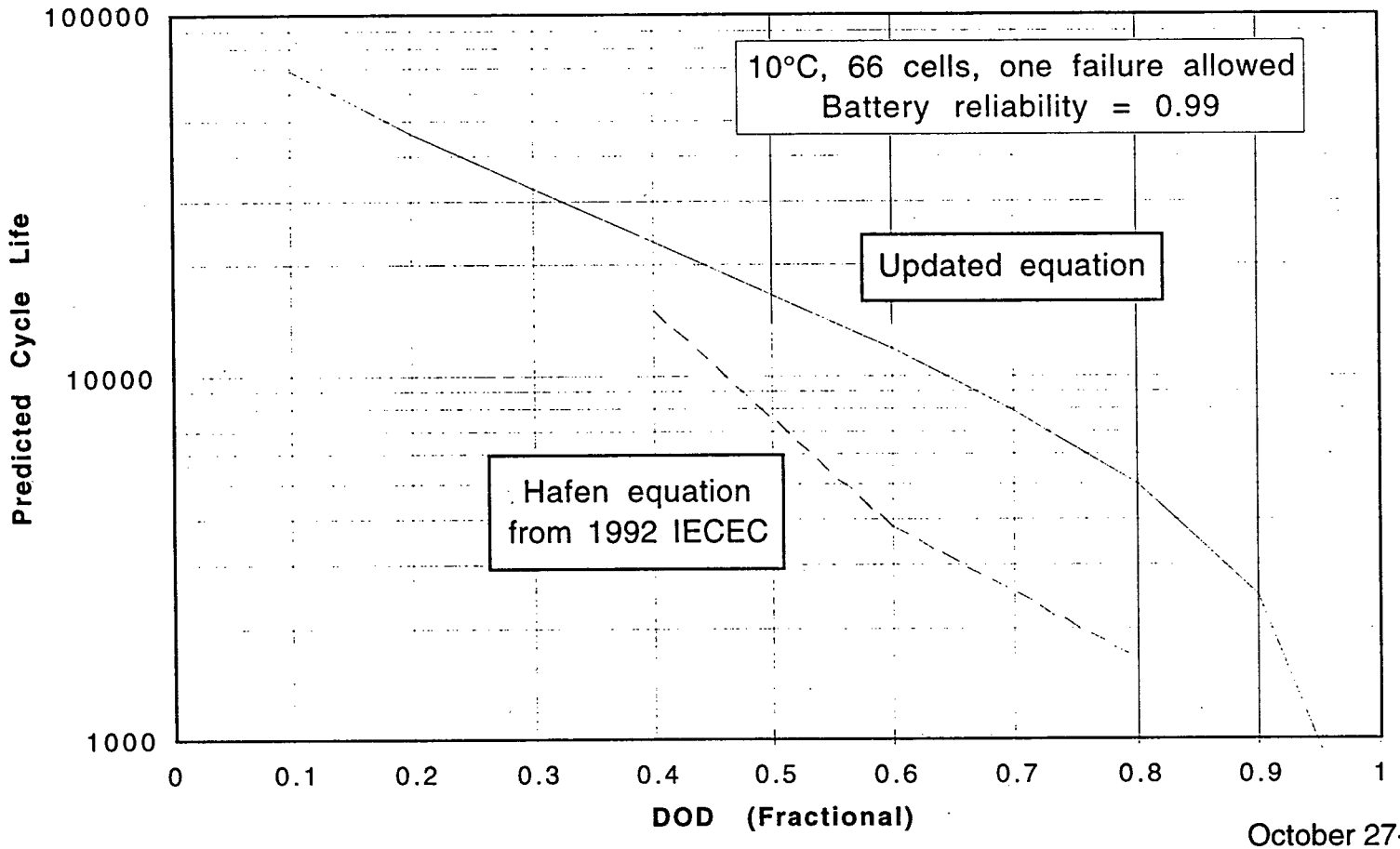

October 27- 29, 1998

LOCKHEED MARTIN
Missiles & Space

NiH_2 Battery Reliability Update

APPLICATION TO HST

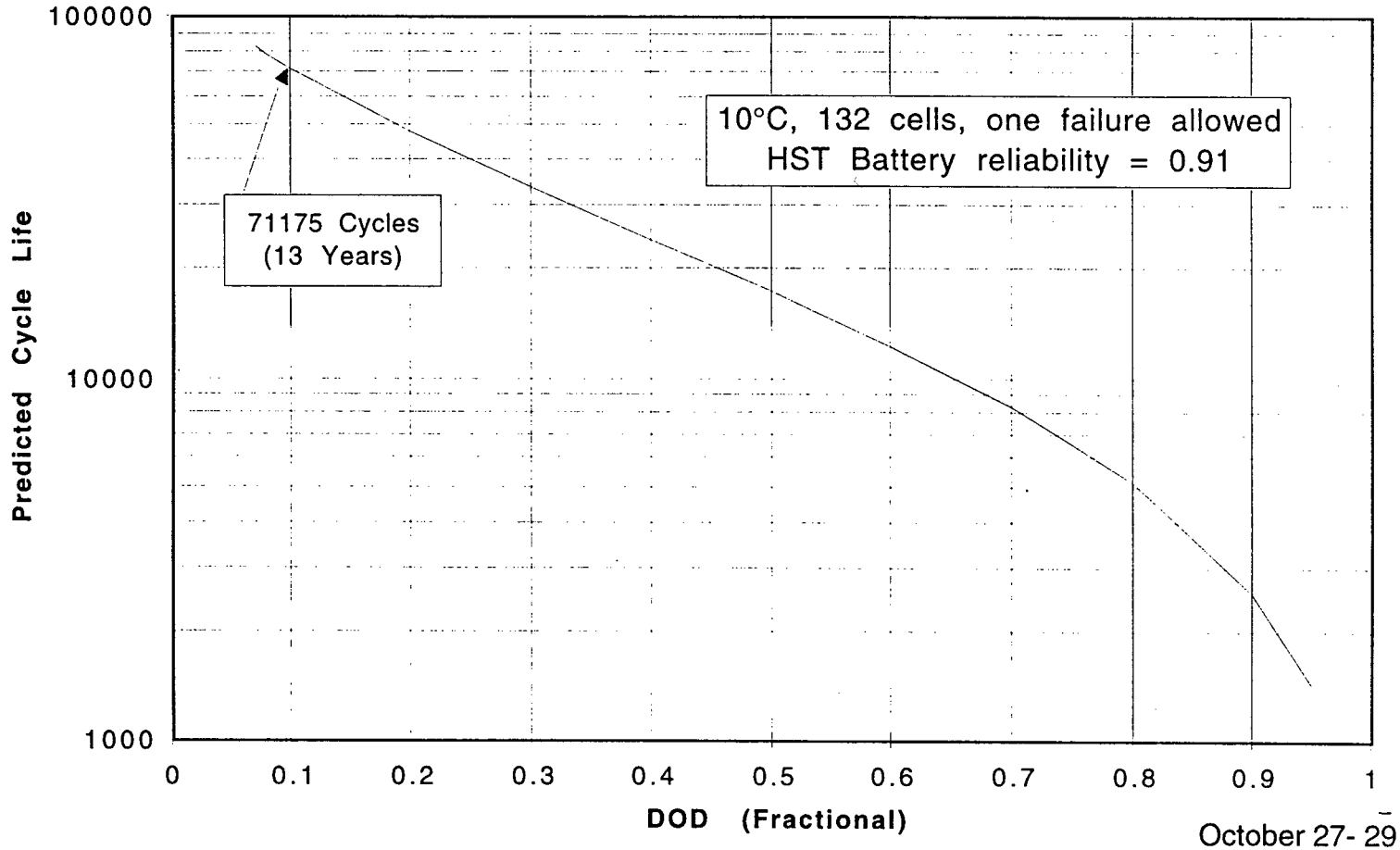

October 27- 29, 1998

NiH_2 Battery Reliability Update

CONCLUSIONS

- A RELIABILITY EQUATION HAS BEEN DEVELOPED FOR STATE-OF-THE-ART NICKEL HYDROGEN CELLS, SUCH AS USED ON HUBBLE SPACE TELESCOPE.
- THE EQUATION IS A RELATIONSHIP BETWEEN OPERATING DOD, CYCLES EXPERIENCED, BATTERY RELIABILITY, NUMBER OF BATTERIES/CELLS AND ALLOWABLE FAILURES.
- TYPICALLY THE SOLUTION BEING SOUGHT IS EITHER BATTERY RELIABILITY, MAXIMUM ALLOWABLE DOD, OR CYCLE LIFE WITH FOUR KNOWN QUANTITIES.
- OTHER RELATIONSHIPS SUCH AS PROBABILITY OF SUCCESS VS. CYCLE LIFE MAY ALSO BE DEVELOPED.
- THE EQUATION SET WILL NOT APPLY IF A LESS THAN OPTIMUM DESIGN IS USED. THALLER'S 1998 IECEC PAPER HAS A DISCUSSION OF CELL DESIGNS WHICH ARE EXPECTED TO HAVE LESS THAN OPTIMUM LIFE.

NiH_2 Battery Reliability Update

REFERENCES

Fox, C., Francisco, J., Ames, K., and Repplinger, R., 1997, "Life Cycling Testing of Spaceflight Qualified Nickel-Hydrogen Battery Cells", 1997 NASA Aerospace Battery Workshop Proceedings, NASA Conference Publication CP-1998-208536, pp. 429-456.

Hafen, D., 1992, "Comparison of Nickel-Hydrogen and Nickel-Cadmium Reliability for Low-Earth-Orbit Batteries", Proceedings of the 27th IECEC, IECEC Paper 929257.

Moore, B.A., Brown, H.M., and Hill, C.A., 1997, "Air Force Nickel-Hydrogen Testing at NAVSURFWARCENDIV Crane", Proceedings of the 32nd IECEC, pp. 186-191, IECEC Paper 97263.

Nelson, W., 1969, "Hazard Plotting for Incomplete Failure Data", J. Quality Tech., Vol. 1, pp. 27-52.

Thaller, L.H., 1993, "Cycle Life vs. Depth of Discharge Update on Modeling Studies", 1993 NASA Aerospace Battery Workshop Proceedings.

Thaller, L.H., 1998a, "Status of Degradation Rates and Mechanisms in Nickel-Hydrogen Cells", Proceedings of the 33rd IECEC, IECEC Paper 98-1043.

Thaller, L.H., 1998b, "Nickel-Hydrogen Cell Designs for Deep DOD LEO Applications", 1998 Space Power Workshop.

HIGH DOD LEO LIFE CYCLE TESTING

Jeff Dermott

Eagle-Picher Technologies, LLC

Joplin, Missouri

Background

- ✦ Life Test at 70% DOD was started 4 years ago.
- ✦ Original intent was to qualify cells produced at the Range Line Facility (RLF).
- ✦ Test data is useful for high DOD cell design.

Test Set-up

- ✦ Standard Acceptance Test cooling cart.
- ✦ Cells mounted in aluminum cooling blocks (minimize dome to dome thermal gradients).
- ✦ Test temperature controlled at 0C based on average upper dome temperature.
- ✦ Nameplate capacity of cells is 56 AH.

EAGLE PICHER
Eagle-Picher Technologies, LLC

POWER Subsystems
Range Line Facility

Life Test Cycle Regime

- ✦ **Test Uses High Rate 70% DOD Cycles to Accumulate Wear on the Cells**
- ✦ **Every 1000 Cycles the Cells are Run for 100 Cycles at 40% DOD as a Health Check**

EAGLE PICHER
Eagle-Picher Technologies, LLC

POWER Subsystems
Range Line Facility

Life Test Cycle Regime

- **Test Temperature = 0C**
- **70% DOD Cycles:**
  - **Charge at a C Rate With a Taper at the End of Charge**
  - **Discharge at a 1.2C Rate for 35 Minutes**
  - **RR = 110%, Total Cycle Time = 90 Minutes**
- **40% DOD Cycles:**
  - **Charge at a C/2 Rate With a Taper at the End of Charge**
  - **Discharge at a C/1.45 Rate for 35 Minutes**
  - **RR = 105%, Total Cycle Time = 90 Minutes**

EAGLE PICHER
Eagle-Picher Technologies, LLC

POWER Subsystems
Range Line Facility

Description of Cells in Test

Cell Lot	Identifier	Positive Porosity	Positive Thick.	Electrolyte (% KOH)	# of Cells
Boiler Plate	Control	80%	0.030"	31%	3
Boiler Plate	BP-V3	80%	0.035"	26%	4
Boiler Plate	BP-V4	84%	0.035"	26%	4
Engineer. Models	EM-V2	80%	0.035"	31%	3

- ✦All cells are in pressure vessels.
- ✦All cells contain slurry plaque from EPT's Range Line Facility

EAGLE PICHER
Eagle-Picher Technologies, LLC

POWER Subsystems
Range Line Facility

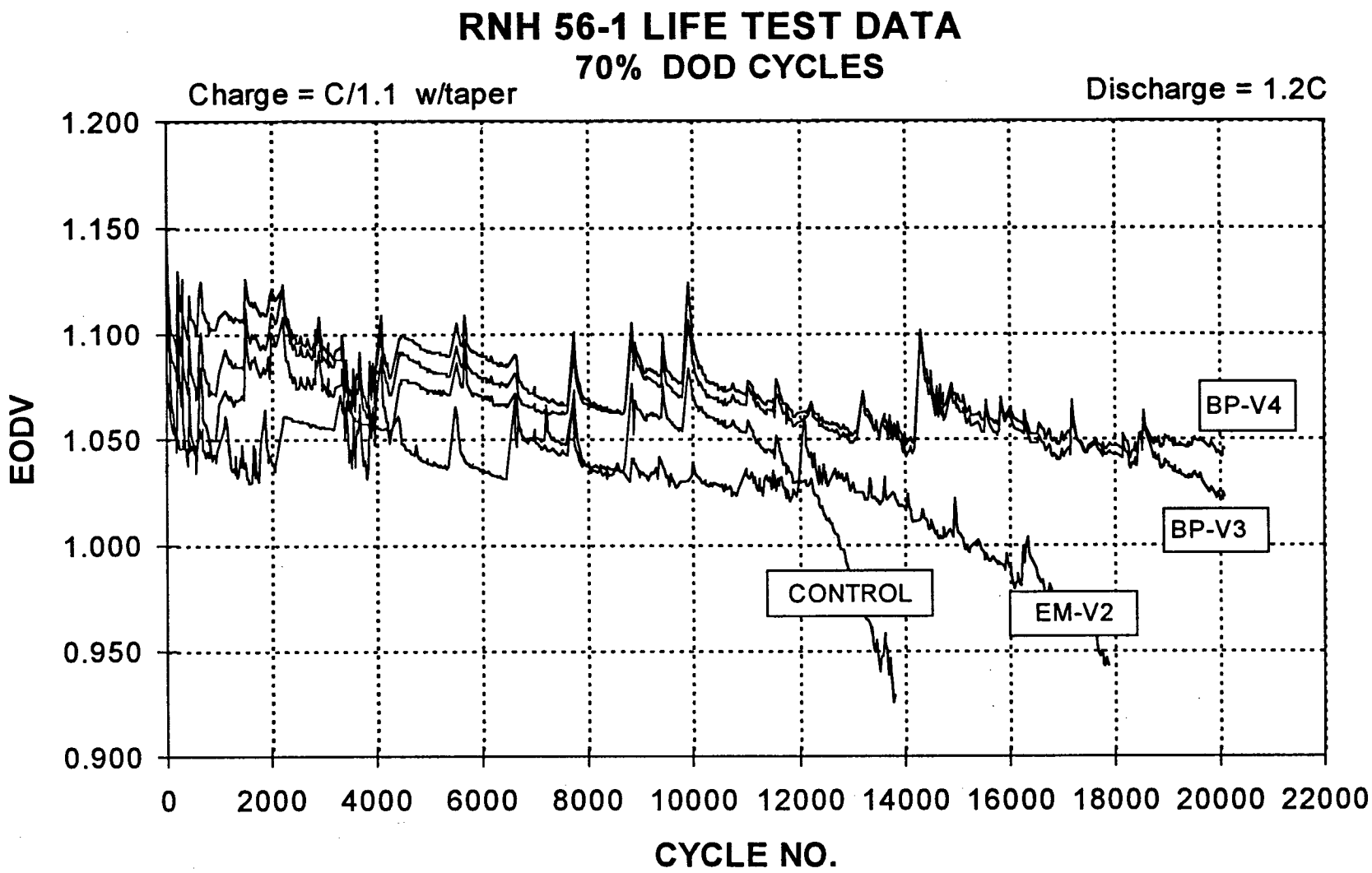

EAGLE PICHER
Eagle-Picher Technologies, LLC

POWER Subsystems
Range Line Facility

RNH 56-1 LIFE TEST DATA
70% DOD CYCLES

Charge = C/1.1 w/taper

Discharge = 1.2C

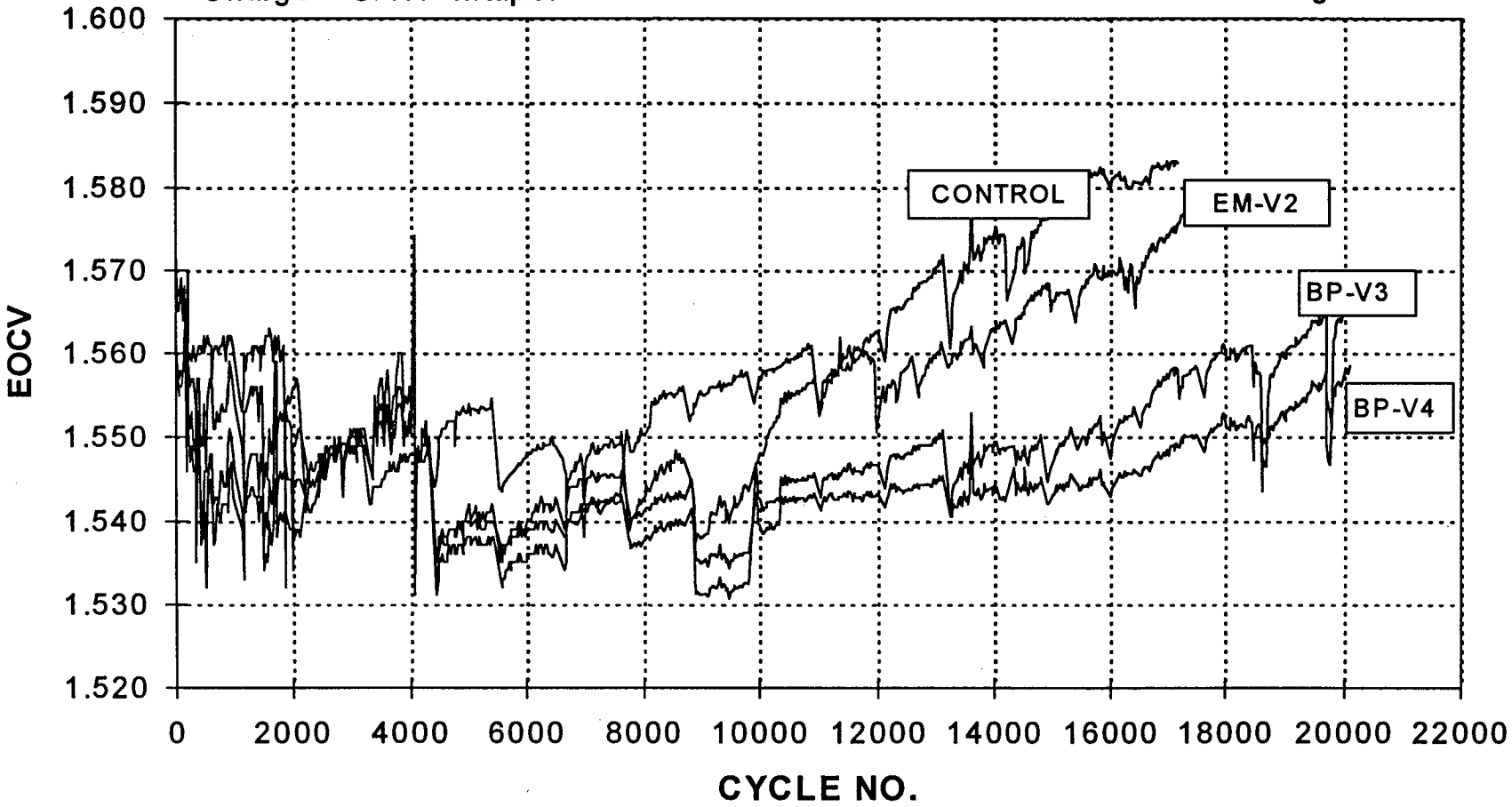

Test Status

- Two cells were removed from the test @cycle 15,800 for EOL performance characterization.
- These cells were a Control and BP-V4.
- The BOL Acceptance test was repeated on the cells.
- A DPA of each cell was also performed.

EAGLE PICHER
Eagle-Picher Technologies, LLC

POWER Subsystems
Range Line Facility

RNH 56-1 LIFE TEST DATA

40% DOD, CYCLE 15,800

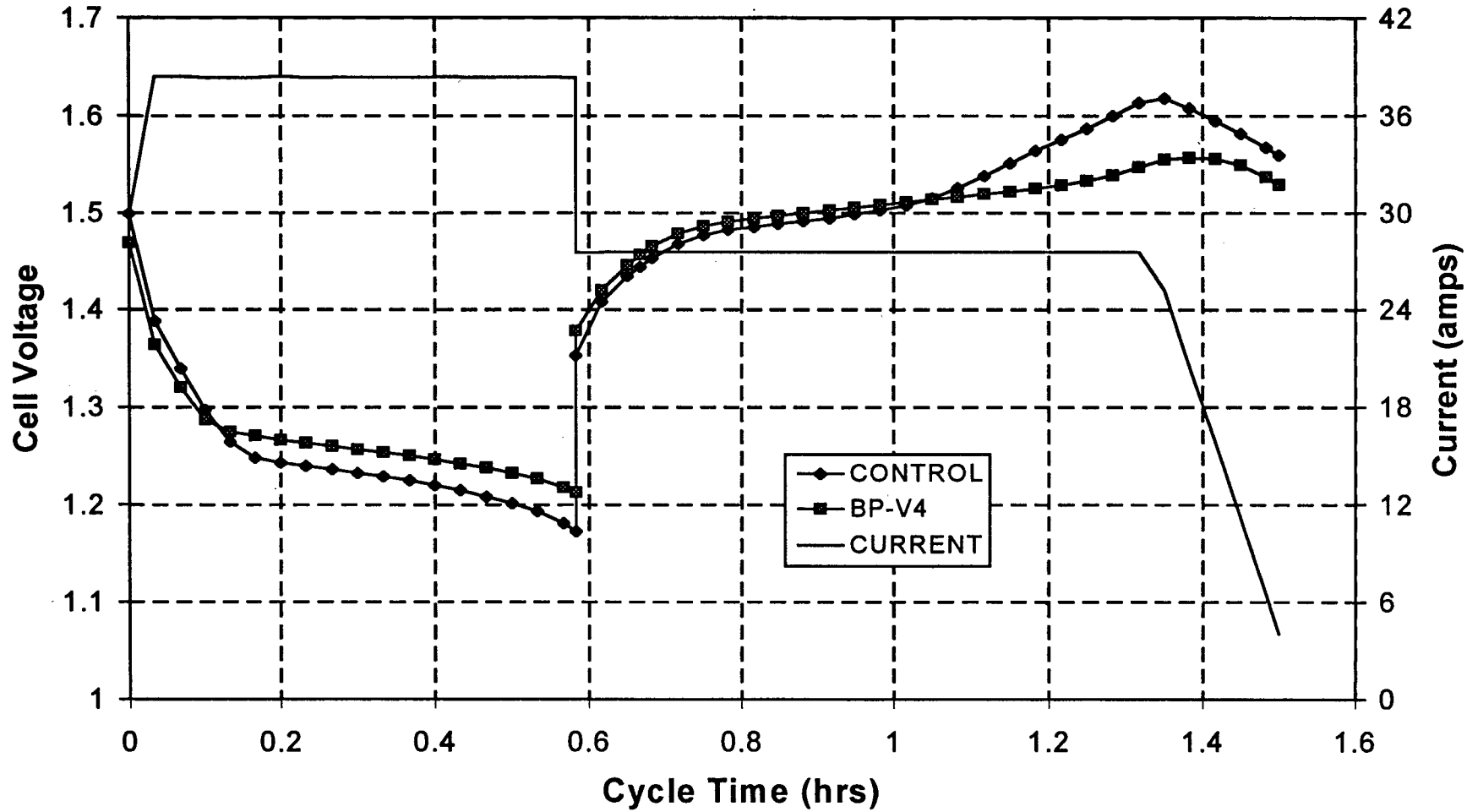

EAGLE PICHER
Eagle-Picher Technologies, LLC

POWER Subsystems
Range Line Facility

CAPACITY DATA

CAPACITY TO 1.0V

CELL	0 deg C (AH)			10 deg C (AH)			20 deg C (AH)	
	BOL	EOL		BOL	EOL		BOL	EOL
Control	67.4	40.3		63.1	41.9		53.4	38.5
BP-V4	64.2	50.6		60.1	49.2		52.3	43.9

- ✦ **Cells showed EOC pressure increase of 100 psig.**
- ✦ **BOL Specific Energy = 50 whr/kg (Control)**
- ✦ **BOL Specific Energy = 53 whr/kg (BP-V4)**

EAGLE PICHER
Eagle-Picher Technologies, LLC

POWER Subsystems
Range Line Facility

DPA Summary

- Stack components of both cells were in good physical condition.
- Electrode Growth
  - Control Cell = 0.003 inches
  - BP-V4 Cell = 0.008 inches
- Electrolyte analysis is being conducted (concentration and distribution)
- Flooded capacity of positive electrodes will be performed.

EAGLE PICHER
Eagle-Picher Technologies, LLC

POWER Subsystems
Range Line Facility

Conclusions

- 35mil electrode cells are providing equivalent cycle life to the 30mil electrodes.
- 26% KOH cells, with 35mil electrodes have shown superior cycle life with equivalent BOL energy densities to 30mil, 31%KOH cells.
- Cycle count is significant and can be used to update existing cycle life models.

EAGLE PICHER
Eagle-Picher Technologies, LLC

POWER Subsystems
Range Line Facility

Acknowledgments

- ✦ *Chris Guilfoyle:* **Eagle-Picher Technologies, LLC**
- ✦ *David Judd:* **Eagle-Picher Technologies, LLC**
- ✦ *Dan DeBiccari:* **Space Systems/Loral**

Ni- H_2 Batteries Performance on Communication and Broadcasting Engineering Test Satellite

1998 NASA Aerospace Battery Workshop
October 27～29,1998

H.Kusawake, Y.Sone, K.Kanno, T.Nakamura, & S.Kuwajima

National Space Development Agency of Japan

Ni- H_2 Batteries Performance on COMETS

1998 NASA Aerospace
Battery Workshop
October 27-29, 1998

CONTENTS

Communication and Broadcasting Engineering Test Satellite

Major Performance, On-Board

Topics(Boost Maneuver Operation)

Performance on Ground Test

Communication and Broadcasting Engineering Test Satellite

1998 NASA Aerospace
Battery Workshop
October 27-29, 1998

Configuration	Structure 2m×3m×3m Box shape Solar paddle 3m×15m(cantilever)
Weight	3.9 tons at lift off 2 tons at Initial geostationary stage
Power	GaAs Solar Cell - Flexible Solar Paddle Approx. 5.5kW(EOL) Ni-H2 Battery DOD≦70%
Attitude Control	Three-axis stabilized Controlled bias momentum type
Unified Propulsion	1700N Apogee kick engine NTO, N2H4-Bi-propellant 50N Thruster × 4 1N Thruster × 8 (redundant) N2H4-mono-propellant
Design Life	3 years
Launch Vehicle	H-Ⅱ rocket
Mission	Inter-orbit Communication Mission Advanced Satellite Broadcasting Mission Advanced Mobile Satellite Communication Mission

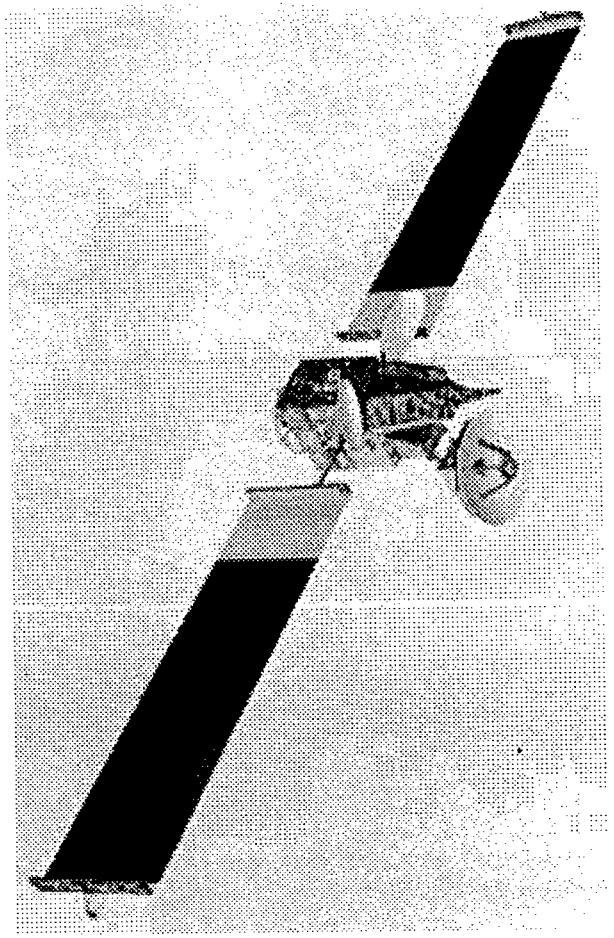

35Ah SPACE Ni-H2 CELL

1998 NASA Aerospace
Battery Workshop
October 27-29, 1998

Cell Major Specifications

Rated Capacity		35Ah
Life	GEO(DOD80%)	10Years, 1000cycle
	LEO(DOD40%)	5Years, 30000cycle
Weight		max. 1076g
Energy Density		40Wh/kg
Mechanical Strength	Burst Pressure	min. 140kgf/cm2
	Pressure Cycling	5000cycle(14-70kgf/cm2)

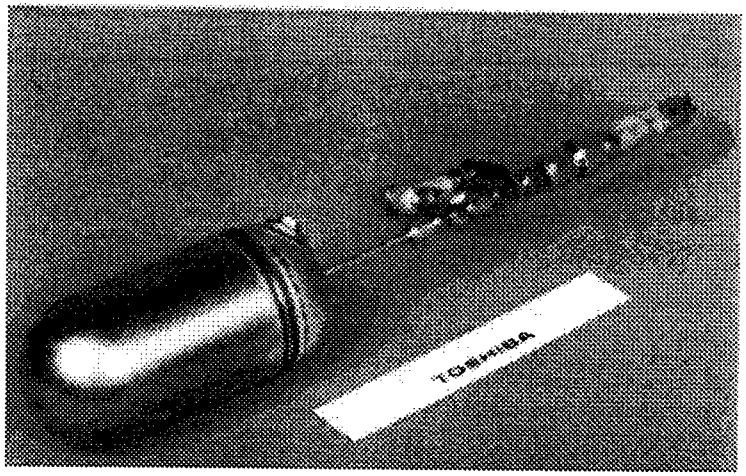

COMETS Ni-H_2 Battery (unit B)

1998 NASA Aerospace
Battery Workshop
October 27-29, 1998

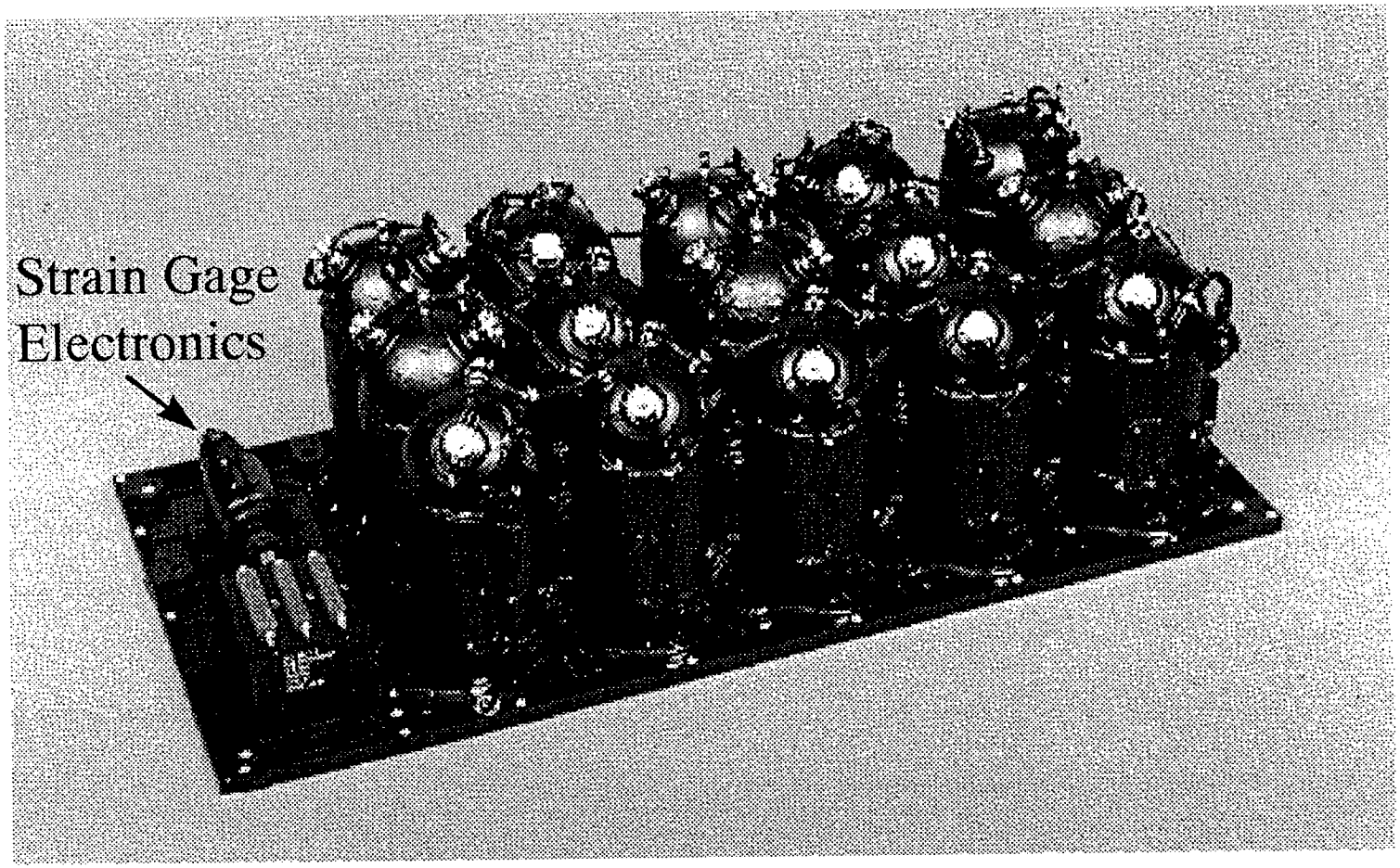

NASDA

National Space Development Agency of Japan

Main Specifications of 35Ah Ni-H_2 Battery

Cell	Toshiba 35Ah
Weight	22.95kg/unit A(16cell)
	22.05kg/unit A(15cell)
Volume	315(T) * 650(W) * 203(H) mm/unit
Charge Scheme	Full/Trickle
	(Command & Automatic by temp.)
Full Charge Rate	2.1 ± 0.6A
Trickle Charge Rate	0.7 ± 0.2A
Max. Discharge Rate	20.4A(normally parallel)
Max. Depth of Discharge	70%(@72min)
Mission Life	Longer than 3years(@GEO)
Reconditioning Load	60.6 Ω
Operating Temperature	-10 ~ 35° C

COMETS uses 4 batteries, consists of unit A & B.

NASDA

National Space Development Agency of Japan

Simplified Block Diagram of COMETS EPS

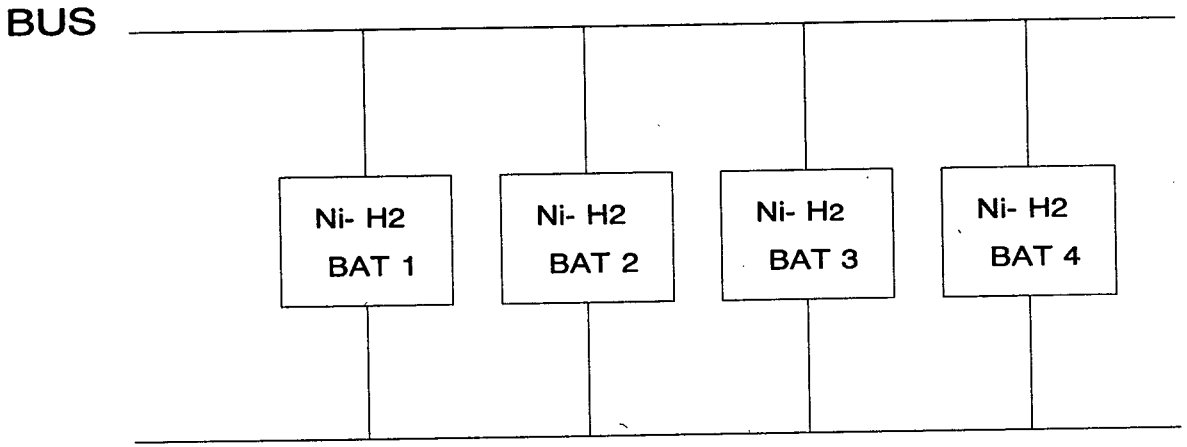

All Ni-H2 batteries are charged during sunshine time and discharged during eclipse time simultaneously.

Boost Maneuver Operation (1/2)

COMETS was not injected into the expected geostationary transfer orbit in February 1998, because of launch vehicle failure.

We decided 7 times maneuvers for getting higher apogee altitude using apogee engine to realize the longer experimental conditions.

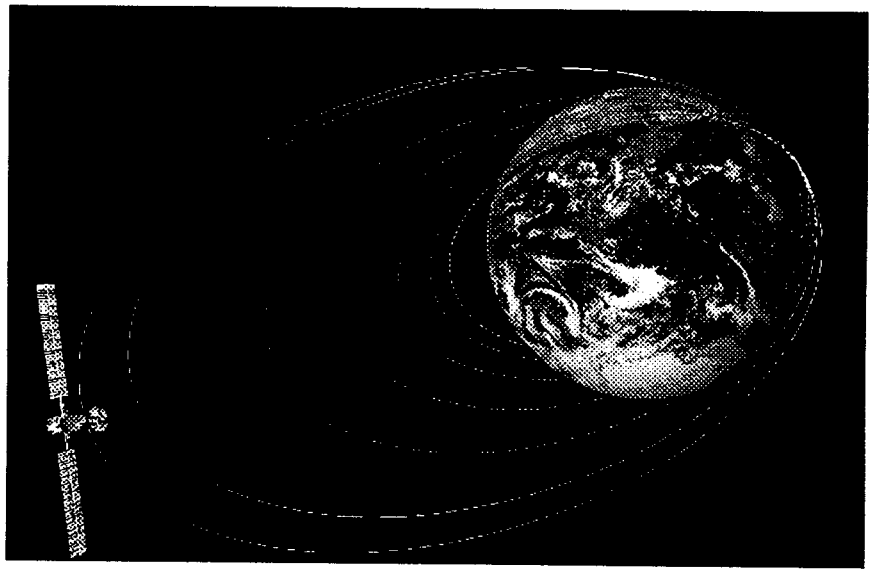

Boost Maneuvers Operation

1998 NASA Aerospace
Battery Workshop
October 27-29, 1998

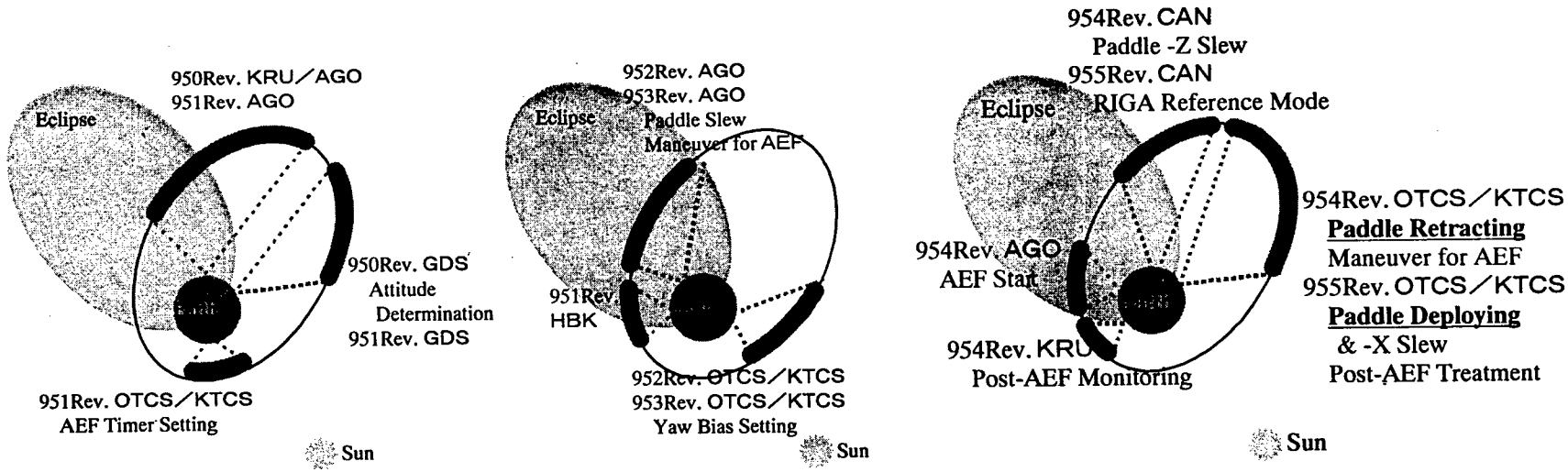

Relations between visibility of ground stations and orbit trajectory
"Discrete operations" for maneuvers #3

Battery Operations

- Ni-H2 Batteries are charged by charge arrays, thus charge rate was not enough to balance charge amount with discharge amount, until Boost Maneuver Operation finished.
- We decided a special heater operation which saved the discharge amount of batteries.
- DOD on Boost Maneuver Operation was Max. 70%. DOD was estimated by pressure of batteries.
- Ni-H2 Batteries are continuing to work over 1700 cycles at DOD 15%, average.

Boost Maneuver Operation (2/2)

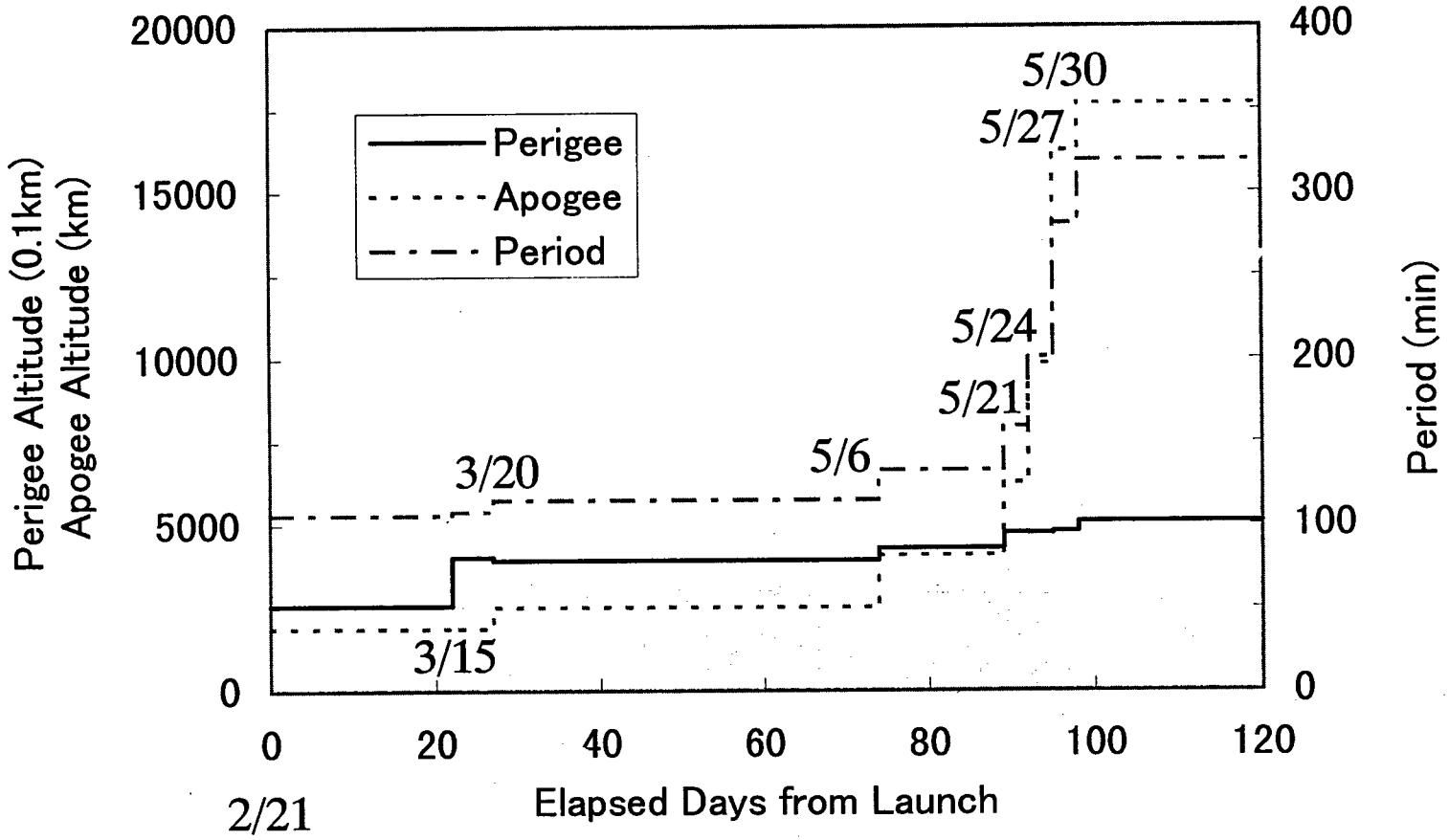

Orbital Eclipse Profile

1998 NASA Aerospace
Battery Workshop
October 27-29, 1998

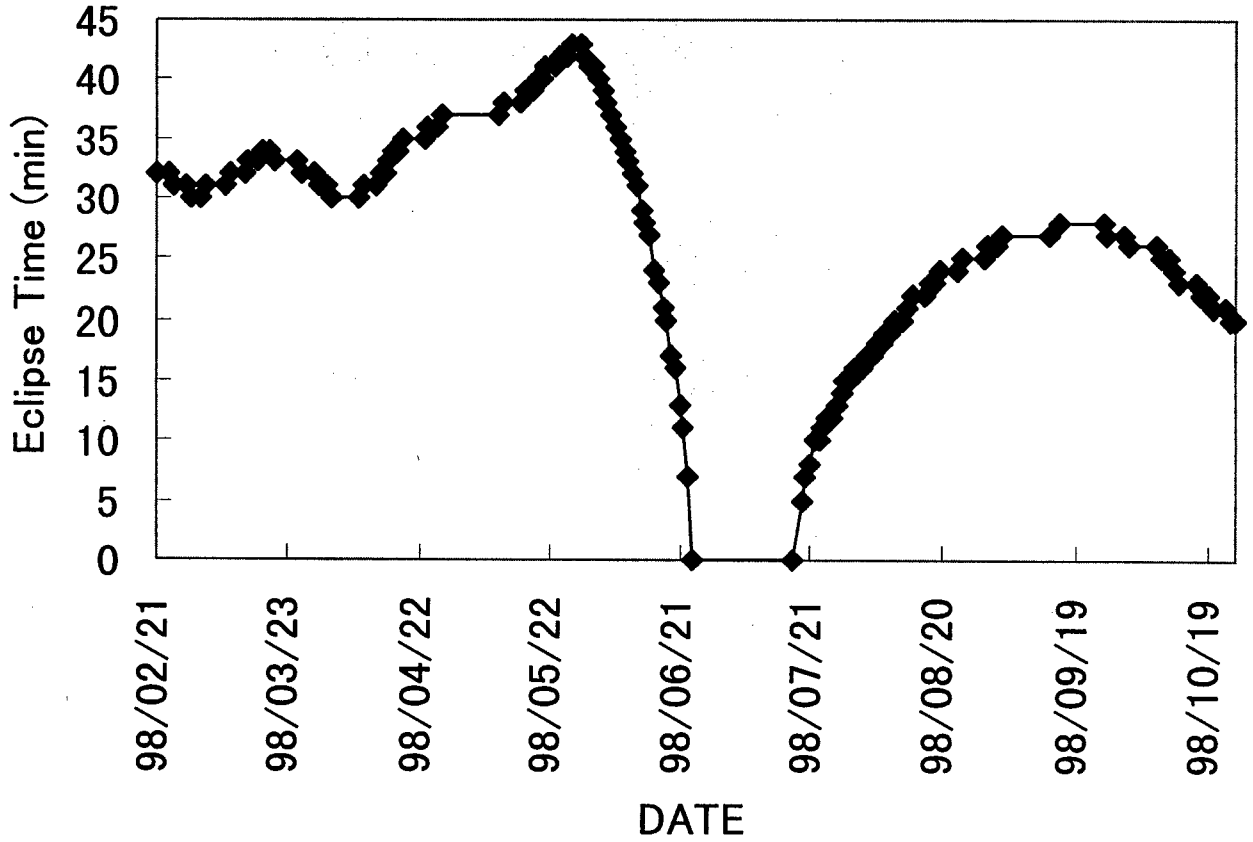

Generated Power

1998 NASA Aerospace
Battery Workshop
October 27-29, 1998

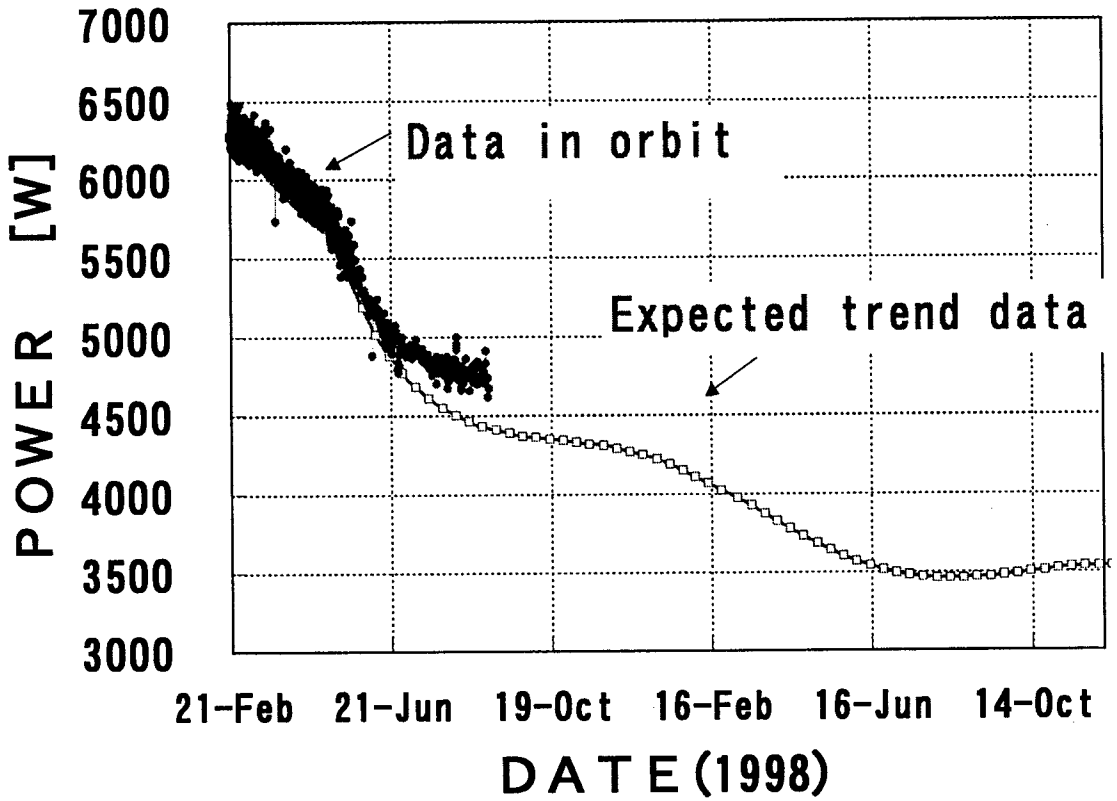

COMETS goes through the Van Allen(radiation) belts.
Thus generated power decreases remarkably.

Progress of Operation on Orbit

	1998 2 3 4 5 6 7 8 9			
EVENT	▲ LAUNCH ▲ ▲ Boost Maneuvers ▲ Operation ▲▲▲▲			
Orbital profile		1st eclipse season	1st full sun season	2nd eclipse season
Operation of Ni-H2 batteries		1289cyc	trickle charge	≧ 400cyc

Trend of 35Ah Ni-H2 Batteries

1998 NASA Aerospace
Battery Workshop
October 27-29, 1998

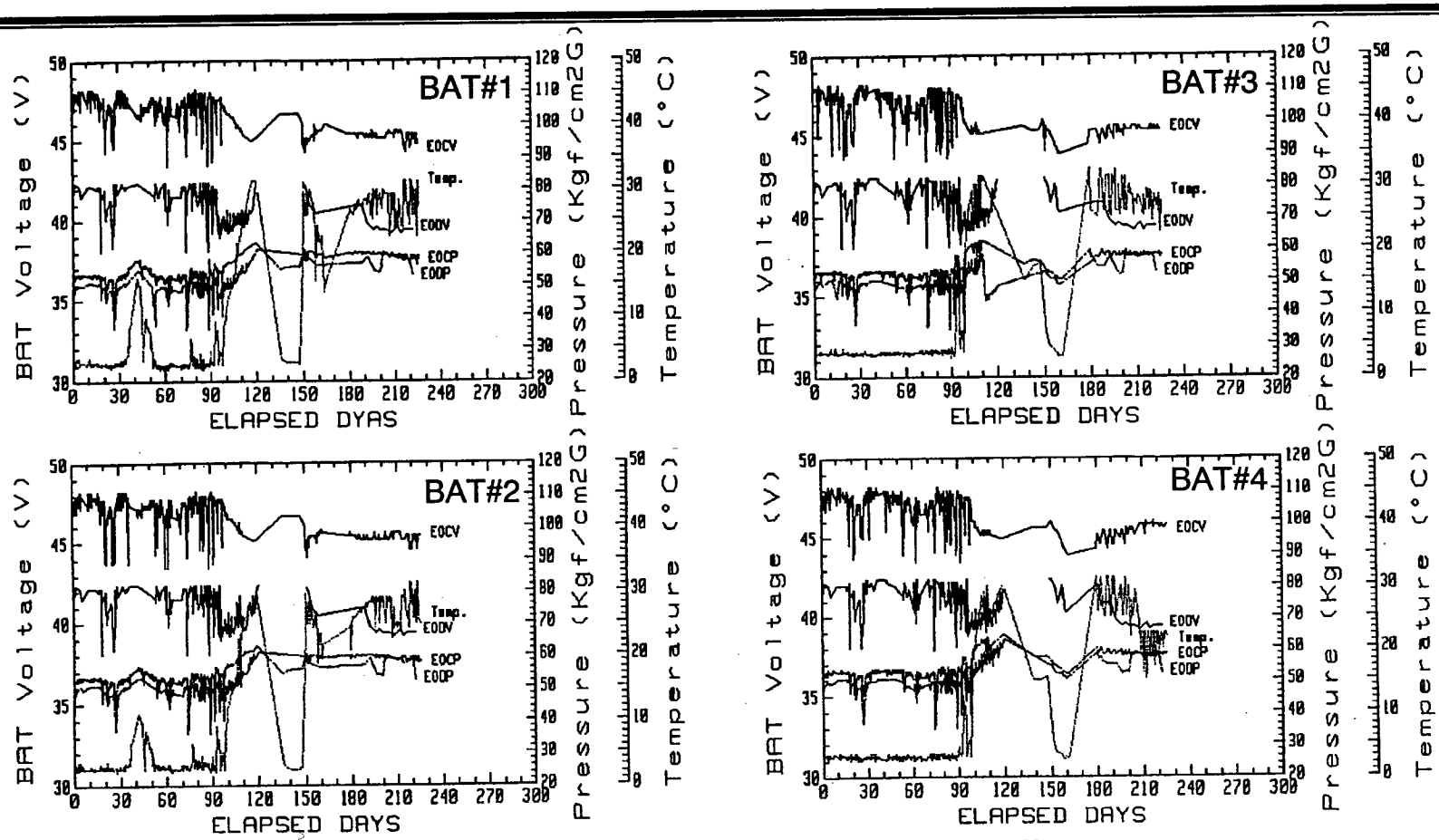

All batteries had good performance until now.

EOCV & EODV of Ni-H2 Cells(2nd Eclipse Season)

1998 NASA Aerospace Battery Workshop
October 27-29, 1998

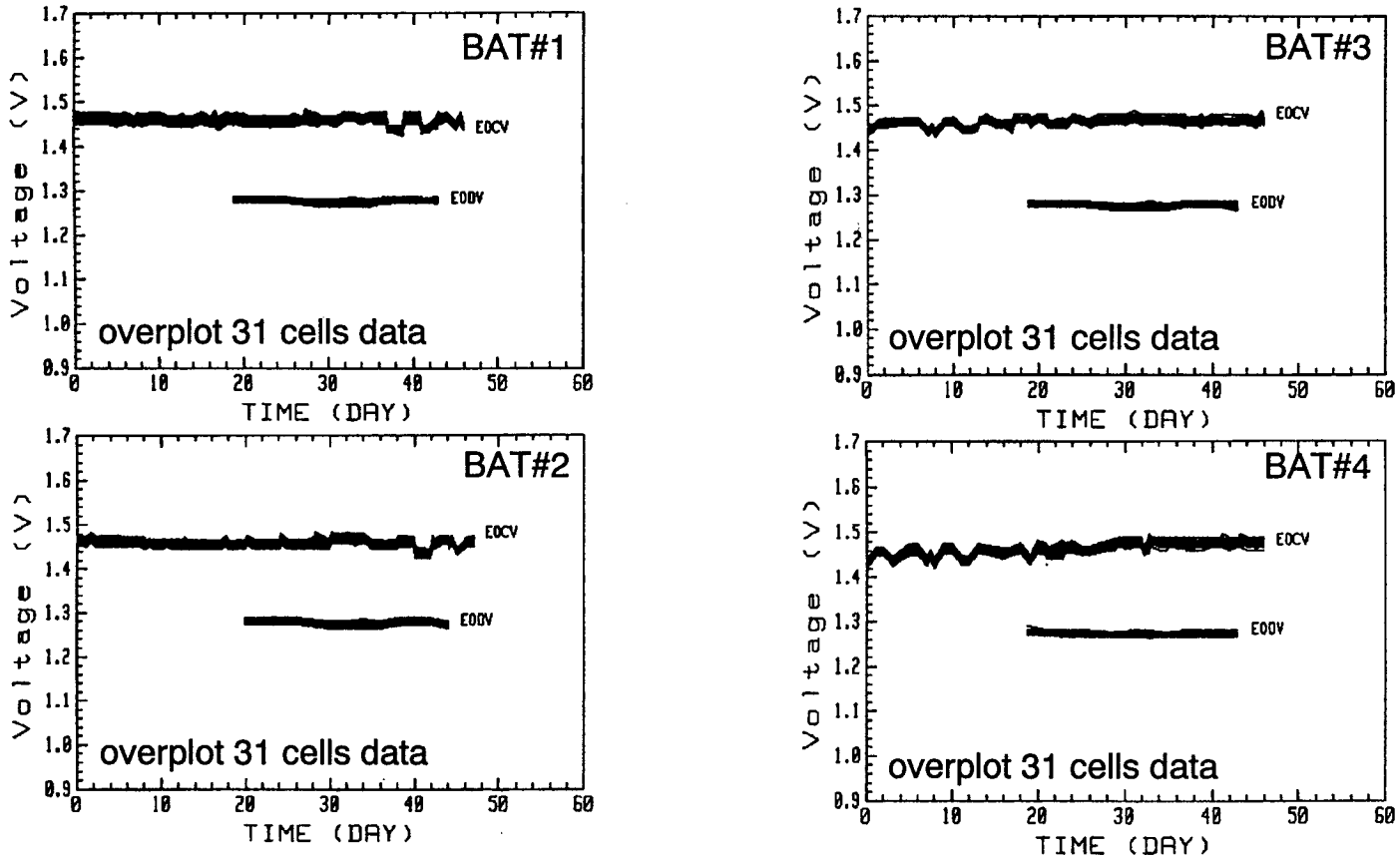

The EOCV and EODV of battery cells coincides with each other.

Trend of 35Ah Ni-H2 Batteries(1st Full Sunshine Season)

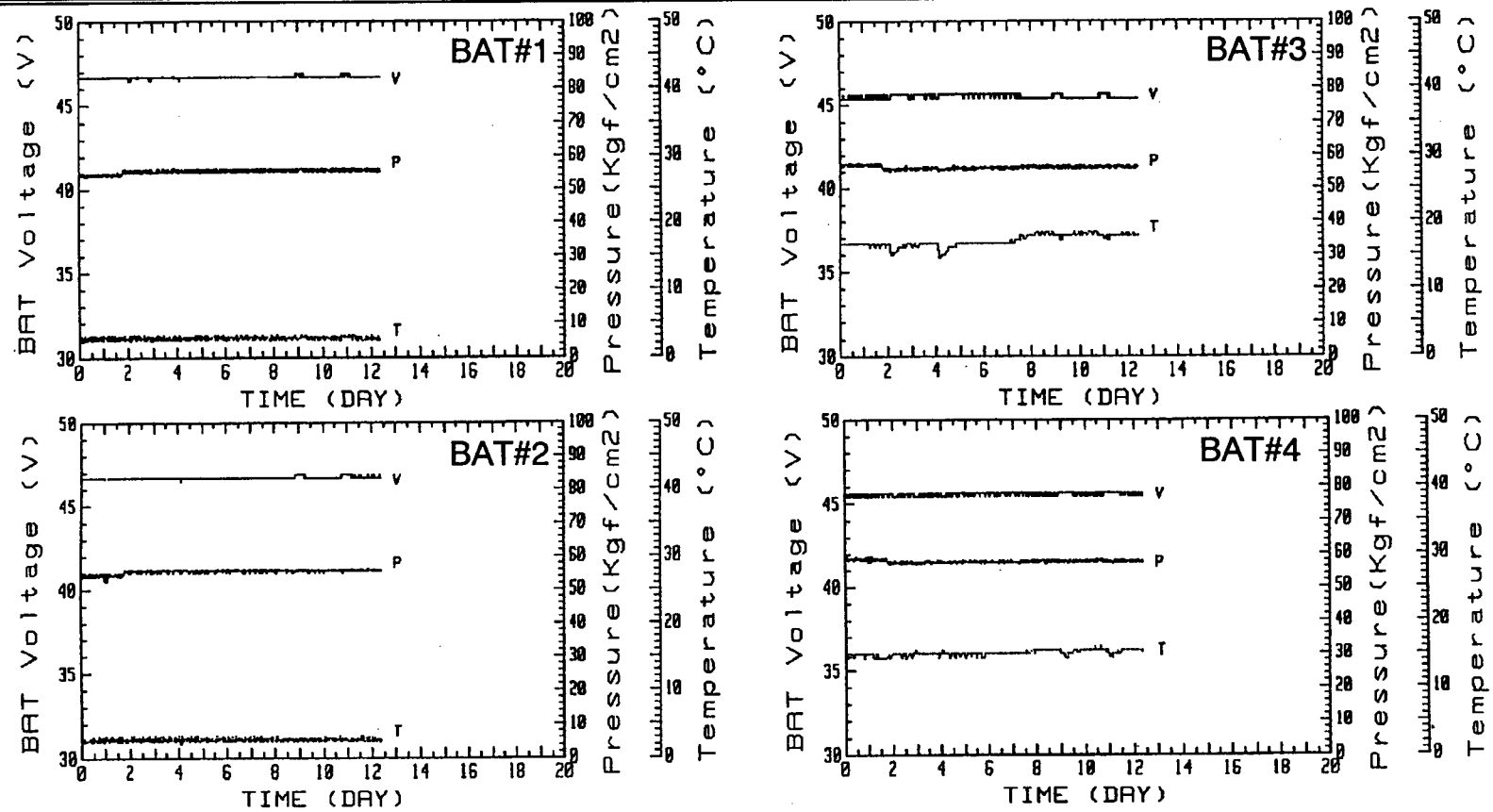

All batteries had stable performance during full sunshine season.

Charge & Discharge Characteristics

1998 NASA Aerospace
Battery Workshop
October 27-29, 1998

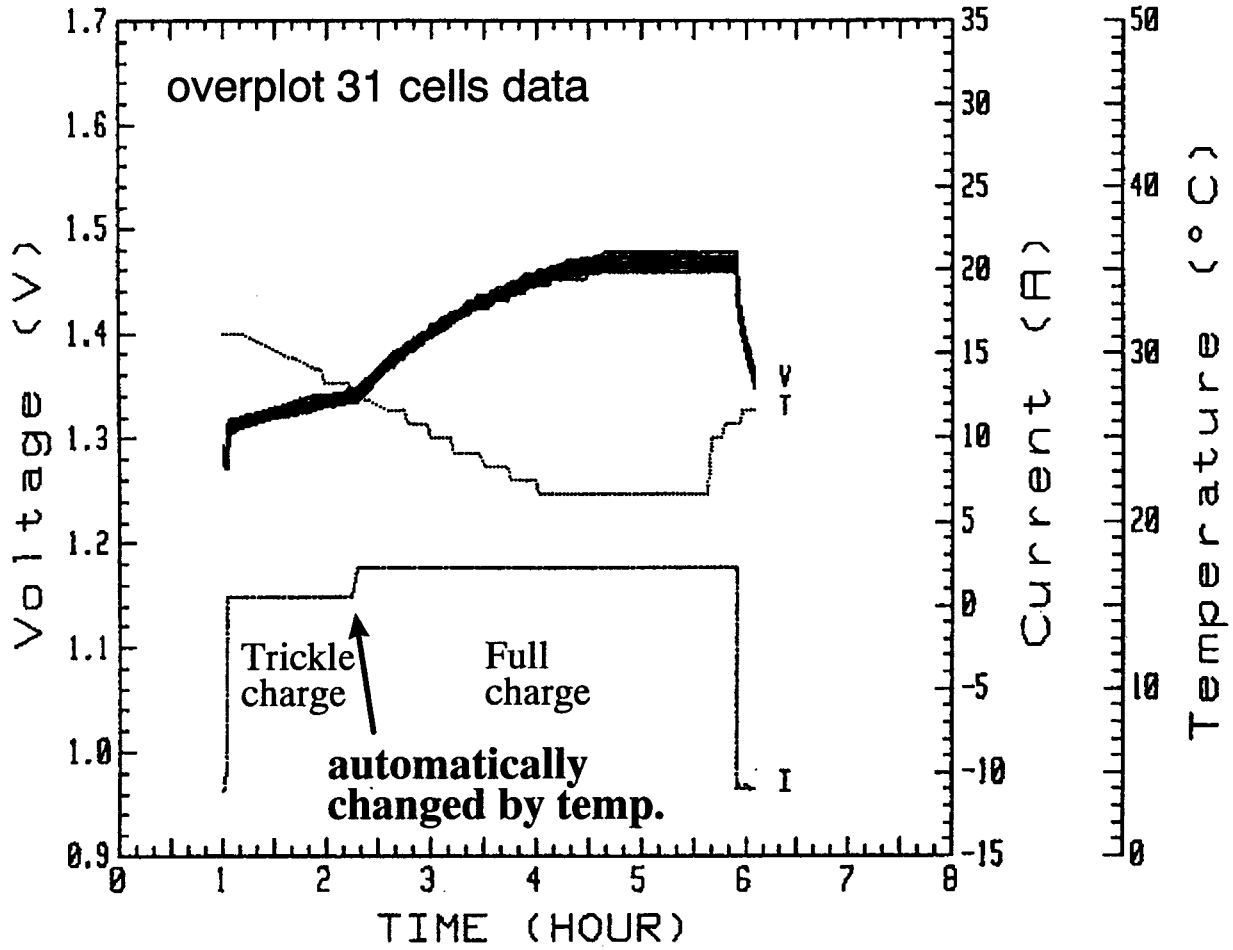

NASDA

National Space Development Agency of Japan

Ni-H2 Battery performance on the Maneuver

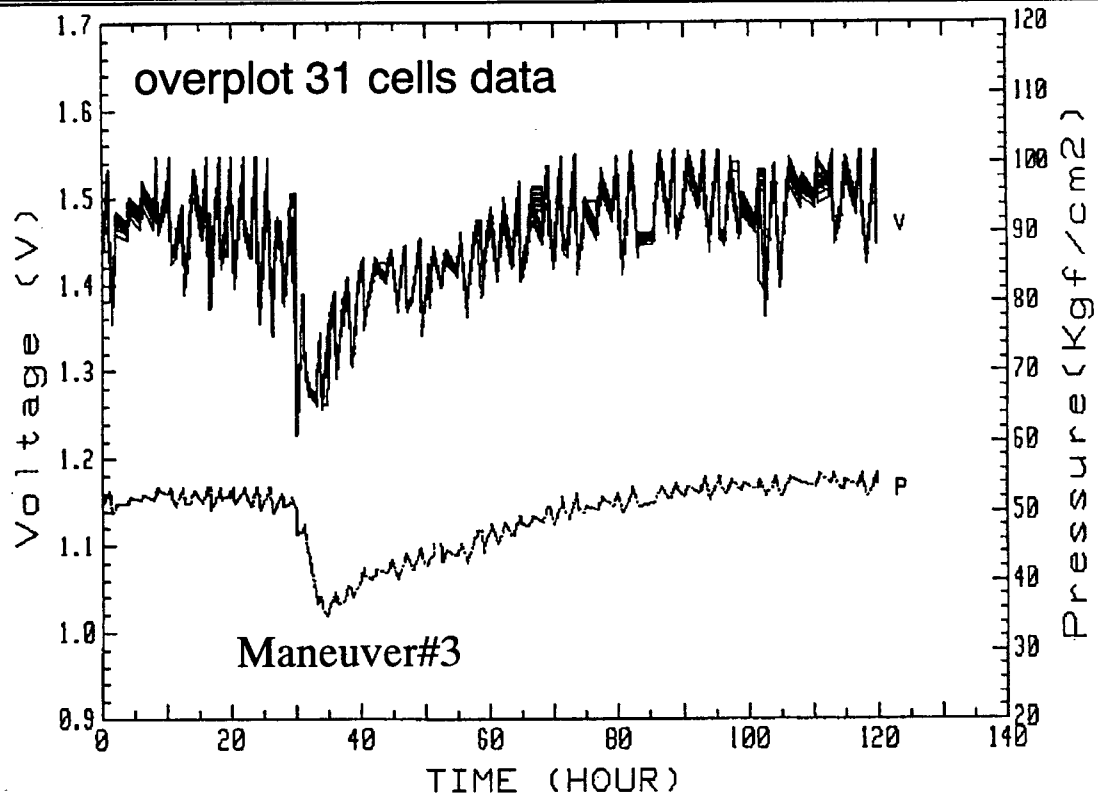

Ni-H2 Battery worked well during Boost Maneuver Operation.

Transition of Depth of Discharge

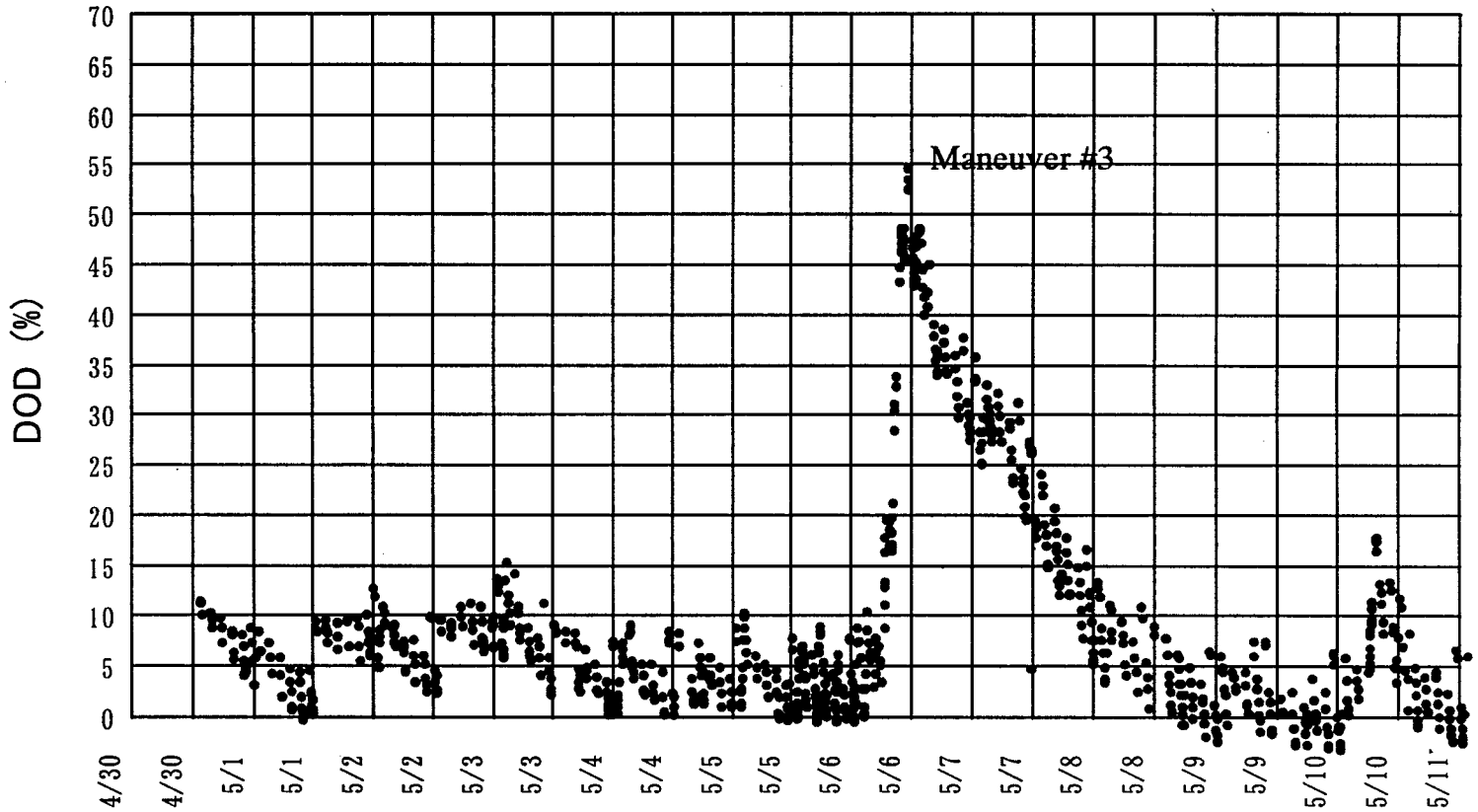

DOD was estimated by pressure of batteries.

Re-deployment of Flexible Paddle

1998 NASA Aerospace
Battery Workshop
October 27-29, 1998

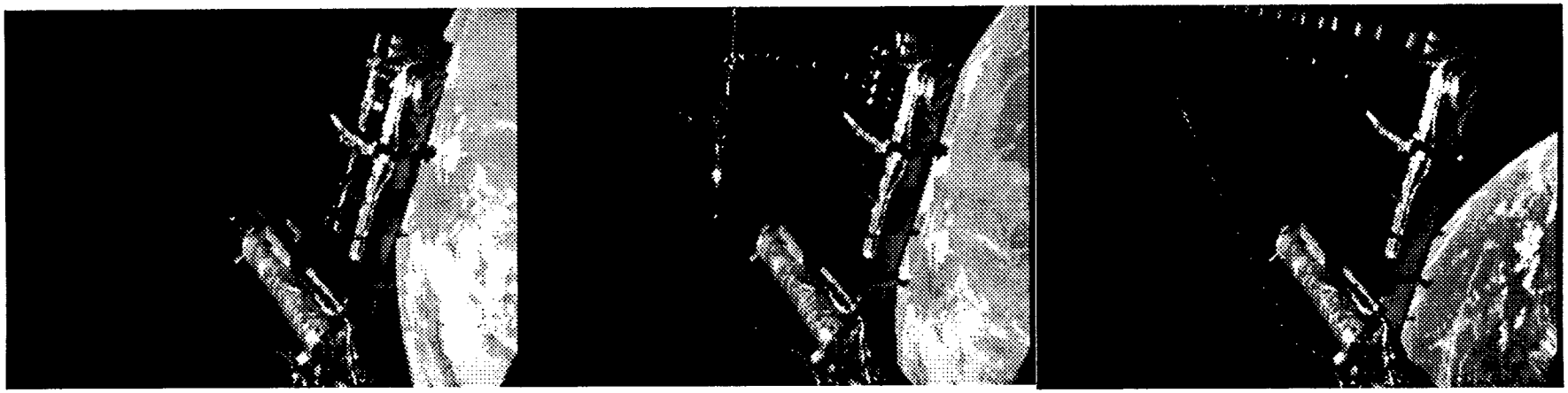

Just after | 2min. after | Completion of

20 May on maneuver #4

NASDA

National Space Development Agency of Japan

Ground Test Data of QT Ni-H2 Cell

1998 NASA Aerospace
Battery Workshop
October 27-29, 1998

DOD80% GEO

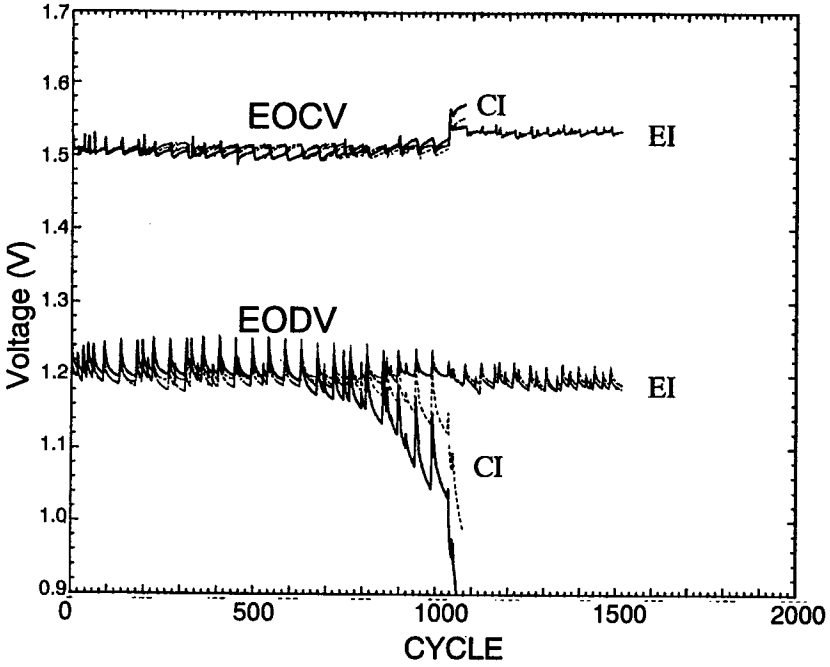

DOD40% LEO

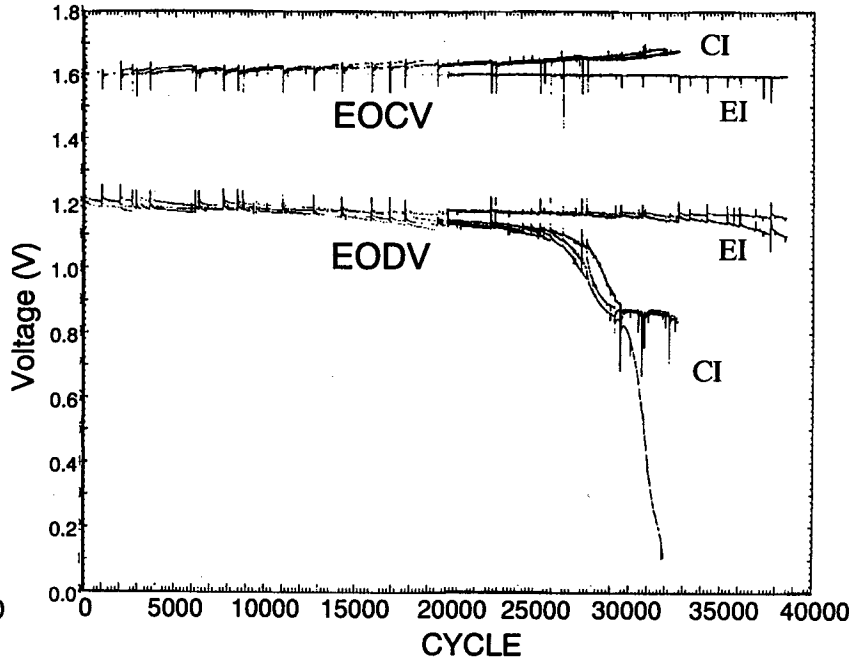

Ni-H2 cell satisfied 1500 cycle on GEO & 35000 cycle on LEO.

Schedule of Battery Development in NASDA

1998 NASA Aerospace
Battery Workshop
October 27-29, 1998

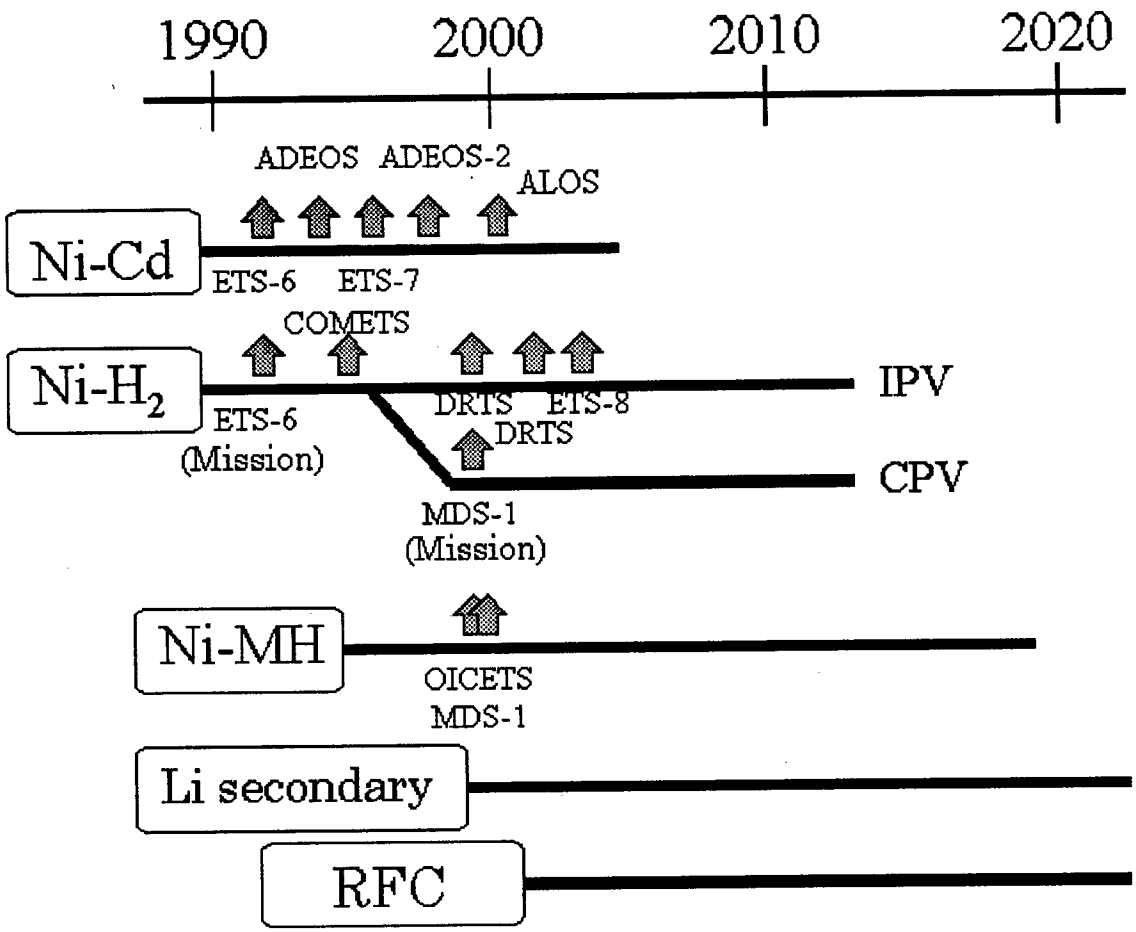

NASDA

National Space Development Agency of Japan

CONCLUSION

- COMETS has 35Ah Ni-H2 batteries as bus equipment. All batteries are continuing to work well during over 8 months on high elliptical orbit.

- It is confirmed that Ni-H2 cells must satisfy requirements, based on COMETS flight results as well as ground test results.

- 50Ah Ni-H2 cells will be used for Data Relay Test Satellite (DRTS-E) to be launched in 2000, and DRTS-W to be launched in 2002.

- 100Ah Ni-H2 cells will be used for Engineering Test Satellite-Ⅷ(ETS-Ⅷ) to be launched in 2002.

- CPV Ni-H2 cells(5Ah × 16 series) will be tested on-board Mission Demonstration Test Satellite-1(MDS-1) to be launched in 2000.

EAGLE PICHER
Eagle-Picher Technologies, LLC

POWER Subsystems

REVERSAL AS A TOOL FOR ASSESSING PRECHARGE OF NICKEL HYDROGEN CELLS

Jack N. Brill
Ron Smith

Technology Concerns

- Extended Wet Storage Has Increased Concern With Respect to a Nickel Hydrogen Cell's Precharge.
  - Positive Precharge Prevents the Capacity Fade Seen in Early Cell Designs Using Hydrogen Precharge.
  - Evidence of Loss of Positive Precharge During Ground Use Has Led to an Interest in Identifying a Precharge Signature.

- Knowing the Cell's Precharge Allows the User to Better Define Storage Methods.

Test Procedure

- Two Cells Were Tested to Determine the Voltage Signature When in Reversal at Low Rates.
  - Fully Charged Cells Were Discharged to 0.9 Volts Per Cell.
  - The Discharge Then Continued at a C/100 Rate Until a Voltage of -1.20 Volts Was Reached.
  - Capacities Between 0.9 And 0.0 Volts and 0.0 To -0.6 Volts Were Recorded.
  - Each Cell Was Charged at a C/100 Rate to 0.7 Volts
  - The Cells Were Fully Charged and Then Discharged to 0.9 Volts.
  - Each Cell Was Then Resistor (0.2 ohms) Drained to 0.1 Volts.
  - The Cells Were Opened and Discharged Under a Constant Hydrogen Supply With 0.2 Ohm Resistors to 0.1 Volts.
  - The Cells Were Sealed With a Hydrogen Precharge Established.
  - The Above Procedure Was Repeated.

EAGLE PICHER
Eagle-Picher Technologies, LLC

POWER Subsystems

Conditioning Discharge With Positive Precharge

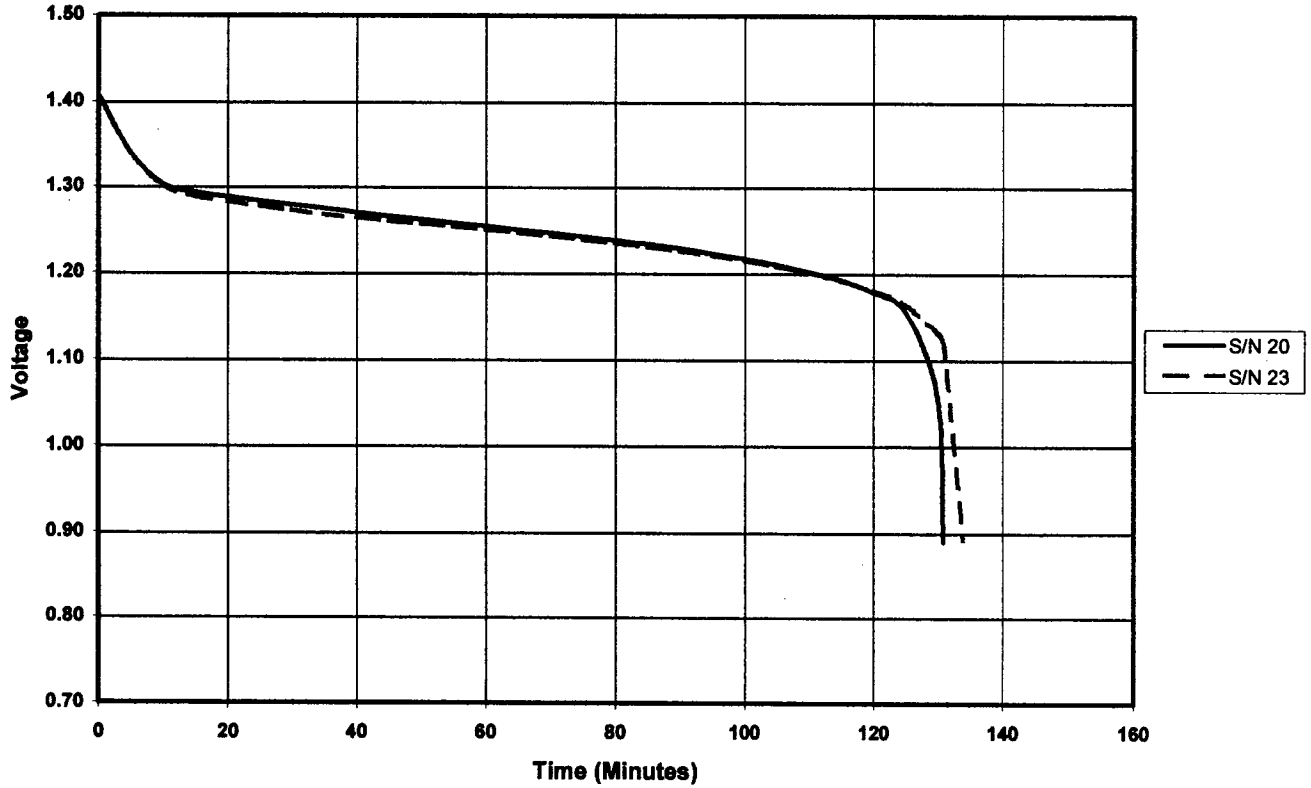

Typical Discharge Curve for a Positive Precharge Cell. The Sharp Voltage Fall off at the End of Discharge Is Characteristic of a Cell Having Positive Precharge.

EAGLE PICHER
Eagle-Picher Technologies, LLC

POWER Subsystems

Low Rate Discharge (Cell Reversal) With Positive Precharge

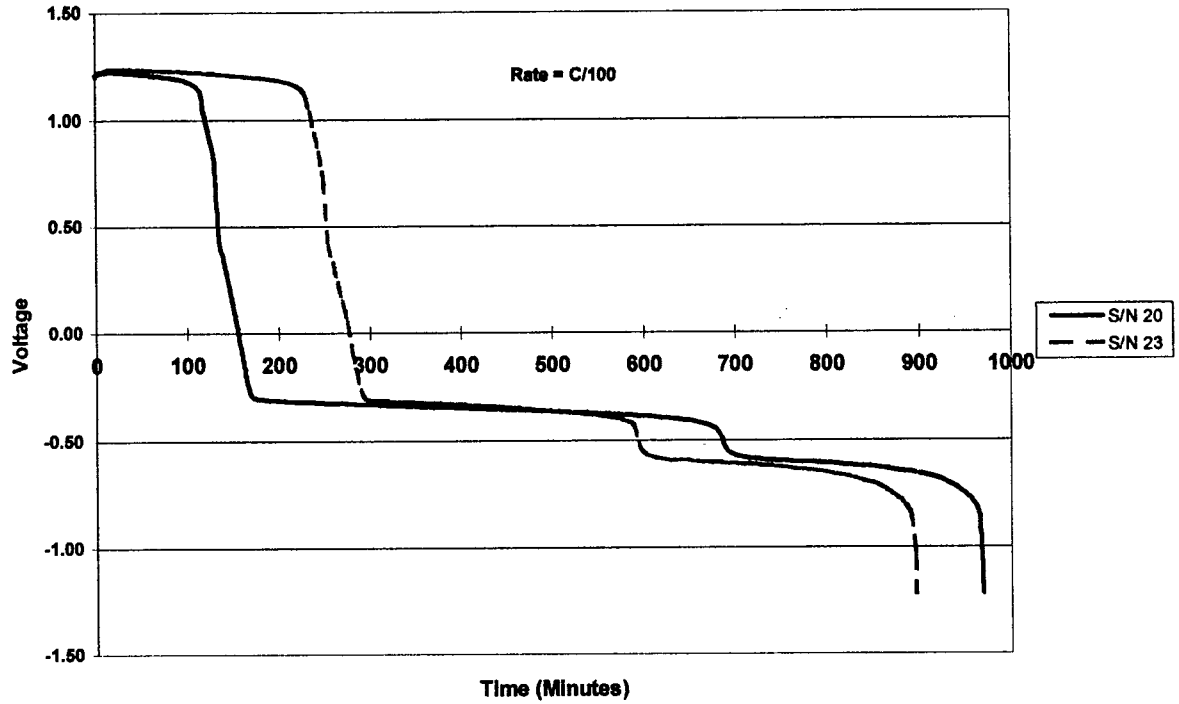

The Early Voltage Reversal and Prolonged Plateau Are Characteristic of Positive Precharge. The Plateaus Below 0.0 Volts Represent Different Phases of the Active Nickel Material. During Reversal Oxygen Is Generated Until the Positive Material Is Exhausted at Which Time Hydrolysis of Water Is Taking Place. The Test Should Terminate at This Time to Prevent Loss of Platinum.

EAGLE PICHER
Eagle-Picher Technologies, LLC

POWER Subsystems

Low Rate Charge after Reversal with Positive Precharge

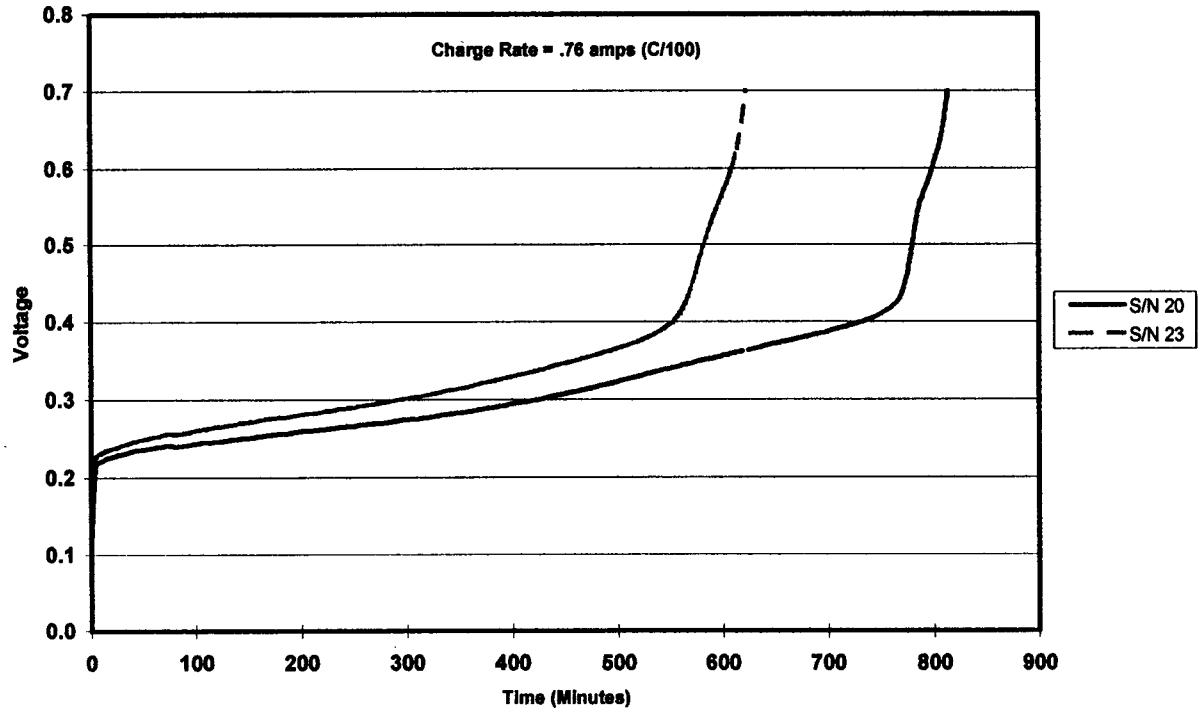

During the Low Rate Charge Oxygen Is Reduced by the Hydrogen Generated. Once All Oxygen Is Consumed the Hydrogen Voltage Is Seen and the Voltage Rises Rapidly to 0.7 Volts. By Characterizing the Time Required to Reach 0.7 Volts the Presence of Positive Precharge Can Be Readily Recognized.

EAGLE PICHER
Eagle-Picher Technologies, LLC

POWER Subsystems

Resistor Drain with Hydrogen Supplied

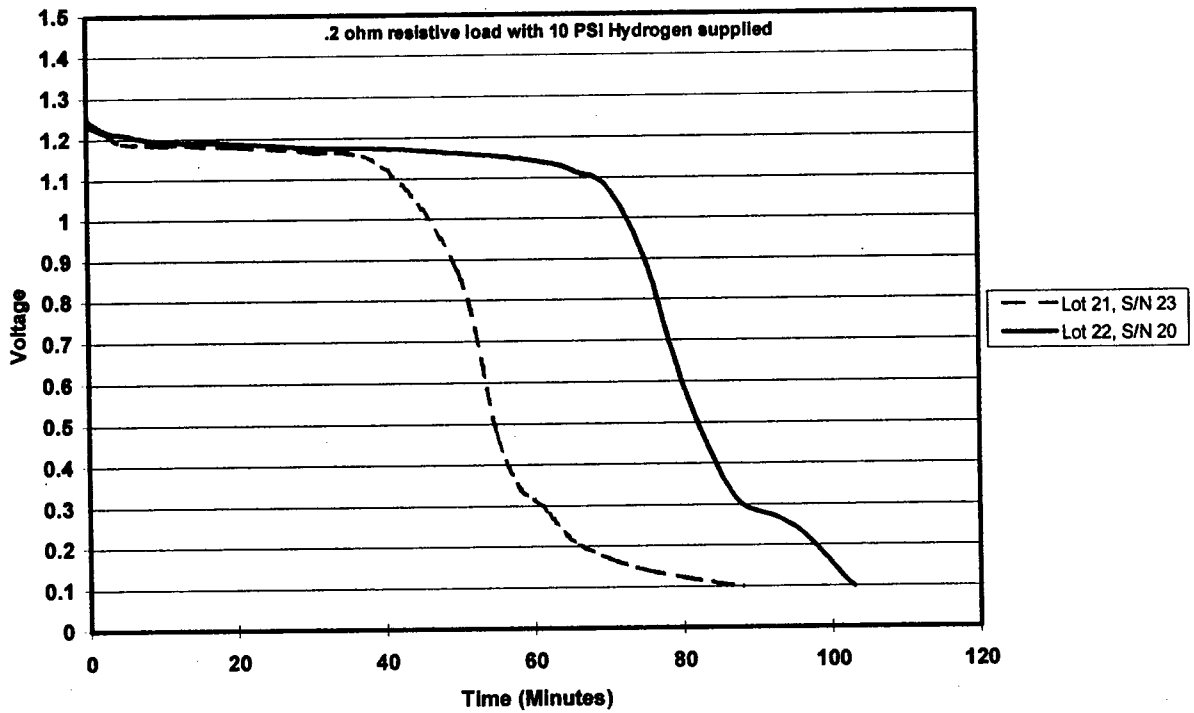

This Voltage Profile During the Resistor Drain Is Characteristic of a Cell Having Hydrogen Precharge. Positive Precharge Is Identified by a More Rapid Fall off in Voltage. Because the Drain Was Terminated at 0.1 Volts the Subsequent Precharge Established Was Slightly Positive Due to the Residual Nickel Capacity to 0.0 Volts. The Intent Was to Establish a Hydrogen Precharge.

EAGLE PICHER
Eagle-Picher Technologies, LLC

POWER Subsystems

Conditioning Discharge (with Near H2 Precharge)

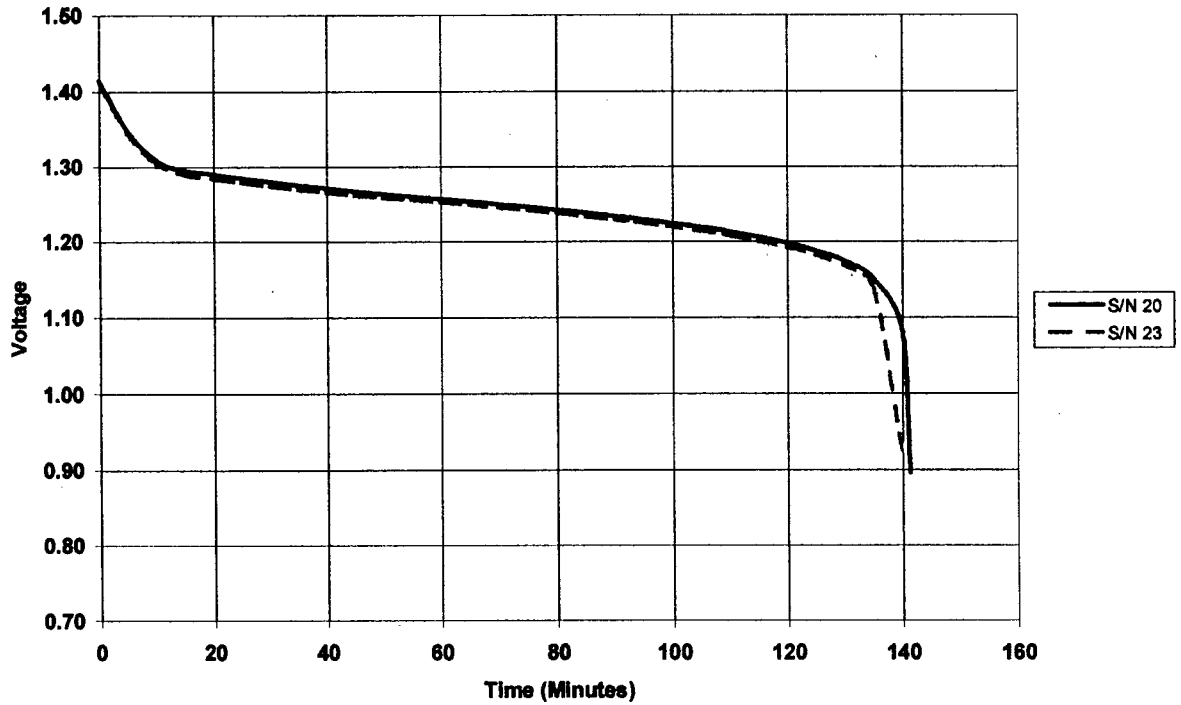

Since the Precharge Was Not Completely Hydrogen As Planned, This Discharge Is More Indicative of a Cell Having Positive Precharge. Normally Hydrogen Precharge Is Repesented by a More Gradual Taper at the End of Discharge, Especially at Lower Rates.

EAGLE PICHER
Eagle-Picher Technologies, LLC

POWER Subsystems

Low Rate Discharge (Cell Reversal with Near H2 Precharge)

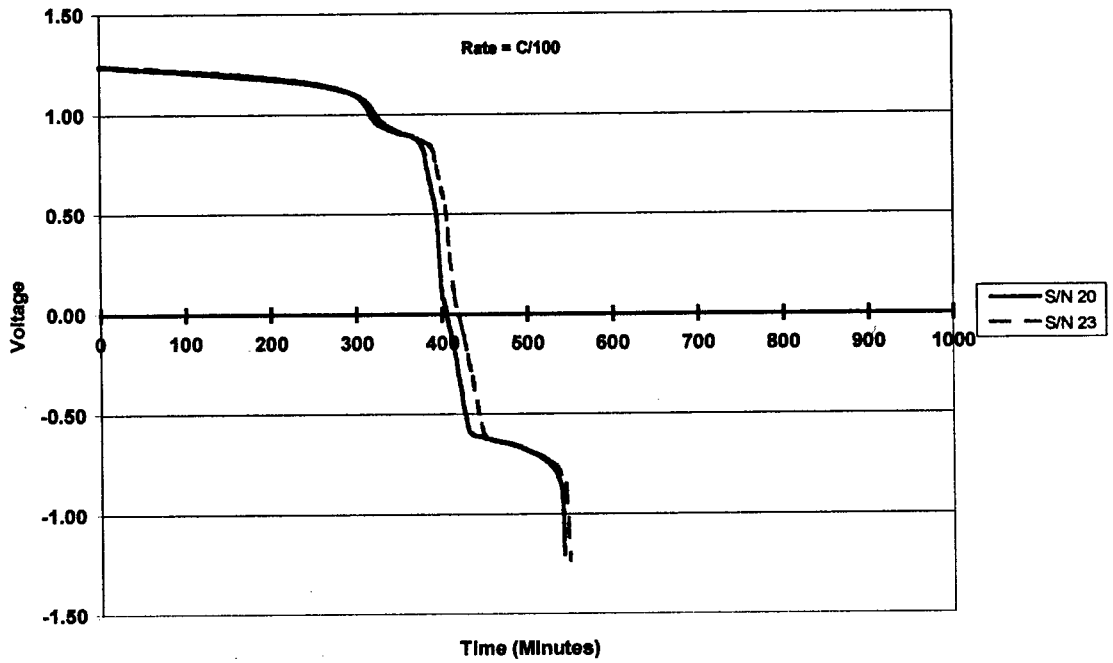

With a Near Hydrogen Precharge the Voltage Remains Above 0.0 Volts Longer and Drops off to -1.20 Volts Earlier Due to the Decreased Available Positive Capacity Beyond Exhaustion of Hydrogen. The Presence of Voltage Below 0.0 Volts Indicates the Presence of a Degree of Positive Precharge. If a Complete Hydrogen Precharge Were Present the Voltage Would Fall to and Remain Near 0.0 Volts.

EAGLE PICHER
Eagle-Picher Technologies, LLC

POWER Subsystems

Low Rate Charge after Reversal (with H2 Precharge)

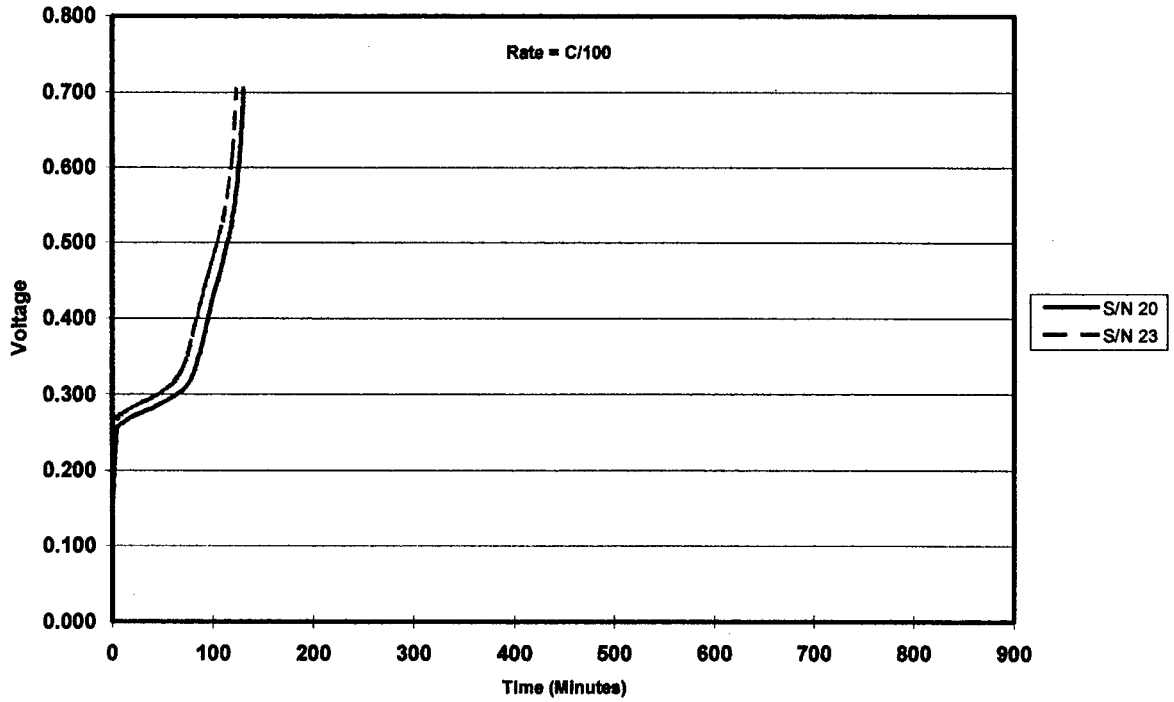

The Brevity of the Time Required to Reach 0.7 Volts During the Low Rate Charge Indicates Less Positive Precharge. Were the Cell at a Hydrogen Precharge the Voltage Would Rise Almost Immediately to 0.7 Volts.

EAGLE PICHER
Eagle-Picher Technologies, LLC

POWER Subsystems

0.2 ohm Resistor Drain with Positive Precharge

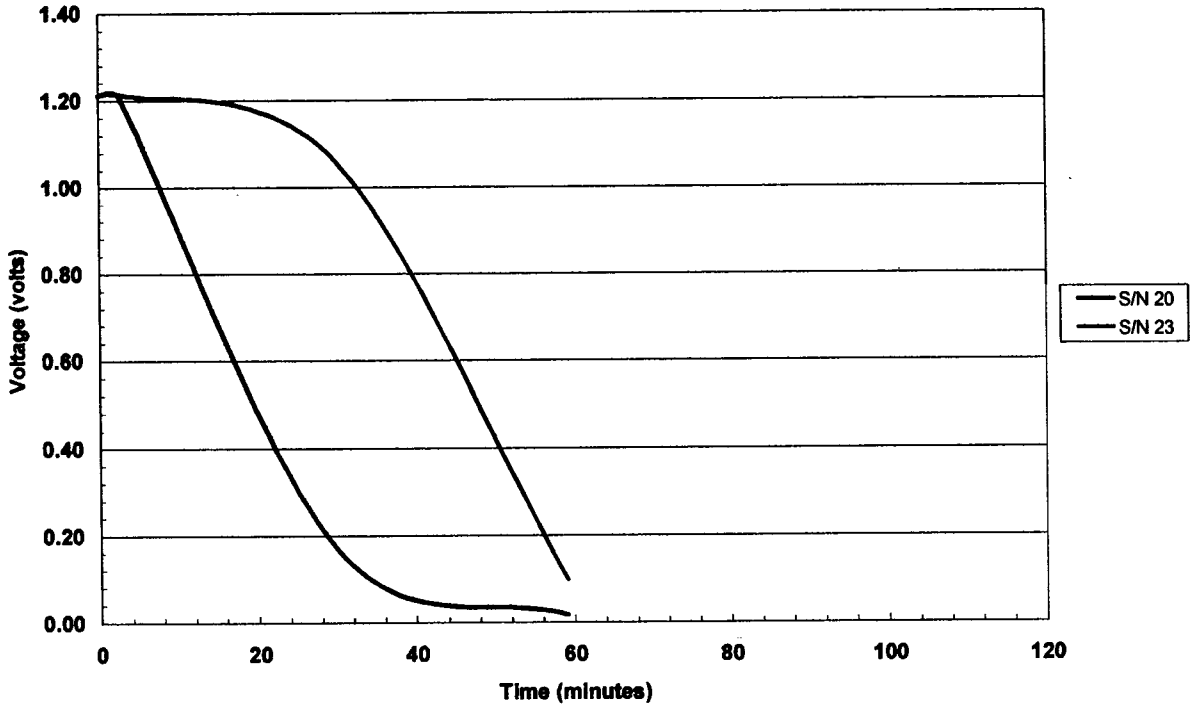

This Chart Compared to the Next Demonstrates the Slope of the Voltage Expected at Different Precharges. With Hydrogen Present the Decay Is More Extended.

EAGLE PICHER
Eagle-Picher Technologies, LLC

POWER Subsystems

0.2 ohm Resistor Drain with Hydrogen Precharge

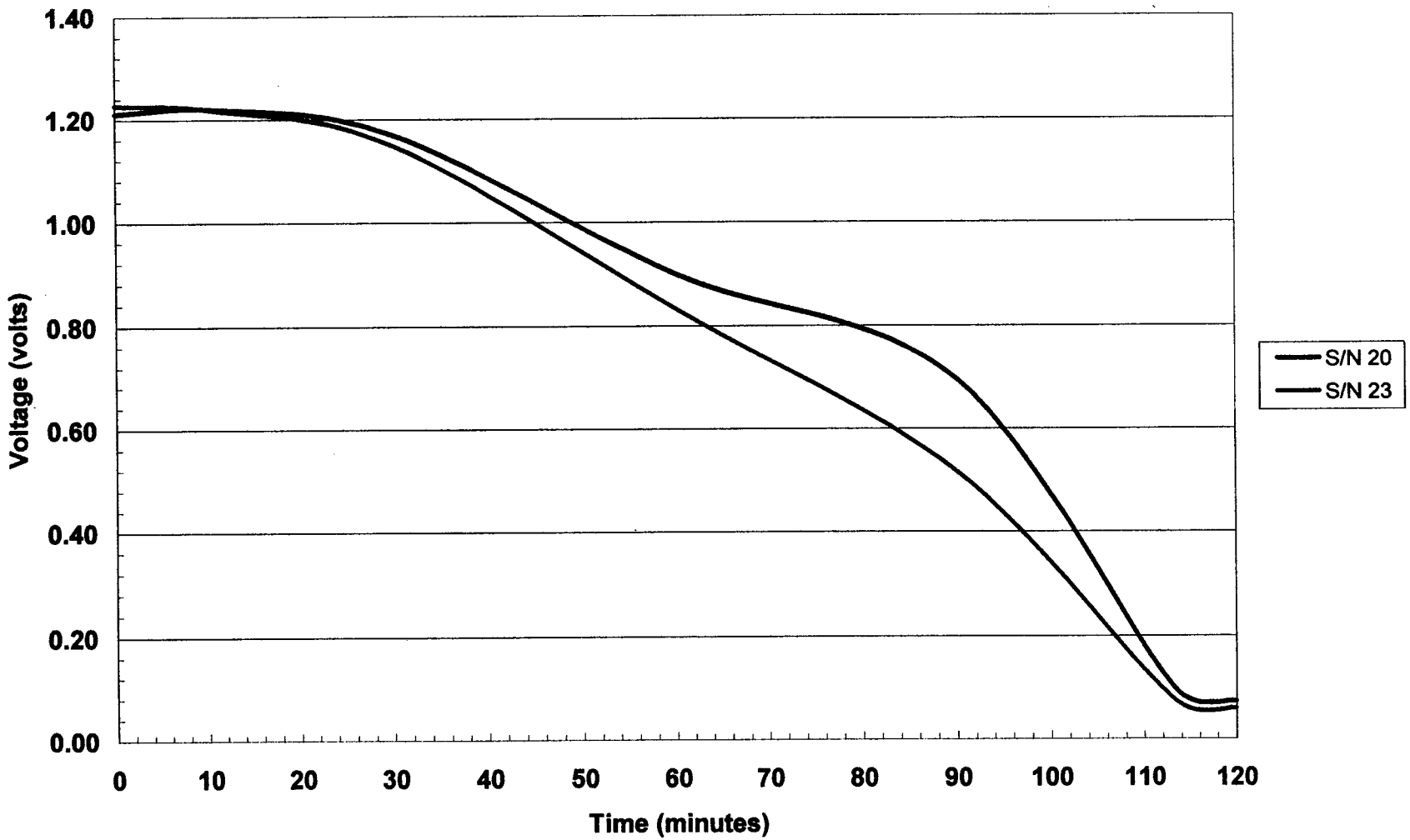

EAGLE PICHER
Eagle-Picher Technologies, LLC

POWER Subsystems

0.2 Ohm Resistor Drains for Positive and Hydrogen Precharged Cells

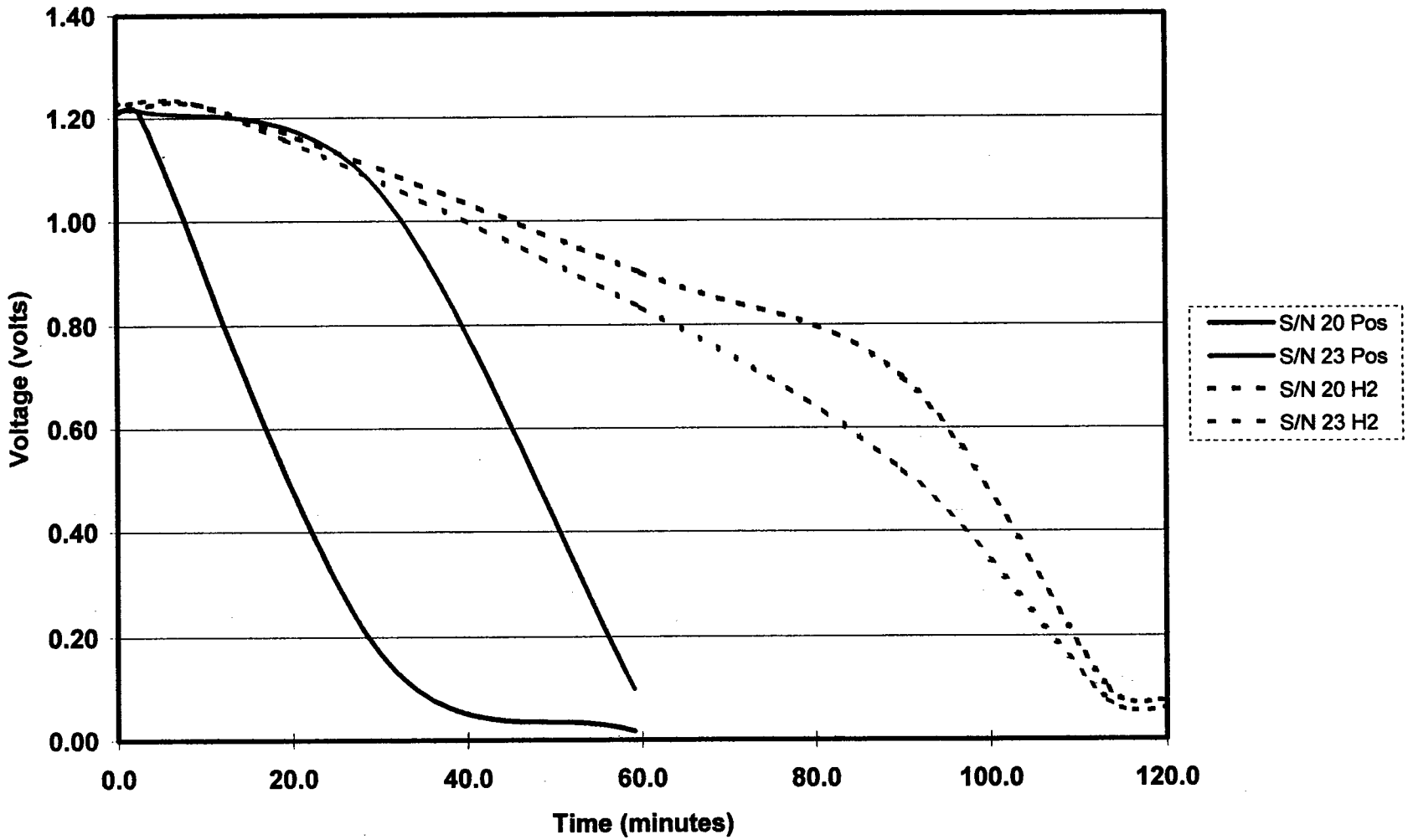

Reversal Test on Cells After 96 Months Storage

- 8 Cells Were Tested for Reversal Characteristics After 96 Months of Storage at 5°C.
  - The Same Test Procedure Was Used As for the Previous Two Cells.
  - These Cells Were Stored With Positive Precharge.
  - Capacity Measurements at Intervals of Approximately 2 Years Were 105 AH.

EAGLE PICHER
Eagle-Picher Technologies, LLC

POWER Subsystems

Low Rate Discharge (Cell Reversal) After 96 Months Storage

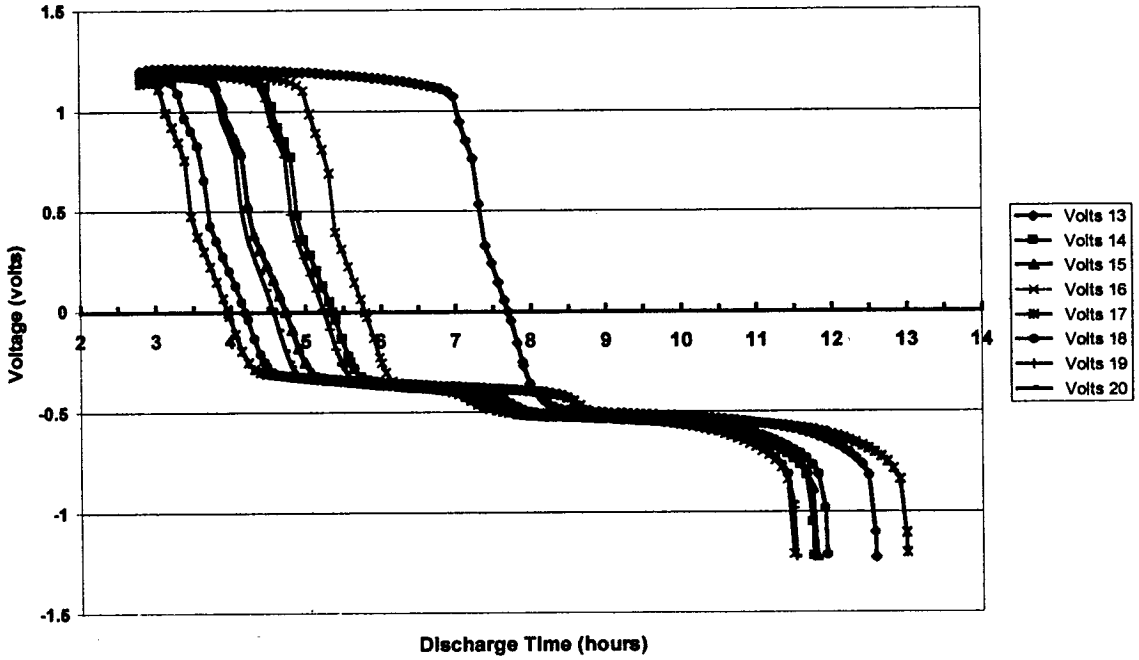

All Cells Have the Characteristics of Positive Precharge As Evidenced by Voltages Below 0.0 Volts.

EAGLE PICHER
Eagle-Picher Technologies, LLC

POWER Subsystems

Low Rate Charge After Reversal With Positive Precharge

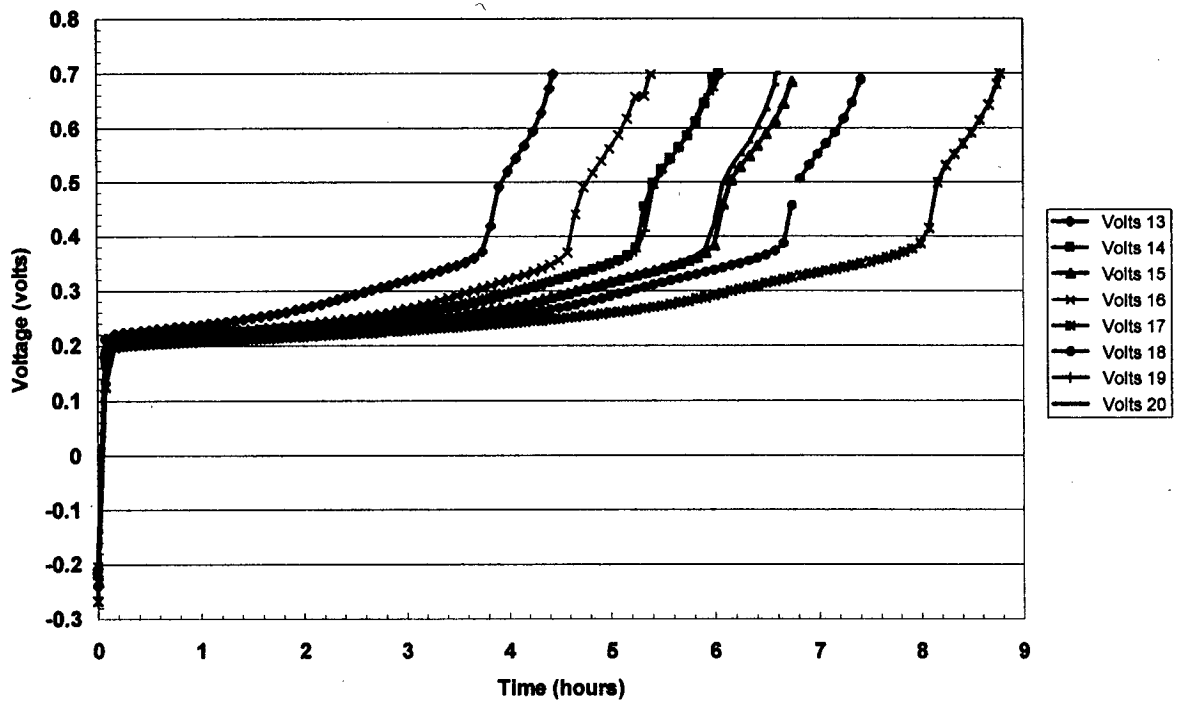

The Low Rate Charge Voltages Are Also Representative of Positive Precharge. The Extended Time Interval to Reach 0.7 Volts Indicates the Presence of a Significant Precharge. By Calculating the Nickel Capacity Under the Low Rate Drain the Per Cent Precharge Can Be Estimated.

Summary

- The Signature of the Voltage Curve at Low Rate Reversal Can Be Used As a Tool to Identify Precharge.
- A Low Rate Charge From a Fully Discharged Cell Can Be Used to Identify Precharge.
- Periodic Assessment During Ground Storage or Use Can Identify a Pattern for Identifying Precharge and Evaluating Storage Needs.
- Knowing the Precharge Will Allow the User to Properly Store the Batteries.

EAGLE PICHER
Eagle-Picher Technologies, LLC

POWER Subsystems

Low Rate Reversal with Positive and Near Hydrogen Precharge

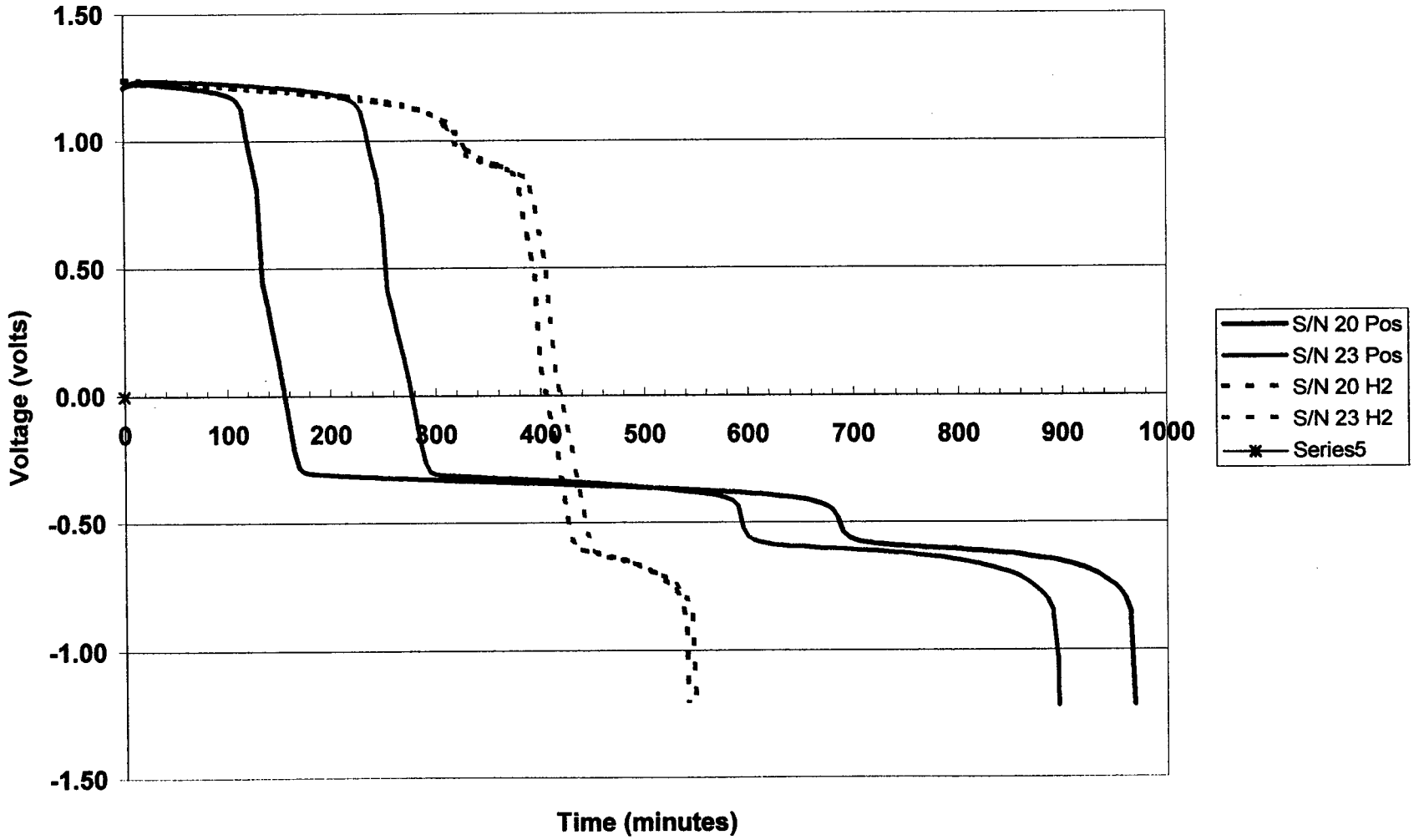

EAGLE PICHER
Eagle-Picher Technologies, LLC

POWER Subsystems

Low Rate Charge with Positive and Near Hydrogen Precharge

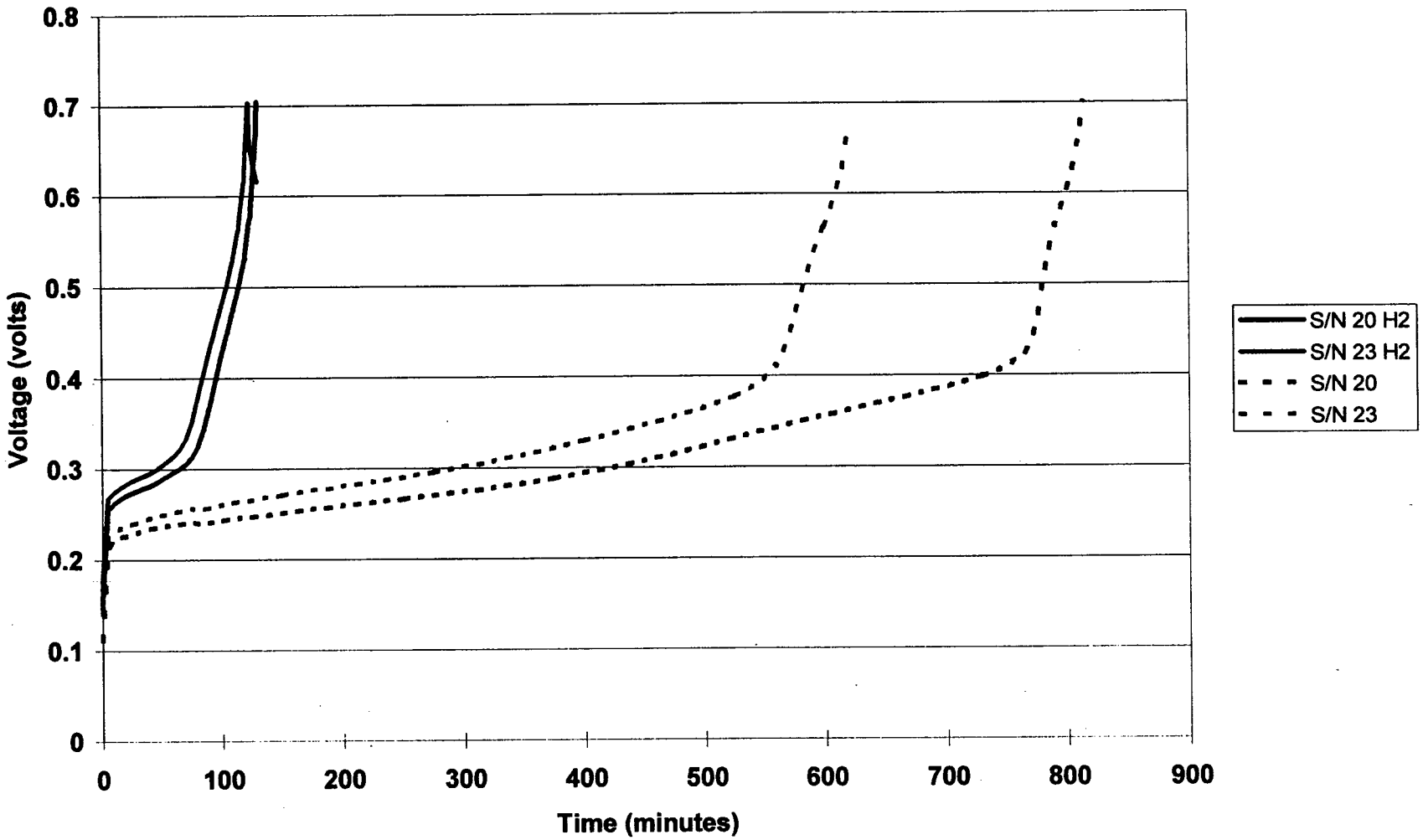

Advanced Nickel-Hydrogen / Silver-Hydrogen Session

MGS 2-CELL CPV NiH_2 BATTERIES

JPL

PRESENTED
BY
SAL Di STEFANO

NASA AEROSPACE BATTERY WOKSHOP
MARSHALL SPACE FLIGHT CENTER
OCTOBER 27-29
HUNTSVILLE, ALABAMA

CONTRIBUTORS:
D. PERRONE, B.V. RATNAKUMAR, T. VALDEZ, L. WHITCANACK - JPL
R. ZERCHER, J. BYERS, S. WALKER - LMA

TOPICS

- BACKGROUND
- MGS BATTERY DESCRIPTION
- TYPICAL PERFORMANCE CHARACTERISTICS
- IN-FLIGHT PERFORMANCE
- OUTLOOK

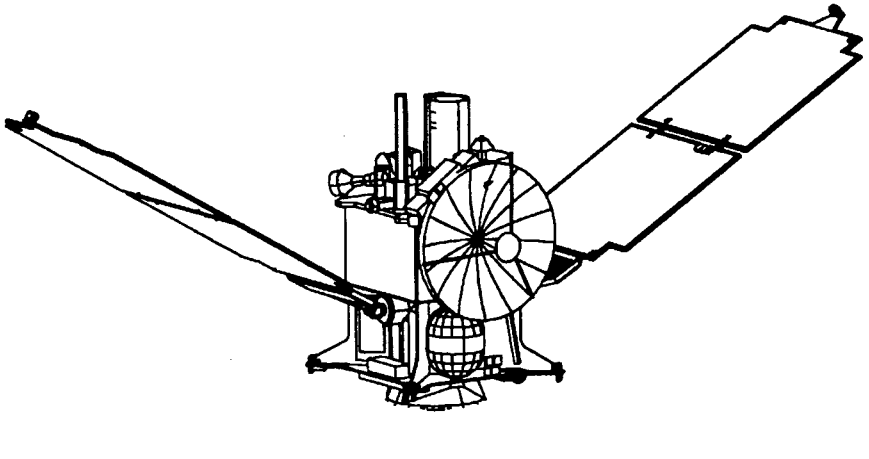

Mars Global Surveyor

After a mission elapsed time of 659 days from launch, Surveyor is 223.34 million miles (359.43 million kilometers) from the Earth and in an orbit around Mars with a high point of 11,098 miles (17,861km), a low point of 108.0 miles (173.8 km), and a period of 11.6 hours.

http://mars.jpl.nasa.gov

MARS GLOBAL SURVEYOR(MGS)
Electric Power Subsystem

- Much of the hardware was modified from the Mars Observer Mission Flight spares
- Direct Energy Transfer System with Boost Regulator
  - Regulated to 28 Volts ±2% (+0.56/-0.3 Volts)
  - 361 Watt Orbital Average Load (Mapping Phase)
- Hybrid GaAs/Si Solar Array Provides Energy Balance During Mission
  - 12 M2 Panel Produces > 664 W at Mapping Aphelion
- NiH2 2-Cell CPV Batteries (2) Provide 20 AH Each
- Linear Battery Charger Controls Battery Recharge
  - Charge Rates of 0.85A, 7.5A, 10.0A and 12.5A
  - 8 VT Limits with Capability to Shift All Down for 1 Cell Failure
- C/100 Trickle Charge Circuit from Regulated Bus
- Boost Regulator Processes up to 24 A With 4 out of 5 Redundancy
- Partial Shunt Assemblies Dump Excess Energy - Up to 3.3 A Each
- Fuse Board Assemblies (2) Protect Pwr Bus with Redundant Fuses

MGS 20 AH Cell Design

- EPI MANTECH
- 23 mil PRESSURE VESSELS
- COMMON PRESSURE VESSEL
- RABBIT EAR TERMINALS (60° INCLUDED ANGLE)
- 30 mil SLURRY POSITIVES
- 32 ELECTRODE COUPLES (16 PER STACK)
- DOUBLE LAYER ZIRCAR
- ZIRCONIUM WALL WICK
- TEFLON COATED WELD RING (INHIBITS ELECTROLYTE MIGRATION)
- 31% KOH
- NICKEL PRECHARGED
- 800 PSI @ MAXIMUM EXPECTED
- MASS: 1291g MAX / CELL

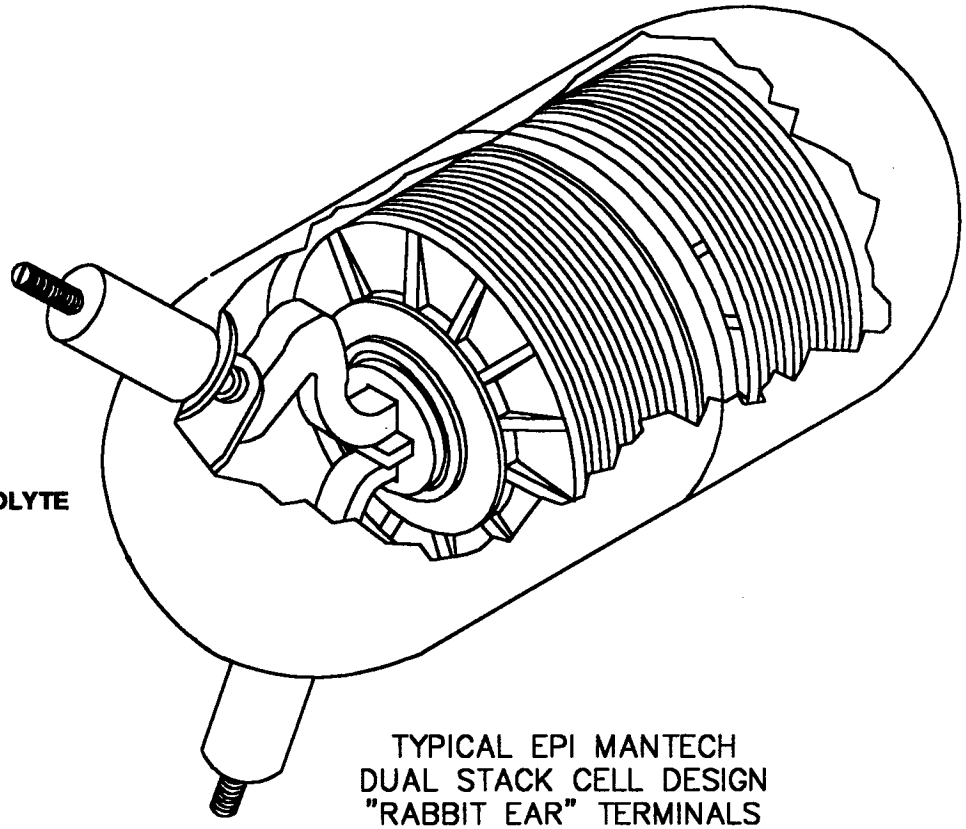

TYPICAL EPI MANTECH
DUAL STACK CELL DESIGN
"RABBIT EAR" TERMINALS

Characteristic C/10) Charge @ 10°C

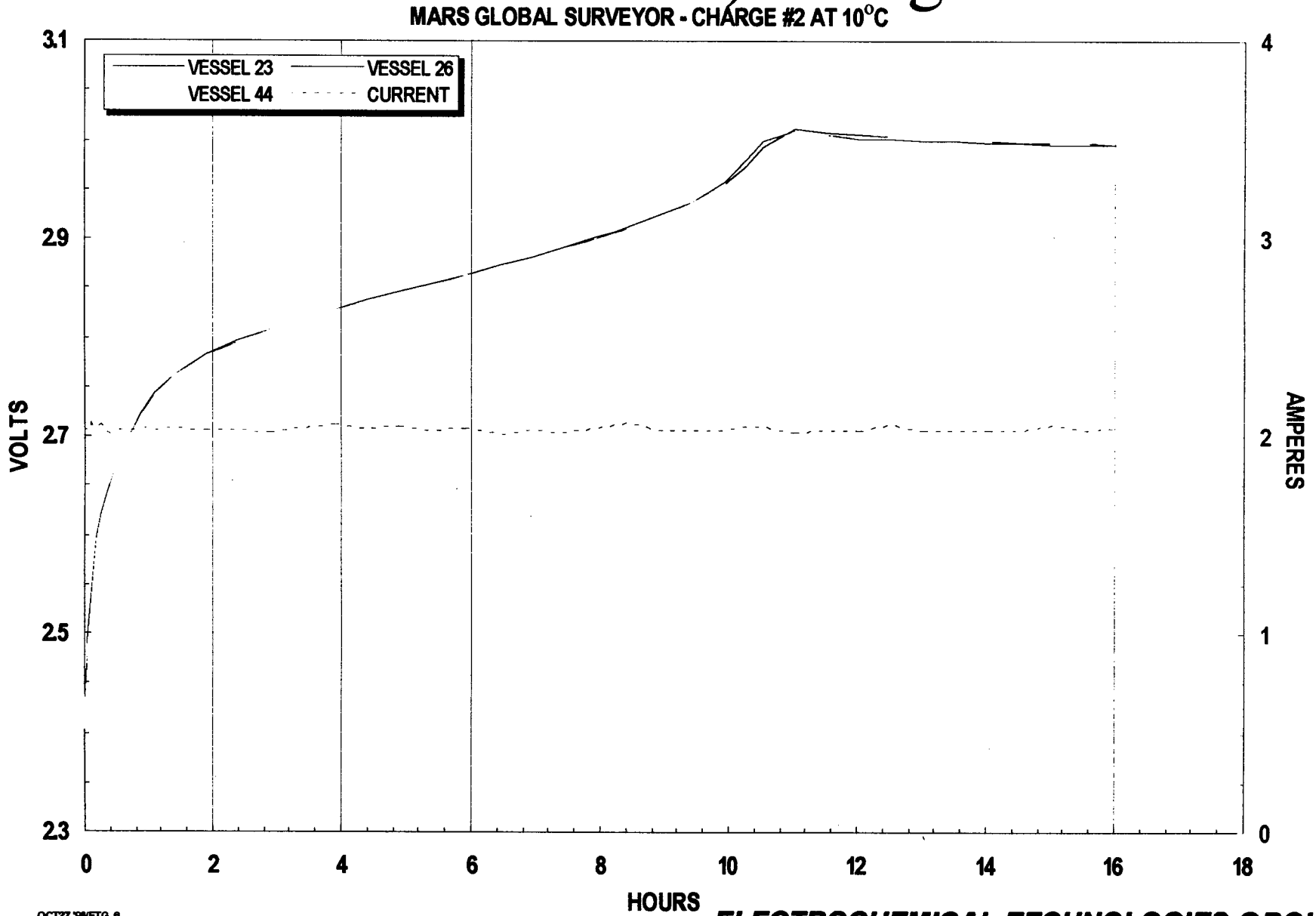

OCT27.98/ETG 6

ELECTROCHEMICAL TECHNOLOGIES GROUP

Characteristic C/2 Discharge @ 10°C

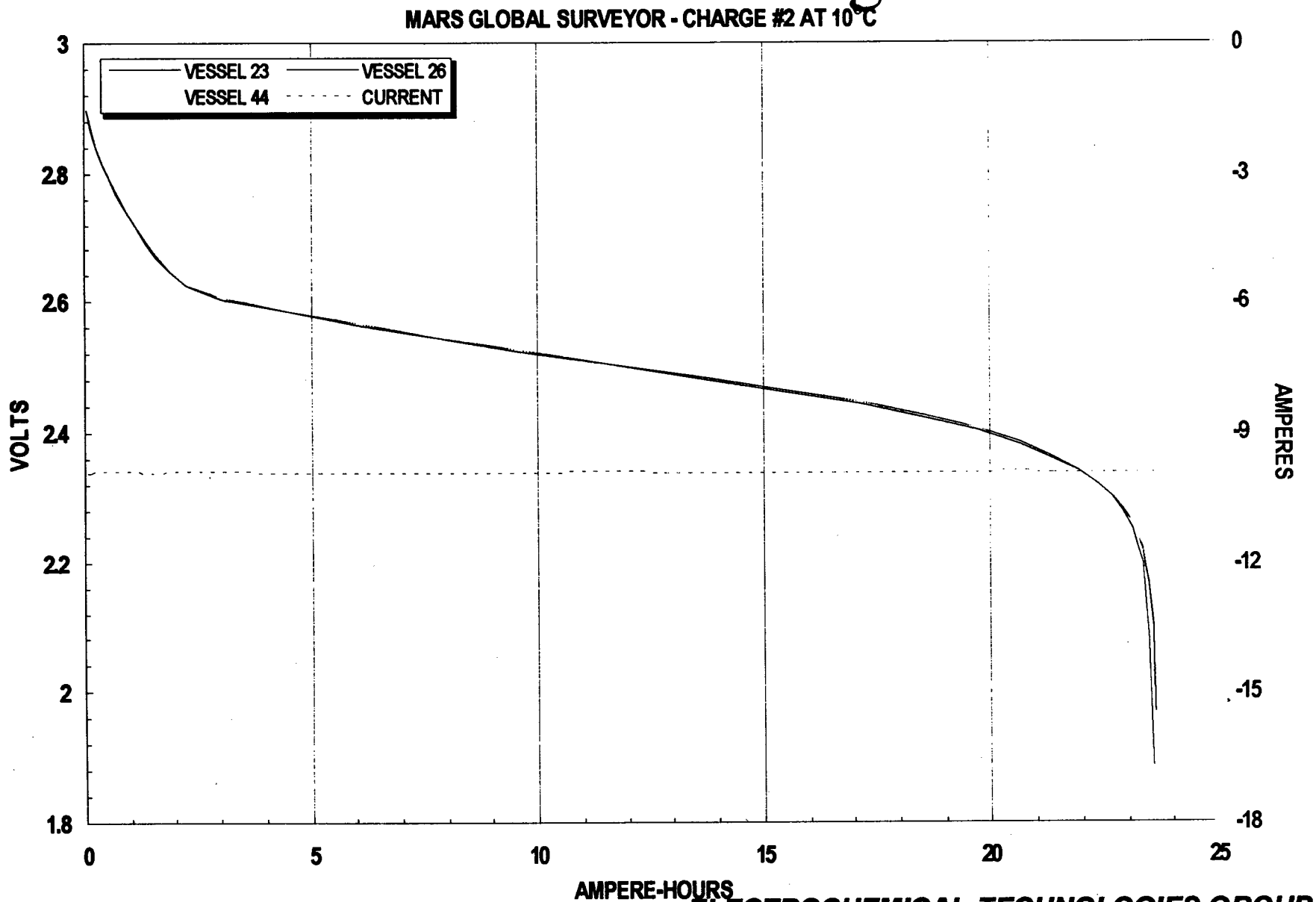

OCT27.98ETG 7

ELECTROCHEMICAL TECHNOLOGIES GROUP

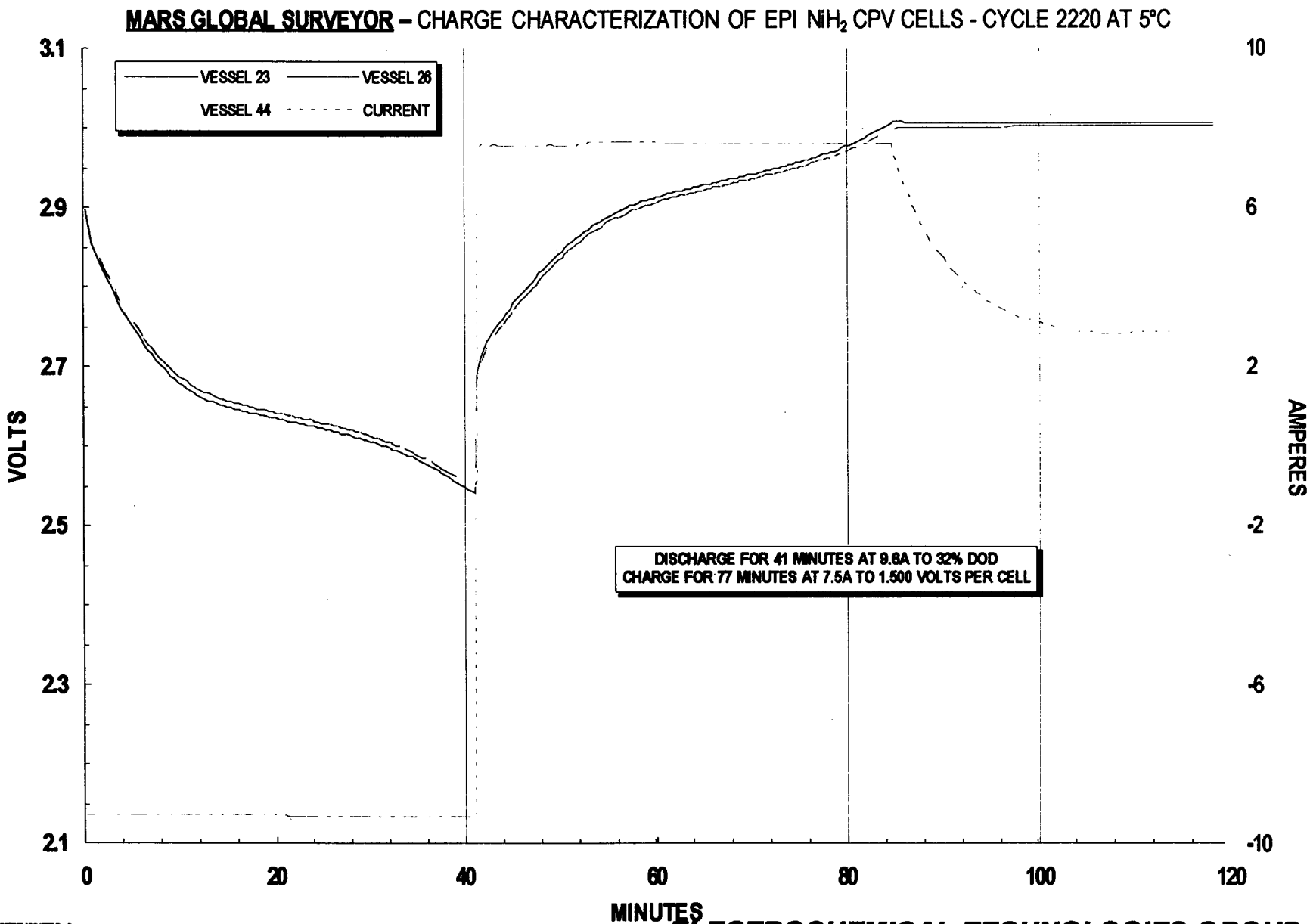
MARS GLOBAL SURVEYOR – CHARGE CHARACTERIZATION OF EPI NiH2 CPV CELLS - CYCLE 2220 AT 5°C
VESSEL 23
VESSEL 28
VESSEL 44
CURRENT
DISCHARGE FOR 41 MINUTES AT 9.6A TO 32% DOD
CHARGE FOR 77 MINUTES AT 7.5A TO 1.500 VOLTS PER CELL
VOLTS
3.1
2.9
2.7
2.5
2.3
2.1
AMPERES
10
6
2
-2
-6
-10
0
20
40
60
80
100
120
MINUTES

V/T curves

- Developed for charge control of LEO (Low Earth Orbit) satellites using NiCd batteries
- Allows for fast charging of batteries
  - minimizes overcharge
  - prevents thermal runaway
- Relatively simple to implement in hardware
- Range of V/T curves can be constructed to take battery aging into account

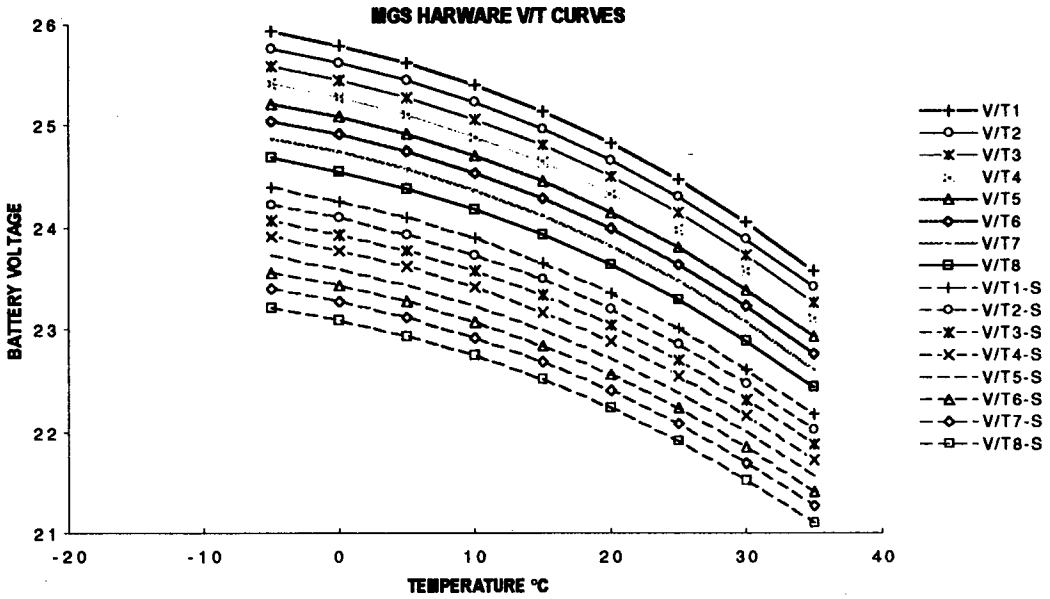

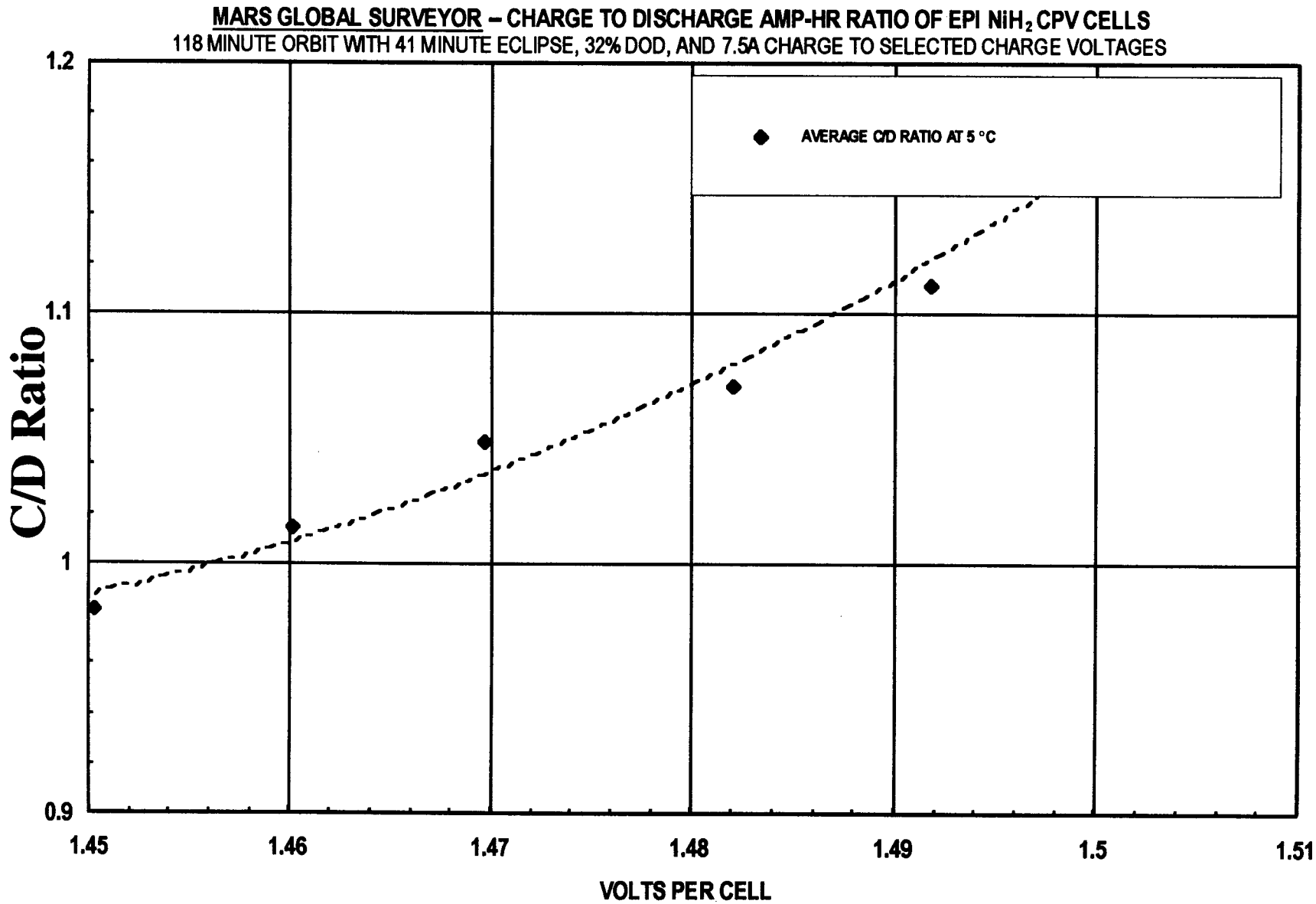
MARS GLOBAL SURVEYOR – CHARGE TO DISCHARGE AMP-HR RATIO OF EPI NiH2 CPV CELLS
118 MINUTE ORBIT WITH 41 MINUTE ECLIPSE, 32% DOD, AND 7.5A CHARGE TO SELECTED CHARGE VOLTAGES
AVERAGE C/D RATIO AT 5 °C
C/D Ratio
1.2
1.1
1
0.9
1.45
1.46
1.47
1.48
1.49
1.5
1.51
VOLTS PER CELL

MARS GLOBAL SURVEYOR – CHARGE TO DISCHARGE AMP-HR RATIO OF EPI NiH_2 CPV CELLS

118 MINUTE ORBIT WITH 41 MINUTE ECLIPSE, 32% DOD, AND 7.5A CHARGE TO SELECTED CHARGE VOLTAGES

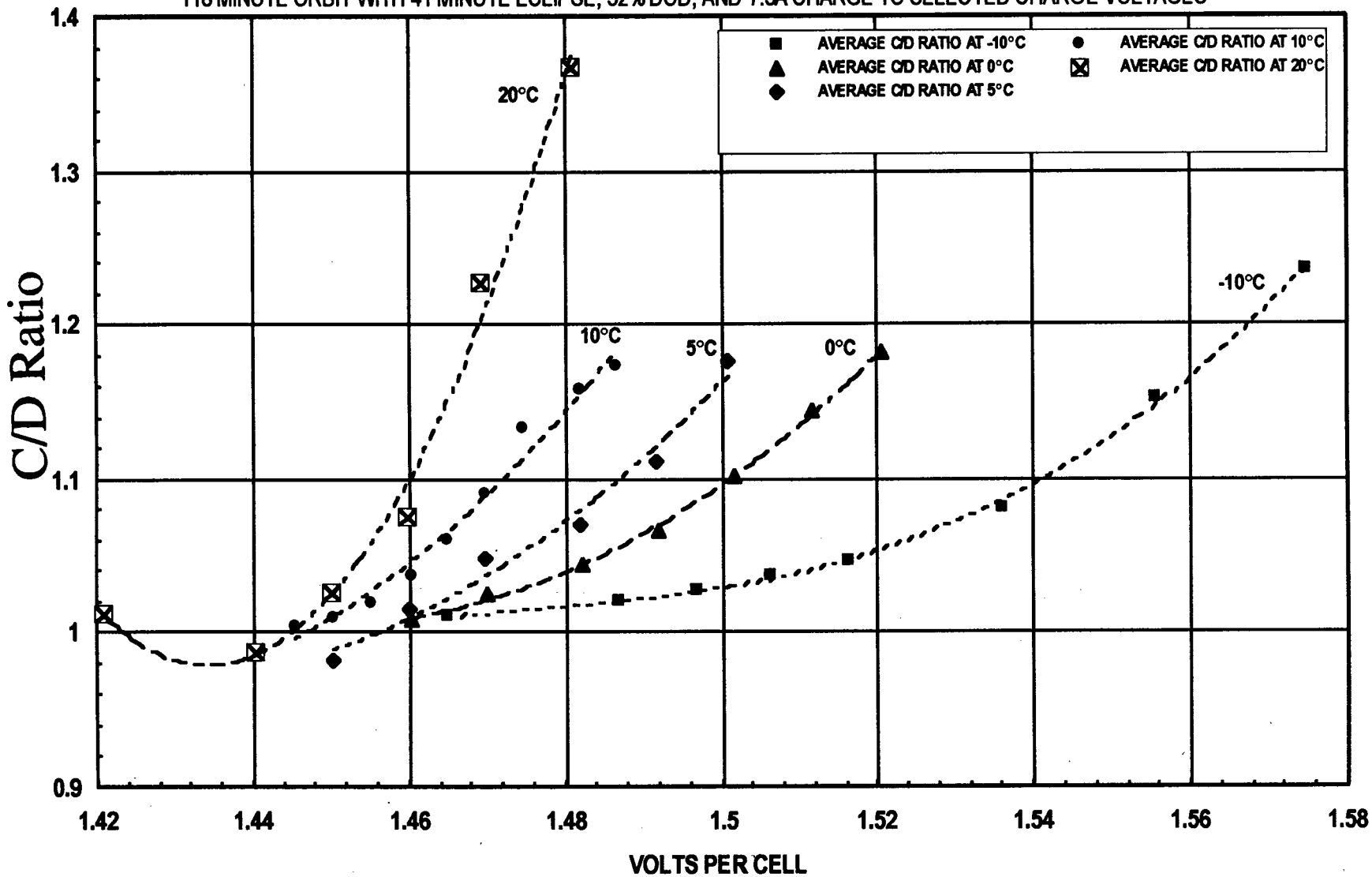

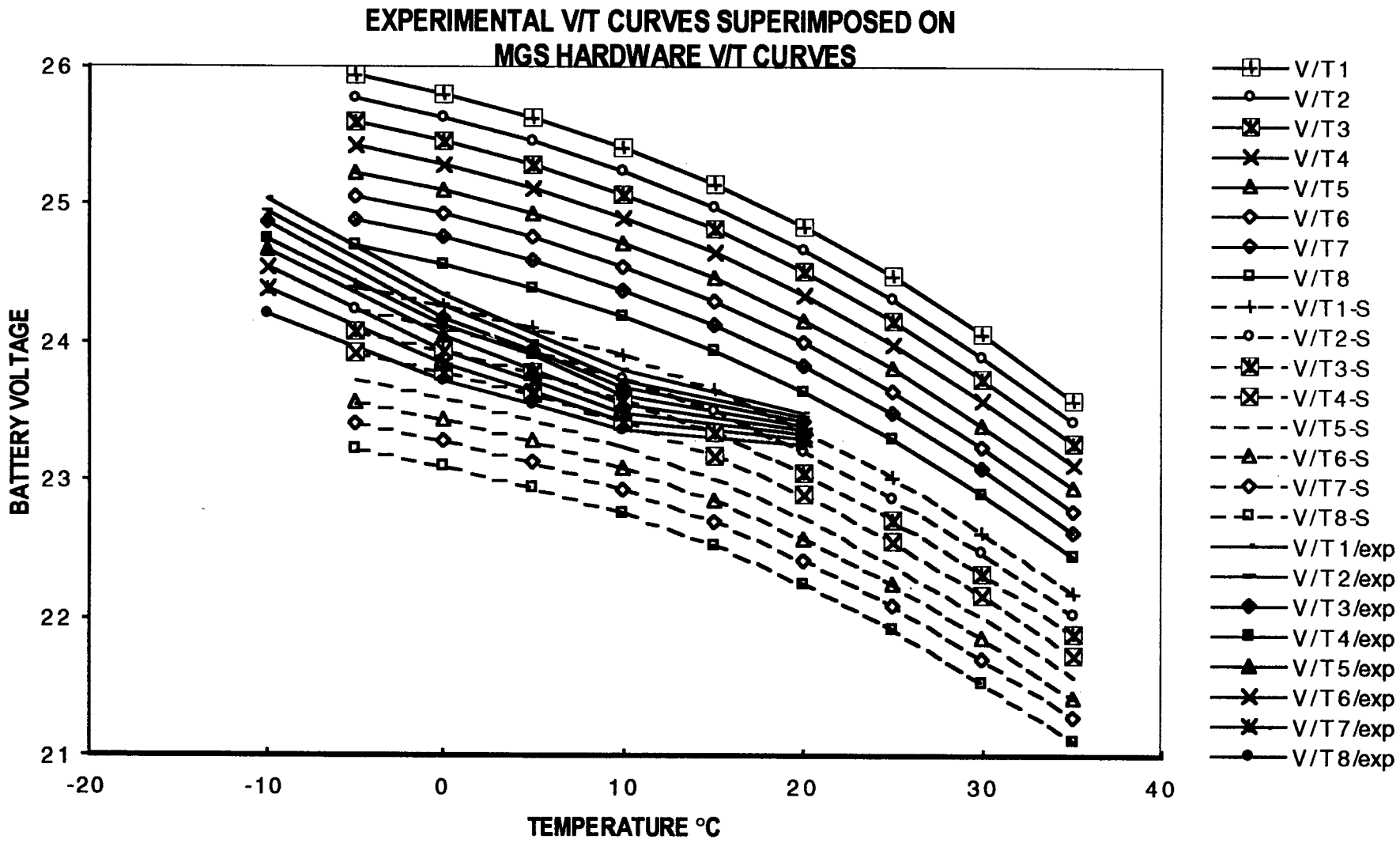
EXPERIMENTAL V/T CURVES SUPERIMPOSED ON
MGS HARDWARE V/T CURVES
BATTERY VOLTAGE
26
25
24
23
22
21
-20
-10
0
10
20
30
40
TEMPERATURE °C
V/T1
V/T2
V/T3
V/T4
V/T5
V/T6
V/T7
V/T8
V/T1-S
V/T2-S
V/T3-S
V/T4-S
V/T5-S
V/T6-S
V/T7-S
V/T8-S
V/T1/exp
V/T2/exp
V/T3/exp
V/T4/exp
V/T5/exp
V/T6/exp
V/T7/exp
V/T8/exp

Characteristic Cruise Performance

Mars Global Surveyor – EPI 20 Ampere-Hour CPV NiH_2 Cells

Cruise Simulation – 0.2A "Trickle Charge" At 5°C

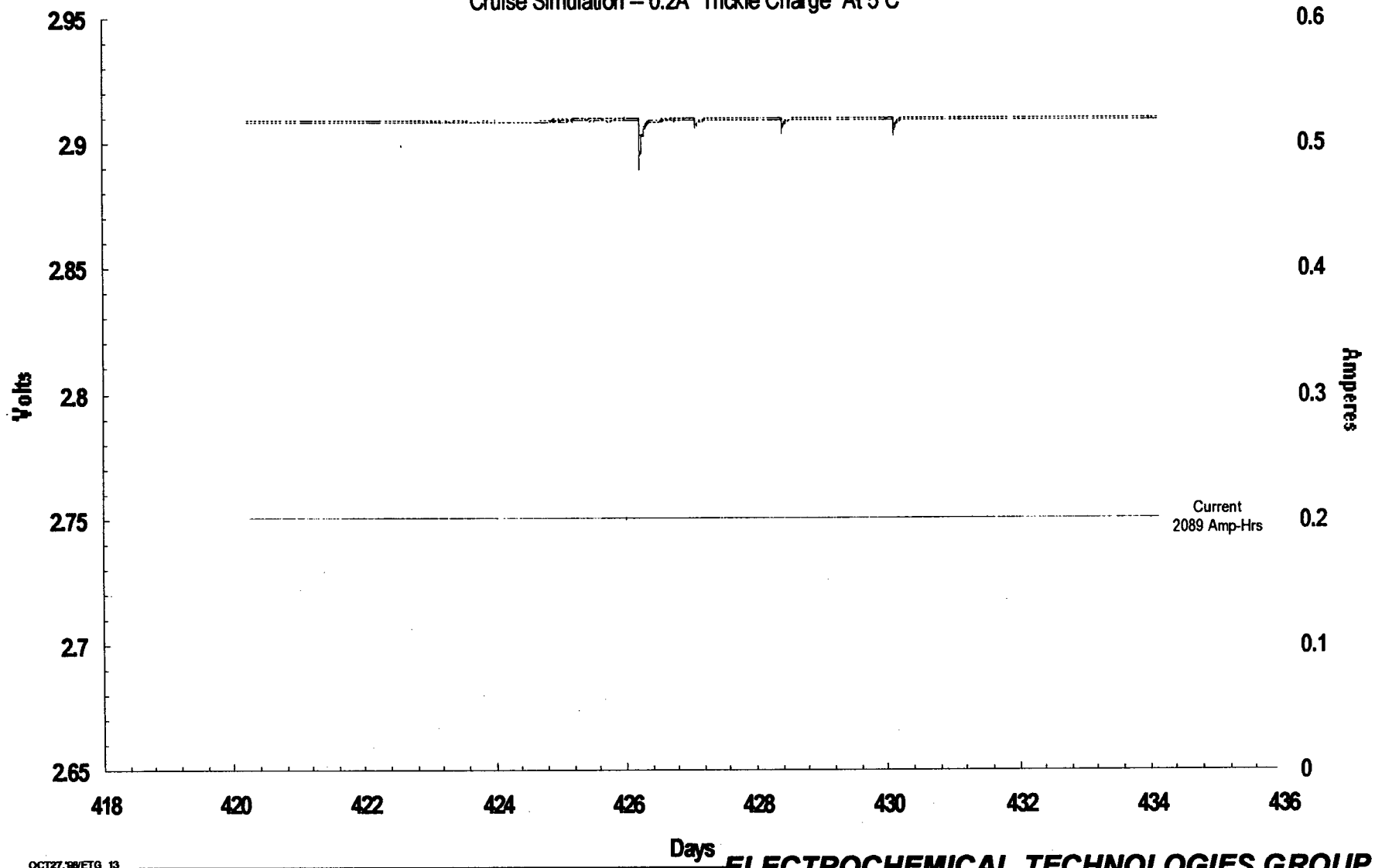

OCT27.98/ETG 13

ELECTROCHEMICAL TECHNOLOGIES GROUP

Characteristic Cruise Performance

Mars Global Surveyor – EPI 20 Ampere-Hour CPV NiH_2 Cells

Cruise Simulation – 0.2A "Trickle Charge" At 5°C

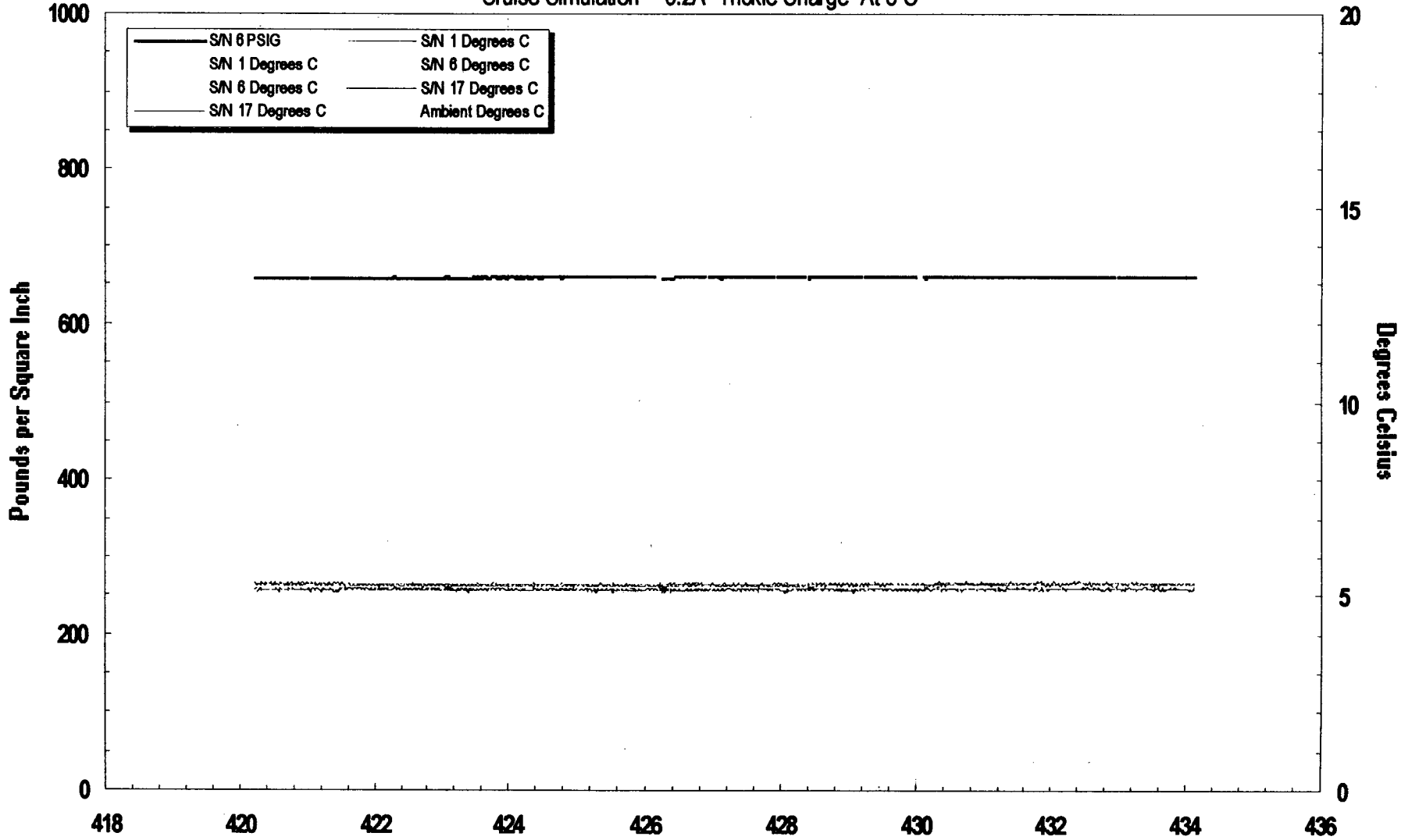

OCT27.98/ETG 14

ELECTROCHEMICAL TECHNOLOGIES GROUP

JPL

Characteristic Aerobraking Orbit Simulation

MGS Simulation(Ni-H2) Orbit # 392

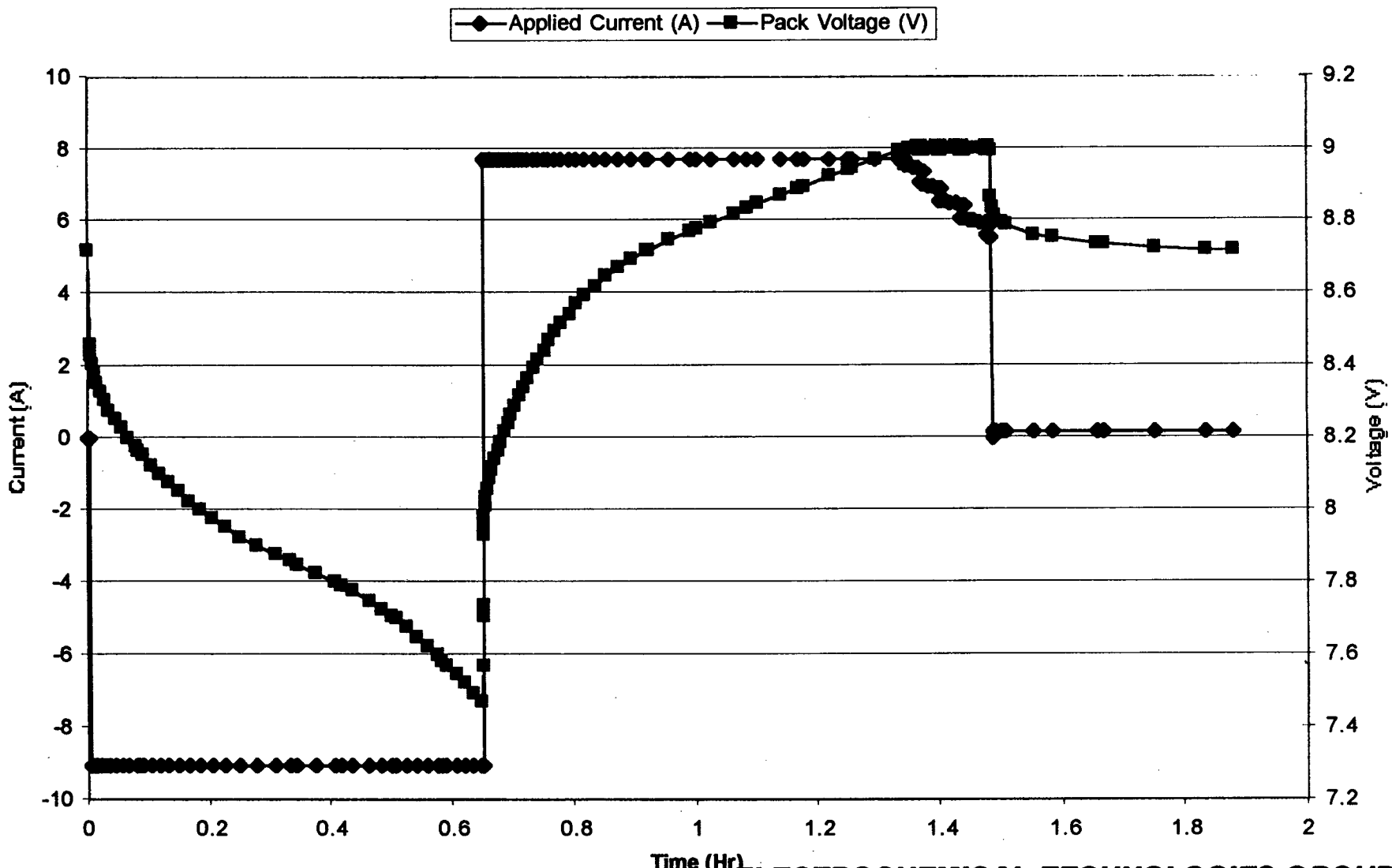

ELECTROCHEMICAL TECHNOLOGIES GROUP

JPL

Trend Analysis

- For Each Day The Highest and Lowest Value for Each Telemetry Channel is Recorded
  - Pressure (4), Temperature (2 of 4), Voltage (2) Follow
- Pressures Have Been Normalized by Dividing Subsequent Readings by the Initial Post-Launch Values
  - Show a 15% Increase Over Time
    - ~4% Due to Trickle Charging for 560 Days
    - ~4% Due to Single Event Overcharge at 7.5 amps to 30°C Overtemperature Cutoff Upon Entering Safe Mode During Cruise
    - 7% Due to 200 Discharge/Charge Cycles Averaging ~30% DOD, 50% Maximum

JPL

NORMALIZED PRESSURE HISTORY CHART

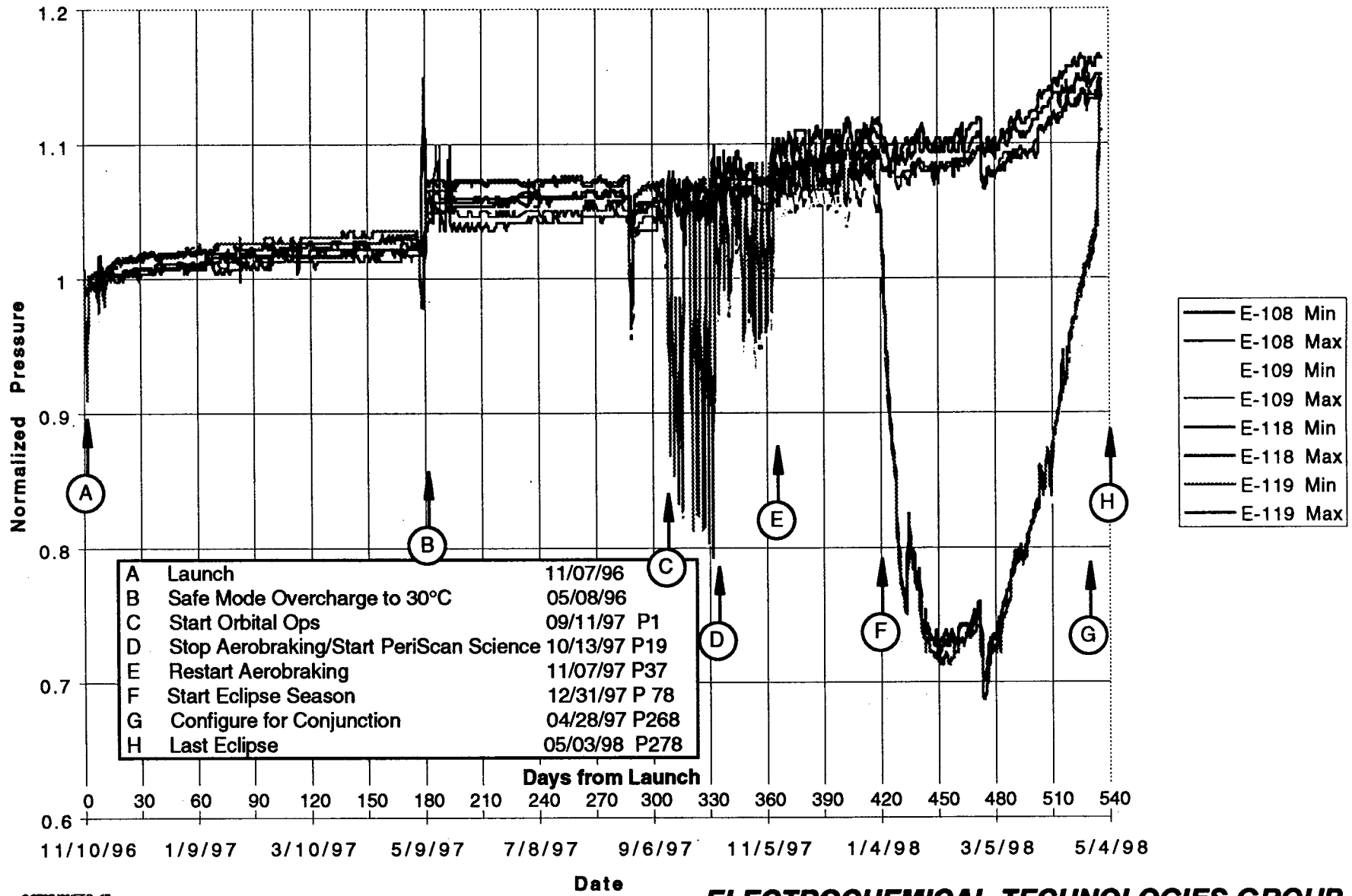

SUMMARY OF PRESSURE TREND DATA

- Data Below Reflects Pressures at Constant Charge Rate (C/100) & Temperature (~2°C) from Beginning of Life to Present
- MGS Pressure Measurements Saturate at 792 psi (6.6%) 812 psi (1.5%), 817 psi (5.4%) and 861 psi (4.5%)

	Beginning of Mission			Current Values (PSI)			Delta Increases (%)		
	Min	Max	Mean	Min	Max	Mean	Min	Max	Mean
Battery 1									
Temperature:	2.6°/2.4° on D97-017			1.4°/0.5° on D98-124					
Pressure 1 (E-0108)	621.8	652.9	628.3	705.8	743.1	712.6	13.5%	13.8%	13.4%
Pressure 2 (E-0109)	656.1	681.5	663.2	745.2	800.7	750.0	13.6%	17.5%	13.1%
Battery 2									
Temperature:	3.2°/1.8° on D96-319			1.6/1.7° on D98-124					
Pressure 1 (E-0118)	628.2	663.5	638.5	734.0	775.7	738.9	16.8%	16.9%	15.7%
Pressure 2 (E-0119)	668.9	699.3	681.9	790.5	824.3	799.0	18.2%	17.9%	17.2%
AVERAGE							15.5%	16.5%	14.9%
AVERAGE								15.6%	

Summary

- Charge control of MGS 2-Cell CPV NiH_2 Battery using modified NiCd charge control system appears to be working well - Not recommended
- Unexpected increase in pressure observed in flight
- Operations have been modified to further minimize overcharge
- The pressure increase not expected to impact mission

Mars Surveyor Operations

Pressure History Since 5/1/98

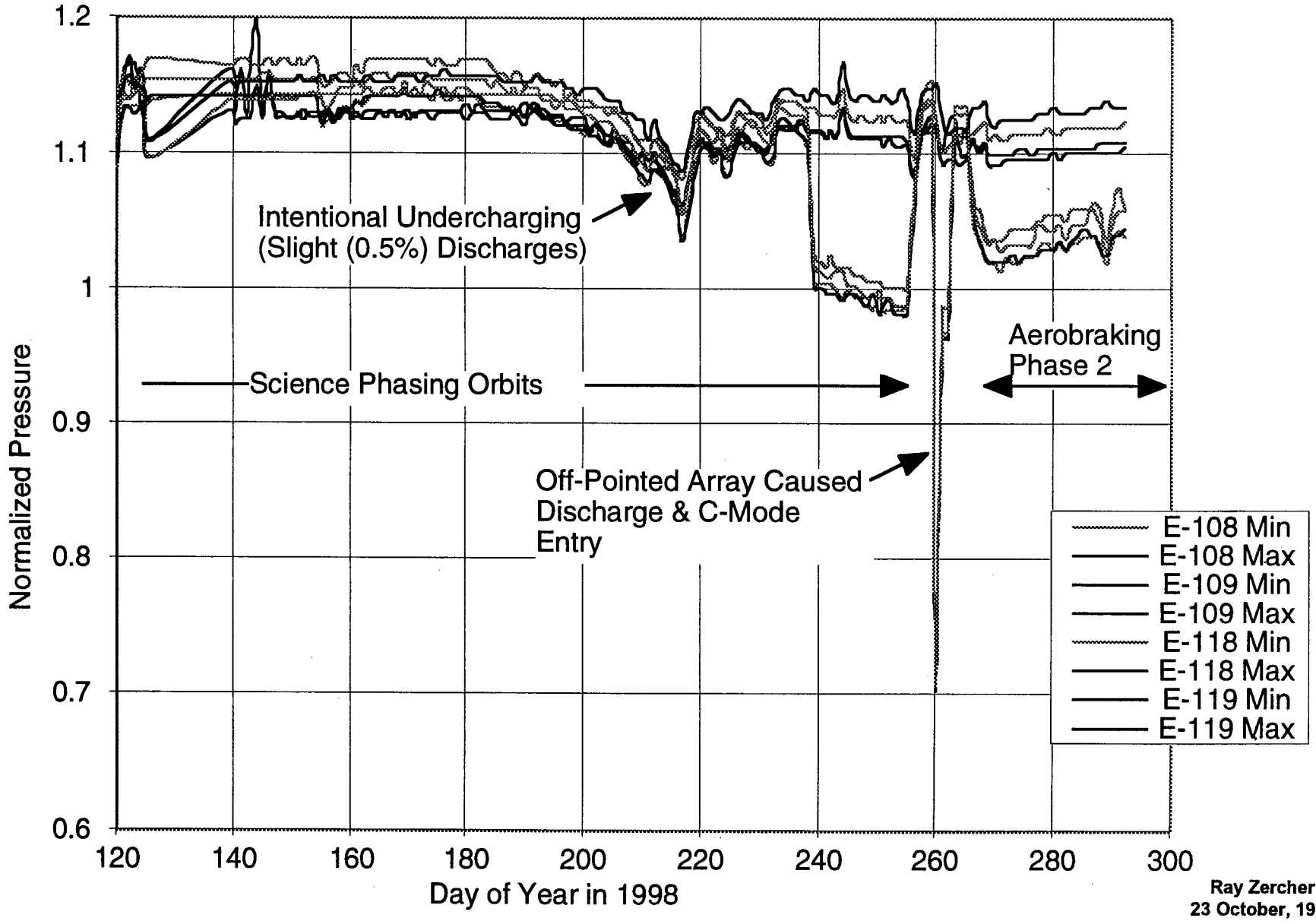

Ray Zercher -2
23 October, 1998

MGS Battery Pressure Data

Mars Surveyor Operations

Temperature History Since 5/1/98

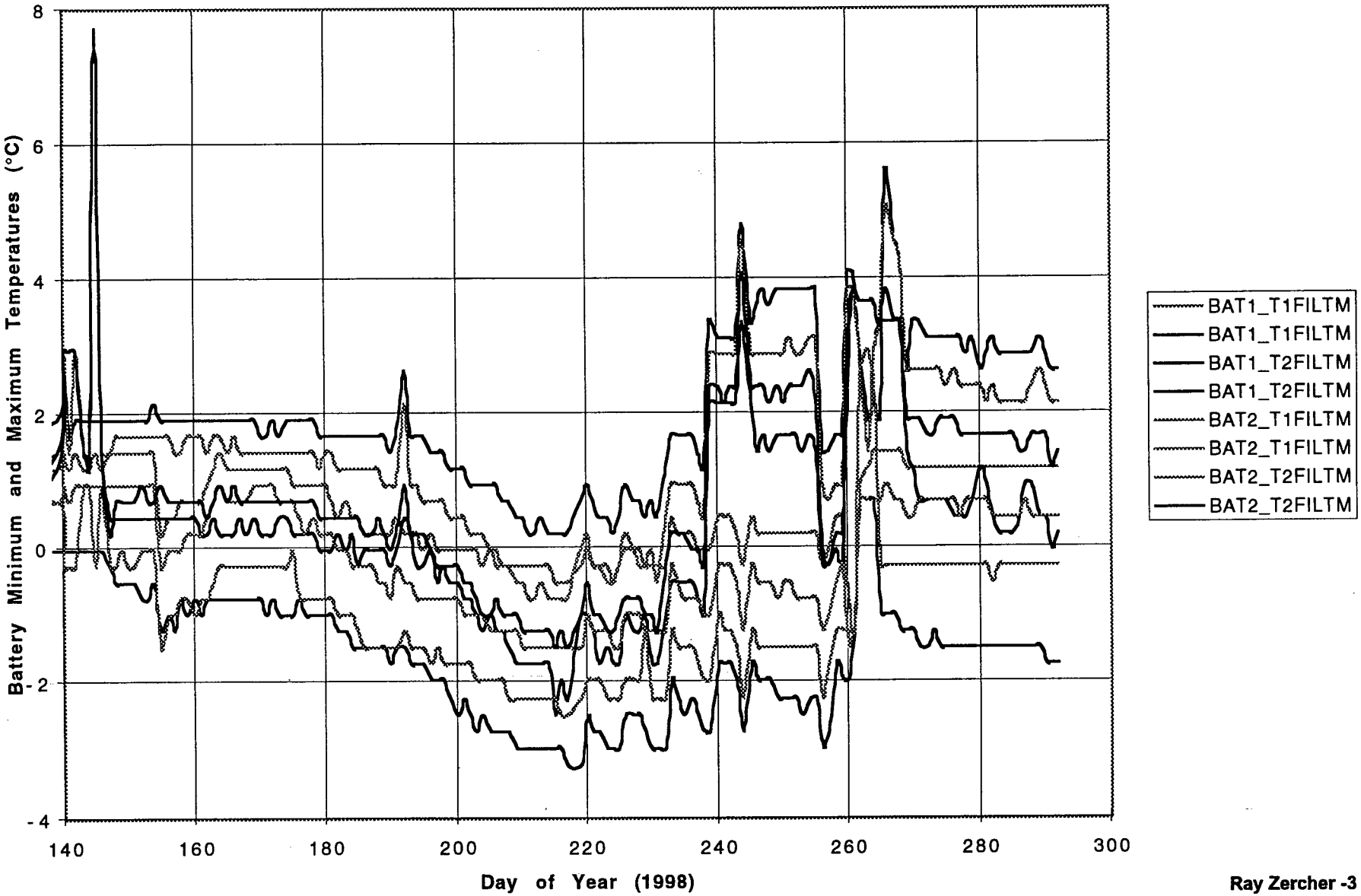

Ray Zercher -3
23 October, 1998

MGS Battery Pressure Data

ACKNOWLEDGMENT

This work was carried out at the Jet Propulsion Laboratory, California Institute of Technology, under contract with the National Aeronautics and Space Administration and was sponsored by:
NASA Code QT (Office of Safety and Mission Assurance)
NASA Code AE (Chief Engineer's Office) and the
MGS Project.

MGS Battery

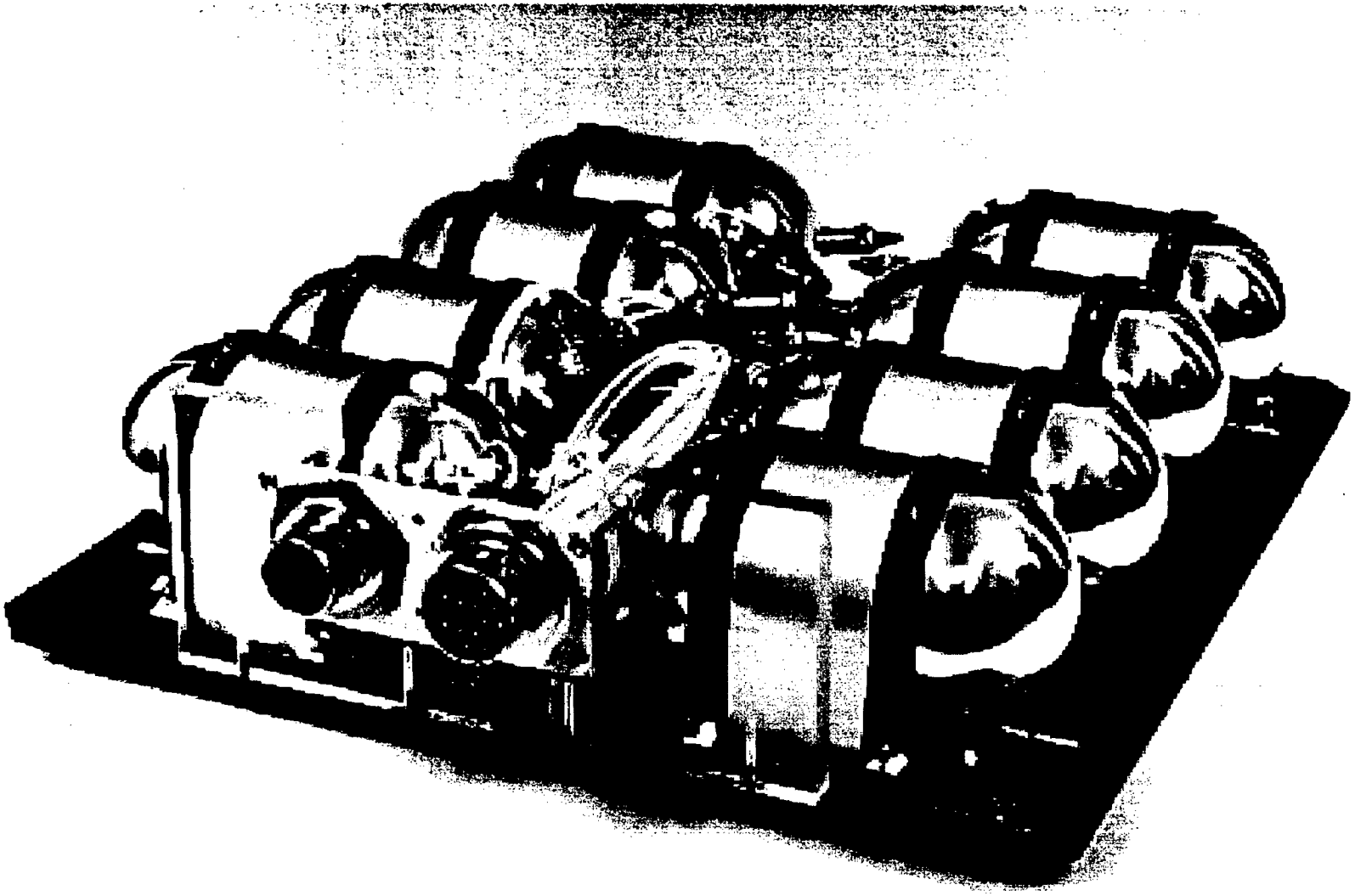

EAGLE PICHER Technologies,LLC

1998 NASA BATTERY WORKSHOP

CPV FLIGHT EXPERIENCE

by

William Cook and Jack Brill

Eagle Picher Technologies, LLC

Joplin Mo.

10-18-98 b.c

EAGLE PICHER Technologies,LLC

1998 NASA BATTERY WORKSHOP

PRESENTATION OUTLINE

- CPV HISTORY
- CPV IN FLIGHT
- DATA ON EXISTING FLIGHTS
- FUTURE FLIGHTS
- CPV ONGOING PROGRAMS
- UNIQUE CPV/IPV BATTERY

10-18-98 b.c

EAGLE PICHER Technologies,LLC

1998 NASA BATTERY WORKSHOP

CPV SAMPLE CELL

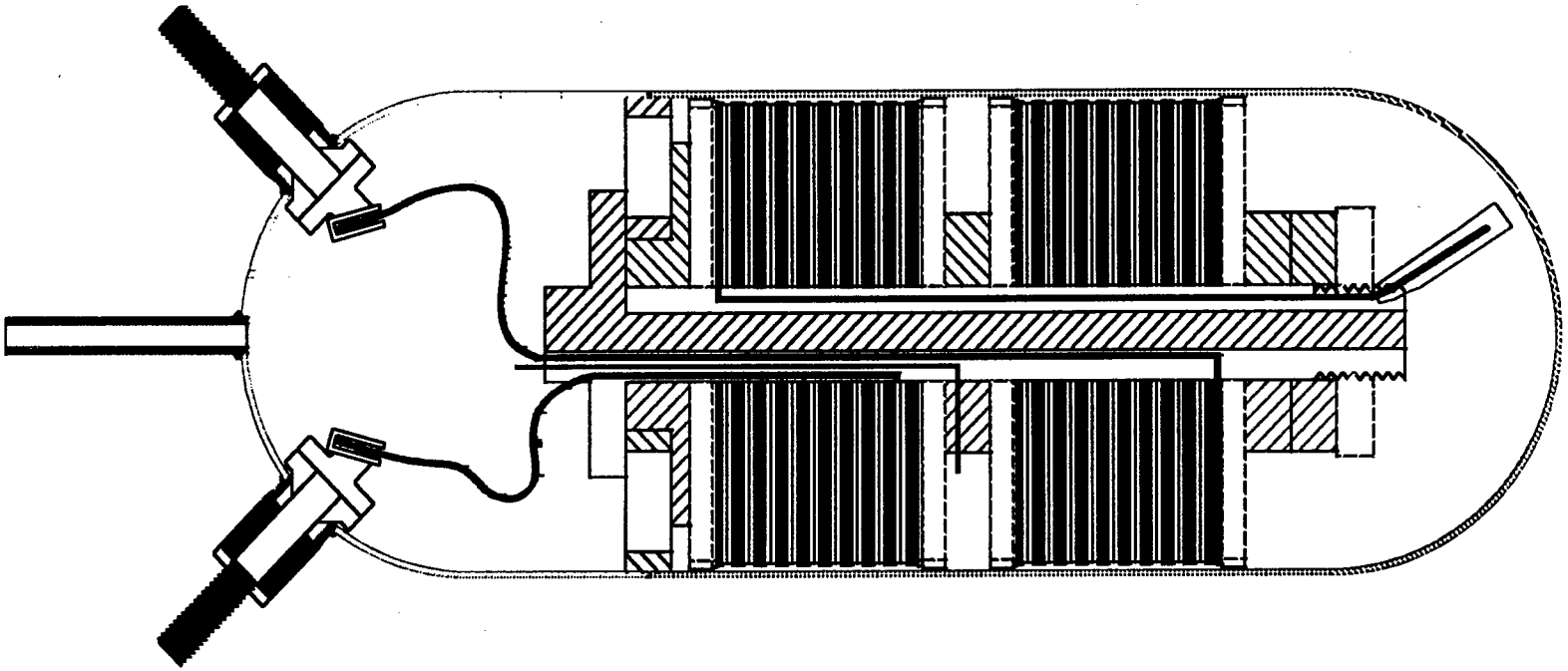

10-18-98 b.c

EAGLE PICHER Technologies,LLC

CPV'S ATTRIBUTE

- INCONEL OF STAINLESS PRESSURE VESSEL
- 30 MIL SLURRY POSITIVES
- TWO LAYER ZIRCAR SEPARATOR
- RABBIT EAR, AXIAL
- TEFLON OR ZIRCONIUM OXIDE WALL WICK
- VARIETY OF BATTERY CONFIGURATIONS

10-18-98 b.c

EAGLE PICHER Technologies,LLC

EAGLE PICHER CPV EFFORT

•1984	BUILT RNHC40 STUDY FOR ROCKWELL	REPORTED 1990 BATTERY CONF.
•1989	BUILT RNHC12-1 CPV FOR INTRASPACE	CELL DELIVERED BUT PROGRAM CANCELLED
•1990	EAGLE PICHER STARTED 2.5"CPV	REPORT IECEC 1990
•1992	EAGLE PICHER CONTRACTED WITH OSC FOR APEX AND SEASTAR PROGRAM	DELIVERED/ SMALL SAT CONF. FRANCE 1992
•1993	CONTRACTED FOR TUBSAT PROGRAM	DELIVERED LAUNCHED ON 1/25/94

10-18-98 b.c

EAGLE PICHER Technologies,LLC

1998 NASA BATTERY WORKSHOP

CPV FLIGHT 2.5"

Battery/ Cell	Program Name	Vehicle Launch Date	Termination Date	Nominal Capacity	Cycles/ Year	Total Cycle	# of Bat	CPV's/ Battery	Total CPV's	Total Cells
RNHC-6-1	TUBSAT-B	25-Jan-94	5-Mar-94	6	5,840	987	1	4	4	8
SAR-10037 (RNHC-10-1)	MSTI-2	8-May-94	5-July-94	10	5,840	1488	1	11	11	22
SAR-10027 (RNHC-6-1)	APEX	3-Aug-94		6	5,400	22,760	1	10	10	20
RNHC-10-1	ORBCOMM F1	3-Apr-95		10	5,475	19,432	1	5	5	10
RNHC-10-1	ORBCOMM F2	3-Apr-95		10	5,475	19,432	1	5	5	10
RNHC-10-1	MICROLAB F1	3-Apr-95		10	5,475	19,432	1	5	5	10
RNHC-10-1	MSTI-3	16-May-96	11-Dec-97	10	5,475	3472	1	11	11	22
SAR-10035 (RNHC-10-1)	SEASTAR	2-Aug-97		10	5,475	6,652	1	10	10	20
RNHC-10-1	ORBCOMM	24-Dec-97		10	5,256	4,312	1	5	5	10
RNHC-10-1	ORBCOMM	24-Dec-97		10	5,256	4,312	1	5	5	10
RNHC-10-1	ORBCOMM	24-Dec-97		10	5,256	4,312	1	5	5	10
RNHC-10-1	ORBCOMM	24-Dec-97		10	5,256	4,312	1	5	5	10
RNHC-10-1	ORBCOMM	24-Dec-97		10	5,256	4,312	1	5	5	10
RNHC-10-1	ORBCOMM	24-Dec-97		10	5,256	4,312	1	5	5	10
RNHC-10-1	ORBCOMM	24-Dec-97		10	5,256	4,312	1	5	5	10
RNHC-10-1	ORBCOMM	10-Feb-98		10	5,475	3,772	1	5	5	10
RNHC-10-1	ORBCOMM	10-Feb-98		10	5,475	3,772	1	5	5	10
RNHC-10-1	TELEDESIC T1	26-Feb-98		10	5,475	3,532	1	5	5	10

10-18-98 b.c

EAGLE PICHER Technologies,LLC

1998 NASA BATTERY WORKSHOP

CPV FLIGHT 2.5" CONT

SAR10077 (RNHC-4-1)	SAFIR-2 (OHB)	9-July-98		4	5400	1,920	1	10	10	20
RNHC-10-1	ORBCOMM	2-Aug-98		10	5,256	1,130	1	5	5	10
RNHC-10-1	ORBCOMM	2-Aug-98		10	5,256	1,130	1	5	5	10
RNHC-10-1	ORBCOMM	2-Aug-98		10	5,256	1,130	1	5	5	10
RNHC-10-1	ORBCOMM	2-Aug-98		10	5,256	1,130	1	5	5	10
RNHC-10-1	ORBCOMM	2-Aug-98		10	5,256	1,130	1	5	5	10
RNHC-10-1	ORBCOMM	2-Aug-98		10	5,256	1,130	1	5	5	10
RNHC-10-1	ORBCOMM	2-Aug-98		10	5,256	1,130	1	5	5	10
RNHC-10-1	ORBCOMM	2-Aug-98		10	5,256	1,130	1	5	5	10
RNHC-10-1	ORBCOMM	2-Aug-98		10	5,256	1,130	1	5	5	10
RNHC-10-1	ORBCOMM	2-Aug-98		10	5,256	1,130	1	5	5	10
RNHC-10-1	ORBCOMM	2-Aug-98		10	5,256	1,130	1	5	5	10
RNHC-10-1	ORBCOMM	2-Aug-98		10	5,256	1,130	1	5	5	10
RNHC-10-1	ORBCOMM	2-Aug-98		10	5,256	1,130	1	5	5	10

EAGLE PICHER Technologies,LLC

1998 NASA BATTERY WORKSHOP

CPV FLIGHT 3.5"

Battery/ Cell	Program Name	Vehicle Launch Date	Termination Date	Nominal Capacity	Cycles/ Year	Total Cycle	# of Batteries	CPV's/ Battery
SAR10061 (RNHC20-1)	MGS	7-Nov-96		20	2,000	3,898	2	8
RNHC-23-1	LEWIS	22-Aug-97	30-Sep-97	23	5,533	6,419	1	12
RNHC-20-3	GEOSAT Follow-on	10-Feb-98		20	5,309	3,657	1	11

10-18-98 b.c

EAGLE PICHER Technologies,LLC

1998 NASA BATTERY WORKSHOP

FLIGHT SUMMARY

- FORTY(40) CPV BATTERIES LAUNCHED TO DATE
- ONE 4AH BATTERY
- TWO 6 AH BATTERIES
- THIRTY- THREE 10AH BATTERIES
- THREE 20AH BATTERIES
- ONE 23 AH BATTERY
- ALL LEO APPLICATION

10-18-98 b.c

EAGLE PICHER Technologies,LLC

NEAR TERM CPV PROGRAMS

PROGRAM	PLANNED LAUNCH DATE	NOM. CAP.	VOLTAGE	COMMENTS
ORBCOMM-2	4/28/98	10	12.5	CPV DELIVERED 8 BATTERIES
QUICKBIRD	7/1/98	40	28	CPV DELIVERED 4 BATTERIES
DLR-TUBSAT	9/1/98	12	10	CPV DELIVERED 1 BATTERY
ORBITER	12/10/98	16	28	EPI 11-CPV BATTERY DELIVERED
LANDER	1/1/99	16	29	EPI 11-CPV/1 IPV BATT DEL
STARDUST	2/6/99	16	28	11-CPV BATTERY DELIVERED
ORBVIEW-3	6/1/99	20	28	11-CPV BATTERY, BUILDING
ORBVIEW-4	12/1/99	16	28	11-CPV BATTERY, BUILDING
CHAMP	12/1/99	16	28	11 CELLS FOR BATTERY BUILDING
MAP	8/1/00	23	28	11-CPV BATTERY, BUILDING
HISSI	99	15	28	11-CPV BATTERY, BUILDING
2001	99	16	28	11-CPV BATTERY, BUILDING
MITA	99	7	28	11-CPV BATTERY, BUILDING
DEEP SPACE	98	12	25	10-CPV BATTERY, BUILDING
GENISIS	99	16	28	11 CPV BATTERY, BUILDING
GRACE	99	16	28	11 CPV BATTERY, BUILDING
SAC-C	99	12	28	11 CPV BATTERY, BUILDING

10-18-98 b.c

EAGLE PICHER Technologies,LLC

1998 NASA BATTERY WORKSHOP

CPV ONGOING PROGRAMS

NOM. CAP.	CELL/BATTERY	PROGRAM	LAUNCH DATE	VOLTAGE	COMMENTS
100	RNHC 100-1	IR&D	N/A	N/A	(10) 40%DOD 1.04RR 5C 503 CYCLES
10	RNHC 10-1	LIFE TEST	N/A	N/A	11 CELLS, 40% DOD, 1.04 RR 23k CYCLES
16	RNHC 16-9	NASA LEWIS	N/A	N/A	31%KOH TOROSPHERICAL ZIRCONIUM OXIDE WALL WICK
16	RNHC 16-11	NASA LEWIS	N/A	N/A	26KOH TOROSPHERICAL ZIRCONIUM OXIDE WALL WICK
16	RNHC 16-13	NASA LEWIS	N/A	N/A	26%KOH TOROSPHERICAL ZIRCONIUM OXIDE WALL WICK WITH CATALYST STRIPS

10-18-98 b.c

EAGLE PICHER Technologies,LLC

1998 NASA BATTERY WORKSHOP

CPV/IPV BATTERY DESIGN

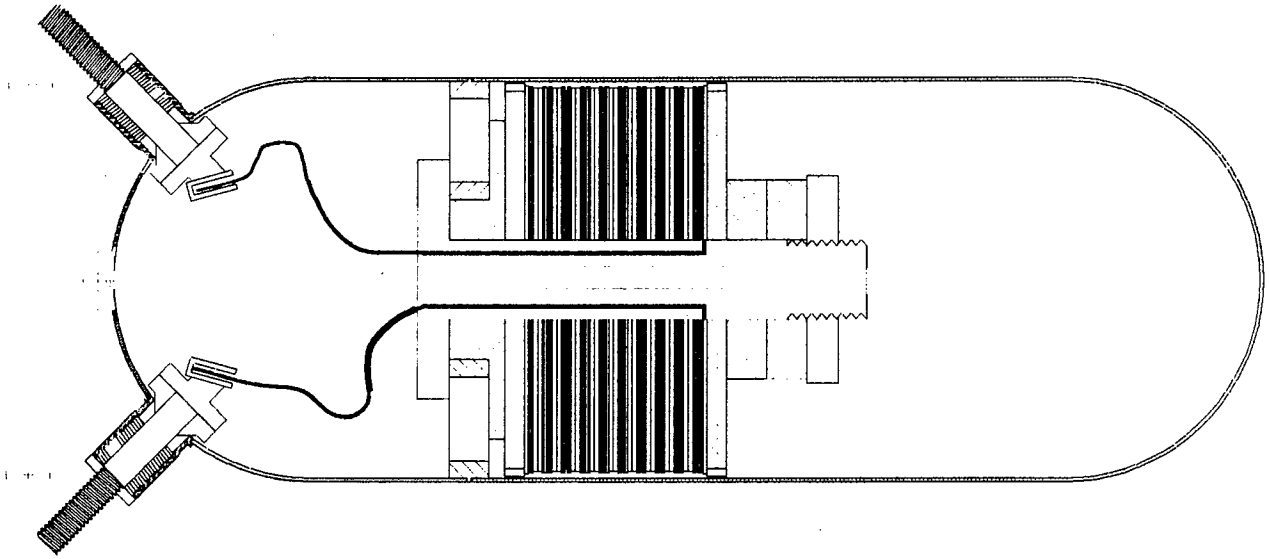

10-18-98 b.c

EAGLE PICHER Technologies,LLC

1998 NASA BATTERY WORKSHOP

CPV/IPV BATTERY DESIGN

8 b.c

EAGLE PICHER Technologies,LLC

1998 NASA BATTERY WORKSHOP

BATTERY DESIGNS

TYPICAL SMALL SPACECRAFT CPV BATTERY DESIGNS

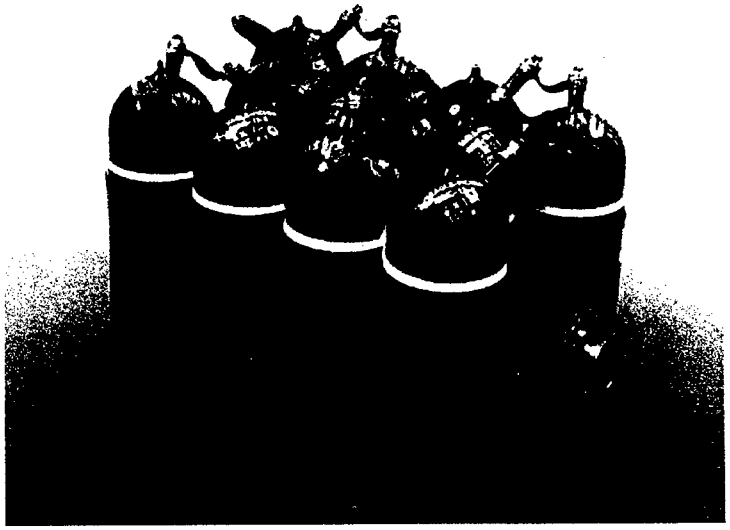

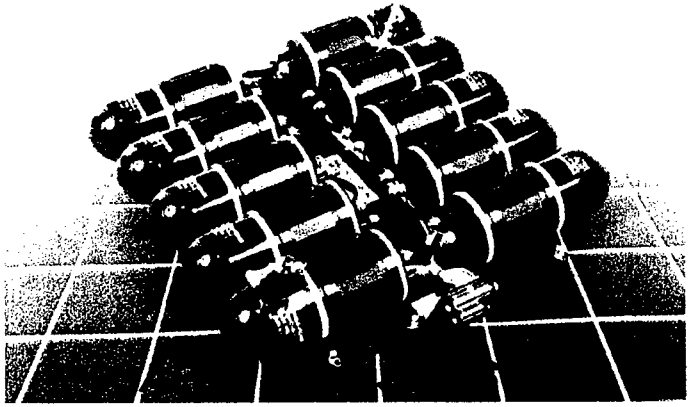

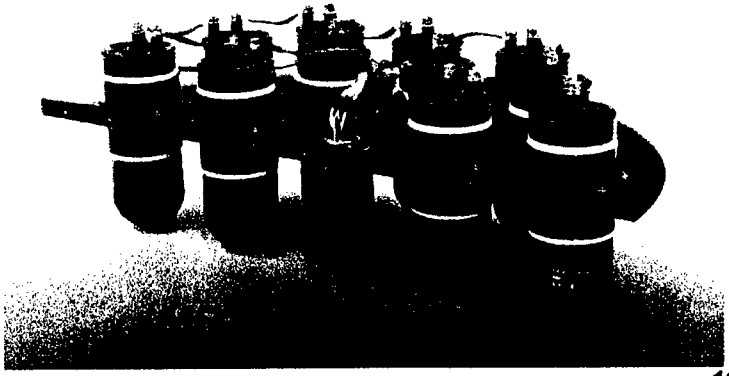

10-18-98 b.c

EAGLE PICHER Technologies,LLC

1998 NASA BATTERY WORKSHOP

SUMMARY

- 36 CPV BATTERIES LAUNCHED UTILIZING 2.5" TECHNOLOGY
- 4 CPV BATTERIES LAUNCHED UTILIZING 3.5 " TECHNOLOGY
- 26 CPV BATTERIES SCHEDULED TO LAUNCH IN NEAR FUTURE
- INCREASE RELIABILITY DUE TO LESS PARTS COUNT
- REDUCED FOOTPRINT
- REDUCED WEIGHT
- CPV HAS ESTABLISHED ITSELF IN THE SATELLITE MARKET

10-18-98 b.c

STATUS OF SPV/CPV TESTING

NAVAL SEA SYSTEMS COMMAND

NSWC

Naval Surface Warfare Center

CRANE DIVISION

Authors: Harry Brown & Steve Hall

1998 NASA AEROSPACE BATTERY WORKSHOP
October 27-29 1998 Huntsville Al.

Introduction Slide.

NAVAL SEA SYSTEMS COMMAND
NSWC
Naval Surface Warfare Center
CRANE DIVISION

STATUS OF SPV/CPV Testing At CRANE DIVISION NSWC

OUTLINE

Common Pressure Vessel (CPV)

- 10 Ahr, 2.5 in. Stainless Steel vessel - RNHC 10-1
  - Pack 3002L - >23600 (4.0 years) -- NASA Lewis Battery Program
- 45 Ahr. 3.5 in Heritage Cells
  - Pack 3005L - >12892 (2.2 years) -- Air Force Research Laboratory
  - Pack 3006L - > 13375(2.3 years) -- Air Force Research Laboratory
  - Pack 3007L - > 14 Accel. GEO cycles -- Air Force Research Laboratory
- 45 Ahr. 3.5 in Heritage Cells w/26% KOH and Wall Wick
  - Pack aaaaa - Catalyzed Wall Wick-- NASA Lewis Battery Program
  - Pack bbbbb - Non-Catalyzed Wall Wick
- 16 Ahr. 2.5 in Heritage Cells w/26% and 36% KOH
  - Pack ccccc -- NASA Lewis Battery Program
- 16 Ahr. 2.5 in Heritage Cells w/Design improvements
  - Pack ddddd 31% KOH -- NASA Lewis Battery Program
  - Pack ddddd 26% KOH
  - Pack ddddd 26% KOH and Catalyzed Wall Wick

Single Pressure Vessel (SPV) 50 Ahr, 10 inch diameter

- Pack 3003L - >20615 (3.5 years) -- NASA Lewis Space Station Program
- Pack 3004L - >13336 (2.3 years) -- Air Force Research Laboratory

This slide summarizes the SPV and CPV test that are on going or planned at Crane.

The SPV's will be covered in detail. Both NASA and Air Force have a battery under test.

The CPV's 2.5 in RNHC 10-1 design is a part of NASA Lewis CPV Technology program.

The 45 Ahr. 3.5 in Heritage cells were purchased by Air Force as a commercial procurement without a government spec. These tests are also a part of a NASA/ Air Force Joint program to evaluate CPV designs.

The remaining tests are planned. These cells evaluate the Design improvements that NASA has been evaluating on IPV cells. One group 16 Ahrs also includes design improvements incorporated by the manufacturer EP.

STATUS OF SPV/CPV Testing At
CRANE DIVISION NSWC

CPV - RNHC10-1 Pack 3002L

NASA Lewis Battery - Pack 3002L
Quantity - 10 cells (1 removed for DPA)
Orbit 90 Minute LEO
Test Temperature = 10°C
DoD = 40%
Discharge Current =
6.71 Amps for 36 Minutes
Recharge - 104%
Charge Current =
4.64 Amps for 54 Minutes

Completed 23582 cycles 4 yrs
as of 10/1/98

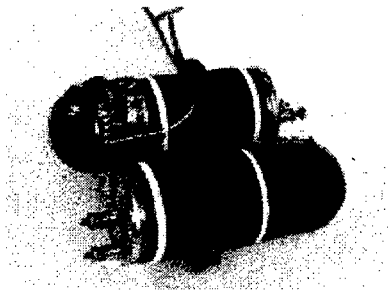

This Pack has completed 4 yrs of cycling under a LEO regime.

At 2 yrs one cell was removed and subjected to DPA. No anomalies were found.

Picture and cell design to be included..

This test sponsored by NASA Lewis CPV Technology Program.

POC Mr. Tom Miller

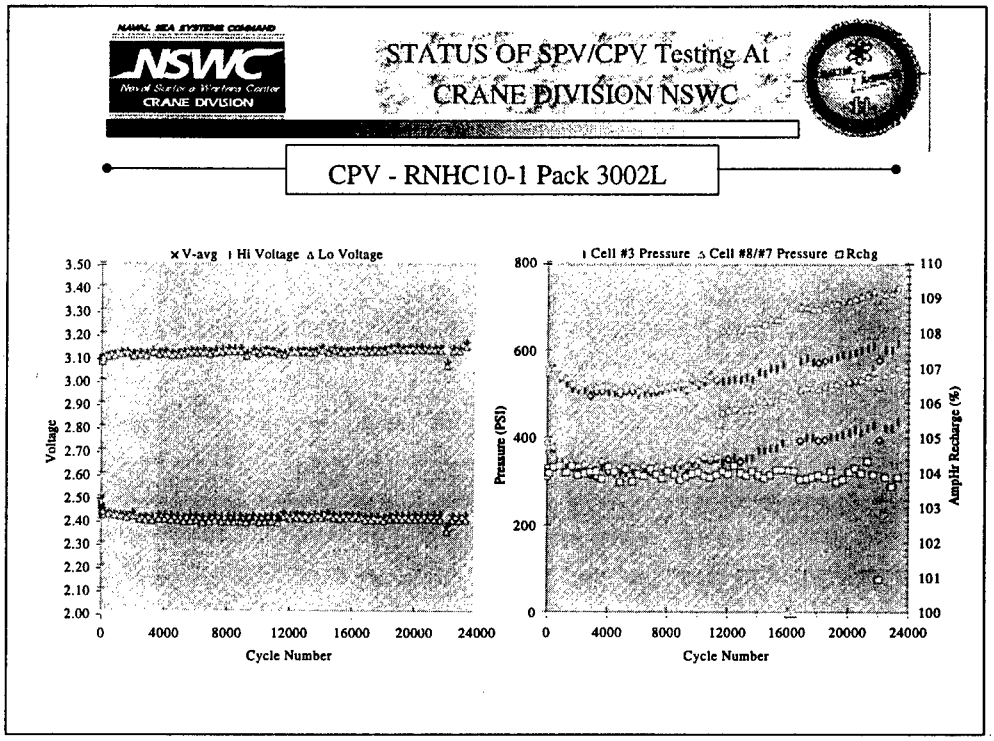

Life cycle voltage and pressure trend plot for Pack 3002L.

There has been little change in the end of discharge and charge voltages of the cells over the 23500 cycles. The change in pressure is due to a change in the measuring strain gage. Cell 8 (original pressure measurement) was removed for DPA. The step increase in the pressure curve occurred when Cell 7 replaced Cell 8 in recording data.

This test sponsored by NASA Lewis CPV Technology Program.

POC Mr. Tom Miller

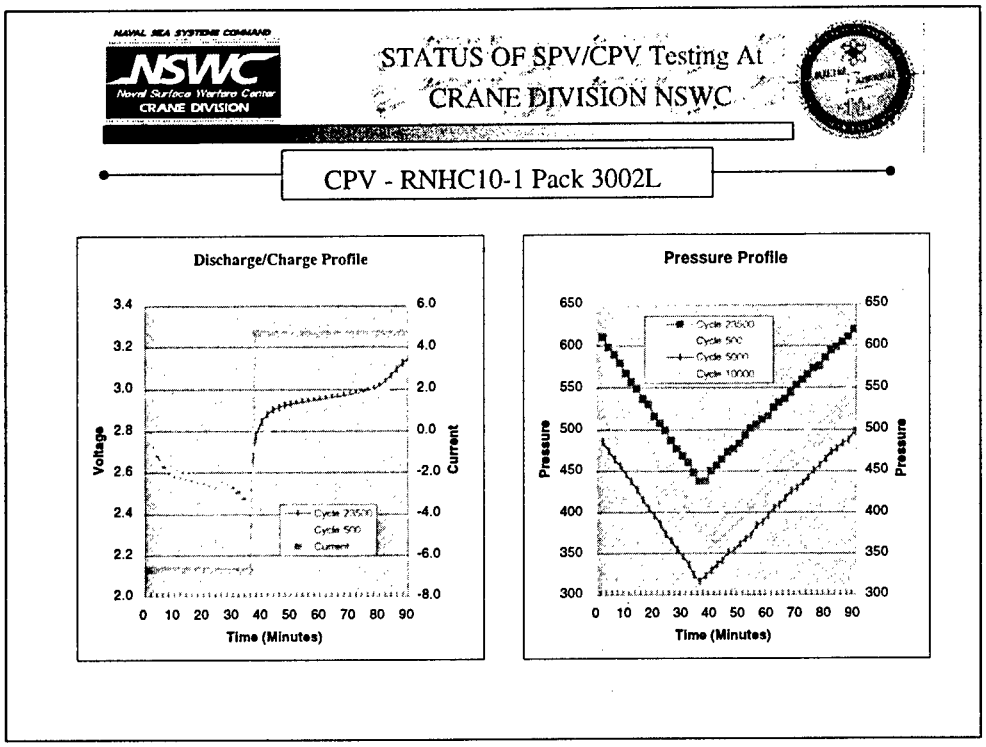

Voltage and Pressure Plot of cycle 500 and 23500. NOTE there is no significant change in the discharge/charge curve and no change in the end of discharge voltage. One would expect a drop in the EOD voltage with life. The Pressure plot is normal in that pressure decreases initially then increases with cycling.

This test sponsored by NASA Lewis CPV Technology Program.

POC Mr. Tom Miller

NAVAL SEA SYSTEMS COMMAND
NSWC
Naval Surface Warfare Center
CRANE DIVISION

STATUS OF SPV/CPV Testing At
CRANE DIVISION NSWC

CPV 45 Ahr Air Force RNHC 45-1

Manuf. Eagle-Picher (Joplin)
Model: RNHC 45-1
Capacity 45 Ahr.
Weight 2.66 Kg Length 13.9 in.
Diameter 3.5 in.
Plates 35 mils Thick
Back to Back
2 layer ZIRCAR
31% KOH
Received 8/95

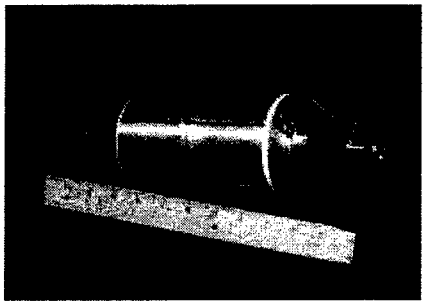

Test Conditions
18 cells were divided into 3 test packs.

The design parameters for the CPV cells was taken from Eagle-Picher commercial specification.

This test sponsored by Air Force Research Laboratory.
POC Mr. Ralph James, Dan Radzykewycz.
Technical Direction: The Aerospace Corporation
POC Ms. Carole Hill

NAVAL SEA SYSTEMS COMMAND
NSWC
David Taylor Model Basin
CRANE DIVISION

STATUS OF SPV/CPV Testing At
CRANE DIVISION NSWC

CPV 45 Ahr Air Force RNHC 45-1

LIFE CYCLE TEST CONDITIONS

	Pack 3005L	Pack 3006L	Pack 3007L
Quantity	6 Cells	6 Cells	6 Cells
Orbit	LEO 90 Min.	LEO 90 Min	Accel. GEO- 24Hrs 42 Day Cycle, 14 Day Trickle Charge
Test Temp	10 °C	-5 °C	10 °C
DoD	40%	40%	15%-75%-15%
Discharge	36 Amps for 30 Min		28.12 Amps
Recharge	104%	104%	110%
Charge	23.50 Amps for 46 Min		2.25 (C/20) to 100%
Trickle Charge	3.10 Amps for 14 Min		C/100 for remainder 24 Hrs
Status10/1/98	12900	13375	784 (14 Seasons)

The cells are being subjected to conditions shown. The LEO Packs have completed over 2 years of test with no anomalies. The GEO pack has completed 14 accelerated seasons.

This test sponsored by Air Force Research Laboratory

POC Mr. Ralph James, Dan Radzykewycz.

Technical Direction: The Aerospace Corporation

POC Ms. Carole Hill

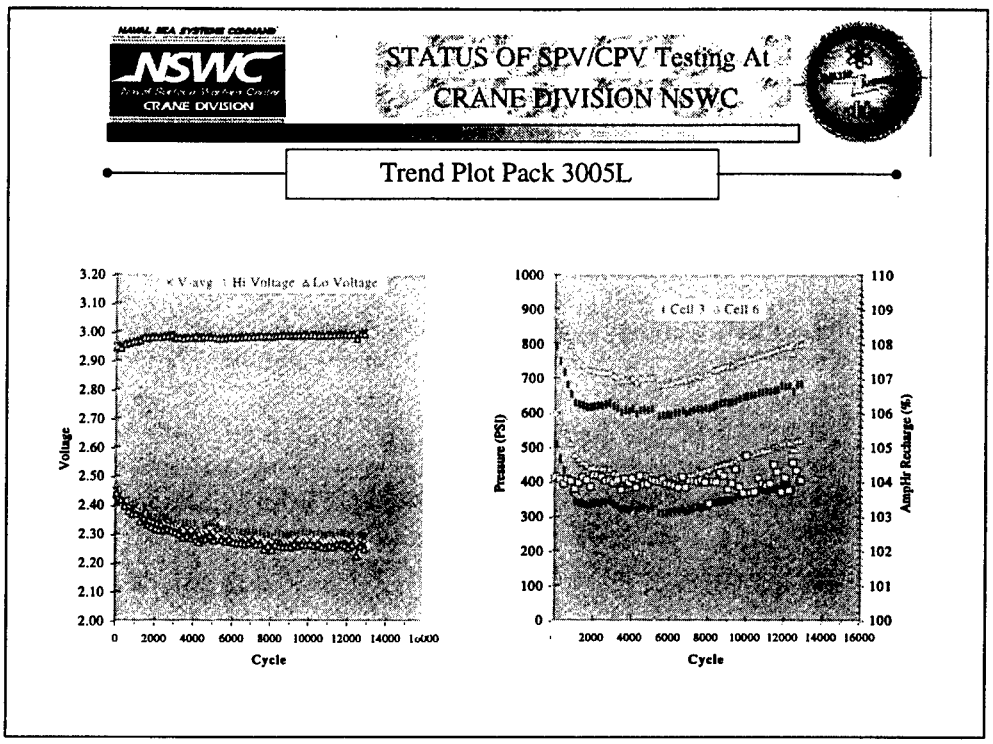

Life cycle voltage trend plot of Pack 3005L.

Life Cycle Pressure and Recharge Trend plot of Pack 3005L

This test sponsored by Air Force Research Laboratory.

POC Mr. Ralph James, Dan Radzykewycz.

Technical Direction: The Aerospace Corporation

POC Ms. Carole Hill

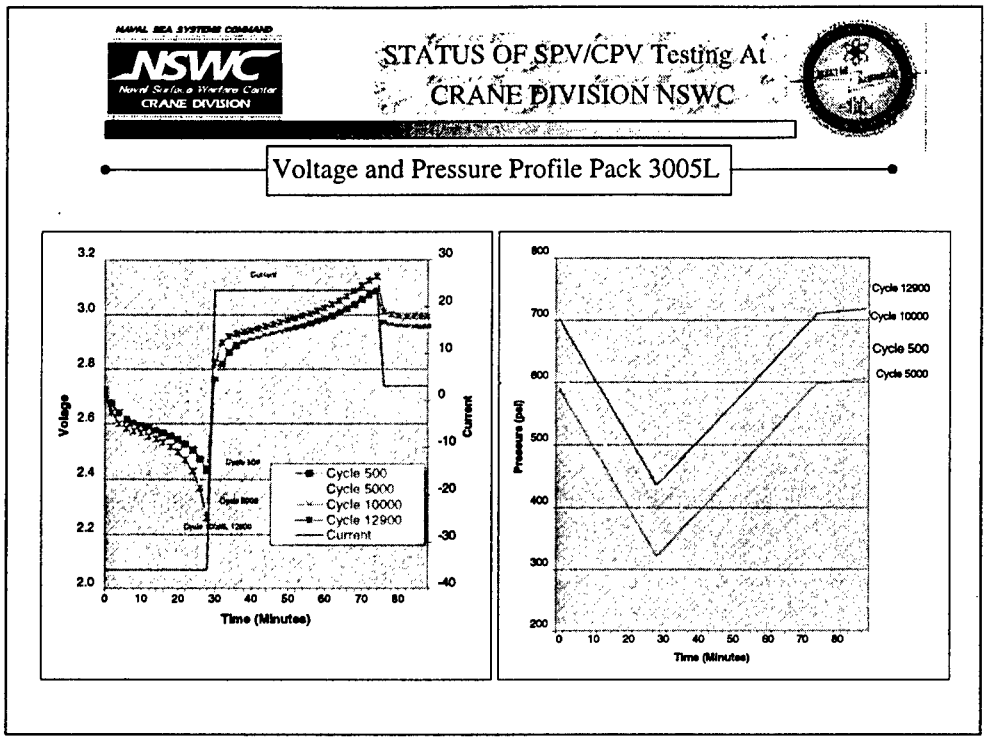

Typical discharge/charge cycle for Pack 3005L.

Typical pressure cycle for Pack 3005L

This test sponsored by Air Force Research Laboratory.

POC Mr. Ralph James, Dan Radzykewycz.

Technical Direction: The Aerospace Corporation

POC Ms. Carole Hill

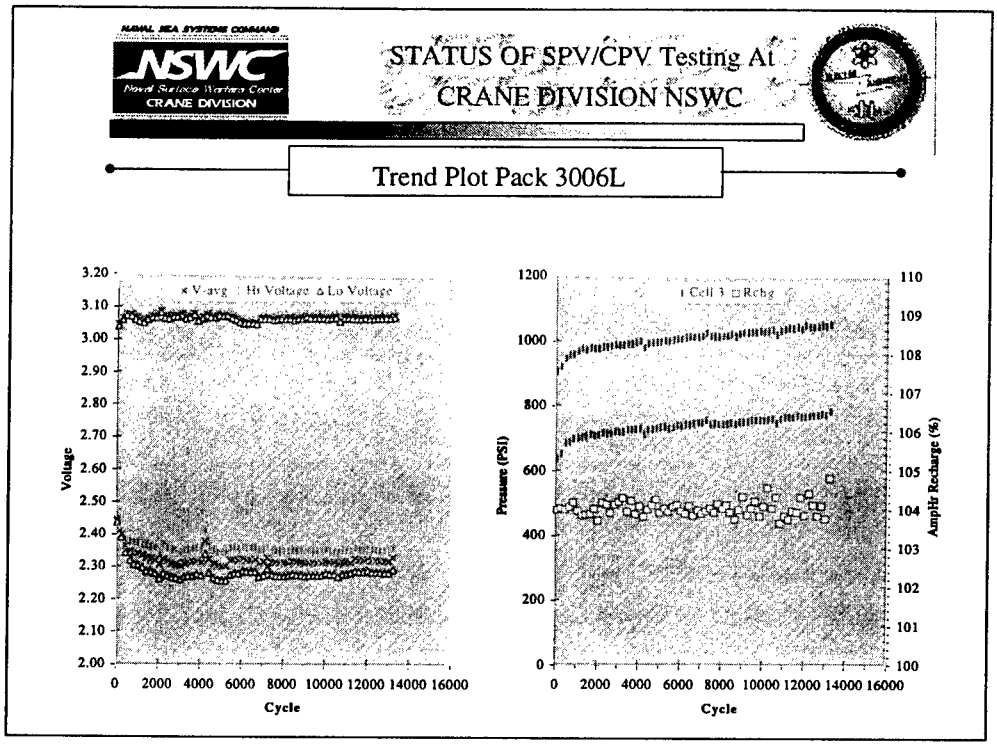

Life Cycle voltage trend plot of Pack 3006L. The pressure curve for this pack is different from that of Pack 3005L. The only difference between the two packs is the temperatue. Pack 3006L is tested at -5C.

This test sponsored by Air Force Research Laboratory.

POC Mr. Ralph James, Dan Radzykewycz.

Technical Direction: The Aerospace Corporation

POC Ms. Carole Hill

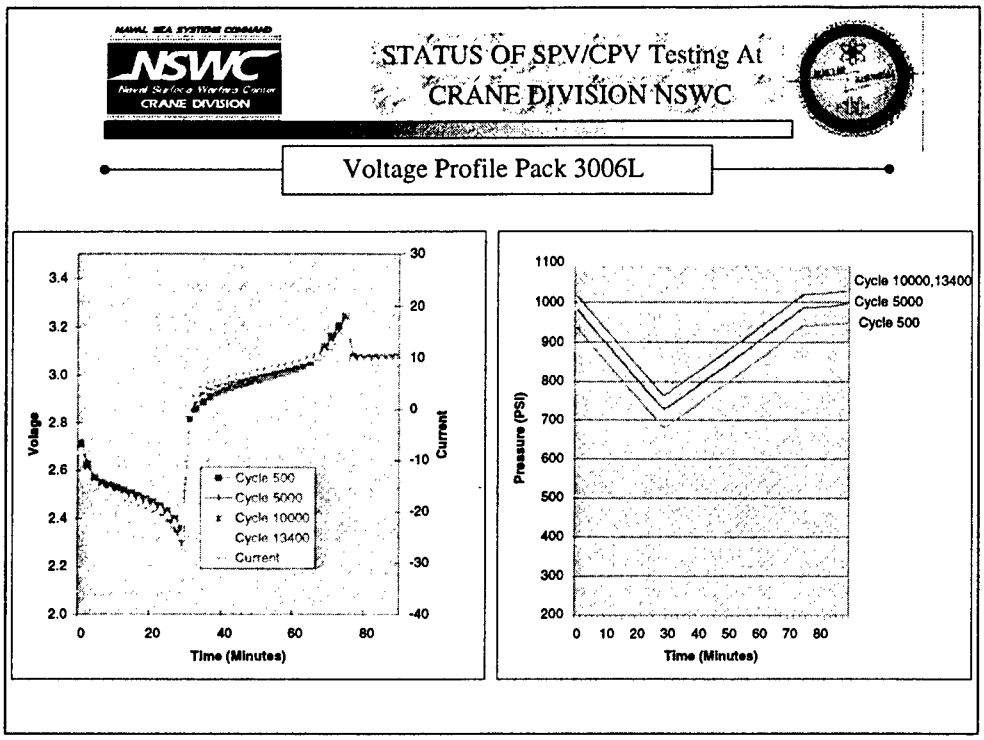

Typical discharge/charge curve for Pack 3006L

Typical pressure plot for Pack 3006L. This pack does not exhibit the characteristic pressure profile decrease from 500 to 5000 then increase for the remainder of life.

This test sponsored by Air Force Research Laboratory.

POC Mr. Ralph James, Dan Radzykewycz.

Technical Direction: The Aerospace Corporation

POC Ms. Carole Hill

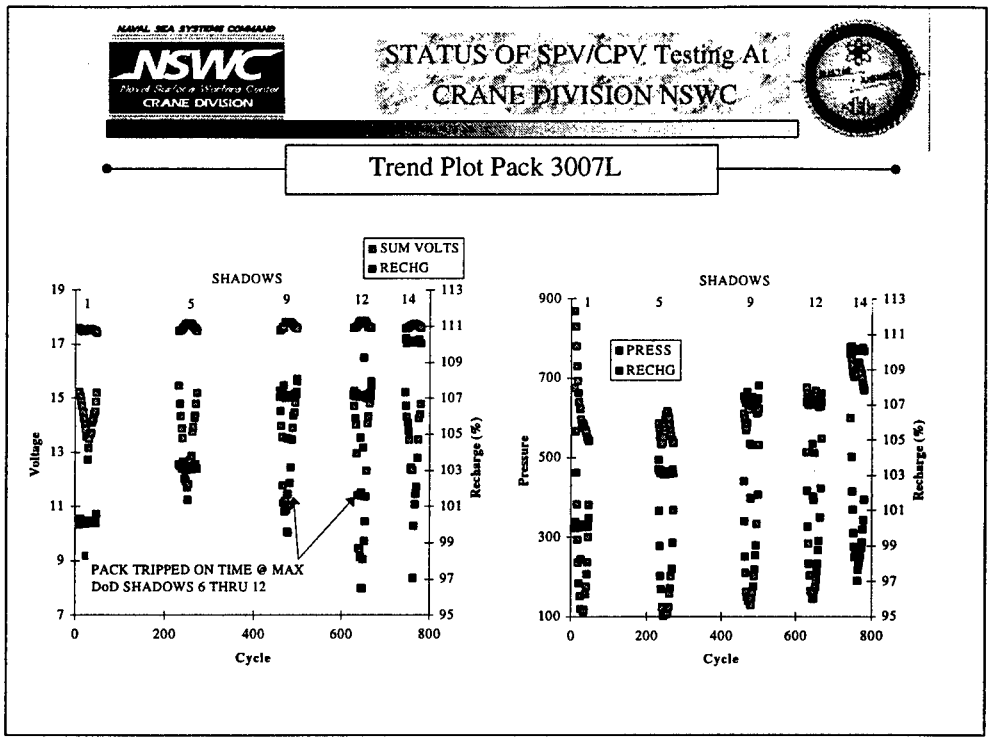

Life Cycle Trend plot for Pack 3007L. The curves represent the discharge during the shadow period from 15% to 75% to 15% DoD.

This test sponsored by Air Force Research Laboratory.

POC Mr. Ralph James, Dan Radzykewycz.

Technical Direction: The Aerospace Corporation

POC Ms. Carole Hill

NAVAL SEA SYSTEMS COMMAND
NSWC
Naval Surface Warfare Center
CRANE DIVISION

STATUS OF SPV/CPV Testing At
CRANE DIVISION NSWC

CPV RNHC 45-1 (Heritage)

Manufacturer Eagle-Picher Joplin
Plates: 80% slurry sinter,
35 mils thick from
EP Colorado Springs
Separator: Double layer ZIRCAR
Wall wick: Zirconium-oxide
Vessel wall Thickness - 0.030"
Terminal Design - Axial
Electrolyte - 26%

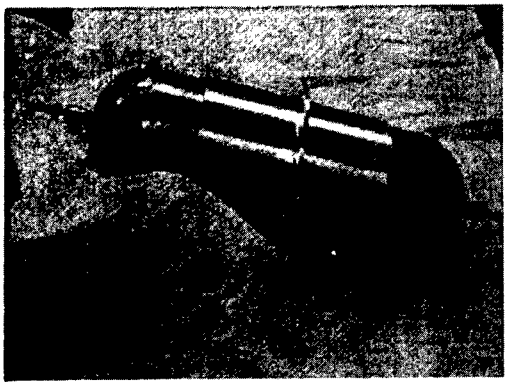

RNHC 45-7 - Non-catalyzed
RNHC 45-9 - Catalyzed

Status: Received Sep 98 Awaiting Test Plan

Design parameters for RNHC 45-7 and 9 cells. The RNHC 45-1 Heritage design is the design previously shown in test as Packs 3005L, 3006L, and 3007L.

This test sponsored by NASA Lewis CPV Technology Program.

POC Mr. Tom Miller

NAVAL SEA SYSTEMS COMMAND
NSWC
Naval Surface Warfare Center
CRANE DIVISION

STATUS OF SPV/CPV Testing At
CRANE DIVISION NSWC

CPV RNHC 16-1 (Heritage)

Plates: 80% slurry sinter,
30 mils thick from
EP Colorado Springs
Separator: Double layer ZIRCAR
PV Wall: Teflonated
Vessel wall Thickness - 0.026"
Terminal Design - Rabbit-ear
Electrolyte - RNHC 16-5 26%
RNHC 16-7 31%

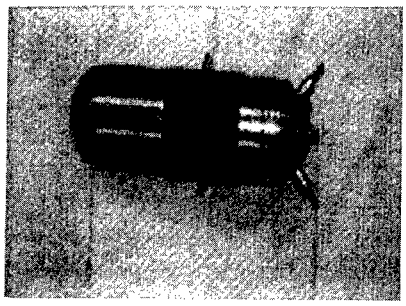

STATUS: Received Sep 98 Awaiting Test Plan

This test will evaluate the RNHC 16-1 design with modification of the electrolyte concentration to evaluate using 26% KOH in the cell.

This test sponsored by NASA Lewis CPV Technology Program.

POC Mr. Tom Miller

STATUS OF SPV/CPV Testing At CRANE DIVISION NSWC

CPV RNHC 16-9 New Design

Plates: 80% slurry sinter,
30 mils thick from
EP Colorado Springs
Separator: Double layer ZIRCAR
PV Wall: Teflonated
Vessel wall Thickness - 0.023"
Terminal Design - Rabbit-ear
Electrolyte - RNHC 16-9 31%
RNHC 16-11 26%
RNHC 16-13 26% & Catalyzed Wall Wick

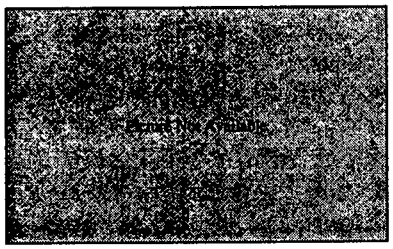

STATUS: Delivery scheduled for March 99

This test will evaluate design changes incorporated by the manufacturer and NASA improvements - 26% KOH and catalyzed wall wick

There are several design changes in the RNHC 16-9 cell. These include:

Incorporation of the fill tube in the positive terminal.

ZrO_2 coating of the CPV wall

Geometry change in the pressure vessel (Hydroformed/Spherical to Deep Drawn/Torospherical.

Other changes that may be proprietary to EP. Contact EP for details.

This test sponsored by NASA Lewis CPV Technology Program.
POC Mr. Tom Miller

STATUS OF SPV/CPV Testing At
CRANE DIVISION NSWC

Introduction - SPV

- 50 Ahr SPV
  - Eagle-Picher (JCI design) 28050SCP — NASA Lewis Research Center, International Space Station, Tom Miller
  - Eagle-Picher (Modified JCI) SAR-10067 — Air Force Research Laboratory, Ralph James, Dan Radzykewycz, Carole Hill (Aerospace Corp)

Eagle-Picher (JCI Design) - This battery is completely a Johnson Controls Industry (JCI) design, manufactured, assembled, and tested at the JCI facility in Butler, WI. The battery was delivered in Nov 1994. This was after EP purchased the facility.

Eagle-Picher (Modified JCI) - This battery was contracted from EP in 1994 before the move from Butler. The battery was originally bid as the JCI design, but in Jan 95 EP moved the facility from Butler, WI to Joplin, MO. Parts for the battery had been manufactured at Butler but the battery had not been assembled. The plate handling during the move was suspect. Thus EP manufactured new plates using the EP process at Joplin and modified the battery size.

NAVAL SEA SYSTEMS COMMAND
NSWC
CRANE DIVISION

STATUS OF SPV/CPV Testing At
CRANE DIVISION NSWC

Design - SPV

NASA LEWIS Pack 3003L		Air Force Pack 3004L	
Manuf.	Eagle-Picher (Bulter)	Manuf.	Eagle-Picher (Joplin)
Model:	28050SCP	Model:	SAR-10067
S/N	S-154	S/N	S-164
Capacity	50 Ahr.	Capacity	50 Ahr.
Weight	27.9Kg	Weight	29.4Kg
Length	29.968 in.	Length	24.682 in.
Diameter	10.104 in.	Diameter	10.139 in.
Cells	22 Flexible Containment Back to Back 2 layer ZIRCAR 31% KOH	Cells	22 Flexible Containment Back to Back 2 layer ZIRCAR 31% KOH
Design	Johnson Controls	Design	JC modified by EP
Plates	Slurry - Johnson Controls	Plates	Eagle-Picher (Joplin)
Assembly	Johnson Controls	Assembly	Eagle-Picher (Joplin) using JC materials and molds.
Received	11/94	Received	11/95

The differences in the design are shown in this slide. The AF battery is about 5 inches shorter and the plates were manufactured at Joplin. The assembly was at Joplin facility using the JCI materials and molds.

The design modification (shorter) reflect changes implemented in the commercial contract.

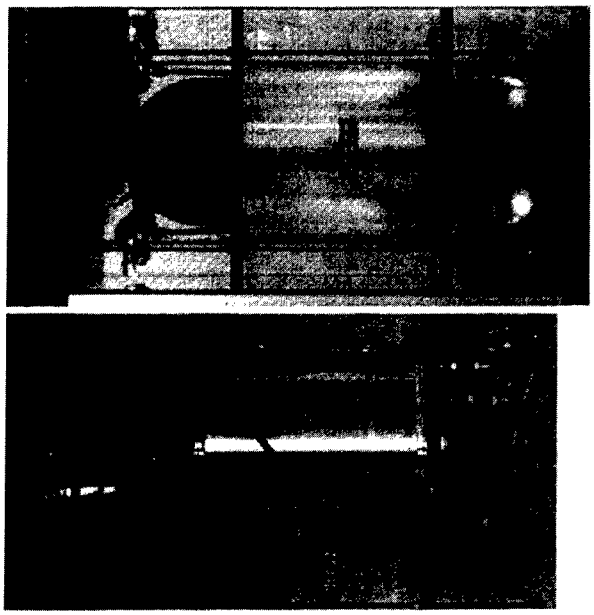

NASA LEWIS
Pack 3003L

Air Force
Pack 3004L

The differences in the design are shown in this slide. The EP design is about 5 inches shorter and the plates are manufactured at Joplin. The assembly was at Joplin facility using the JC materials and molds.

STATUS OF SPV/CPV Testing At CRANE DIVISION NSWC

Acceptance Test

NASA Lewis Battery - Pack 3003L
Conditioning 20 cycles 43 Ahr
Capacity Test 10°C

Rate	Ahr to 22.0v	Ahr to 11.0v
C/2	43.09	C/10 8.71
C	43.09	C/10 8.70
1.4C	44.72	C/10 8.37
2C	42.63	C/10 9.88

Charge Retention 0°C

C/2	37.97	C/10 2.94

Air Force Battery - Pack 3004L
Conditioning 16 cycles 61. Ahr
Capacity Test 10 °C 60.80 Ahr

Temp/Rate	Ahr to 22.0v	Ahr. to 11.0v
-5 °C @ C	69.71	1.69
10°C @ C	63.94	1.51
10°C @ C/2	64.85	1.51
20°C @ C/2	59.44	2.43
30°C @ C/2	55.07	2.65

Overcharge Capacity

0°C @ C/2	75.13	3.43

Charge Retention 10°C

C/2	59.98	1.34

Pack 3003L - After 20 conditioning cycles the battery delivered on 43 Ahr. This was less then at the manufacturer's acceptance test. The battery had provided 54.6 Ahr. After some discussion it was decided to go ahead and test the battery.

Pack 3004L - This battery gave no problems during acceptance tests.

NAVAL SEA SYSTEMS COMMAND
NSWC
CRANE DIVISION

STATUS OF SPV/CPV Testing At
CRANE DIVISION NSWC

Life Cycle Conditions

NASA Lewis Battery - Pack 3003L
Orbit 90 Minute LEO
Test Temperature = 10°C
DoD = 35%
Discharge Current =
29.17 Amps for 36 Minutes
Recharge - 104%
Charge Current =
20.22 Amps for 54 Minutes

Completed 20615 cycles 3.5 yrs
as of 10/1/98

Air Force Battery - Pack 3004L
Orbit 90 Minute LEO
Test Temperature = 10°C
DoD = 40%
Discharge Current =
40 Amps for 30 Minutes
Recharge - 104%
Charge Current =
26.12 Amps for 46 Minutes
3.41 Amps for 14 Minutes
Completed 13336 cycles 2.3 yrs
as of 10/1/98

The Life Cycle test conditions are shown above.

The batteries although on slightly different regimes can be compared.

In terms of life the batteries are cycling 1 year apart.

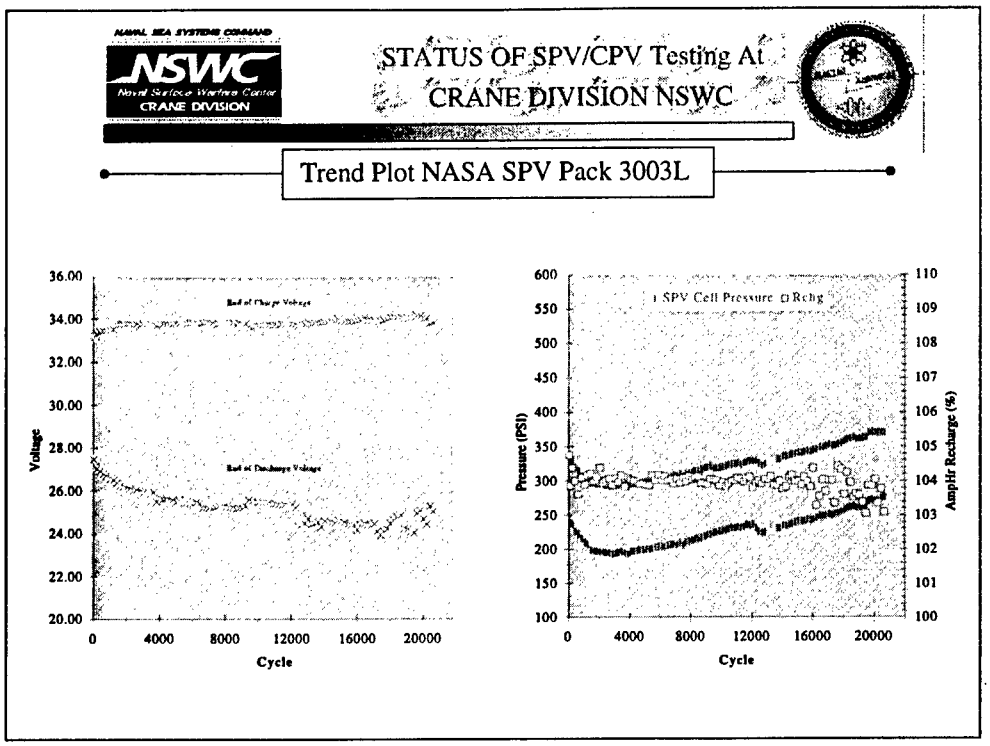

Trend Plot of Voltage vs Cycle for Pack 3003L.

The top line is the End-of-Charge (EOC) voltage.

The bottom line is the End-of-Discharge (EOD) voltage

At 26 volts EOD = 1.18 v/cell

At 34 volts EOC = 1.54 v/cell

Trend Plot of Pressure and Recharge vs Cycle for Pack 3003L.

The lower % Recharge may have caused the lower difference in EOD note in previous slide around 20000.

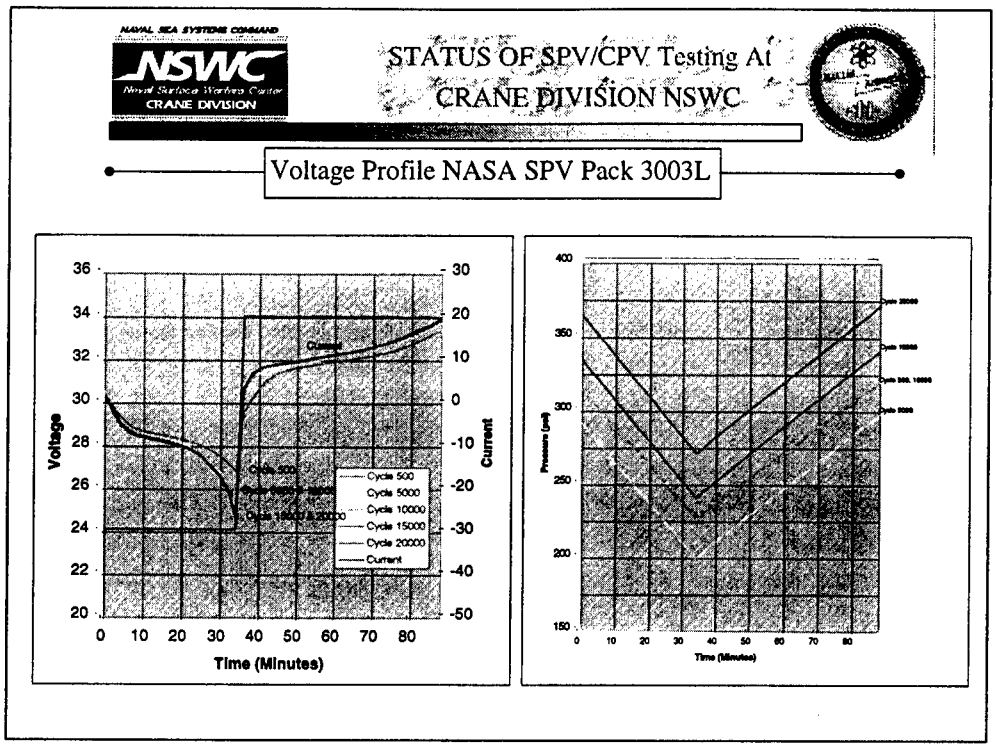

If the curves are not in color: The lowest EOD curve is cycles 20000 and 15000.

Cycles 5000 and 10000 are in the middle, and cycle 500 is the top curve.

Note that the as the EOD is lower, EOC increases.

Cycle	EOD	EOC
500	26.86	33.43
5000		
10000	25.42	33.67
15000		
20000	24.77	33.99

Pressure change is very consistent. The pressure changes in the first 500 cycles. The curves remain linear. If Pressure is used as a state of charge, a recalibration must be done overtime.

Cycle	EOC	EDO
500	314	227
5000	292	200
10000	314	227
15000	335	241
20000	365	271

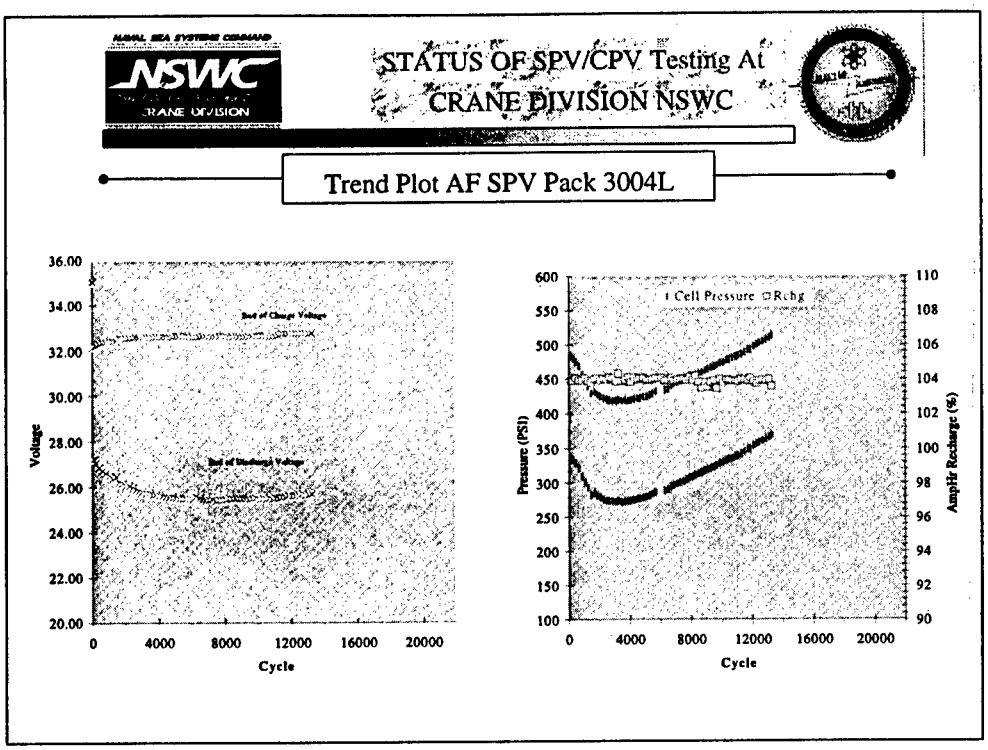

Voltage, Pressure and % Recharge Trend Plot for PACK 3004L

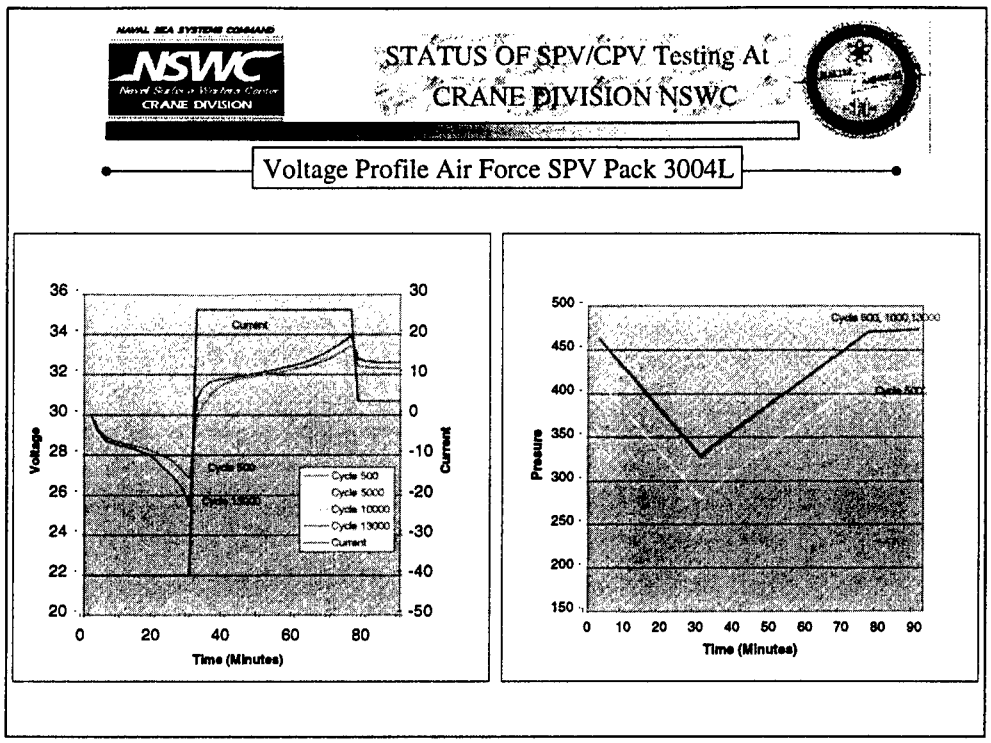

Voltage Profile for Cycles 500, 5000,10000, and 13000

Cycle 500 EOD = 26.82 EOC High Rate = 33.44 Trickle = 32.31

Cycle 13000 EOD = 25.47 EOC High Rate = 33.90 Trickle = 32.61

Pressure Profiles for the cycles

Cycles 500, 10000 and 13000 are the upper curve

Cycle 5000 is the lower curve

Cycle	EOD	EOC
500	329	464
5000	280	405
10000	329	464
15000	329	464

STATUS OF SPV/CPV Testing At
CRANE DIVISION NSWC

ACKNOWLEDGEMENT

SPONSORS:

NASA Lewis Research Center

NASA Aerospace Battery Systems Programs - Michelle Manzo

Nickel Hydrogen CPV Technology Evaluation - Tom Miller

Air Force Research Laboratory

Battery Program - Ralph James, Dan Radzykewycz

Technical Direction (Air Force)

The Aerospace Corporation - Carole Hill

EAGLE PICHER
Technologies, LLC

Nickel-Hydrogen Single Pressure Vessel (SPV) Battery Test Results

Steve Sterz, Beth Parmley, and Dwight Caldwell
Eagle-Picher Technologies, LLC
P. O. Box 47, Joplin, MO 64802

EAGLE PICHER Technologies, LLC

Nickel-Hydrogen

Single Pressure Vessel (SPV)

TRADITIONAL NiH_2 BATTERY CONFIGURATION

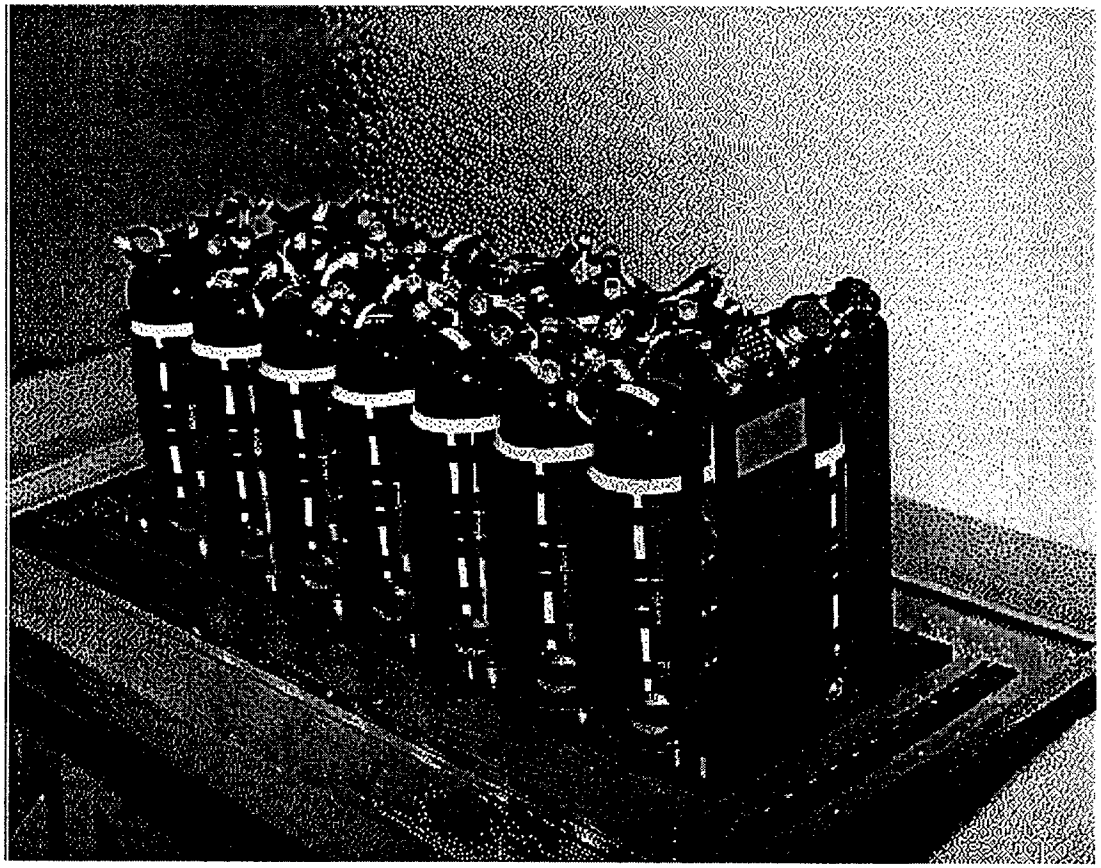

SPV NiH_2 BATTERY CONFIGURATION

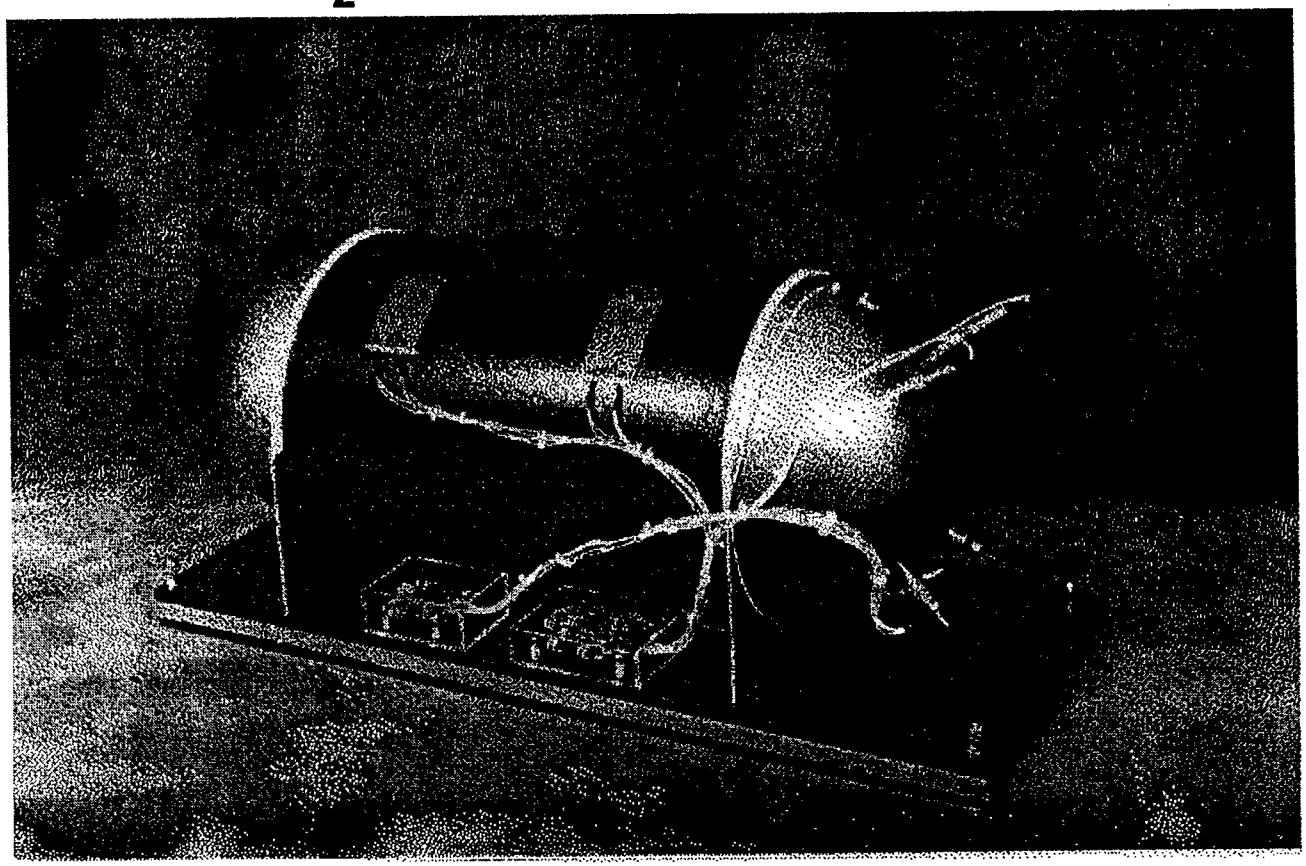

EAGLE PICHER Technologies, LLC

Nickel-Hydrogen Single Pressure Vessel (SPV)

SPV BATTERY DESIGN SUMMARY

- Battery type SAR 10081
- Nominal Voltage 27.5 V
- Rated Capacity 60 Ah
- Actual Capacity 70 Ah
- Weight 80.0 Lb (36.3 Kg)
- Spec. Energy 53.4 Wh/Kg
- Diameter 10.17"
- Length 25.2"
- Vessel Wall Thickness .056"
- Max. Expected Operating Pressure 800 psi
- Vessel Safety Factor >2.0

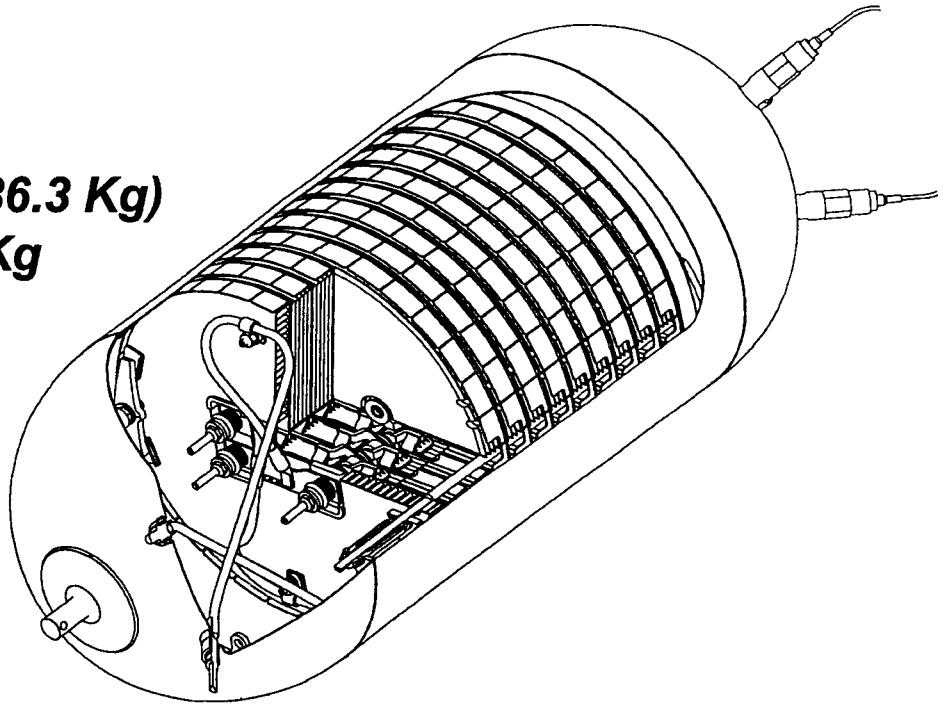

NICKEL-HYDROGEN SPV TESTING

- *Impedance vs. Depth-of-Discharge*
- *Capacity vs. Discharge Rate*
- *Mid Discharge Voltage vs. Discharge Rate*
- *Charge Retention vs. Open Circuit Time*
- *Charge Efficiency vs. Temperature*
- *Parallel Batteries on One Controller*

Impedance vs. Depth-of-Discharge (DOD)

- ***C/10 charge for 16 hours***
- ***C/2 discharge with 3C/2 pulses at 20, 40, 60 and 80% DOD***
- ***Impedance calculated by $\Delta V/\Delta I$ on the leading edge of the pulse***
- ***-10, 0, 10°C Test temperatures***

Depth of Discharge (%)	-10° C Impedance (mOhms/cell)	0° C Impedance (mOhms/cell)	10° C Impedance (mOhms/cell)
20	0.985	0.871	0.780
40	1.015	0.864	0.773
60	1.106	0.916	0.773
80	1.235	1.008	0.833

EAGLE PICHER Technologies, LLC

Nickel-Hydrogen

Single Pressure Vessel (SPV)

Impedance vs. Depth-of-Disharge

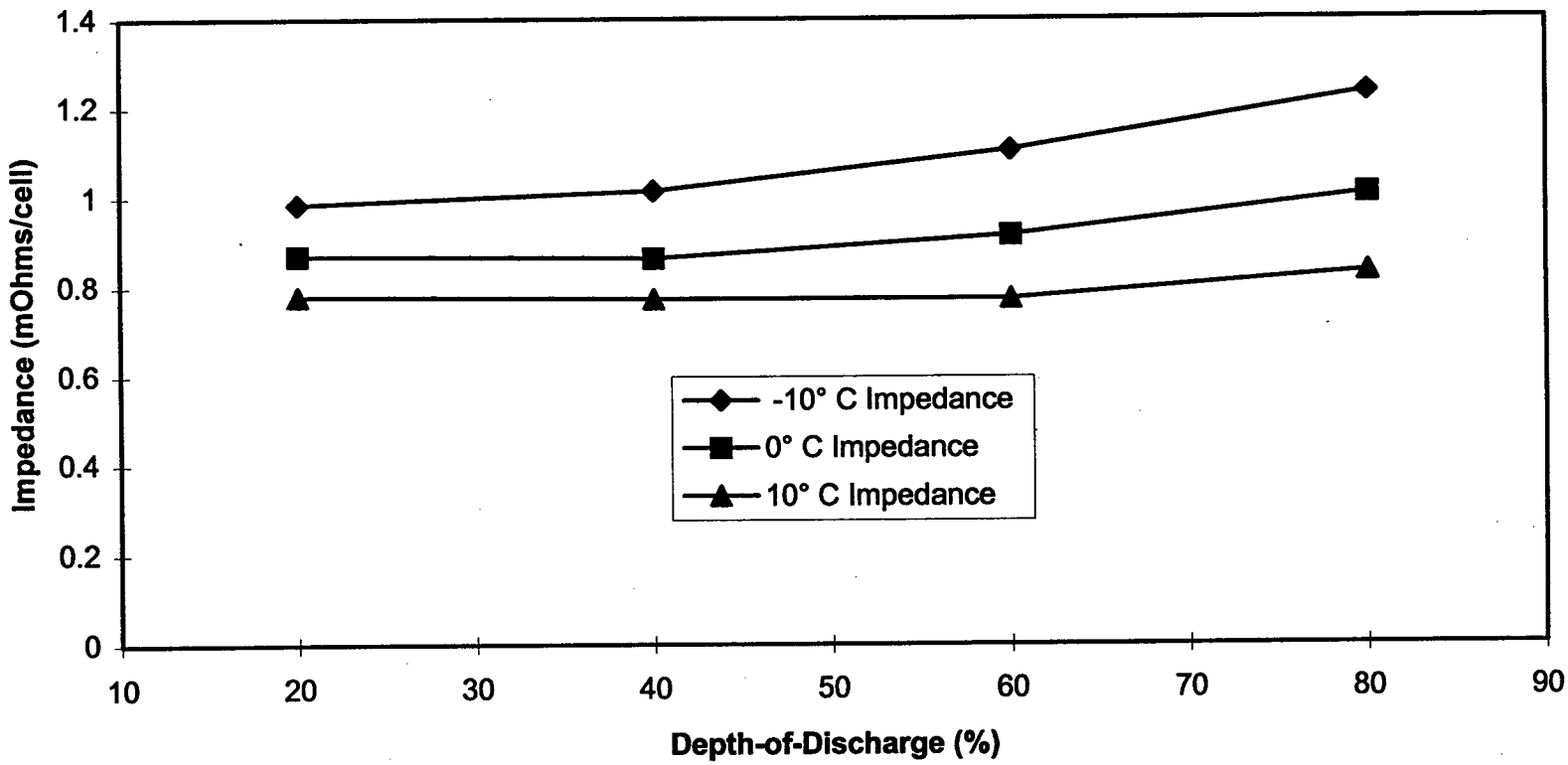

EAGLE PICHER Technologies, LLC

Nickel-Hydrogen Single Pressure Vessel (SPV) Battery Test Results

Capacity vs. Discharge Rate

- *C/10 charge for 16 hours*
- *C/2, C and 2C discharge rates*
- *Capacity measured to 1 volt/cell*
- *-10, 0, 10°C Test temperatures*

Rate of Discharge (C)	-10° C Capacity (Ah)	0° C Capacity (Ah)	10° C Capacity (Ah)
0.5	78.9	78.3	75.3
1	78.2	77.7	74.8
2	75.5	75.5	73.8

EAGLE PICHER Technologies, LLC

Nickel-Hydrogen

Single Pressure Vessel (SPV)

Capacity vs. Discharge Rate

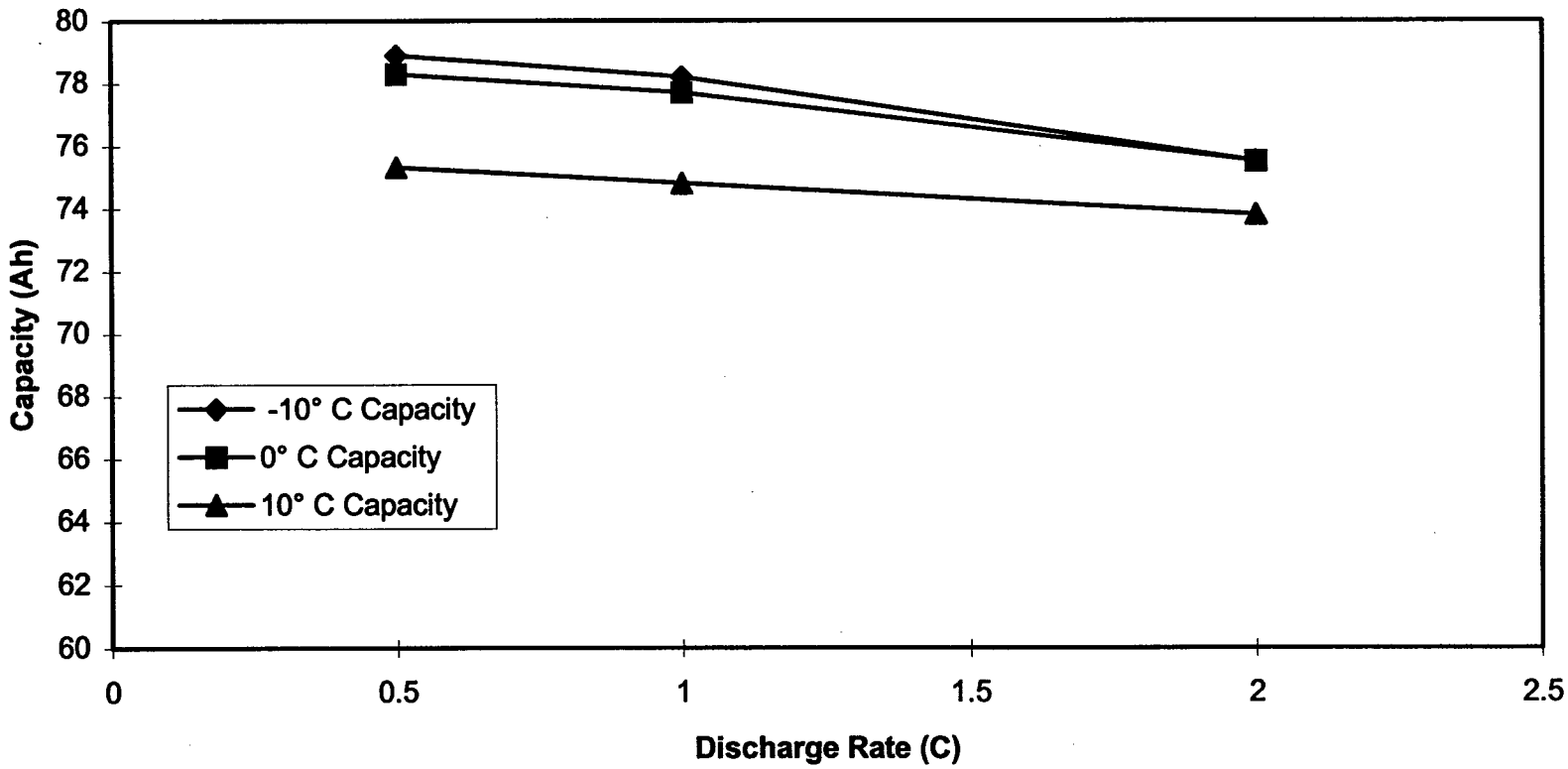

EAGLE PICHER Technologies, LLC

Nickel-Hydrogen Single Pressure Vessel (SPV) Battery Test Results

Mid Discharge Voltage vs. Discharge Rate

- *C/10 charge for 16 hours*
- *C/2, C and 2C discharge rates*
- *Capacity measured to 1 volt/cell*
- *-10, 0, 10°C Test temperatures*
- *Watt-hours out divided by Amp-hours out*

Rate of Discharge (C)	-10° C MDV (Volts/Cell)	0° C MDV (Volts/Cell)	10° C MDV (Volts/Cell)
0.5	1.26	1.27	1.27
1	1.21	1.23	1.24
2	1.15	1.16	1.17

EAGLE PICHER Technologies, LLC

Nickel-Hydrogen

Single Pressure Vessel (SPV)

Mid Discharge Voltage vs. Discharge Rate

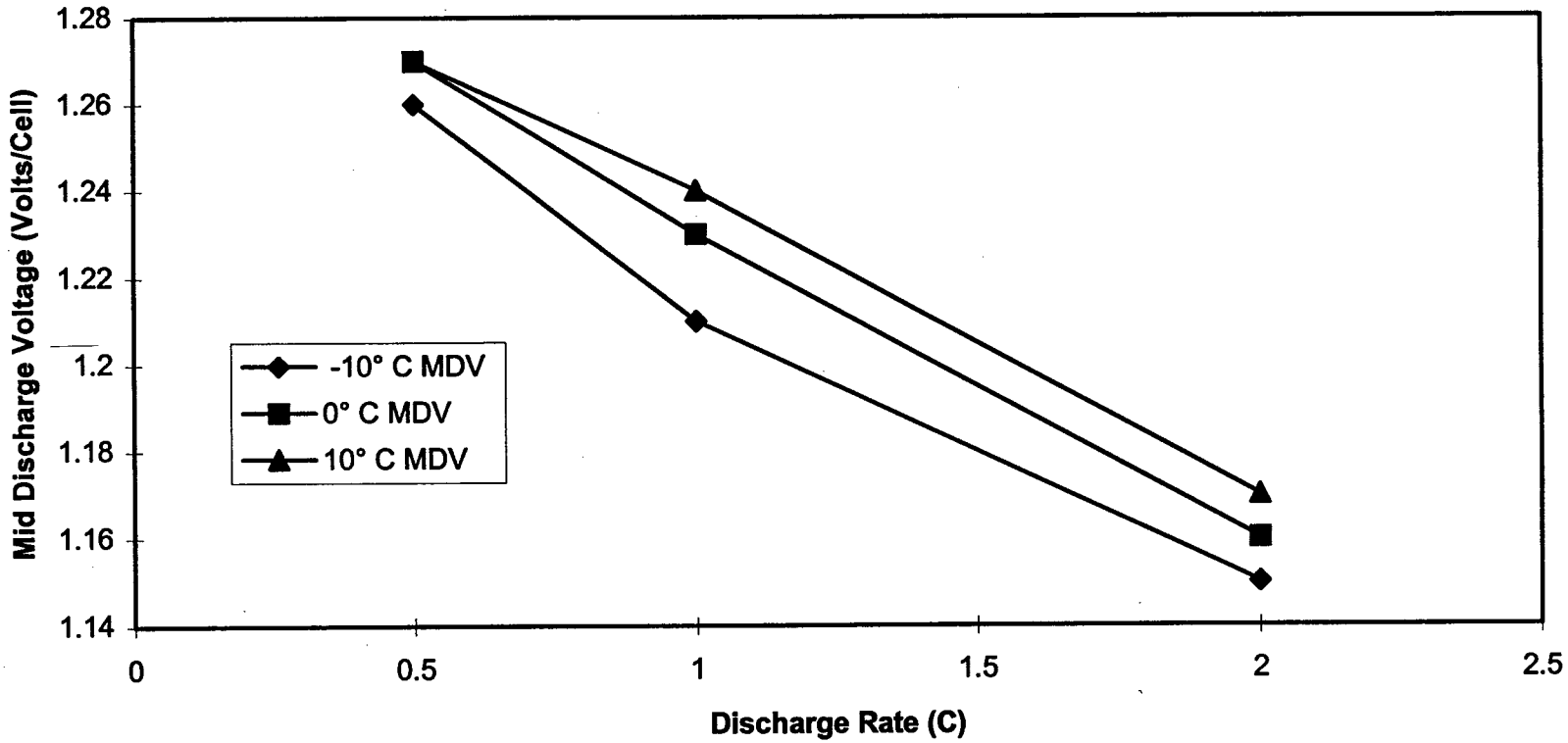

EAGLE PICHER Technologies, LLC

Nickel-Hydrogen Single Pressure Vessel (SPV) Battery Test Results

Charge Retention vs. Open Circuit Time

- *C/10 charge for 16 hours*
- *72, 96 and 120 hour open circuit times*
- *C/2 discharge to 1 volt/cell*
- *-10, 0, 10°C Test temperatures*
- *Open circuit discharge capacity divided by standard capacity*

Open Circuit Time (Hours)	-10° C Charge Retention (%)	0° C Charge Retention (%)	10° C Charge Retention (%)
72	90.4	89.7	86.9
96	90.4	88.3	85.3
120	89.3	87.9	82.8

EAGLE PICHER Technologies, LLC

Nickel-Hydrogen

Charge Retention vs. Open Circuit Time

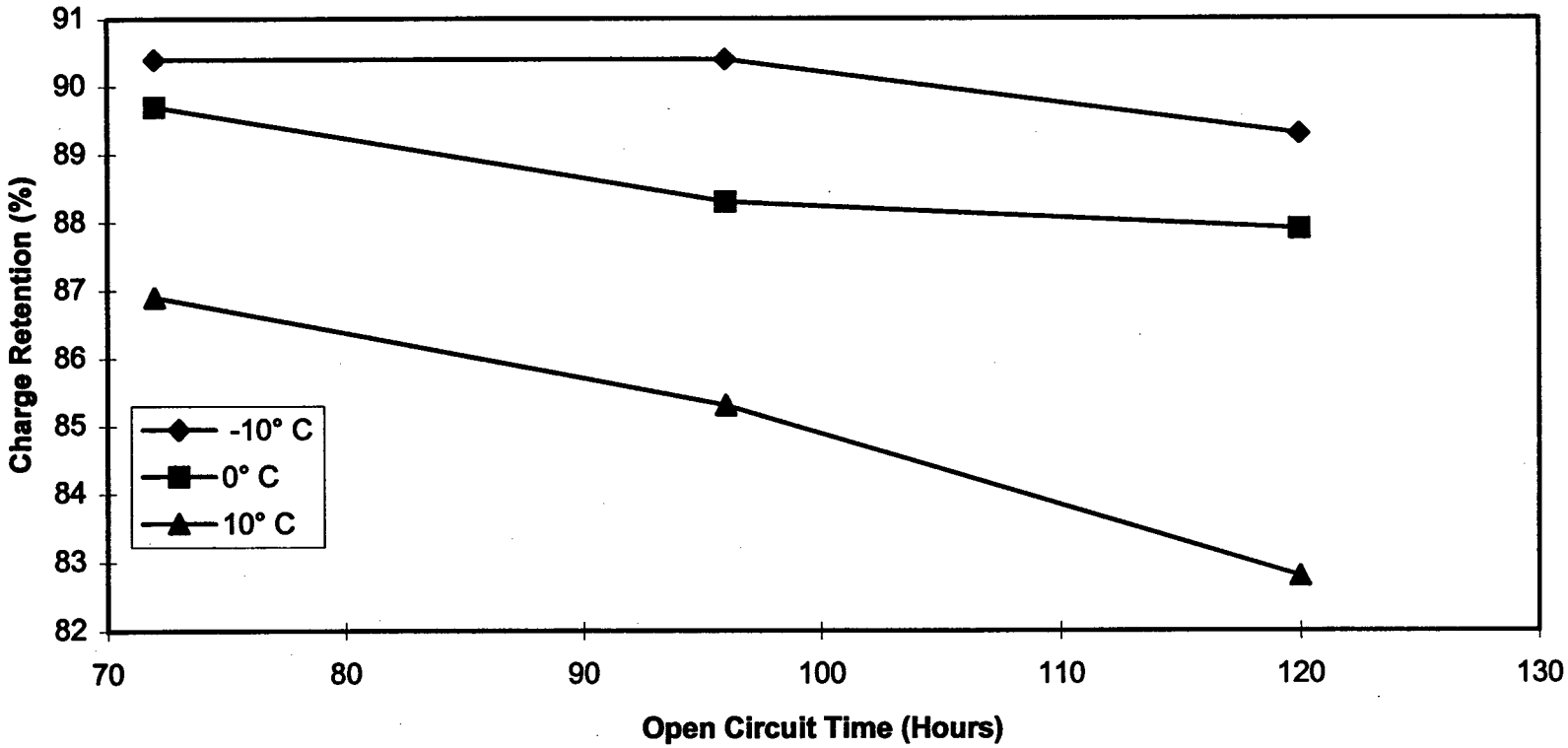

EAGLE PICHER Technologies, LLC

Nickel-Hydrogen Single Pressure Vessel (SPV) Battery Test Results

Charge Efficiency vs.Temperature

- *C/10 charge*
- *C/2 discharge*
- *-10, 0, 10, 20, 30°C Test temperatures*
- *Measure between 300 and 400 psia*
- *Watt-hours on discharge divided by watt-hours on charge*
- *Amp-hours on discharge divided by amp-hours on charge*

Temperature (°C)	Watt-Hour Efficiency (%)	Ampere-Hour Efficiency (%)
-10	81	96
0	83	94
10	83	94
20	83	94
30	81	91

EAGLE PICHER Technologies, LLC

Nickel-Hydrogen

Charge Efficiency vs. Temperature

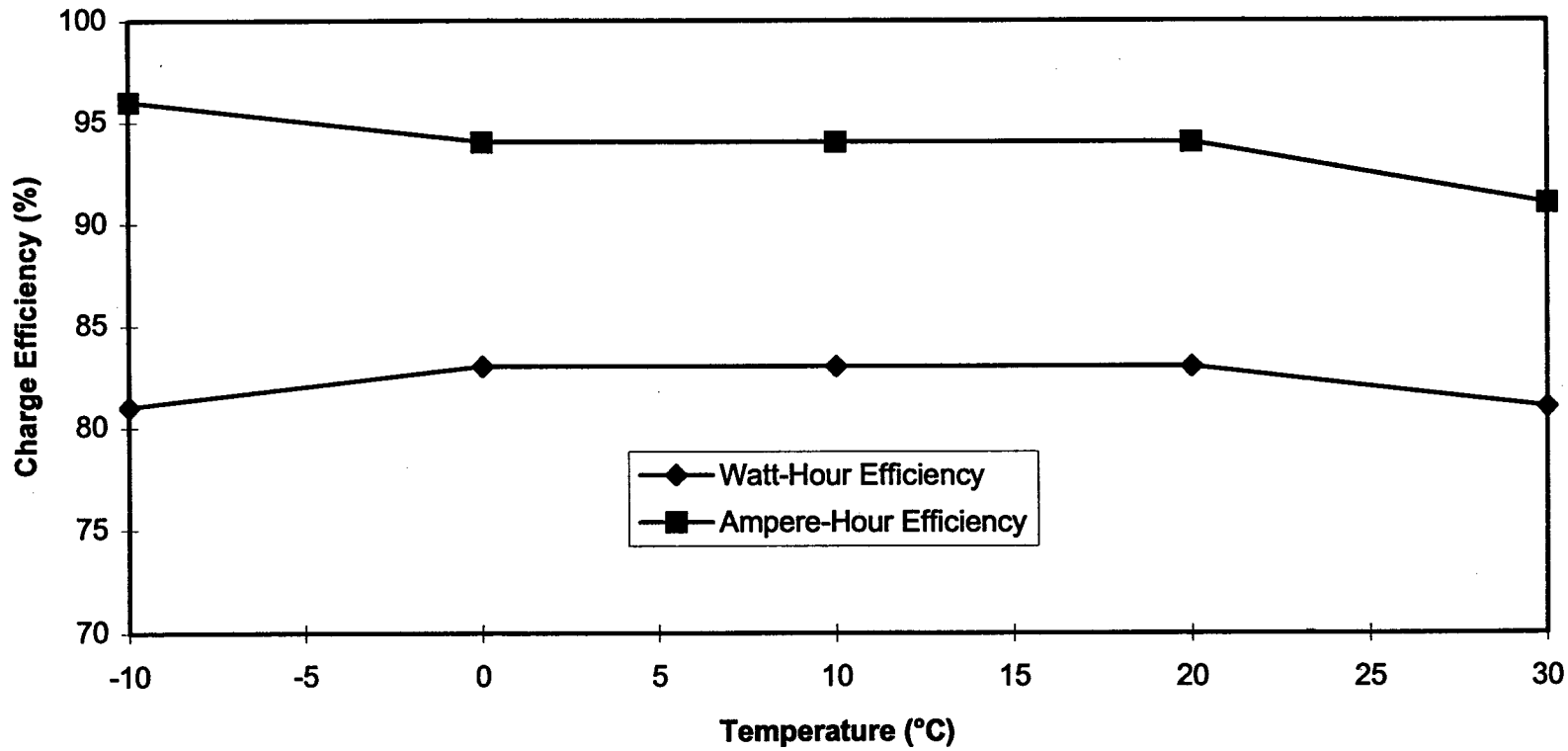

EAGLE PICHER Technologies, LLC

Nickel-Hydrogen Single Pressure Vessel (SPV) Battery Test Results

High-Rate Charge Efficiency vs.Temperature

- *C/2 charge*
- *C/2 discharge*
- *-10, 0, 10°C Test temperatures*
- *Measure between 300 and 400 psia*
- *Watt-hours on discharge divided by watt-hours on charge*
- *Amp-hours on discharge divided by amp-hours on charge*

Temperature (°C)	Watt-Hour Efficiency (%)	Ampere-Hour Efficiency (%)
-10	78	96
0	82	97
10	83	97

EAGLE PICHER Technologies, LLC

Nickel-Hydrogen

High-Rate Charge Efficiency vs. Temperature

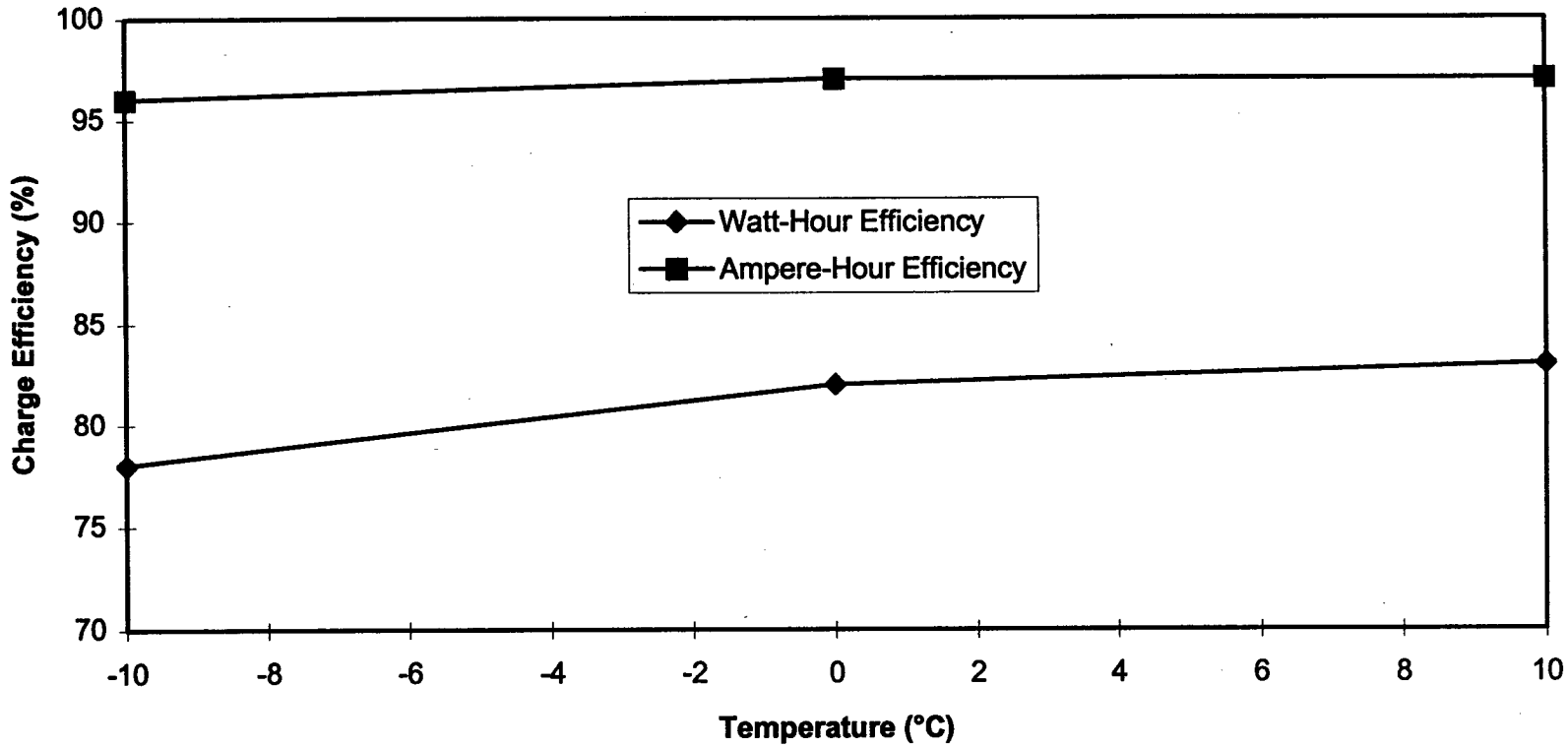

EAGLE PICHER Technologies, LLC

Nickel-Hydrogen Single Pressure Vessel (SPV) Battery Test Results

Parallel Battery Test

- *Two 60 Ah batteries in parallel*
- *One test console*
- *100 minute 40% DOD (48 Ah) LEO cycle*
- *One battery held at -5°C the other at 10°C*

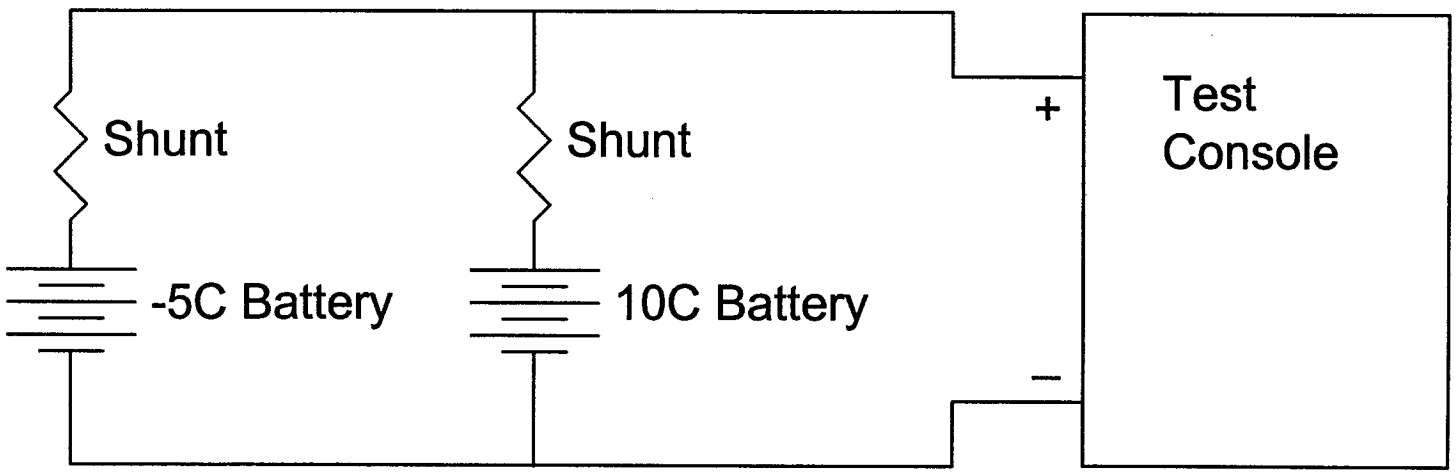

Parallel Battery Test

- *-5°C Battery reached 72% state-of-charge (SOC)*
- *10°C Battery reached 90% SOC (used as charge-control cut-off)*
- *-5°C Battery cycled at 35% depth-of-discharge (DOD)*
- *10°C Battery cycled at 45% DOD*

Summary

- *Impedance*
  - *Increases as depth-of-discharge increases*
  - *Decreases as temperature (-10 to 10°C) increases*
- *Capacity*
  - *Decreases as discharge rate increases*
  - *Decreases as temperature (-10 to 10°C) increases*
- *Mid discharge voltage*
  - *Decreases as discharge rate increases*
  - *Increases as temperature (-10 to 10°C) increases*

Summary (continued)

- *Charge retention*
  - *Decreases as open circuit time increases*
  - *Decreases as temperature (-10 to 10°C) increases*
- *Charge efficiency*
  - *Watt-hour efficiency peaks between 0 and 20°C*
  - *Amp-hour eff. decreases as temperature (-10 to 30°C) increases*
- *Parallel batteries at different temps (-5 to 10°C) share loads unequally*
- *Test results generally agree with individual pressure vessel (IPV) data*

CONCLUSIONS

- SPV BATTERY TESTS DELIVER VERY GOOD, PREDICTABLE, CONSISTENT RESULTS COMPARED WITH EXTENSIVE IPV BATTERY EXPERIENCE
- SAME ELECTROCHEMISTRY, SO PROVEN PERFORMANCE AND DURABILITY FEATURES ARE RETAINED
- SPV ADVANTAGES ARE DERIVED FROM THE FOLLOWING:
  - IMPROVED PRODUCIBILITY
  - HIGH RELIABILITY
  - LOWER COST
  - REDUCED WEIGHT

Lightweight Silver-Hydrogen Cell Design

D. K. Coates, S. C. Cooper and D. P. Bemis
Eagle-Picher Technologies, LLC
Joplin, MO 64801

Abstract

Silver-hydrogen was investigated in the early 1970's as a potential source of energy storage for spacecraft applications and some promising results were obtained. However, development of the silver-hydrogen system was discontinued in favor of the nickel-hydrogen system, which has since become extremely successful in aerospace applications. Problems encountered with the silver-hydrogen system included electrolyte management and silver migration. The silver-hydrogen system is being re-evaluated in light of the developments and advances in technology over the past 20 years. The nickel-hydrogen system has been well developed and engineered and excellent results have been obtained within the past few years with the silver-metal hydride system. The combination of these technologies would yield a battery system capable of competing with lithium-ion on a weight basis. Silver-hydrogen has many advantages over the nickel-hydrogen system, including higher specific energy. This makes reconsideration of the silver-hydrogen system worthwhile. Design evaluation and testing has been performed at the electrode level and boilerplate cell level. Component development has included a radiation grafted three-layer laminate separator, developed by Pall-RAI, which functions well as a silver migration barrier. Flightweight silver-hydrogen cells have been fabricated and are currently undergoing electrical characterization testing. A computer model has been developed to aid in flight cell design analysis and optimization. Cycle life evaluation testing and a thermal performance analysis of the system are also planned.

This Page Left Blank Intentionally

AgH_2 CELL REACTIONS

$2\,AgO + H_2O + 2\,e^- = Ag_2O + 2\,OH^-$	[1]	$\varepsilon° = 0.607V$
$Ag_2O + H_2O + 2\,e^- = 2\,Ag + 2\,OH^-$	[2]	$\varepsilon° = 0.342V$
$H_2 + 2\,OH^- = 2\,H_2O + 2\,e^-$	[3]	$\varepsilon° = 0.828V$
$AgO + H_2 = Ag_2O + H_2O$	[4]	$\varepsilon° = 1.435V$
$Ag_2O + H_2 = 2Ag + H_2O$	[5]	$\varepsilon° = 1.170V$
$4\,OH^- = O_2 + 2\,H_2O + 4\,e^-$	[6]	$\varepsilon° = -0.401$

SILVER-HYDROGEN ELECTROLYTE CONCENTRATION vs. SOC

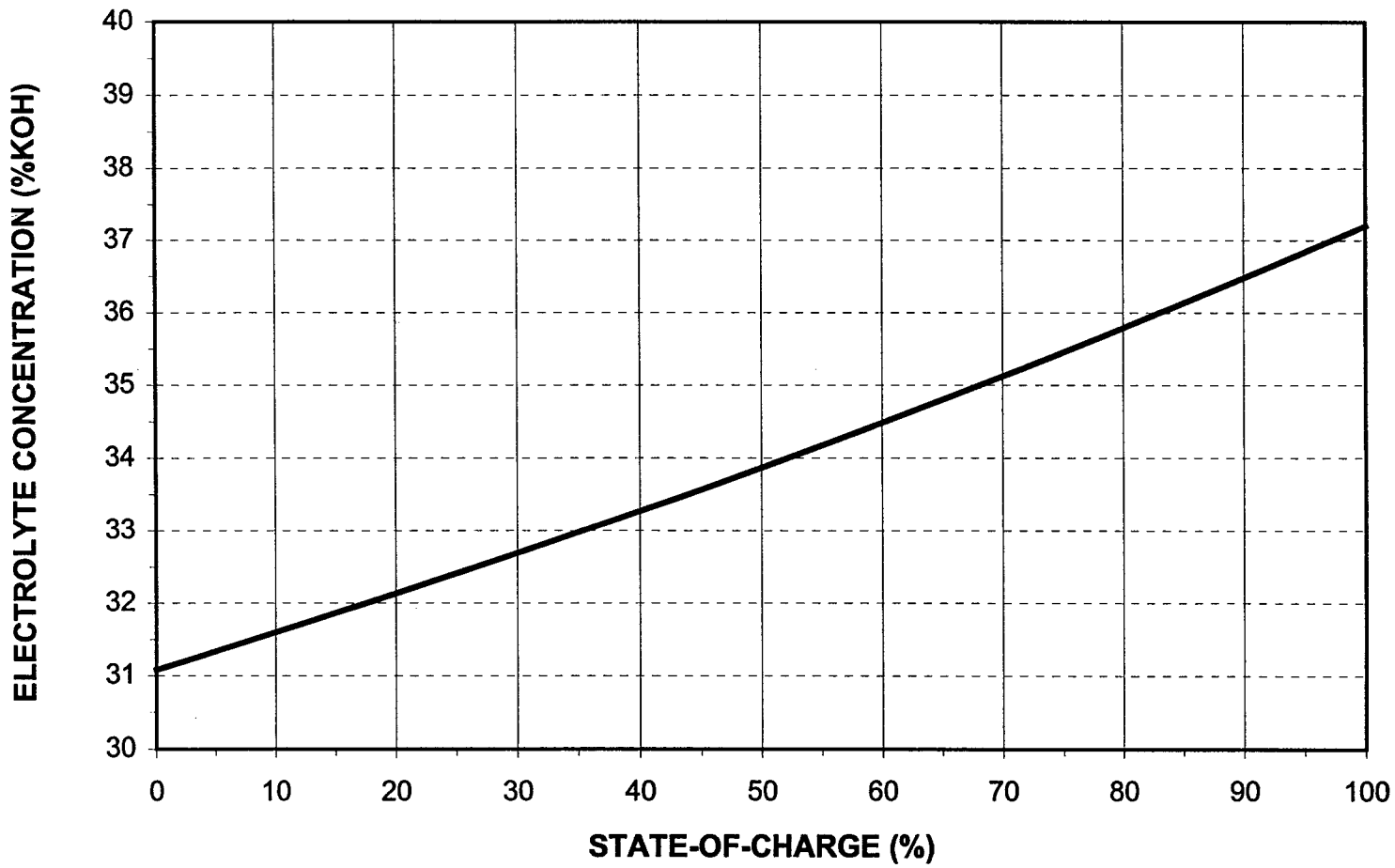

ELECTROLYTE CONCENTRATION VARIES AS A FUNCTION OF STATE-OF-CHARGE. THE SILVER-HYDROGEN SYSTEM IS NOT "WATER BALANCED" LIKE THE NICKEL-HYDROGEN SYSTEM. COMPUTER MODELING SUGGESTS THE ELECTROLYTE CONCENTRATION WILL VARY APPROXIMATELY 6% FROM THE FULLY DISCHARGED TO THE FULLY CHARGED STATE. ELECTROLYTE MANAGEMENT IS THEREFORE A CENTRAL ISSUE IN OPTIMIZING CELL CYCLE LIFE.

SILVER-HYDROGEN CELL DESIGN RATIONALE

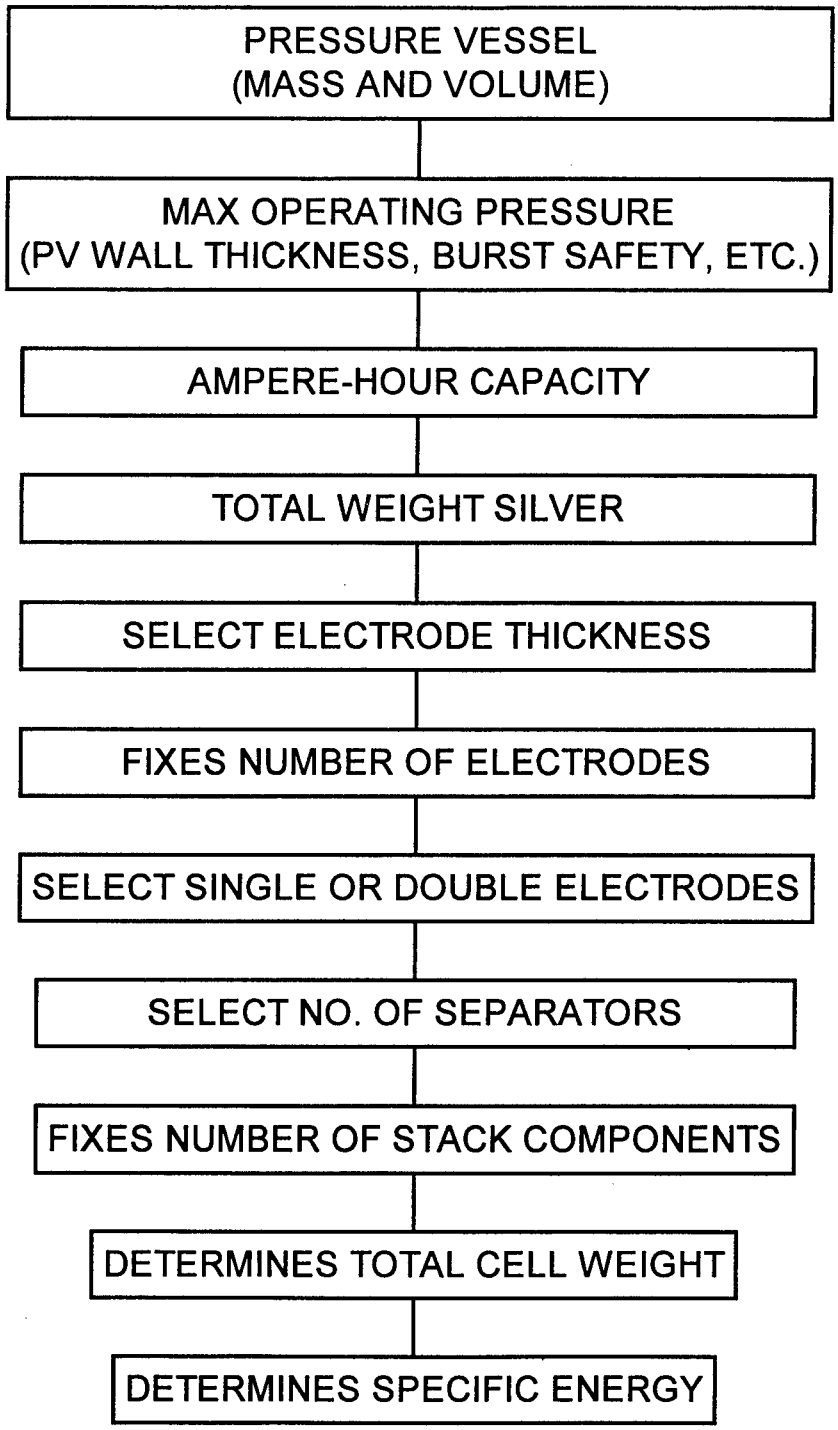

Silver-Hydrogen Cell Design				
	3.5"	%	3.5"	%
Cell Capacity	60		65	
Nominal Output Voltage (Volts)	1.15		1.15	
Maximum Operating Pressure (psi)	670		670	
Pressure Vessel w. wick (g)	270	26.4	270	29.3
Weld Ring (g)	45	4.4	45	4.9
Number Electrodes	20		10	
Silver ElectrodeTotal Weight (g)	234	22.9	234	25.4
Silver Electrode Thickness (in)	0.020		0.040	
Hydrogen Electrode Total Weight (g)	14.8	1.4	7	0.8
Separator Total Weight (g)	80	7.8	60	6.5
Electrolyte Weight (g)	157	15.4	128	13.8
Electrolyte per Ampere-hour (g/Ah)	2.6		2.0	
Gas Screen Weight (g)	6	0.6	4	0.4
End Plates (g)	53	5.2	53	5.7
Core (g)	12	1.2	12	1.3
Terminals (g)	30	2.9	30	3.3
Conductor Weight (g)	60	5.9	40	3.3
Misc. Weight (g)	40	3.9	40	4.3
Fixed Inert Weight (g)	510	49.9	490	53.1
Total Cell Weight (g)	1002		912	
Specific Energy (Wh/kg)	69		81	

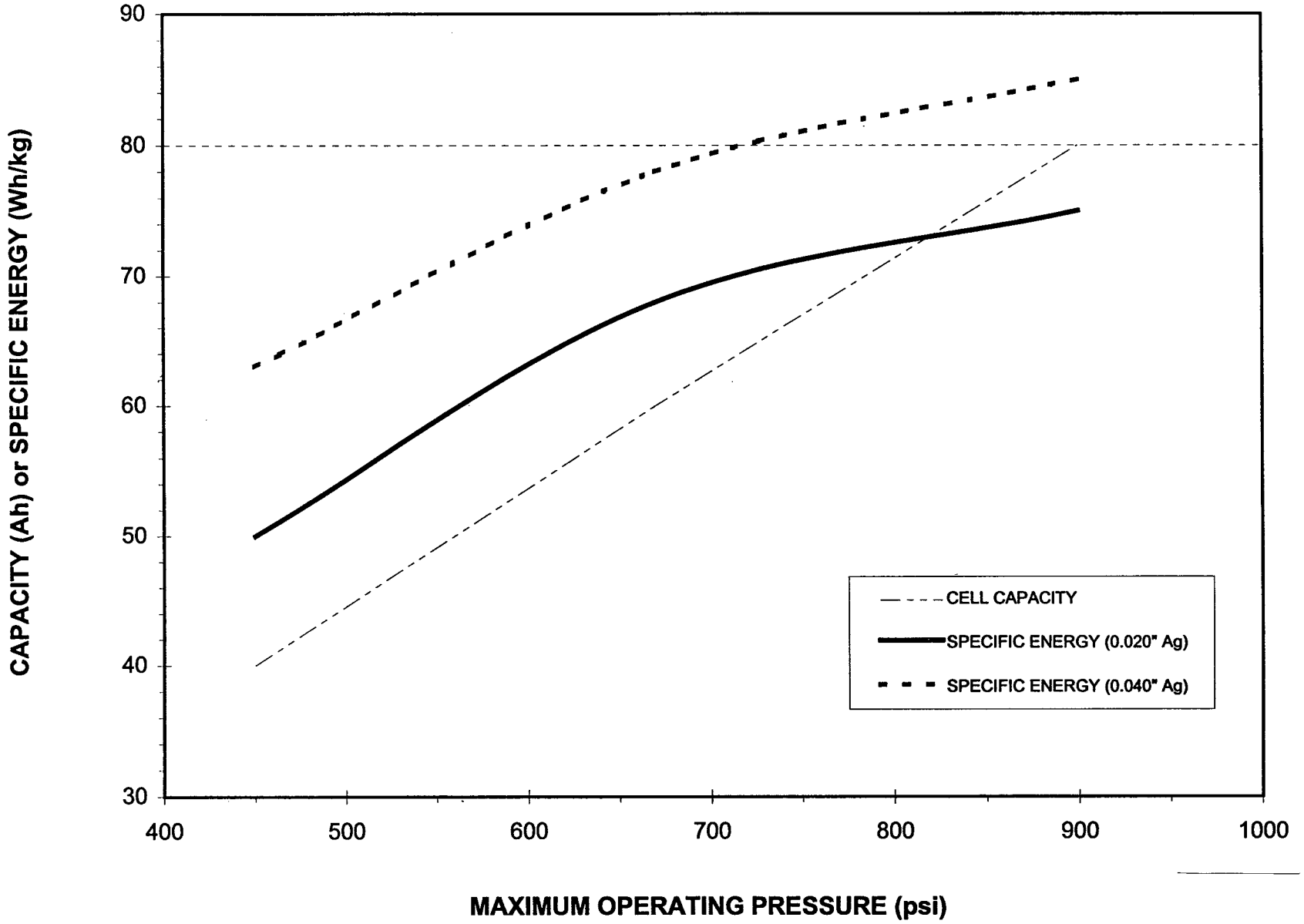
90
80
70
60
50
40
30
400
500
600
700
800
900
1000
CAPACITY (Ah) or SPECIFIC ENERGY (Wh/kg)
MAXIMUM OPERATING PRESSURE (psi)
CELL CAPACITY
SPECIFIC ENERGY (0.020" Ag)
SPECIFIC ENERGY (0.040" Ag)

A SPREAD-SHEET BASED COMPUTER MODEL WAS DEVELOPED TO EVALUATE THE EFFECT OF DESIGN VARIABLES ON FINISHED CELL SPECIFIC ENERGY. THE PRESSURE VESSEL IS A SIGNIFICANT PROPORTION OF CELL WEIGHT (UP TO 26%). THEREFORE, HIGHER SPECIFIC ENERGY CAN ONLY BE OBTAINED BY PACKAGING MORE CAPACITY WITHIN THAT PRESSURE VESSEL AND THEREBY DECREASING ITS WEIGHT IMPACT ON THE CELL. MORE HYDROGEN, AND THEREFORE A HIGHER PRESSURE, IS REQUIRED TO INCREASE CELL CAPACITY. THE CHART SHOWS THE REALTIONSHIP BETWEEN MAXIMUM CELL OPERATING PRESSURE AND SPECIFIC ENERGY FOR TWO CELL DESIGN VARIATIONS, AS PREDICTED BY THE MODEL. TAKING 800 PSI AS THE MAXIMUM PRACTICAL OPERATING PRESSURE FIXES THE CELL SPECIFIC ENERGY AT ABOUT 70 Wh/kg FOR A CONSERVATIVE DESIGN APPROACH AND ABOUT 82 Wh/kg FOR THE MORE ADVANCED DESIGN.

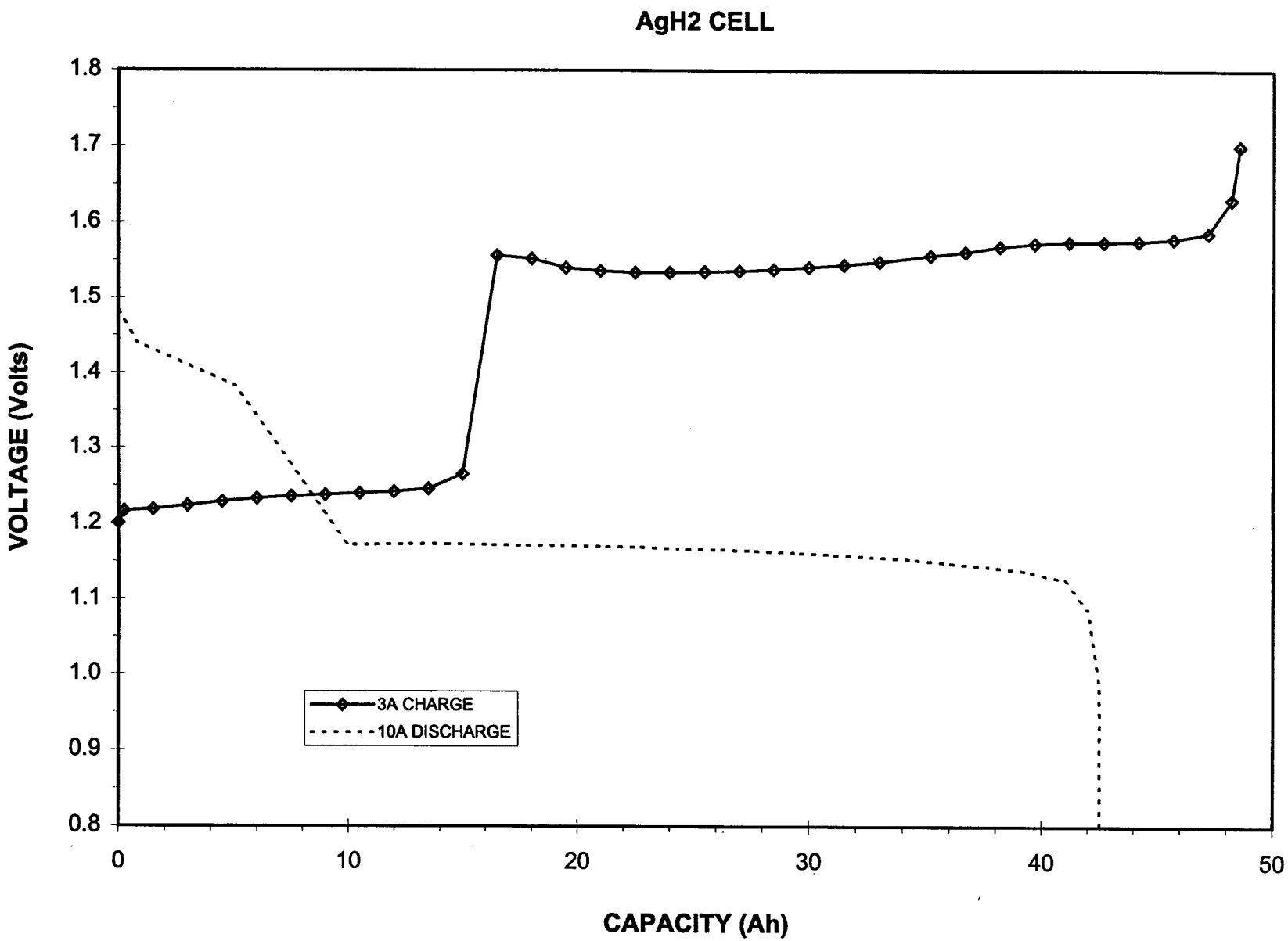
AgH2 CELL
VOLTAGE (Volts)
1.8
1.7
1.6
1.5
1.4
1.3
1.2
1.1
1.0
0.9
0.8
0
10
20
30
40
50
CAPACITY (Ah)
3A CHARGE
10A DISCHARGE

THIS IS A TYPICAL CHARGE/DISCHARGE VOLTAGE PROFILE FOR THE SILVER-HYDROGEN SYSTEM, SHOWN FOR A 42 AMPERE-HOUR FLIGHT-WEIGHT CELL. THE TWO-STEP PROCESS IS CLEARLY SHOWN IN THE CHARGE CURVE. THE LOWER PLATEAU IS THE TRANSITION FROM METALLIC SILVER TO SILVER (+1) AND THE UPPER PLATEAU IS SILVER (+1) TO SILVER (+2). THE UPWARD TAIL AT THE END-OF-CHARGE IS THE POTENTIAL MOVING TOWARDS THAT OF OXYGEN EVOLUTION. A SIMILAR TWO-STEP EFFECT IS EVIDENT IN THE DISCHARGE CURVE ALTHOUGH LESS PRONOUNCED. THE LENGTH AND POSTION OF THE TWO PLATEAUS ARE STRONGLY AFFECTED BY CHARGE AND DISCHARGE RATE AND TEMPERATURE. IN SOME CASES ONLY ONE DISCHARGE PLATEAU, AT THE LOWER VOLTAGE, IS OBSERVED. AT HIGH CHARGE RATES THE LOWER VOLTAGE PLATEAU IS EITHER GREATLY SHORTENED OR MISSING, AND THE CELL CHARGES AT THE HIGHER VOLTAGE.

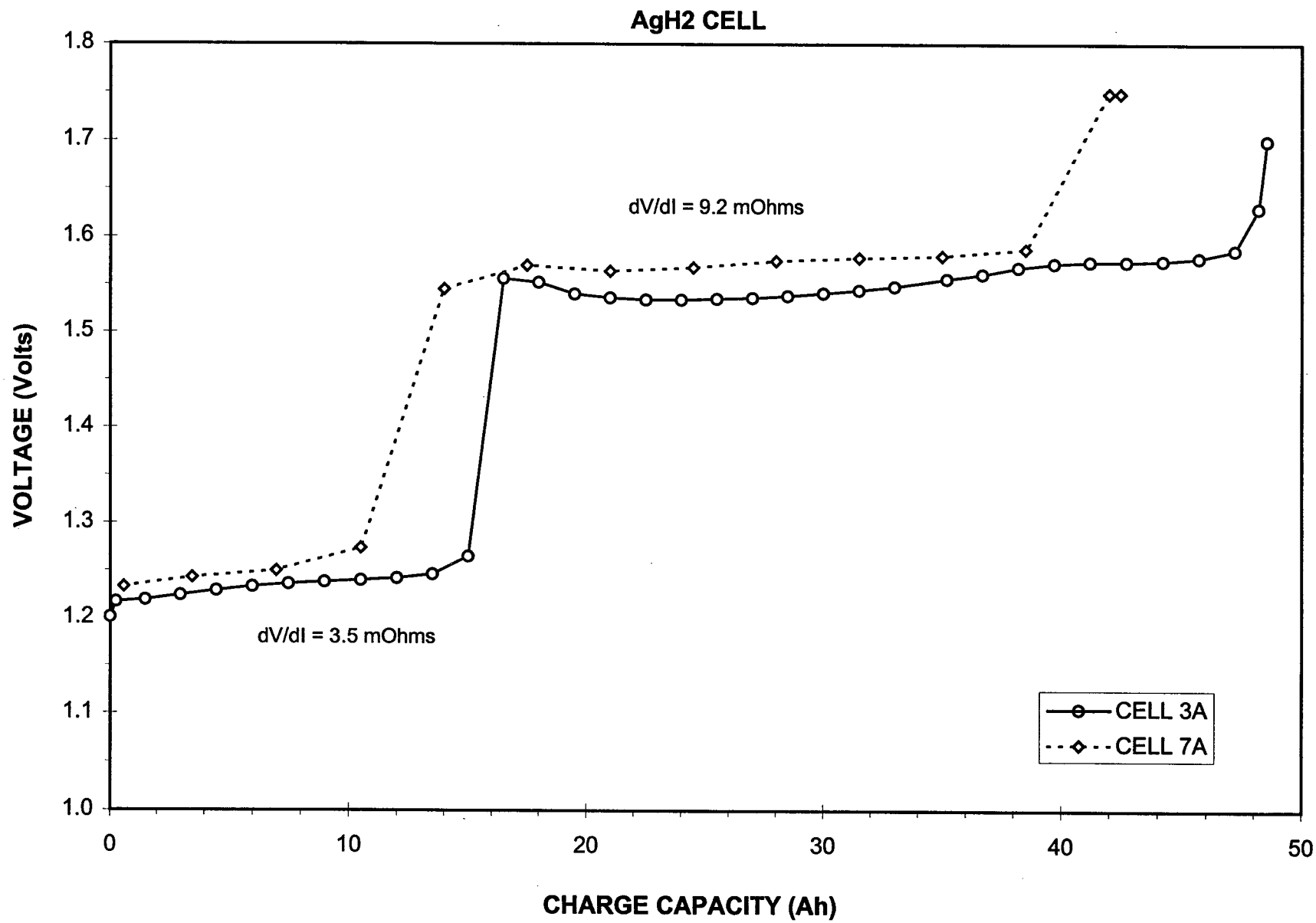
AgH2 CELL
VOLTAGE (Volts)
1.8
1.7
1.6
1.5
1.4
1.3
1.2
1.1
1.0
0
10
20
30
40
50
CHARGE CAPACITY (Ah)
dV/dI = 9.2 mOhms
dV/dI = 3.5 mOhms
CELL 3A
CELL 7A

THIS CHART COMPARES CHARGING AT TWO DIFFERENT RATES (3 AMPERES AND 7 AMPERES) ON A 42 AMPERE-HOUR FLIGHT-WEIGHT CELL. THE VOLTAGE PROFILES SHOW THE EFFECT OF CHARGE RATE ON THE TWO PLATEAUS. THE TRANSITION POINT TO THE UPPER PLATEAU (Ag^{++}) OCCURS EARLIER (AT A LOWER SOC) AT THE HIGHER RATE THAN AT THE LOWER RATE. ALSO AT THE HIGHER RATE, OXYGEN EVOLUTION OCCURS AT A LOWER SOC WHICH DECREASES THE CHARGE EFFICIENCY OF THE CELL. THE $\Delta V/\Delta I$ IMPEDANCE CALCULATED IS 3.5 MILLIOHMS FOR THE Ag/Ag^{+} PLATEAU AND 9.2 MILLIOHMS FOR THE UPPER Ag^{+}/Ag^{++} PLATEAU. AS THE SILVER ELECTRODE IS CHARGED, METALLIC SILVER IS CONVERTED TO LESS CONDUCTIVE SILVER-OXIDE WHICH INCREASES THE IMPEDANCE OF THE ELECTRODE.

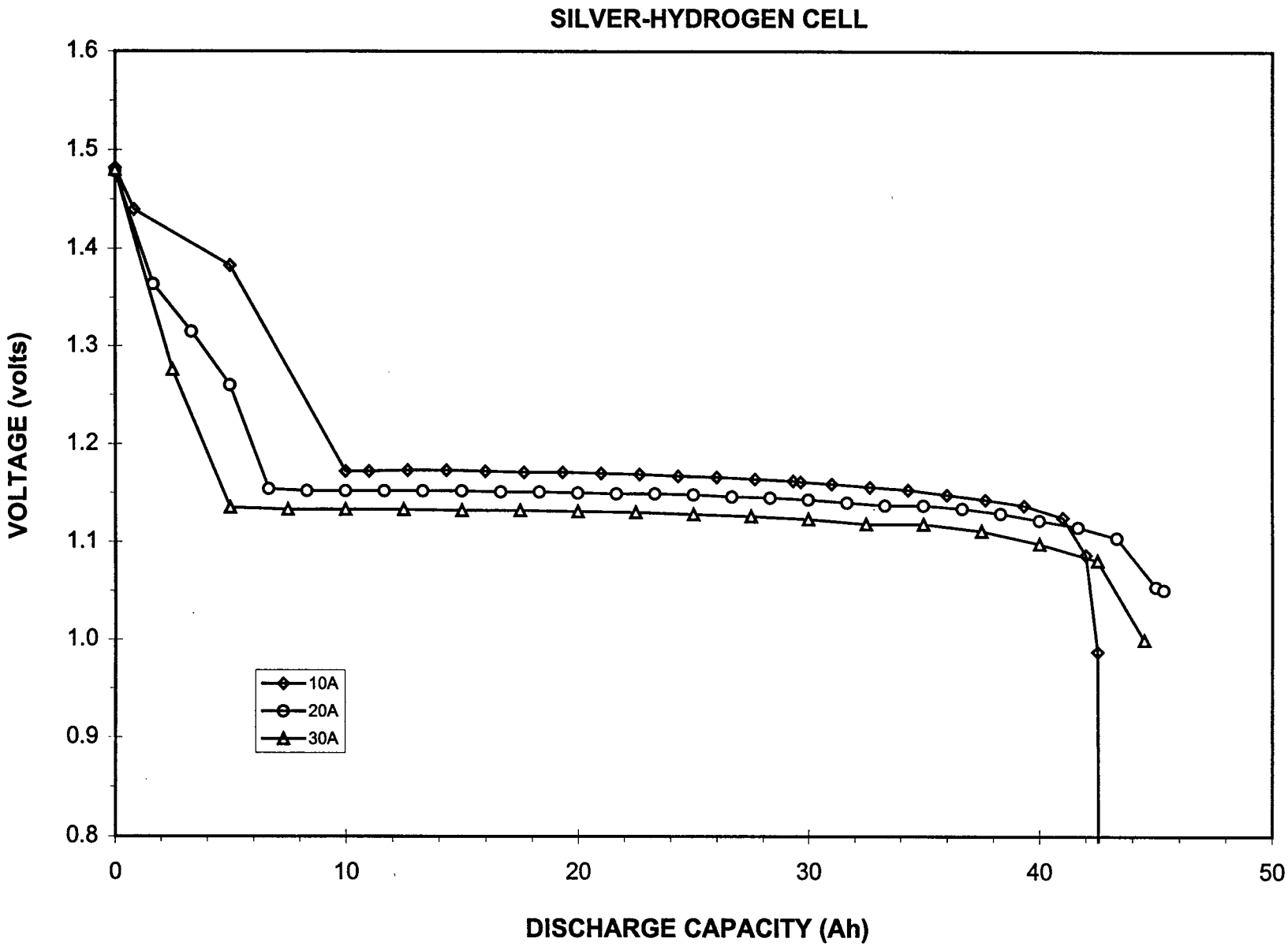
SILVER-HYDROGEN CELL
VOLTAGE (volts)
1.6
1.5
1.4
1.3
1.2
1.1
1.0
0.9
0.8
0
10
20
30
40
50
DISCHARGE CAPACITY (Ah)
10A
20A
30A

THIS CHART SHOWS DISCHARGE VOLTAGE AS A FUNCTION OF DISCHARGE RATE ON THE SAME 42 AMPERE-HOUR FLIGHTWEIGHT CELL. THE UPPER PLATEAU, WHICH CORRESPONDS TO THE REDUCTION OF Ag^{++} TO Ag^{+} IS GREATLY DIMINISHED AS THE DISCHARGE RATE IS INCREASED. AT THE C RATE AND ABOVE ONLY A SINGLE DISCHARGE PLATEAU IS OBSERVED. THIS EFFECT IS ALSO SOMEWHAT DEPENDENT ON THE CHARGE CONDITIONS AS WELL. IN THIS CASE, THE CHARGE CONDITIONS WERE NEARLY CONSTANT FOR EACH DISCHARGE. THE CELL WAS CHARGED AT A 0.1C RATE WITH ABOUT 10% OVERCHARGE PRIOR TO THE 10 AMPERE DISCHARGE. THE CELL WAS CHARGED AT THE SAME RATE FOR THE OTHER TWO DISCHARGES BUT RECEIVED ABOUT 20% OVERCHARGE, WHICH ACCOUNTS FOR THE SLIGHT INCREASE IN DISCHARGE CAPACITY. IT IS APPARENT THAT THE DROP IN DISCHARGE PLATEAU VOLTAGE IS RELATIVELY CONSTANT AS THE RATE INCREASES. CELL CAPACITY IS VIRTUALLY UNAFFECTED BY DISCHARGE RATE UP TO THE C RATE.

SILVER-HYDROGEN FLIGHTWEIGHT CELL

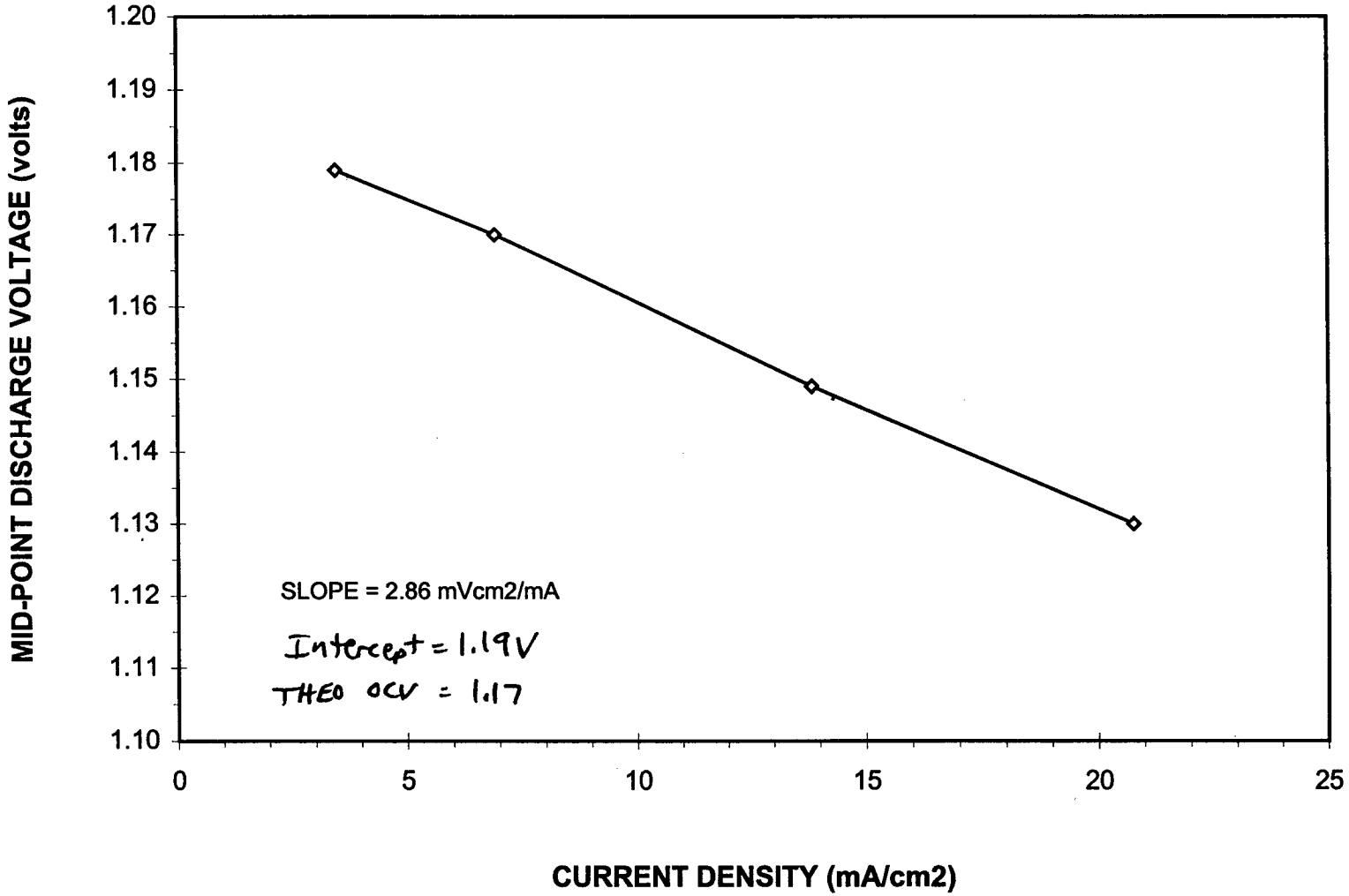

THE MID-POINT DISCHARGE VOLTAGE IS PLOTTED AS A FUNCTION OF CURRENT DENSITY, BASED ON THE DATA FROM THE PREVIOUS CHART. THE VOLTAGE IS LINEAR AS A FUNCTION OF CURRENT. THIS IMPLIES THAT THE LOW-FIELD APPROXIMATION OF THE BUTLER-VOLMER EQUATION IS IN EFFECT. THE CELL IS NOT BEING DRIVEN TO EXCESSIVE OVERPOTENTIALS AT THESE RATES (UP TO 0.75C). THE IMPEDANCE CALCULTED FROM THE LINEAR SLOPE OF THIS DATA IS 1.9 MILLIOHMS, WHICH IS ESSENTIALLY A $\Delta V/\Delta I$ CALCULATION. EXTRAPOLATION OF THE LINE TO ZERO CURRENT DENSITY YIELDS AN INTERCEPT VALUE OF 1.19 VOLTS. THE THEORETICAL OPEN-CIRCUIT VOLTAGE FOR THE CELL (USING THE E^0 FOR Ag/Ag^+) IS 1.17 VOLTS. THE 20 MILLIVOLT OFFSET MAY BE AN INDICATION OF SOME SMALL AMOUNT OF RESIDUAL HIGHER VALENCE SILVER OR IT MAY BE AN ARTIFACT OF THE TESTING OR OTHER POLARIZATION ISSUES.

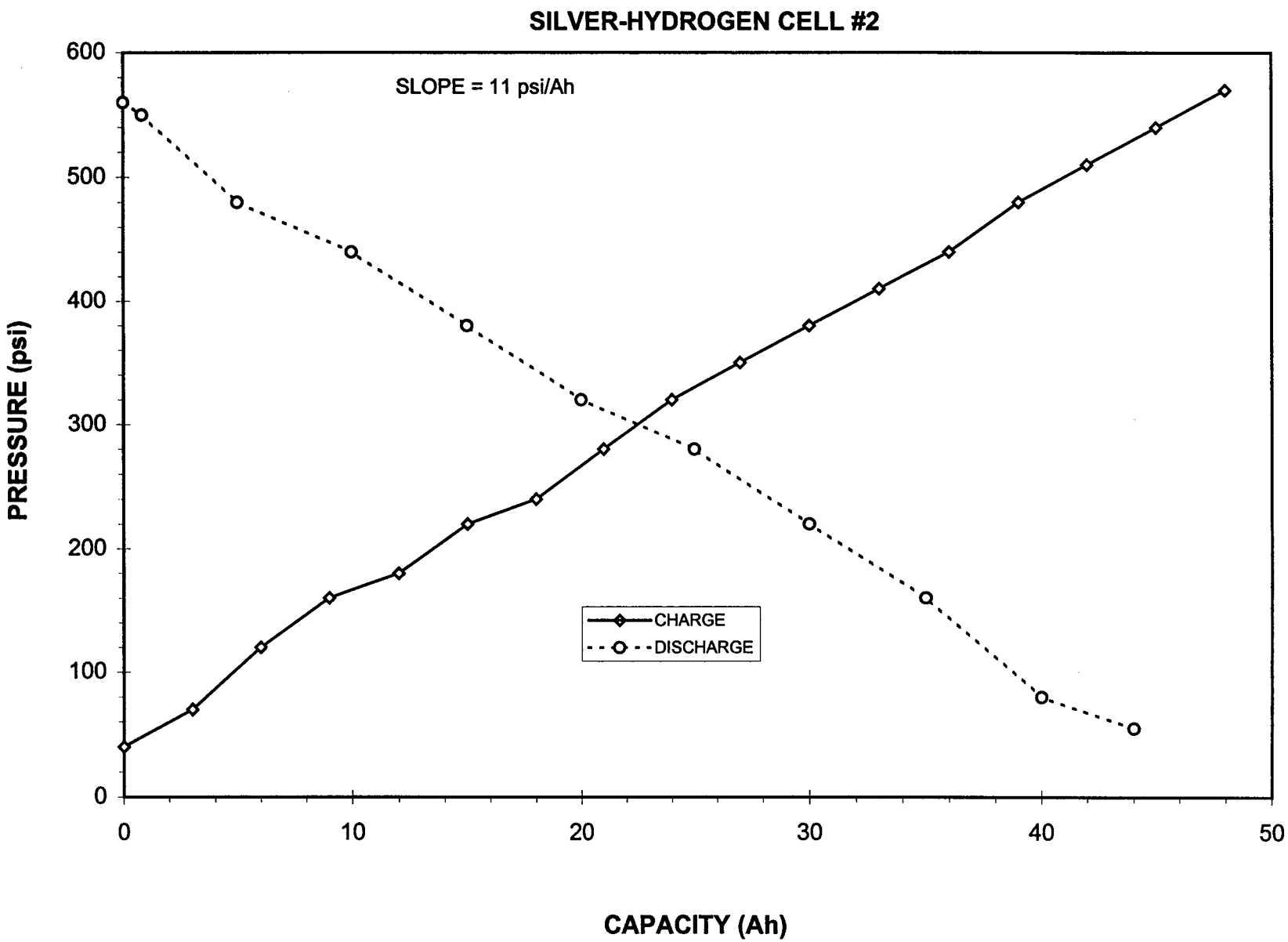
SILVER-HYDROGEN CELL #2
SLOPE = 11 psi/Ah
PRESSURE (psi)
CAPACITY (Ah)
CHARGE
DISCHARGE
0
100
200
300
400
500
600
0
10
20
30
40
50

THE OVERALL CELL REACTIONS INDICATE THAT EVEN THOUGH THE CELL IS NOT WATER BALANCED, HYDROGEN PRESSURE SHOULD BE LINEAR AS A FUNCTION OF STATE-OF-CHARGE AS IN THE NICKEL-HYDROGEN SYSTEM. PRESSURE VERSUS CAPACITY (SOC) DATA IS SHOWN FOR A TYPICAL CONSTANT CURRENT CHARGE AND DISCHARGE. THE CELL WAS CHARGED AT 0.1C AND DISCHARGED AT 0.25C, BOTH AT ROOM TEMPERATURE. THE CHARGE AND DISCHARGE DATA ARE LINEAR WITH A SLOPE OF 11 PSI/AMPERE-HOUR IN BOTH CASES.

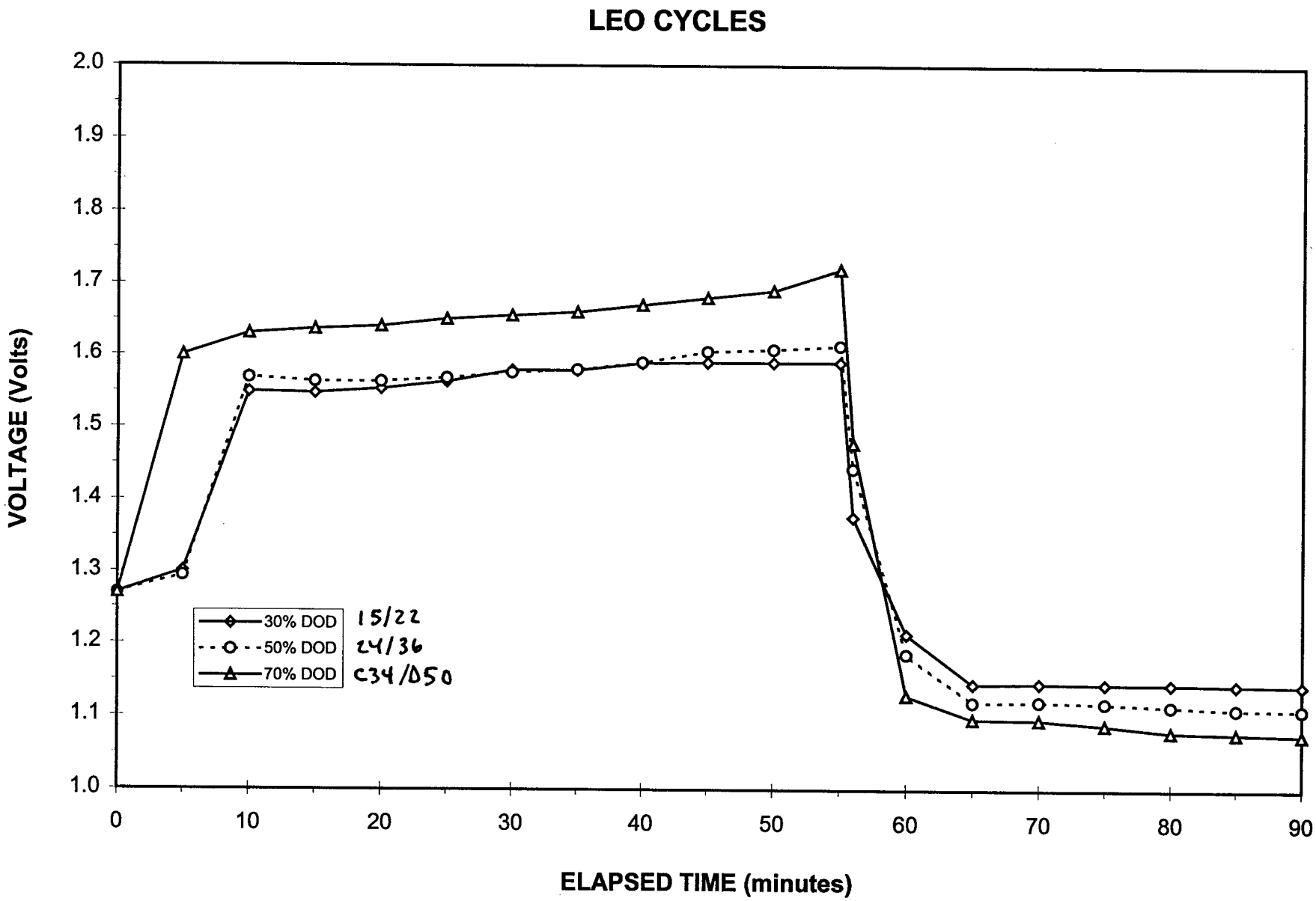
LEO CYCLES
VOLTAGE (Volts)
2.0
1.9
1.8
1.7
1.6
1.5
1.4
1.3
1.2
1.1
1.0
0
10
20
30
40
50
60
70
80
90
ELAPSED TIME (minutes)
30% DOD 15/22
50% DOD 24/36
70% DOD C34/D50

LOW-EARTH-ORBIT (LEO) TESTING WAS PERFORMED TO DETERMINE HOW THE SILVER-HYDROGEN SYSTEM WOULD PERFORM UNDER THIS REGIME. THREE DEPTHS-OF-DISCHARGE (DOD) WERE EVALUATED, 30% DOD, 50% DOD AND 70% DOD. A 55 MINUTE CHARGE AND 35 MINUTE DISCHARGE CYCLE REGIME WAS SELECTED AND REMAINED CONSTANT THROUGHOUT TESTING. 30% DOD CORRESPONDS TO A CHARGE RATE OF 15 AMPERES AND A DISCHARGE RATE OF 22 AMPERES (ABOUT 0.5C). 50% DOD CORRESPONDS TO A 24 AMPERE CHARGE/36 AMPERE DISCHARGE. 70% DOD CORRESPONDS TO A 34 AMPERE CHARGE AND A 50 AMPERE DISCHARGE (MORE THAN A C RATE). THE DISCHARGE DATA LOOKS TYPICAL WITH A SMALL DEPRESSION IN THE DISCHARGE VOLTAGE OCCURING AS THE DOD, AND THEREFORE THE DISCHARGE RATE, IS INCREASED. THE CELL EASILY MAINTAINED DISCHARGE VOLTAGE AT THE 70% DOD RATE. THE CHARGE VOLTAGE SHOWS ALMOST NO EFFECT INCREASING THE DOD FROM 30% TO 50%. THE INITIAL LOWER VOLTAGE CHARGE PLATEAU IS VIRTUALLY UNAFECTED UNDER THIS TEST REGIME AS IS THE ACTUAL CHARGING VOLTAGE. THE END-OF-CHARGE VOLTAGE IS ONLY SLIGHTLY HIGHER AT THE HIGHER DOD. HOWEVER, THE CHARGING VOLTAGE AT 70% DOD IS ABNORMALLY HIGHER THAN THE OTHERS. THIS CORRESPONDS TO INCREASING THE CHARGE RATE FROM 24 AMPERES AT 50% DOD TO 34 AMPERES AT 70% DOD. THE INCREASED CHARGE VOLTAGE APPEARS TO BE DUE TO A LARGE INCREASE IN POLARIZATION OF THE CELL. THE CELL IMPEDANCE IS RELATIVELY HIGH AT THIS POINT AS SILVER IS BEING CONVERTED TO THE LESS CONDUCTIVE OXIDE.

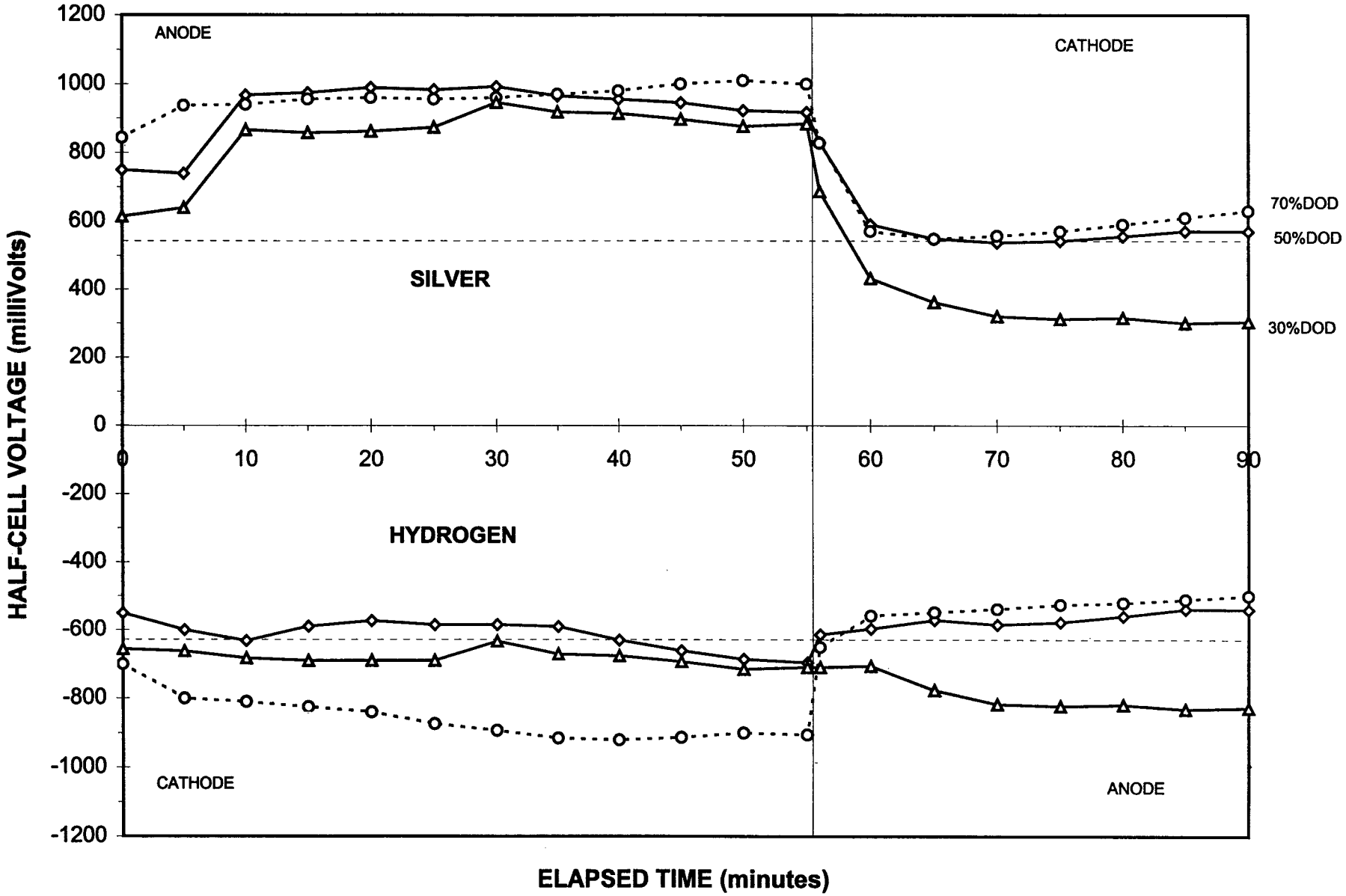
ANODE
CATHODE
SILVER
HYDROGEN
CATHODE
ANODE
70%DOD
50%DOD
30%DOD
HALF-CELL VOLTAGE (milliVolts)
ELAPSED TIME (minutes)
1200
1000
800
600
400
200
0
-200
-400
-600
-800
-1000
-1200
0
10
20
30
40
50
60
70
80
90

IN ORDER TO DETERMINE WHICH ELECTRODE IS RESPONSIBLE FOR THE LARGE INCREASE IN CELL POLARIZATION OBSERVED AT THE HIGH CHARGE RATE IN LEO TESTING, HALF-CELL VOLTAGES WERE MEASURED USING THE CELL PRESSURE VESSEL AS A QUASI-REFERENCE ELECTRODE. THE CHARGE VOLTAGES MEASURED AT THE SILVER ELECTRODE ALL SHOW A RELATIVELY UNIFORM DISPLACEMENT FROM EQUILIBRIUM REGARDLESS OF THE CHARGE RATE. HOWEVER, THE CHARGE VOLTAGE BEHAVIOR OF THE HYDROGEN ELECTRODE SHOWS A MARKED INCREASE IN POLARIZATION AT THE 70% DOD CHARGE RATE. THE EQUILIBRIUM VALUE FOR THE HYDROGEN ELECTRODE VERSUS INCONEL IS APPROXIMATELY -628 MILLIVOLTS. THE VOLTAGE IS CLOSE TO THIS VALUE THROUGHOUT CHARGE AT THE 30% DOD AND 50% DOD CHARGE RATES. THE CHARGE VOLTAGE OF THE HYDROGEN ELECTRODE VERSUS INCONEL IS POLARIZED TO GREATER THAN -900 MILLIVOLTS AT THE 70% DOD CHARGE RATE. THIS ABNORMALLY HIGH VOLTAGE MAY BE CONCENTRATION POLARIZATION DUE TO THE INCREASING CONCENTRATION OF THE ELECTROLYTE (CORRESPONDING TO A DECREASING CONCENTRATION OF WATER) DURING CHARGE.

SILVER-HYDROGEN HALF-CELL VOLTAGES

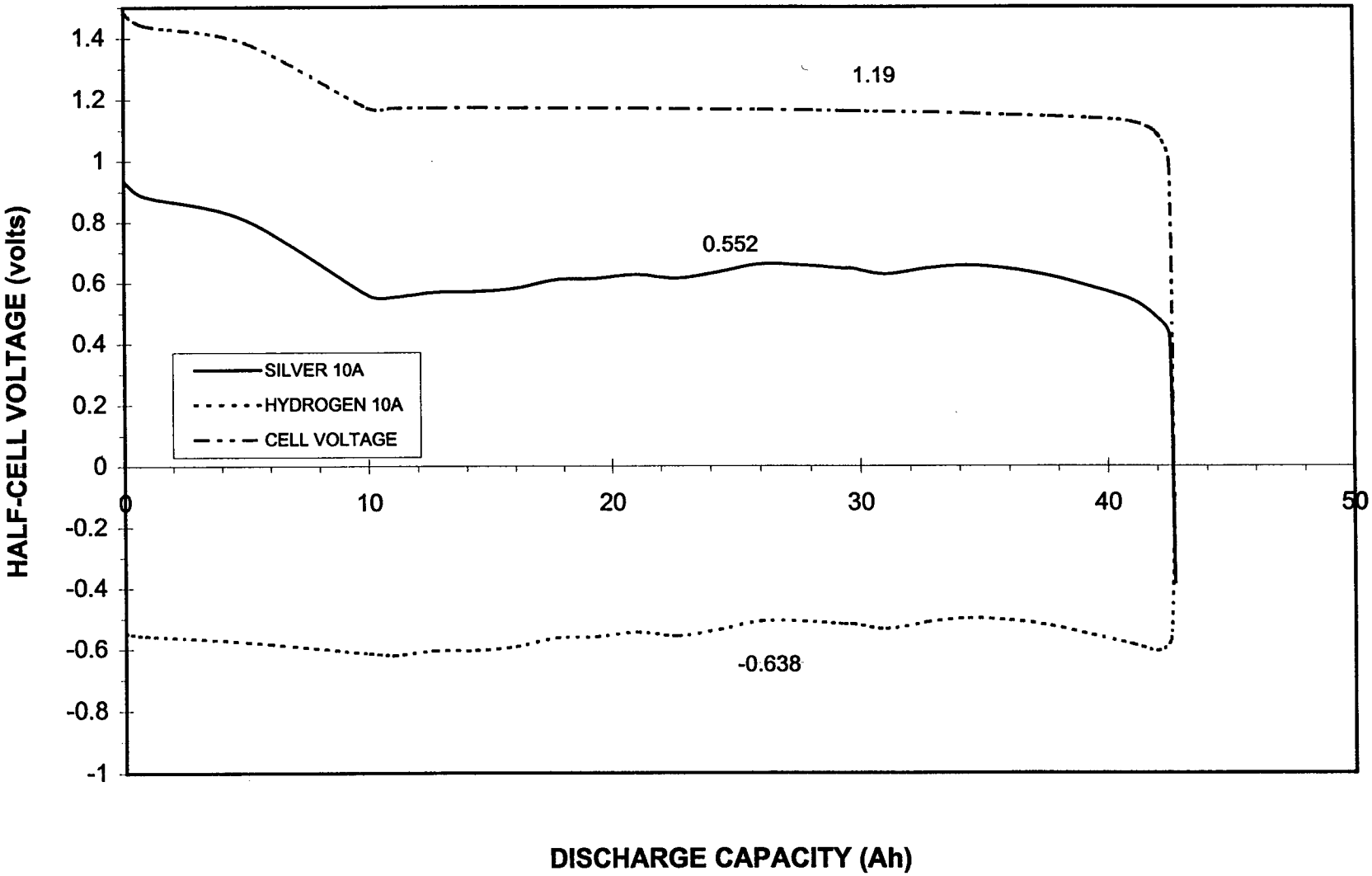

THIS CHART SHOWS TYPICAL HALF-CELL DISCHARGE VOLTAGES OBTAINED WHEN TAKEN VERSUS THE INCONEL PRESSURE VESSEL. THE CELL IS DISCHARGED AT 10 AMPERES AT ROOM TEMPERATURE. THE SILVER ELECTRODE AVERAGES ABOUT 552 MILLIVOLTS AND THE HYDROGEN ELECTRODE IS ABOUT -638 MILLIVOLTS. BOTH ELECTRODES ARE DISPLACED ABOUT 10 MILLIVOLTS FROM THEIR EQUILIBRIUM VALUES AT THE 10 AMPERE DISCHARGE RATE. THIS INDICATES THAT THE IMPEDANCE OF THE TWO ELECTRODES IS NEARLY EQUAL AT THIS RELATIVELY LOW RATE. THE TWO HALF-CELL VOLTAGES ARE EXACTLY ADDITIVE TO YIELD THE SAME CELL VOLTAGE AS MEASURED FROM TERMINAL TO TERMINAL. THE HIGHER VOLTAGE PLATEAU ($Ag^{++} \rightarrow Ag^{+}$) CAN BE SEEN IN THE SILVER HALF-CELL VOLTAGE WHILE THE HYDROGEN ELECTRODE VOLTAGE IS ESSENTIALLY FLAT.

SILVER-HYDROGEN POTENTIAL DIAGRAM USING THE PRESSURE VESSEL AS A REFERENCE

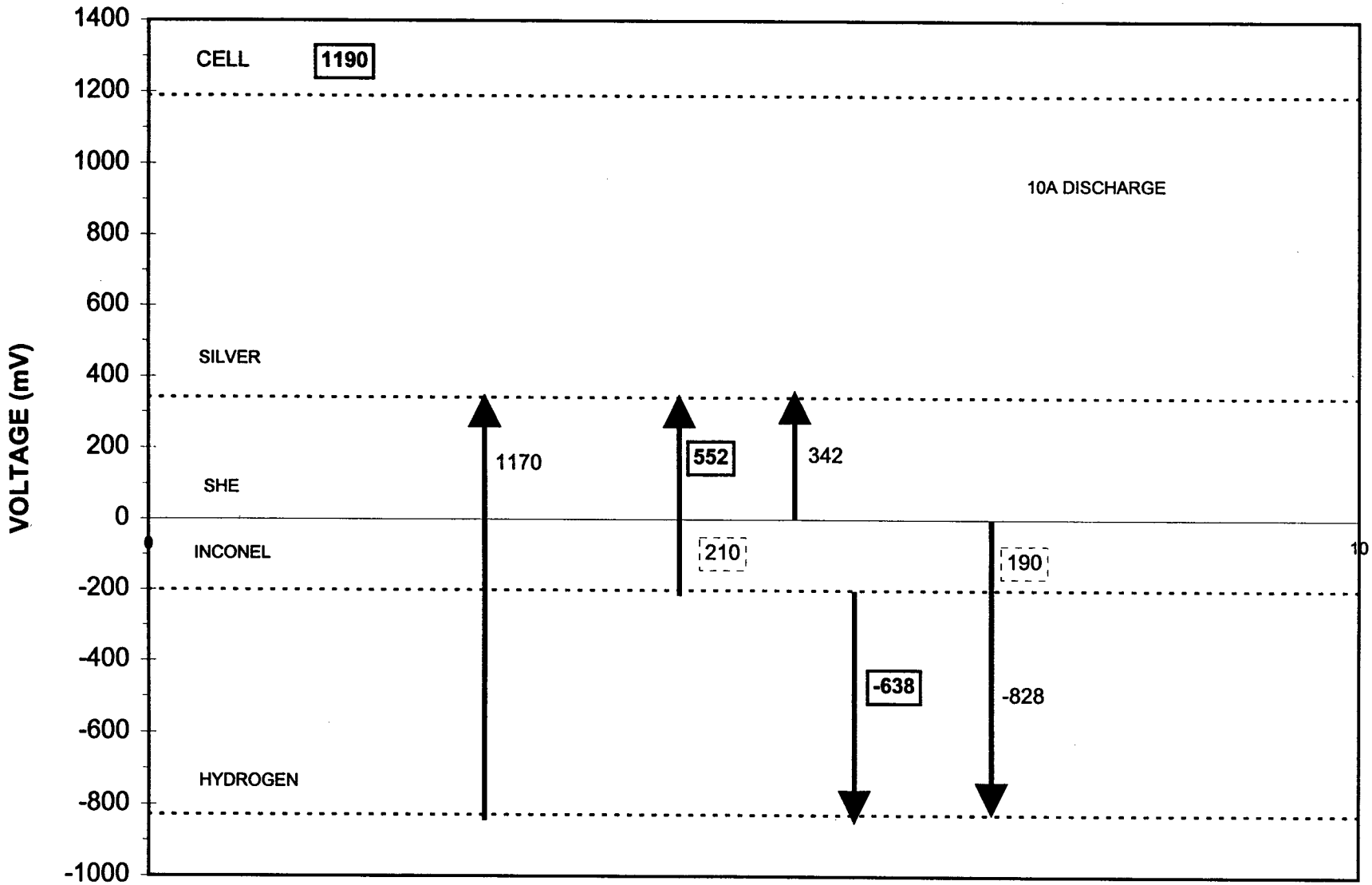

A POTENTIAL DIAGRAM WAS CONSTRUCTED FROM THE 10 AMPERE DISCHARGE DATA TO DETERMINE THE STANDARD POTENTIAL OF THE TWO HALF-CELLS VERSUS INCONEL. THE MEASURED VALUES OF THE HALF-CELL VOLTAGES CAN BE COMPARED TO THE THEORETICAL E^0 VALUES VERSUS THE STANDARD HYDROGEN ELECTRODE (SHE). THE POTENTIAL OF INCONEL VERSUS SHE CAN BE ESTIMATED FROM THE KNOWN THEORETICAL POTENTIALS AND THE EXPERIMENTALLY MEASURED HALF-CELL POTENTIALS. USING THE SILVER ELECTRODE VALUE, A POTENTIAL OF -210 MILLIVOLTS CAN BE CALCULATED FOR INCONEL VERSUS SHE. LIKEWISE, USING THE HYDROGEN ELECTRODE DATA A POTENTIAL OF -190 MILLIVOLTS CAN BE CALCULATED. THE APPARENT DISCREPANCY OF 20 MILLIVOLTS CAN BE ACCOUNTED FOR BY THE FACT THAT THE MEASURED HALF-CELL POTENTIALS ARE DYNAMIC MEASUREMENTS UNDER A 10 AMPERE LOAD. THE E^0 VALUES ARE EQUILIBRIUM POTENTIALS. IF THE MEASURED HALF-CELL POTENTIALS ARE CORRECTED FOR THE POLARIZATION VOLTAGE DROP AT 10 AMPERES (i.e. 10 MILLIVOLTS AS DETERMINED IN A PREVIOUS CHART) BOTH SETS OF DATA AGREE TO WITHIN ONE MILLIVOLT. THEREFORE, THE POTENTIAL OF INCONEL VERSUS SHE IN THE SILVER-HYDROGEN CELL IS ESTIMATED TO BE -200 MILLIVOLTS.

INCONEL POTENTIAL DIAGRAM USING Hg/HgO AND Hg/Hg2Cl2 AS A REFERENCE

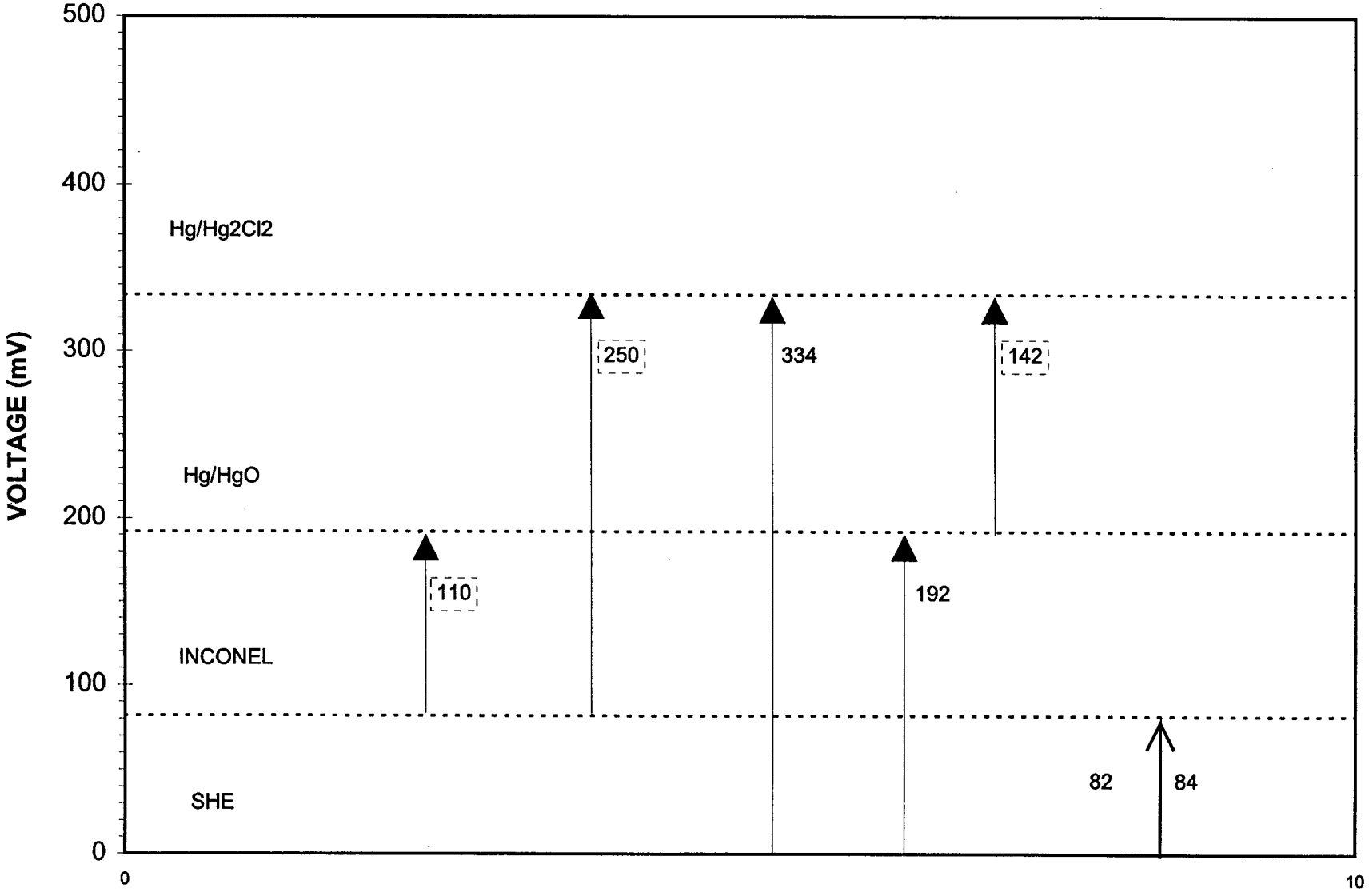

OTHER EXPERIMENTS WERE CONDUCTED TO INVESTIGATE THE POTENTIAL OF INCONEL IN VARIOUS ELECTROCHEMICAL SYSTEMS. THIS POTENTIAL DIAGRAM SHOWS A ZIRCONIA FLAMESPRAYED INCONEL COUPON MEASURED VERSUS A STANDARD CALOMEL (Hg/Hg_2Cl_2) REFERENCE ELECTRODE AND A MERCURY/MERCURY-OXIDE (Hg/HgO) REFERENCE ELECTRODE. A COMMERCIAL CALOMEL ELECTRODE WAS USED WHILE THE MERCURY OXIDE REFERENCE WAS FABRICATED AND CALIBRATED LOCALLY. THIS TEST WAS DONE WITH ALL THREE ELECTRODES IN AN OPEN BEAKER OF 31% KOH (NO HYDROGEN ATMOSPHERE). TWO STANDARD REFERENCE ELECTRODES WERE USED AS A WAY TO CROSS-CHECK RESULTS BECAUSE THE POTENTIAL BETWEEN CALOMEL AND MERCURY-OXIDE IS A KNOWN VALUE. EQUILIBRIUM MEASUREMENTS ARE SHOWN IN THE POTENTIAL DIAGRAM ALTHOUGH DYNAMIC TESTING WAS ALSO DONE. THE INCONEL WAS REFERENCED TO BOTH THE CALOMEL AND MERCURY-OXIDE ELECTRODES. INCONEL WAS MEASURED AT AN EQUILIBRIUM POTENTIAL OF 82 MILLIVOLTS ABOVE SHE WHEN COMPARED TO THE MERCURY-OXIDE REFERENCE ELECTRODE. A VALUE OF 84 MILLIVOLTS IS CALCULATED WHEN INCONEL IS REFERENCED TO THE CALOMEL ELECTRODE. THE AGREEMENT WITHIN 2 MILLIVOLTS IS CONSIDERED WITHIN THE EXPERIMENTAL ERROR OF THE SYSTEM. THEREFORE, THE EQUILIBRIUM POTENTIAL OF THE INCONEL VERSUS SHE IS ASSIGNED A VALUE OF 83 MILLIVOLTS.

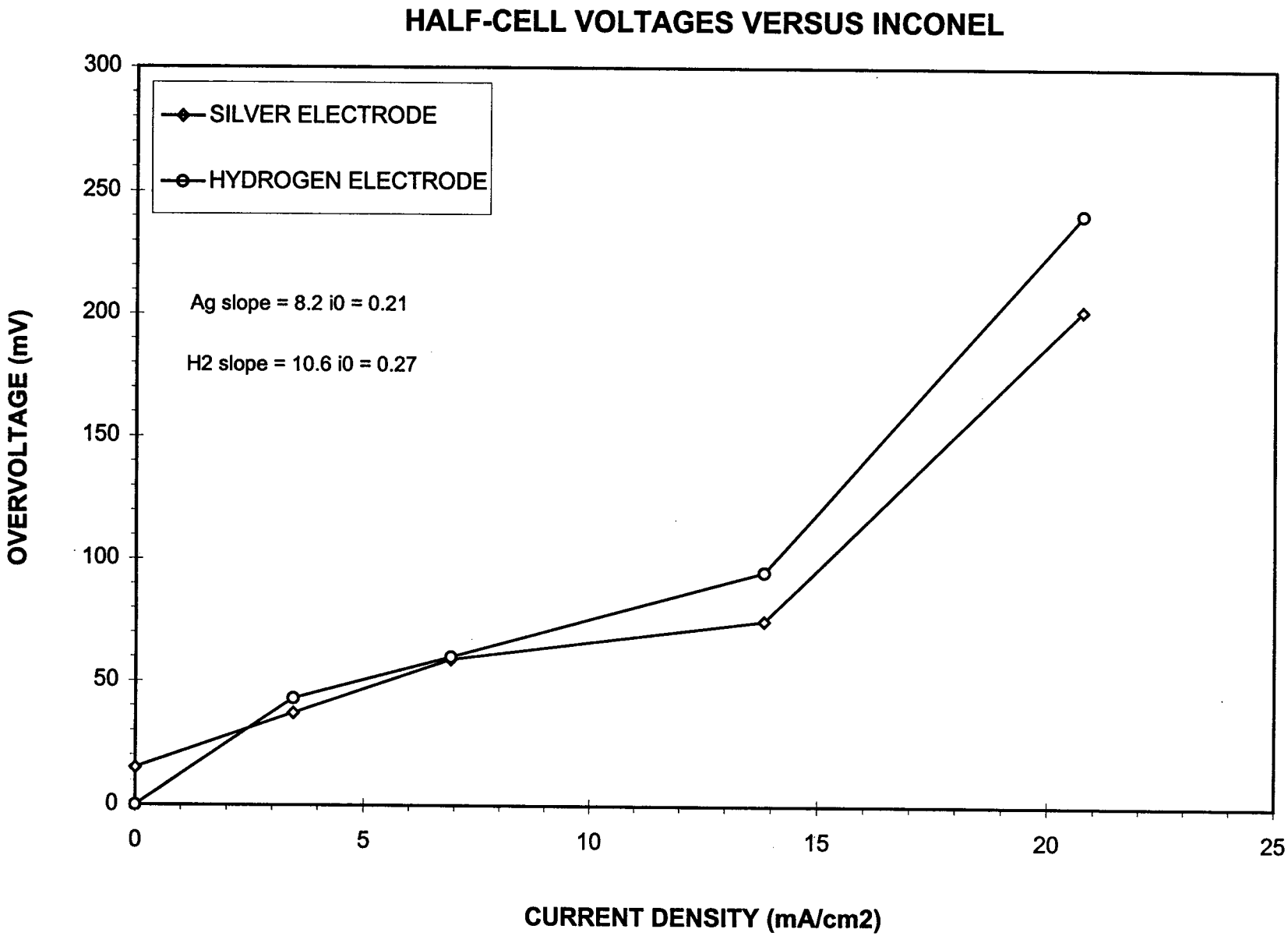
HALF-CELL VOLTAGES VERSUS INCONEL
SILVER ELECTRODE
HYDROGEN ELECTRODE
Ag slope = 8.2 i0 = 0.21
H2 slope = 10.6 i0 = 0.27
OVERVOLTAGE (mV)
300
250
200
150
100
50
0
0
5
10
15
20
25
CURRENT DENSITY (mA/cm2)

STANDARD EQUILIBRIUM POTENTIALS WERE ESTABLISHED FOR BOTH THE SILVER AND HYDROGEN ELECTRODES VERSUS INCONEL. SILVER IS 542 MILLIVOLTS VERSUS INCONEL AND HYDROGEN IS -628 MILLIVOLTS VERSUS INCONEL (AS MEASURED IN THE SILVER-HYDROGEN CELL ENVIRONMENT AT ROOM TEMPERATURE). THESE EQUILIBRIUM POTENTIALS WERE USED TO CALCULATE THE OVERPOTENTIAL FOR EACH ELECTRODE AS A FUNCTION OF CURRENT DENSITY. THIS DATA IS SHOWN IN THE FIGURE. BOTH THE SILVER AND HYDROGEN ELECTRODE SHOW AN APPROXIMATE LINEAR RELATIONSHIP WITH CURRENT DENSITY UP TO ABOUT 15 MILLIAMPERES PER SQUARE CENTIMETER. THIS OBEYS THE LOW-FIELD APPROXIMATION OF THE BUTLER-VOLMER EQUATION. THIS INDICATES THAT THE ELECTRODES ARE NOT BEING DRIVEN FAR FROM EQUILIBRIUM AT THESE RATES. ABOVE 15 MILLIAMPERES PER SQUARE CENTIMETER THE RELATIONSHIP MOVES TOWARD THE EXPONENTIAL OR HIGH-FIELD BUTLER-VOLMER RELATIONSHIP. THE SLOPE OF THE HYDROGEN OVERPOTENTIAL IS SLIGHTLY LARGER THAN THAT OF THE SILVER INDICATING THAT THE HYDROGEN ELECTRODE IS POLARIZED TO A LARGER OVERPOTENTIAL THAN THE SILVER ELECTRODE FOR AN EQUIVALENT CURRENT DENSITY.

INDIVIDUAL ELECTRODE IMPEDANCE (CHARGE)

ΔV/ΔI CALCULATION FOR 3A AND 7A CHARGE
LOWER PLATEAU (Ag^+)

SILVER ELECTRODE

$R_{Ag} = \Delta V/\Delta I = 5.0\ m\Omega$

HYDROGEN ELECTRODE

$R_{H2} = \Delta V/\Delta I = 55.0\ m\Omega$

PARALLEL COMBINATION

$1/R_{CELL} = 1/R_{Ag} + 1/R_{H2}$

$R_{CELL} = 4.6\ m\Omega$

ΔV/ΔI CALCULATION BASED ON FULL CELL VOLTAGE = 3.5 mΩ

ΔV/ΔI CALCULATION FOR 3A AND 7A CHARGE
UPPER PLATEAU (Ag^{++})

SILVER ELECTRODE

$R_{Ag} = \Delta V/\Delta I = 10.0\ m\Omega$

HYDROGEN ELECTRODE

$R_{H2} = \Delta V/\Delta I = 70.0\ m\Omega$

PARALLEL COMBINATION

$1/R_{CELL} = 1/R_{Ag} + 1/R_{H2}$

$R_{CELL} = 8.75 m\Omega$

ΔV/ΔI CALCULATION BASED ON FULL CELL VOLTÁGE = 9.2 mΩ

INDIVIDUAL ELECTRODE IMPEDANCE

ΔV/ΔI CALCULATION FOR 10A AND 20A DISCHARGE

SILVER ELECTRODE

$R_{Ag} = \Delta V/\Delta I = 2.8\ m\Omega$

HYDROGEN ELECTRODE

$R_{H2} = \Delta V/\Delta I = 5.9\ m\Omega$

PARALLEL COMBINATION

$1/R_{CELL} = 1/R_{Ag} + 1/R_{H2}$

$R_{CELL} = 1.90\ m\Omega$

ΔV/ΔI CALCULATION FOR 10A AND 5A DISCHARGE

SILVER ELECTRODE

$R_{Ag} = \Delta V/\Delta I = 4.4\ m\Omega$

HYDROGEN ELECTRODE

$R_{H2} = \Delta V/\Delta I = 3.4\ m\Omega$

PARALLEL COMBINATION

$1/R_{CELL} = 1/R_{Ag} + 1/R_{H2}$

$R_{CELL} = 1.92\ m\Omega$

ΔV/ΔI CALCULATION BASED ON FULL CELL VOLTAGE = 2.0 mΩ

CONCLUSIONS

FLIGHTWEIGHT SILVER- HYDROGEN CELLS HAVE BEEN BUILT BASED ON EXISTING FLIGHT QUALIFIED NICKEL-HYDROGEN CELL CESIGNS

SILVER-HYDROGEN IS CAPABLE OF PROVIDING UP TO 80 Wh/kg

DISCHARGE VOLTAGE IS 1.19 VOLTS AT NORMAL RATES (<0.5C)

CELL IMPEDANCE IS 2.0 MILLIOHMS ($\Delta V/\Delta I$)

ELECTROLYTE MANAGEMENT IS IMPORTANT TO CELL DESIGN

CHARGING BECOMES LIMITING FACTOR ABOVE 50% DOD

HYDROGEN ELECTRODE IS LIMITING DURING HIGH-RATE CHARGE

> 50% DOD MAY REQUIRE INCREASED THERMAL MANAGEMENT

THE PRESSURE VESSEL CAN BE USED AS A QUASI-REFERENCE ELECTRODE TO MEASURE HALF-CELL VOLTAGES

INCONEL/HYDROGEN IS 200mV ABOVE SHE

INCONEL/AIR IS 83mV ABOVE SHE (110mV BELOW Hg/HgO)

INDIVIDUAL ELECTRODE IMPEDANCE CAN BE CALCULATED BASED ON HALF-CELL VOLTAGES

AT RATES BELOW C/2, DISCHARGE VOLTAGE IS A LINEAR FUNCTION OF CURRENT DENSITY (LOW FIELD APPROXIMATION)

CYCLE LIFE IS A FUNCTION OF SEPARATOR/SILVER BARRIER

ERRATA

Original paper published in
The 1997 NASA Aerospace Battery Workshop Proceedings
NASA/CP-1998-208536, pages 83-112

PERFORMANCE OF NICKEL-CADMIUM BATTERIES ON THE GOES I-K SERIES OF WEATHER SATELLITES

Sat P. Singhal
Computer Sciences Corporation

Walter G. Alsbach
Jackson & Tull

Gopalakrishna M. Rao
NASA/Goddard Space Flight Center

A minor change was made to the second equation on page 98 and Table 4 (Page 102) was revised during the final preparation of the paper. These changes were inadvertently left out of the final proceedings. Corrected pages 98 and 102 are reproduced here in their entirety.

Battery Reconditioning

Spacecraft Batteries are reconditioned prior to the start of each eclipse season. The batteries are individually reconditioned by use of the following sequence after verifying that the other battery is connected to the spacecraft bus.

a. Turn off battery charging
b. Open battery discharge relay number 2
c. Inhibit the battery under voltage protection
d. Turn on battery reconditioning

The 139.6 ohm resistive load is connected across the battery, resulting in an initial C/48 (0.25 A) reconditioning discharge rate. The individual cell voltages of the selected battery are monitored throughout the reconditioning discharge period. When the first cell voltage reaches 0.5 ± 0.1 V, the reconditioning discharge is terminated. Figure 6 shows the battery reconditioning circuitry.

On-orbit reconditioning has been performed prior to 7 eclipse seasons for GOES-8, and 5 eclipse seasons for GOES-9. The batteries on GOES-10 were not reconditioned prior to the fall 1997 eclipse season.

Charge removed from the batteries during reconditioning was calculated using a different approach than that described earlier. During reconditioning, the nominal discharge current has a value of 0.25 A (C/48 rate). However, the step size for the discharge current telemetry is 0.06 A, too coarse to show discharge current changes as the battery voltage changes. Since the battery is being discharged by connecting it to a constant resistor (139.6 Ohms), the discharge current is given by the use of Ohm's law

$$I = V/R$$

and the charge removed as an integral of battery voltage, i.e.,

$$D\ (Ah) = (1/R) \int (V - 0\ 6)\ dt$$

where 0.6 represents voltage drop across the diode on discharge relay. In addition, since the reconditioning process continues for 60 - 65 hours, the voltage data for integration is sampled at 1-minute intervals at the beginning and end of the process (where the voltage is changing comparatively rapidly) and at 5-minute intervals during the middle 48 hour period.

Figure 7 shows the performance of GOES-8 battery 1 during its first reconditioning cycle (Fall 1994). The reconditioning was terminated when cell 12 voltage dropped to a value of 0.5 V. Corresponding data for battery 2 is shown in Figure 8.

Table 4 compares the results from all reconditioning cycles to date: seven for GOES-8 and five for GOES-9. The data show that the battery capacity has improved with time. The table also shows the end of discharge (EOD) battery voltage for each case.

Table 4. Battery Reconditioning Results for GOES-8 and -9.

		GOES-8		GOES-9	
		Ah Removed	EOD Voltage	Ah Removed	EOD Voltage
Fall 1994	Battery 1	13.89	25.1		
	Battery 2	13.97	23.9		
Spring 1995	Battery 1	14.98	19.7		
	Battery 2	15.14	19.1		
Fall 1995	Battery 1	15.05	20.3	13.81	22.9
	Battery 2	15.33	19.7	13.57	27.5
Spring 1996	Battery 1	15.62	18.1	14.96	18.9
	Battery 2	15.65	18.3	14.87	19.7
Fall 1996	Battery 1	15.30	19.3	15.03	19.3
	Battery 2	15.45	18.9	15.04	20.1
Spring 1997	Battery 1	15.72	16.3	15.49	17.7
	Battery 2	15.81	17.1	15.32	19.5
Fall 1997	Battery 1	15.41	18.9	15.13	18.7
	Battery 2	15.42	19.5	14.99	19.7

1998 NASA Aerospace Battery Workshop Attendance List

Jon D. Armantrout
Lockheed Martin Missiles & Space
B/149 D/E7-90
POB 3504
Sunnyvale, CA 94088-3504
Ph: (408) 742-1800 Fax: (408) 756-0645
E-mail: jon.armantrout@lmco.com

L. Krista Barker
The Boeing Company
14261 East 4th Avenue
Bldg 6, Suite 100
Aurora, CO 80011
Ph: (303) 677-3265 Fax:
E-mail: rtcurtis@gte.net

Doug Bearden
Marshall Space Flight Center
EB12
Marshall Space Flight Center, AL 35812

Bob Bechtel
Marshall Space Flight Center
EB11
Marshall Space Flight Center, AL 35812
Ph: (256) 544-3294 Fax: (256) 544-5841

Jim Bell
Hughes Space & Communications
MS 1514 / Bldg. 231
POB 2999
Torrance, CA 90509
Ph: (310) 517-7607 Fax: (310) 517-7676
E-mail: jebell1@ccgate.hac.com

Charles W. Bennett
Lockheed Martin Astro Space
230 E. Mall Blvd.
King of Prussia, PA 19406-2995
Ph: (610) 354-6155 Fax: (610) 354-3434
E-mail: ebennett@voicenet.com

Matt Bolling
AZ Technology
4901 Corporate Dr., Suite 101
Huntsville, AL 35805
Ph: (256) 837-9877 x138 Fax:

Ron W. Bounds
Gorca Systems
423 Terhune Rd.
Princton, NJ 08540
Ph: (609) 642-1900 x160 Fax: (609) 642-1901
E-mail: boundsrw@gorca.com

Rita Brazier
Marshall Space Flight Center
EB11
Marshall Space Flight Center, AL 35812
Ph: (256) 544-3295 Fax: (256) 544-5841

Jeffrey C. Brewer
Marshall Space Flight Center
EB12
Marshall Space Flight Center, AL 35812
Ph: (256) 544-3345 Fax: (256) 544-5841
E-mail: jeff.brewer@msfc.nasa.gov

Jack Brill
Eagle-Picher Technologies, LLC
1216 W. C Street
Joplin, MO 64801
Ph: (417) 623-8000 X346 Fax: (417) 623-8000 X441

Harry Brown
Naval Surface Warfare Center - Crane Div.
Code 6095 B2949
300 Highway 361
Crane, IN 47522
Ph: (812) 854-6149 Fax: (812) 854-3589
E-mail: brown_harry@crane.navy.mil

John Bush
Marshall Space Flight Center
EB12
Marshall Space Flight Center, AL 35812
Ph: (256) 544-3305 Fax:

Shirley Butler
Marshall Space Flight Center
EB12
Marshall Space Flight Center, AL 35812
Ph: (256) 544-3298 Fax:

1998 NASA Aerospace Battery Workshop Attendance List

Dwight Caldwell
Eagle-Picher Technologies, LLC
1216 W. C St.
Joplin, MO 64801
Ph: (417) 623-8000 x378 Fax: (417) 623-5319
E-mail: pwrsubsys@epi-tech.com

Bill Carpenter
Harris Government Communications Division
MS 22-5840
POB 91000
Melbourne, FL 32901
Ph: (407) 729-7881 Fax:
E-mail: bcarpe01@harris.com

John E. Casey
Lockheed Martin Space Mission Sys & Services
2400 NASA Rd. 1, EP5
Houston, TX 77058-3799
Ph: (281) 483-0446 Fax: (281) 483-3096
E-mail: john.e.casey1@jsc.nasa.gov

Barbara Clark
SAFT R&D Center
107 Beaver Ct.
Cockeysville, MD 21030
Ph: (410) 771-3200 Fax: (410) 771-0234
E-mail: barbara.clark@saftamerica.com

Estelle Clavelli
Socius Consulting
1624 Woodridge Rd.
Tuscaloosa, AL 35406
Ph: (205) 759-2339 Fax:

Dwaine Coates
Eagle-Picher Technologies, LLC
1216 W. C Street
Joplin, MO 64801
Ph: (417) 623-8000 Fax:

John Cole
Electro Energy, Inc.
22 Shelter Rock Lane
Danbury, CT 06810
Ph: (203) 797-2699 Fax: (203) 797-2697

William D. Cook
Eagle-Picher Technologies, LLC
1216 W. C Street
Joplin, MO 64801
Ph: (417) 623-8000 Fax:

William L. Crabtree
Marshall Space Flight Center
EB12
Marshall Space Flight Center, AL 35812
Ph: (256) 544-5305 Fax: (256) 544-5841

Karen Cunningham
Marshall Space Flight Center
EB12
Marshall Space Flight Center, AL 35812
Ph: (256) 544-5618 Fax:

Robert Curtis
The Boeing Company
14261 East 4th Avenue
Bldg. 6, Suite 100
Aurora, CO 80011
Ph: (303) 677-3265 Fax:
E-mail: rtcurtis@gte.net

Eric C. Darcy
Johnson Space Center
MS EP5
Houston, TX 77058
Ph: (281) 483-9055 Fax: (281) 483-3096
E-mail: edarcy@ems.jsc.nasa.gov

Jeff Dermott
Eagle-Picher Technologies, LLC
POB 47
Joplin, MO 64801
Ph: (417) 623-8333 Fax: (417) 623-0233

Sal Di Stefano
Jet Propulsion Laboratory
MS 277-212
4800 Oak Grove Drive
Pasadena, CA 91109
Ph: (818) 354-6320 Fax: (818) 393-6951

1998 NASA Aerospace Battery Workshop Attendance List

Andrew F. Dunnet
Fraser-Dunnet Consulting
5112 Bradford Drive
Annandale, VA 22003
Ph: (703) 256-4092 Fax: (703) 256-4094
E-mail: adunnet@aol.com

Ted Edge
Marshall Space Flight Center
EB12
Marshall Space Flight Center, AL 35812
Ph: (256) 544-3381 Fax:

Michel Fabre
ALCATEL
100, Bd du Midi
06150 Cannes La Bocca
France
Ph: (33) 4 92927391 Fax: (33) 4 92926190

Jerry L. Fausz
US Air Force Research Lab
AFRL/VSDV
3550 Aberdeen Ave. SE
Kirtland AFB, NM 87117-5776
Ph: (505) 846-7890 Fax: (505) 846-0320
E-mail: fauszj@plk.af.mil

Joseph P. Fellner
USAF
AFRL/PRPB
1950 Fifth Street
Bldg 18, Rm G-33
Wright-Patterson AFB, OH 45433-7251
Ph: (937) 255-7770 Fax: (937) 656-7529
E-mail: fellnejp@possum.appl.wpafb.af.mil

Mike Flowers
The Boeing Company
499 Boeing Blvd.
POB 240002
Bldg 48-19, MS JC-32
Huntsville, AL 35758
Ph: (256) 461-5182 Fax: (256) 461-5981
E-mail: michael.w.flowers@boeing.com

Christopher L. Fox
Eagle-Picher Technologies, LLC
C & Porter Streets
Joplin, MO 64801
Ph: (417) 623-8000 X367 Fax: (417) 781-1910
E-mail: cfox@epi-tech.com

Pete George
Marshall Space Flight Center
EB12
Marshall Space Flight Center, AL 35812
Ph: (256) 544-3331 Fax:

Sophie Guilbert
SAFT Space and Defense Division
Rue G. Leclanche
BP1039
86060 Poitiers Cedex
France
Ph: 33 549 55 4575 Fax: 33 549 55 4780
E-mail: sophie.guilbert@saft.alcatel.fr

Doug Hafen
Lockheed Martin Missile and Space
B/149 D/E7-90
POB 3504
Sunnyvale, CA 94088-3504
Ph: (408) 743-7220 Fax: (408) 756-0645
E-mail: doug.hafen@lmco.com

Charles Hall
1105 Lyngate Dr.
Huntsville, AL 35803
Ph: (256) 880-9927 Fax:

David Hall
Marshall Space Flight Center
EB12
Marshall Space Flight Center, AL 35812
Ph: (256) 544-4215 Fax:

Jeff Hayden
Eagle-Picher Technologies, LLC
3820 South Hancock Expressway
Colorado Springs, CO 80911
Ph: (719) 392-4266 Fax: (719) 392-5103

Albert Himy
Navy / JJMA
2341 Jefferson Davis Highway
Suite 715
Arlington, VA 22202
Ph: (703) 418-4257 Fax: (703) 418-4269

1998 NASA Aerospace Battery Workshop Attendance List

Scott Hoover
Orion Satellite Corporation
2440 Research Blvd.
Suite 160
Rockville, MD 20850
Ph: (301) 258-3325 Fax: (301) 258-3319
E-mail: shoover@loralorion.com

Greg Hoshal
IST
4704 Moore St.
Okemos, MI 48864
Ph: (517) 349-8487 Fax: (517) 349-8469

Sam Hwangbo
Boeing North American Inc.
12214 Lakewood Blvd
Downey, CA 90242-2693
Ph: (562) 922-0252 Fax: (562) 922-5379
E-mail: sam.y.hwangbo@boeing.com

Nathan Isaacs
Mine Safety Appliances Company
38 Loveton Circle
Sparks, MD 21152
Ph: (410) 472-7710 Fax: (410) 472-7800
E-mail: nedizakmsa@aol.com

Lorna Jackson
Marshall Space Flight Center
EB12
Marshall Space Flight Center, AL 35812
Ph: (256) 544-3318 Fax:

Thierry Jamin
CNES / AE / SE / AC
18 Avenue Edouard Belin
31055 Toulouse Cedex
France
Ph: 05 61 27 49 38 Fax: 05 61 28 21 62
E-mail: jamin@shetland.cst.cnes.fr

Judith A. Jeevarajan
Lockheed Martin
2101, NASA Rd 1
Mail Stop EP5
Houston, TX 77058
Ph: (281) 483-4528 Fax: (281) 483-3096
E-mail: jjeevara@ems.jsc.nasa.gov

Chad O. Kelly
Eagle-Picher Technologies, LLC
C & Porter
Joplin, MO 64801
Ph: (417) 623-8000 x436 Fax: (417) 626-2078
E-mail: eplion@aol.com

Jim W. Kennedy
Marshall Space Flight Center
MS EA01
Marshall Space Flight Center, AL 35812
Ph: (256) 544-1002 Fax:
E-mail: jim.w.kennedy@msfc.nasa.gov

Ken King
AZ Technology
4901 Corporate Dr., Suite 101
Huntsville, AL 35805
Ph: (256) 837-9877 x106 Fax:

Martin Klein
Electro Energy Inc.
22 Shelter Rock Lane
Danbury, CT 06810
Ph: (203) 797-2699 Fax: (203) 797-2697

John C. Lambert
Design Automation Associates, Inc.
276 Hazard Avenue
Enfield, CT 06082
Ph: (860) 749-3832 Fax:
E-mail: www.daasolutions.com

Dr. Harlan L. Lewis
Naval Surface Warfare Center - Crane Div.
300 Highway 361
Crane, IN 47522-5001
Ph: (812) 854-4104 Fax: (812) 854-4104

Eric Lowery
Marshall Space Flight Center
EB12
Marshall Space Flight Center, AL 35812
Ph: (256) 544-0080 Fax:

1998 NASA Aerospace Battery Workshop Attendance List

Chuck Lurie
TRW
MS R4/1082
One Space Park
Redondo Beach, CA 90278
Ph: (310) 813-4888 Fax: (310) 812-4978
E-mail: chuck.lurie@trw.com

Dr. Tyler X. Mahy
U.S. Government
c/o OTS, NHB
Washington, DC 20505
Ph: (703) 874-0739 Fax: (703) 641-9830

Michelle Manzo
Lewis Research Center
MS 309-1
21000 Brookpark Rd.
Cleveland, OH 44135
Ph: (216) 433-5261 Fax: (216) 433-6160

Jeff Martin
Marshall Space Flight Center
EB12
Marshall Space Flight Center, AL 35812

Dean W. Maurer
Loral Skynet
292 Johnston Dr.
Watchung, NJ 07060
Ph: (908) 470-2310 Fax: (908) 470-2457
E-mail: dwm@loralskynet.com

Louis C. Maus
Marshall Space Flight Center
PD11
Marshall Space Flight Center, AL 35812
Ph: (256) 544-0484 Fax: (256) 544-4225

Kurt McCall
Marshall Space Flight Center
EB12
Marshall Space Flight Center, AL 35812
Ph: (256) 961-4501 Fax:

Dr. Walter McCracken
Eagle-Picher Industries
POB 47
Joplin, MO 64802
Ph: (417) 623-8000 Fax: (417) 623-0850
E-mail: wmccracken@epi-tech.com

George Methlie
2120 Natahoa Ct.
Falls Church, VA 22043
Ph: (202) 965-3420 Fax: (703) 641-9830

Martin Milden
2212 So. Beverwil Dr.
Los Angeles, CA 90034-1034
Ph: (310) 836-7794 Fax: (310) 836-4494
E-mail: mmilden@worldnet.att.net

Tom Miller
Lewis Research Center
MS 309-1
21000 Brookpark Rd.
Cleveland, OH 44135

Thomas R. Newbauer
SMC / AXEN
SMC / AXE
160 Skynet St.
Los Angeles, CA 90245-4683
Ph: (310) 363-5176 Fax: (310) 363-2532
E-mail: tom.newbauer@losangeles.af.mil

David O'Dell
Marshall Space Flight Center
EB12
Marshall Space Flight Center, AL 35812
Ph: (256) 544-3416 Fax:

Burton Otzinger
Jet Propulsion Laboratory
4800 Oak Grove Drive
Pasadena, CA 91109
Ph: (626) 354-2351 Fax:

1998 NASA Aerospace Battery Workshop Attendance List

Paul Panneton
JHU Applied Physics Lab
11100 Johns Hopkins Rd.
Laurel, MD 20723-6099
Ph: (443) 778-5649 Fax: (443) 778-6556
E-mail: paul.panneton@jhuapl.edu

Gopal Rao
Goddard Space Flight Center
Code 563
Greenbelt, MD 20771
Ph: (301) 286-6654 Fax: (301) 286-1751
E-mail: grao@pop700.gsfc.nasa.gov

Janet Rayl
AZ Technology
4901 Corporate Dr., Suite 101
Huntsville, AL 35805
Ph: (256) 837-9877 x114 Fax:

Ron Repplinger
Eagle-Picher Technologies, LLC
POB 47
Joplin, MO 64802
Ph: (417) 623-8000 Fax: (417) 623-5319

Lee Saylors
Vaughn Associates, Inc.
8801 Willow Hills Dr.
Huntsville, AL 35801
Ph: (256) 881-5706 Fax:

Frank Scalici
INTELSAT
3400 International Dr. NW
Washington, DC 20008
Ph: (202) 944-7353 Fax: (202) 944-7333
E-mail: frank.scalici@intelsat.int

George Schwartz
Boeing
320 Lake St. #104
Huntington Beach, CA 92648
Ph: (562) 922-3050 Fax: (562) 922-1034

Sat P. Singhal
Computer Sciences Corporation
7404 Executive Place
Seabrook, MD 20706
Ph: 301 464-7453 Fax: 301 464-3352
E-mail: ssinghal@csc.com

Yoshitsugu Sone
National Space Development Agency of Japan
Tsukuba Space Center
2-1-1 Sengen, Tsukuba-city
Ibaraki-pref. 305-8505 Japan
Ph: 81-(0)298-52-2285 Fax: 81-(0)298-52-2299
E-mail: sone.yoshitsugu@nasda.go.jp

David M. Spillman
Wilson Greatbatch Ltd.
10000 Wehrle Drive
Clarence, NY 14031
Ph: (716) 759-5378 Fax: (716) 759-8579
E-mail: dspillman@greatbatch.com

Joe Stockel
National Reconnesance Office
14675 Lee Rd.
Chantilly, VA 20151
Ph: (703) 808-4088 Fax:
E-mail: joeskl@ucia.gov

Bradley Strangways
Symmetry Resources, Inc.
POB 785
Arab, AL 35016
Ph: (205) 586-8911 Fax: (205) 586-9443
E-mail: symm@bmtc.mindspring.com

Rao Surampudi
Jet Propulsion Laboratory
4800 Oak Grove Dr.
Pasadena, CA 91109
Ph: (818) 354-0352 Fax: (818) 393-6951
E-mail: rao.surampudi@jpl.nasa.gov

Lawrence Thaller
The Aerospace Corporation
MS M2/275
POB 92957
Los Angeles, CA 90009
Ph: (310) 336-5180 Fax: (310) 336-1636

1998 NASA Aerospace Battery Workshop Attendance List

Robert F. Tobias
TRW
MS R4/1074
One Space Park
Redondo Beach, CA 90278
Ph: (310) 813-5784 Fax:

Walter A. Tracinski
Applied Power International
1236 N. Columbus Ave., #41
Glendale, CA 91202-1672
Ph: (818) 243-3127 Fax: (818) 243-3127
E-mail: watracinski@earthlink.net

Dr. Hari Vaidyanathan
COMSAT Laboratories
22300 Comsat Dr.
Clarksburg, MD 20871
Ph: (301) 428-4507 Fax: (301) 428-3686
E-mail: hari.vaidyanathan@comsat.com

Russell Vaughn
Vaughn Associates, Inc.
3313 Memorial Pkwy., Suite 125
Huntsville, AL 35801
Ph: (256) 881-1494 Fax:

Philippe Vermeiren
VITO
Boeretang 200
B-2400 MOL
Belgium
E-mail: vermeirp@vito.be

Harry Wajsgras
Goddard Space Flight Center
Code 563
Greenbelt, MD 20771
Ph: (301) 286-6158 Fax:

Harry Wannemacher
Jackson & Tull
3502 Moylan Dr.
Bowie, MD 20715
Ph: (301) 805-6095 x749 Fax: (301) 805-6099
E-mail: harry.wan@jnt.com

Marvin Warshay
Lewis Research Center
MS 301-2
21000 Brookpark Rd.
Cleveland, OH 44135
Ph: (216) 433-6126 Fax: (216) 433-8311
E-mail: marvin.warshay@lerc.nasa.gov

Margot Wasz
The Aerospace Corporation
MS M2/275
POB 92957
Los Angeles, CA 90009
Ph: (310) 336-2141 Fax: (310) 336-5846

Steve Wharton
NSWC, Crane Division
Code 6095 B2949
300 Hwy 361
Crane, IN 47522-5001
Ph: (812) 854-4381 Fax: (812) 854-3589
E-mail: wharton_s@crane.navy.mil

James R. Wheeler
Eagle-Picher Industries, Inc.
POB 47
Joplin, MO 64801
Ph: (417) 623-8000 X359 Fax: (417) 623-6661

Tom Whitt
Marshall Space Flight Center
EB12
Marshall Space Flight Center, AL 35812
Ph: (256) 544-3313 Fax:

Doug Willowby
Marshall Space Flight Center
EB12
Marshall Space Flight Center, AL 35812
Ph: (256) 544-3334 Fax:

Albert H. Zimmerman
The Aerospace Corporation
MS M2/275
POB 92957
Los Angeles, CA 90009-2957
Ph: (310) 336-7415 Fax: (310) 336-1636

REPORT DOCUMENTATION PAGE

Form Approved
OMB No. 0704-0188

Public reporting burden for this collection of information is estimated to average 1 hour per response, including the time for reviewing instructions, searching existing data sources, gathering and maintaining the data needed, and completing and reviewing the collection of information. Send comments regarding this burden estimate or any other aspect of this collection of information, including suggestions for reducing this burden, to Washington Headquarters Services, Directorate for Information Operation and Reports, 1215 Jefferson Davis Highway, Suite 1204, Arlington, VA 22202-4302, and to the Office of Management and Budget, Paperwork Reduction Project (0704-0188), Washington, DC 20503

1. AGENCY USE ONLY *(Leave Blank)*

2. REPORT DATE
February 1999

3. REPORT TYPE AND DATES COVERED
Conference Publication

4. TITLE AND SUBTITLE
The 1998 NASA Aerospace Battery Workshop

5. FUNDING NUMBERS

6. AUTHORS
J.C. Brewer, Compiler

7. PERFORMING ORGANIZATION NAMES(S) AND ADDRESS(ES)
George C. Marshall Space Flight Center
Marshall Space Flight Center, AL 35812

8. PERFORMING ORGANIZATION REPORT NUMBER
M–912

9. SPONSORING/MONITORING AGENCY NAME(S) AND ADDRESS(ES)
National Aeronautics and Space Administration
Washington, DC 20546–0001

10. SPONSORING/MONITORING AGENCY REPORT NUMBER
NASA/CP—1999–209144

11. SUPPLEMENTARY NOTES
Proceedings of a workshop sponsored by the NASA Aerospace Flight Battery Systems Program, hosted by the Marshall Space Flight Center, and held at the Huntsville Hilton on October 27–29, 1998.

12a. DISTRIBUTION/AVAILABILITY STATEMENT
Unclassified–Unlimited
Subject Category 44
Standard Distribution

12b. DISTRIBUTION CODE

13. ABSTRACT *(Maximum 200 words)*

This document contains the proceedings of the 31st annual NASA Aerospace Battery Workshop, hosted by the Marshall Space Flight Center on October 27–29, 1998. The workshop was attended by scientists and engineers from various agencies of the U.S. Government, aerospace contractors, and battery manufacturers, as well as international participation in like kind from a number of countries around the world.

The subjects covered included nickel-hydrogen, silver-hydrogen, nickel-metal hydride, and lithium-based technologies, as well as results from destructive physical analyses on various cell chemistries.

14. SUBJECT TERMS
battery, cell, nickel-hydrogen, silver hydrogen, nickel-metal hydride, lithium, lithium-ion, destructive physical analysis

15. NUMBER OF PAGES
724

16. PRICE CODE
A99

17. SECURITY CLASSIFICATION OF REPORT
Unclassified

18. SECURITY CLASSIFICATION OF THIS PAGE
Unclassified

19. SECURITY CLASSIFICATION OF ABSTRACT
Unclassified

20. LIMITATION OF ABSTRACT
Unlimited